UNCLASSIFIED

AD 273 512

Reproduced
by the

ARMED SERVICES TECHNICAL INFORMATION AGENCY
ARLINGTON HALL STATION
ARLINGTON 12, VIRGINIA

UNCLASSIFIED

ASD TECHNICAL REPORT 61-70

Theoretical and Experimental Investigation
of Photochromic Memory Techniques and Devices

THE NATIONAL CASH REGISTER COMPANY
ELECTRONIC DIVISION
HAWTHORNE, CALIFORNIA

DECEMBER 1961

AERONAUTICAL SYSTEMS DIVISION

NO OTS

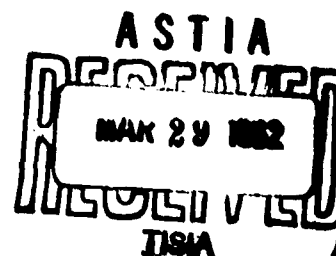## NOTICES

ASD TECHNICAL REPORT 61-70

Theoretical and Experimental Investigation of Photochromic Memory Techniques and Devices

The National Cash Register Company
Electronic Division
Hawthorne, California

December 1961

Electronic Technology Laboratory
Contract No. AF 33(616)-6205
Project 7062
Project 70921

AERONAUTICAL SYSTEMS DIVISION
AIR FORCE SYSTEMS COMMAND
UNITED STATES AIR FORCE
WRIGHT-PATTERSON AIR FORCE BASE, OHIO

FOREWORD

ABSTRACT

This is the final report on the theoretical and experimental investigation of photochromic memory techniques and devices, Contract No. AF33(616)-6205. The report describes the theoretical and experimental investigations which were undertaken, both with respect to photochromic materials and with respect to the associated equipment necessary for the realization of a photochromic memory.

Results are presented on the basic sensitivity and resolution capabilities of photochromic materials. Temperature and fatigue characteristics are also discussed, with special attention given the stability of the colored state with temperature. Chemical data is presented on the light sensitive materials, the solvents, and the coatings.

The additional studies described included light sources, light shutters, cathode-ray tubes, optics and resolution, accessing techniques and systems configurations. Light source studies include an evaluation of the laser (optical maser) for use with photochromic materials. A detailed theoretical and experimental study of the ultrasonic diffraction grating light shutter is presented. Maximum operating speeds and modes of operation with cathode-ray tubes are described. Resolution capabilities of lenses, photochromic coatings, photographic film, Kalvar film, and the effects of illumination for optically storing digital information on light sensitive media are discussed. The systems studies include descriptions of a cathode-ray tube - photochromic memory system and a system for up-dating photographic (permanent) memories.

The final section of the report contains a summary and conclusion of the work undertaken. Volume II contains all the Appendixes referred to in the main body of the report.

PUBLICATION REVIEW

The content of this report represents the scientific findings of an Air Force sponsored program. It does not direct any specific application thereof. The report is approved for publication to achieve an exchange and stimulation of ideas.

FOR THE COMMANDER:

LEONARD M. BUTSCH, Jr.
Lt Colonel, USAF
Chief, Bionics & Computer Branch
Electronic Technology Laboratory

TABLE OF CONTENTS

SECTION I. PURPOSE OF PROJECT AND OBJECTIVES

SECTION II. THE NATIONAL CASH REGISTER COMPANY PHOTOCHROMIC MEMORY PROGRAM PRIOR TO THE RECEIPT OF WADD CONTRACT AF33(616)-6205

TABLE OF CONTENTS

ASD TR 61-70

LIST OF ILLUSTRATIONS

ASD TR 61-70

ASD TR 61-70

xiv

ASD TR 61-70

LIST OF ILLUSTRATIONS

ASD TR 61-70

ASD TR 61-70

ASD TR 61-70

ASD TR 61-70

LIST OF TABLES

xxiv

LIST OF TABLES

SECTION I

PURPOSE OF PROJECT AND OBJECTIVES

A. THE PHOTOCHROMIC MEMORY CONCEPT

Photochromic coatings are similar to photographic emulsions in that they exhibit a change in transmission with excitation by light of the proper spectral distribution. Photochromic coatings differ, however, in two respects: they do not require a development process and they exhibit a reversal of state (return to the first state) when illuminated by light of a second spectral distribution. In this reversal of state, photochromic coatings are similar, superficially at least, to magnetic coatings.

Photochromic surface storage then includes certain characteristics of both photographic and magnetic surface storage. The similarity to photographic storage lies in high information packing density, beam-of-light accessing, high-speed readout, and the promise of low over-all cost per bit. The similarity to magnetic storage lies primarily in the possibility of dynamic operation, i.e., writing and erasing as well as reading.

Although the photochromic memory promised certain unique and desirable features, it was recognized that other inherent characteristics might exist which would make it appear less attractive than alternate storage schemes. In order that the pertinent factors, both pro and con, might be properly weighed from a systems point of view, the photochromic memory program

---

1

was organized to first obtain the basic data which would allow for such an evaluation before undertaking the preliminary systems design.

A more detailed introduction to photochromism and the photochromic memory concept can be obtained by reference to the appendixes. Appendix I is an early paper (February 1958) on the subject of the photochromic memory. It is followed by a discussion of basic principles for the encapsulated materials (Appendix II), encapsulation (Appendixes III and IV) and NCR Photochromism research (Appendixes V and VI).

B. PURPOSE OF PROJECT

This project was initiated to establish the practical feasibility of the photochromic memory concept by both theoretical and experimental investigations. These investigations were to provide the necessary data for the detailed preliminary design of a feasibility model of an optimum realizable photochromic memory system. The program was divided into two phases: a materials research program (not sponsored by this contract) to provide the photochromic materials, and a techniques and components research program (under this contract) to develop, obtain data on, and adapt the necessary techniques and components required for a photochromic memory system. The data thus obtained was to be used in the preliminary design of the feasibility model.

"The commercial devices and materials used during the research were not developed to meet either Air Force requirements of the requirements of the research reported herein. Therefore, if results obtained with such commercial items did not meet requirements, such failures cannot be construed as derogatory to any item or its manufacturer."

C. INITIAL OBJECTIVES

It was agreed that, ultimately, the project would be directed toward a feasibility design which would be classified as general purpose and which would satisfy to the greatest possible extent the following criteria:

1) Simplicity of design
2) Reliability
3) Minimum random access time to stored information

2

4) High volumetric storage density

5) Low over-all weight

6) Low over-all power consumption

7) Insensitivity to shock, vibration, temperature variations, power supply fluctuations, nuclear radiation and other environmental conditions likely to be encountered in high altitude flight.

8) Low cost

It was understood that in obtaining the necessary data for the preliminary design it would not be possible, under this contract, to fully consider all the above criteria. However, it was recommended that where possible, these criteria should be given at least cursory consideration.

D. REORIENTATION OF PROGRAM

Toward the final phases of this program, it was recognized from the data obtained that the preliminary design of a realizable photochromic memory would lead to a device that, from an over-all systems point of view, was not competitive with other general purpose storage devices. The most serious limitations proved to be a slow write-erase speed (due to light source intensity limitations and high photochromic exposure requirements) and a fatiguing (i. e., wearing out) of the coatings under dynamic switching operations. From a systems viewpoint, the latter problem is much more serious than the former. Simple postulation of a faster write-erase speed (e. g., through use of a continuous laser) and/or non-fatiguing materials would not lead to a design that was realizable; such an approach, therefore, was rejected.

Discussions were held with contracting agency technical personnel with respect to the final phase of the program. Since no general purpose or special purpose applications could be found which were compatible with the present characteristics of photochromic coatings and available auxiliary components, it was decided to modify the original goals. The objectives

3

selected for the final effort were to define a photographic memory up-
dating system using photochromic materials and to define a cathode-ray
tube-photochromic memory system designed around the limitations of
present photochromic materials.

E. FINAL OBJECTIVES

Because of the limitations associated with present photochromic ma-
terials, the original concept of a high speed, non-fatiguing memory was
found to be unfeasible. The final goals were modified accordingly, and
it was agreed by those concerned that the final report would include:

1) The synthesis of a system which would provide for the
up-dating of a permanent photographic-type memory through
the use of bulk transfer to a light reversible photochromic
surface on which corrections and/or deletions could be made.
The updated information would then be bulk transferred back
to a photographic-type material exhibiting permanency. It
was understood that, where possible, chemical processing
would be eliminated (e. g. , through use of a heat develop-
able film such as made by the Kalvar Corporation).

2) A preliminary system using cathode-ray tubes for operating
light sources, but with the additional feature of bulk transfer
of data to the photochromic surface included. Though
somewhat impractical at the present state-of-the-art, the
ultimate merits of a cathode-ray tube system seemed such
as to warrant a preliminary study based on this technique.

4

SECTION II

THE NATIONAL CASH REGISTER COMPANY
PHOTOCHROMIC MEMORY PROGRAM PRIOR TO THE RECEIPT OF
WADD CONTRACT AF33(616)-6205

A. GENERAL REVIEW

The National Cash Register Company began an active photochromic
memory research program in June 1957. This program was divided into
two phases: a photochromic materials phase, and a memory techniques
and components phase. The materials phase was assigned to the NCR
Research Department at Dayton, Ohio, and the memory techniques and
components phase was assigned to the NCR Electronics Division at
Hawthorne, California.

Although an ultimate photochromic memory was the goal of the program,
NCR personnel involved at the start of the program felt that the state of
the materials research had not reached the point where reasonable esti-
mates might be made concerning the important characteristics of the
ultimate encapsulated photochromic materials for the memory applica-
tion. As a result, the Electronics Division (Hawthorne) work was pri-
marily directed toward determining which of the many possible opt'cal
and control components (i.e., from light sources to photodetectors)
would most likely meet the needs of the over-all system. A secondary
Hawthorne objective was to formulate systems concepts, making use of
the data available, and to update these systems concepts as new data be-
came available. This approach, it was anticipated, would lead to a work-
ing memory with a minimum of time between the establishment of a final
photochromic material and the production of the prototype memory.

5

In spite of the distance separating the materials and techniques and components groups, a fairly close working relationship was established. Information was exchanged regularly by means of the mail, the telephone, and numerous personal contacts. Regularly scheduled trips were made between the two facilities by members of both groups. This approach led to important changes of emphasis in materials synthesis as the important aspects of material characteristics for the memory application became more well defined.

B. PHOTOCHROMIC MATERIALS PROGRAM

1. Materials

Photochromic behavior of a compound refers to an observable spectral absorption change in the material as a result of incident electromagnetic radiation. Therefore, if such a compound shows a reversible photochromic change and the thermal stability in the two states is long, the compound can be considered analogous to an "on" or "off" switch and function as a memory device. Should this photochromic change be of a permanent nature, the material functions as a recording device or a so-called photographic system. On the other hand, if the photochromic change can only be observed during illumination or only for a very short time thereafter, one has a self attenuating light filter. Although the properties mentioned above depend upon the photochromic behavior of each material, the ultimate applications are quite divorced from one another and depend upon the characteristics of the respective "extremes" of behavior.

In literature on the subject various photochromic materials have been reported; however, at The National Cash Register Company, research was mainly devoted to the thermochromic ethylenes and spiropyrans. All thermochromic ethylenes appeared to be capable of undergoing a non-reversible reaction with light, which eliminated them for applications requiring reversible reactions.

6

Another class of materials which were investigated included the spiropy-
rans,. compounds in which a single atom is a common member of two rings
with three or more members. A general reaction can be written for the
photochromic behavior of these spiropyrans:
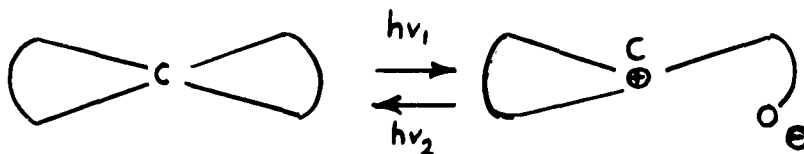
This reaction can be followed spectrophotometrically, since the ring
opening results in the formation of a highly colored material compared to
a colorless or almost colorless material represented by the closed form.
Generally the rate of closure is followed which is dependent upon the sub-
stituent groups attached to the molecule, the solvent, and temperature.

Values (called σ-values) can be assigned to substituent groups which give
a measure of their relative effects on a reaction. This empirical rela-
tionship is known as Hammett's Equation and has been applied to many
systematic investigations of organic reactions. In the synthesis of the
spiropyrans Hammett's σ-values were used as a guide to give improved
thermal stability.

Since the open structure of the spiropyran is more polar compared to
the closed form, its stability in polar solvents (e.g., ethanol) is greater
than in non-polar solvents (e.g., benzene). This was verified by the
rate studies. As expected, the effect of temperature on the rate con-
stants followed the standard thermodynamic relationships.

The evaluation and testing of the various spiropyrans required on general
grounds, the determination of the rate constants under numerous envi-
ronmental conditions. As stated previously, these rates were followed
spectrophotometrically which necessitated the prior determination of the
absorption maxima from the spectra of the respective compound. It was

7

also of importance that as much information concerning the spectral sensitivity and quantum yield be determined; that is to say, the relationship of the photochromic behavior of the spiropyrans to different wavelengths of light.

Since the application of the photochromic material required reversibility, it was required to investigate the stability of the compound under continuous cycling (writing-erasing). Fatigue of the sample meant that it has lost its switching property due to the breakdown or chemical inactivation of the compound. Here again, environmental conditions were proven to be one of the controlling factors in the fatigue studies. By the commencement date of the contract, however, the exact mechanism of this irreversible change had not been determined. Studies of samples by exhaustive illumination methods (representing accelerated cycling), however, had appeared to give some basic data for the understanding of fatigue.

For the utilization of the photochromic spiropyrans for photographic applications, it was required that a fixed print be obtained. Three methods appeared feasible for the stabilization: (1) removal of the solvent, since the switching occurs only (almost all cases) in solution; (2) precipitation of the colored form - this depends upon the relative solubility of the two species in a solvent; and (3) adsorption of the colored form from solution by an absorbent. Process (3) in a way was related to (2); the absorption of the spiropyrans on adsorbents was also dependent upon the compound (functional groups) and solvent. A more detailed discussion is included in Appendix VI.

2.   Encapsulation and Coatings

To restrict the photochemical reaction of the spiropyran to a very small area, the encapsulation process was used. The internal phase of the capsules was varied in respect to compound and solvent to give the required characteristics to the solution. By the encapsulation of the

8

photochromic system of microscopic size, one had, in a way, a very close
analogy to the grain in silver-halide photography. The capsulated material
had been coated on various substrates such as paper, plastics, and glass.
Transparent capsular coatings were obtained when the refractive index of
a secondary coating of a lacquer or similar material was matched with
the initial coating. A more complete treatment of encapsulation is given
in Appendixes III and IV.

Thin transparent films of photochromic materials had also been prepared
by casting a melt of the compound in a polymer, or laminating a highly
viscous solution between two transparent sheets (glass, Coronar film
base, etc.).

3. Testing and Evaluation

Standard chemical and photometric testing of photochromic materials
had taken place as described in Appendixes VI and VII. Data of particular
interest had been collected on the ultraviolet and visible spectra of the
materials, the effect of substituents, solvents, thermal stability, spec-
tral sensitivity, and quantum yield. For certain applications the sta-
bilization of the colored state (fixing) was investigated. This involved
studies of adsorbents, solvents, spiropyran interactions, solvent removal,
and irreversible precipitation of the colored state.

The efforts just prior to the contract concerned dynamic fatigue studies
and involved the design and construction of special fatigue testing appara-
tus (described in Appendixes VI and VII). These studies were concerned
with fatigue as the result of continuous cycling between the written and
unwritten states, under different environmental conditions, under exhaus-
tive illumination, and analyses of fatigue products for theoretical inter-
pretations of the fatigue mechanism.

9

d. PHOTOCHROMIC MEMORY TECHNIQUES AND COMPONENTS PROGRAM

1. Objectives

Since most engineering ventures are a series of compromises dictated by system and component specifications, incomplete component data and limited time schedules ordinarily bring forth "worst" case assumptions in order to maximize the probability of a successful conclusion to such ventures. If a better-than-the-worst-case assumption offers special advantages, such an assumption might be made with a subsequent increase in the risk of failure. If possible, a better course to follow would be to cover both contingencies by carrying on parallel programs with as little duplication of fundamental effort as possible.

The philosophy of the latter approach was adopted for the photochromic memory program. This philosophy stemmed from light source-light shutter considerations and the fact that a greater possibility exists for meeting the broad objectives of the research program with what was felt to be the less desirable of the two most promising approaches. The most desirable approach called for the use of a cathode-ray tube to include both light source and light shutter functions as well as to provide an easily controlled beam for accurate accessing. The other alternative relied on the use of a high-speed ultrasonic light shutter which could be operated continuously and which could be used in conjunction with any available light source. While, in this case, many of the CRT limitations were bypassed, other problems were introduced, one of the most formidable being concerned with accurate fast access. It was entirely possible that both approaches might be found acceptable. It would then be possible to pick the best approach for the specific application.

2. Light Sources

The light source studies began with a literature survey. Numerous contacts were made with manufacturers of light source equipment to

10

obtain information on reliable, high energy light sources with the anticipated spectral characteristics for the photochromic memory application. This was followed by a theoretical study (see Appendix VIII) which indicated that the useful energy output/unit area of the light source was the parameter of greatest importance for rapid switching when the light source was imaged on the photochromic surface. It was also discovered that the total light output became significant when the light was used to illuminate a surface larger than the source to a maximum brightness, and that a subsequent reimaging of this larger surface takes place on the photochromic material (as in one mode of operation of an ultrasonic diffraction grating light shutter). In other words, even with demagnification, optical systems could not create an image with an energy per unit area greater than that of the object. In order to be practical, it was assumed that the condition of equality in brightness could only be approached. (At the time of this study, the coherent optical laser had not as yet been demonstrated practically).

The light sources chosen for writing studies consisted of the Osram HBO-109 and the GE-H6, P16, and P24 phosphors. The Osram HBO-109 was used in source imaging studies, the GE-H6 was used in certain ultrasonic diffraction grating light shutter studies, and the P16 phosphor was used in CRT studies. Additional write and erase sources were obtained which were useful for experimental work. These included electronic flash lamps, a Blak Ray XX-4, and a GE sun lamp.

Other light sources were also found useful in conducting experimental work. These included the tungsten ribbon filament lamp, the Zirconium arc point source, a P15 CRT with servo control (accessing studies), and some other general purpose lamps.

P16 cathode-ray tube studies were conducted with the RCA C-73687A pulsed light source (a non-focused CRT) and a standard Tektronix oscilloscope P16 CRT. Neither source produced visible writing through a quartz optical system although both wrote when photochromic coatings

11

were held against the CRT faceplates. Calculations made from the experiment on the oscilloscope indicated that writing was occurring at the rate of about 40 microseconds per square mil. Phosphor aging, burn, and resolution were serious problems when the equipment was operated at high energy levels. The P16 phosphor rise and fall times measured better than 0.25 microsecond. (Further CRT experimentation of a more quantitative nature was later to be conducted with higher voltage CRT's (15 KV-30KV) in order to obtain high brightness while maintaining good resolution). Design and construction of the hardware for the CRT laboratory program was started prior to the WADD contract. The equipment was designed to accommodate advanced CRT accessing studies as well.

CRT brightness can be increased by a factor of from two to three by going to an air-cooled metal plate-backed phosphor. The phosphor is placed at 45 degrees to the optical axis of the electron gun and is viewed through the side of the CRT which can be fitted with an optically flat window. There was no need to investigate this CRT since the manufacturer, DuMont, claimed that extrapolation by two or three was quite valid. For certain borderline applications of the photochromic memory, such an increase might make an otherwise unacceptable system acceptable.

Writing with the Osram HBO-109 and the GE-H6 lamps indicated at least millisecond writing rates. The use of mechanical shutters limited the shutter speed to from two to three milliseconds. The Osram HBO-109 was used as the writing source in a series of fatigue studies in Hawthorne and also in Dayton.

Alternating current ripple had been noted in most sources that were not powered by a well-filtered d-c power supply. Although this did not interfere with initial gross tests, it was a source of difficulty for the more refined tests at fast shutter speeds. Batteries were used when conducting tests requiring ripple free sources.

12

ASD TR 61-70

Equipment for testing light sources was purchased. This included a grating spectograph, a thermopile and galvanometer, and a calibrated light source. It was found that unless great care was used in the thermopile energy measurements, erroneous results would be obtained. The greatest problem was concerned with heating of the thermopile from infrared radiation.

Light source studies had not been very active just prior to the receipt of the WADD contract. This was related to the fact that new photochromic material was being developed which would most likely have slightly different spectral energy requirements from that of the first material studied, a material which exhibited excessive fatigue under dynamic use. Past experience had indicated that light source energy studies should most logically be carried out simultaneously with writing energy studies. The properties of the photochromic material could then dictate modifications in the testing program to make the data obtained more meaningful.

3. Light Shutters

The investigation of light shutters began with a survey of high speed photography to determine if any of the techniques used in this field would be suitable. In general high speed photography makes use of two schemes: very fast shuttering of high intensity sources and motion compensation by which a moving object is made to appear stationary through an opposing motion in the optical system. Although interesting, the high speed photography study did not come up with any technique or techniques that looked very promising. For example, two shutters that are used in high speed photography are the Kerr cell shutter and the Baird electro-optic shutter. These devices ordinarily operate on a single shot basis. They operate from charged capacitors which are charged over a relatively long interval of time and are discharged over a relatively short interval of time. Even if power supplies were available to operate such shutters at megacycle rates, the shutters would

13

abso:b enough energy to cause over-heating. In addition, commercial Kerr cells do not pass the ultraviolet spectrum. The Baird electro-optic shutter is useful only over a small angular field and it passes only from 10 to 25 percent of the incident light. The on-off contrast is about 100 to 1. (Monitoring of developments in magneto-and electro-optic light shutters, as well as other types, were to continue).

The cathode-ray tube seemed to be the shutter that would have the best characteristics. The reason, however, that a cathode-ray tube did not seem useful for the intended application was the limitation of acceptable phosphors.

The ultrasonic diffraction grating light shutter had been found capable of operating continuously in the microsecond region and yet it did not require excessive power for operation as compared to the electro-optic and magneto-optic devices. A commercial contact was made with reference to furnishing such a light shutter, but the price was found prohibitive.[1] As a consequence, construction of the shutter was undertaken on the project. It was found that the construction of a working model did not require too great a research effort. However, this did not mean to imply that a working model of the calibre that might be required for a photochromic memory would not require a great deal of additional research effort. The theoretical treatment of the ultrasonic light shutter can be found in Appendix IX.

In view of the foregoing, it was decided to concentrate effort on two light shutters for the photochromic memory. The first, and most desirable, was the CRT which would be easily controlled for accessing and act as a light source as well. The other shutter, the ultrasonic diffraction grating, was to be used with a high intensity continuous light source. The ultrasonic shutter had an additional feature. This had to do with automatic filtering possibilities when transmitting light. In other words, this shutter could be operated as a switchable filter and an

14

ultrasonic light shutter simultaneously. The filtering property was a function of the ultrasonic excitation frequency and the shuttering property a function of the amplitude of the particular excitation frequency at any given time.

4. Optics

The optical problems associated with a photochromic material were found to be rather severe. Primarily, the requirement was to transfer the light from a light source to the photochromic surface with a minimum loss of intensity. It was very difficult to decide on specific optical components until the general design (or at least the layout) of the over-all memory had been completed. In other words, should the memory be a drum, disk, tape, stationary surface, scanned by a CRT beam, etc. Most of the conceivable systems would require working off-axis optically as well as on-axis; thus, it was very important to determine just how much a field would be covered by the system. A number of lenses were purchased, some for special applications and others as general purpose lenses. (The general problem of transferring the light from the source to the surface is covered in a paper in Appendix VIII and was discussed under light sources).

Much of the optical equipment required for the project was of a special purpose type. The higher quality lenses were purchased for the ultrasonic application, as this study had proceeded far enough to determine some of the parameters that had to be met by specific optical components. The plans were always to use standard optics whenever possible until the parameters of the system were determined more fully. At that time, project members were to go into consultation with lens designers and lens manufacturers in order to determine the proper specifications of special lenses which would be manufactured to meet the requirements of the photochromic memory. Contacts were made with optical designers and manufacturers.

15

Shortly before receipt of the WADD contract, some investigations which were a direct result of the ultrasonic diffraction grating research led to a more thorough theoretical and experimental investigation of the operation of optical systems. This study was from the point of view of optical information theory rather than that of geometrical optics. This study appeared to be bearing fruit with respect to fundamental optical limitations. The work also indicated that if a photochromic memory could be set up in some very special ways, there was a strong possibility that the contrast of the pattern written on the photochromic material might be materially increased.

Experience with the supposedly high quality lenses that were obtained indicated that it was necessary for users to thoroughly test the lenses. Standard methods used for testing lenses appeared to be inadequate for the type of high resolution operation required. This question was discussed with a number of people, notably scientists working in this field at the National Bureau of Standards. They all seemed to agree that the best method for testing lenses was through sine wave testing or response, which closely correlated with the work in optical information theory mentioned previously. Plans at the end of the period prior to the start of the WADD contract were to continue the optical investigation from the more theoretical approach of optical information theory, which included advanced concepts of sine wave testing and optical spatial filtering.

5. Accessing

There are two ways of accessing photochromic memories. These can be called, generally, open-loop and closed-loop (feedback) accessing. The merits of open-loop accessing are simplicity and a minimum of equipment. However, open-loop schemes require precise mechanical equipment for high resolution. Closed-loop accessing, although it does require more complex equipment, allows for very accurate access schemes and high packing densities for the stored information. The project was organized to place primary importance on closed-loop accessing schemes

16

to obtain both the ultimate pulse packing density that is possible with photochromic material and the optimum rapid access to a specific location. Even though closed-loop schemes were to receive emphasis, possibilities for open-loop accessing were not to be ignored.

The accessing schemes which were studied in the laboratory had to do with the use of a CRT for the light source in an edge locking servo operation. Accessing with the ultrasonic diffraction grating light shutter was considered in one proposed application of such a shutter in a photochromic memory. A more complete coverage of these prior accessing schemes can be found in Appendix XVII.

At the beginning of this contract, a number of pieces of accessing equipment were on hand. One, the Optron, a servoed CRT spot device, had been purchased and modified, and design work was begun on an automatic transistorized accessing system. The design goal was to allow different types of accessing schemes to be programmed with the same components by means of patch cords. This system was to make use of a scheme which counted tracks to the desired track position and then locked on the edge of the track by edge locking servo action.

6. Systems Concepts

Application of photochromic materials to memory systems was approached from the basis of four important points:

1) cost
2) capacity
3) access time
4) transfer rate

Although premature in a sense, members of the project were asked to prepare two random access memory proposals making assumptions

ASD TR 61-70

where necessary and using the most optimum assumptions when such
assumptions were required. The first proposal suggested use of a CRT
with a photochromic disk to give a total system capacity of about 50
million bits. The second proposal advanced the use of a rather novel
drum and the ultrasonic light shutter. Servoing was to be accomplished
with a low inertia mirror. The proposals are described in Appendix
XVIII. No further work was done on these photochromic memory schemes
because of lack of quantitative data on photochromic materials.

7.   Testing and Evaluation of Photochromic Materials

The testing and evaluation of photochromic materials by the Hawthorne
group was rather limited. However, some time was spent in the manu-
facture of photochromic coatings for evaluation in Hawthorne both by
the Dayton and Hawthorne laboratories. This work revealed that the
production of uniform high-quality coatings was by no means a small
task. Some of this work is described in Appendix VII along with pic-
torial data concerning some of the results which were obtained on the
coating techniques. The testing of materials that took place in Hawthorne
had not been too conclusive because of the poor capsule structure of
some of the samples that were received.

In the process of conducting tests on the switching of photochromic
materials, the failure to get repeatability in results led to an investi-
gation of the possible causes of this condition. The investigation was
carried out by a special testing set-up to determine if the
materials were weakening because of fatigue. This work is described
in detail in Appendix VII, and it revealed that the photochromic ma-
terial was suffering from two types of fatigue. The cause of one of
these types of fatigue was determined, and subsequently eliminated.
Work on the other type of fatigue appeared to indicate that it too could
also be eliminated. Work on fatigue just prior to the contract revealed
an improvement by a factor of from 100 to 1000 times over the initial

18

samples. A similar, but more elaborate, testing set-up was built by the Dayton group for automatic fatigue testing.

SECTION III

PHOTOCHROMIC MATERIALS
RESEARCH CONDUCTED IN DAYTON*

A.   ROLE OF THE FUNDAMENTAL RESEARCH DEPARTMENT (DAYTON)

The Dayton research and development program on photochromic materials and coatings was not supported under this contract. However, it was understood that the Fundamental Research Department of The National Cash Register Company at Dayton, Ohio, would prepare, partially evaluate, and make available photochromic materials and coatings as they were required by the photochromic memory project. In addition, regular consultations were to take place between the groups in order to properly define the most optimum realizable material for the memory application. This, in turn, was to help guide the chemists in their efforts to synthesize better materials. The role of the Fundamental Research Department during the course of this contract was carried out as described, but with a greater effort than had been anticipated would be required.

B.   MATERIALS EVALUATION AT THE ELECTRONICS DIVISION (HAWTHORNE)

The evaluation of photochromic materials by the group supported under this contract was to be limited to tests on coatings and bulk encapsulated materials as provided by Fundamental Research. The encapsulated

---

*The work described in this section was carried out in the Fundamental Research Department of The National Cash Register Company at Dayton, Ohio and was not supported by this contract.

20

ASD TR 61-70

materials in bulk were to be included in a coating study at the Electronics
Division if time and manpower permitted. Aside from an additional
brief attempt at the coating of encapsulated photochromic materials
beyond that reported in Appendix VII (which indicated a talk of greater
magnitude than could be adequately handled with the group available),
the materials evaulation was concentrated on the coatings which were
supplied by Dayton, and the coating problem was left with Fundamental
Research. The Hawthorne studies are presented in Section IV of this
report.

C. TECHNICAL DISCUSSION

1. Introduction

The original choice of encapsulated photochromic materials for the
photochromic memory application was dictated by the use of liquid
system. The availability of a microencapsulation process made the
concept of a high resolution liquid photochromic memory practical.

During the latter part of the contract, work on other programs demon-
strated that non-capsular types of coatings could be manufactured with
some very desirable characteristics. These coatings could be written
to higher optical densities, exhibited extremely high resolution and good
optical qualities, and were much simpler to coat on glass substrates
when optimum clarity and uniformity were required. As a result of this
turn of events, the capsular coatings were de-emphasized and the final
portion of the contract made use of non-capsular coatings.

Section II of this report includes a brief description of what is believed
to be the basic photochemical mechanism responsible for the photochromic
behavior of the materials synthesized for this project. Appendixes II
through VII treat the subjects of photochromic chemistry and encapsulation

21

ASD TR 61-70

in much greater detail. The subject of this section of the report will have
to do with the developments in photochromic chemistry and coatings
during the course of this contract.

The desirability of developing photochromic materials for room tempera-
ture operation is obvious. However, with the number of other material
problems which required investigation, the availability of photochromic
systems which would operate within the range of relatively simple
refrigeration equipment delegated this consideration to one of secondary
importance. Indeed, the temperature characteristics had received
vigorous research previously and appeared to be reaching the point of
diminishing returns.

The research conducted on photochromic materials in regard to their
use in a memory device was directed toward the following goals:

1) The synthesis of photochromic materials exhibiting stability
   in two states with reasonable temperature characteristics

2) The synthesis of photochromic materials which exhibited
   reversibility from one state to the other with a minimum
   light energy required for switching

3) The synthesis of photochromic materials with good static
   and dynamic fatigue characteristics

4) To help evaluate the photochromic materials synthesized
   for the memory application

2. Liquid and Capsular Systems

Much of the photochromic materials research and evaluation was con-
ducted with liquid systems, i.e., the photochromic material was dissolved
in a solvent and the resulting liquid placed in a suitable container for

22

study. This approach considerably speeded up research and the results obtained could be extrapolated to the coated systems generally, if the proper precautions were taken.

At the beginning of this contract materials were known with thermal decay times (disappearance of the colored state) at reduced temperatures ($0^{\circ}C$-$10^{\circ}C$) in terms of months. Some could be extrapolated to years, granted that the assumptions made were accurate. In general, however, no one photochromic material was optimum in all its characteristics as compared to another material, for any given application. It was then necessary to select the best material from those available which came closest to providing the best compromise for the particular application. This was the case for the photochromic memory application. A detailed evaluation of available materials was made to provide a selection and some data relatively early in the contractual period.

a. Selection of a Photochromic Material

The first selection of a material for detailed study in the memory program was based on data assembled from the kinetics of the thermal disappearance of color. Some of the photochromic spiropyrans synthesized and their respective rate constants in ethanol and toluene are listed in Table I. The σ-values were used as a guide for synthesis according to the Hammett relationship discussed in the Appendix VI. Although the last compound listed in the table exhibited the best rate constant, the material failed to meet the requirement of light reversibility. The 5', 7'-dichloro-6'-nitro BIPS compound did meet the latter requirement and was therefore selected as the material for use in the memory program. It should be noted, however, that other compounds might have been synthesized with better properties, but the above choice had to be made on the available compounds.

23

TABLE I

THERMAL COLOR DISAPPEARANCE AT $6^{\circ}C$

(1,3,3-Trimethylindolinobenzopyrylospirans)

Substituent	$\Sigma \sigma$	$k(sec^{-1})$ in Ethanol	$k(sec^{-1})$ in Toluene
6'-methoxy-8'-nitro	0.01	1.32×10^{-2}	2.01×10^{-2}
6',8'-dibromo	0.36	3.97×10^{-3}	
5'-nitro-8'-methoxy	0.28	2.52×10^{-3}	2.38×10^{-2}
7'-chloro	0.40	1.26×10^{-3}	
6'-chloro	0.11	1.01×10^{-3}	
5'-nitro	0.66	7.48×10^{-4}	1.93×10^{-2}
6'-nitro-8'-methoxy	0.37	5.53×10^{-4}	4.41×10^{-3}
6'-nitro-8'-methyl	0.62	3.51×10^{-4}	
6'-nitro-8'-allyl	0.62	2.10×10^{-4}	
7'-nitro	0.67	7.11×10^{-5}	1.20×10^{-2}
8'-nitro	0.80	6.30×10^{-5}	1.14×10^{-2}
6'-nitro	0.79	4.28×10^{-5}	1.30×10^{-2}
6'-bromo	0.15	3.98×10^{-5}	
6'-chloro-8'-nitro	0.91	2.27×10^{-5}	2.97×10^{-2}
6'-bromo-8'-nitro	0.95	1.70×10^{-5}	2.53×10^{-2}
6'-nitro-8'-fluoro	1.03	6.33×10^{-6}	5.01×10^{-2}
6'-nitro-8'-bromo	1.00	3.67×10^{-6}	
5'-chloro-6'-nitro	1.15	1.13×10^{-6}	
5'-bromo-6'-nitro	1.17	8.46×10^{-7}	
5',7'-dichloro-6'-nitro	1.52	3.92×10^{-7}	1.70×10^{-4}
5',6'-dinitro-8'-methoxy	1.05	2.34×10^{-7}	

24

b. Selection of a Solvent System.

After the selection of 5', 7'-dichloro-6'-nitro BIPS, more extensive studies were carried out in regard to its behavior in solvents. The kinetic data obtained on numerous solvent systems at various temperatures are tabulated in Table II. Figure 1 clearly illustrates the variations observed in photochromic material-solvent systems. Appendix VI describes the treatment of the kinetic data in regard to the Arrhenius temperature dependance and the determination of the activation energy.

A study of the rates of photochemical color formation for the various solvent systems was also made. This data is given in Table III and was obtained from experiments carried out with low intensity monochromatic light. The correlation of this data with energy measurements made with a light source compatible with a memory device would be misleading due to the wide variations in light intensity and spectral distribution of the source. It does, however, illustrate the importance of choosing the proper light source to provide the biggest optical density changes with the energy input, as is indicated by the photostationary state reached with various wavelengths of light. All the before-mentioned data were obtained in dilute liquid systems and, though useful, did not necessarily define the system to be used in the memory device.

The data in Figure 1 indicated that of all the solvents tested to that date and found suitable for the photochromic memory application, the solvent 1:1 decanol-dimethylcyclohexane possessed the best stability at reduced temperature. Using a straight line extrapolation (somewhat risky), the decay time increases roughly an order of magnitude for each $6^\circ C$ drop in temperature. This calculates to 417 days at $5^\circ C$ and 11-1/2 years at $-1^\circ C$. These results should be used with caution since a non-linear relationship could exist over such long time intervals.

25

TABLE II

5',7'-DICHLORO-6'-NITRO BIPS

RATES OF THERMAL COLOR DISAPPEARANCE

Solvent	Temp. (^{o}C)	λ max. (mμ)	Conc. (M)	k (sec.$^{-1}$)	t 1/2 (min.)
Ethanol	6.0	533	2.5×10^{-4}	3.92×10^{-7}	1155
Energy of Activation* equals 26.78 K cal/mole	25.0	535		9.95×10^{-6}	
	43.2	535	5.8×10^{-5}	2.00×10^{-4}	
	50.4	535	5.8×10^{-5}	4.76×10^{-3}	
*Taken from activation energy plot	63.1	535	5.8×10^{-5}	1.49×10^{-3}	
	70.9	535	5.8×10^{-5}	3.32×10^{-3}	
	72.5	535	5.8×10^{-5}	4.47×10^{-3}	
Methylcyclohexane	10.0	568	5.80×10^{-5}	3.25×10^{-3}	
Energy of Activation equals 21.82 K cal/mole	15.	565	3.11×10^{-5}	5.48×10^{-3}	
	16.4	568	5.80×10^{-5}	7.92×10^{-3}	
	20.9	568	5.80×10^{-5}	1.36×10^{-2}	
	30.3	568	5.80×10^{-5}	3.74×10^{-2}	
	35.4	568	5.80×10^{-5}	7.82×10^{-2}	
2:1 (m/w) Arochlor-Magnaflux Oil	4.5	562,590	3.69×10^{-5}	$4.45 \times 10^{-5}, 4.65 \times 10^{-5}$	258,247
	16.5	562,590	3.69×10^{-5}	$2.35 \times 10^{-4}, 2.37 \times 10^{-4}$	48, 48
Energy of Activation equals 26.17 K cal/mole (for both peaks)	25.0	562,590	3.69×10^{-5}	$9.60 \times 10^{-4}, 1.04 \times 10^{-3}$	11.9,11.1
	33.1	562,590	3.69×10^{-5}	$3.25 \times 10^{-3}, 3.15 \times 10^{-3}$	3.5, 3.6
	39.7	562,590	3.69×10^{-5}	$6.98 \times 10^{-3}, 8.32 \times 10^{-3}$	, 1.4
	48.5	562,590	3.69×10^{-5}	$2.35 \times 10^{-2}, 2.48 \times 10^{-2}$	0.5, 0.5
	58.7	562,590	3.69×10^{-5}	$6.27 \times 10^{-2}, 6.52 \times 10^{-2}$	0.18,0.17

26

TABLE II (Cont'd.)

5',7'-DICHLORO-6'-NITRO BIPS

RATES OF THERMAL COLOR DISAPPEARANCE

Solvent	Temp. (0°C)	λ max. (mμ)	Conc. (M)	k (sec.$^{-1}$)	t 1/2 (min.)
Benzene	10	590	3.11×10^{-5}	4.13×10^{-4}	
	15	590	3.11×10^{-5}	7.33×10^{-4}	
p-Fluorotoluene	10	585	3.11×10^{-5}	7.98×10^{-5}	
1:1 (V/V) Decanol-Dimethy-Cyclohexane	10	540	1.0×10^{-4}		
	25	540	3.12×10^{-5}	6.28×10^{-5}	
	25	540	1.0×10^{-4}	6.6×10^{-5}	
	35	540	1.0×10^{-4}	3.24×10^{-4}	
4:1 (V/V) Decanol-Dimethyl-Cyclohexane	25	540		4.92×10^{-5}	
C_{15} Alcohol	10	540	2.0×10^{-4}		
	25	540	3.11×10^{-4}	1.9×10^{-4}	
	35	540	3.11×10^{-4}	4.03×10^{-4}	
Nitro Cyclohexane	35	555	1.5×10^{-4}	3.6×10^{-4}	
1:4:1 (V/V/V) Toluene-Dimethyl Cyclohexane-Methylcyclohexanol	25	560	3.20×10^{-5}	4.67×10^{-4}	

27
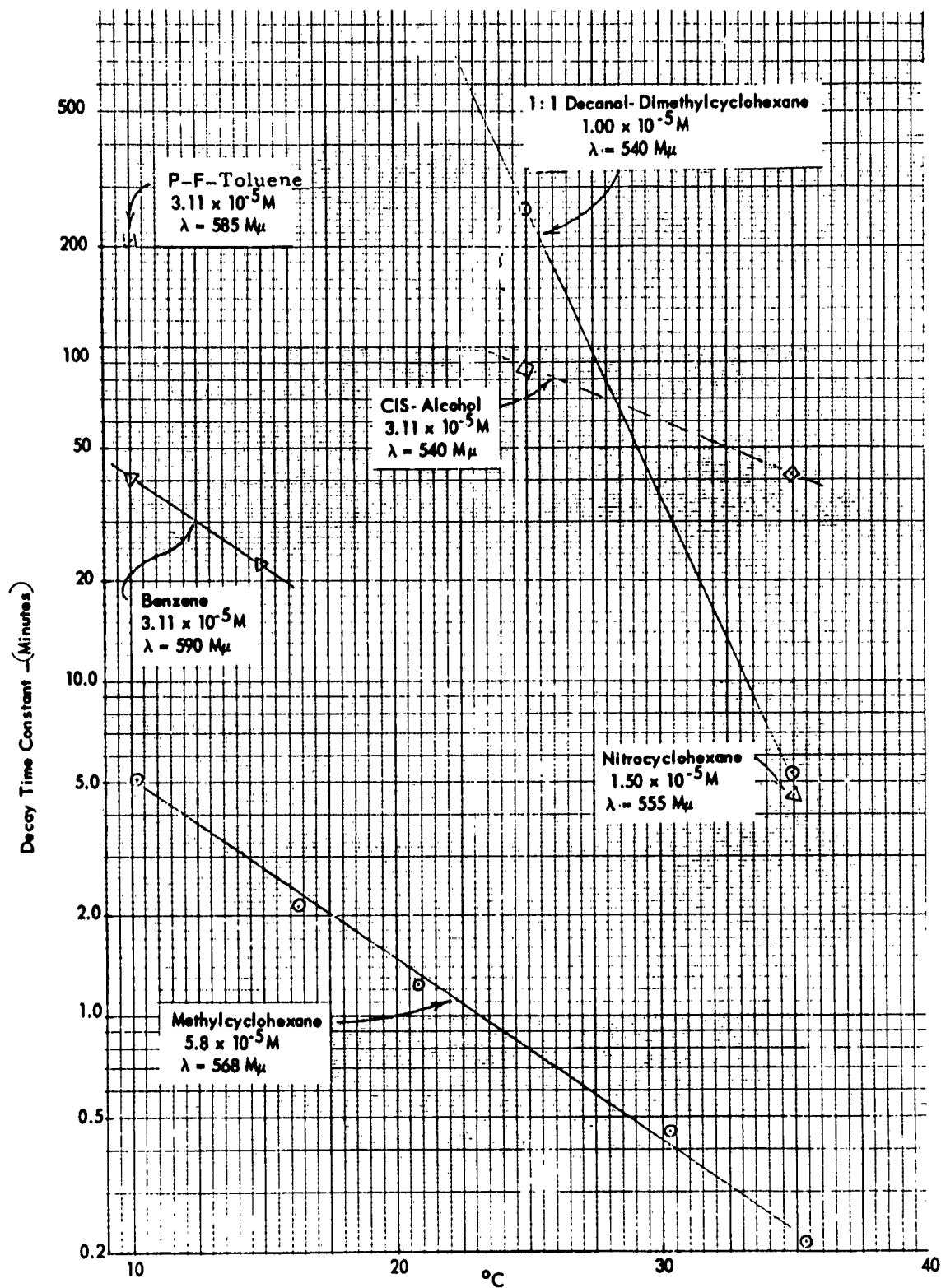
Figure 1. Rate of Color Decay vs. Temperature.

TABLE III

5', 7'-DICHLORO-6'-NITRO BIPS

RATES OF PHOTOCHEMICAL COLOR FORMATION

Solvent	Temp °C	Conc. (M)	λ Exposure	Exposure Intensity (Thermopile Response)	Photochemical Equil. Absorbance	k (sec.⁻¹)
Ethanol	25°	3.11×10^{-5}	366 mμ	33.60 μV	0.263	1.16×10^{-3}
	25°	3.11×10^{-5}	334	2.59	0.550	1.65×10^{-4}
	25°	3.11×10^{-5}	313	22.20	0.835	1.04×10^{-3}
	25°	3.11×10^{-5}	296	11.07	0.922	5.08×10^{-4}
	25°	3.11×10^{-5}	265	7.94	0.891	6.58×10^{-4}
	25°	3.11×10^{-5}	253	5.08	0.826	4.60×10^{-4}
	25°	3.11×10^{-5}	405	8.91	0.128	1.77×10^{-4}
1:1 (V/V) Decanol-Dimethyl-Cyclohexane	25°	1.0×10^{-4}	366	31.42	0.889	6.3×10^{-4}
	25°	1.0×10^{-4}	313	20.33	0.727	8.83×10^{-4}
	25°	1.25×10^{-4}	366	31.50	0.616	7.2×10^{-4}
	25°	1.5×10^{-4}	366	31.08	1.075	7.3×10^{-4}
	25°	5×10^{-5}	366	31.63	0.341	7.1×10^{-4}
	25°	5×10^{-5}	313	20.40	0.894	8.45×10^{-4}
1:1 (V/V) Decanol - Nitro-Cyclohexane	15°	3.13×10^{-5}	366	49.18	0.201	4.99×10^{-4}
2:1 (V/V) Decanol - p-Fluorotoluene	10°	3.15×10^{-5}	366	50.75	0.183	1.67×10^{-3}
Nitrocyclohexane (Impure)	25	1.5×10^{-4}	313	19.93	0.143	1.33×10^{-4}
(Impure)	25°	3.11×10^{-4}	313	20.59	0.320	
(Distilled)	25°	3.10×10^{-4}	366	36.29	0.179	2.4×10^{-4}
(Distilled)	25°	3.15×10^{-5}	313	22.02	0.023	

29

TABLE III (Cont'd)

5',7'-DICHLORO-6'-NITRO BIPS

RATES OF PHOTOCHEMICAL COLOR FORMATION

Solvent	Temp. °C	Conc. (M)	λ Exposure	Exposure Intensity (Thermopile Response)	Photochemical (E mil. Absorbance)	k (sec.$^{-1}$)
p-Fluorotoluene	10°	3.17×10^{-5}	366 mμ	34.68	1.364	8.58×10^{-4}
	10°	2.98×10^{-5}	313	21.70	1.885	1.28×10^{-3}
2:1 (V/V) p-Fluorotoluene-Decanol	10°	3.22×10^{-5}	313	30.22	0.752	8.90×10^{-4}
Phenylethyl Alcohol	10°	3.17×10^{-5}	366	33.22	0.195	7.49×10^{-4}
	10°	3.17×10^{-5}	313	22.33	0.603	8.77×10^{-4}
Benzene	10°	3.12×10^{-5}	366	34.10	1.005	9.49×10^{-4}
	10°	3.11×10^{-5}	313	21.13	1.353	1.90×10^{-3}
n - Butanol	25°	3.13×10^{-5}	366	30.62	0.193	5.7×10^{-4}
	25°	3.13×10^{-5}	313	21.32	0.839	6.66×10^{-4}
	25°	3.13×10^{-5}	313	32.27	0.680	1.23×10^{-3}
α,α-Dimethylbenzyl Alcohol	25°	3.18×10^{-5}	366	36.18	0.288	9.42×10^{-4}
	25°	3.18×10^{-5}	313	33.49	0.818	3.40×10^{-4}
	25°	3.18×10^{-5}	296	18.12	0.178	
1:3 (V/V) 2-Methylcyclohexanol-Methylcyclohexane	25°	3.13×10^{-5}	366	49.84	0.293	1.46×10^{-3}
	25°	3.13×10^{-5}	313	32.32	0.605	1.71×10^{-3}
1:2 (V/V) "	25°	3.12×10^{-5}	366	46.97	0.240	1.80×10^{-3}
	25°	3.09×10^{-5}	313	30.00	0.733	2.01×10^{-3}
1:1 (V/V) "	25°	3.12×10^{-5}	366	49.39	0.288	1.92×10^{-3}
	25°	3.12×10^{-5}	313	32.57	0.738	1.72×10^{-3}

30

TABLE III (Cont'd)

5',7'-DICHLORO-6'-NITRO BIPS

RATES OF PHOTOCHEMICAL COLOR FORMATION

Solvent	Temp. °C	Conc. (M)	λ Exposure	Exposure Intensity (Thermopile Response)	Photochemical Equil. Absorbance	k (sec.$^{-1}$)
1:4:1 (V/V/V) Toluene-Dimethylcyclohexane-2-Methylcyclohexanol	25°	3.20×10^{-5}	313	30.54	0.662	2.35×10^{-3}
2:1 (W/W) Arochlor-Magnaflux Oil	16.5°	3.69×10^{-5}	405	12.82	0.071	9.71×10^{-4}
	16.5°	3.69×10^{-5}	334	4.06	0.057	4.48×10^{-4}

31

Soon after the choice of 1:1 decanol-dimethylcyclohexane as the solvent, it was determined to be poorer in sensitivity to incident radiation and in resistance to fatigue than some of the newer solvents investigated. These solvents were, in general, combinations of dimethylcyclohexane and methylcyclohexanol. Toluene was also noted to increase resistance to fatigue when added to the solvent system.

Capsular photochromic coatings were prepared of the solvent systems which were most feasible for encapsulation. Table IV describes the capsular coatings submitted for test. It is important to note that the choice of the solvent system for encapsulations required that the final coating be transparentized before use. This necessitated a matching in the indices of refraction between the encapsulated system and the over-coating which automatically limited the choice of systems for study. In general, the liquid and capsular samples gave similar results. Following initial testing at Hawthorne, spectral curves of the HSP-208 coatings were run on a double beam spectrophotometer and are shown in Figures 2 and 3.

TABLE IV.   CAPSULAR PHOTOCHROMIC COATINGS*

Designation	Solvents	Solvent Ratios
HSP-208	Arochlor; magnaflux oil	2:1
HSP-209	Methylcyclohexanol; toluene; methylcyclohexane	1:1:8
HSP-210	Methylcyclohexanol; toluene; demethylcyclohexane	1:1:4

* Photochromic material: 1 percent 5'7' dichloro 6' nitro BIPS
  Capsule size: 2-3 microns
  Aggregation: capsules aggregated to form 5-7 micron aggregates
  Overcoating (Transparentizing): Acryloid AT-50
  Dry coating thicknesses: 1-3 mils (approximate)

32
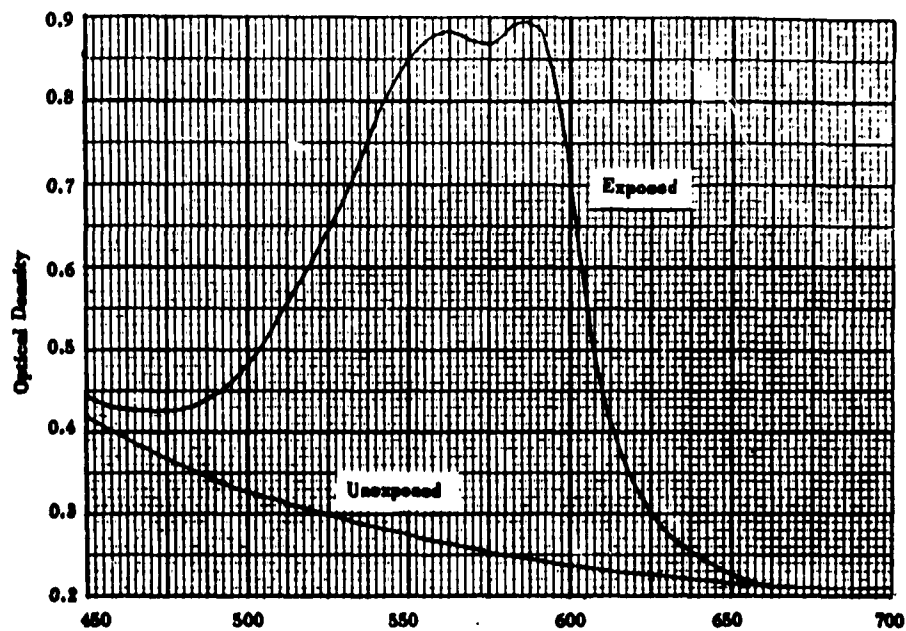
Figure 2. "Clear" and "Exposed" Curves for Transparentized
HSP-208 with Air as a Reference.
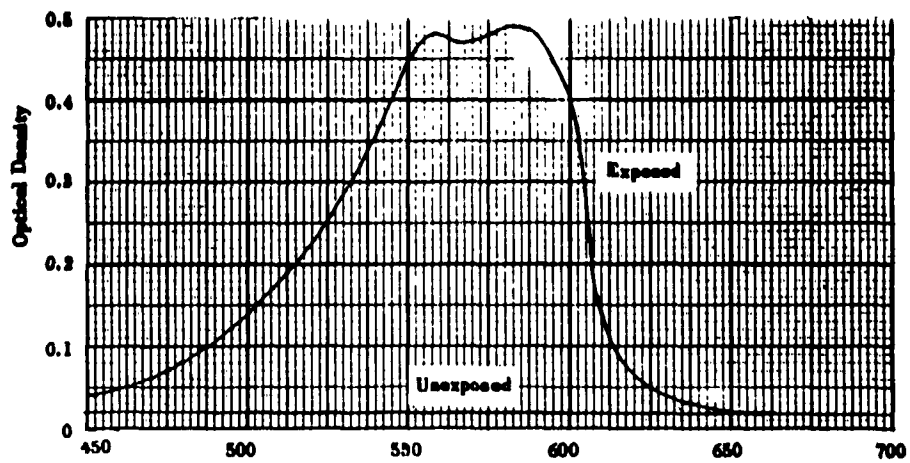
Figure 3. "Clear" and "Exposed" Curves for Transparentized
HSP-208 with HSP-208 as a Reference.

33

ASD TR 61-70

The interest in HSP-208 led to a colored state decay investigation over the range 4.5°C to 58.7°C using a 3.69×15^{-5} molar solution. The results are shown in Figure 4. The effect of dye concentration in obtaining optical density for a typical liquid system is shown in Figure 5. There appears to be no point in exceeding 0.005 molar for this solution. The concentration must be adjusted to minimize precipitation of the colored form in a practical system, so the HSP-208 capsules were manufactured with a 0.001 molar solution rather than some higher value. Tests indicated that a precipitation of some photochromic materials definitely occurred at 0.005 molar. A 0.001 molar concentration appeared to be generally adequate as a safety factor for avoiding precipitation of the colored form for most materials. An increase in optical density of about 25 percent could have been obtained by going to 0.0025 or 0.003 molar with the added risk of a slight degree of precipitation.

3. Non-Capsular Systems (Polymeric Films)

As a result of other programs, techniques were developed for the preparation of non-capsular (solid-solution) coatings. Results obtained with these coatings showed promise for the photochromic memory application. Samples of various coatings were submitted to the Hawthorne group for testing. The Hawthorne evaluation is included in Section IV and shows that an order of magnitude less exposure was required for the non-capsular coatings tested to reach a given optical density as compared to the capsular variety tested.

Non-image forming illumination of the non-capsular samples using varying coating thicknesses indicated that very little increase in optical density was achieved through the use of thicker coatings. Thus, the coloring occurred near the surface and was relatively insensitive to variations in coating thickness over a given sample slide.

34
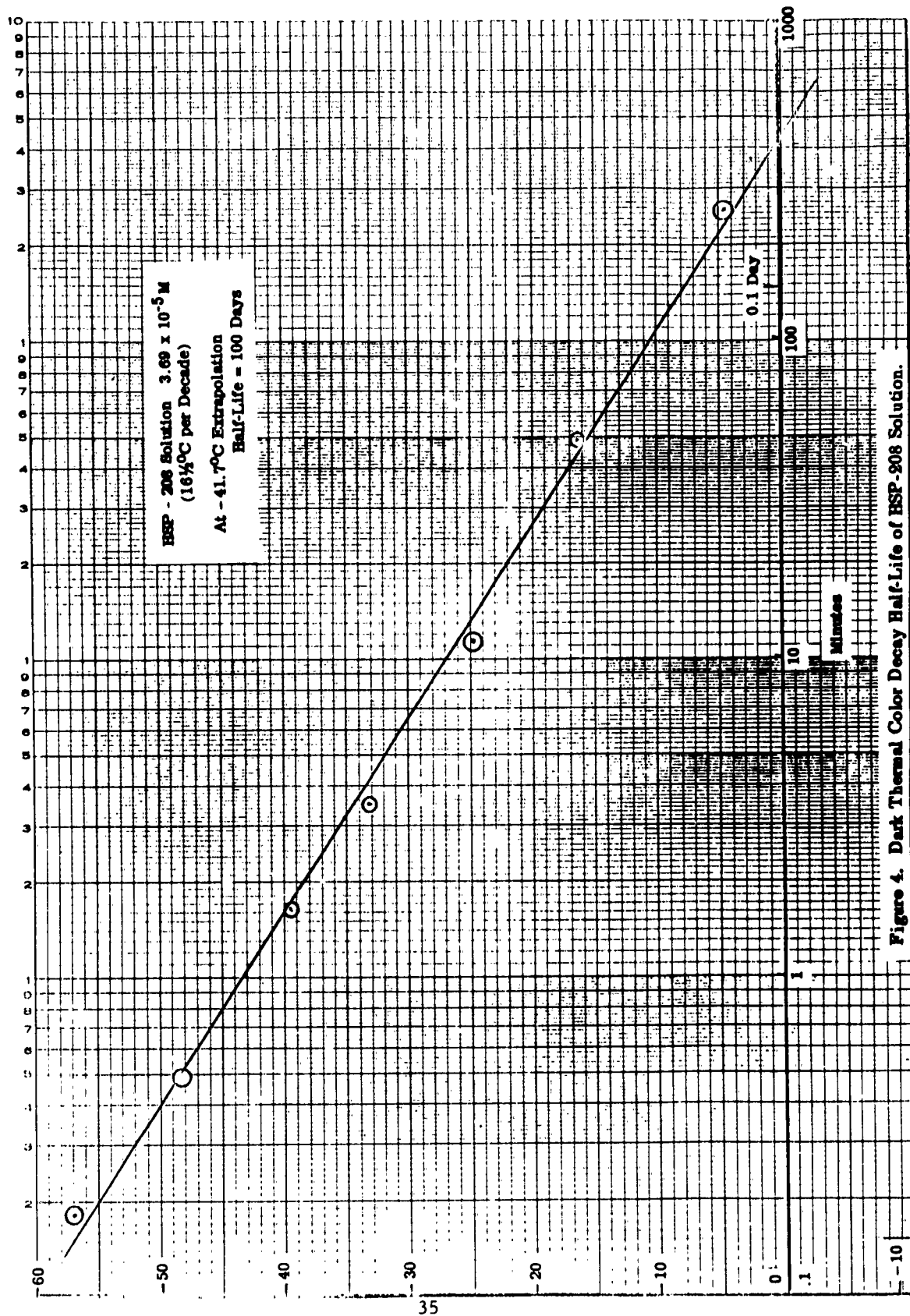
Figure 4. Dark Thermal Color Decay Half-Life of BSP-208 Solution.

BSP - 208 Solution 3.69 x 10⁻⁵ M
(16½°C per Decade)

At – 41.7°C Extrapolation
Half-Life = 100 Days

Figure 5. Concentration vs. Liquid Cell Thickness (6'NO$_2$ BIPS in Toluol).

Sample 1961:

3A. 0.0001 molar
3B. 0.0005 molar
3C. 0.001 molar
3D. 0.005 molar
3E. 0.01 molar
3F. 0.05 molar
3G. 0.1 molar

Optical density achieved by one flash —
(81 watt seconds) at 900 volts, 200 µfd.

36

Tests were run over a period of one month to determine the effect of the loss of the volatile solvent with time on coating sensitivity. The sensitivity of the coating was found to be relatively unchanged on aging over this period. Maximum storage life, or shelf life aging, was not determined.

Measurements made on the polymeric films (without photochromic dye) to below 300 millimicrons indicated that these films were just as good transmitters of the near ultraviolet (300 to 400 mμ) as they were of the visible spectrum. Thus, the sensitivity of the dye-bearing coating to writing illumination does not suffer because of absorption by the film carrier. Table V describes the polymeric films which were submitted to the Hawthorne group for testing. Figure 6 gives the dark thermal color decay for four of the samples.

4. Research on Improving the Characteristics of Photochromic Coatings

In addition to synthesizing and evaluating known materials for the photochromic memory application, a continuing research and development program was conducted at the Fundamental Research Department's laboratory in Dayton with respect to developing new photochromic materials for the memory application. This program was aimed at improving those characteristics which imposed the most severe limitations on the intended use of the materials. The following discussion describes some of the characteristics investigated and the results obtained.

a. Static Fatigue

Only a limited amount of data on static fatigue was collected during the program. The few tests that were run indicated that as long as the bulk photochromic solutions were kept protected from the atmosphere and U.V. radiation they were stable. These tests were limited to periods of a few months duration. Other materials which were kept in slide boxes

37

Figure 6. Dark Thermal Color Decay Half-Life of Photochromic Samples H-62, P-105, P-112 and P-113.
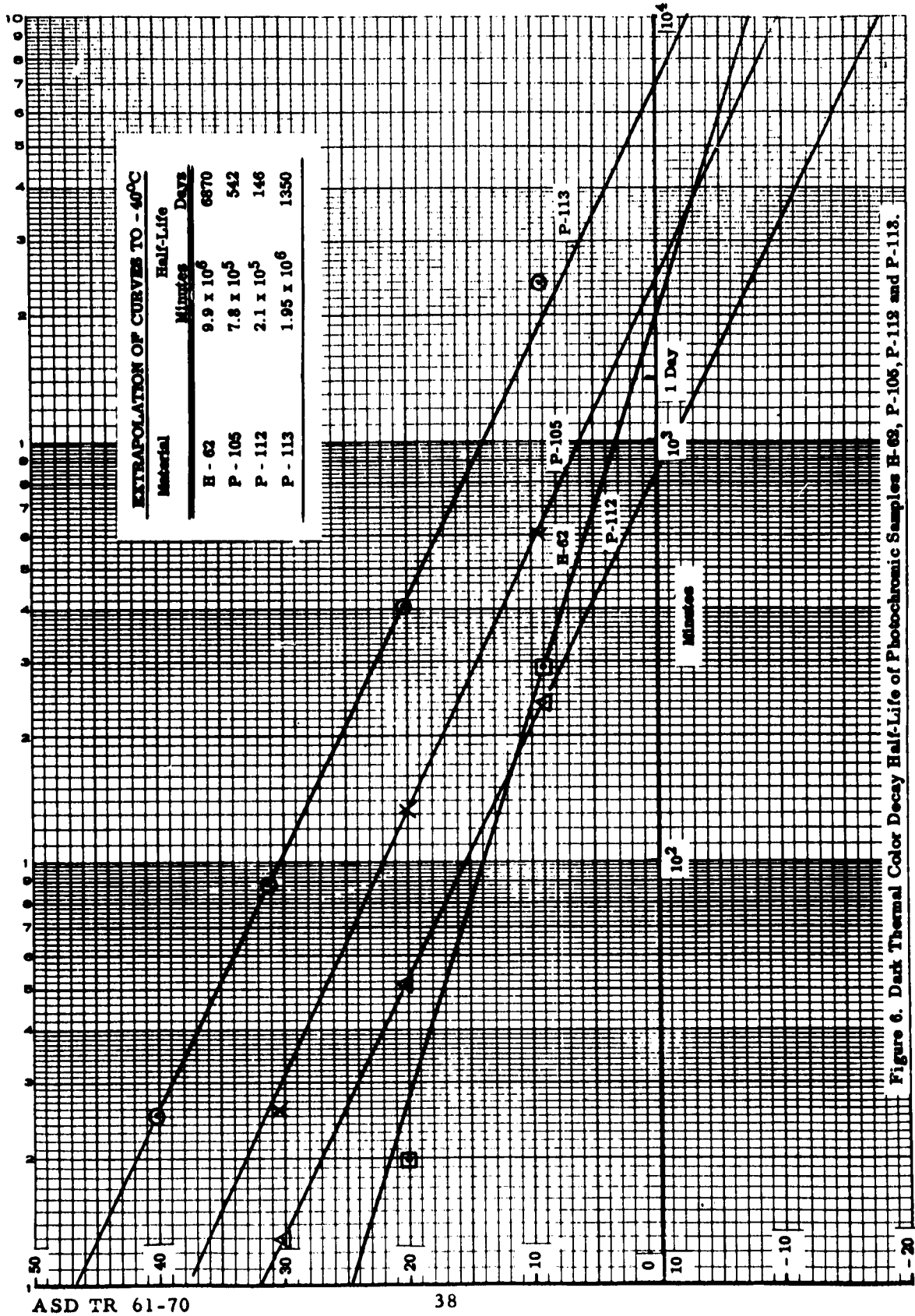
TABLE V

POLYMERIC FILMS

Coating	Photochromic Dye	Resin	Solvent and Plastic
P 102	6'-nitro-8'-methoxyBIPS	Acryloid B-72	Toluene
P 105	6'-nitroBIPS	Acryloid B-72	Mesitylene
P 108	5'-bromo-6'-methoxy-8'-nitroBIPS	Acryloid B-72	Mesitylene
P 112 (also called 94)	5'-bromo-6'-nitro-8'-methoxyBIPS	Acryloid B-72	Toluene
P 113	5'-7'-dichloro-6'-nitroBIPS	Acryloid B-72	Toluene
H 62	5'-bromo-6'-nitro-8'-methoxyBIPS	Ethocel 50 cps	Toluene, ethanol

39

without special precautions offered no problems for periods over a year. At one time a group of slides was found to have become completely insensitive in a fairly short period, but this was traced back to a faulty encapsulation run. In particular, the liquid system used in the HSP-208 coating was determined to suffer no ill effects after a one-month storage period in the dark in a closed container. An HSP-208 coating made in November, 1959 was tested in January, 1960 and again in February, 1961. Both tests gave approximately the same results.

b. Dynamic Fatigue

Dynamic fatigue is the term applied to the wearing out of photochromic materials with use. It is the result of changes which occur within the photochromic systems when they are continuously or repeatedly subjected to the radiation bands used for reading or for switching the material between the two states. Other spectral bands are not of any great importance since there is no necessity for subjecting the photochromic materials to those bands (in a working memory).

It was established just prior to the receipt of this contract that photochromic material was subject to fatigue upon exposure to the ultraviolet writing illumination. As the contract began, there was in progress an attack on this fatigue problem through the study of fatigue in liquid systems. Appendix VI describes the fatigue tester that was under construction at that time for aiding in these studies. In addition, the prolonged exposure of large samples of the liquid systems in the chemical laboratory continued and these results were to be compared to those from the fatigue testing device.

The chemical laboratory fatigue studies indicated that water and oxygen were major factors in the fatigue of systems under study. Water was also noted to affect the rate of decay from the colored to the colorless state (thermal decay). The use of anti-oxidants appeared to reduce fatigue.

40

Results were obtained where a liquid system was fatigued in a closed container, followed by a vacuum distillation process. In this process, it was hoped that the fatigued material plus the fatigue producing agent might be left behind. No improvement in fatigue was obtained.

Later fluctuations as great as 20 percent were noted in the special fatigue tester. After some time, this non-reproducibility was traced to the use of a test cell which had a liquid sample thickness of 30 mils.

It appeared that only that portion of the photochromic liquid system nearest the light source was colored (i.e., the coloring did not penetrate the cell to any great extent) during exposure and the rotating disk holding the cell produced a mixing which, as would be expected, was not reproducible. For more concentrated solutions, a precipitation of the colored form occurred which was often accompanied by a clumping action. This led to even more erratic results. A cell thickness reduction to five mils removed the tendency for these serious convection effects to occur within the cell. This was determined by repeating tests and checking for reproducibility.

With the debugged set-up for checking fatigue, the useful life data for dynamic operation dropped from previously determined values (on this equipment) in the thousands of switching cycles down to hundreds of switching cycles. The convection occurring in the 30-mil cell was apparently replenishing the material continuously, thus leading to a greatly increased apparent life.

Testing with ultraviolet radiation shorter than 313 millimicrons resulted in a rapid fatiguing of the samples. Due to equipment limitations, the region between 313 and 334 millimicrons was not included in this test.

41

Just past the mid point of the contract an expanded fatigue study was initiated in the Fundamental Research Department. At this time it was fair to assume that the following played a role in the fatigue mechanism:

1) water
2) oxygen
3) equilibrium reaction of the starting materials
4) intramolecular rearrangement
5) action of UV on solvent
6) temperature

It was postulated that a 25 percent increase in life could be expected by excluding water. This result is to be expected because water is a part of the equilibrium reaction between the starting materials of the organic synthesis. The starting materials of the synthesis are also subject to air oxidation so photochromic materials are expected to exhibit improved life with oxygen exclusion.

Study of oxygen take-up during continuous exposure of Fischer's Base, a starting material, showed that oxindole was formed by the photochemical process. Continuous U. V. exposure in a nitrogen atmosphere extended the life of Fischer's Base two and a half times and the photochromic system tested approximately four times.

A recent publication[*] showed that Fischer's Base could undergo internal rearrangement under certain conditions. It appeared that such a re-arrangement might occur during ring opening of the spiropyran and lead to a non-light sensitive product. This investigation, however, was not completed by the expiration date of this contract.

---

* Nasao, Nakazaki, et al, Bulletin of the Chemical Society of Japan, pp 461-474 (1960).

ASD TR 61-70

A very interesting experiment was performed late in the program in which a large volume of photochromic material was fatigued. Subsequent analysis revealed that nearly 97 percent of the starting materials were still present, although the sample exhibited complete fatigue. The respective salicylaldehyde and salicylic acid were isolated and definitely identified in the sample. When the corresponding salicylaldehyde or salicylic acid was added to a fresh photochromic solution in the proportions found in the fatigues sample, the fresh sample exhibited the characteristics of a nearly fatigued sample.

The action of U.V. light on the solvent in the presence of photochromic dyes was not investigated.

Although a slight loss in sensitivity occurred, it was found that the useful life of the material was doubled when the temperature was lowered from $+25°C$ to $-10°C$.

Several benzene solutions of 6'-nitro BIPS, one of the structures on which much data was available, were fatigued under slightly different conditions for the purpose of isolating and identifying the fatigue products. A Gates U.V. lamp, a sun lamp, and a conventional incandescent lamp used in various combinations showed that the nature of the fatigue products did not vary significantly with the light source. The decomposition products isolated accounted for less than 4 percent of the starting material and the remaining 96 percent was recovered in either its colored or colorless form. The approximate percentages of starting materials accounted for as decomposition products were as follows:

0.3 percent	5-nitro salicylic acid
1.0 percent	5-nitro salicylaldehyde
0.6 percent	1, 3, 3-trimethyloxindole
< 0.1 percent	1, 3, 3-trimethyl-2-methylene- -hydroxy indoline
0.5 percent	as yet, unidentified tar

43

Qualitative tests indicated that the above products (with the exception of the tar which was not tested) inhibit photochemical color development in decreasing degree as listed above.

A comparison of the vapor phase chromatographs of the benzene used as a solvent and of the distillate obtained from the fatigued solution showed no apparent differences. Therefore, any decomposition products from the solvent must either have been volitilized during exposure or absorbed by the tar.

The findings from the above work indicate that fatigue is essentially a desensitizing action due to small amounts of decomposition products (in cases where complete precipitation of the colored form is not apparent). The next step in the analysis of fatigue will be to determine the concentration of the various decomposition products which can be tolerated without loss of sensitivity. Such information will indicate whether or not fatigue, or rather fatigue products, are directly involved in the sensitivity of fresh BIPS solutions. If trace amounts of decomposition products do not decrease sensitivity, the solution of the fatigue problem can be safely deferred while more emphasis is placed on sensitivity directly.

c. Sensitivity to Switching Radiation

The Fundamental Research Department's investigation of photochromic sensitivity to switching radiation included tests with practical light sources as well as monochromatic radiation. In general, the photochromic sensitivity was found to be slightly better than what was typical for diazo materials.

It was recognized from the start that what was required was a high-speed light source - photochromic material system. Thus, a low intensity

44

source, high-speed material combination would be no better than a high-intensity source, low-speed material. In line with this philosophy, the program included light source intensity and spectrum investigations along with the basic photochromic sensitivity measurements.

The switching radiation used in the fatigue tester consisted of Xenon flash tubes operated in the 50 to 110 watt-second-per-flash region. The between-pulse interval was about three seconds. The spectral quality was controlled by write and erase filters.

Apparent inconsistencies in the data on degrees of sensitivity were noted between the Hawthorne and Dayton groups. This was at least partially due to some extrapolation of monochromatic radiation data from samples in liquid cells. For example, measurements indicated that a 10 microwatt-second/cm^2 exposure at 366 millimicrons of a three mil thick liquid sample could produce a change of 0.3 in optical density when read by tungsten light. The sample consisted of 5'7'-dichloro-6'-nitro BIPS at 0.001 moles in nitrocyclohexane.

The liquid systems were found to be more sensitive than the capsular and non-capsular coatings, which were about equal in sensitivity. To reach an optical density of 2.5 took about 2.5 times as much energy for the coatings than for the liquid sample. At lower densities the energy difference was less; at higher densities the energy difference was greater. All samples were run at very high concentrations.

Many of the results obtained in sensitivity experimentation at Dayton indicated greater sensitivity than the Hawthorne results by about a factor of 3. Higher obtainable optical densities were also observed. It was also noted that the figures from both research groups were more in line when they were normalized about the maximum density as 100 percent. In these tests, an optical density of 1.0 was chosen as the end point of the writing test at Dayton. With the coatings exhibiting very little penetration

45

to writing energy, it appeared quite likely that the convergence angle of the test beam and its plane of focus (if a lens was so used) would contribute to faster or slower writing on photochromic coatings. The calibration of the test beams did not take such effects into account, but merely provided the energy density at the minimum beam cross-section. Thus, somewhat different experimental set-ups could provide somewhat different results.

A detailed experimental study of the sensitivity of the coatings supplied to Hawthorne and a comparison of the results of the two laboratories was undertaken. These studies led to an agreement that the general sensitivity of these coatings were written to near full density was of the order of 1/3 watt-second per cm^2 in the 300 - 4-- millimicron range of the spectrum. Detailed data is included in Section IV of this report.

To obtain high optical densities with a single flash of a Xenon flash tube (EG and G FX-1) required flashes in the hundreds of watts-seconds per flash input. This demonstrated the impracticality of operating at high flashing rates with such tubes.

d.   Contrast Limitations

One of the problems encountered in attempting to achieve high optical densities in photochromic materials was the tendency of the colored form to precipitate from the higher concentration samples. The precipitate was non-reversible and caused a background build-up (described in Appendixes VI and VII). The generally safe concentration for no precipitation of the photochromic dye in the solvent is about 0.001 molar. As this concentration is raised, the background effect gradually became noticeable. However, in the form of plastic coatings the dye concentrations were as high as four percent and this effect did not occur.

46

Much of the experimental work was carried out at higher than the standard concentration (0.001 molar). It was found expedient to run many of the tests at the higher concentrations in order to obtain a higher optical density with the write operation. Because of this, the results obtained were not always directly applicable to the lower concentrations, but only served to indicate what might be expected at these lower concentrations.

The other effect causing background build-up, the yellowing of the solvent, was a relatively minor effect. It was found to cause only slight changes in optical density, and served as a past-history marking for coatings. In this respect, it was useful in the experimental programs.

The presence of a photostationary state offered difficulties in choosing optimum conditions for high contrast operations without complete data on this effect.

e. Single Capsule Structures

Prior to the start of the contract it had been noted that capsules of the diameter of interest for the memory application, five microns or less, tended to agglomerate (stick together as clumps). Such structures were difficult to coat and tended to produce effective grains the size of the agglomerate rather than capsule size. The surface of the coating was also rougher than it would be with a non-agglomerating material, and when an agglomerated grain stuck to the coating bar, streaks were drawn in the coating surface.

The production of single capsule structures (no agglomeration) down to 3 microns showed promise for coatings of much improved quality. There was promise that the optical technique of spatial filtering (to be described under Optical Studies in Section IV) could be used with these coatings to produce enhanced contrast of the patterns stored upon them. In any case, the production of single capsule structures was considered a major breakthrough in capsular technology.

ASD TR 61-70

f.   Preparation of Capsular Coatings

The procedure for making capsular coatings for the photochromic memory device was to dissolve the dye in a suitable solvent at a convenient concentration. This solution (internal phase of I. P.) was then encapsulated in gelatin by the NCR microencapsulation procedure. The capsule solution was concentrated (by removal of water) to a suitable coating consistency (about the consistency of Karo syrup). Draw-down coatings were made on uniformly thick 2 x 3 inch microscope slides using a Baker film applicator (Gardner Laboratory, Inc.) at a wet film thickness of five mils. The coatings were force dried in an oven at 150°F for 5 to 10 minutes. These coatings were transparentized by overcoating with a 40 percent solution of Acryloid B-72 (Rohm and Haas Company) and toluene. The Acryloid was coated at a wet film thickness of five mils and was allowed to air dry.

g.   Preparation of Non-Capsular Coatings

The method used in fabricating photochromic filters was to place a solution of the dye in a polymeric film. The formulations of these filters contained dyes, organic solvents, and resins. A screening program for the dyes was conducted in which approximately 200 spyropyran compounds were tested for their color reactions in various solvents when exposed to ultraviolet light. The spectral characteristics of these compounds were compared between 400 mμ and 700 mμ. The selection of the most appropriate dyes was made from this group.

The selection of dyes to be tested at Dayton and Hawthorne was based on the following considerations:

1)   A marked difference in color should exist between the
     exposed (colored) and the unexposed (uncolored) states.

48

2) The material should have a high sensitivity.

3) The dyes should not fatigue readily.

4) The colored state could be reversed to the colorless
    state, preferably by light energy.

5) The colored state should have a long lifetime, i.e., the
    rate of color decay should be very small.

6) Precipitation of the colored form from solution should
    not occur upon exposure to U.V. light.

(1) Solvents. Commercial grade and analytical reagent grade, organic
solvents were used to dissolve the dyes and resins. Both polar and non-
polar solvents were tested in the formulation for photochromic films.
Emperical solubility parameters* were used as a guide for the selection
of suitable solvents for the resins.

(2) Resins. The main criteria for the selection of resins used as film
formers and carriers of the dye were that 1), the resins be soluble in
common organic solvents, 2), the resins form clear, colorless, trans-
parent films, and 3), the resins be compatible with the dye.

(3) Support Media. Photochromic films were coated on 2 x 3 x 3/64 inch
soft glass microscope slides.

(4) Coatings. Formulations for coatings essentially consisted of the dye
dissolved in a polymeric solution. A typical formulation consisted of one
part (by weight) of dye to 60 parts solvent and 40 parts resin. Coatings
were made by drawing down a thin film of the viscous solution over a
glass slide substrate by means of a Baker film applicator. Wet-coating
thicknesses of 5 to 10 mils were made by this technique. Generally a

---

* H. Burrell, "Solubility Parameters for Film Formers,"
  Optical Digest, pp. 726-758, October 1955.

49

wet-coating thickness of five mils was made which resulted in a dry film
thickness of approximately one mil.

The quality of coatings was governed by the selection of the proper formu-
lation viscosity, purity (free from non-soluble contaminants) of the dye,
and by physically preventing dust particles from settling on the films
during drying.

50

SECTION IV
PHOTOCHROMIC MEMORY TECHNIQUES AND DEVICES
(HAWTHORNE)

A.   INTRODUCTION

With the limited number of project personnel (one to four people at any given time) on this contract, it was not possible to investigate the various techniques and components to the extent originally intended.   The major efforts were concentrated on those areas offering the greatest concern for the realization of a photochromic memory.

Much of the work in the various areas investigated is inter-related. To avoid confusion, as much as possible, it has been necessary to isolate each area for purposes of discussion.   Within each area, the presentation is, more or less, chronological and follows the trend of the project from start to finish.   This type of organization should be helpful to the reader whenever it is necessary to refer from one section of the report to another.

B.   EVAULATION OF COATINGS

A major part of the effort on this contract had to do with the evaluation of coatings as they were received from the Fundamental Research Department in Dayton.   This work included some repetition of the work in Dayton, but was undertaken with the intended application in mind and the evaluation was handled accordingly.   The Dayton studies, as intended, were of a more fundamental nature.

51

1.   Capsular Coatings

a.   General Characteristics

The attainment of coatings of good optical clarity and uniformity has al-
ways been considered a high priority item in the photochromic memory
project. Such coatings are a necessity for achieving the optimum signal-
to-noise ratio, or, in another sense, the minimum useful optical density
for the written marks. This became of even greater importance when
the technique of spatial filtering (to be described subsequently under
Optics) came under consideration as a method for improving the relia-
bility of read-out of information recorded at relatively low optical den-
sities.

During the first phase of the contract period, transparentized "uniform"
capsular coatings were received from Dayton. These were judged by
eye and did, indeed, look quite good. On projecting an image of these
coatings through a spatial filtering system, the uniformity was replaced
by a very irregular structure. The two situations in the optical image
planes were recorded on positive photographic paper (negative picture)
and are shown in Figure 7. The magnification is about 1.5.

The spatial filtering set-up is spatially "coherent" (makes use of a point
source of light) and was used to make both pictures in Figure 7. Thus,
as is well known in photography for specular illumination, even Figure 7
(a), which is without spatial filtering, appears rather sensitive to dirt
and imperfections. The schlerien-type photograph of Figure 7 (b)
reveals non-uniformities in coatings due to changes in refractive index,
transmission, surface shape, and pitting. The effect of such non-
uniformities in a system is dependent on the optical configuration used,
and most non-coherent systems would be rather insensitive to the many
imperfections seen in Figure 7. However, the extreme sensitivity of
the technique made it an excellent one for judging coating uniformity.

52

(a) "Uniform" Capsular Coating (Negative Picture).

(b) Same Coating as Above After Spatial Filtering.

Figure 7.

The evaluation described above was followed by a study of an additional series of coatings supplied by Fundamental Research, Dayton. As was standard practice, these coatings were supplied on 2 x 3 inch microscope slides. Both microscopic examination and spatial filtering were used for evaluating these slides. In addition to capsular structures, one coating was non-capsular in order to ascertain the additional degradation suffered by the capsular structures over the non-capsular species.

The capsular coatings were made up of non-aggregating five micron capsules with a transparentizing overcoating. Figure 8 shows a series of contact photographs made from negatives exposed in the spatial filtering set-up mentioned previously. The image of the scale not only indicates the magnification used (25X), but it also indicates the resolution obtained with the objective lens of this system, somewhat less than 0.001 inch.

Coating (c), the non-capsular coating, is excellent. If it were not for the edges of the coating, it would be difficult to detect its existence (the black spots are specks of dirt). Coating (b) is quite poor and, in fact, could be rejected by simple unaided visual inspection. Coating (a) looked quite good to the unaided eye, except for a few isolated clumps and holes. The spatially filtered picture indicates that there could be some problems in recording and reading back information marks of the order of one or two mils or less in this type of an optical system.

The three slides described above were scanned with a 0.2-mil spot by rotating the slides through the stationary spot. The transmitted light was captured by a multiplier phototube. The results indicated that the coating structure had very little effect on beam intensity when read in this fashion. Coating (b) did appear to introduce a slight bit of "grainy" stationary noise, but even this was quite small. Thus, it was determined that in the non-coherent reading system, coating uniformity is important only with respect to introducing variations in optical density of written spots, defocussing by causing changes in the lens to coating distance,

ASD TR 61-70
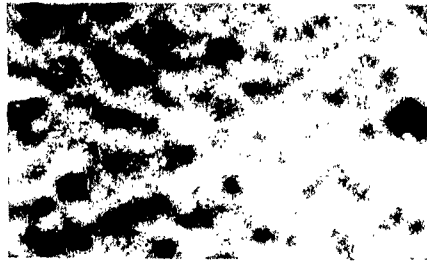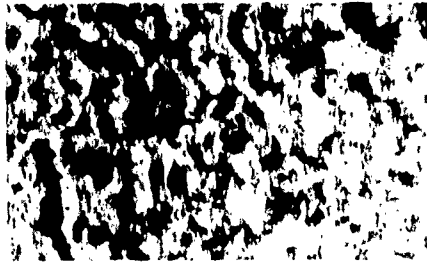
<table>
<tr><td>(a)</td></tr>
<tr><td>(b)</td></tr>
<tr><td>(c)</td></tr>
</table>

With Spatial Filtering   No Spatial Filtering

0   ,1
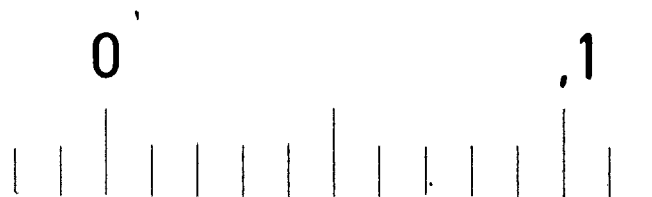
Scale of Photographs
1 small division = 0.010 inch

Figure 8. Photographic Investigation of Coating Uniformity.

55

and reducing the resolution of written spots through reflection, refraction, and diffraction scattering effects on the incoming writing beam. In the coherent, spatially filtered systems, coatings should approach the quality of the non-capsular sample, coating (c).

Although a refrigeration unit was purchased for below room temperature studies, the building of a refrigeration chamber was eventually felt to be an unnecessary complication and was ruled out for the initial studies. This decision stemmed from the receipt of coatings which had a sufficiently long colored state decay at room temperature to allow the pertinent data to be collected before appreciable decay occurred.

Writing tests were run with the first material selected for the memory application, 5'7' dichloro-6' nitro BIPS in 1:1 decanol-dimethylcyclo-hexane. Some of the coatings were manufactured in Hawthorne from thinned out bulk capsular material. These were evaporation-type coatings as described in Appendix VII. Other higher quality transparentized coatings supplied by Dayton were also used. The results indicated a change in optical density between the written and unwritten states of from 0.2 to 0.4. These results indicated that either higher optical densities should be achieved or systems should be developed to operate reliably on fairly small differences in optical density.

On the examination by spatial filtering of additional capsular slides provided by Fundamental Research, Dayton, none were found to be of the optical quality required to perform contrast enhancement by spatial filtering without simultaneously introducing a great deal of noise. These slides included a number of capsular systems, including the chosen system 5'7' dichloro-6' nitro BIPS in 1:1 decanol-dimethylcyclohexane. The best samples appeared to have about one-half the apparent irregularity of structure of that shown in (a) Figure 8. This result called for a de-emphasis of the spatial filtering approach to contrast enhancement

56

until coatings of high optical quality were demonstrated to be feasible with capsular systems (at this point in the project non-capsular materials were not considered feasible). This decision was further enhanced by the relatively good results obtained with the HSP-208 type of coating to be described next.

With the advent of more promising solvent systems, a number of these (designated as HSP-208, HSP-209, and HSP-210) were chosen for evaluation with the selected photochromic material. The chemical characteristics of these systems are described in Section III of this report, which includes spectral data on the HSP-208 capsular coating.

b.   Experimental Evaluation of Capsular Photochromic Coatings
        HSP-208, HSP-209, and HSP-210

The detailed description of the experimental set-up used for obtaining the data to be discussed in this section of the report is contained in the Appendix XI. Briefly, the slides containing the capsular coatings were mounted on a disk and exposed to a nine mil spot (or spots) of ultraviolet light while the disk was held stationary. The disk was then rotated past a "read" station which scanned the exposed plate with a 1/2 mil spot of light from a tungsten source. The light transmitted through the coating was sensed by a multiplier phototube whose output was monitored on an oscilloscope.

(1) Test No. 1 - Relative Optical Densities. First, all the samples were quickly run through so that any large variation in sensitivity from one type of coating to another could be detected. It was found that all the coatings required about the same amount of light to write to maximum density and, therefore, the relative sensitivities were considered to be the same. However, the maximum density differed slightly and is shown in Figure 9 (photographs (a), (b), and (c), representing coatings HSP-208 , HSP-209 and HSP-210, respectively). To the left of each trace is a density ref-

57

erence level having a neutral density of 0.2. Thus, since the density
reference level was maintained the same for each coating, the maximum
density for each sample was as indicated in Table VI.

TABLE VI.

RESULTS OF TEST NO. 1

Material	Photograph Figure 9	Maximum Density At Full Exposure
HSP-208	(a)	0.31
HSP-209	(b)	0.22
HSP-210	(c)	0.25

(a) HSP-208

(b) HSP-209

(c) HSP-210
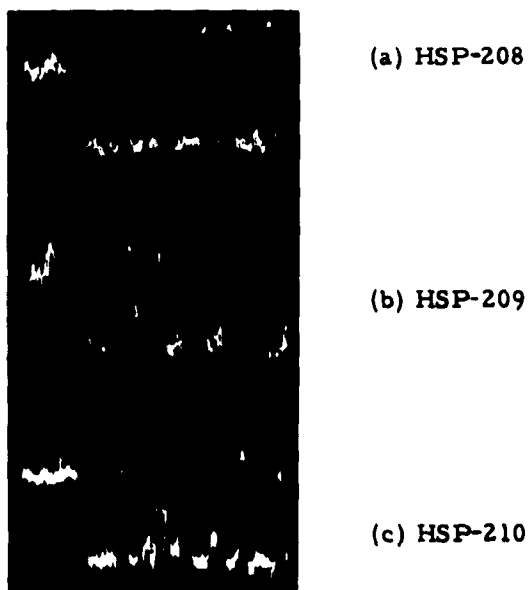
Figure 9. Relative Density Capabilities of Non-Transparentized
Photochromic Coatings.

The thickness for each coating was 0.01 inch (wet) and the non-trans-parentized material was used. Results indicated that HSP - 208 could be written to the greatest density and with the least amount of grain noise. Since the speeds of all the coatings were similar, HSP-208 was selected for the next test.

(2) Test No. 2 - D Log E Curve for HSP-208. To find how the density changed with exposure, a conventional D Log E curve was plotted for HSP-208. Figure 10 shows the results over a wide range of exposures, and the subset photographs represent the photographic data from which the curve was plotted. Subset (a) shows exposures increasing from left to right and exhibiting a maximum density before beginning to fall off with longer exposures. Optimum exposure density for HSP-208 was selected at 0.31 units since the curve begins to turn over after this point. Energy density of the imaged spot during exposure was measured at 0.66 watt secs/cm^2. The graph shows that a density of 0.31 was reached in 0.45 second (4.5T). Therefore, the energy density was approximately 0.3 watt secs/cm^2.

It was surmised at the time of the experiment that the fall-off in maximum density at long exposure times was due to erasure through overheating of the coating. This tends to be verified in subset (b) of Figure 10 which indicates that the center of the written spot (the point of maximum heat concentration) on the right-hand side of the photograph is definitely de-pressed. Further verification was noted through microscopic investigation of spots obtained after relatively long exposures. Figure 11 is a photomicrograph of an overexposed spot which has experienced erasure at the center. Subsequently, it was determined that fatigue was the most important factor here and not overheating.

(3) Test No. 3 - Relative Coating Noise. Tests were made on the non-transparentized coatings (0.01 inch wet) to determine the relative noise of each coating. Photographs (a), (b), and (c) in Figure 12 show noise
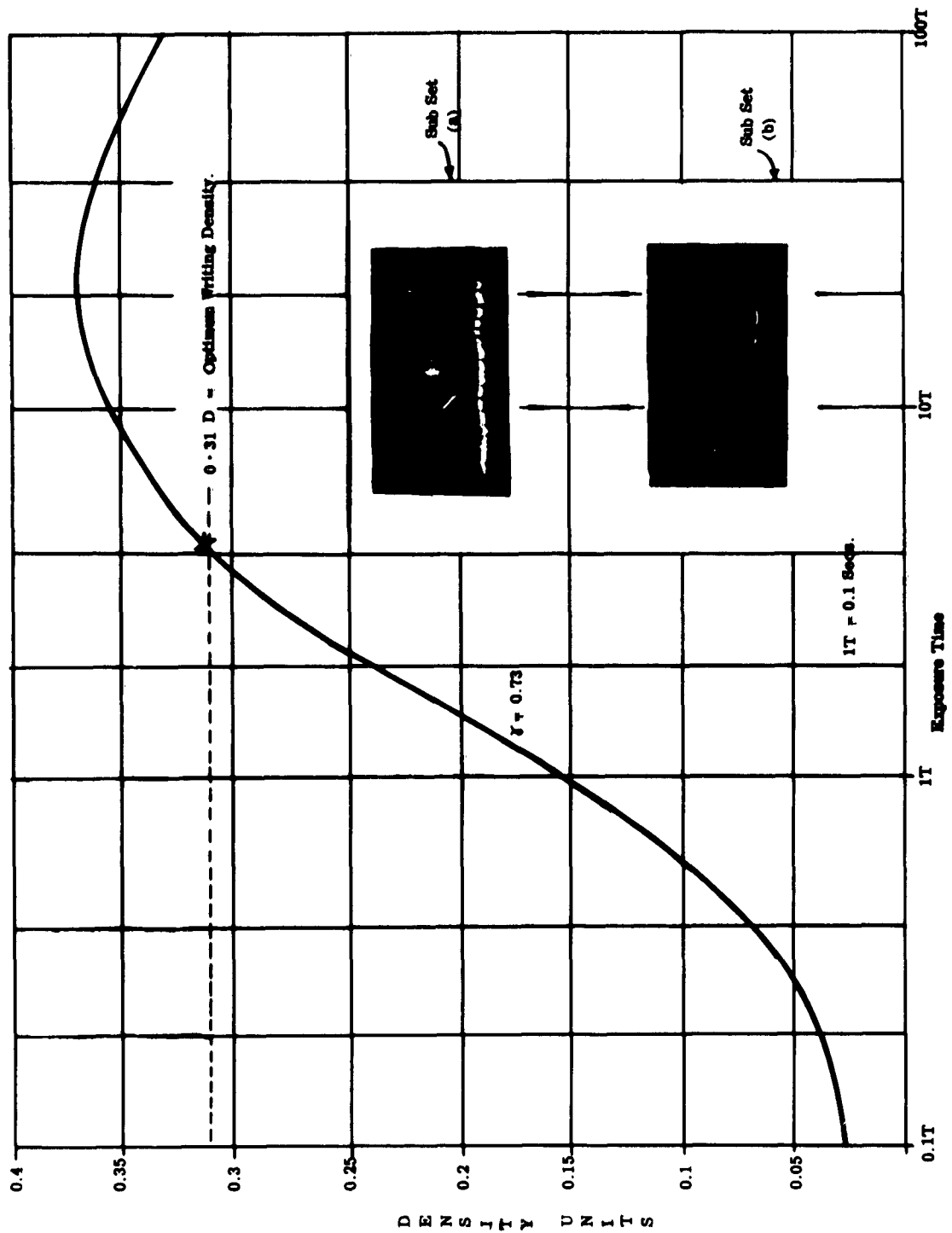
Figure 10.   Graph of Density vs. Log Exposure for HSP-208 10-Mil 10-Mil Coated with AT-50 10 Mil.

0 - 31 D = Optimum Writing Density.

Sub Set (a)

Sub Set (b)

γ = 0.73

1T = 0.1 Secs.

1T   Exposure Time

0.1T   1T   10T   100T

0.4   0.35   0.3   0.25   0.2   0.15   0.1   0.05

D E N S I T Y   U N I T S
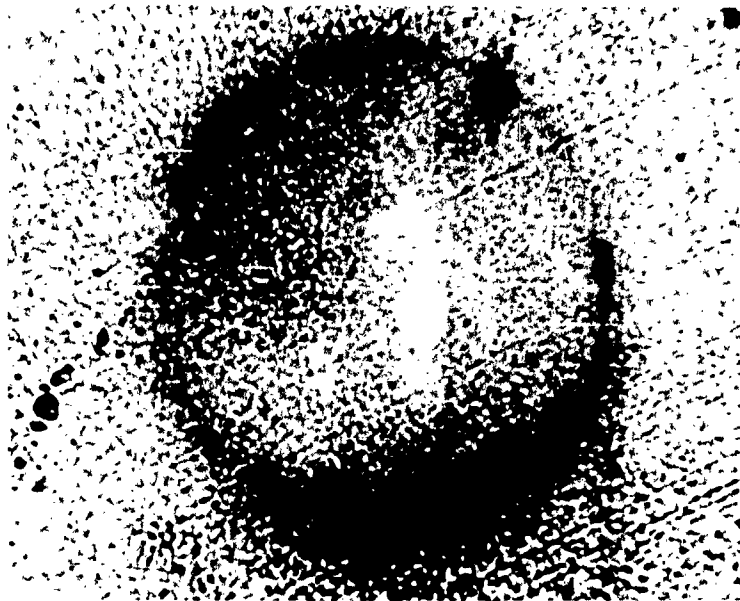
Figure 11. Result of Prolonged Exposure of a
Photochromic Coating.

levels on coatings HSP-208, HSP-209, and HSP-210, respectively.

(a) HSP 208
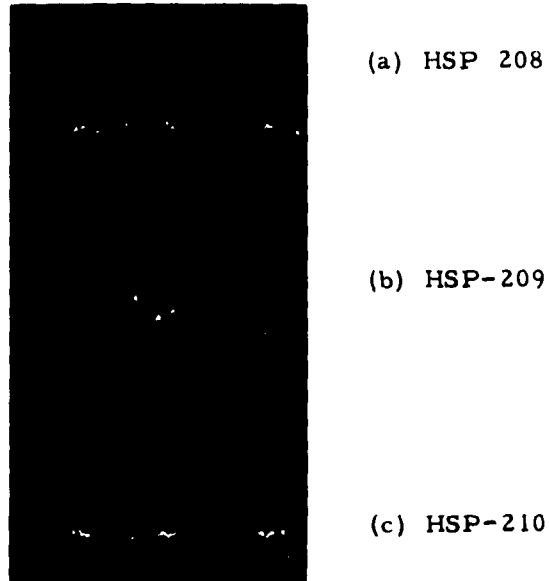
(b) HSP-209

(c) HSP-210

Figure 12. Relative Coating Noise.

From the data the coatings can be graded as indicated in Table VII.

TABLE VII

RESULTS OF TEST NO. 3

Coating	Photograph	Support Marks With Signal/Noise Ratio
HSP-208	(a)	5:1
HSP-209	(b)	2:1
HSP-210	(c)	3. 5:1

From the results obtained, it was evident that HSP-208 was the least affected by noise.

(4) Test No. 4 - Non-Transparentized and Transparentized Coatings. This test showed that the overcoating AT-50, at a thickness of 0.01 inch wet did not provide an improvement for all coatings. Figure 13 (a) and (b) show untreated and overcoated HSP-208 coatings, respectively. A tremendous improvement in signal-to-noise was effected and 0.009 inch diameter marks recorded and read with an improvement in signal-to-noise ratio by practically an order of magnitude. Figure 14 (a) and (b) show untreated and overcoated HSP-209 coatings, respectively. An improvement was discernible but not by as large a factor as for HSP-208. Figure 15 (a) and (b) show untreated and overcoated HSP-210 coatings, respectively, indicating no noticeable improvement in the signal-to-noise ratio. The reason for such variations in improvement was traced

(a)
Untreated

(b)
Transparentized

Figure 13. Untreated and Overcoated HSP-208 Coatings.

Figure 14. Untreated and Overcoated HSP-209 Coatings.

63

(a) Untreated

(b) Transparentized
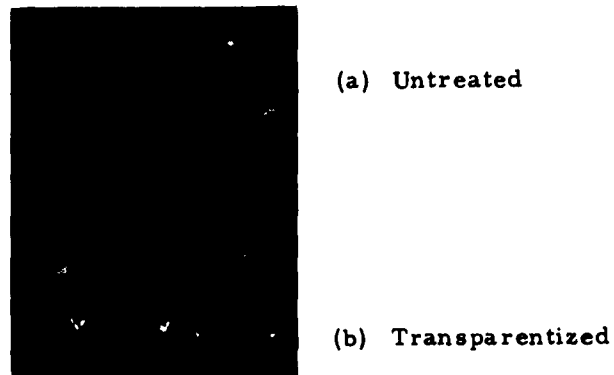
Figure 15. Untreated and Overcoated
HSP-210 Coatings.

to the refractive index match between the overcoating and the coating.
For HSP-208, it provided good improvement because the match looked
good, even to the eye. However, on HSP-209 and HSP-210, the over-
coating had not caused the coating to become truly transparent. Never-
theless, results indicated that overcoating, when refractive indexes were
matched, provided a signal-to-noise improvement in the region of an
order of magnitude.

(5) Test No. 5 - Effective of Coating Thickness (Preliminary Results).
The HSP-208 material was supplied in two grades of wet thickness, 0.005
inch and 0.01 inch. Figure 16 (a) and (b) show the effects of thickness
changes and represent coatings 0.005 inch and 0.01 inch thick, before
drying respectively. The density improved from 0.18 to 0.31 units by
increasing the thickness with no measurable loss in resolution. To the
left of each picture is a neutral density reference level of 0.2 density
units which enables a direct comparison to be made.

64

(a) 0.005 inch wet thick coating

(b) 0.01 inch wet thick coating

HSP-208 Transparentized capsular coating

Figure 16. Effect of Coating Thickness.

(6) **Test No. 6 - Peak Density.** Since HSP-208 (0.01 inch thick wet) gave the best all-around results, an effort was made to spectrally match the reader to see what improvement could be achieved in effective density. A dichroic filter having a very narrow band pass of some five to ten millimicrons and peaking at 552 millimicrons was placed over the reading lamp source. Since it had been ascertained that 552 millimicrons was just within the absorption peak of the exposed marks, a peak density figure was established. To show the effective improvement in density, two photographs were recorded as shown in Figure 17 and 18, showing the effect of the filter. Figure 17, with no filter, shows a seric of marks with reference to a 0.2 neutral density reference marker, a id pictures (a), (b) and (c) are exposures of the same marks at different time base sweeps. The density of the marks in Figure 17 is equal to 0.31 unit. Figure 18 shows the same marks when read with the dichroic filter with the density of the marks equal to 0.56 unit.

This test demonstrated peak density. Since the dichroic filter had such a narrow band, the poor signal-to-noise ratio was to be expected.

65

Figure 17.
Peak Density Without Filter.

Figure 18.
Peak Density With Filter.

The resolution could not be judged either with the dichroic filter, since
the electrical bandwidth of the phototube was reduced to make Figure 18
possible, and evidence of this can be seen by comparing the (c) sweeps
in each photograph.

(7) <u>Test No. 7 - Resolution.</u> The resolution of HSP-208 overcoated with AT-50
was assessed by careful focussing of both the exposing mark and the
reading light spot. Figure 19 represents the best solutions thus far obtain-
able with a 0.009 inch diameter mark. From this it is certain that 0.002
inch marks could easily be resolved, and not too much difficulty should be
encountered in obtaining 0.001 inch marks.

0.009 inch dia. Photochromic mark,
read with 0.0005 inch dia. spot.

Figure 19. Resolution Test of HSP-208.

Photomicrographs were taken of single and multiple written spots with a glass, reference scale overlay. These are shown in Figure 20 and 21. The smallest divisions on the scale are spaced on 10-mil centers. The streaks appearing on the photographs are due to scratches on the reference scale surface. The focus was adjusted with reference to the circular spots so the reference scale was slightly out of focus.

(8) Conclusions Concerning Tests on HSP-208, HSP-209, and HSP-210 Coatings.

(a) HSP-208, 0.01 inch wet and overcoated with AT-50 0.01 inch thick, provided the best results from the samples submitted.

(b) Overcoatings will help most when the coatings refractive index is matched to that of the coating capsules. Under these conditions an improvement in signal-to-noise ratio of an order of magnitude may be expected.

(c) The writing density increases with thickness without any noticeable deterioration in resolution.

(d) Marks some 0.002 inch in size can be written and resolved with a signal-to-noise ratio of 30:1. Marks some 0.001 inch are
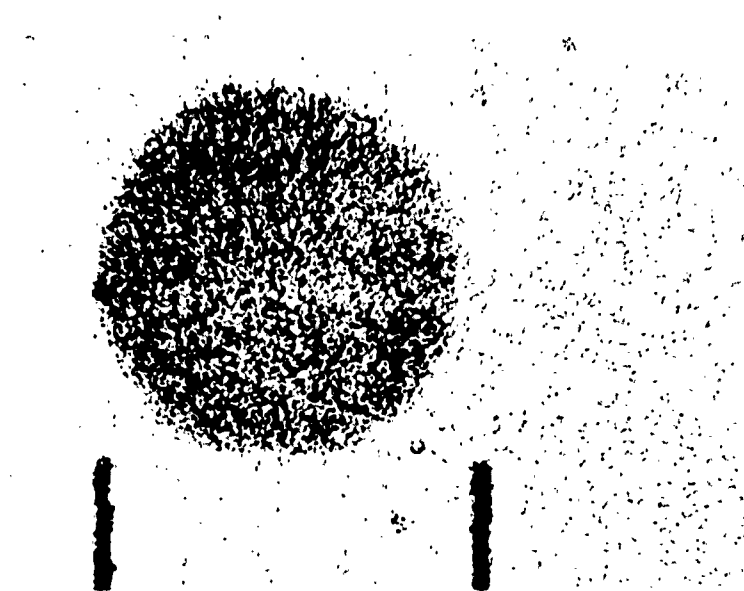
Figure 20.   Photomicrograph of a Nine Mil Spot Written on HSP-208.
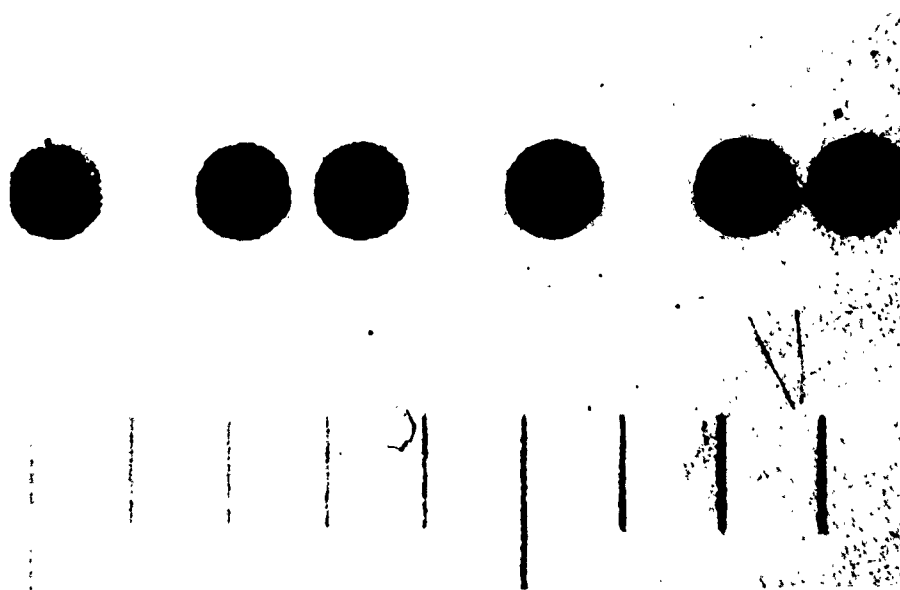
Figure 21.   Photomicrograph of a Series of Nine Mil Spots
Written on HS P-208.

quite realistic, but with some sacrifice in signal-to-noise ratio.

(e) Matching the reading light source to the photochromic material spectral characteristics is desirable and will yield, in general, a factor of two in signal amplitude.

Although not conclusive, the studies at this point tended to indicate that the best patterns stored on capsular coatings are created at some depth within the coatings. Since the read spot is not imaged on the non-uniform upper and lower coating surfaces, the noise due to surface structure is minimized. The surface dirt and dust problems are also minimized for the same reason.

c. Additional Tests To Determine The Resolution Of HSP-208 Photochromic Coatings

As described above, the HSP 208 photochromic coatings gave rather encouraging results as far as resolution was concerned. The purpose of the experiments to be described next was to establish preliminary resolution capabilities of this coating in terms which will be meaningful as far as storage information packing density is concerned.

Some confusion usually results when an attempt is made to quote resolution in numerical form. To appreciate this, one only has to examine some of the units generally used. Lines per inch is popular, but, generally the inspection of lines is subjective. T. V. lines and optical lines become confusing and the former when coupled with what is known as a shrinking raster technique provides yet another figure of dubious value. It seemed sensible, therefore, to avoid a specific numerical quantity based on any of the known confusing units and to determine only the figures that were directly applicable to the intended application.

Since it was proposed to store information in the form of "marks", what better basic unit could be used? For this application the limit of

resolution was defined as the number of marks that could be written per unit area in such a fashion that they could be recovered or recognized by "state of the art" techniques with acceptable reliability. When resolution is measured in marks per unit area, it must be remembered that the final storage capacity in bits per unit area depends upon the manner in which the marks are used to designate a bit. At the time of the study, the best way of doing this was not discussed since it would imply a preconceived system design. Since the definition of resolution implied recovery of the information, it was taken for granted that no appreciable loss was sustained during recovery. The electronics and optics used for this were working well within their capabilities and the limit actually did exist in the recording of data. To be sure of this, suitable tests were made with photographic high resolution plates on marks packed to a far higher density than possible with the photochromic material and no loss in recovery of data was observed. Several photographs of readout traces supported the experiments, and in every case the effective reading spot size was verified as 0.0003 inch diameter, which was small compared with the marks being read.

By stating this, it is not meant to imply that a small reading spot size compared to mark size provides the best ultimate way of reading the marks. Depending upon how the marks are used to designate a bit, there should be an optimum spot size for best signal-to-noise ratio and under certain circumstances can result in a reading spot somewhat larger than the marks. Since we were primarily concerned with the resolution limits of the material, the small reading spot size facilitated this measurement.

(1) <u>Testing Procedure.</u> First, it was necessary to establish a starting point for resolution test. To do this, circular spots were written on the emulsion commencing at 0.01 inch diameter and descending in size until they were just being fully resolved by the reading spot. This occurred at 0.0025 inch diameter spots. Figures 22 and 23 show microphotographs

70

of written spots, accompanied by their respective oscilloscope read-
but traces, for spot diameters of 0.01 inch and 0.0025 inch in diameter,
respectively.

Careful interpretation of the data in Figure 23 enabled the dimensions to
be placed on the photograph. From the oscilloscope trace the read spot
size was determined and apparent edge sharpness of the spots assessed.
The calibration scale on the photograph is in units of 0.01 inch and dim-
ensions in thousandths of an inch have been delineated on the photograph.
The following relationships from these dimensions can be shown:

(2) Calibration of Photomicrograph Against Oscilloscope Trace. From
Figure 23,

        22.5 mils (a) = 14.6 divisions on the oscilloscope trace
    . ˙. one division on the oscilloscope trace = 1.54 mils

Also,

        14.2 mils (b) = 9 divisions on oscilloscope trace
    . ˙. one division on the oscilloscope trace = 1.58 mils

Therefore, the average calibration of one oscilloscope trace division
= 1.56 mils.

(3) Analysis of Oscilloscope Wave Form. For any one mark,

        Width of trace at base of mark   =   3 Divisions = 4.67 mils
        Width of trace at center of mark =   2 Divisions = 3.12 mils
        Width of trace at top of mark   = 1.2 Divisions = 1.87 mils

From the above data, we can compute the read spot size.

71

Actual size of mark   =   2.5 mils

Read spot hidden for   =   1.87 mils

Read spot size = $\dfrac{2.5 - 1.87}{2}$ = 0.315 mils

which checks with other methods of measurement.

For a perfectly defined spot, the width of the trace at the bottom of the mark would be spot size + two read spot diameters, i.e., 2.5 + 2 x 0.315 = 3.13 mils.

Actual measured size of trace   =   4.67 mils

Additional spread = 4.67 - 3.13 = 1.53 mils for both sides.

Therefore, one edge takes 0.765 mils to go from full exposure to clear base density.

The edge spread of 0.765 mils gives a good indication of the resolving properties of the coating, providing no portion of the spread can be attributed to the optical system.

(4) **Discussion of Results and Verification.** From the definition exhibited by the 0.0025 inch diameter spot with an edge sharpness of 0.765 mil, the smallest mark size for complete resolution must exceed twice the figure plus the read spot size, i.e., 1.53 + 0.312 = 1.842 mils. This dictates that the optimum mark packing density for complete resolution using a 0.312 mil read spot would be made by dark marks of 0.312 mil in size placed on 2.154 mil centers. Reading of such a pattern should yield a sine wave reaching full limits of amplitude. Such a pattern could easily be made on a photographic plate and reduced on to the photochromic emulsion for verification. Figure 24 shows a drawing of such a photographic mask which would give the optimum recording pattern together with the expected result and probable output trace.

A starting point had been established for further tests and it was now

72
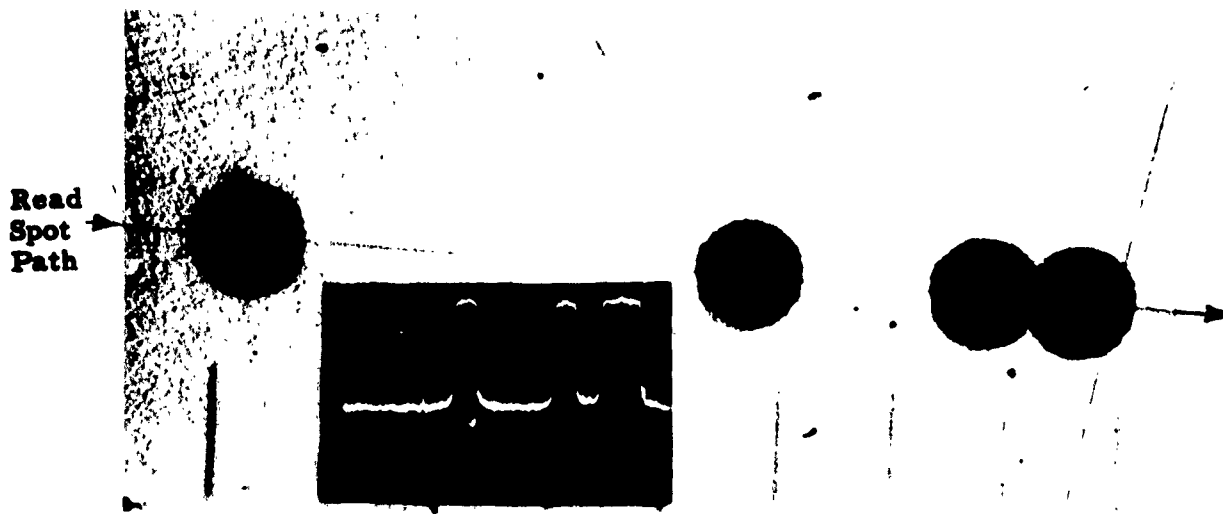
Figure 22.   0.01 Inch Diameter Spot and Associated Read Trace.
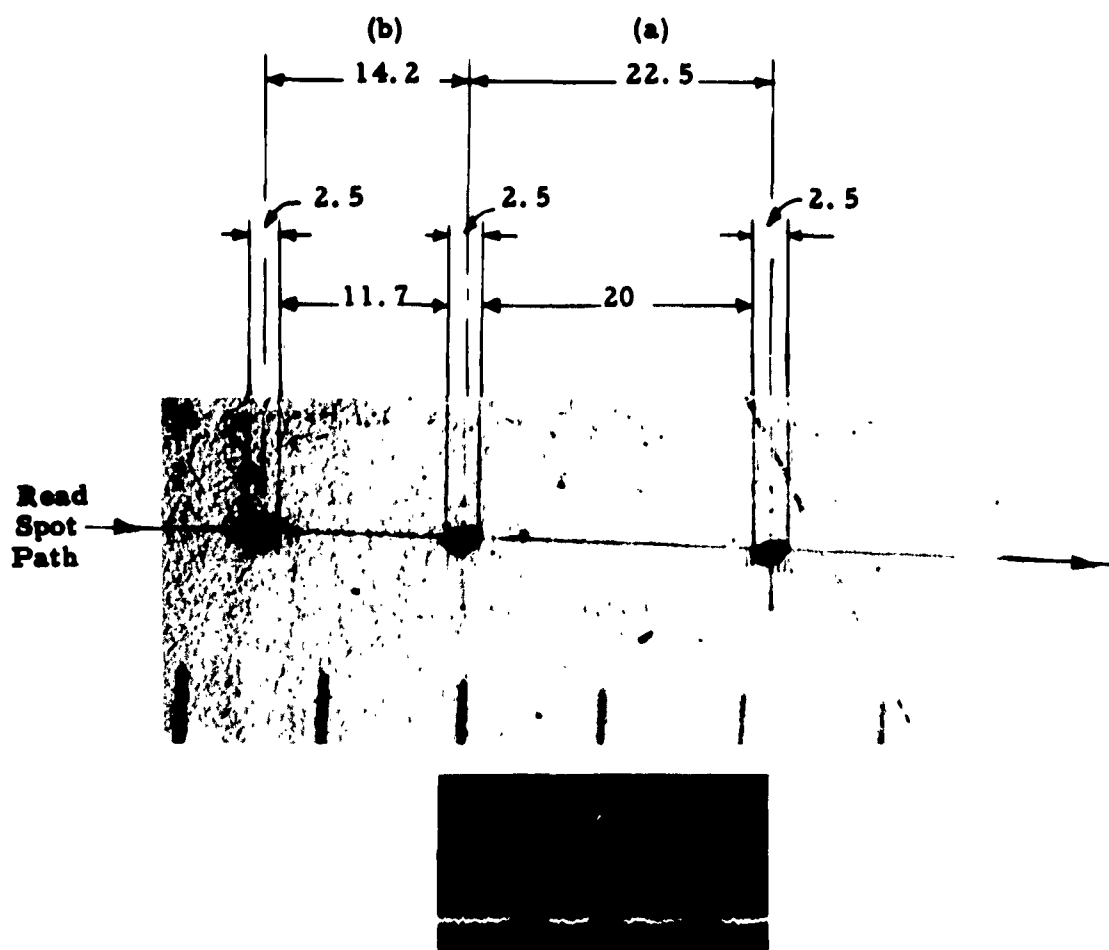
Figure 23.   0.0025 Inch Diameter Spots and Associated Read Trace.
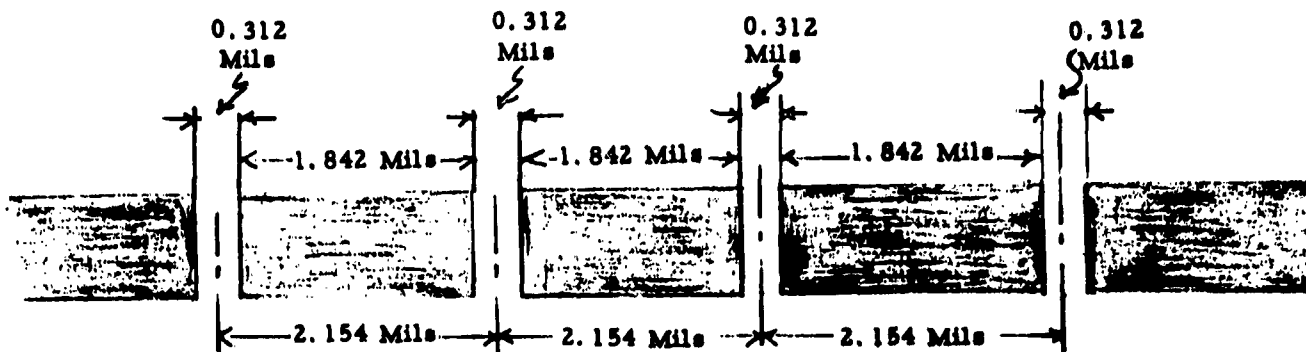
Dimensions for Photographic Mask for Optimum Transfer of Marks
To Photochromic Material for 0.312 Mil Read Spot.
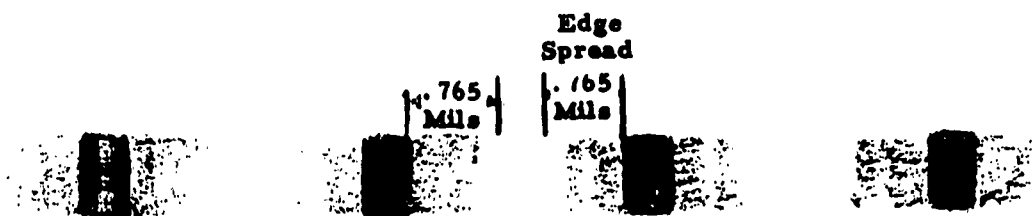
Anticipated Exposure Pattern on Photochromic Material
From Transfer of Above Photographic Mask Showing
Spread Effect (In Lateral Directions Only.)
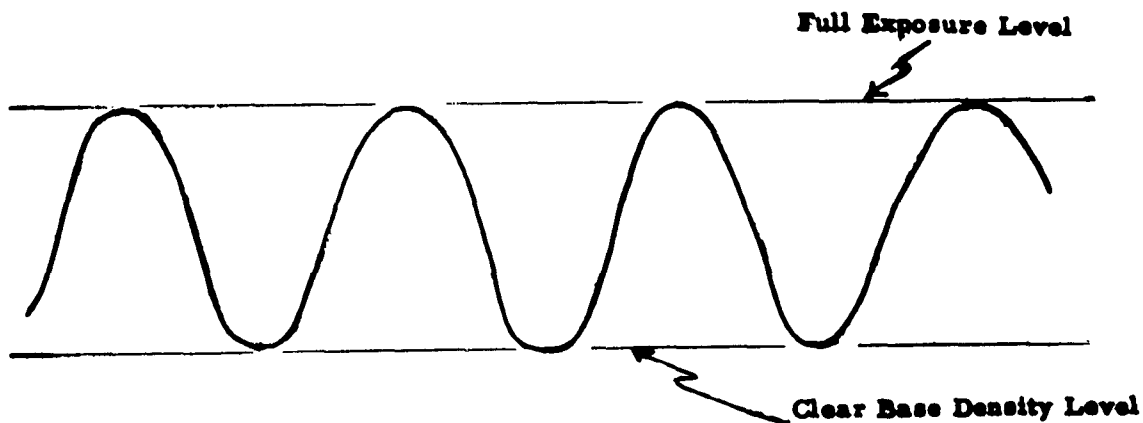
Phototube Readout of Photochromic Marks

Figure 24. Optimum Recording Pattern.

necessary to find how the output signals would be effected by making the masks smaller, which will verify the previous workings. To do this a series of marks, similar to any that could ultimately be used for any real system, was used. These marks were square and uniformly spaced, varied randomly by a factor of two. For convenience several tracks were used and, in addition, black and white borders run on each side of the marks, which were also exactly one mark in size. The master mask for these marks is shown in Figure 25 at full size where each mask is 0.02 inch square. This master mask was used to transfer and at the same time reduce the pattern to required size onto the photochromic coating.

Since earlier tests showed that two mil marks could only be fully resolved with the aid of marks specially spaced on photographic masks, the master mask as shown in Figure 25 was reduced so that each mark was approximately 1.7 mils. This insured that the resolution limits of the material would be exceeded. This pattern was placed on the photochromic slide in such a fashion that any one track of marks could be traversed by the read spot.

Figure 26 shows a microphotograph of such a transferred pattern and Figure 27 shows an oscilloscope trace reading the track marked on the photomicrograph. Several such patterns were recorded which represented the field of the microscope lens. Figure 28 shows an oscilloscope trace sweeping through several complete patterns together with a neutral density reference marker of 0.2 density unit. These scope traces indicated that the read-out was not fully resolved inasmuch as the read spot did not reach full white at any time during the read cycle, with the result that the marks appeared to sit on a pedestal. The degree of the pedestal amplitude was dependent upon the edge fill-in of the white areas of the marks, which was a function of the edge spread in the material. Since the pattern represented marks, 1.7 mil square, and the previously estimated spread from each black mark was 0.765 mil, the only area left in the

75
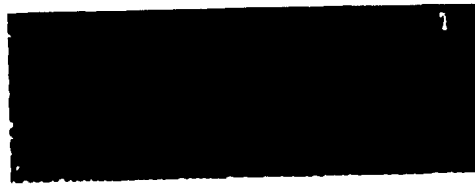
Figure 25.   Master Mask Used for Transfer to Marks to
Photochromic Material.
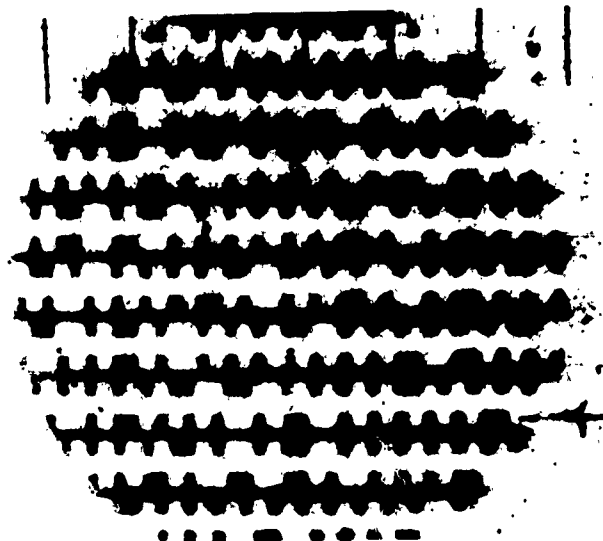
Figure 26.   Microphotograph 1.7 Mil Marks.
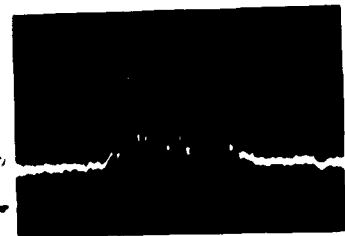
Figure 27.   Read-Out of Track
Shown in Figure 26.
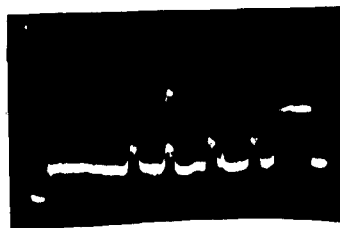
Figure 28.   Read-Out Trace of Several Microscope Fields
1.7 Mil Marks.

white marks where the read spot could be fully seen was 1.7 - 1.53 = 0.17 mil. Since the read spot was 0.3 mil, the whites were not fully resolved. The area between the double white marks showed that more light penetrated through; the oscilloscope trace indicated the intensity of the light that reached full white. Since the distance between edges of a double white mark equaled 3.4 mil and the edge spread consumed 1.53 mil, this left 1.87 mil for the spot to get through, and it being 0.3 mil would show the double whites fully resolved to 1.87 - 0.6 or 1.27 mil. The photograph shows that this was not the case, indications were that the whites were not resolved because of an edge spread of the border exposure, which also spread 0.765 mil. The read spot was adjusted to read in the center of the marks, i.e., $\frac{1.7}{2}$ or 0.86 from the border so that the spot would over-cap into the edge spread of the border. Read-out of the 1.7 mil marks resulted in a signal-to-noise ratio of about 15:1.

This pattern was reduced still further so that the mark size was 1.28 mil square. Figures 29, 30, and 31 show oscilloscope traces of such marks where a signal-to-noise ratio of about 8:1 was obtained. It must be remembered that no attempt was made to spectrally match the read-out. Previous investigations showed that at least an improvement by a factor of two could be expected from such a match.

Thus far, small marks had been made with reasonable success. It was necessary to see if any improvement in edge spreading could be effected by changing optical elements of the system, and to learn how the image was being placed in the photochromic emulsion.

To do this the mark size was maintained constant at 1.7 mil, three different power microscope objectives were used to form the image, and the photographic master mask was moved accordingly to provide the necessary reduction ratios so that the image mark size was held constant. The effect of this was to change the angle of convergence of the image, which could very well affect the edge spreading effect and ultimately the resolution.

ASD TR 61-70
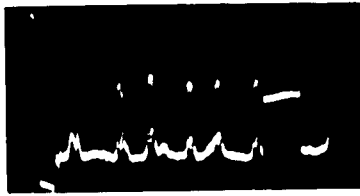
Figure 29.
Several Microscope Fields.

Figure 30.
Two Fields.

Figure 31.
One Field.

Figure 32.
1. 7 Mil Marks by 10X
American Optical
Objective.
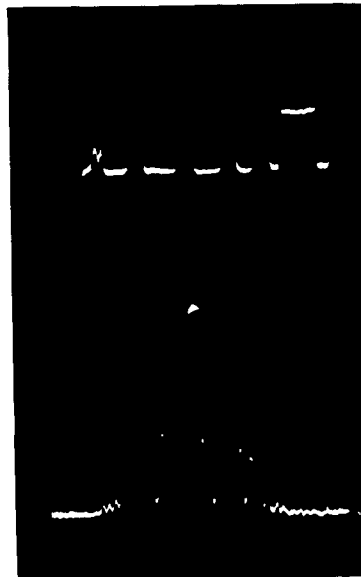
Figure 33.
1. 7 Mil Marks by 5X
American Optical
Objective.
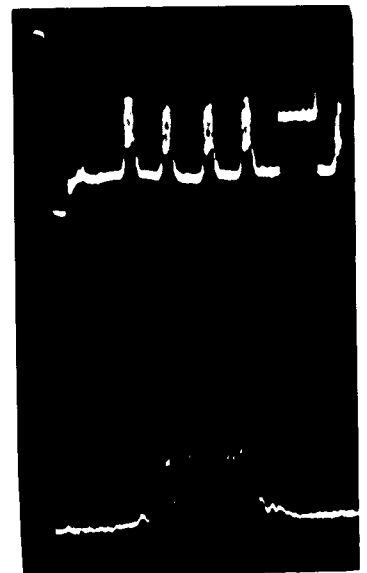
Figure 34.
1. 7 Mil Marks by 3. 2X
American Optical
Objective.

Figures 32, 33, and 34 show the oscilloscope traces made with the three different microscope objectives, which were all produced by the same manufacturer, American Optical Co., and corresponded to 10 x, 5x and 3. 2x lenses, respectively. Results indicated that the edge spreading got worse as the angle of convergence was decreased. Generally speaking, the lenses did not appreciably affect the resolution by any great amount which more or less confirmed our belief that the edge spreading was a function of the material and not the lens.

(5) Conclusions Concerning Resolution Capabilities of HSP-208 Coatings.

    (a) 1. 7 and 1. 28 mil marks can be written and recovered with a signal-to-noise ratio of 15:1 and 8:1, respectively. Spectral matching of the read-out would improve this to 30:1 and 16:1, respectively.

    (b) Since the above packing density was achieved when the format used for making the marks was not optimized, it seems reasonable to postulate that one mil marks (0.001" square) could be written and recovered with a signal-to-noise ratio of 10:1 with a spectrally matched reading system. This would imply that the marks would be laid down in such a manner as to make optimum use of the edge spread in the coating.

    (c) At present, therefore, a practical maximum mark storage capacity (signal/noise 10:1) promises to be in the vicinity of 10^6 marks/in^2 with capsular coatings of the type tested. A reasonable system might require two-four marks to designate one bit, so a practical storage figure is some 330,000 bits per in^2.

79

d. Sensitivity of Photochromic Materials HSP-208 and HSP-216 as a
   Function of Coating Thickness

Previous data indicated that about 0.3 watt secs/cm^2 was required to
reach a reasonable density with the capsular coatings. Subsequent tests
showed this figure to be reliable, but they were made using an Osram
high pressure mercury lamp and a spectral energy distribution of that pro-
vided by the Corning 7-60 filter. Following these tests some additional
tests were run on two photochromic coatings with calibrated energy
densities. Figure 35 shows D log E curves for HSP-208 for varying
thicknesses and the effect of thickness on speed. Thickness is graded
in "wet mils," and for a density of 0.2 to tungsten light, HSP-208 showed
the ranges indicated in Table VIII.

TABLE VIII

SENSITIVITY vs. COATING THICKNESS

Wet Coating Thickness	Density to Tungsten	Energy Required Watt Sec/cm^2
5 mils	0.2	0.5
10 mils	0.2	0.15
20 mils	0.2	0.1
30 mils	0.2	0.065

These results amounted to a variation of some 10:1 in effective sensit-
ivity and must be considered at lease a help in effecting an increase of
sensitivity.

Figure 36 shows a graph of D log E curves for photochromic coating
HSP-216, a coating received from Dayton as worthy of evaluation. It
had the same effective speed variations as HSP-208, but was slightly
slower in over-all sensitivity.

80
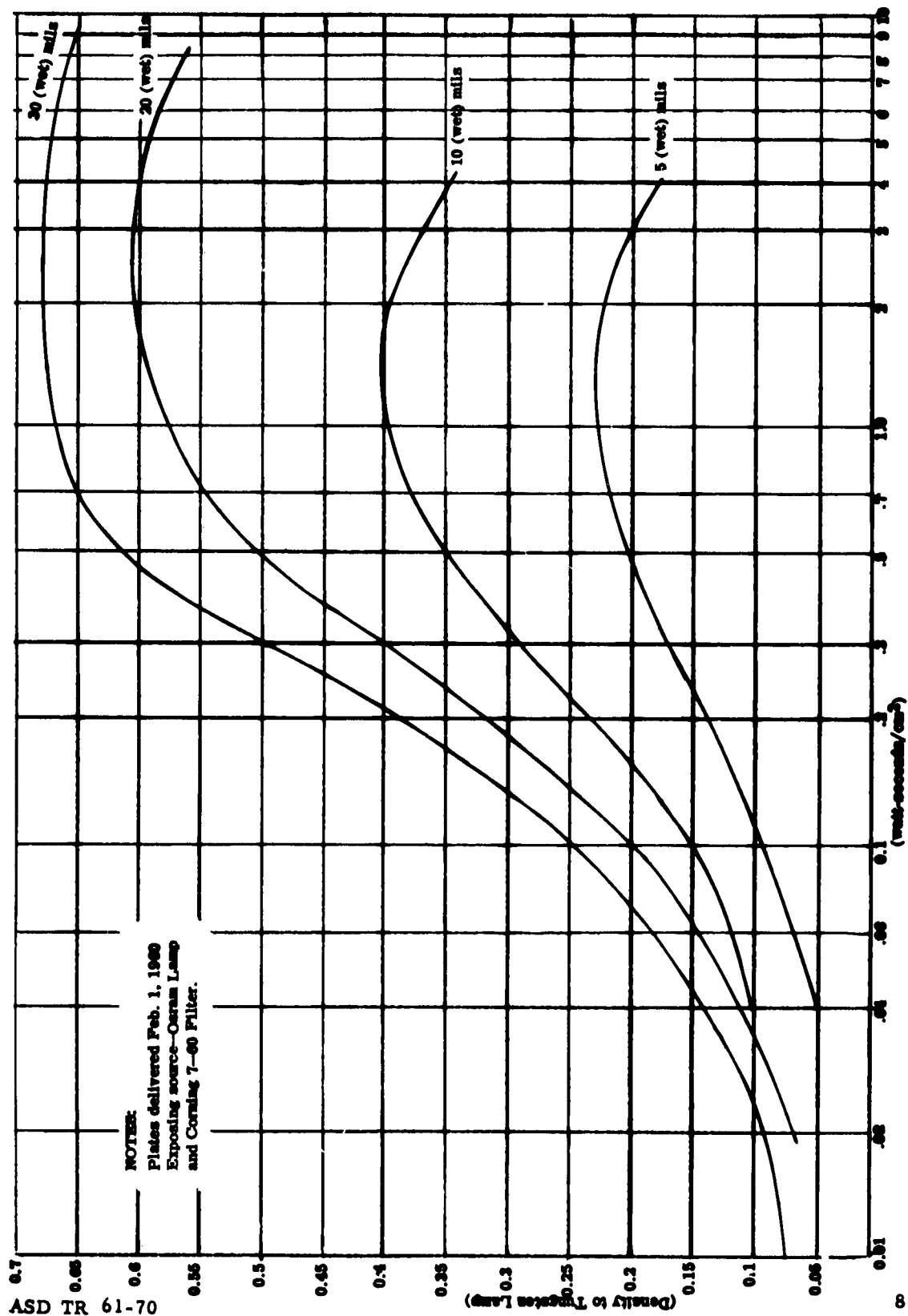
Figure 35. D Log E Characteristics for HSP-208 at Various Emulsion Thicknesses.

NOTES:
Plates delivered Feb. 1, 1960
Exposing source—Osram Lamp
and Corning 7—60 Filter.
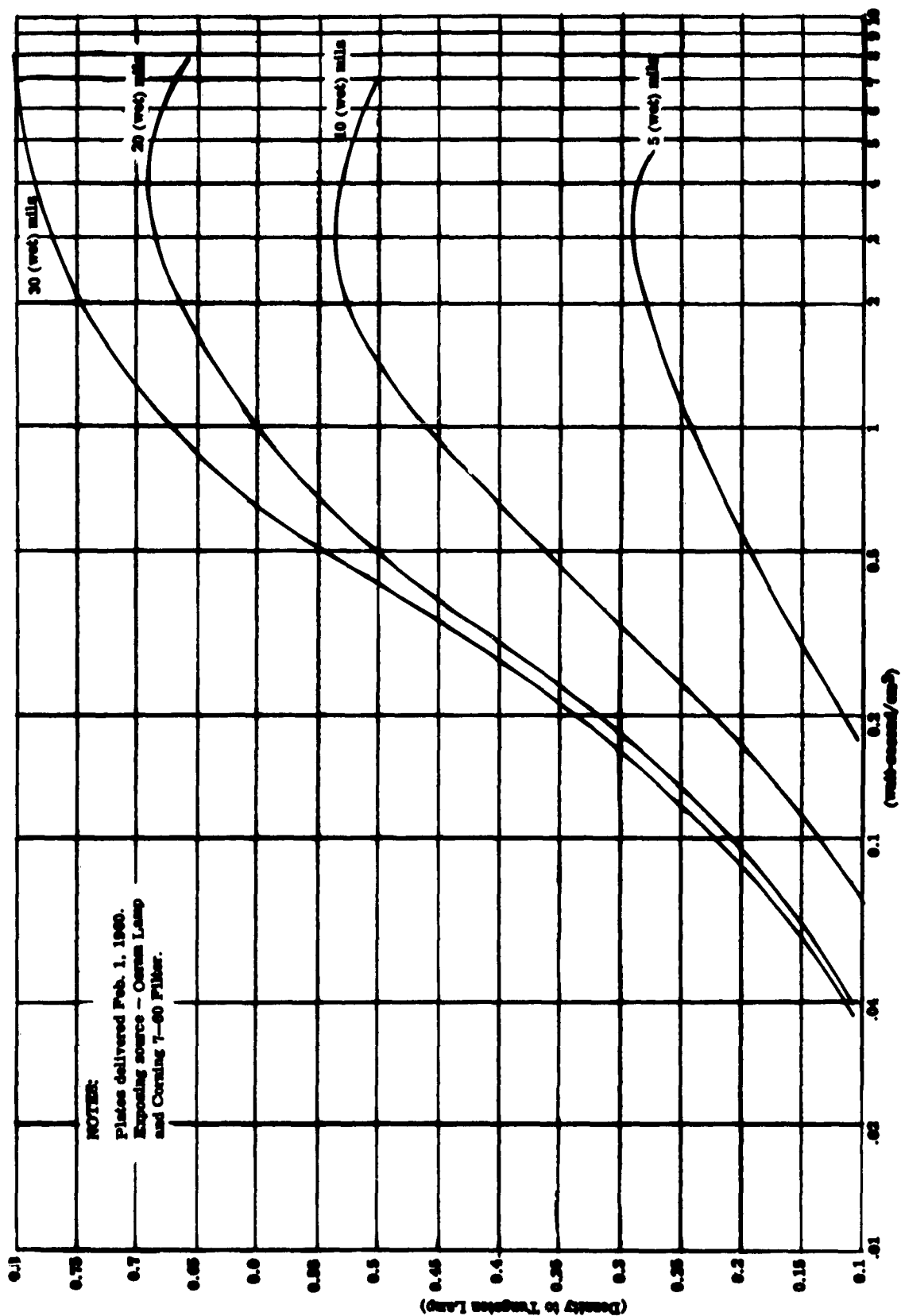
Figure 36. D Log E Characteristics for HSP-216 at Various Emulsion Thicknesses.

e. Verification of the Sensitivity of HSP-208 Capsular Coating

A question was raised by the Fundamental Research group at Dayton regarding the accuracy of the writing energy measurements on the HSP-208 capsular coatings as obtained at Hawthorne. These measurements were carefully re-run and the result 0.32 watt seconds/cm^2 compared within experimental error with the previous result 0.33 watt seconds/cm^2. The detailed results and calculations were reviewed at a joint meeting in Dayton at which time additional measurements were made with the identical sample evaluated at Hawthorne. This meeting resulted in the conclusion that, within experimental error, the two groups were in agreement with the sensitivity of HSP-208 coatings, i.e., nominally 1/3 watt second/cm^2 in the 330-380 millimicron band of the spectrum.

2. Non-Capsular Photochromic Coatings

a. Introduction to Non-Capsular Coatings

It had been noted during experimental studies on other projects that many non-capsular photochromic coatings appeared to be somewhat more sensitive than the capsular variety. In addition, these coatings tended to exhibit molecular resolution capabilities, i.e., such coatings were optics limited. Solid-solution coatings were made by dissolving the photochromic material in a solution which, after deposition on the substrate to be used was allowed to dry into a relatively tough film. Since the molecules were not confined to a given small volume (as in the capsular materials), a problem with diffusion appeared likely when recording and storing patterns of very fine detail. The diffusion problem (also referred to as a "bleeding" of recorded information) was previously considered to be severe enough to make the non-capsular coatings unsatisfactory for the photochromic memory application.

One of the most serious limitations of photochromic capsular coatings was the low sensitivity to switching radiation. Since non-encapsulated photochromic coatings appeared to exhibit a higher sensitivity and optical density, and had been under development at our Dayton facility for other

applications, it was decided that they should be studied experimentally for possible use in a memory. It was recognized that such coatings might tend to exhibit "bleeding" for information stored at high packing densities over a considerable period of time. However, the extent to which bleed might occur had not been determined. It appeared possible that a slight bleed might eventually turn out to be a small price to pay for increased sensitivity and contrast.

b. Non-Capsular Coatings D Log E Curves.

Experimental data were obtained on solid solution coatings and included D log E curves, resolution capabilities, and fatigue characteristics. Figure 37 shows the typical results obtained for D log E plots of both encapsulated and unencapsulated coatings. It can be seen that roughly the same total exposure is required to obtain maximum contrast for both types of coatings, but that the increased density of the solid solutions provides a given optical density with roughly an order of magnitude less exposure.

The only important difference between the solid solution materials tested in this program were the base densities, which ranged between 0.06 and 0.38 density units, and the maximum densities which ranged between 1.1 and 2.3 density units. The best incremental density change was associated with the material designated at No. 94 (which is included in Figure 37).

The experimental data used in the construction of Figure 37 is included in Appendix XII. This appendix includes the data and curves on five other solid solution coatings. In general, these coatings range from one and one-half to two mils thick. The results were not very sensitive to changes in coating thickness.

c. Resolution Capabilities of Non-Capsular Photochromic Coatings

Since the non-capsular coatings have molecular dispersion of the photochromic material, their resolving power is inherently very high. In tests to date, they have matched, in general, high resolution photographic slides which are in the 1000-2000 lines/mm class.

84
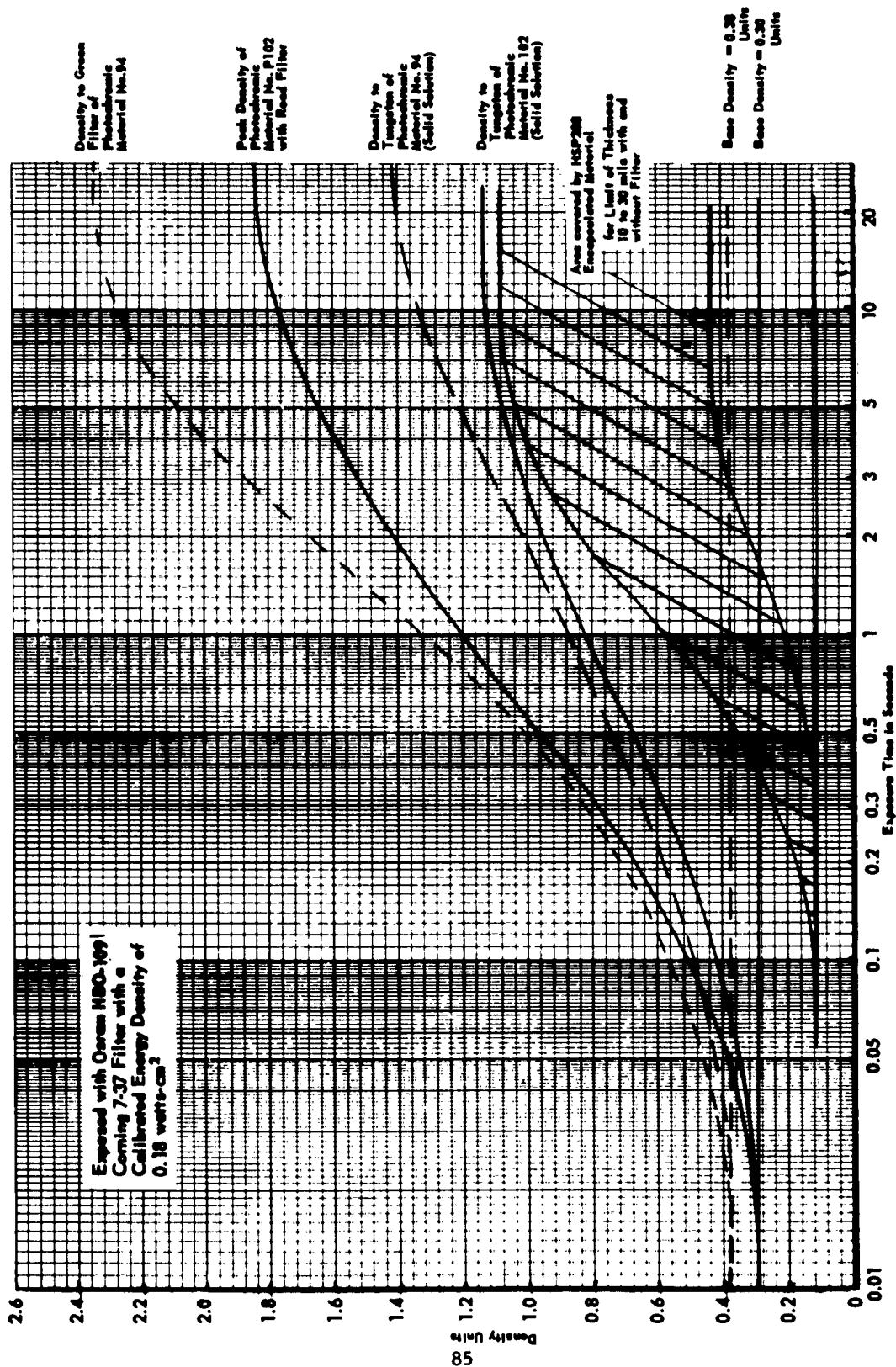
Figure 37. Density of Photochromic Materials No. 94 and No. P102.

85

ASD TR 61-70

Testing in this region (or greater than 500 lines/mm) becomes difficult without special equipment, and it is somewhat more practical to conduct the experimentation with respect to the intended application.

Resolution measurements on the HSP-208 coating were reported under capsular coatings. It was felt that a comparative measurement would be informative as to the increased resolution possible with non-capsular coatings. It should also be recalled that an extrapolation indicated that marks as small as one mil square looked feasible for a practical system with capsular coatings.

P-105, one of the better solid solution coatings, was selected for the comparative test. The same master mask, pattern used with the HSP-208 was used for transferring a digital pattern to the coating. However, the reduction ratio was considerably increased. This resulted in digital marks as small as 0.000456 inch on the photochromic surface as compared to the 0.0017 inch marks on the HSP-208. Thus, the linear packing density was increased 3.5 times or 12 times greater on an area basis.

Figure 38 is a photomicrograph of the recorded pattern described above. The same 0.01 inch calibration marks were used on this slide as in the HSP-208 photomicrograph. Since 22 of the smaller marks were contained in 0.01 inch, the mark size was the stated 0.456 mil. By eye, the definition of these marks is excellent, and they are by far preferable to the much larger 1.7 mil marks in the HSP 208 figure. Inspection should be restricted to the center of the field as the lens is introducing edge-of-field deterioration of the image.

A more useful measure of definition was associated with a reading wave-form generated by a scanning spot as would be used in a digital store. Experimentation along this line yielded negative results due to too large a reading spot. The test equipment which had been developed for the coarser capsular patterns was not of sufficient resolution to adequately scan fine patterns on high resolution solid solution coatings. Also noteworthy was the lack of grainy background which appeared on the HSP-208
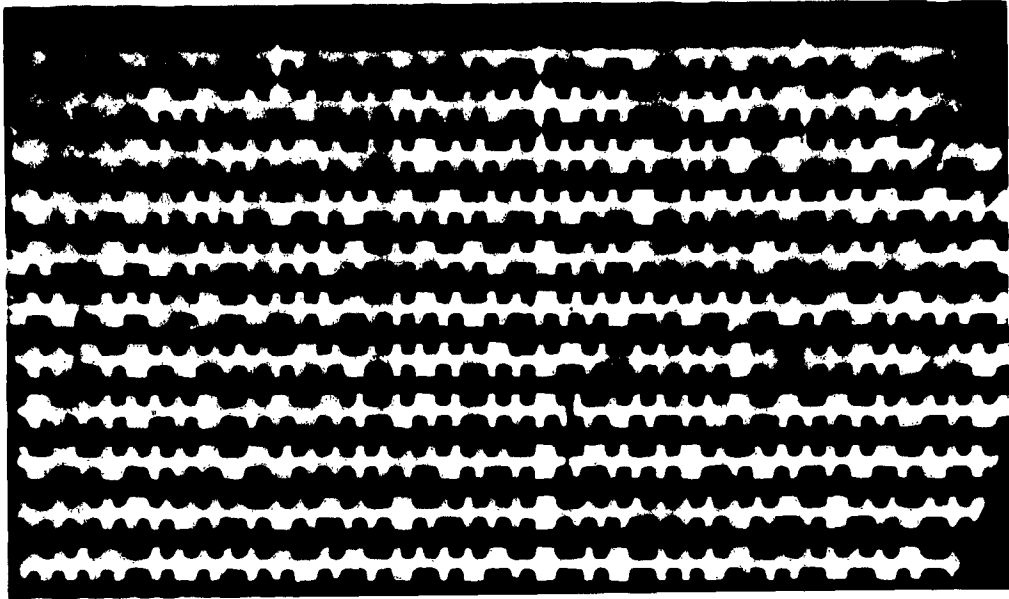
Figure 38. Photomicrograph of 0.456 Mil Marks on a
Non-Capsular Photochromic Coating.

photograph. The improved resolution was, moreover, accompanied
by an improved signal-to-noise ratio. As stated before, the signal-to-
noise ratio determines the ultimate packing density that a memory can
use.

From the above considerations it was concluded that the resolution of the
solid solution coatings was the limiting factor in the ultimate design of a
photochromic memory using these coatings. The limit would be determined
by optical considerations, mechanical tolerances and registrations, and
signal-to-noise limitations.

It is noteworthly that at the time this study was underway some non-
capsular coatings with recorded patterns stored for a few weeks at $20^{\circ}F$

87

in a standard refrigerator had not shown any tendency to bleed.

d. Fatigue Measurements of Non-Capsular Photochromic Coatings

Fatigue testing is ordinarily a very time-consuming process. In order
to obtain a rough fatigue comparison of solid solution photochromic
samples in a short time, a relatively fast, order of magnitude testing
device was checked out and served the purpose quite well. This device
had been used to check out some solid solution coatings and indicated
reversible switching lifes in the range from 1,000 to 10,000 cycles for
solid solution materials. A description of the testing device and the first
experimental results are given in Appendix XIII.

It is important to note that these samples were fatigue tested at room
temperature, and with a rather unusual erasing feature. Past experi-
ence had indicated that fatigue was primarily a function of the total
ultra violet exposure, if serious heating was not present. In this case,
the results obtained were representative of what might be obtained under
actual operating conditions. However, the data indicated that this con-
clusion might not be entirely valid. An appreciable difference in fatigue
to visual illumination was noted and appeared to be a function of both
intensity and spectral distribution. Also, in an actual photochromic
memory, the ambient temperature would not be room temperature
but much colder ($<0^{\circ}C$). Therefore, the effect of temperature, if any,
is another factor to be considered.

e. Non-Capsular Coatings Selected for Study

Of the great variety of non-capsular coatings available from the Fundame-
ntal Research group in Dayton, four were selected for further study
under the Hawthorne program. These included H-62, P-112, P-113 and
P-105. The first two were essentially heat erasable, and the latter two
were of the light erasable category. It is to be noted that coating 94 used
earlier and P-112 were actually made from the same type of coatings.
Most of the experimental work made use of the two coatings P-112 and

88

P-105. The P-105 coating was chosen because of its higher optical
density over P-113.

f. Additional Resolution Investigations

Improved optical set-ups have demonstrated that the non-capsular coatings
are capable of resolving over 700 lines per millimeter. The only limiting
factor has been the available optics.

To obtain the resolution at the reader, the experimental technique was
modified. The recorded data was first transferred at 20X magnification
to 35 mm film. It was ascertained that very little additional loss was
encountered at this step. The 35 mm film was then placed on the reader
(PEDAL) and rotated past the microscope objective projection station.
The illumination source (HBO-109) was imaged on the microscope ob-
jective. The projected image of the rotating film was made to fall on
a small hole located on axis so as to obtain use of the center of the
field of the microscope objective. A phototube placed behind the hole
then responded to the light level variations as the recorded pattern on
the transparency traversed the hole. In all cases, the scanning aperture
was kept to less than 1/10 the width of the finest pattern in the projected
image. The reader was tested with known width opaque lines of 0.4
mil and gave excellent square pulses at the output.

The 700 lines per millimeter quoted above is primarily for comparative
purposes as this is the way resolution is ordinarily expressed in the
fields of optics and photography. It corresponds to a contrast (or es-
ponse) of about 10 or 20 percent of that of very coarse patterns (of the
same original optical density as the fine patterns) when imaged through
the same system.

With the advent of the necessity of bulk transfer (parallel writing of
many bits over a given image field), investigations of resolution vs.
field were undertaken. A mottled appearance was noted when images

89

were written at lower optical densities and this effect gave a ragged appearance to edges of marks at any density. It did affect resolution, but not in a uniform way which made the resolution difficult to judge by eye. The reader tended to sense this effect only as a slight noise. One cause of this defect was traced to the condenser lens in the optical system and is described further in the optics section of this report.

On correcting the defect in the optical system, a definite improvement was noted. However, there was still a slight background mottle in the patterns recorded on the P-105-type coatings. No appreciable mottle was noted in either the P-112 or P-113 coatings.

An interesting experiment was undertaken during a search for the solution to the mottling defect. This involved a prior heating of the photochromic coating to 250° - 300° F in order to allow surface tension to smooth out any imperfections in the coating surface. There did appear to be an improvement in the pre-heated coatings, but this conclusion does not tend to be borne out by the result obtained after changing condensers. This approach is noted as a matter of record as a possible means for clearing surface irregularities in photochromic coatings. Kalvar film makes use of such an effect and, incidentally, is the source of the inspiration to try this approach.

g. Decay of the Colored State

Patterns stored on non-capsular coating P-105 at 20° F for six months were still visible. More important, no bleeding, or diffusion of edges was noted. There was a contrast loss, however.

With the arrival of specially designed refrigeration units, a new series of experiments was started with the P-105 coatings stored at four different temperatures: 40°F, 20°F, 0°F and -20°F. The coatings were first written with both high resolution patterns and a step wedge. The latter

90

allowed ready evaluation of contrast loss with a densitometer when the sample was removed from the refrigeration unit. The former allowed assessment of bleeding effects. The evaulation of the P-113 coatings was held up because of an insufficient quantity of slides for the refrigeration test program. The tests on P-113 were about to be started just prior to the termination date of the present contract and no data (besides that generated in Dayton, see section III) is available.

Preliminary results of the P-105 refrigeration tests are given in Table IX. Since the slides were removed from their chambers for testing and were rapidly warmed to room temperature (to minimize condensation from the water vapor in the air), they were not put back into the chambers. Each test, then, required a new slide with a slightly different initial density than any of the others. The data obtained was smoothed and adjusted where necessary, for an initial density of 1.0.

The preliminary results indicate that although the thermal color decay is quite sensitive to temperature, a thermal color decay in terms of a year or years is not unreasonable with relatively modest refrigeration equipment. Long term tests are required to establish that other factors, such as aging (i.e., through chemical change), do not appear which could cause unpredictable effects to occur after extended periods of time.

TABLE IX
P-105 REFRIGERATION TEST DATA[*]

| Days | Decrease in Optical Density | | |
	20°F	0°F	-20°F
7	0.23	0.08	0.03
18			
21	0.39	0.12	
32	0.45		
38			0.05
41		0.15	
42	0.48		

[*] Initial optical density (nominal) equals 1.0.

91

C. LIGHT SOURCES AND SPECTRORADIOMETRY

1. General Remarks

As described in Section II of this report (Prior Work), a number of light sources were originally used with photochromic materials. During the course of this contract, these were reduced to those most suitable for the investigation undertaken at any particular time. These are best classed (but not rigorously) as continuous, pulsed, and cathode-ray tubes.

With the D log E curves available in the previous section, the characteristics of the light sources (along with the particular optical system used) allow the calculation of writing speed for a particular photochromic material-light source combination. Since there is very little prospect for increasing the sensitivity of photochromic coatings as much as an order of magnitude, the attainment of maximum intensity in the light source, and at the proper spectral bands, is of paramount importance for the realization of a photochromic memory with reasonable writing speeds.

Although no experimental work or systems studies were undertaken on the laser (optical maser), a very recent development, practically speaking, the potential of a laser light source appeared so great for the photochromic memory application that a preliminary theoretical study was made concerning this device. This study, just completed at the end of the contract, is included as Appendix XIV of this report. The conclusions reached in Appendix VIII concerning light sources are not applicable to the laser, which is a coherent source (electromagnetic as well as spatial coherency can be achieved with laser).

Before taking up the work with light sources, it is well to note the conclusion of Appendix VIII for electromagnetically incoherent light

92

sources. This is that the power density of the imaged source with a
reasonable f/no. lens (f/1.6), a demagnification of ten or more and
a two thirds transmission loss is about one-tenth the brightness of
the source when the source brightness is in terms of power density
per steradian.

To eliminate the need for constant reference to the D log E curves
given previously, a value of 1/3 watt—seconds per cm^2 can be used
as the writing energy requirement for photochromic coatings. This
exposure leads to optical densities in the 1.0 - 2.0 range for typical
non-capsular coatings as can be ascertained by reference to the
curves in Appendix XII and Figure 37.

A summary of the characteristics of a number of light sources is
included in Table X. It will be a convenient reference while review-
ing this section of the report. Although not strictly valid, all
increments of the 300-400 millimicron region are assumed to be
equally effective in producing switching to the colored state. This
is also the case for the 500-600 millimicron region of spectrum which
is used for switching back to the colorless state.

2. Spectroradiometric Studies

The need for further spectroradiometric data for all types of light
sources was apparent after initial spectroradiometric studies and
experimental evaluation of light sources. Not only is data required
in narrow spectral bands, but the time rate of change of radiant flux
in these bands is also required for pulsed sources.

Initially, an attempt at a rather modest piece of equipment underwent
preliminary design for obtaining accurate spectroradiometric data
for continuous sources. Objections were raised to this design which
led to serious consideration for the design and construction of a double
beam instrument capable of evaluating both pulsed and continuous light
sources.

93

TABLE X

LIGHT SOURCE DATA

Light Source	Type	Input, Watts	V, Volts	I, Amps	Life, Hours	Source, Quoted MM	Brightness		
							Stilb	Watts cm^2 steradian 500-600 mμ	Watts cm^2 steradian 300-400 mμ
HBO-109?	Hg	100	20	5	100	0.3x0.3	140,000	200	500
HBO-200	Hg	200	57	3.5	200	2.5x1.3	25,000	36.5	50
GE-AH6*	Hg	1000	840	1.4	100	2.5x2.5	30,000	110	135
XBO-501	Xenon	450	20	23	1500	1.2x2.4	25,500	37	26
C 2	Zircon-ium Arc	2	37	0.055	100	0.076	7,300	10	1.2
5ZP16**	CRT	5.4	27KV	0.0002	1000	0.254	—	—	35***
5AUP24**	CRT	5.4	27KV	0.0002	1000	0.254	—	70	—****

* Gross assumptions were made on the GE-AH6 to get the following data.

** Typical operating conditions in a flying spot scanner were used for the calculations here. See Cathode-Ray Tube studies in part E of this section for more details on these tubes.

*** Two percent efficiency.

**** Four percent efficiency.

The above CRT brightness calculations are for the stated efficiencies in radiating over 2π steradians. Note that the CRT beams cannot be held stationary under the above conditions.

94

Additional work on spectroradiometric techniques indicated that a modification of the Beckman DK-1 spectrophotometer would be preferable to building a spectroradiometer from the ground up. The Beckman representatives kindly allowed a modification on a factory instrument in order to determine whether the signal-to-noise ratio with the proposed modification would be sufficient to detect one microsecond pulses of light reliably. The electrical modification amounted to raising the multiplier phototube voltage and changing the load resistor after disconnecting the automatic recording portion of the instrument. Using the reflectance attachment, the pulse from the unknown source is than compared with a pulse (chopper) reference light standard on a video bandwidth oscilloscope.

The results of the experiment indicated that for ten millimicron bandwidths, fairly reliable results could be obtained. It also indicated that useful U. V. could be obtained from a tungsten reference over the range of interest.

A recommendation was made for the purchase of a Beckman DK-1 with the reflectance attachment and modifications. Although the data previously obtained appeared to be reasonably accurate, it was considered desirable to look at the various mechanisms occurring in the photochromic material-light source combinations under different operating conditions in the greatest detail possible with more precise measurement.

A recent decision was made to purchase the Beckman DK-1 spectrophotometer with the modicications to be provided by Beckman Instruments. The instrument had not been received by the termination date of this contract. It will be used for future studies of light sources and photochromic materials.

3.   Continuous Sources

a.   Sylvania Zirconium Concentrated Arc

This source appeared to offer great promise as a visible spectrum
point source of high intensity and also because of its size, low power
requirements. However, it was found unsatisfactory as a read or
erase source because of a lack of constancy in position and brightness.
The shift in position was found to be comparable to the spot size and
not to a small fraction of the spot size as indicated by the published
data on this light source. Another lamp of the same general type was
tried with similar results. In general, however, the availability
of this source in the lab has proved quite useful for general optical
studies where the lack of constancy in position and brightness is not
troublesome.

Since the evaluation of the zirconium arc, Sylvania has introduced the
equivalent in a tungsten cathode which is claimed to have absolute sta-
bility. These lamps have about 72 percent the intensity of the zircon-
ium variety. The tungsten lamp was not evaluated experimentally.

b.   Tungsten Filament Light Sources

Tungsten filament sources provide excellent read sources if the parti-
cular set-up in which they are used allow these sources to remain
stationary. Coil filaments, the most common configuration, are a
problem if it is necessary to image one of the coil elements on a hole
in a mask, a common requirement. In this mode, the lamp can be
quite small, since the filament only need be large enough to encompass
the hole when imaged.

Writing has been obtained with tungsten filaments when used with U. V.
filters. The exposure time, however, is in terms of many seconds
and minutes.

96

A-c ripple is a problem when reading spots with tungsten lamps. This problem was eventually solved by use of small lamps which can be powered by a regulated transistor power supply. Since the filament itself is imaged on a small hole, the actual lamp rating is of no consequence. With the cost of the lamps used (6 volt pilot lamps) reduced to a negligible quantity, it was feasible to run them at high temperatures with an associated reduced life. For such applications, a straight wire filament is preferable to the coil filament (for ease in alignment). However, the only straight wire filament lamp located was quite expensive, and one would not consider burning these up at a relatively high rate. Such a straight filament lamp with a pre-focus base selling for under one dollar should prove quite valuable for many instrument applications.

c. Osram HBO-109 Mercury Arc

This source is a typical arc source with a negative resistance characteristic. With the regular Gates supply it was found that severe fluctuations in light output occur due to ripple in the rectifier source. A ripple in voltage of about 2 percent across the source is seen as a 50 percent ripple in light level. The problem was partially solved by purchase of a ripple filter to go with the Gates supply. Use of negative feedback for ripple suppression was attempted, but the circuitry which evolved was found to require a greater d-c source voltage then was readily available from the d-c supplies on hand. A relatively small, high current d-c supply of 100 volts or greater with a 6 amp capability was not found which fell within budget limitations.

With the recognition that high speed writing was not feasible, the problem of freedom from ripple became less urgent. The present capability of writing to a good density at about 100 spots per second with the HBO-109 has not been accompanied by any noticeable variation in contrast from spot-to-spot. Use of the ripple filter should provide adequate ripple suppression for the speeds of operation anticipated in the foreseeable future.

97

d. G. E. H-6 Mercury Arc

This source was capable of much greater total radiant output than the HBO-109, but it is of lower brightness. It was the source planned for use with the ultrasonic switch where the pulse train in the cell was to be imaged on the photochromic material. It was used as a slit source in this mode of operation. The same ripple problems as occurred with the HBO-109 also occur with this source. With the recognition that the sensitivity of photochromic materials are not compatible with the ultrasonic cell, this source was relegated to an inactive status.

e. Xenon Arc Source

Use of a continuous Xenon arc was not attempted due to its much lower writing efficiency as compared to a mercury arc. Since Xenon is used in standard flash tubes, it was used as the source for flash tube studies.

f. Black Light

Low intensity near U. V. lamps, commonly called black-lights, have been used to provide over-all exposure of photochromic materials, or to make contact prints where optimum transfer of information is not of any great significance. They are a valuable asset in the laboratory, but they are not of such an intensity to be of any great interest to the photochromic memory program as a source within a working memory.

4. Pulsed Sources

The pulsed sources used were the Xenon flash lamps and cathode-ray tubes. Since the latter sources are considered in a separate section, they will not be dealt with further here.

98

a.   Xenon Flash Lamps

Xenon flash lamps were used extensively in the equipment and studies carried on in Dayton. The studies in Hawthorne were much more restricted with respect to this type of lamp. Any breakthrough with this light source in conjunction with photochromic materials at the Dayton facility would have been reported to the Hawthorne group, and we could have taken advantage of it.

The flash tubes were used with input powers of from 50 to 110 watt-seconds. The flashing rate was always quite low, generally about one flash every three seconds on the automatic test equipment used in Dayton. Pulse duration of the radiant pulse can be controlled by variations in the capacity and voltage of the charge storage circuit. Although flashes as short as one microsecond have been achieved, the flashes used are generally of the order of one to two milliseconds.

Flash tubes generally can dissipate from 3 to 20 watts of power, depending upon expected life. Flashing rate is then determined by finding total input power vs. permissible power dissipation. For shorter life, say 5000 flashes, power rating may be increased to 40 watts. The tubes of smaller physical size suffer a corresponding decrease in permissible power and energy per flash.

b.   Other Pulsed Sources

The use of other pulsed sources, such as a mercury arc or a carbon arc, presents essentially the same drawbacks as described above. The carbon arc is generally being abandoned in favor of the high pressure small arc tubes. Since there appeared to be no advantage in conducting additional investigations with these other sources, the experimental work was confined : ） the sources described previously.

99

5. The Laser

The laser (Light Amplification by the Stimulated Emission of Radiation) is a light source capable of emitting coherent radiation in an electromagnetic sense. As mentioned above, the laser is treated in some detail in Appendix XIV. The importance of the laser is associated with its ability to produce a parallel, in-phase beam of light of an essentially mono-chromatic character. Such a beam can be focused to a minute point of light and produce energy densities of the order of a megawatt/cm^2 or more.

An ideal laser for photochromic materials would be capable of being switched on and off at a megacycle rate or more, it would radiate either in the near U.V. or between 500-600 millimicrons, and it would be capable of operating over long periods of time with a minimum of care. Such a laser has not as yet been realized. Once it is realized, a photochromic memory operating at video rates should be possible. It would still fail to be a general purpose memory, however, because of the dynamic fatigue of photochromic materials. In fact, the effect of coherent radiation on photochromic materials is not known and would have to be investigated. In addition, such a source would be practically ideal for all types of reciprocity failure investigations, photographic as well as photochromic.

100

D. LIGHT SHUTTERS

1. Introduction

As outlined in Section II, Prior Work, the original emphasis was to obtain and/or develop a high speed light shutter capable of operating in the micro-second region on a continuous basis. It was desirable to have a shutter capable of operating with continuous light sources as an alternative to the cathode-ray tube, which had also been slated for investigation in this pro-gram. It was justly feared that available cathode-ray tubes and phosphors might not be within the capabilities required by a high speed photochromic memory system. Cathode ray tubes are considered separately under Part E of this section titled "CATHODE-RAY TUBES STUDIES."

The importance of the high-speed light shutter was dependent on the realiza-tion of a suitably rapid light source-photochromic material combination. When the capabilities in this area were finally recognized to be a relatively slow write-erase operation, the fast shutter requirement became superfluous. However, the major shutter effort, the ultrasonic light shutter, had been completed as described below. The slow-speed limitations presently inherent in available light sources are well within the capabilities of mechanical shutters and offer no serious problem.

2. Pulsed Source Shutters

A common means for shuttering a light beam is to electrically pulse the source on and off. This method has found extensive use in high spe d photography. The source intensity characteristics were considered under Part C of this section; general shuttering characteristics will be considered here.

The pulsed source, or flash tube, has been developed for use primarily in high speed photography, and, to a lesser extent, in stroboscopes. In these applications, the lack of a very high degree of reliability is not serious. The

tendency for electronic flash tubes to misfire is looked upon as a nuisance rather than a serious handicap. Such would not be the case for a computer application and is a reason for having some reservations concerning their use in such systems. Another more obvious reason is associated with a limited life in terms of the number of flashes possible. The projected high operating speeds for the photochromic memory (in microseconds) would have led to a very short life indeed.

When operating at the high pulse powers required to write and erase photochromic materials as they are known at the present time, it has been found necessary to operate at a very low pulsing rate to keep within the operating temperature of flash tubes, as well as to keep the power supplies to reasonable size. For example, 50 watt-seconds input per flash and up has been found to be rather representative in the experimental programs. A hundred flashes per second leads to 5000 watt-seconds/second or a five kilowatt power supply at the very least, and an overheated flash tube.

Electronic flash lamps have served quite well in a number of laboratory programs for experimental purposes. On a one-shot, or a few-shot, basis they have been quite useful.

The results of the photochromic memory program have not revealed writing sources capable of orders of magnitude higher writing speeds than can be obtained with Xenon flash tubes at the present time. Thus, if a slow write-erase system without cathode-ray tubes were desirable, the electronic flash tubes merit another look. The limited number of flashes is not as serious in this case. For example, a continuous pulsing over a one week interval at one pulse per second leads to 604,800 pulses, a reasonable life for some present-day flash tubes.

3. Magneto- and Electro-Optic Shutters

The general conclusions reached in Section II, (relating to prior work), concerning magneto-optic and electro-optic shutters, did not change appreciably

during the course of this contract. It was felt that the ultrasonic light shutter was of sufficient speed and far more practical to use in a continuous fashion than those of the crossed polaroid variety.

4. The Ultrasonic Light Shutter

a. Introduction

The preliminary work on this shutter is described in Section II (Prior Work). The more detailed theoretical concepts are presented in Appendix IX. A general introduction to the subject, along with the experimental work, will be described below.

b. The Ultrasonic Diffraction Grating

The decision to construct an ultrasonic shutter was made after it was determined that the price asked by the Fairchild Controls Corporation for their commercial unit was beyond the budget of the project, and after a literature search indicated that such an undertaking would not be overly difficult. This shutter appeared to have fewer obvious drawbacks than any of the others considered, except, possibly, the cathode-ray tube, which was to receive study also.

The primary properties of the ultrasonic shutter which were of interest to the photochromic memory project were — ease of switching with relatively low power, electronic light filter control, a possibility for making use of the inherent pulse scan motion through the cell and very little heating while operating at megacycle rates.

When a collimated beam of light passes through normal to a beam of ultrasonic waves, a diffraction phenomena results. The pattern obtained is, in some respects, similar to the pattern obtained by a diffraction grating. A typical experimental arrangement is shown in Figure 39.
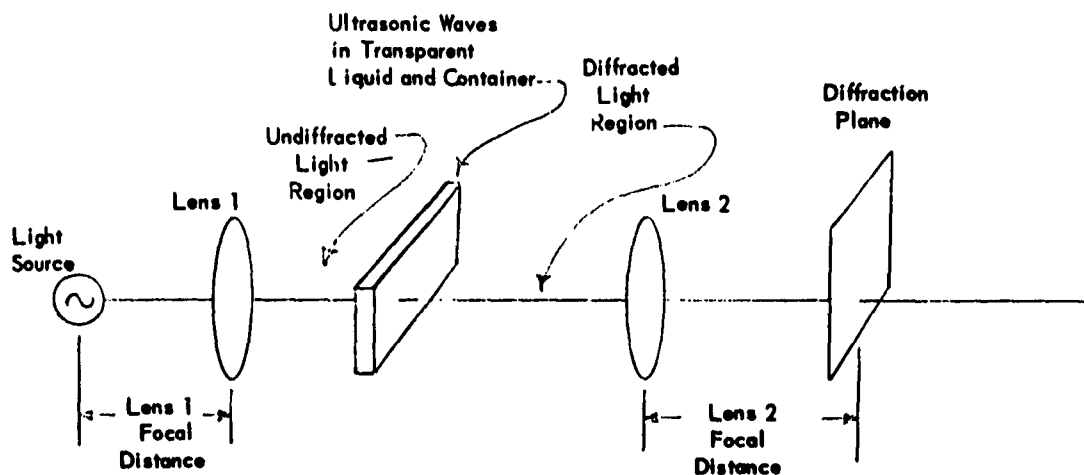
Figure 39. Typical Ultrasonic Grating
Experimental Set-Up.

The ultrasonic wave is propagated by condensations and rarefactions
of the medium through which it is traveling. These changes in density
result in corresponding changes in the index of refraction of the
medium. Thus, adjacent portions of the incident plane wave-front (of
light) traverse different optical paths in the ultrasonic medium. The
emerging wave-front is transformed into a complex surface.

Figure 40 compares the transmission properties of an ordinary diffrac-
tion grating with the refractive properties of an ultrasonic "grating."

The transmission properties of the diffraction grating consist of a large
amplitude "step-function." Maximum and minimum transmission
approaches 100 percent to 0 percent, respectively.

The index of refraction of the ultrasonic "grating" changes as a small
amplitude sine wave. The variation from maximum to minimum re-
fractive index is small. The spacings of orders in the diffraction
pattern obtained from an ultrasonic "grating" is similar to the spacings
obtained from an ordinary diffraction grating. The respective formulas
are given as follows:

104
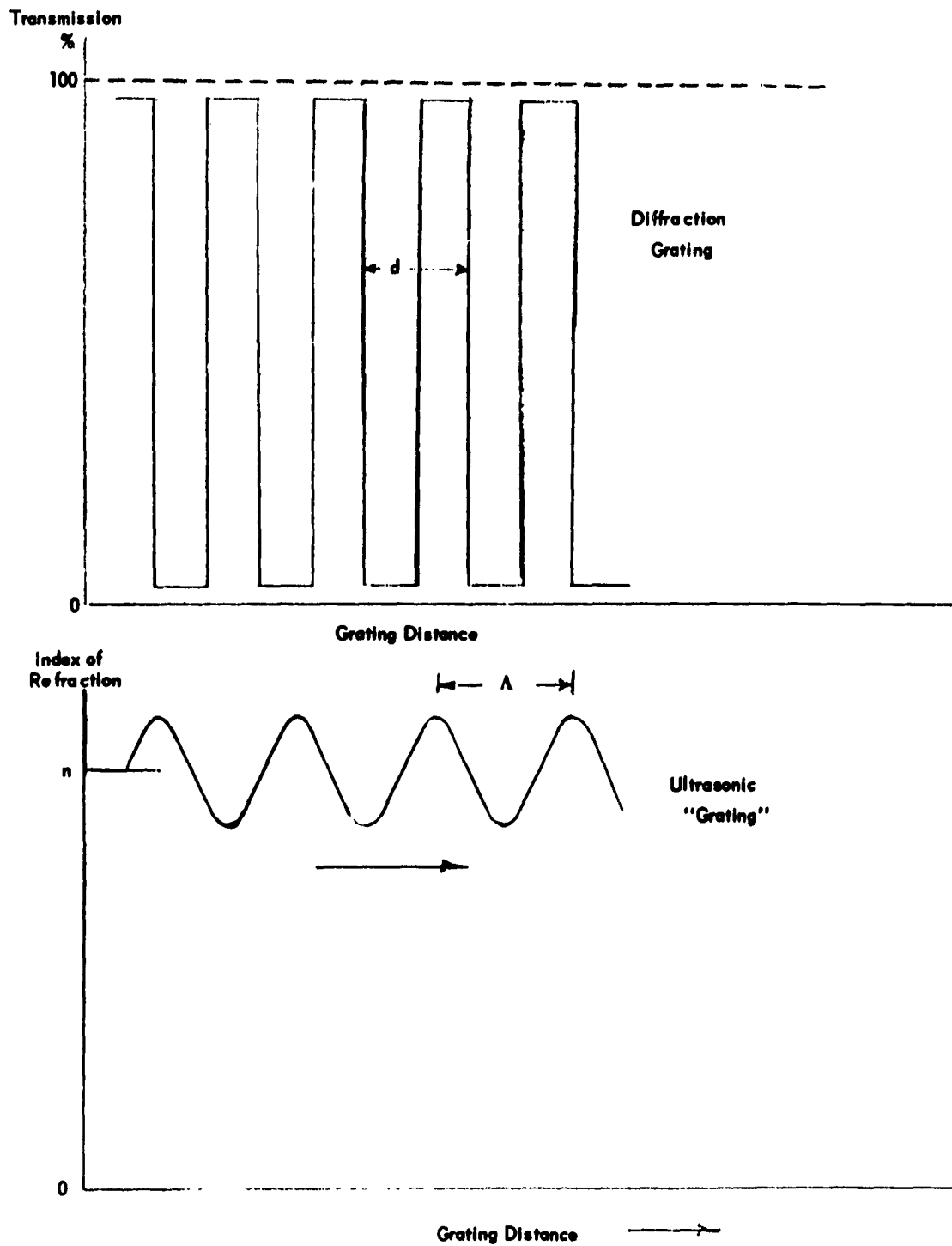
Figure 40. Transmission and Refraction Gratings.

1) Ultrasonic "grating":

$$\Lambda \sin \theta_n = n\lambda$$

2) Diffraction grating:

$$d \sin \theta_n = n\lambda$$

where,

λ = wave-length of the incident light

Λ = wave-length of the ultrasonic waves

θ_n = angular displacement of the nth order

n = order number

A most interesting (and important) feature of the diffraction pattern obtained with an ultrasonic "grating" is the variation of relative intensisties of the various orders, in a manner not at all like a conventional diffraction pattern. The variations are a function of the ultrasonic intensity, and by varying this intensity it is possible to reduce the intensity of the central order of the ultrasonic diffraction pattern far below the intensity of some of the higher orders. This is not possible with an ordinary diffraction grating, where the central order is always maximum.

The fact that a "grating" exists only when ultrasonic waves are present in the medium suggests a possible application as a light shutter.

Figure 41 illustrates an experimental set-up.
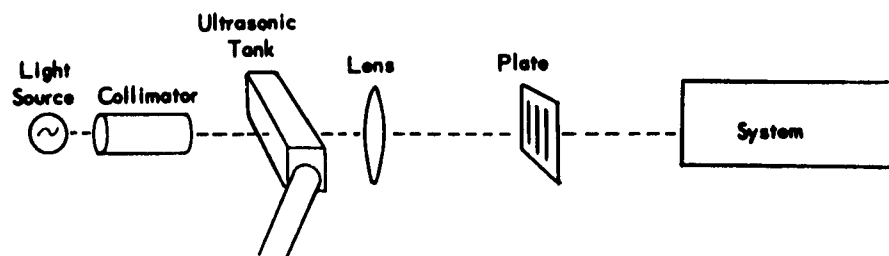
Figure 41. Ultrasonic Grating Light Shutter.

106

c. Modes of Operation

The diffraction pattern appears on the plate which contains various slits to transmit individual orders. There are many possible modes of opera-tion.

(1) Mode No. 1. The plate consists of an opaque region to block the central order and a transparent region to pass the higher orders. With no ultrasonic energy in the ultrasonic tank, only the central order exists and minimum light energy is transferred to the system. When ultrasonic energy is applied to the ultrasonic tank, higher orders are formed and light energy passes around the opaque region and on to the system.

(2) Mode No. 2. The plate consists of a transparent region to pass the central order and an opaque region to block the higher orders. With no ultrasonic energy in the tank, only the central order exists and maximum light energy is transferred to the system. At a particular value of ultra-sonic energy, the central order reaches a null with most of the energy transferred to the higher orders which are blocked by the plate. When in this state, a minimum amount of light energy is transferred to the system.

(3) Mode No. 3. The plate consists of a regular pattern of transparent slits (central order opaque) which are spaced to intercept a particular region of the spectrum when the ultrasonic "grating" is excited by a predetermined frequency. Thus the "grating" acts simultaneously as a diffraction plane shutter and light filter.

(4) Mode No. 4. The plate is divided into two independent plates, an upper plate and a lower plate. Two light accepting systems are used, one above the other, so that each receives light only from one of the plates. Both plates have slits (like Mode No. 3), but of a different spatial arrangement. The upper plate will pass spectral band f_1, and the lower plate passes spectral band f_2. This a single source and grating can provide multiple shuttering and filtering in a simultaneous fashion.

(5) <u>Mode No. 5.</u> When operating as in Mode No. 3, it is possible to "shift" the filter to a new portion of the spectrum by altering the ultrasonic drive frequency to correspond to the desired pass band. In particular, a pulsed shutter can be made to pass alternately (or at random) band f_1 and then band f_2 by switching the ultrasonic drive frequency during the "off" portions of the cycle. Ultrasonic frequency changes during the "on" portions of the cycle would be accompanied by a switching transient in which a whole range of frequencies would sweep past the slits as the spectrum readjusted to the changed conditions.

d. Experimental Results with the Ultrasonic Grating

The quartz ultrasonic cell was constructed by Texas Instruments Co. to fairly close tolerances. Some difficulty was experienced in the first cell mount, and this was rebuilt. The proper mounting of an electrical contract to the crystal transducer has been a source of difficulty. Very little information was found in the literature concerning the <u>practical</u> aspects of designing a crystal mount for the type of an arrangement used, and it was found necessary to make modifications as the program has progressed.

After it was determined that an ultrasonic cell transducer driver would be required to deliver a few hundred watts because of the inherently poor match between the crystal and the liquid in the cell, the Viking Adventurer and Courier amateur radio equipment was obtained to provide the driving power. The Courier was not used in experimentation, as it led to arcing at the crystal mount and crystal fracture whenever it was connected for use as a driver and proper load adjustments attempted. However, except for a lack of power, the Adventurer performed quite well. With this unit, and the crystal transducer operating alternately at the seventh and ninth harmonics, power was available to reach only the first null of the Bessel function - type diffraction spectrum. Initially, there were serious switching transients from the Aventurer, but an internal change in coupling and bypass capacitors cleared up the trouble. The

108

Adventurer was excited by a specially designed reactance tube oscillator chassis which could be switched rapidly between two independently adjustable frequencies. The oscillator could be turned on and off rapidly as well. The Adventurer could also be excited by a standard laboratory signal generator, if this was desired.

The basic arrangement of the components is shown clearly in Figure 42. A GE-H6 lamp, one of the lamps used in its housing is at the far end of the bench. This light source imaged on an adjustable slit. The light passing through the slit is collimated by the first large lens. The collimated beam is diffracted by the ultrasonic grating (shown with the shield for the coil which resonates with the crystal transducer) and reimaged into a slit diffraction pattern at the plane of diffraction plate holder. This holder can be adjusted vertically and horizontally, and provisions are available for rotating the particular diffraction plate in use. The Adventurer driver is shown in front, but the other equipment is not shown.

Optical alignment of the cell was not as critical as indicated in the literature and there were a number of effects in the diffraction pattern which did not appear to be satisfactorily explained. These departatures from expected performance led to a more comprehensive study of the literature (Appendix IX) and to further experiments to reconcile the theory and the experimental observations. To obtain better experimental data, and to minimize the need for further modification of the driver circuitry, a crystal operating at a fundamental frequency of 8.2 mc/s, the seventh harmonic of the previous crystal, was ordered. Fundamental operation of the crystal ordinarily increases the available power into the liquid by a large factor.

A slit light filter plate for use with a slit light source was made to be placed in the diffraction plane. It was to pass ultraviolet light at one ultrasonic cell excitation frequency and green light at another frequency (8.2 mc/s and 10.5 mc/s). Although it worked to some extent, the

109
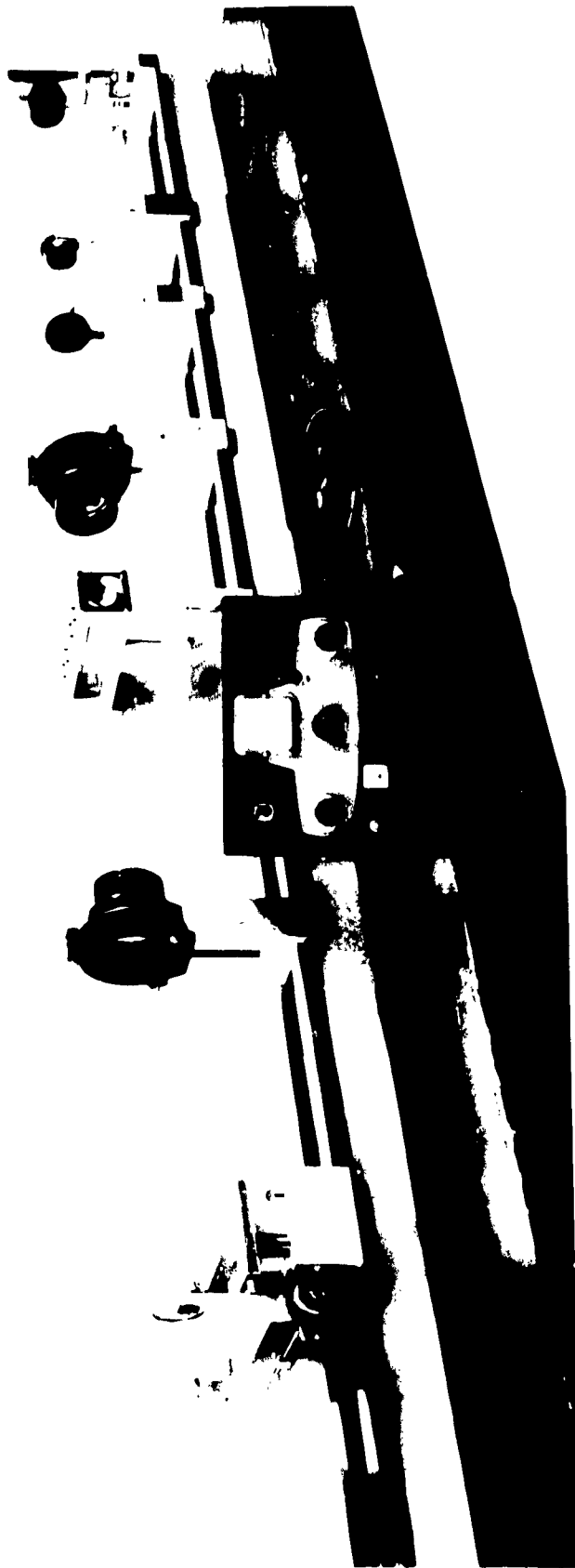
Figure 42. Ultrasonic Diffraction Grating Light Shutter.

accuracy was less than that required. A better method of constructing such filters is through photographic means. Figure 43 (a) indicates how this is done in conjunction with a narrow band dichroic filter at the slit. Figure 43 (b) is a result obtained with three different narrow band filters (bandwidth 5 millimicrons) and an undeviated, unfiltered beam. The photographic plate was displaced vertically after each exposure and the filter's were changed.

Figure 44 contains a series of RF envelopes which were measured at the crystal transducer and the associated output of a photomultiplier (located after the diffraction plate). The top traces in each photograph were oscilloscope superpositions of the RF envelope and the photomultiplier output. The RF envelope — photomultiplier phase relationship has no significance. Figures 44 (a) through 44 (c) were taken in a modified Mode No. 1 set-up, described above, and Figure 44 (d) was taken in the Mode No. 2 set-up. Series (a) to (c) included a reimaging of the ultrasonic cell on a narrow slit before passing the light on to the photomultiplier. Therefore, the output signal is actually a response from the unresolved pulse train as the moving image passed the slit. In (d), the signal is present as long as the train remains in the field of the lens (a 2 inch path). Figures 45 and 46 are photographs of the experimental set-ups.

The outputs of the switchable frequency and gated oscillator chassis are shown in Figure 47 for the condition where the two frequencies, 8.2 mc/s and 10.5 mc/s, are interleaved. The frequency is switched during the "off" part of the cycle. The same signals at the crystal transducer are somewhat deteriorated because of the Adventurer bandwidth limitations. The pulsed oscillator circuit is shown in Figure 48.

The mounting of the new crystal was associated with the following conditions. The sound beam was produced in a small quartz tank (I.D. 1 inch x 1 inch x 6 inch) encased in a steel housing. The piezoelectric 71° X-cut quartz crystal was mounted in an air-backed holder at one end of the tank.

111
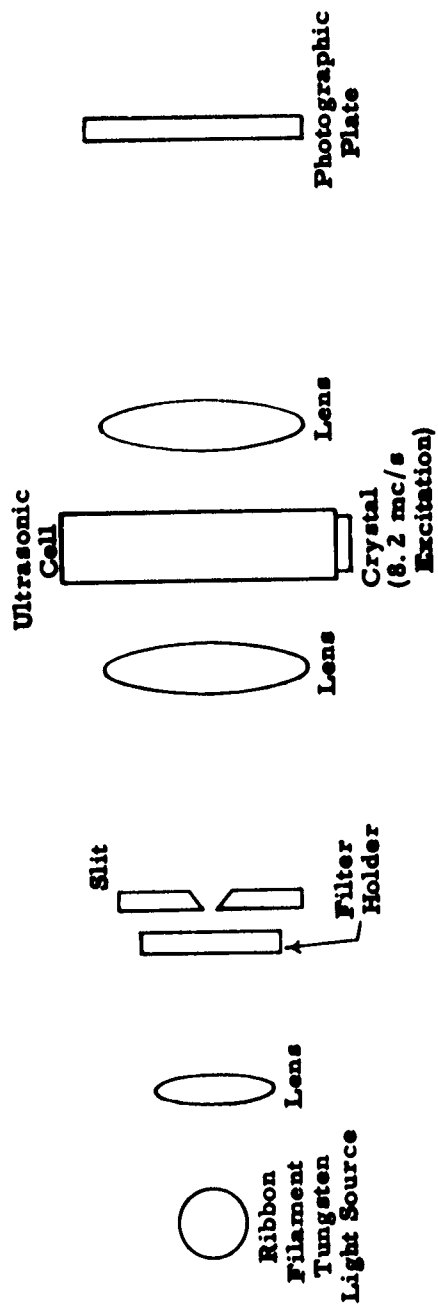
(a) Sketch of Setup to obtain narrow Spectral Lines on a Photographic Plate.

(b) Ultrasonic Diffraction Grating Diffraction Patterns.

Figure 43.   Ultrasonic Diffraction Grating Setup.

112

(a) 2 μsec/cm
10 μsec pulse

(b) 20 μsec/cm
40 μsec pulse

(c) 200 μsec/cm
280 μsec pulse
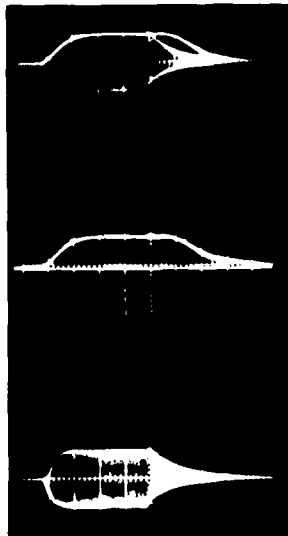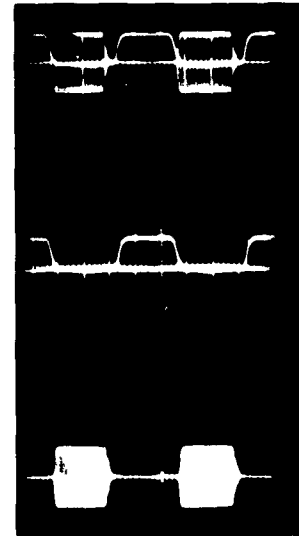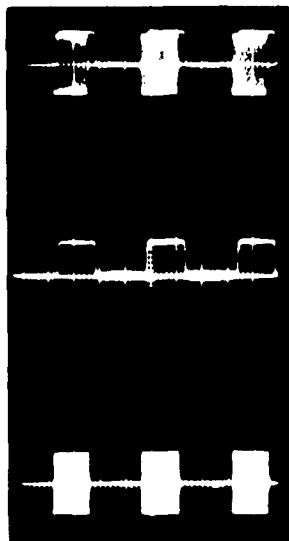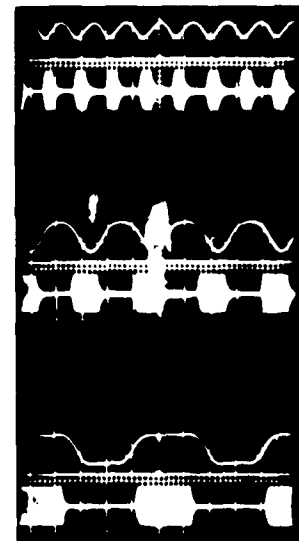
(d) 20 μsec/cm

Figure 44. Waveforms from Ultrasonic Cell Pulsed Operation Setup.
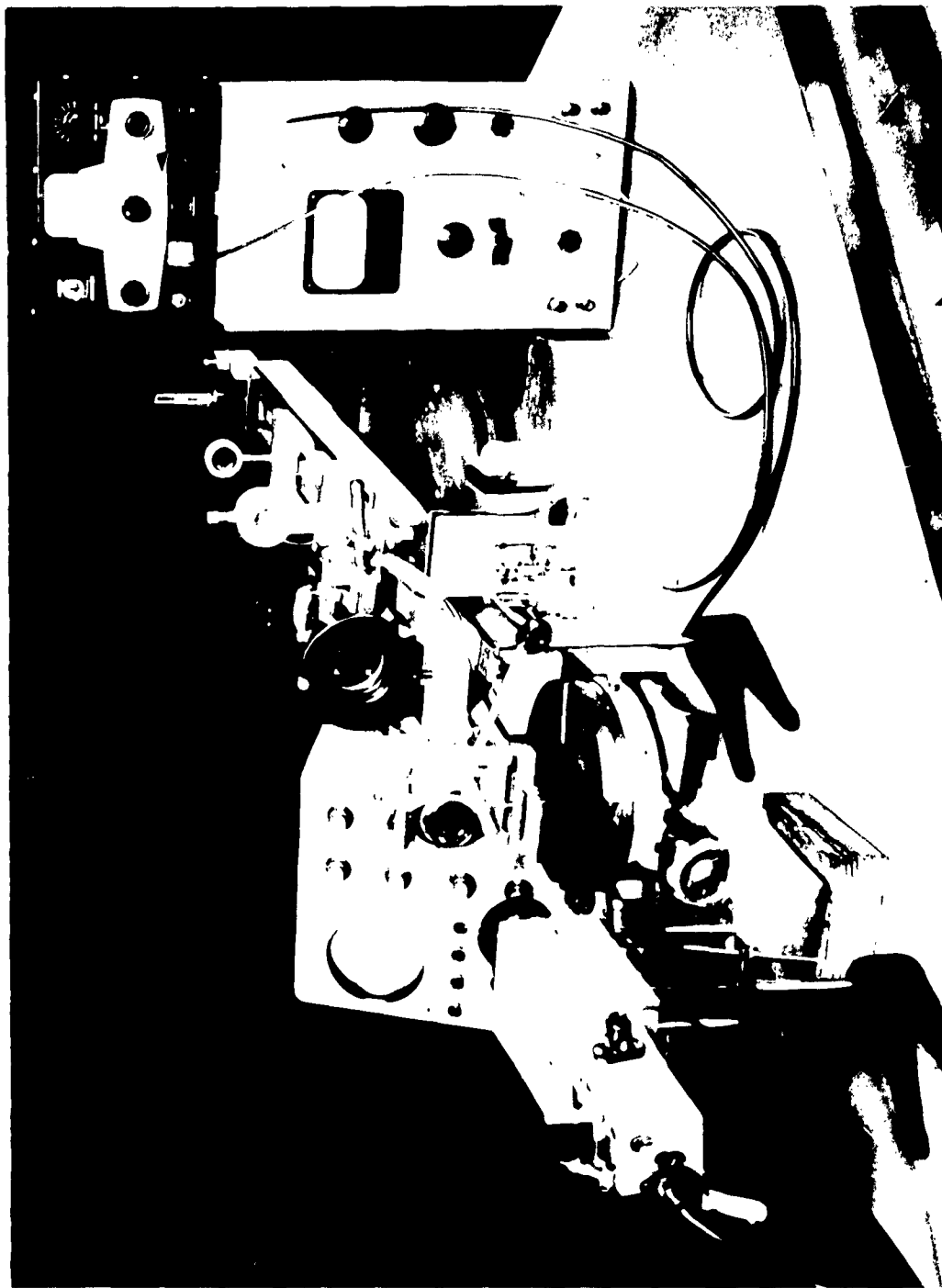
Figure 45. Ultrasonic Light Switch (Mode No. 1)

114
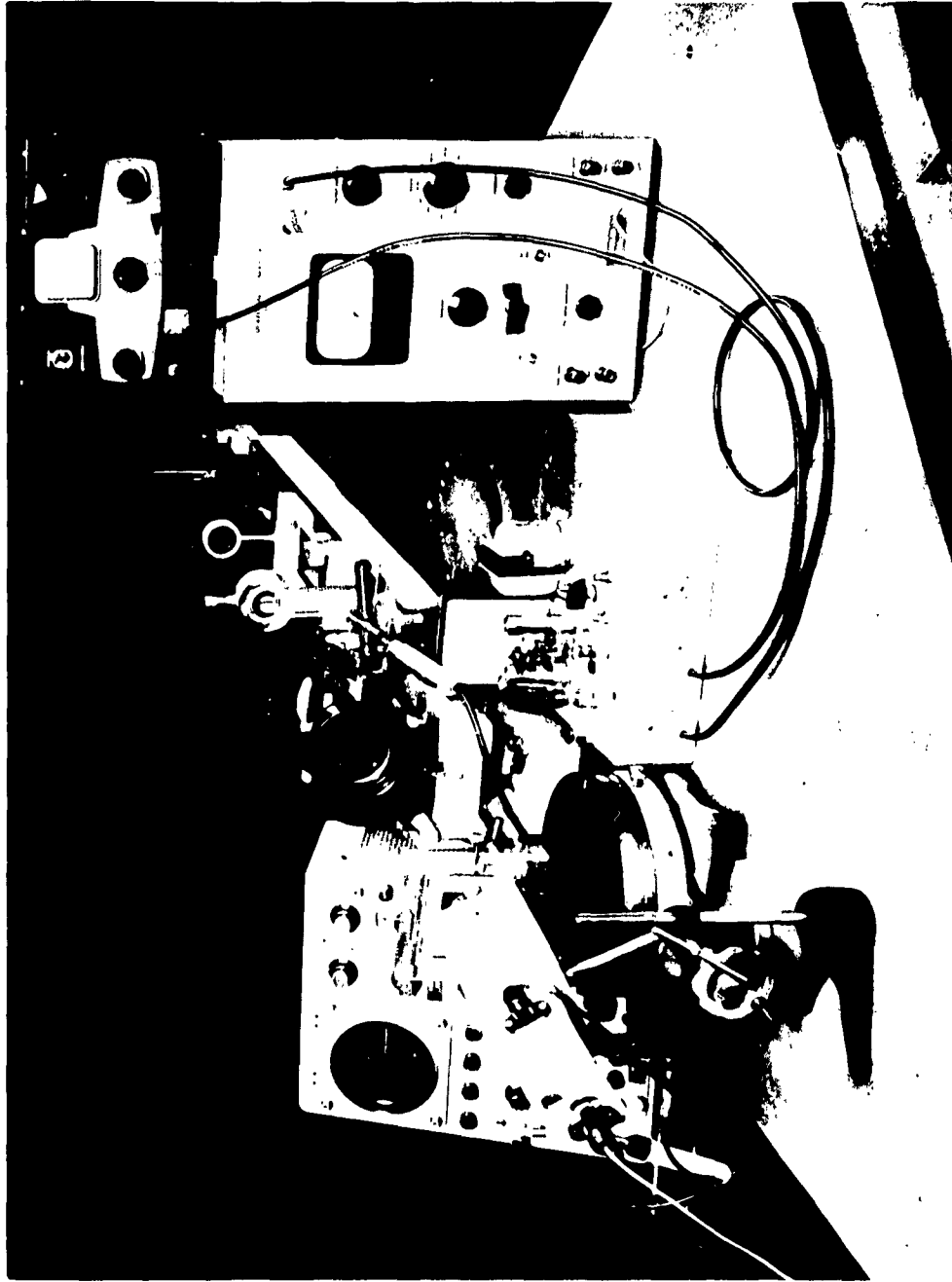
Figure 46. Ultrasonic Light Switch (Mode No. 2)

| 8.2 and 10.5 Mc Interleaved | 8.2 and 10.5 Mc Interleaved |
| -10 Microsecond Bursts | -200 Microsecond Bursts |

Figure 47. Outputs of Switchable Frequency and Gated Oscillator.

At the other end of the tank a multiple-layer screen mesh was mounted to break up the incident wave fronts thereby eliminating reflections. The crystal was driven at its fundamental frequency of 8.19 Mc. by a Viking Adventurer CW Transmitter (input power 50 watts) whose output circuits were modified for better impedance match to the quartz crystal.

Difficulty was encountered in getting a good conductive coating on the washer used to mount the quartz crystal. Some coatings would crack when deformed, while others had poor conductivity. A good coating was found in the form of a mixture of finely powdered silver in a lacquer base. This coating did not crack and had only 1/4 ohm resistance.

The use of a vibrating quartz crystal would appear to introduce some experimental error, since it has been shown that the surface does not vibrate at all points with equal amplitude. The photograph in Figure 49 was taken by Dye [*] and reproduced from Bergmann's [**] book.

---

[*] W. D. Dye, Proc. Roy . Soc. Lond., A138, 1 (1932).

[**] L. Bergmann, Der Ultraschall und Seine Anwendung in Wissenschaft und Teknik, p. 263 (1954).
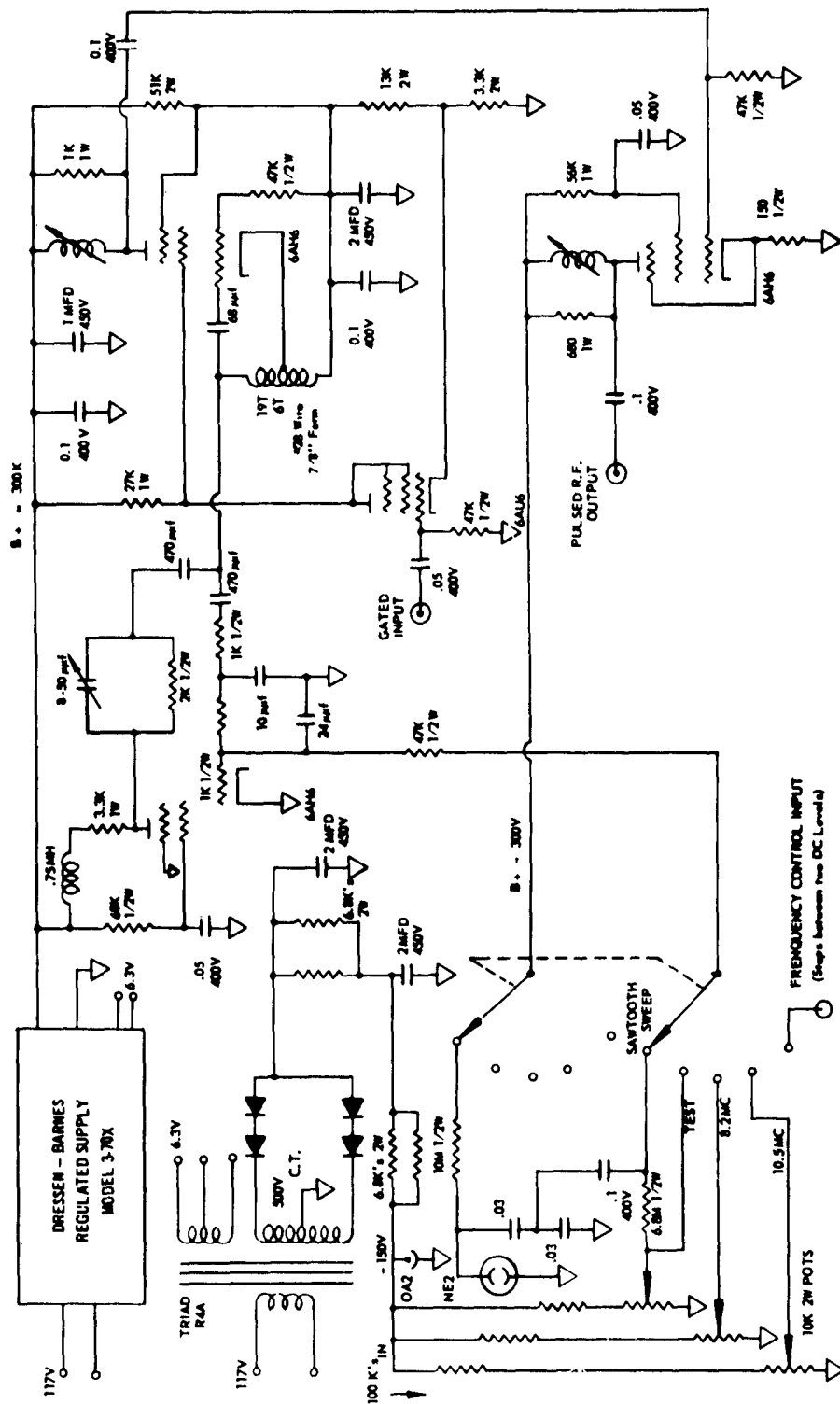
Figure 48. Gated and Switchable Frequency Oscillator.

ASD TR G1-70
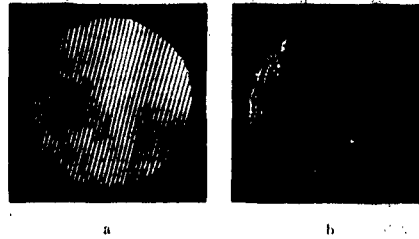
Figure 49. Interference Bands on (a) Stationary Quartz Crystal
and (b) Vibrating Quartz Crystal (Dye).

Part (a) is a photograph of interference bands set up on the surface of
the crystal with the crystal motionless. Part (b) was photographed
with the crystal vibrating. If all parts of the crystal were vibrating
uniformly, we would expect to find some sort of uniform blurring of
the interference bands. Part (b) clearly shows that this is not the
case.

However, if the amplitude variations are much less than one wave length,
the error introduced is negligible. It has been shown by Lord Rayleigh
(see Ditchburn - p. 249)[*] that corrugations in a plane wave of amplitude
(or phase) much less than one wave length will die out exponentially as
the wave front advances.

For the crystal used, the displacement of the surface is given by:

$$\xi = (2.32 \times 10^{-10})V$$

For V = 3000 volts

$$\xi = 7 \times 10^{-7} \text{ meters}$$

* R. W. Ditchburn, <u>Light</u>, Interscience Publishers, 1957.

Since the wave length of the ultrasonic beam (at 8.19 Mc) is 1.8×10^{-4} meter in water, the displacement is indeed small compared to the wave length. Thus, no appreciable error results from the non-uniform vibration of the crystal surface.

The equivalent circuits of the 8.19 Mc. crystal are shown in Figure 50.
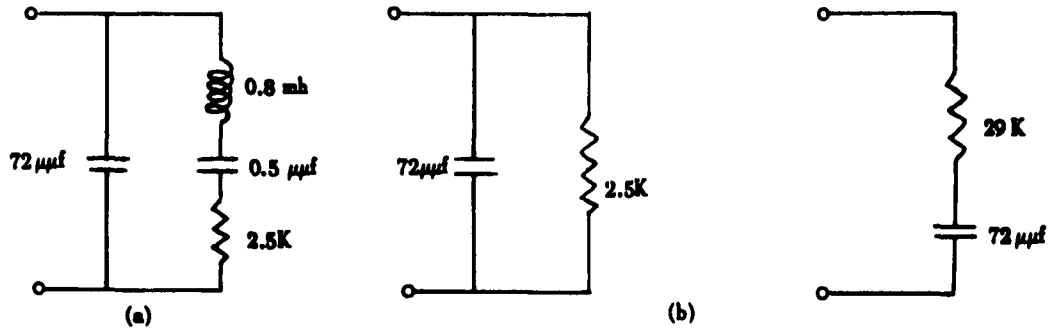
Figure 50. Equivalent Circuits for the 8.19 Mc. Crystal.

Part (a) is the general equivalent circuit and part (b) is the parallel and series equivalent at resonance.

A series inductance of 5.2 μ-henries was constructed to form a resonant circuit with the crystal capacitance, at the natural resonant frequency of 8.19 Mc. The output matching circuit of the transmitter was modified to match the 29 ohm equivalent load.

An experimental set-up was devised for providing the Bessel-function ultrasonic shutter output directly on an oscilloscope for photographic recording. This method was used in studies rather than the tedious method of measuring the energy in each part of the spectrum, directly or indirectly, and computing the Bessel-function spectrum from such measurements (as has been done by other investigators in the past).

119

When a rotating mirror is placed between the ultrasonic grating and the lens which forms the diffraction pattern, and when the system is bent as shown in Figure 51, a moving diffraction pattern is created at the focal point of the latter lens. If a slit is placed at this focal plane with a photo-multiplier tube behind it, as shown, the photomultiplier output is just that which corresponds to the intensity of the diffraction pattern. Figure 52 contains oscilloscope trace photographs from such an arrangement, which aids materially in the research studies. The literature indicates that such data formerly was taken point-by-point.

It has been determined that if a point source was used in place of the slit source above, and imaged through a small hole instead of a slit, the experimental ultrasonic grating work would be greatly simplified from an alignment point of view. It was also determined that the accompanying low light level could be counteracted by use of the Osram HBO-109 point source with a UV reject filter. In going to this source in the experimental set-up, very poor results were obtained because of a strong hum in the source itself. This was found to be due to inadequate filtering in the Osram d.c. power supply. Although the major ripple was eventually eliminated, a different source was used to expedite this work.

The intensity distribution of the diffracted orders (calculated by Raman and Nath in their first paper) is discussed in Section A of Appendix IX. The waveforms of Figure 52 may be compared to the data in that Appendix by considering the comparative intensities for photographs No. 1 through No. 8 to be respectively:

$$0, \ 0.05, \ 0.2, \ 0.4, \ 0.8, \ 1.2, \ 1.8, \ 2.4$$

The reason for these unequal normalized intervals is that the photographs were taken with successive, equal amplitude transducer voltage increments, which are porportional to the square root of the intensities.

120
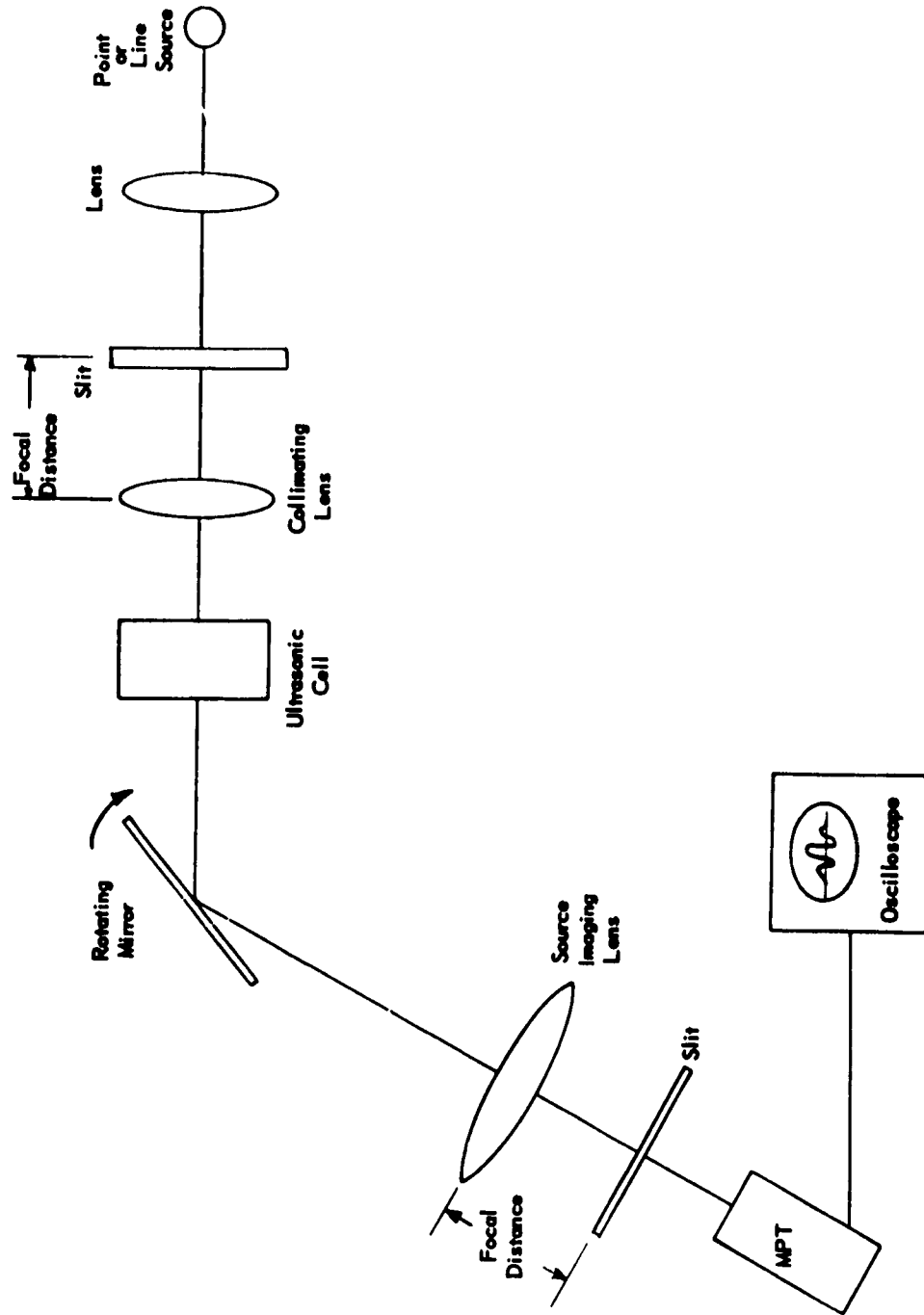
Figure 51. Arrangement for Producing an Intensity Plot of the Ultrasonic Grating Diffraction Pattern.

121

Figure 52. Ultrasonic Diffraction Grating Bessel Function-Type Spectra for Varying Transducer Drive.

122

No quantitative comparison has been made because a subsequent experiment revealed that the slit limiting the cross-section of the parallel light beam was not properly located to tranverse an essentially uniform cross-section of the sonic beam, thus introducing an experimental error that would be difficult to calculate.

A technique for determining the uniformity of the sonic beam is to pass many small bundles of parallel light through the sonic beam. To do this, a photograph was taken of an array of black dots on a white background. This resulted in a negative having transparent dots on a black background. This negative was placed directly in front of the ultrasonic tank in the parallel light beam. Thus, most of the parallel beam was blocked out except for small "pencils" of light. An image of the "dot pattern" was focused upon a screen. The experimental set-up is shown in Figure 53.
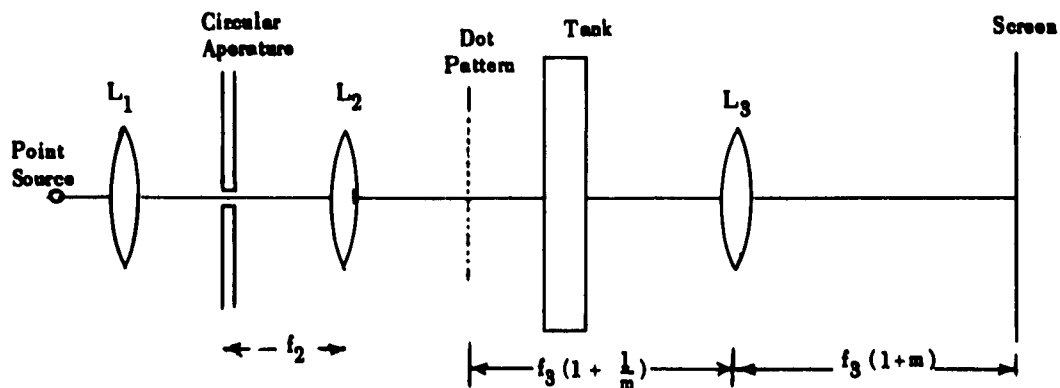
Figure 53. Experimental Set-up for Testing Uniformity of Ultrasonic Beam.

The photograph in Figure 54 (a) was taken of the image on the screen with no ultrasonic beam present in the tank. Photograph 54 (b) was taken with an ultrasonic beam in the tank showing that each "dot" exhibits diffraction effects. Previous photos showed some "dots" with

123

little or no diffraction effects present, indicating operation in a non-uniform portion of the ultrasonic beam due to mis-alignment.

(a)   (b)

Figure 54. Image of "Dot Pattern".
(a) Without and (b) With Ultrasonic
Excitation in Tank.

With the apparatus set up in Figure 55, contrast ratios were measured for the "zeroth" and "first" orders.
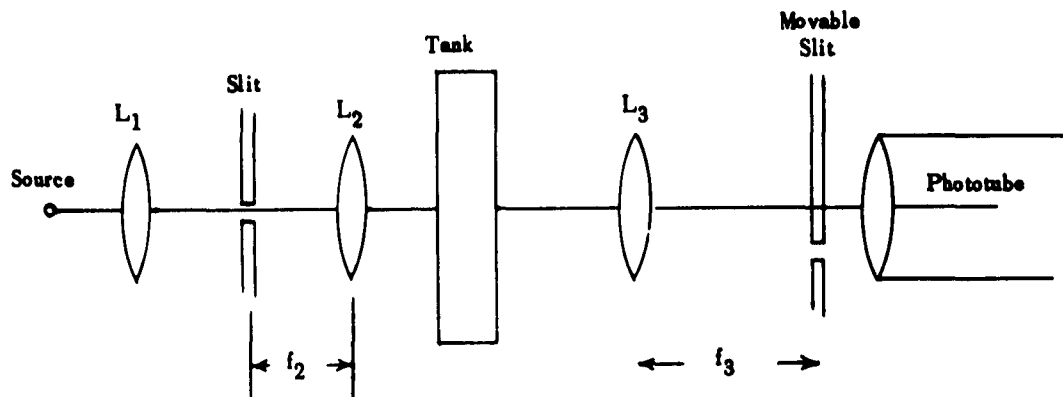
Figure 55. Experimental Set-up to Measure Contrast Ratios.

Photo 56 (a) was taken with the slit adjusted to pass only the "zeroth" order. The output of the phototube was monitored by an oscilloscope with its horizontal sweep free-running. The top line of the grid

represents "zero" light intensity, since it represents the output of the phototube with an opaque stop inserted in the system. The two lower line traces correspond respectively to the minimum and maximum transmission, as determined by adjusting the ultrasonic energy in the tank. The contrast ratio is poor, being approximately 7:1.

(a)   (b)

Figure 56. Contrast Ratios for (a) Zeroth Orders
and (b) First Order.

Photo 56 (b) was taken under similar conditions with the slit adjusted to pass only the first order. This contrast ratio is much better, being approximately 50:1.

e.   Summary

1)   In reviewing the series of five papers by C. V. Raman and Nagandra Nath, it appears that the general complex differential-difference equation has been derived rigorously and that its solution would completely describe the phenomenon of diffraction of light by ultrasonic waves.

2)   It has been shown in Appendix IX that the validity of the solution obtained by Raman and Nath for their simplified equation becomes doubtful as the ultrasonic frequency used approaches the mega-cycle region. This is a direct consequence of eliminating one term from the general equation as being negligible.

125

3) Nagadra Nath[*] has solved the differential-difference equation for both normal and oblique incidence in the form of a complex alternating series. Van Cittert[**] has obtained a system of differential equations for normal incidence and has solved them in a series of Bessel functions.

4) Rao[***] has shown that the results of Nagandra Nath and Van Cittert are identical and has extended Van Cittert's solution to the case of oblique incidence.

5) The series solution of Nagandra Nath (and Van Cittert) converges more slowly with increasing frequency, and is therefore of limited usefulness. At very high frequencies (Rao[****]) the series does not converge.

6) A solution of the general equation in either closed form or as a rapidly converging series would probably prove useful for future theoretical advances in ultrasonic diffraction phenomena at high frequencies.

7) Agreement of experiment with theory is limited by the following conditions:

(a) Non-uniform cross-section and diffuse boundary of the acoustic beam due to Fresnel Diffraction.

(b) Distortion of the accoustic field due to motional perturbations of the liquid medium.

(c) Reflection of light occurring at the inner surface of the exit portion of the tank due to change of index of refraction. This can be minimized by using a liquid such as xylol (n $\approx$ 1.5) which closely matches the index of refraction of the quartz.

---

[*]   N. S. Nagendra Nath, Proc. Ind. Acad. Sci., 4, 222 (1936).
[**] P. H. Van Cittert, Physica, 4, 590 (1937).
[***] K. Nagabhushana Rao, Proc. Ind. Acad. Sci., 8, 124 (1938).
[****] S. Bhagavantan and B. Ramachandra Rao, Proc. Ind. Acad. Sci., 54, July 1948.

(d) Reflections of light occurring at the outer surface of the exit portion of the tank. This can be minimized by coating the outer surface with a quartz wave length non-reflection film.

(e) At higher ultrasonic intensity, the sinusoidal disturbance of the medium becomes distorted, being equivalent to the presence of harmonics (by Fourier analysis). This results in a superposition of diffraction patterns.

8) In using this phenomenon for a binary light switch, it is recommended that one of the first orders of the diffraction pattern be allowed to pass through the diffraction plane for light propagation. This results in the following conditions:

(a) A good contrast ratio results even for poor experimental conditions.

(b) Approximately 20 percent to 30 percent of the light of that of the non-diffracted image is utilized.

(c) Since an image of the source is being used, the brightness of the final image is limited by the brightness of the source.

f. Conclusions

The primary result of the ultrasonic diffraction-grating study has been to establish that the diffraction pattern intensity distribution for ultrasonic drive frequencies in the megacycle region (the region of interest for our application) can not be accurately predicted from purely theoretical considerations at the present state-of-the-art. The only solutions to the general equation describing the operation in this region are infinite series solutions in which the proof of the convergence of the series is difficult to establish. In addition, the general equation does not take into account such effects as Fresnel diffraction of the ultrasonic waves in the tank, harmonic distortion of these waves, etc.

127

The literature studies have indicated that there is some confusion and disagreement concerning the ultrasonic diffraction phenomenon. Some of the authors did not appear to be aware of the complete Raman and Nath studies which include both the approximate and 'exact' cases.

The experimental studies did not turn out to be as extensive as originally anticipated since most were to be designed to conform to the optimum conditions as predicted by theory. Without an adequate theoretical prediction of results in the megacycle region (5 mc/s to 15 mc/s), a more or less empirical approach suffices. From our past experimental studies, as well as studies of others reported in the literature, the complete diffraction of light out of the central order of the diffraction pattern does not appear to be realizable. Thus, what was felt to be the most efficient mode of operation for light utilization must be rejected unless very special memory mechanizations could be developed to be compatible with a fairly "leaky" light shutter.

As a consequence of these factors, the ultrasonic light shutter, if compatible with photochromic materials was to receive primary consideration as a diffraction shutter in which the central order of the diffraction pattern is rejected by an opaque spatial filter. This would permit operation with a good "on-off" contrast ratio and would permit the use of switched ultrasonic drive frequencies for spectral filtering. The loss of available light for the write and erase operations (70 percent to 80 percent) was to be made up by increased exposure time.

5. Mechanical Shutters

Initially, ordinary camera shutters were in use on the project to aid in experimental work, but they were not contemplated for use in the memory. Eventually, however, they were found to be adequate for maximum speed writing with sources such as the Osram HBO-109. For example, with this source at 1/400 second shutter speed, writing occurs, but it is of low optical density. Thus, the present speed capabilities of our light source-photochromic coating combinations are quite compatible with standard shutters.

128

A likely shutter for an operating system would be the electrostrictive
shutter put out by Mullenback and described by Critchlow and Litz. It
is rated at 50×10^6 flexures, which at its maximum operating speed
(as high as 200 cycles per second) leads to an acceptably long life.
Since at no time did a system which would be compatible with this shutter
appear acceptable to the contracting agency, there was no attempt to
obtain one for research evaluation. This is classified as a mechanical
shutter since it operates by physically (mechanically) moving an opaque
object into and out of the beam.

129

E. CATHODE-RAY TUBES

1. Introduction

The ultimate light source for the photochromic memory was felt to be the cathode ray tube if it were capable of providing sufficiently intense spots for writing and erasing photochromic materials at high speeds. Not only would it allow for high speed access and high speed, reliable servoed spot operation, but it also would provide a simple rapid means for shuttering the spot. For certain modes of operation, the resolution capabilities of cathode ray tubes are adequate, but the attainment of still higher resolutions held promise for more powerful systems.

In the investigations to be described below, the items of interest were primarily resolution capabilities and spot intensity within given spectral bands. To be even more meaningful, the latter investigations were carried out in conjunction with actual photochromic coatings.

2. Experimental Evaluation of the CBS 5BYP16

a. Introduction

A rather detailed comparison of the high resolution CBS 5BYP16 cathode-ray tube was made with respect to the capabilities of a 5ZP16 cathode-ray tube. Although the CBS tube (made available on loan) was not quite up to published specifications, and the 5ZP16 was a used tube, it was felt that these tubes would provide enough data to indicate somewhat better than order-of-magnitude capabilities of the respective tubes.

CBS Electronics was manufacturing a series of "high resolution" cathode-ray tubes. These tubes are of the 5BYP-series. The advertised resolution capability of these tubes is of the order of 5000 to 10,000 lines across a diameter as measured by the television "shrinking raster" method. Usual cathode-ray tube resolutions by the same method of resolution

130

measurement are between 500 and 2000 lines for a 5 inch tube. The CBS 5BYP-series of cathode-ray tubes departs somewhat in its construction from conventional magnetic deflection tubes. The most significant change is that of the use of "immersion optics" for the focus and deflection system and a small angle of beam deflection. The term "immersion optics" indicates that the magnetic fields used for focus and deflection are continuous throughout the path of the electron beam from the gun exit to the phosphor surface. "Immersion optics" necessitates very long focus and deflection coil windings and these special coils are necessary for its operation. In addition the tube has an optically flat faceplate and very uniform phosphor deposition.

The 5ZP16 cathode-ray tube is advertised as an 800 line tube, "shrinking raster method." On another program (Air Force Contract AF33(616)-6085) for the visual analysis of high density stored pictorial data, this tube had been evaluated by the "knife edge test." In this "knife edge" test the imaged cathode-ray tube stop is moved from behind an opaque edge in a direction normal to the edge, and the distance required for full light level is the over-all dimension of the spot along the direction of motion. Of interest, particularly for application concerning the photochromic memory, was the brightness, or energy per unit area, as well as spot size and some data concerning the variation of spot size with beam current and brightness.

An important consideration was that the 5BYP16 was still a prototype tube in that CBS had not previously made the 5BY series in a P16 phosphor. Most of their efforts had been with the P5 phosphors. As different phosphors have different physical and chemical properties, test data from a particular phosphor may not apply to any other. This is an added complication for the production of a fine spot size above that of producing a well defined electron beam by the gun and electron optics.

The following is some additional data obtained in a telephone communication with Dr. Hambilton of CBS Electronics concerning the CBS high resolution CRT.

131

1) Conditions for exposure of Royal Pan film to an optical
    density of 1.9 to 2.0.

    Line Sweep Length: 2 inches
    Time per single Sweep: 68 μsec
    Beam Current: 15 μamp (0.0 = 1.9)
                           24 μamp (0.0 = 2.0)

2) Maximum drive conditions (for single line sweep of (a) above).

    High Voltage: 20 KV
    Beam Current: 25 μa

3) Resolution

    1000 lines/inch: 1 μa
    800 lines/inch: 24 μa

4) Method of Testing Resolution ("Shrinking Raster" type test)

    Compressed raster method with a 500 line wedge test pattern.
    Raster reduced until bottom of wedge disappears visually.

5) Sine wave response tests for CRT's were being worked on.

6) Grain size for different phosphors varies and makes comparisons
    difficult.

7) CBS was setting up to measure absolute energy outputs of
    CRT's by spectroradiometric means and according to military
    specifications.

b. Testing Method

The spot size measurement made use of the "knife edge" test. The equip-
ment constructed under Contract AF33(616)6085 was readily adaptable for

132

this purpose. Raster generation and the scanning of a selected line across the CRT screen with a known rate was already implemented. The projection lens, transparency mount, and multiplier-phototube were installed and operating. The only requirement was to make suitable edges (knife edges) for measurements and install them in the transparency mount, to break the Ultor lead to the cathode-ray tube, install an ammeter, and install the CBS cathord-ray tube. A diagramatic sketch of the equipment is shown in Figure 57. For more information concerning the equipment refer to the "Final Technical Report, Visual Analysis of High Density Stored Pictorial Data," Contract AF33(616)6085, WADC-TR-59-2.

The testing method used was as follows: The CBS cathode-ray tube was installed on the optical bench constructed under Contract AF33(616)6085 and described in WADC-TR-59-2. The image of the cathode-ray tube screen was projected 1:1 onto the knife edge. The raster times and lengths were measured and converted to beam duty cycle and rate in inches of beam travel per second. The multiplier phototube output signal was displayed upon an oscilloscope with known sensitivity and time coordinates. Measurements of the average beam current using a microammeter in the high voltage Ultor voltage was set at 20,000 volts. The observed oscilloscope waveforms of the multiplier phototube output signals, as the projected image of the trace passed by a knife edge, changed from the dark level to the light level of illumination of the multiplier phototube. The time of this change is a measure of the time and thus the distance that the spot moved during this time. The distance for a change from no light to maximum light is the over-all dimension of the cathode-ray tube spot along the direction of travel. The "spot size" was measured for many values of beam current. As the multiplier phototube is essentially linear with respect to output current with changes in light level between limits of the noise level and saturation, a measure of the relative light level as a function of beam current and a measure of relative brightness with changes of beam current can be obtained from the amplitude of the multiplier phototube signal as observed on the oscilloscope.

133
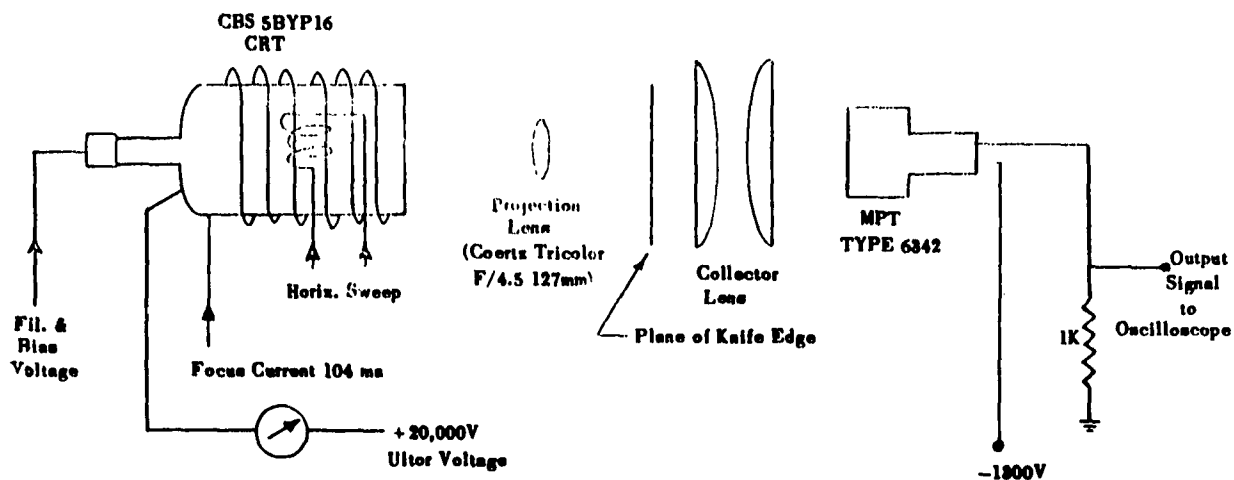
Figure 57. "Knife Edge" Test Equipment.

The beam current was set at a particular value and focused and the oscilloscope waveforms of the multiplier phototube signals observed. The time for the spot to move from behind the knife edge and the amplitude of the change was taken from the resultant signal. Difficulty was experienced in determining the exact point at which the beam started to emerge and completed its emergence. The 10 percent and 90 percent points were used.

Displayed in Section C are the curves of beam current (peak) versus spot size and relative illumination. As similar data had been obtained for a type 5ZP16 tube, this is also presented for comparison.

Subsequent measurements of radiant energy output of the 5ZP16 as a function of beam current under conditions similar to that for the relative brightness measurements afford some degree of correlation of relative brightness and absolute brightness. As the measurements of the 5ZP16 and 5BYP16 for relative brightness were made under essentially identical conditions, some degree of correlation may be inferred.

134

c.   Test Results

The CBS 5BYP16 was subjected to the following raster test configuration:
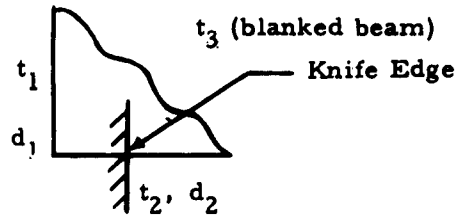
where

$$t1 = 2900 \ \mu sec \qquad d1 = 1 \ inch$$
$$t2 = 1260 \ \mu sec \qquad d2 = 1 \ inch$$
$$t3 = 9440 \ \mu sec$$

The beam current duty cycle was equal to

$$\frac{t1 + t2}{t1 + t2 + t3} = \frac{2900 + 1260}{2900 + 1260 + 9440}$$

$$= \frac{4160}{13600} = 0.305.$$

The results of the raster tests are plotted in Figures 58 through 61.

d.   Discussion

The spot size measurements as indicated in Figures 58 through 61 for the particular 5BYP16 and the 5ZP16 units used are seemingly in marked disagreement with the manufacturers' ratings of 10,000 line and 800 line tubes respectively.

Taking the manufacturers' specifications at face value would seem to indicate a line width of 5 inches/10,000 or 0.0005 inch for the 5BYP16 and 5 inches/800 or 0.00625 inch for the 5ZP16 where the measured over-all spot size, using a "knife edge" test, is about 0.004 inch for the 5BYP16

135
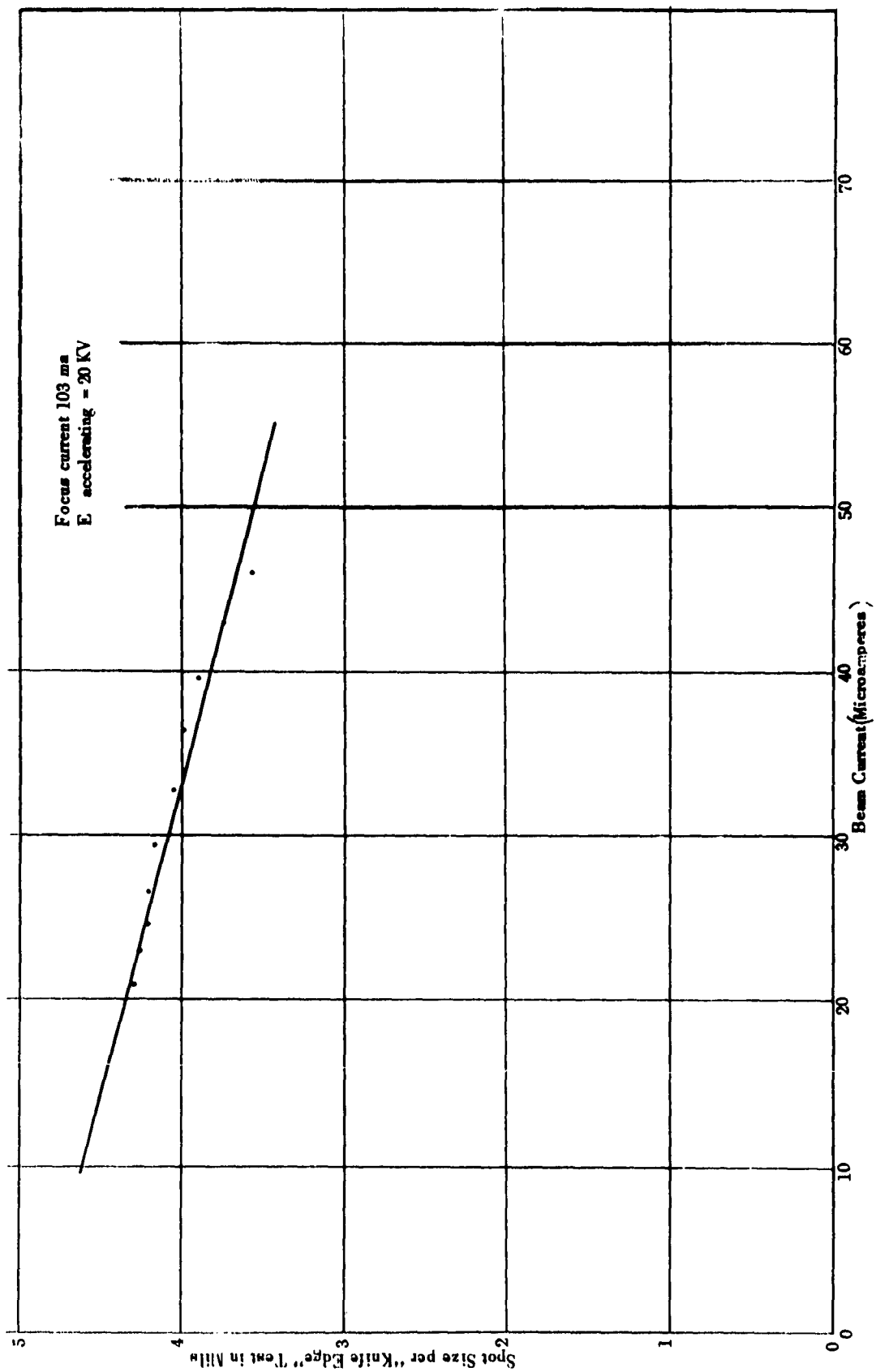
Figure 58. Variation of Beam Spot Size With Beam Current for 5BYP16 Cathode-Ray Tube Using "Knife Edge" Test.
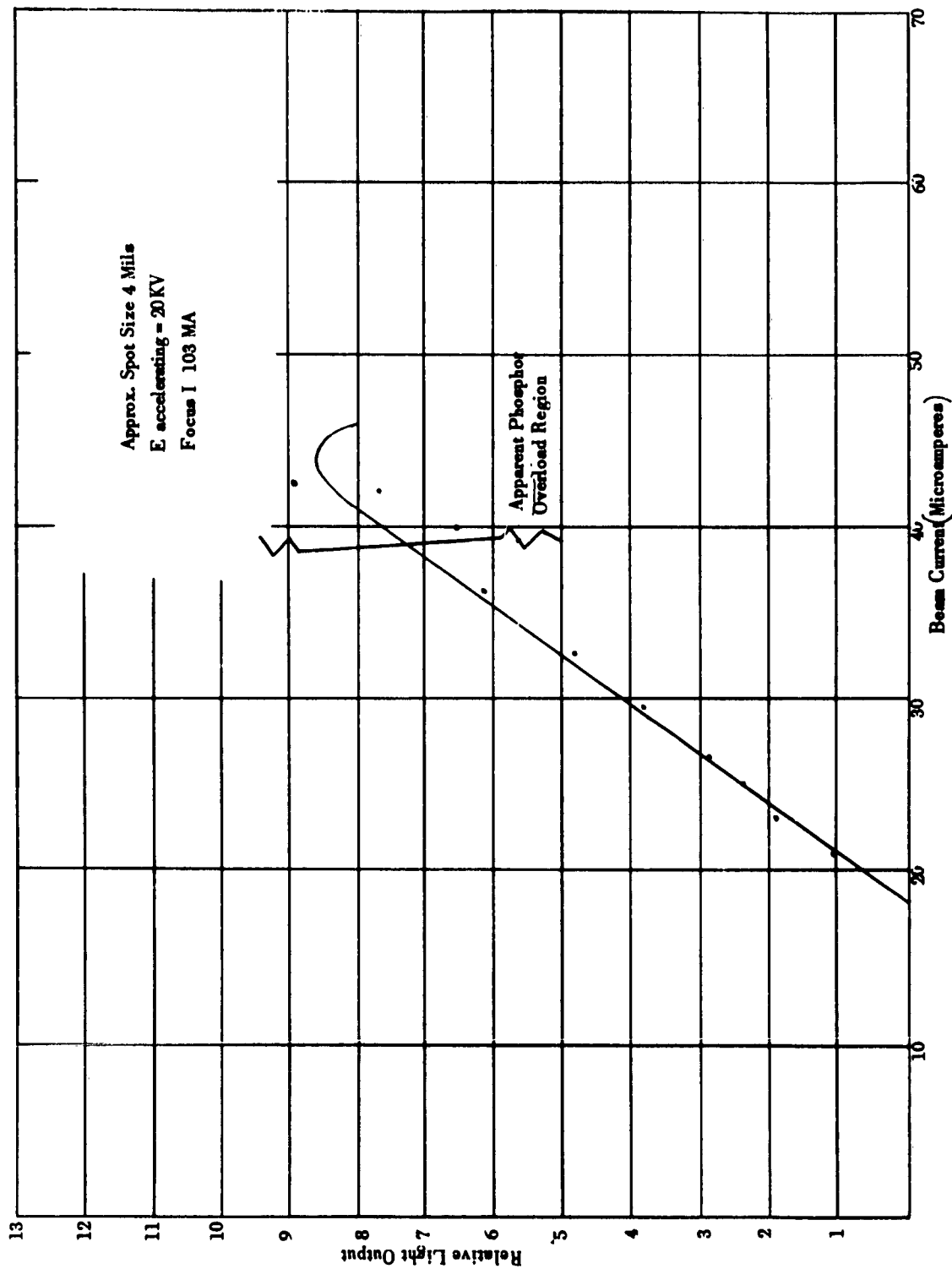
Figure 59. Variation of Relative Light Output with Beam Current for 5BYP16 Cathode-Ray Tube.

137

ASD TR 61-70
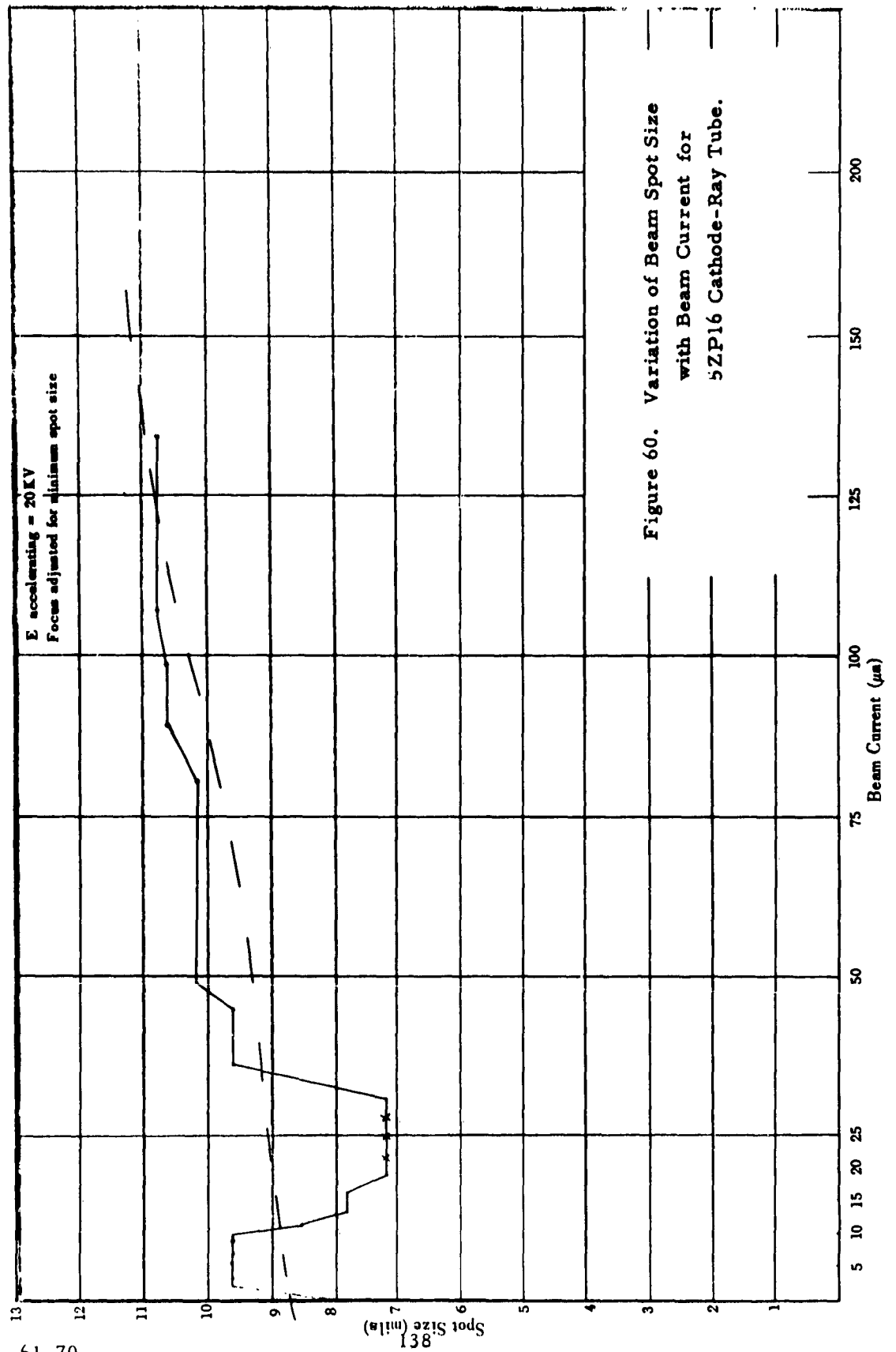
Figure 60. Variation of Beam Spot Size with Beam Current for 5ZP16 Cathode-Ray Tube.

E accelerating = 20 KV
Focus adjusted for minimum spot size

Spot Size (mils)
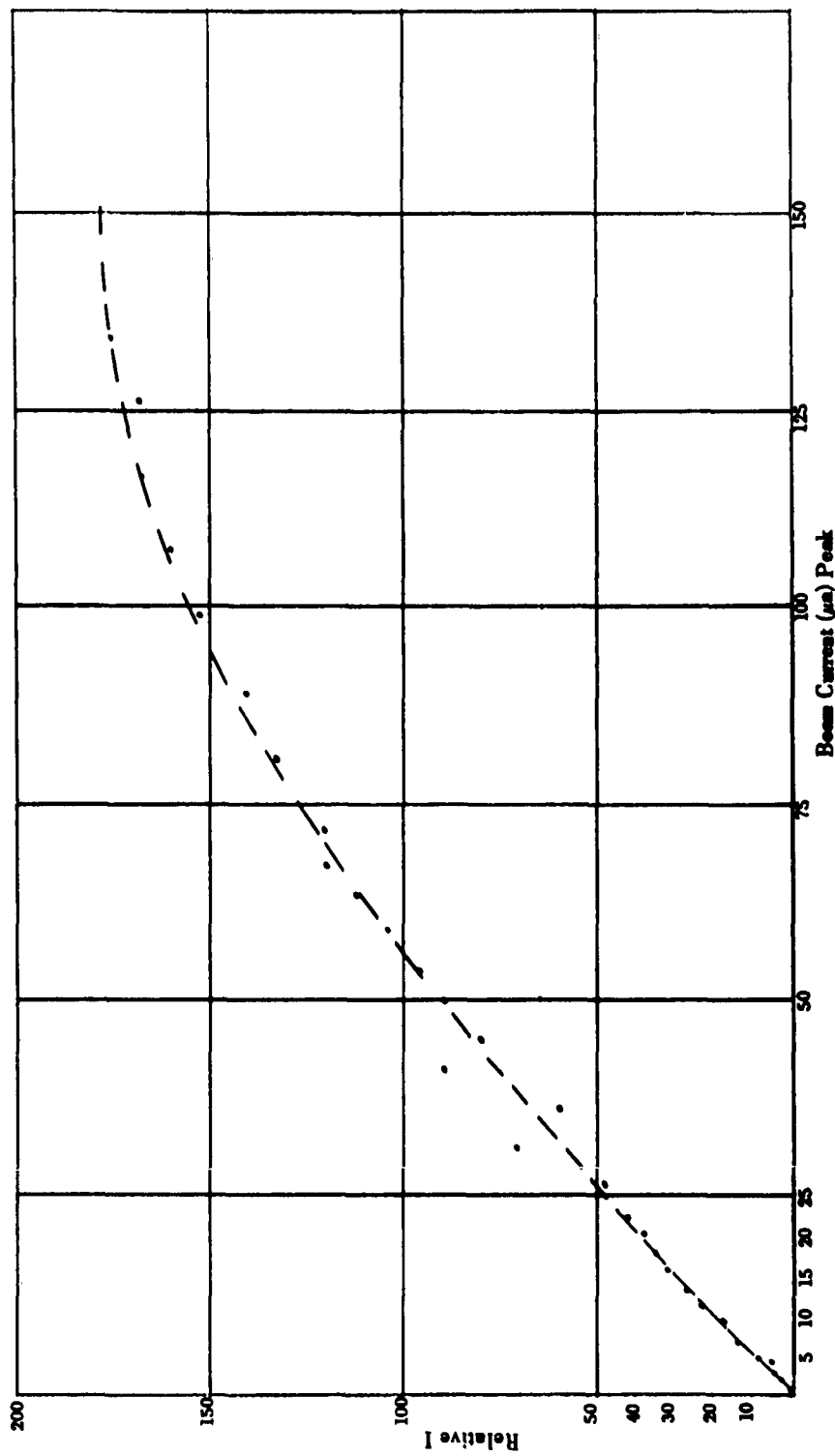
Beam Current (µa)

Figure 61. Variation of Relative Light Output with Beam Current for 5ZP16 Cathode-Ray Tube.

139

and about 0.010 inch for the 5ZP16. The fact that very different results, using the "knife edge" test method, are obtained is not surprising as both tubes are supposedly rated by the "shrinking raster" method, or equivalent. The "shrinking raster" method ordinarily uses a known number of horizontal lines of scan upon the tube face in the same manner as a T.V. raster is generated, and calls for reducing the vertical drive until the separation between the individual lines is no longer discernible to an observer. It is then not surprising that a large difference in spot size measurement would occur, depending on whether the "shrinking raster" or "knife edge" method was used.

However, the very large difference in advertised resolution using the "shrinking raster" method between the 5BYP16 and the 5ZP16, 10,000 lines and 800 lines, respectively, would seem to yield a large difference in spot size on resolution capability when using another method of testing such as the "knife edge" test. This is not the case. The "knife edge" test indicates a higher resolution only of the order of two for the 5BYP16 over the 5ZP16 where the "shrinking raster" method, as advertised by the manufacturers, indicates an increase of resolution capability of over ten times.

It may well be, as the "shrinking raster" method of cathode-ray tube resolution measurement is dependent upon an observer's judgement, that the resolution figures quoted by different manufacturers are subject to wide fluctuations. A more probable cause in this case is that the 5BYP16 used for these tests was a prototype tube and not really capable of the best resolution. CBS Electronics had indicated previously that the use of P16 phosphor presented some problems in the deposition of phosphor of sufficiently small grain size and thickness to obtain high resolution results. It is quite possible that the 10,000 line resolution quoted for the 5BYP5 can never be obtained using a P16 phosphor due to the characteristics of the phosphor.

The relative light level outputs as a function of beam current yield somewhat sketchy data upon what can be expected in the way of light levels and the maximum light levels obtainable for the 5BYP16 and 5ZP16 cathode-ray tubes. The most important factor is to understand the maximum power that can be put into the phosphor without damage to the phosphor for the particular minimum obtainable spot size in use. The curve of the 5BYP16 indicates a maximum phosphor loading at the sweep rate of 0.0008 inch/microsecond, at about 40 to 50 micro-amps. This point is easily determined from Figure 59 by noting the point at which an increase in beam current results in a decrease in light output. Any further increase in beam power will result in destruction of the phosphor due to heat.

The curve of Figure 59 does not pass through the origin. This fact would indicate that some beam current is necessary before any detectable light output can be obtained. Beam current during this experiment was controlled by means of varying the bias on the cathode-ray tube grid. The beam current could be brought to zero by means of this bias; therefore, it was not external leakage causing the offset reading. Figure 61, the curve for a 5ZP16, gives a detectable light output for very low beam currents (1 μa). The explanation for this result is not known at this time. It seems reasonable to assume, however, that the offset reading should be subtracted from the measured value in order to determine the actual beam current striking the phosphor, as experiments with other cathode-ray tubes indicate that currents of one micro-amp yield visible light on the phosphor. The importance of this factor is in calculating the power input and output of the phosphor.

The P16 type phosphor usually falls between 2 percent and 4 percent efficiency for radiant energy output compared with the beam power input. At the 20,000 volts accelerating voltage, a measured current of 40 micro-amps and an 18 micro-amp offset yields (22) (10^{-6}) (20) (10^3) watts or 440 milliwatts of power input.

141

From experiments not connected with this one, it appears for some as
yet unexplained reason, that at the higher phosphor loading and small
spot size, the lower efficiency prevails. Using the two percent figure,
the radiant power output is $(0.02)(440)(10^{-3})$ or 8.8 milliwatts of
radiated light for the 5BYP16 for the particular conditions of the test.
As the spot size is of the order of 0.004 inch, if uniform illumination
over the spot is assumed for purposes of calculation, the intensity of
the spot is $(8.8)/(10^3)(0.002)^2(\pi)$ watts/in^2 or about 700 watts/in^2. As
the spot illumination is not uniform, the peak light intensities must be
much higher than this.

For the 5ZP16 the maximum phosphor loading could not be determined
as precisely as that for the 5BYP16. The spot size was much larger and
undoubtedly the phosphor screen characteristics in particular size and
thickness significantly different. However, Figure 61 indicates that the
maximum phosphor loading was beginning to be approached at about 100
micro-amps. The spot size at this point was about 0.010 inch. The
beam velocity was 0.0024 inch/microsecond. At a 20 KV voltage, the
power input was $(20 \times 103)(100)(10^{-6})$ or about 2 watts. Again using
the figure of 2 percent efficiency, the radiant power output is $(0.02)(2)$
or 40 milliwatts. In terms of watts/in^2 for a 0.010 inch spot, again
assuming uniform illumination over the spot area, the power rate is $(40)/$
$(10^3)(25)(\pi)(10^{-6})$ or about 500 watts/in^2.

The points of maximum phosphor loading on power input for both tubes,
5BYP16 and 5ZP16, are reasonably close (700 watts/in^2 and 500 watts/in^2)
considering the large amount of experimental error probable, the assump-
tions as to uniformity of spot illumination, and the probability of large
differences in screen coatings. These power regions are of course only
valid for the particular conditions of the test. The spot dwell time for
both tubes, if the beam size measurements are reasonably correct, is
about 5 microseconds, and the cycle time or "dead time" between reenergiz-
ing the spot again is about 13 milliseconds. At lower dwell time on a

142

particular spot and/or longer times between energizing a particular area, greater peak power levels should be obtainable as the only apparent limit is the heating of the phosphor by the beam input power. Naturally the inverse is also true.

e. Conclusions

Results of CRT experiments have produced resolution measurements using the "knife edge" test in comparison with the manufacturers method of testing and a reasonably accurate measurement of maximum power input and output to the cathode-ray tube screen. The resolution measurements have yielded conflicting results. The conclusion from this test is that a reliable specification of cathode-ray tube resolution capabilities is difficult if not impossible to obtain from the manufacturers. Testing of the tubes in the intended application is a virtual necessity.

The screen power measurements seem to be in reasonably close agreement between the 5BYP16 and the 5ZP16. This is more reasonable as the power input is readily calculated, and the same phosphor and accelerating voltage are used. The major difference between the two tubes in this respect is the phosphor grain size and screen thickness. The data obtained should then be useful for estimating the probable performance of any cathode-ray tube using P16 phosphor and a similar accelerating voltage.

3. Further Experimental Evaluations of Cathode-Ray Tubes

a. Preliminary Tests

On completion of the CRT investigations described above, further tests were conducted with respect to switching photochromic materials to the colored state by use of the RCA 5ZP16 tube. These tests indicated that if P16 phosphor was heated to its maximum temperature

ASD TR 61-70

in five microseconds, the brightness obtainable promised to be sufficient to switch photochromic materials. It was only possible to do this with a small spot on the tube since it required some 100 microamperes of beam current.

Using a small spot presented many difficulties, the worst one being that the distribution of light over the spot was at the mercy of the electron beam, and always resulted in a very bright center and gradually decreasing brilliance towards the edge. To overcome this difficulty (which leads to premature burning of the phosphor) it was necessary to de-focus the beam and spread the available electrons over a greater area.

Careful adjustment of a focus coil can produce a spot of light with extremely uniform intensities in varying diameters. Spots from 0.25 inch to some 1 inch in diameter can be achieved in this manner. Since the area of the phosphor of a normal spot is in the neighborhood of some 2×10^{-5} square inch, and the smallest uniform spot size some 5×10^{-2} square inch, it was obvious that a proportional amount of beam current would be required to raise the temperature of the phosphor to some 300° in 5 microseconds in each case.

Most average high-resolution flying spot scanner types of tubes have peak beam current limitations on the order of 1 milliampere, and in order to heat an area of phosphor some 5×10^{-2} square inch, peak beam currents on the order of 250 to 500 ma are necessary. This required a specially constructed gun.

b. High Beam Current Cathode-Ray Tube

Preliminary investigations revealed that Mr. Norman Fyler (Litton Industries) felt that he could design such a gun. The cost, he said, would be some $2000, which appeared to be quite reasonable. It also was possible to have the phosphor rescreened at any time for $50, which meant that experiments could be conducted to the burning point with a minimum expenditure for screen replacement.

144

The initial contact with Mr. Fyler was followed up by a visit to Litton Industries, Electron Tube Division, Emeryville, California. The purpose of the meeting was to discuss the manufacture of the special cathode-ray tube and to make certain that Mr. Fyler knew exactly what the requirements were for such a tube.

First, recent measurements made with an RCA 5ZP16 tube were described and it was estimated that a tube producing some 400 times more light would enable photochromic emulsions to be exposed in a reasonably short time (microseconds). The RCA tube provided a peak pulse current of one milliampere, and Mr. Fyler re-confirmed that they could design a gun to develop peak pulse currents of 500 milliamperes. By placing a tungsten mesh over the cathode he proposed that the phosphor would be evenly illuminated over the area concerned, and the control grid could safely be driven positive. Some relaxation of the duty cycle, required originally, appeared necessary to keep the cathode and power supply requirements within reasonable bounds and it was agreed that 500 milliamperes at a duty cycle rate of 1000:1 would be acceptable.

Other methods of producing greater intensities from the phosphor were discussed and it was shown that a factor of at least five could be obtained by an unorthodox design, but unfortunately other undesirable restrictions that such a design would impose made it unattractive for consideration at this time.

Mr. Fyler felt that the price of $2000 on a "best-efforts" basis would represent some $4000 worth of work inasmuch as Litton supports such projects on a "match" basis; as often, the results benefit them as well as the user.

A request was made for some guidance in assessing the temperature of the phosphor when run within its cooling time constant limits. It was interesting to note that Mr. Fyler was not able to provide any data, since he explained that it was not known, as of yet, just how the heat leaves the

145

phosphor. They felt that, with the tube, careful measurements may shed some light on these calculations, and to that end they would provide some additional data concerned, specifically, with the weight and thickness of phosphor on the screen, the metal plate backing, and the glass face plate.

Mr. Fyler felt that the limitation might not be the heat of the phosphor, but rather the decomposition of the metal backing and this deserved careful attention.

Mr. Fyler agreed that an increase of some 400 times the light output ought to be available from the tube, with a reservation that the duty cycle was not to exceed 1000:1. It was hoped that a duty cycle of 100:1 would be obtained; however, it really was very difficult to assess accurately just what would be available. It was sufficient at that time to ensure that peak beam currents of 500 ma, minimum, would be available.

Litton personnel seemed very interested in making this tube and made offers of assistance in many areas. Some useful data on phosphor screen thickness and weight relationships were obtained.

The special cathode-ray tube was ordered. While awaiting delivery, it was decided to continue experimentation with the available cathode-ray tubes.

c. Evaluation of the 5ZP16 and 5AUP24

Cathode-ray tube operating times necessary to make a photochromic memory practical have real limits. A superficial investigation into memory systems and applications indicated that the longest tolerable exposure time was a millisecond, resulting in a system of greatly restricted merits. The shortest exposure time can only be described as "the shorter the better" with a general understanding that anything from 5 to 10 microseconds would be highly satisfactory and desirable.

146

Subsequent references to pulses will therefore imply that they are within the range of useful limits of 5 to 1000 microseconds.

Measurements were made upon two commercially available CRT's manufactured by R.C.A., viz., 5ZP16, and the 5AUP24. The choice of these two cathode-ray tubes was dictated by the fact that the spectral emission curves of the phosphors are the closest available match to the write and erase spectrum requirements of the photochromic materials, respectively. Only the 5ZP16 measurements will be discussed and fully analyzed since results show that the only difference between the two phosphors is the efficiency value, P24 being approximately twice as efficient as P16. The experiments were designed to measure the limitation of the phosphor rather than the tube as a whole and consequently may be applicable to other P16 and P24 tubes providing the coating density of the phosphor screen is roughly the same.

It seems, in order to explain why it is difficult to theoretically compute the data desired, a consideration of maximum brightness will help. Maximum light output occurs when the phosphor is heated to the maximum temperature (T_{max}) it can withstand without loss of light output. This is reached just before permanent damage is sustained by the phosphor in the form of burning. Several sources of information may provide numerical quantities concerning the heat capacity, thermal conductivity, screen coating density and T_{max}[*] so together with

---

* Heat capacity of Phosphor approximately 0.2 cals/gram per degree centigrade. Refer to text by Leverenz, Luminescence of Solids, p. 398.

Thermal Conductivity of Phosphor in avaccuo, quoted by chief engineer of C.B.S., CRT Division, as 2.74×10^{-4} cals/gram, per square centimeter cross section, per centimeter per degree centigrade.

Phosphor Screen Coating Densities vary in commercially available tubes from 5 to 10 milligrams per cm^2. See Leverenz-Luminescence of Solids, p. 439; Bell Labs. Tech. Journal - Sept. 1958, p. 1190.

T_{max} for P16 and P24 phosphor reputed to be in the neighborhood of 300°C, verbally confirmed by C.B.S. engineers. Leverenz, Luminescence of Solids, p. 344, confirms that this could be reasonable.

147

regulation of the electrical beam power input, it would seem a relatively simple thermodynamic problem to compute the maximum brightness obtainable. In principle it is as simple as that, but complicated by the following factors:

1) Electrical energy in the electron beam is easily measured, but wide differences in opinion (supported by virtually no data) are existent concerning the relationship of electron beam size to visible spot size. Hence, the energy density of the electron beam cannot be reliably established. This immediately makes it difficult to confidently pursue the thermodynamic solution to the phosphor loading problem .

2) Assuming the above problem could be overcome, it would be possible to calculate the required electrical energy to raise the phosphor to T_{max}. One is then immediately faced with the problem of how long it takes to return to ambient temperature. This is a function of heat flow from the spot, some goes via the phosphor, some by the glass, some by radiation, and some by convection. To try and theoretically reckon with these factors is difficult. What looked like a relatively simple analysis has turned into a complex problem. It is for these reasons that a study in measurement of radiant energy from the CRT is most readily accomplished by careful experimental measurement.

(1) <u>Measurement of Problems.</u> Since the measurement of interest is energy density, it is preferable that the CRT be illuminated in a uniform manner. The natural focused spot created by the electron beam is generally accepted to have a gaussian distribution, and hence would complicate the measurement of energy density since T_{max} would only be reached by a relatively small area of the visible spot. To overcome this problem it was proposed to pulse operate the tube in such a fashion

148

that a relatively large, uniformally illuminated spot some 0.375 inch in diameter is produced. Unfortunately, insufficient beam power becomes available with this mode of operation to reach T_{max}, but it does afford accurate measurements approaching this value of temperature.

Under certain conditions it is possible to reach another limit known as "phosphor saturation" before T_{max} is reached. This occurs with a value of beam current density that excites every available phosphor excitation center. Any further increase in beam current density beyond this maximum would yield no further increase in brightness, and consequently should be detected experimentally with a fall off in efficiency. Results clearly indicate that limitation due to phosphor saturation was not reached over the limits tested under pulsed conditions.

(2) **Method of Measurement.** Figure 62 shows a block diagram of the manner in which the pulsed operation was achieved, and shows all relevant dimensions. The instrument used to measure the radiant energy was a thermopile, which was placed some 4.0625 inches from the face plate of the CRT. The output of the thermopile activated a galvanometer, and this combination was calibrated against a standard NBS lamp. Normally, the CRT was cut off by the -150 volts on the control grid (G_1) from the output of the pulse amplifier. The cathode was returned to a few volts positive to ensure that the tube was turned fully on during pulse time. This was adjusted during operation to give uniform illumination of the spot.[*] G_2 was returned to a +150 volt power supply and G_3 was electrostatically focused for a small spot. A magnetic focus coil was connected to a variable d-c power supply and current adjusted through the coil so that the spot was defocused magnetically to 0.375 inch diameter. The average beam current was measured by a microammeter in the ultor lead, and was varied only by changes in either the pulse repetition rate or pulse duration.

---

[*] Adjusted here means by eye, and subsequently tested by exposure of a photographic plate, for uniform illumination. Best uniformity occurs when the grid is driven slightly ($\approx$ 1 volt) positive with respect to the cathode.

149
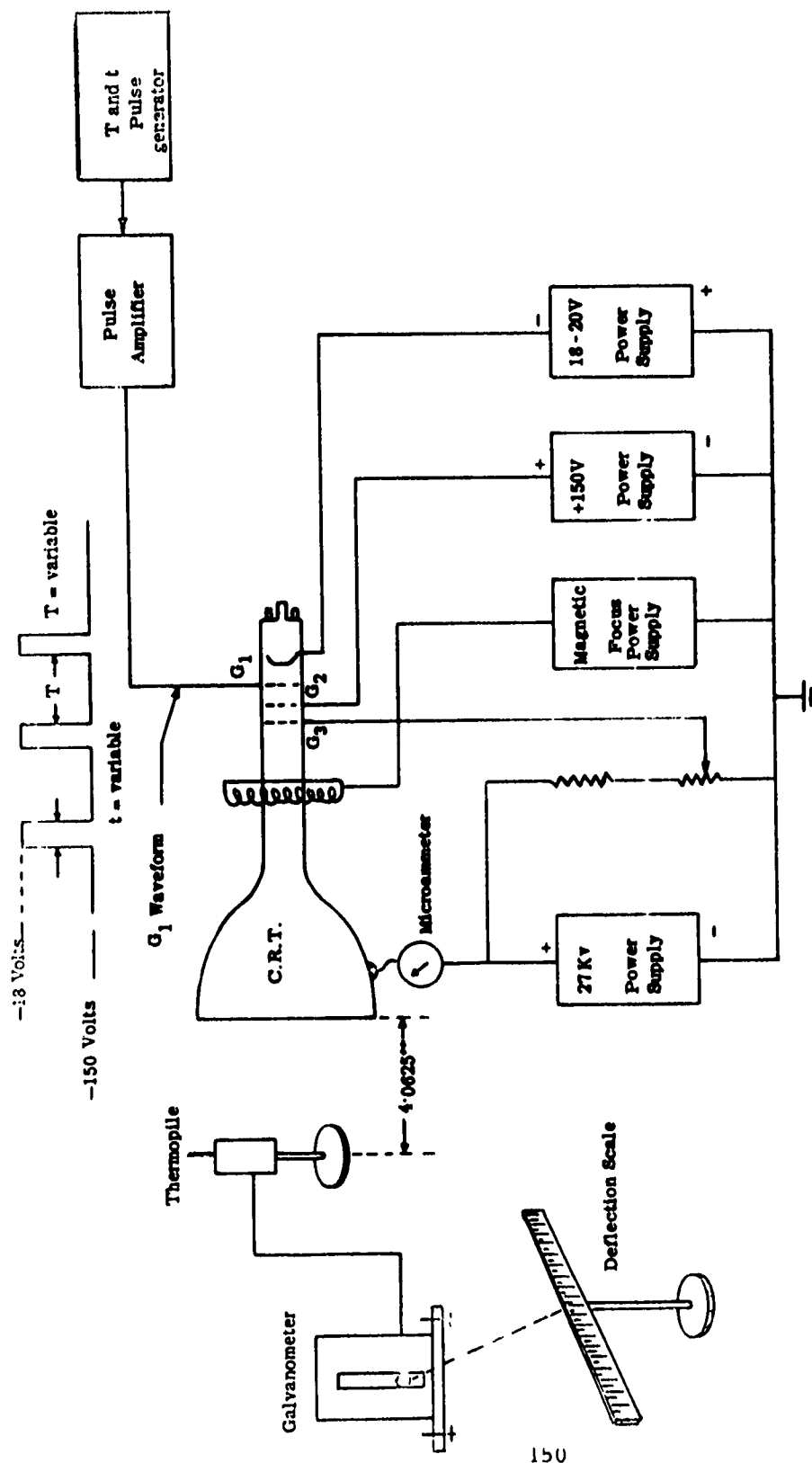
Figure 62. System used in Measurement of Pulsed Energy.

ASD TR 61-70

(3) **Objectives of Measurements.** Having arranged the operation of the tube
in such a fashion as to evenly illuminate a known area, it was possible to
introduce electrical energy into this area by varying the pulse repetition
rate and/or pulse duration.

Preliminary testing of the test system revealed that the maximum beam
current available fro n the gun was influenced by the geometric position
of the magnetic focus coil over the gun structure. Different positions
produced peak available beam current ranges from 0.7 ma in the generally
accepted "normal" position up to 3.5 ma when moved closer to the rear of
the tube. Tests were conducted in both positions. Since both the thermo-
pile and beam current microammeter measured average values, the duty
cycle, in turn controlled by pulse duration and repetition rate, enabled
the peak values of beam current and energy density to be computed. The
objective of varying the manner in which energy is introduced to the phosphor
is to ascertain whether or not this affects the efficiency of the phosphor in
converting the electrical energy to radiant energy. Four such tests were
run and results are shown in Test Data Sheets I, II, III, and IV in
Appendix XVI. Inspection will show a wide variety of pulse durations and
repetition rates for two values of peak beam current.

(4) **Evaluation of Pulsed Tests.** To evaluate the tests, a graph of galvano-
meter deflection against average beam current was plotted for each test.
This showed that no matter what the pulsed condition was, a given average
beam current always produced the same deflection on the galvanometer,
and Figure 63 shows the result. This, of course, was true for the ranges
tested only, but it does show that, within reasonable limits, one pulse
can be made to contain a very exact amount of energy, and it does represent
a very high intensity per unit area within the duration of the pulse.

Tests were made with pulse durations of 5, 10, and 50 microseconds,
and it was possible to state the amount of energy contained in each and to
compare efficiencies. Calculations and solutions in Section A of Appendix XVI
demonstrate how these figures were obtained from the measurements.

151
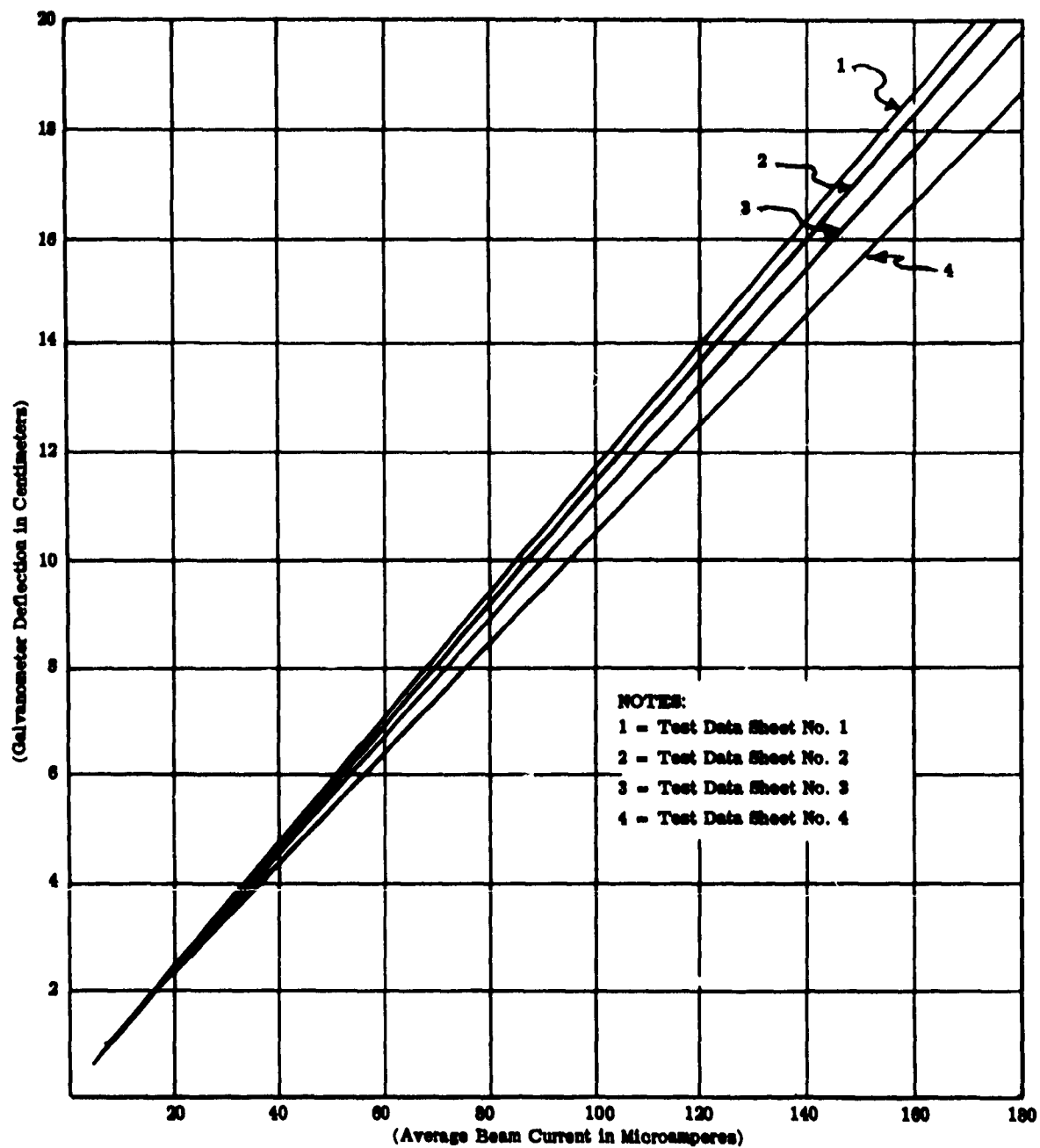
Figure 63. Results of Tests 1, 2, 3, and 4.

ASD TR 61-70

These tests showed a linear increase of radiant energy density per pulse with increase in pulse duration. The fourth test, where the peak beam current had been increased from some 0.7 ma to 3.0 ma, showed the relationship to be linear for change of peak beam current. Both relationships being linear over the range tested indicates that, for a fixed spot size, radiant energy density is proportional to the electrical input beam power and that this takes place with an efficiency of 2.25 percent. Having established that in all cases approximately two percent of the beam power is converted to radiant energy, it is necessary to devise some way of raising the phosphor to T_{max} with a known amount of electrical energy. So far all the tests have failed to heat the phosphor to T_{max} due to the beam current limitation of the gun. T_{max} may be reached in two ways:

(a) By sufficient energy density in one pulse

(b) By average input energy density (i.e., continuous operation).

Neither of these modes provide sufficient average energy to enable the thermopile to register before the phosphor is damaged. However, by using a variation on the theme of (b), by keeping the spot moving we can obtain a high average level suitable for measurement by using a large effective area of phosphor. A new mode of operation will therefore be used which will

(a) Raise the phosphor close to T_{max}

(b) Provide adequate quantity of average radiant energy
    to permit accurate thermopile measurements.

(5) <u>Measurement of Maximum Brightness (Phosphor at or near T_{max})</u>.
To reach maximum brightness the CRT was operated as shown in Figure 64. Two amplifiers were coupled to magnetic deflection coils and each coil was driven with a sine wave of frequency 30 cps. A 90° phase shift was provided between each amplifier, and the net result when the amplitude output of each amplifier was adjusted, was a circular raster upon the face of the CRT. Conventional bias on G_1 controlled the beam current which

153
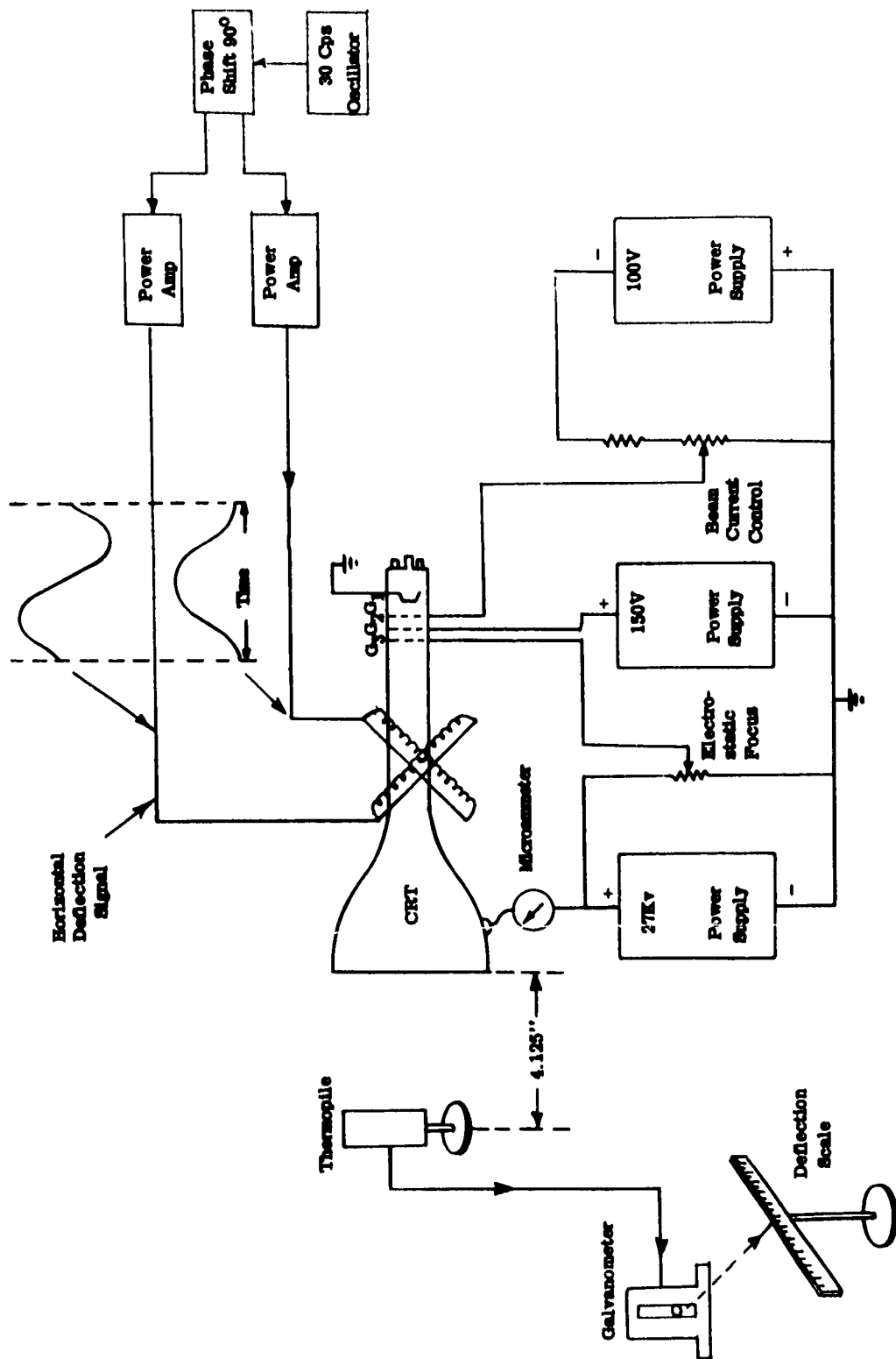
Figure 64. Configuration used to bring Phosphor to T_{max}.

30 Cps Oscillator

Phase Shift 90°

Power Amp

Power Amp

Horizontal Deflection Signal

Time

CRT

$G_1G_2G_3$

Micrometer

Electro-static Focus

Beam Current Control

100V Power Supply

150V Power Supply

27Kv Power Supply

Thermopile

4.125"

Galvanometer

Deflection Scale

154

ASD TR 61-70

was measured with a microammeter in the ultor lead. G_2 and G_3 were set for smallest possible spot diameter, which was assessed to be in the order of 0.015 inch diameter.

The spot was small so that sufficient input electrical energy density was available to raise the phosphor close to T_{max}. This was experimentally verified by increasing the beam current until the raster just damaged the phosphor visually. This occurred with a 2.5 inch diameter raster at about 220 ma of beam current, rotating at 30. Beam current was backed off to 180 ma and it was assessed that the temperature was rising close to T_{max}.

(6) <u>Evaluation of Circular Raster Test.</u> Calculation sheet V in Appendix XVI tabulates the experimental measurements obtained with this mode of operation. Data show that some 39.8 watts/cm^2 of radiant energy were measured.

Caution must be exercised when interpreting this figure as it represents an unusual situation. It represents the summation of energy from the annular area traversed by the spot during the circular sweep. Calculation sheet VI (Appendix XVI) shows this area to be numerically equivalent to 520 spots so that the energy density rate per CRT spot is 76.5 milliwatts/cm^2. This value constitutes the limit of radiant energy available from the P16 phosphor when it is at or near T_{max}. For equivalent pulsed operation this is shown to be 2540 microwatt seconds/cm^2 radiant energy density per pulse.

These are the maximum radiant energy levels that will be used in the next section to determine the time required to expose photochromic materials from P16 phosphor.

It is interesting to note that the phosphor efficiency has "slumped" to near one percent in this mode of operation. To ensure that the limiting value was T_{max} and not phosphor saturation, several other energy readings were taken at various beam currents and Figure 65 shows a graph of galvanometer deflection versus beam current. It is quite linear up to 220 μamps

155

NOTES:

Distance from Thermopile to CRT face = 4.125 inches
Circular raster = 2.5 inches in diameter
High Voltage = 27 Kv
Galvanometer sensitivity = 0.118 cm deflection for
$1 \mu watt/cm^2$ energy density
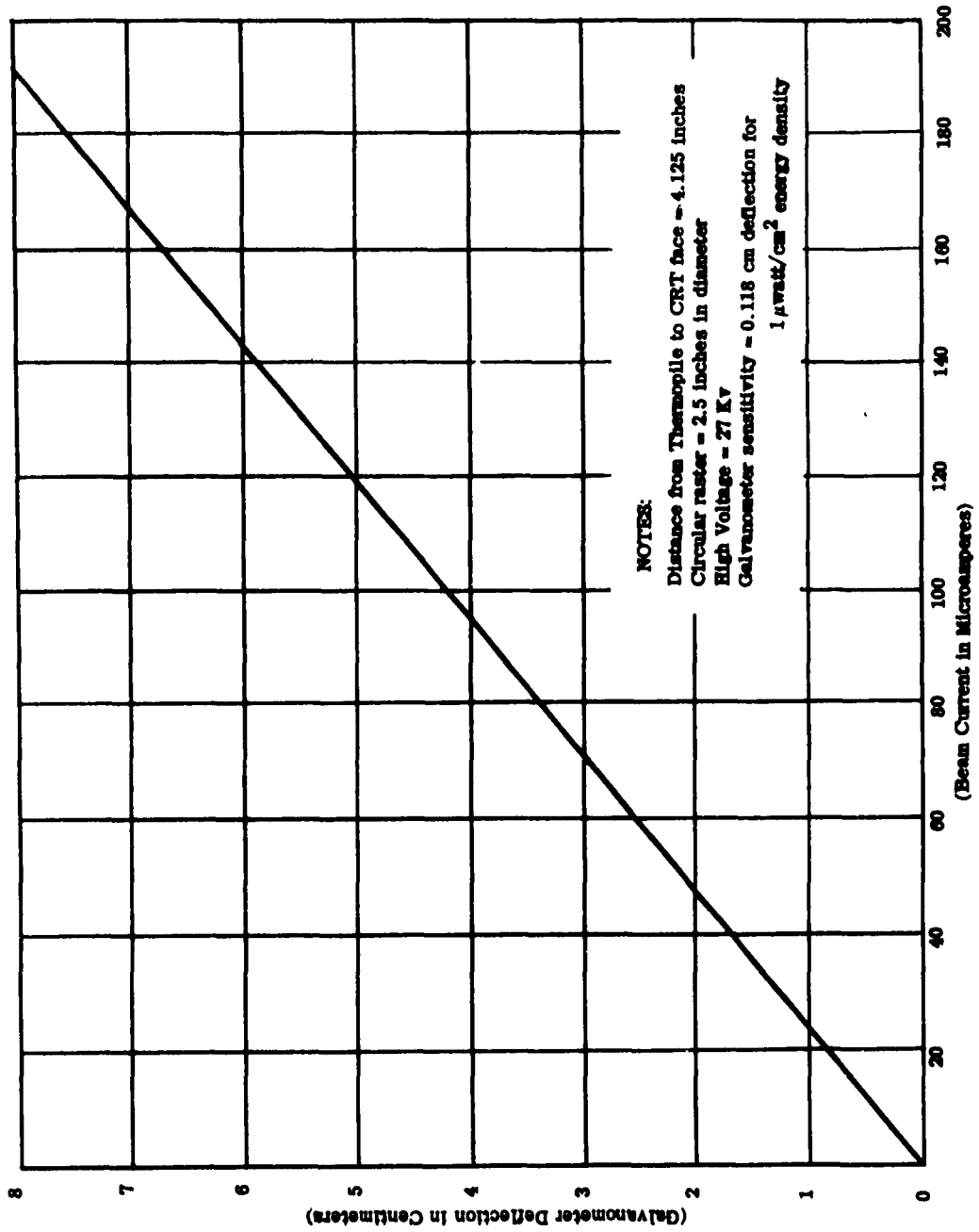
Figure 65. Circular Raster Test.

(Beam Current in Microamperes)

(Galvanometer Deflection in Centimeters)

156

ASD TR 61-70

where permanent damage was observed in the form of burning. Had phosphor saturation occurred, the graph would have turned over sharply indicating this limit. The efficiency of one percent remains constant for all values of beam current. It suggests that the efficiency is somewhat a function of the spot size and beam current density distribution. Earlier pulsed experiments, with a relatively uniform illumination of the spot, indicated two percent efficiency. The small spot is generally accepted to have a gaussian distribution, and this together with the higher operating temperature must account for the fall off of efficiency.[*]

With the maximum energy levels established it is now possible to compute the most efficient manner of attaining T_{max} for any mode of operation. Calculation sheet VII (Appendix XVI) shows the beam current required to bring a large spot 0.375 inch in diameter to T_{max}, and observation of duty cycle permits safe average operation to be computed. Result indicates peak beam current of 0.67 amps for duration of 10 microseconds would settle at T_{max} for a repetition rate of 200 cps. This has assumed a return to two percent efficiency which is probably in order for a large spot where

     (a) Beam size is near spot size, and

     (b) Uniform illumination is ensured.

Where natural beam spot size computations are involved one percent efficiency would be a better practical figure.

(7) __Summary.__ The previous tests revealed the limitation of the phosphor when heated to T_{max} To utilize this, average beam power capabilities of the tubes must not be exceeded, and preliminary calculations

---

[*] Other observers find that generally, as T_{max} is approached, efficiency of the phosphor decreases. No solid explanation is given for this. (See Leverenz, _Luminescence of Solids_, pp. 440-441).

ASD TR 61-70

show that such energy densities can be readily achieved in small spots with the 5ZP16. Larger areas involve a special gun design to provide high peak currents.

It is important to realize that once T_{max} has been reached, the length of time that it becomes available is a function of the mode of operation of the tube. In the circular sweep method, if the spot were followed by a moving lens then it becomes available for 100 percent of the time. This is about the best that can be achieved. Only small improvements can be expected by sweeping larger and larger areas of phosphor, roughly in proportion to the increased area, but limited when the duty cycle "off time" exceeds the cooling time constants of the phosphor.

The next part of this report will show what sort of exposure times can be achieved on photochromic materials when the 5ZP16 is used as a light source.

4. The Compatability of Cathode-Ray Tubes with Capsular Photochromic Coatings

The preceding has defined the maximum brightness that may be obtained from the P16 phosphor, and it is now a relatively simple matter to see what sort of exposure times can be achieved. First it is necessary to define the mode of operation of the tube so that two sets of exposure times can be estimated:

    (a) Using a lens to follow a moving spot at T_{max}

    (b) Pulsing a stationary spot

These two modes of operation represent the extreme cases of exposure times and, dependent upon the mode selected, would greatly influence system design. Mode (a) will undoubtedly yield the shortest exposure times, but relegates the maneuverability of the electron beam to the order of mechanical times that would be required to follow the spot

158

with the lens. Mode (b) still allows fast movement of the spot within the field of the lens being used (which may be large compared with mark sizes). Any mode of operation between (a) and (b) will come from series-parallel writing or rewriting of the mark and will fall somewhere between the two limits.

a. Transfer of Energy from CRT Face to Image Plane

It is reasonable to assume that a lens will be used to transfer the energy from the CRT face to the image plane. Before working out exposure times it is first necessary to know approximately the order of efficiency that may be achieved in such a transfer. This was determined experimentally with the aid of the thermopile and equipment was arranged as shown in Figure 66.

Since we were interested in computing exposure times to P16 phosphor, it was necessary to see how the spectral energy emission of phosphor could affect the speed. To do this D log E curves were run with a calibrated energy density spot on the CRT itself; Figures 67 and 68 show a graph of D log E curves for varying thicknesses of photochromic emulsions of types HSP-208 and -216, respectively. Comparison of these curves with those made with the Osram HBO-109 and Corning 7-60 filter show that the maximum written density is reduced, especially for HSP-216, but that approximately the same amount of exposure energy density is required. Hence, exposure times with P16 phosphor of 0.3 watt sec/cm^2 does provide sufficient energy to cause maximum density to be reached at least with HSP-208. HSP-216 requires slightly more. This figure will next be used to compute the exposure times available with a CRT and P16 phosphor. At the time of these experiments, only capsular coatings were being used.

b. Time Required for CRT P16 Exposure of Capsular Coatings

(1) Mode (a). Mode (a) represents the best possible way to ulilize the brightness available from the CRT. This assumes that some satisfactory mechanical method is found to essentially follow a moving spot on the phosphor which is maintained near T_{max}. Calculation sheet V (Appendix XVI) shows that the

ASD TR 61-70
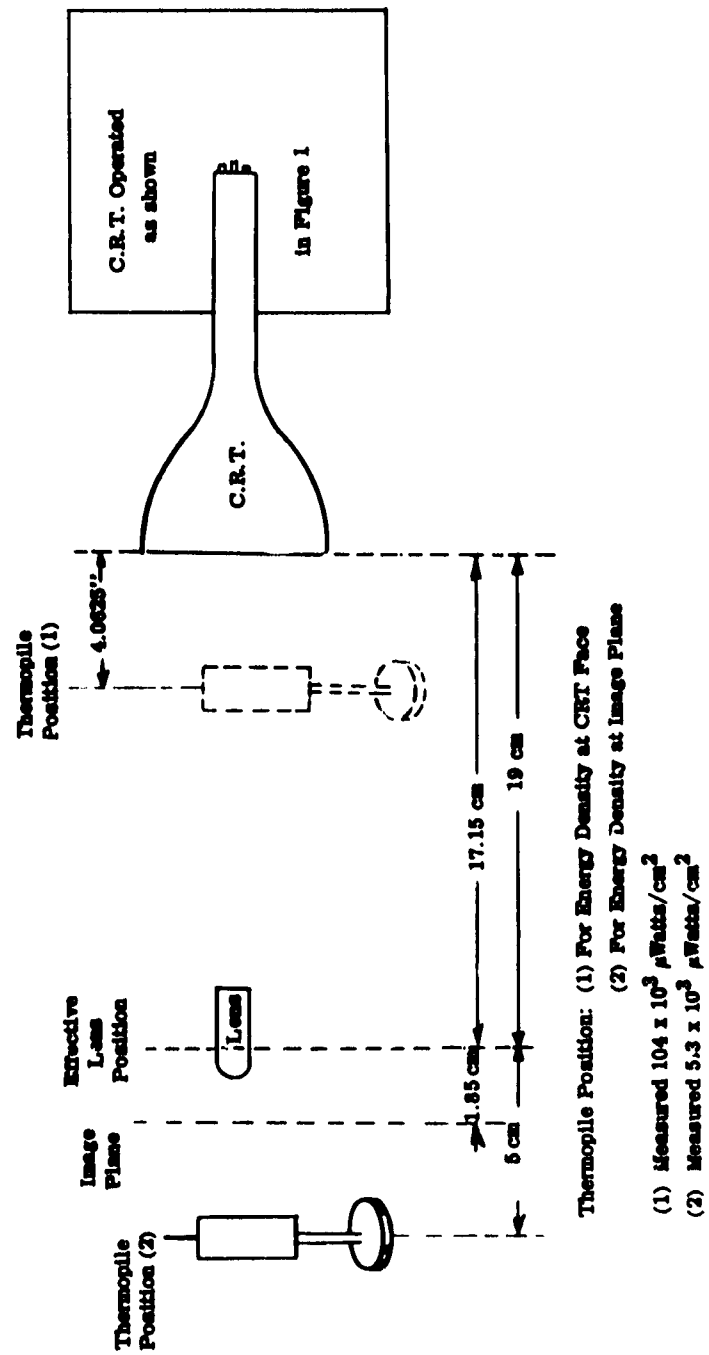
Figure 66. Energy Density Transfer Test Set-Up.

Thermopile Position (1)

Thermopile Position (2)

Thermopile Position: (1) For Energy Density at CRT Face
                     (2) For Energy Density at Image Plane

(1) Measured 104×10^3 μWatts/cm^2
(2) Measured 5.3×10^3 μWatts/cm^2

C.R.T. Operated
as shown

in Figure 1

C.R.T.

Effective
Lens
Position

Image
Plane

Lens

4.0625"

17.15 cm

19 cm

1.85 cm

5 cm

160

ASD TR 61-70
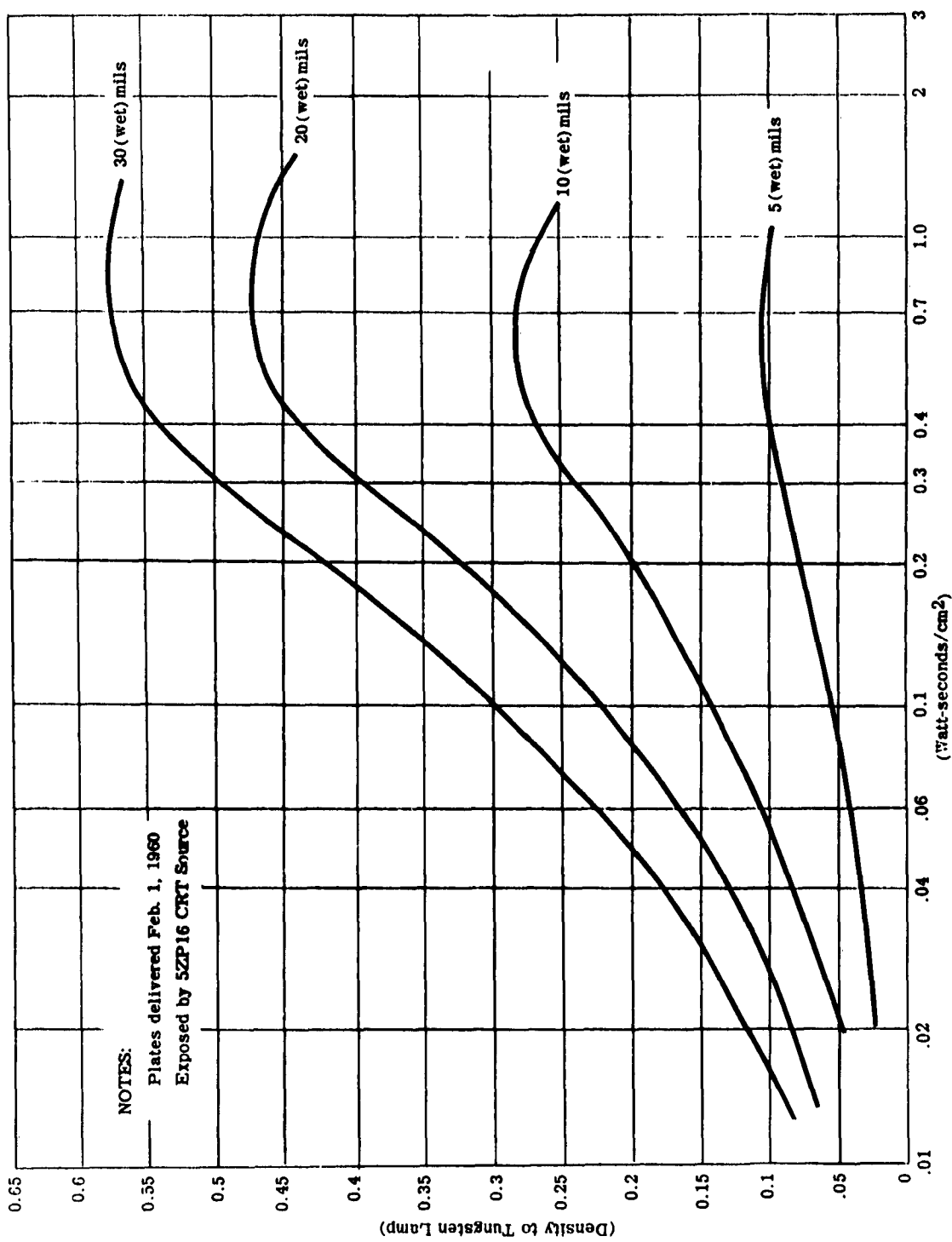
Figure 67. D Log E Curves for HSP-208 at Various Emulsion Thicknesses.

161
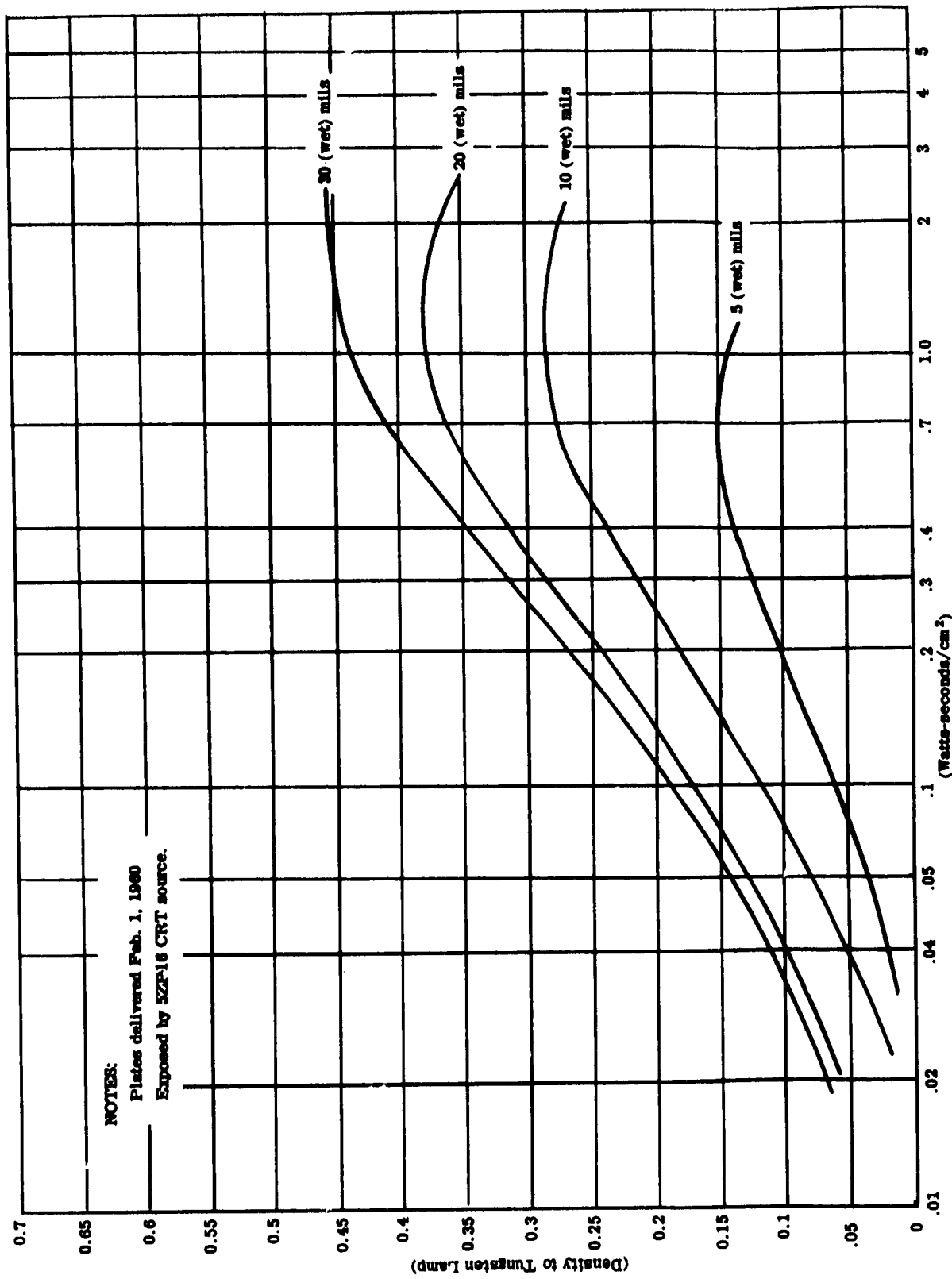
Figure 68. D Log E Curves for HSP-216 at Various Emulsion Thicknesses.

NOTES:
Plates delivered Feb. 1, 1960
Exposed by 5ZP16 CRT source.

162

energy density at the face of the CRT under such circumstances will be in the neighborhood of 40 watts/cm^2 radiant energy. Previous optical tests show that in practice about 1/20 of this will be available at the image plane, i.e., 2 watts/cm^2. Sensitivity tests show that 0.3 watt sec/cm^2 is required, hence the required amount of energy will have been supplied in

$$\frac{0.3}{2} = 150 \text{ milliseconds.}$$

(2) **Mode (b).** This constitutes the most efficient "stationary spot" illumination of the phosphor and is calculated in sheet No. VII. Here each pulse contains the T_{max} limit of energy density of 2540 micro-watt secs per pulse, at the CRT face. At the image plane one-twentieth of this becomes available - 125 micro-watt secs/cm^2. The number of such pulses of energy required to summate the required 0.3 watt secs/cm^2 is

$$\frac{0.3}{0.125 \times 10^{-3}} = 2400 \text{ pulses.}$$

Observations of the cooling time constant of the phosphor sets the maximum rate at which they are available at 200 per second. Hence, time to deliver required energy equals 2400/200 equals 12 seconds.

c.   Conclusion

The most efficient use of P16 phosphor as a light source for exposing photochromic materials of present speed capabilities requires exposure times of 150 milliseconds at best and 12 seconds in a conventionally operated mode. Both of these exposure times represent the most efficient use of the available energy density as far as both phosphor and conventional optics are concerned, when used with conventional cathode-ray tubes.

General purpose memory applications of photochromic materials dictate that the limits of useful exposure times range from 10 microseconds up to the very maximum of one millisecond, the latter imposing heavy restrictions upon both systems design and application. This being the case it must

163

be concluded that CRT's do not possess the required energy densities to make them a satisfactory light source for use with photochromic materials when considered for general purpose memory applications.

A set of similar measurements were conducted on P24 phosphor for the erase application. The efficiency of P24 phosphor is roughly twice that of P16; the erase times obtained with P24 phosphor were approximately the same as exposure times were for P16 phosphor. Experimental tests showed that approximately the same amount of radiant energy density was required to erase as to write the capsular photochromic materials.

Due to the increased densities available, these measurements indicate that the non-capsular coatings have an effective increase in writing rate of an order of magnitude over the above stated values, or somewhat greater, depending upon the useable written density.

5. <u>Special Cathode-Ray Tube Studies</u>

a. Experimental

Additional CRT studies conducted made use of the 5ZP16. It was found possible to transfer a television-type raster to the photochromic material (non-capsular) from the 5ZP16 after minutes of exposure. This could be accomplished by simultaneous projection, but faster writing occurred with the projection beam turned off. In all cases, the contrast of the raster at the photochromic material was quite poor. Much better results were obtained when the raster presentation was replaced by scans which allowed the beam to move a great deal slower and/or to time-share only a fraction of the screen's surface. These results (largely qualitative) are predictable from the data obtained previously on the 5ZP16. The results obtained are summarized in the following table (Table XI) and the layout of the basic experimental set-up is shown in Figure 69.

Although the modification of the set-up of Figure 69 for the digital storage application will be taken up under Systems Studies (Part H) a brief description of the experimental device used is in order here.
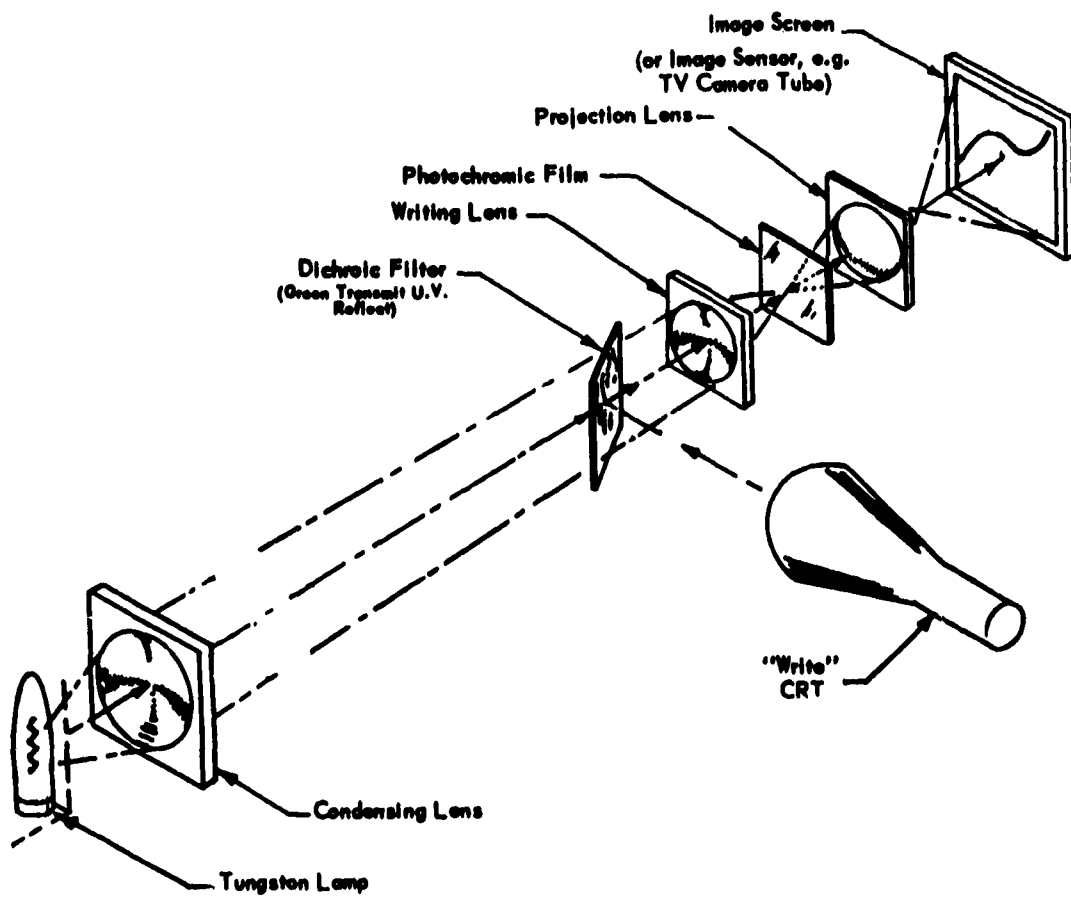
Figure 69. CRT-Photochromic System with Simultaneous Read Capability.

TABLE XI

SUMMARY OF DATA FROM EXPERIMENTATION WITH 5ZP16
WRITING OF (NON-CAPSULAR) PHOTOCHROMIC MATERIAL

CRT Type	5ZP16
High Voltage	27KV
Beam Intensity (focused)*	Adjusted to just below phosphor burn point, where possible. Maximum otherwise.
Writing Lens	f/1.6, 3/4" f.l.
Writing Lens Magnification	<0.1 at all times
Spot Diameters/sec., high contrast writing**	5

* Conditions much more severe on the phosphor and somewhat different than in the "stationary spot" case described previously (which indicated a 12 second exposure time for capsular materials).

** Using simultaneous projection with a 100 W tungsten source.

Referring to Figure 69, two light sources were provided, a 5ZP16 and a 100 watt tungsten lamp. The former is the "write" source and the latter the "read" source. The read and write channels were combined by means of the 45° dichroic filter. This filter reflected the U.V. light from the CRT and passed 500-600 millimicron illumination from the tungsten source. The condenser lens was used to provide a field of illumination which matched the size of the CRT face. Thus, the writing lens could simultaneously image a writing spot of U.V. and illuminate the whole area over which the writing spot was able to traverse. It was also possible to operate in a non-simultaneous mode through the use of shutters in each channel.

For experimental studies, the read beam transmitted through the photo-
chromic sample was intercepted by a projection lens and imaged on a
receiving screen for visual observation. Figures 70 and 71 are two
views of the experimental set-up in operation. The various elements
which are visible in these photographs are individually pointed out. The
projection lens is behind the disk which holds the photochromic slide
and the tungsten source is not within the field of view. Use of a rotatable
disk for holding photochromic slides allowed for the rapid sequencing
of new slides into the beam. The picture on the screen was written by
a few seconds exposure of the photochromic slide to a 60 cycle repetition
rate ellipse on the 5ZP16.

b. A Special Cathode-Ray Tube of Increased Spot Brightness

It was obvious from the results obtained from the CRT investigations that
improved CRT's were necessary in order to write in reasonable times on
photochromic coatings. Of all the types reviewed (on paper) the CBS
rotating anode CRT was felt to be the most promising. The price of this
CRT, $6000 to $8000, was beyond the budget of this project, so the
investigation was limited to discussions with the manufacturers and a
paper study. This tube is the type CL 1001 P16 and is shown in Figure 72.

(1) <u>Tube Data.</u> The following information is taken from the CBS data
sheet.

The Line Scan Tube was created to fulfill the requirement of obtaining the
maximum light output from an electron excited phosphor screen. CBS
Laboratories Type CL-1001 P16 represents one design of Line Scan Tube
that has been established.

In the conventional cathode-ray tube used as a flying spot light source, the
light output is limited by the rate of the heat dissipation of the phosphor.
The phosphor is a semiconductor and therefore has a low rate of heat con-
duction. In the use of flying spot cathode-ray tubes with a raster matrix,

ASD TR 61-70

Figure 70.   Projected CRT Pattern.

Photochromic
Coating

Writing Lens

CRT Face

Condensing
Lens

Dichroic
Filter

Tungsten
Source
(not shown)

Figure 71.   View of CRT Image and Filter.

CAUTION- The operation of this tube at high anode voltages can result in the production of (soft) x-rays. Suitable protection for operating personnel should be provided.

Figure 72.   Special Electron Tube

Type CL-1001 (P16).

169

the duty cycle of phosphor element is such that time is provided for the dissipation of the heat created by the electron beam before the beam returns to the same spot. When the conventional cathode-ray tube is used as a single scanning line light source, the duty cycle has been so greatly increased that the phosphor does not have sufficient time to dissipate the heat caused by the cathode-ray beam striking the surface. The heat will accumulate on repeated scans until it is great enough to destroy the phosphor.

When conventional cathode-ray tubes are used in single line applications it is necessary to reduce the cathode (beam) current to prevent the phosphor destruction. With this condition the light output is greatly reduced so that in many flying spot tube requirements in which a fine spot is needed, the resulting light output is so small that the cathode-ray tube has been found unsatisfactory. It was to solve such a problem requiring an exceedingly small light spot of high brightness that the present Line Scan Tube was created.

The solution of the problem of dissipating the heat on the phosphor has been accomplished by the use of a rotating drum. The phosphor is deposited onto a metal drum which acts as a heat sink and provides a means of rotating the phosphor so that the excited material is continuously removed from the beam scanning area. The heated phosphor does not return to the scanning area until a complete rotation of the drum allowing sufficient time for the phosphor to return to operating temperature before coming into contact with the beam again.

By the use of the phosphor drum an equivalent raster area of 2.25 x 3.14 inches is provided on the C1-1001 P16 enabling the rotating anode tube to produce a single line scan having a spot brightness greater than the spot brightness of a conventional cathode-ray tube using raster scan.

Additional light output is obtained by viewing the same side of the phosphor that is bombarded by the electron beam. Also, obtaining the light from the
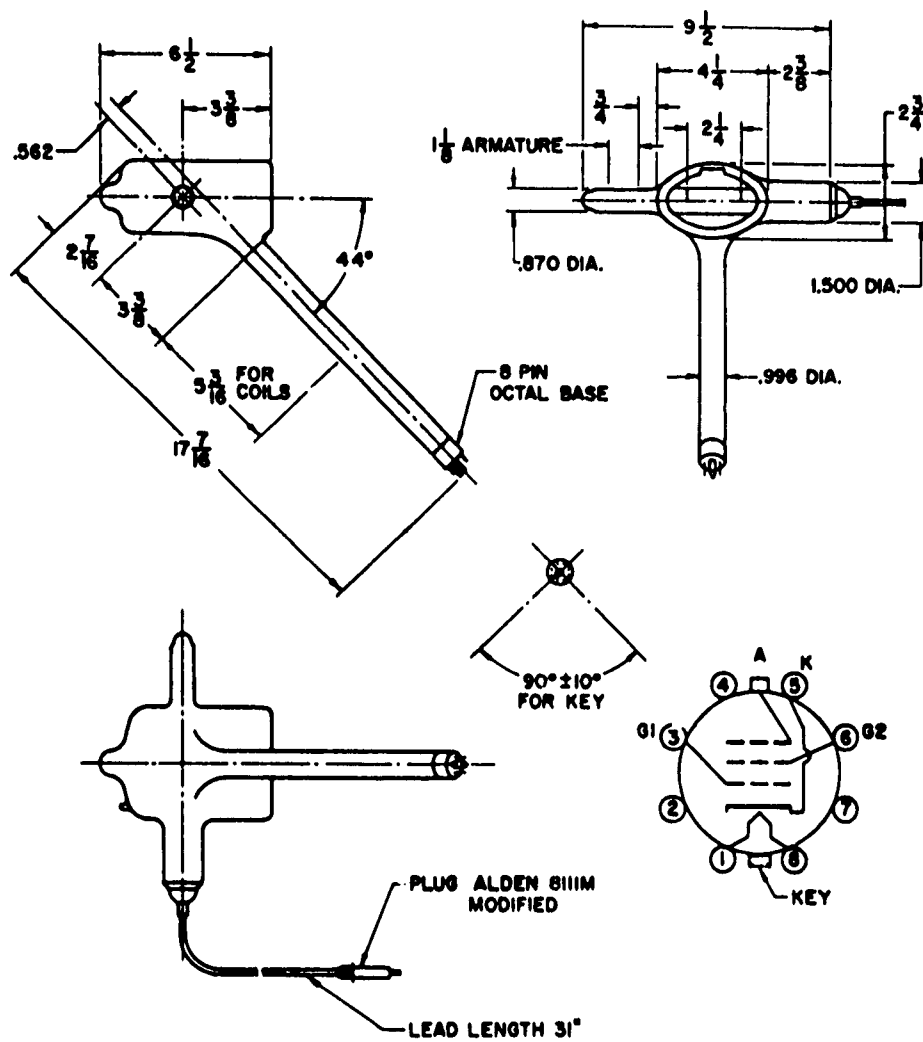
170

CAUTION- The operation of this tube
at high anode voltages con result in
the production of (soft) x-rays.
Suitable protection for operating
personnel should be provided.

Figure 72. Special Electron Tube

Type CL-1001 (P16).

169

electron bombarded side of the phosphor has the advantage of producing a smaller size spot than normally can be obtained from a given electron beam diameter. The usual diffusion of the light through the phosphor in the conventional tube with phosphor deposited on glass is eliminated.

A further advantage of the use of a metal drum is the unique means that it provides for the deposition of the phosphor. The high conductivity of the metal drum enables the use of a method of depositing phosphor from solution by electrodeposition. This method produces a screen of very fine texture without the usual "pin holes" or conglomerates associated with the "spray" or "settling" methods.

One of the very important features of the Line Scan Tube is the elimination of the streaking of the readout film caused by phosphor blemishes. With the conventional cathode-ray tube any blemish in the phosphor of the scan line will produce a streak on the recording film. The Line Scan Tube eliminates this problem by a feature of the rotating phosphor drum which provides a different phosphor area for consecutive scans of the electron beam. Thus phosphor imperfections will appear as an aperiodic dot rather than as a continuous streak. As expressed above, the phosphor depositing method used in the Line Scan Tube eliminates the most common cause of blemishes found in conventional cathode-ray tubes so the resulting recordings will be free of imperfections usually attributed to phosphor.

The CBS Laboratories' type CL-1001(P16) is a single beam, magnetic deflection and focus cathode-ray tube having high light output with fine resolution and especially designed for flying spot applications where a single line scan is used. The tube features a high precision, tetrode, electron gun structure and a fine grain phosphor coated on a revolving drum. General characteristics are given in Table XII.

171

TABLE XII

GENERAL CHARACTERISTICS OF TYPE CL-1001 (P16) TUBE

Electrical

Focusing Method	Magnetic
Deflection Method	Magnetic
Phosphor Drum Drive Motor	2 ∅, 4 pole, induction

Optical

Phosphor*	P16
Fluorescence	Violet
Persistence	Extremely Short
Faceplate	Clear, 7740

Mechanical

Overall Length	17-7/16 inches
Overall Width	10-3/4 inches
Minimum Useful Screen Width	2.25 inches
Connections	SK 1988
Outline Drawing	SK 1988

Maximum Ratings (Absolute Values)

Heater Voltage	6.3 ± 10% volts
Accelerator Electrode Anode Voltage	27000 max. volts DC
Accelerator Electrode Input Power	2.5 max. watts

* Other types available.

172

TABLE XII (Continued)

GENERAL CHARACTERISTICS OF TYPE CL-1001 (P16) TUBE

Control Electrode (Grid No. 1) Voltage

	Max. positive	$\pm$ 0 max. volts
	Max. negative	-150 max. volts
Peak Heater to Cathode Voltage		180 max. volts

Typical Operating Conditions

Heater Voltage	6. 3 VAC
Heater Current	0. 45 $\pm$ 10% A
Accelerator Voltage[1]	24500 VDC
Grid No. 2 Voltage	1000 VDC
Focus Field Strength for Focus[5](approx.)	700 AT
Grid No. 1 Voltage for Cutoff[2]	-50 to -20 VDC
Grid No. 1 "Modulation" Voltage[3]	25 V Max.
Light Output[3,6]	10 μW/cm^2 Min.
Resolution[3,4] (TV elements per scan)	1000
Deflection Angle for Full Deflection	45 Deg.
Drum Speed (approximate)	1700 RPM

Circuit Values

Maximum Grid No. 1 Resistance	1. 5 Max. Megohm

ASD TR 61-70

TABLE XII (Continued)

GENERAL CHARACTERISTICS OF TYPE CL-1001 (P16) TUBE

NOTES: Values given are nominal unless otherwise indicated.

1. "Ground" lead connected to E_b supply return.

2. Visual extinction of focused, undeflected spot.

3. Beam current of 50 μA DC.

4. As measured by observing the light output with a multiplier type phototube having S11 response and a cathode-ray oscillograph when the focused light spot is scanned across a test object having a square wave transmission grid of equal open and closed widths each being one-thousandth of the length between the fiducial marks. The modulation observed on the oscillograph shall be 50% or more of the amplitude from full darkness to full brightness. This is approximately equivalent to a line width of 2.5 mils at the half-amplitude of its light energy distribution.

5. With suitable focus coil configuration.

6. Measured on the optical axis at a distance of 10 cm from the phosphor surface.

A review of the data obtained on this project along with the decreased probability of burn with a rotating anode-type tube has indicated that writing

speed could be increased one to two orders of magnitude with this tube. When operating with an adequate safety factor with respect to burn, indications are that writing could fall in the range from a few to possibly 100 spots per second. The line scan introduces certain systems limitations, of course, but is compatible with a number of possible mechanizations. However, even this CRT is at least an order of magnitude off the one millisecond writing time which was selected as the minimum for a useful system.

6. Status of Litton High Beam Current Cathode-Ray Tube

The special high current CRT, when first tested in the laboratory, failed to meet the high pulse current specifications. The peak beam current was measured as 5.6 milliamps, instead of the required 500 milliamps. With this tube, the light output was found to be no better than that obtained from a standard 5ZP16 operated at 1.5 milliamps. This discrepancy was assumed to be due to the low phosphor coating density, 0.4 milligrams/cm^2 vs. the more standard figure of 3 milligrams/cm^2. The testing was carried no further, and the tube was returned to Litton for gun modification and a thicker P16 phosphor coating.

The Litton high peak beam current tube was modified by Litton with respect to the phosphor coating and electron gun structure and returned for further research studies. On testing this CRT once again, the peak beam current was lower than specified (350 ma instead of 500 ma), but it was considered sufficient for initial experimentation. However, on examination of the enlarged spot on the CRT face, extreme spot non-uniformity was noted. This made the tube unsatisfactory for the experimentation which had been planned. The tube was once again returned to Litton for modification to obtain improved spot uniformity.

By the time the Litton tube had been returned once again to the laboratory, the experimentation with the 5ZP16 had been well under way and this work continued. The data on hand concerning P16 phosphor was felt to be

175

reliable as consistent experimental results had been obtained with the
5ZP16. Thus, the pressure for experimentally determining the pro-
perties of P16 phosphor with the Litton tube was considerably relaxed.
Since the regular CRT tests tend to be quite damaging to the phosphor
coatings, it was decided to put this relatively expensive tube aside until
systems studies were more formalized.

Because of the relatively consistent results obtained with the 5ZP16
experimentation, and with the load of additional work required for this
program, further tests on this cathode-ray tube were not undertaken.
This tube is still capable of providing some relatively important funda-
mental data, but, because such investigations did not appear to offer any
significant implications for the photochromic memory, they were not
undertaken.

F. OPTICS AND RESOLUTION CONSIDERATIONS

1. Introduction

The following discussion is primarily concerned with individual optical
components and techniques. The situations were a number of optical com-
ponents are coordinated with electrical or electronic equipment in experi-
mental equipment or mock-up devices are described under Systems Studies
(part H of this Section).

2. Spatial Filtering

a. Basic Concepts

The developments in optical spatial filtering were a natural outgrowth of
considerations involved in the study of the ultrasonic diffraction grating
and had started shortly before the receipt of the present contract. Referring
again to Figure 42, if the ultrasonic grating is replaced by a black-and-white
photographic transparency, and if this transparency is located at a distance
greater than the focal length from the diffraction pattern forming lens, the

176

latter lens will also form a real image of the transparency in space
beyond the diffraction plane. This arrangement is shown in Figure 73.
It should be noted that the indicated arrangement is closely related to
the arrangement required for obtaining the single slit, double slit, etc.,
Fraunhofer diffraction patterns which are discussed in standard text-
books on optics. This arrangement differs from the textbook arrange-
ment only in that the object-lens two distance is such that a real image
is formed beyond lens two.

With a point source for illumination, and with the object removed, the
diffraction plane contains the L_2 aperture limited image of the point
source, a two dimensional diffraction pattern. When the object
transparency is inserted at the indicated position, the diffraction
pattern changes drastically, and, in effect takes the form of the
two-dimensional spatial frequency Fourier transformation of the object
transparency. This situation has been considered in the literature but,
apparently, was not too well-known until relatively recently.
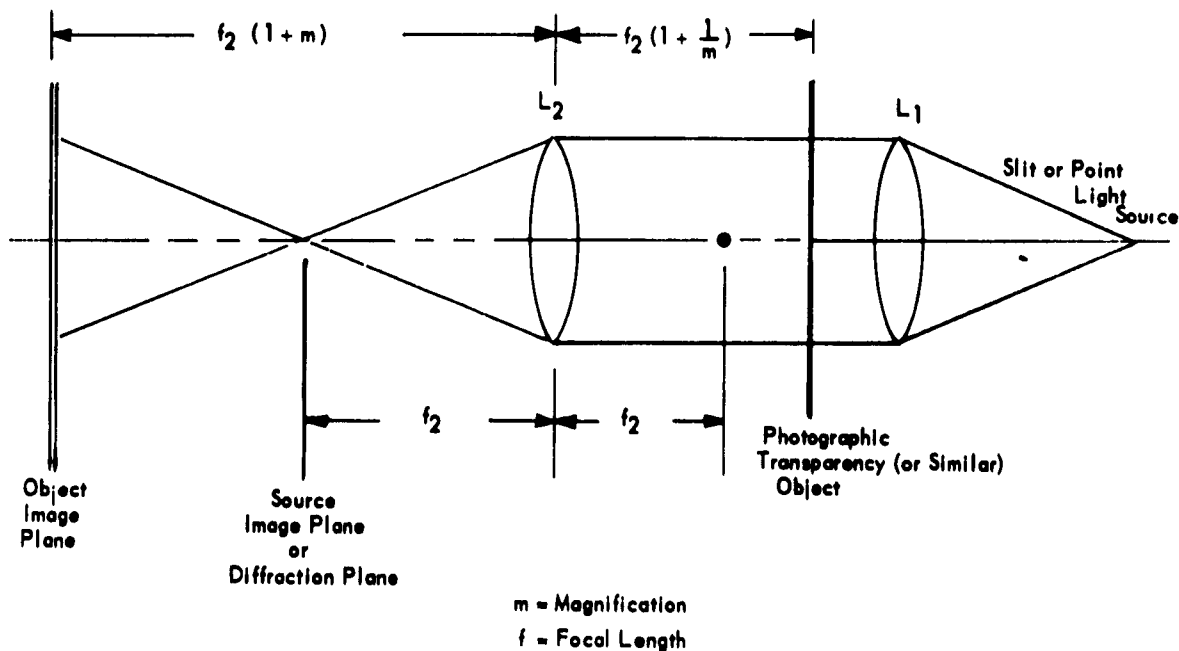
Figure 73.   Optical Set-up for Spatial Filtering Experiments.

177
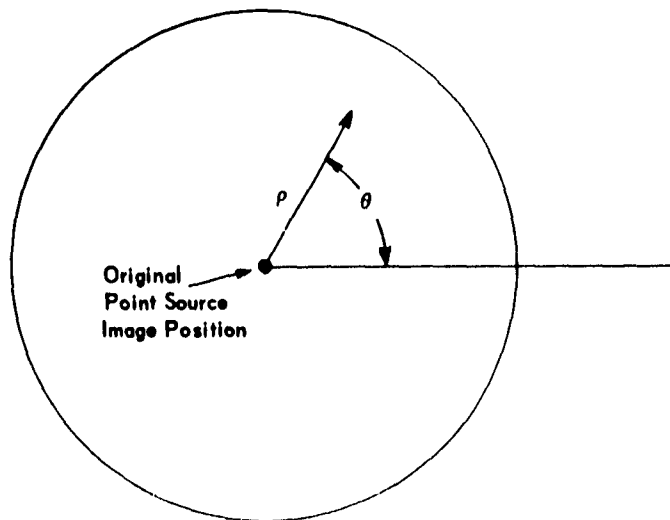
Figure 74.   Coordinates of Spatial Diffraction Pattern.

Figure 74 indicates the coordinates of the spatial diffraction pattern.
Fine details in the transparency (high frequency components) corres-
pond to large values of ρ, large detail to small values of ρ, and the
simple uniform field (no detail) to the point source diffraction pattern,
where most of the energy falls near $\rho = 0$. Since diffraction occurs
at right angles to edges, light falling at an angle θ in the diffraction
plane (with respect to a reference line common to both the object and
diffraction planes) has been diffracted from edges in the object parallel
to a line $90^\circ + \theta$. With such a diffraction pattern existing in space
between the final lens and the image screen, it is a relatively simple
task to remove certain Fourier components from the image by means
of opaque, or partially opaque, spatial filters in the diffraction plane.

The spatially filtered pictures of coatings, described under Evaluation
of Coatings (Part B of this Section), were obtained by simply removing
a portion of the diffraction pattern completely with an opaque plate.
Spatial filtering also offered the promise of increasing the contrast of
low contrast transparencies (or digitally stored photochromic patterns)
by removing the low spatial frequency over-all field components (d-c level)

178

while retaining the light which senses the fine detail. It should be pointed out that the spatially filtered coating pictures were actually made with a slit source which filtered the resultant one-dimensional diffraction pattern at right angles to the slit image in the diffraction plane.

The contrast enhancement potentialities of spatial filtering brought into the realm of possibility the use of much lower written optical densities on photochromic materials, which was an important development. However, this technique requires excellent uniformity of coatings of a quality even higher than that envisioned initially for the memory application. At the time of this experimentation, capsular coatings that were on hand were not of sufficiently high quality for spatial filtering experiments.

b. Further Theoretical and Experimental Studies

During a project review which was held with the WADD Project and Task Scientists, a great deal of interest was shown in the possible application of the techniques of optical spatial filtering to the Photochromic Memory program. It was suggested that a tutorial paper on this subject might be written and included as a part of the Appendixes of one of the quarterly reports. After considering the loss of time that the writing of such a paper would involve, and the fact that quite a few papers have been published on the subject, it was decided to publish the bibliography given in Appendix XV in lieu of the tutorial paper.

The electronically oriented reader would probably benefit from a review of single and multiple slit diffraction theory as given in elementary texts on physical optics before undertaking the study of the papers listed in Appendix XV. References 2, 3, 6, 7, 24, 26, 33 and 34 serve quite well as an introduction to the subject. Most of the publications picture a third lens between the spatial filter and image, which introduces an additional transfer function into the system. Although this third lens offers no conceptual difficulties, experience in the laboratory has shown that the two lens system is much easier to work with for general experimentation.

179

In spatial filtering studies it had been noted that the edges of objects tend to become multiple after a square pass type of spatial filtering operation is performed. The simplest case investigated experimentally is that of the step function, shown in Figure 75. Case (b) illustrates the low pass limited version of case (a). This case is a natural consequences of imaging with a lens, a low pass filter. Case (c) illustrates the action of a high pass spatial filter. The bias light is suppressed to zero and the low spatial frequency components are removed from the image.

What is observed in the image plane is the intensity due to f(x), case (c), or the square of f(x) for this case. When a number of edges are close together in the image, interference effects take place after spatial filtering and it is best to treat each case individually. In the consideration of spatial filtering for the Photochromic Memory application, such optical "ringing" effects would require careful study and spatial filters should be designed to minimize or eliminate such effects.

Figure 76 (b) and (c) are multiplier phototube (MPT) results obtained from the experimental set-up of Figure 76.(a). When the spatial filter is moved out of the region of the image of the slit source, the maximum MPT signal occurs. The noise is seen to be due to the effective light level since very little noise is present when the transmission of the system is stopped by the opaque portion of the disk. When a square pass spatial filter is slowly moved into the image of the slit source the average light level and noise level will drop (middle picture in Figure 76 (b) and (c)). When spatial filtering of the slit source is complete the condition illustrated in Figure 75 occurs for each edge in the field. The noise level is seen to be only slightly greater than for the case of the stopped system. The double fringe effect actually occurs at each edge, but it was not resolved by the experimental image scanning slit. This was determined by visually examining the spatially filtered stationary image under high magnification.

From the investigation conducted to this point, it appeared that the preceding description of some of the effects of spatial filtering was at least qualitatively
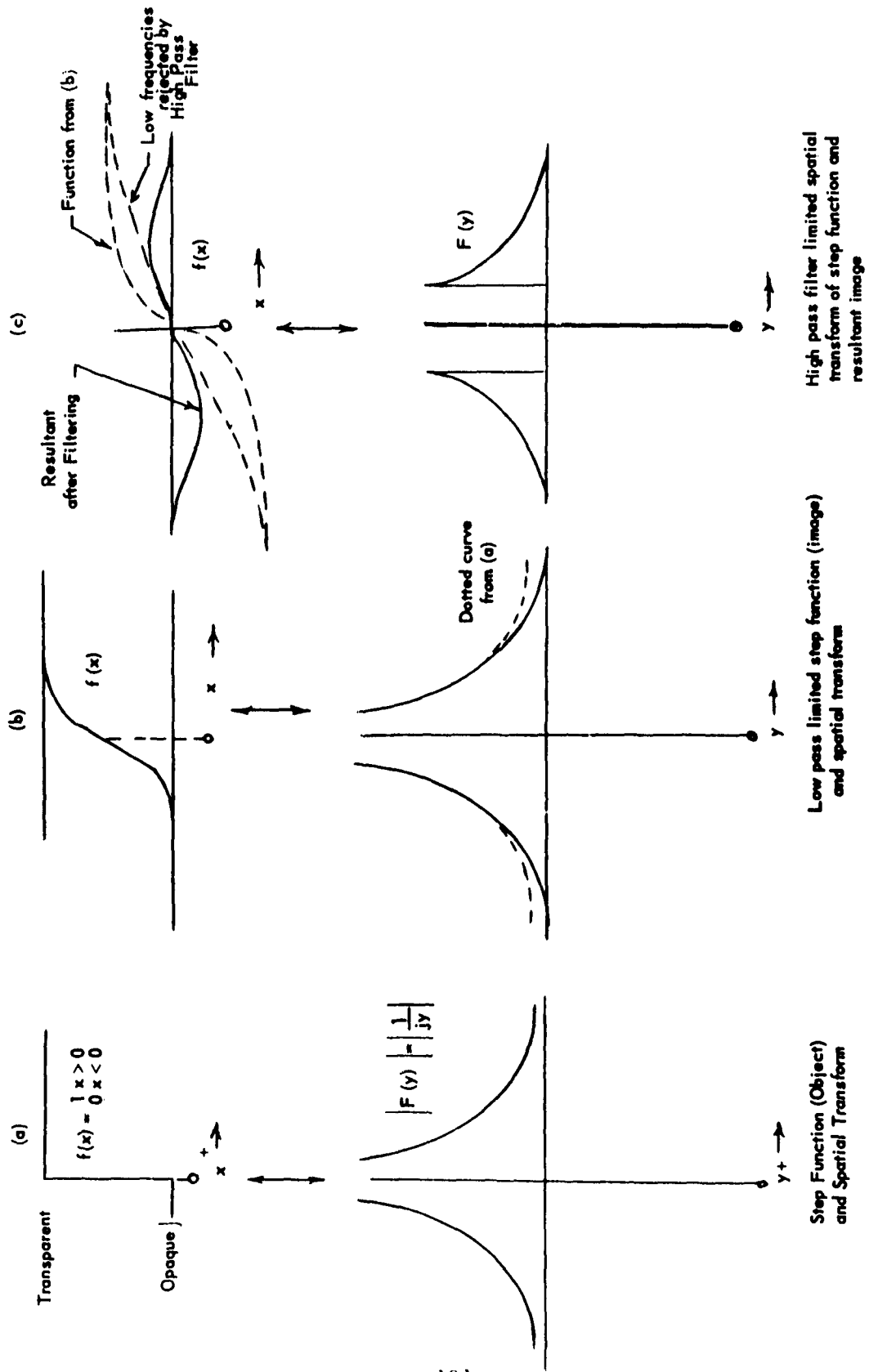
Figure 75. Image Response for Spatially Filtering a Step Function.

181

(a)

Slit
Source

Spatial Filter
Motion

MPT

Spatial
Filter

Rotating
Disk

Transparent
Slit

Double Optical
Density Slit

Slit in
Image Plane
Parallel to Slit
Source

Neutral Optical
Density Filter

Opaque

Hole in Disk

Disk
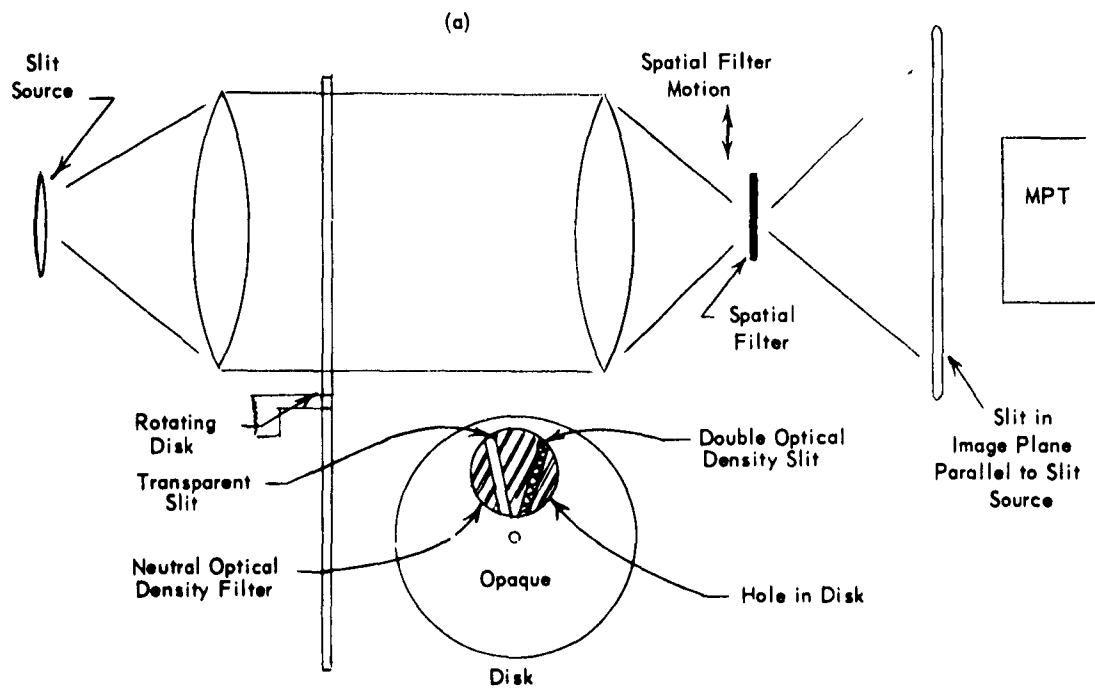
(b)
Dark Slit on a Light Background

(c)
Light Slit on a Dark Background

Figure 76. Multiplier Phototube Noise Reduction by means of Spatial Filtering.

accurate and would allow such schemes to be evaluated for use in the photo-
chromic memory program. Because of limitations in time and the number
of project personnel, rigorous mathematical investigations of spatial filter-
ing phenomena were not undertaken. Fortunately, the semi-quantitative
approximate transfer function approach appeared sufficient to evaluate the
merits of proposed configurations.

c. Final Status of Spatial Filtering

On completion of the studies described above, it was decided to de-emphasize
the spatial filtering approach because of the uniformity problems with the
capsular coatings. This decision was strengthened by the appearance of
the much improved HSP-208 capsular system which offered greater contrast
in the written patterns.

When the emphasis was changed to the non-capsular systems, spatial filtering
appears feasible. However, the contrast capabilities of the non-capsular
coatings were adequate at this time and the difficulties associated with
spatial filtering, practically speaking, dictated that the efforts with available
personnel should be expended on the alternate schemes. From the studies
that were undertaken, it appears that spatial filtering techniques deserve
a great deal of theoretical and experimental study for a variety of applica-
tions. The recent literature indicates that such a trend exists.

3. Filters

a. Types Used

Of the filters used in the research program, only the ultrasonic shutter
filtering scheme could be considered as unique. This subject is treated
under the discussion of the ultrasonic shutter and will not be discussed
further in this section.

The common types of filters used have been the Kodak Wratten filters, colored
gelatine sheets from a number of sources, Corning glass filters, and dichroic-

filters. The latter filters are of greatest interest since they can be designed to specifications in many cases. The advantages and disadvantages of the other filters are well known and data regarding their characteristics can be obtained from the sales literature. They will not be considered further here.

b.. Dichroic Filters

Dichroic, or interference, filters have very valuable characteristics. The filters are made up of multiple layers deposited in such a manner (on a glass substrate) so as to produce interference between the incident and reflected rays of light. By controlling the composition, thickness and the number of interferring layers, these filters can be manufactured to required specifications in most cases. Very little light is absorbed. What is not transmitted tends to be reflected. Thus, they are useful both as transmitting filters and reflecting filters, and they have been used as both simultaneously on this program. The non-fading characteristic (stability) is also important when used with ultraviolet light.

For initial studies three dichroic filters were obtained. Their spectral pass bands are shown in Figure 77.

The filters were manufactured to specifications. They were purchased as general purpose laboratory equipment and have proven to be quite useful during the course of the program, especially the green filter centered at 552 millimicrons. This was the readout filter in most of the studies concerning optimum readout of patterns from photochromic material.

Somewhat later two dichroic filters were obtained which were designed to operate at 45° to the incident illumination. These filters were designed to reflect the near ultraviolet spectrum and to pass the visible spectrum between 500 and 600 millimicrons. No curves were available, but they performed quite satisfactorily in the applications in which they were tried.

184
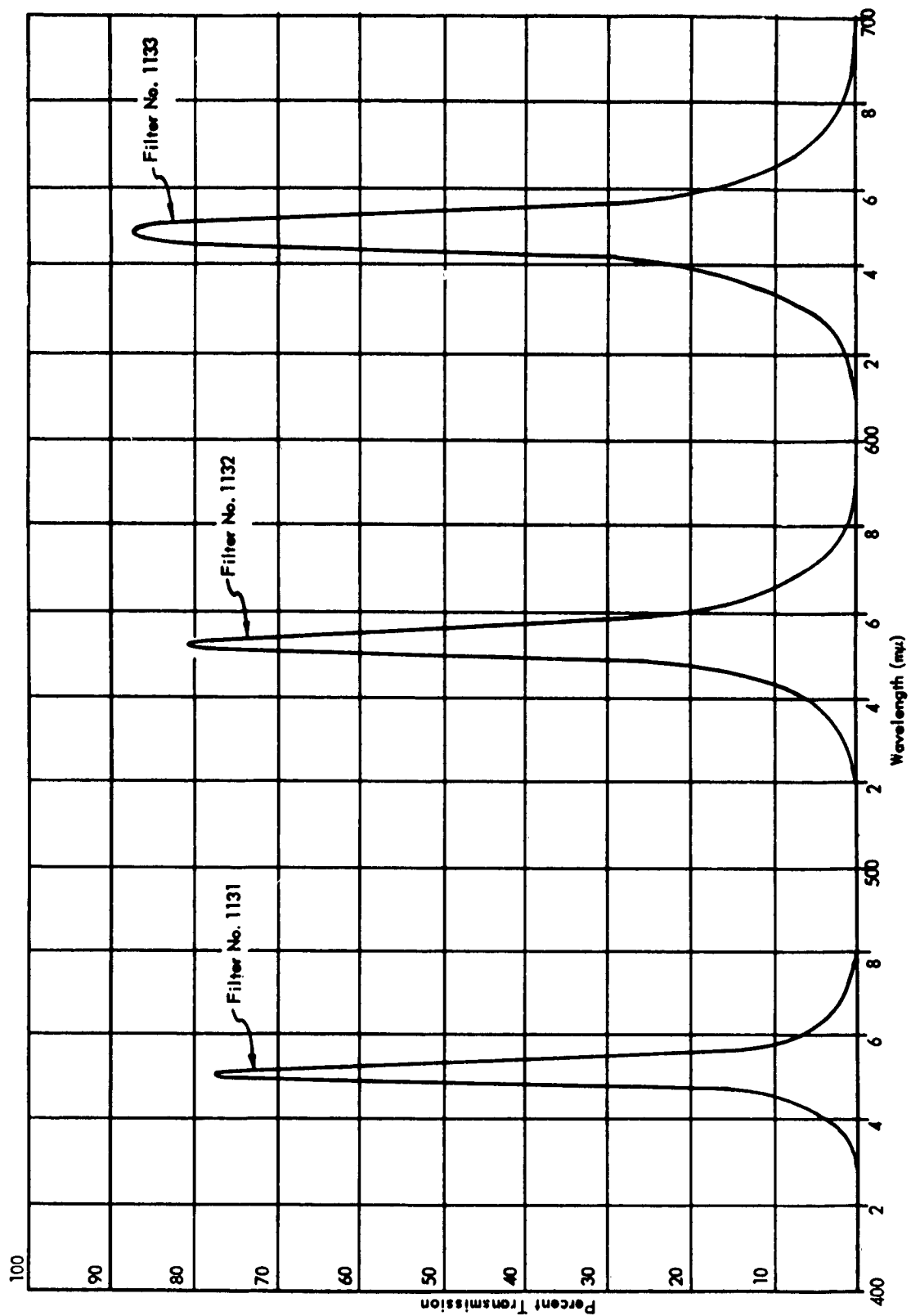
Figure 77. Characteristics of Spectrolab Dichroic Filters.

185

The one major fault noted was the tendency to develop multiple images (ghosts) because of the finite thickness and reflection from the backing glass. The solution to this problem is the use of a thin backing (a pellicle filter) or the use of a dichroic prism.

c. Dichroic Gratings

A dual spectral channel technique for reading and tracking with little, if any, cross-talk is described in Appendix XVII. It is basically very simple. If the tracking information is transparent to read light, the reading channel is not influenced by the presence of tracking information. More important, the tracking channel is not influenced by the presence or absence of stored information if such information is transparent to the tracking illumination. Thus, the result of such a system could lead to an edge locking servo accessing memory with complete freedom in choice of the format by which information is to be stored. An increase in packing density(bits/inch^2) by a factor as large as 4 is possible over previous techniques of edge locking servo accessing through use of this approach.

A major problem in this dual spectrum approach had been the susceptibility to fading that colored photographic dyes experience when exposed to the ultraviolet. A non-fading dichroic filter in the form of a grating would solve this problem. Although an attempt was made to obtain such a grating for evaluation, it was not possible to obtain one during the course of this contract.

186

4. Lenses and Resolution

a. Initial Optical Considerations

Initially it was not known which of a wide variety of optical configurations the photochromic memory might eventually require. A general purpose lens or optical component study was felt to be not too meaningful. Rather, lenses were obtained as the project progressed and evaluated in their particular applications.

In the initial stages, microscope objectives were used for imaging a small spot in order to read written spots on photochromic material, and an optical 8-mm, 3/4 inch f/1.6 projection lens was used for the write-erase operation. No great difficulties were experienced with the latter lens, and, as will be seen later, this lens is actually one of the better lenses of those tested for use with photochromic materials. The read-out of patterns (which were rotated through the imaged spot on PEDAL) by the microscope objectives did offer some difficulties due to flare and scattered light. The explanation for this is apparent when one considers that a spot of light 0.2 mil in diameter in a 100 mil diameter field has an area 250,000 times smaller than that of the field. In this case, uniformly distributed flare and scattered light one-quarter of a million times less intense, on the average, than the spot will contribute just as much light to a photodetector as the spot itself if the phototube views the entire field. Satisfactory read-out was finally obtained by due care in shielding and making liberal use of aperture stops. It was found difficult to create well-defined spots less than the order of 0.2

187

to 0.3 of a mil, but since these were felt to be adequate, no great effort was expended here.

The work with the ultrasonic diffraction grating and spatial filtering required lenses of interferometric quality. Lenses which were not of this quality were immediately sensed by the lack in uniformity of field illumination at the image plane. It was relatively simple to isolate the offending lens in the system by moving or rotating each lens individually and noting corresponding motion in the non-uniformly illuminated field image. Two sets of lenses were obtained which worked quite satisfactorily in these investigations as far as they were pursued, an F/2.5, 7 inch focal length and the Anastigmat F/5.6, 14 inch focal length. In addition to poor quality lenses, dirt, fingerprints, lint, etc. were just as serious in creating problems in the coherent, specularly illuminated systems. With care, however, such problems can be kept within bounds.

A reflecting objective was not found too useful in the experimental program. It was found that in most of the experimental set-ups, the on-axis obstruction, inherent in such a lens, caused difficulties in illuminating the lens properly and allowing checking of the alignment. With the improved equipment available during the latter part of the program, better results could, no doubt, have been obtained. However, because of the previous difficulties with this lens, further testing was put off in favor of further evaluation of some of the promising refracting objectives.

A problem resulting from different focus points for the ultraviolet and visible for most of the lenses was by-passed in the initial studies through use of different optical systems for each of the functions required. With the purchase of an air gauge micro-positioning system, this problem was reduced to one of inconvenience, primarily, since it was only necessary to observe the air gauge dial when changing the settings from visible to ultraviolet imagery, or the reverse. This gauge is accurate to better than 50 microinches when positioning a lens with respect to a plate.

b.   Evaluation of Resolution - General

With the advent of the high resolution, non-capsular photochromic coatings, a new emphasis was put on the optical elements used to print and read such patterns. In all cases investigated, the optical elements themselves appeared to be introducing the limiting resolution. In line with the much tighter tolerances of the higher resolution investigations, improved equipment was built in the form of a highly versatile optical bench with lens holders and auxiliary hardware of much greater rigidity and ease of alignment than is found on ordinary laboratory optical benches.

Though photochromic resolution capabilities appear far out in front of the presently contemplated hardware, the inclusion of the detailed data on high resolution optical systems compatible with photochromic coatings is an important part of the record of this research. This information can help determine the feasibility of photochromic material for advanced systems of the future. For the present program, however, it indicates the degradation (if any) to be expected in data which are optically transferred in bulk and singly in a photochromic memory system.

189

An optical component which caused considerable difficulty in the bulk transfer studies was a defective quartz (probably fused) condenser lens. This lens caused a mottled appearance in the printed patterns which appeared very much like a coating defect. The source of the problem was discovered only after considerable experimentation with the coatings and with the optical hardware. The specularity of the illumination from the mercury arc lamp caused these ordinarily negligible effects to appear.

The condenser defect was found by suitably attenuating the Osram light source through a partially transmitting filter and examining the real image in space through a microscope. When the mottled appearance was noted in the real image in space, it was traced to the condenser by noting the effect as each component in the system was rotated. When the quartz condenser was replaced by a lens of good quality, the mottled appearance of the image cleared up, except for a very slight effect which was in the photochromic coating (P-105). The condenser defect was a common one and appeared in even the best condensers which were available for the laboratory work.

The above account demonstrates the need for good interferometric quality lenses in systems employing specular illumination. Although this requirement was recognized at the outset, the quartz condenser was examined in non-specular illumination which did not reveal the nonuniformity as seen in the transmitted specular illumination.

The projective type of bulk transfer for the loading of the CRT memory described in Systems Studies (Part H of this Section) is limited by both resolution and field considerations of the lens involved. Preliminary system specifications called for a field of 200 x 200 mils, or approximately a 300-mil circular field, with marks on the order of one mil

ASD TR 61-70

across. Laboratory work indicated that a 50-mil square field was achievable with excellent lines of less than 0.25 mil. This led to a 16 fold increase in packing density for a given plate if the 50-mil field is used rather than the larger field of 200-mils.

Figure 78 is an enlargement of a portion of a test chart recorded on a 50-mil field on the photochromic material. To obtain lines per millimeter resolution, the figures must be multiplied by a factor of eight. Although not entirely clear due to the additional losses in the print-out process from the micro-image and the reproduction process used in this report, the lines indicated by 20 ('60 lines/mm) were well resolved over the whole field. These lines are approximately 0.12-mil wide. The lines of the coarsest pattern shown are 0.21-mil in width, a dimension similar to that required to store a 128 x 128 array in a 50-mil field. This work was originally limited to obtaining optimum resolution and field simultaneously by testing various optical arrangements and components and judging the results visually. It was then necessary to obtain more quantitative measurements with respect to the contrast of the high density patterns and to assess the practicality and reliability of the read-out of such densely recorded marks.

c. Evaluation of Resolution - Projection Transfer

In a photochromic memory employing a bulk transfer feature in order to achieve high transfer rates, it will be necessary to externally store the bulk data on a transparent medium. When the preparation and handling of data is considered, the most convenient means for accomplishing such storage appears to be through the use of readily available 35-mm equipment, supplies and techniques. Further discussion of the bulk transfer operation is included in Part H (Systems Studies) of this Section.

The best quantitative technique for the evaluation of the resolution of optical and photographic components is generally accepted to be sine wave response. This subject is covered in many of the papers referenced in Appendix XV. A very lucid and detailed account of optical sine wave

191
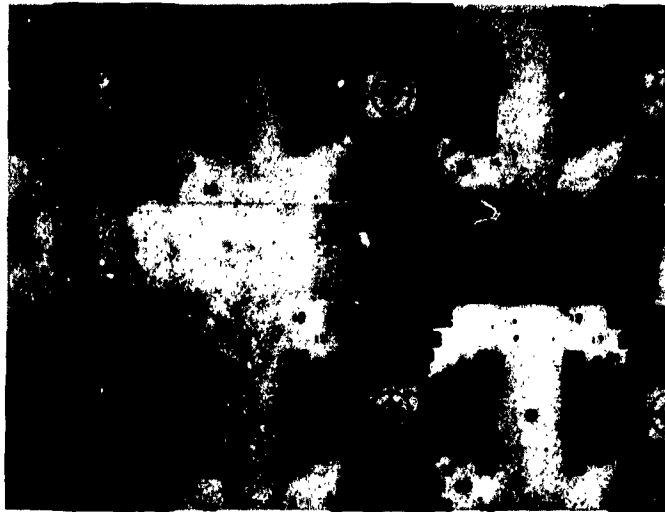
Figure 78.   Preliminary Results - Resolution in 50-Mil Field.

response has appeared in an ASTIA report,[*] which also treats the
case of optical square wave response. Because of the much greater
ease of conducting square wave response measurements, this type
of evaluation was used in the experimental work described below.
Reference will also be made to published sine wave data.

No attempt was made to establish the complete rigor of the methods
used or the conclusions drawn. Rather, with the limited facilities and
manpower available, an   empirical approach using square wave
response was employed. Experimental verification was established,
in general, for predicted results obtained from the square wave response
measurements on individual components or combinations of components.

---

* Wide Angle High Definition Television Systems, Contract X16 onr-
  23605, Radio Corporation of America, ASTIA Document AD-6247.

(1) <u>Kodak Micro-File Film</u>. This film is a high contrast film regularly used in line copy microfilming work. It has the general characteristics that are desirable for storing digital patterns as long as these patterns are not of too small dimensions. This film appeared to be a natural choice for use as the transparency for bulk transfer to a photochromic memory. Figure 79 shows the sine wave response of high quality microfilm.

Since photographic film is ordinarily used with a lens, it is appropriate to also provide a lens curve at this time as well. Figure 80 shows the sine wave response of a perfect lens and the result when an image passes through 6 such lenses. These curves amply illustrate how no system using such components could linearly reproduce an infinite number of generations of an original object, no matter how coarse the detail. However, film inertia (analogous to electronic clipping) and saturation effects can be used for the regeneration of data somewhat analogous to the manner in which digital devices constantly reshape electrical pulses passing through them. This is more or less the manner in which line copy film operates. Because of the non-linear nature of the inertia and saturation effects, it was decided that they should be kept to a minimum if meaningful data were to be generated rapidly. For a number of reasons, practically speaking, no line copy multiple-generation system has yet been achieved which does not degenerate the transferred copy with each generation.

The processing of Micro-File to different gammas (contrast) was investigated with respect to changing the square wave response. Figure 81 illustrates the change in square wave response for a given lens - Micro-file film combination with a change in gamma. Although the high gamma appears desirable for coarser patterns, it is more sensitive to the absolute light levels used and can lead to the clipping or saturation mentioned previously. These effects can produce large changes in the relative sizes of what were originally equal dark and transparent spots. Thus, in the preparation of a digital pattern on Micro-File, high contrast can lead to changes in bit size, a very disturbing feature with most contemplated formats and read-out schemes. The degree to which this will occur is dependent both on projected image quality and the actual bit size within the image.
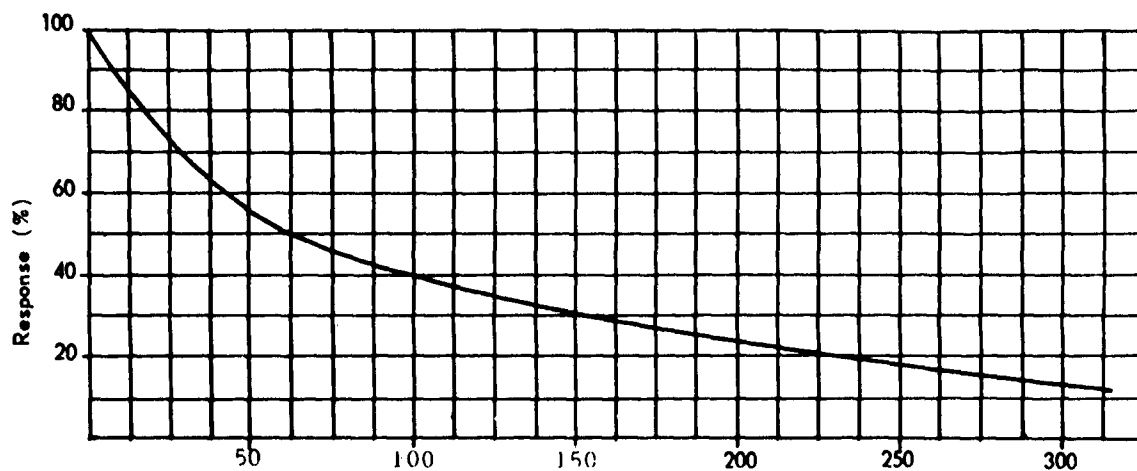
Figure 79. Sine-Wave Response of Microfilm.
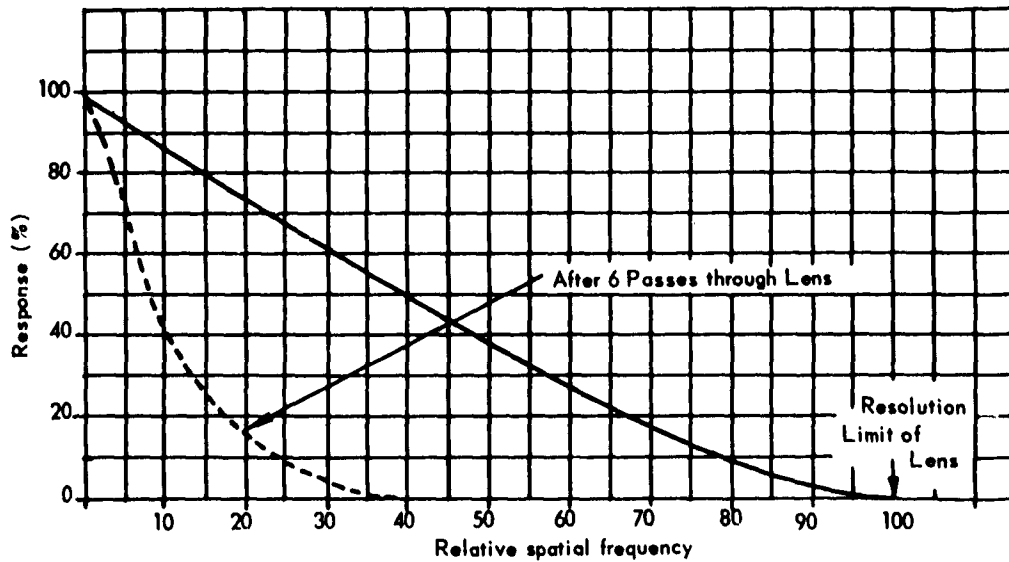
Figure 80. Sine-Wave Response of Perfect Lens.

194

Square Wave Response of Same
Copy Lens and Microfilm For:

(a) High Gamma Processing – 6 to 8

(b) Normal Gamma Processing – 2 to 2.5
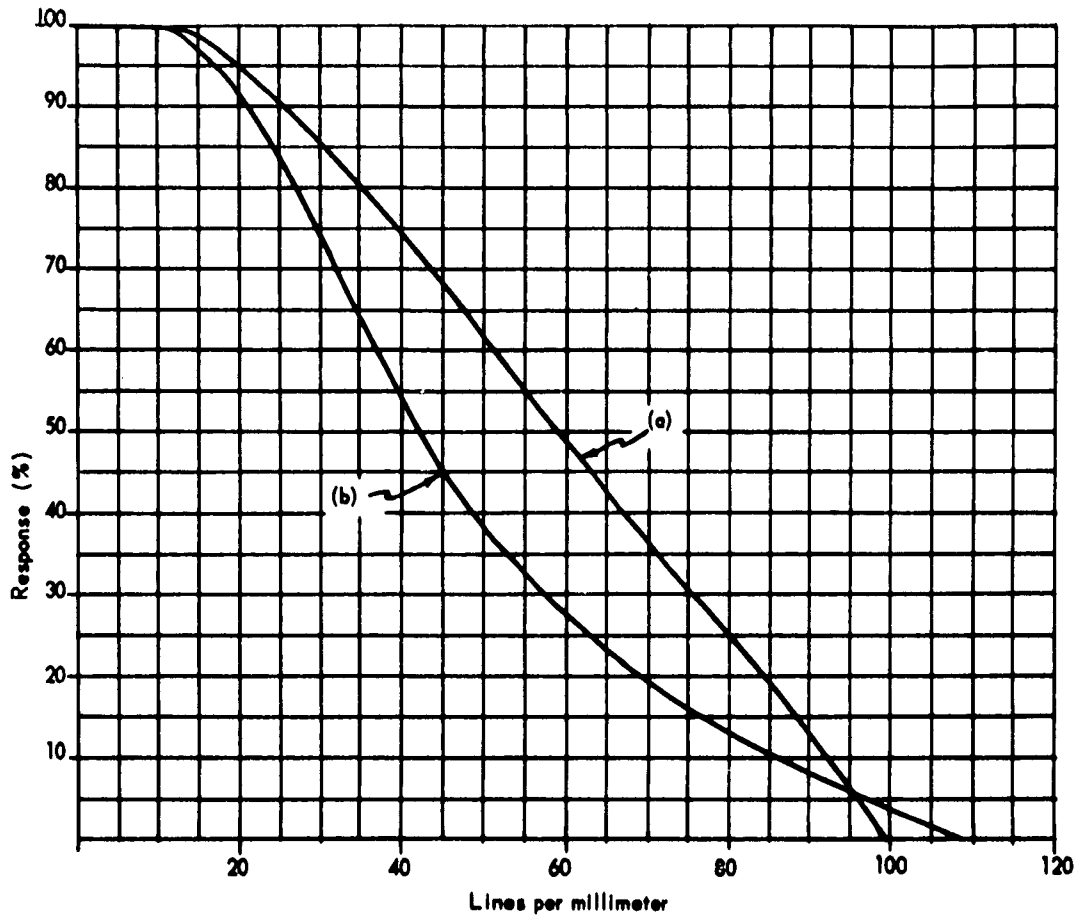
Figure 81. Variation of Square Wave Response with Gamma.

195

In order to relate the sensitivity of exposure and contrast to particular processing techniques which might be employed, D Log E curves were run on Micro-File for different processing methods. Figure 82 presents the results obtained. Such information is not readily available from film manufacturers.

(2) <u>Copy Lenses</u>. The preparation of the master transparencies for bulk transfer could be accomplished in a number of ways. The most promising would use standard 35-mm microfilming equipment which is generally available at most sites. The question then resolved to the point where an evaluation of copy lenses was involved.

A survey of the literature shows that copy lenses of the highest quality will exhibit a uniform and flat field and will be corrected for use at a specific reduction ratio. The combined results of such a lens and Micro-File processed to average gamma is expected to achieve at least 110 lines per millimeter at 15 percent resolution by contrast over the entire field. The claims by some manufacturers of upwards to 150 lines per millimeter probably is for the lens alone and does not include the response of the film. For example, the Kodak Micro-File Ektar, designed as an f/4.5 lens with a fixed mechanical aperture of f/8, is rated to yield 160 lines per millimeter. From the study undertaken, it appears that copy in excess of 100 lines per millimeter, 15 percent resolved by contrast, is not easy to obtain in practice over a 35-mm field. This will then be taken as the figure assumed achievable at an operating site.

(3) <u>Objective Lenses and the Practical Resolution at a Non-Capsular Photo-chromic Coating</u>. In order to evaluate real patterns in miniature on photo-chromic coatings, a 35-mm transparency of the NBS resolution chart was made in which the finest patterns were 85 percent resolved by contrast. This chart is very convenient since it has patterns of varying detail which are long enough in one dimension to allow ready evaluation in the scanning micro densitometer (described in Appendix X). This pattern was a 10:1

196

Figure 82.
Gamma Variation of Microfilm
with Various Processing
Techniques.

LEGEND:

(a) D19 (68°F   5 Mins.)
(b) D19 (68°F   1.5 Mins.)
(c) D19 (68°F   6:1 Diluted 1.5 Mins.)
(d) PS 471 A (45 Secs. 68°F)

ASD TR 61-70
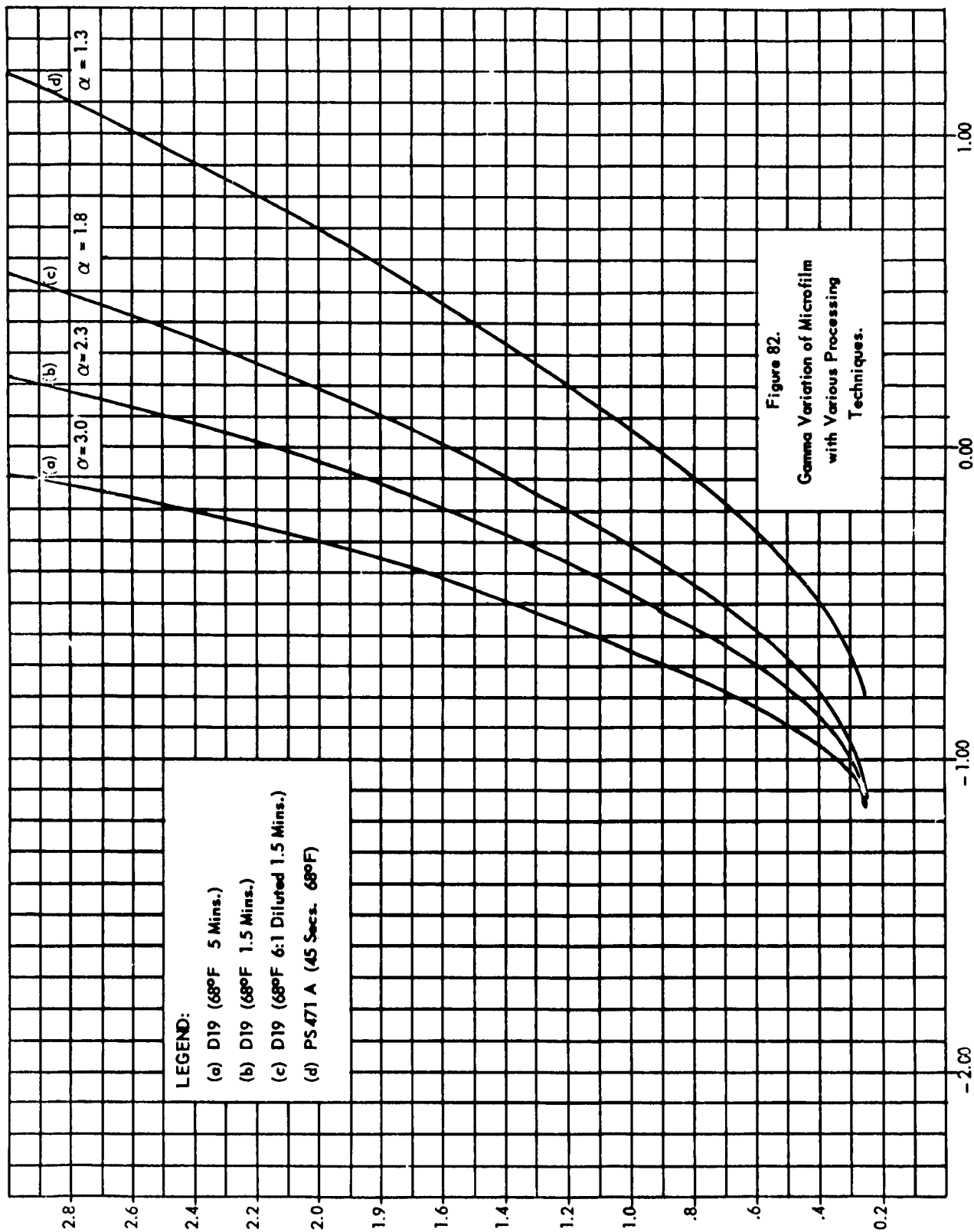
reduction of the original NBS chart. The further reduction of 20:1 was taken on the optical bench to give an overall reduction of 200:1. Thus, the finest lines on the pattern on the photochromic coating were 640 lines per millimeter. Both visual examination under a high powered microscope and microdensitometer scanning were employed. It was assumed that the visual limit of resolution was the point at which the patterns dropped to a 10 percent contrast variation.

As far as could be determined with a number of lenses, the limit of resolution is almost entirely due to the optics. The present discussion, then, is a treatment of a practical system resolution rather than that of the photochromic coating. The useful field was always an important consideration in these studies. Even if an array of only 128 x 128 spots is anticipated, or 128 lines per field (photographic lines), the array would have to be transferred at 5 to 10 times this resolution not to suffer noticeable deterioration during the transfer process. A reasonable goal for the present is then on the order of one thousand lines per field for such an array. In this respect, square wave response is misleading. It is concerned with peak-to-peak contrast change. Edge degradation, which occurs, is not included in an obvious manner.

The shape of the square wave response curve was obtained by photographing back out to microfilm (specially processed for linear transfer, i.e., low gamma) from which the microdensitometer trace was obtained. This procedure was carried out at high power and found to affect image quality only in a relatively negligible manner.

To obtain a flat field with the microscope objectives available, it was found necessary to insert aperture stops within certain of these objectives for best results. Most of the objectives displayed a difference in focus for ultraviolet as compared to visible light. With the availability of an air gauge for focus determination to fractions of a mil, this offered no serious problem.

198

The term optical system is used rather than writing lens or objective since the performance of the objective lens depends upon the method of illuminating the transparency. Optimum performance of a system occurs when the numerical aperture of the illuminating system equals that of the objective lens or lenses when stopped (if necessary) to yield maximum resolution at the center of the field. In practice these conditions are sometimes hard to achieve with limited types and focal length collector lenses available. Another condition which is implied in the description of optimum performance is that the image of the light source formed by the collecting lenses should fill the entrace pupil of the objective lens or lenses.

So far no mention has been made of efficiency, which constitutes achieving the largest possible solid angle between the light source and the collector lens. When testing the lenses to be described, care was taken to try and approach optimum performance at the expense of efficiency. However, there should be no doubt that optimum performance and efficiency will only be obtained with special design of the collector lenses and care in choosing a light source of correct size. It is expected that such a properly designed system is likely to yield superior results to those so far achieved.

It was possible to test a wide variety of lenses for writing on the photochromic coatings and although only two types were evaluated in detail, it is of interest to describe how other types performed. Since a reduction step of some 20 to 25:1 is involved, a lens having optical characteristics similar to a 10x microscope objective was a good starting point from which to conduct tests.

Several 10x achromats of good quality were tried, all having focal lengths of about 15mm and numerical aperatures of 0.25. Tests showed that these objectives were not chromatically corrected over a sufficiently broad spectrum of light to permit good quality images to be formed in the band required (300 to 400 mμ). This was especially noticeable when no filter was used to restrict the visible light and resulted in a prolonged depth of "confused" focus. If a filter was used it was then possible to establish a focus in the 300 to 400 mμ band, but the image quality was inferior to the same image focussed

199

and created in the visible band. None of the objectives were found satisfactory for high resolution recording with photochromic coatings. Next, 10x apochromatic objectives were tried. These yielded far superior results to the achromats, indicating that the chromatic correction's designed in this type of lens must extend into or near the 300 to 400 mμ band. Regular 10x apochromatic microscope objectives when used for reduction without an eye piece produced excellent results at the center of the field but fell off very sharply at the extremities. The use of a compensated eye piece improved this but still gave a very small useable field. Bausch and Lomb suggest the design of a specially corrected eye-piece, although they call it a field correcting lens, to enable a flat field to be obtained.with their regular 10x apochromatic objective. Removal of the visible spectrum by a filter had very little effect upon the focus with apochromatic objectives but a slight improvement in acuity was obtained.

Having observed the results obtained with regular achromats and apochromats, the essential details were forwarded to several optical companies together with a request that they provide use with the optical system that would meet our resolution and field requirements from off the shelf items. Only one company - Carl Zeiss of Germany was able to immediately provide some optics for testing and it is these that were used for measurements and evaluation of resolution. The optical system sent was comprised of a 10x planapochromatic objective of numerical aperature 0:32 and a matching 8x complan eye piece to be used in a tube of length 160 millimeters. This system was tested and produced micro patterns of excellent quality, the resolution observed at the photochromic coating was about 650 lines per millimeter, 10 percent resolved by contrast. The field was extremely flat over the area used which was 50-mils in diameter. This was the largest field that could be illuminated with the collector lenses available. However, the field potentialities of this lens combination will allow a field diameter of 80 mils in diameter when properly illuminated. So far it is not known whether or not the field remains entirely flat over 80-mils diameter but judging by the 50-mil field observed, very little fall-off is expected. In addition to the high resolving power this lens also exhibited good acuity or sharpness yielding the best images formed to date.

200

Carl Zeiss also provided another lens which was also tested and was called a Luminar. It was designed to form a slightly enlarged, spherically and chromatically corrected image of small objects in a useful distance. The focal length is 16-mm and it is fitted with an iris diaphram and has a speed of f/2.5, wide open. When tested this lens performed quite well but only. when a filter removed the visible light. It produced a very flat field over an area 0.1 inch in diameter and produced a resolution of 450 lines/mm over the field at the photochromic coating. Again, collector lens availability and a fixed size light source made illumination difficult for optimum resolution. It is expected that some improvements will be achieved with the lens. It does not require an eye piece as does the apochomatic objective. Results obtained with the Luminar very closely resembles those obtained with the Simpson f/1.6 projector lens used for earlier writing tests.

Apart from resolution and field capabilities, one other important measurement concerning lens performance must be noted, that of depth of focus. The lens ultimately selected for the writing in any system will represent a compromise of the three factors:

(a) resolution

(b) field coverage

(c) depth of focus

For the photochromic memory application, the first two qualities may be combined so that objectives can be more easily compared in merit by the term "lines per field." The depth of focus which is certainly somewhat governed by the resolution can vary depending upon lens design, but in general the higher the resolution the smaller the depth of focus. To date, the depth of focus has been measured as the distance that the lens may be varied from the photochromic coating without noticeable departure from maximum obtainable resolution for the objective in question. In certain cases it would be desirable to know how the resolution varies as lens-to-photochromic-distance tolerance is increased to either side of the true focus point.

ASD TR 61-70

Table XIII lists the observed performances of the objectives tested that showed the greatest promise. These results indicates that the Zeiss

TABLE XIII

OBJECTIVE TEST RESULTS

Writing Lens System	Maximum Resolution at 10 Percent Point	Field Diameter	Lines Per Field	Depth of Focus
Zeiss 10 Planapo- chromat and 8 x K ph Eye piece	700	50	890	± 0. 00005 inch
Zeiss Luminar f=16mm at optimum stop	450	100	1144	± 0. 0002 inch
Simpson f 1. 6/projec- tor lens, stopped at optimum	450	80	910	± 0. 0005 inch
Projected capability of Zeiss 10x Planapo- chromat & 8 x K pl Eye piece with improved illuminating system	700 (up ?)	80	1420 (up ?)	± 0. 00005 inch (down ↓ ?)

Planapochromat will probably eventually out-perform all other lenses so far tested but the depth of focus to achieve this performance may place too heavy a burden upon the mechanical tolerances of some system designs.

The Zeiss planapochromat combination showed an interesting feature in as much as the micro-image itself at the photochromic coating exhibited quite

severe barrel distortion. When the distorted image was recovered with the same optical system, the distortion was equally and oppositely cancelled out yielding a perfectly normal and undistorted read-out. The effect was interesting because the resolution and acuity of the micro-image was not visibly affected by this distortion.

The resolving powers of these optical systems in conjunction with the photochromic coating were derived and plotted in lines per millimeter resolved by contrast and are shown in Figures 83 and 84 for the Zeiss planapochromat and 8x eye piece and Zeiss luminar and Simpson projection lenses, respectively. These curves were derived from a micro-densitometer trace of a recovered N.B.S. resolution chart. The fall off in frequency due to the response of the microfilm at both input and output was removed. The curves may be used to assess the performance of either optical system by combination with the response of the input microfilm and/or cathode-ray tube to give an over-all resolution performance figure.

From Table XIII it can be seen that all the lenses are in the general area of 1000 lines per field except the last one, which is much better. It can be eliminated by the critical focus problem and price. The Simpson f/1.6 lens, inexpensive and with the greatest tolerance, is the lens selected for the systems design. The packing of 128 lines into an 80 mil field leads to 1.6 lines per mil or 64 lines per millimeter. This can be seen to be well resolved on Figure 84 and should lead to a fairly steep relative gradient for edges of recorded data of the selected dimensions.

d.   Contact Bulk Micro-Transfer of High Resolution Digital Patterns

The ability to apply the contact printing procedure to affect a transfer of a group of photochromic micro-patterns directly to high resolution photographic emulsion promises to be a powerful tool. Experiments have shown that this is a reliable method of transfer and measurements have yielded a transfer factor which may be used to evaluate the use of such a method. A great deal of patience and considerable number

203
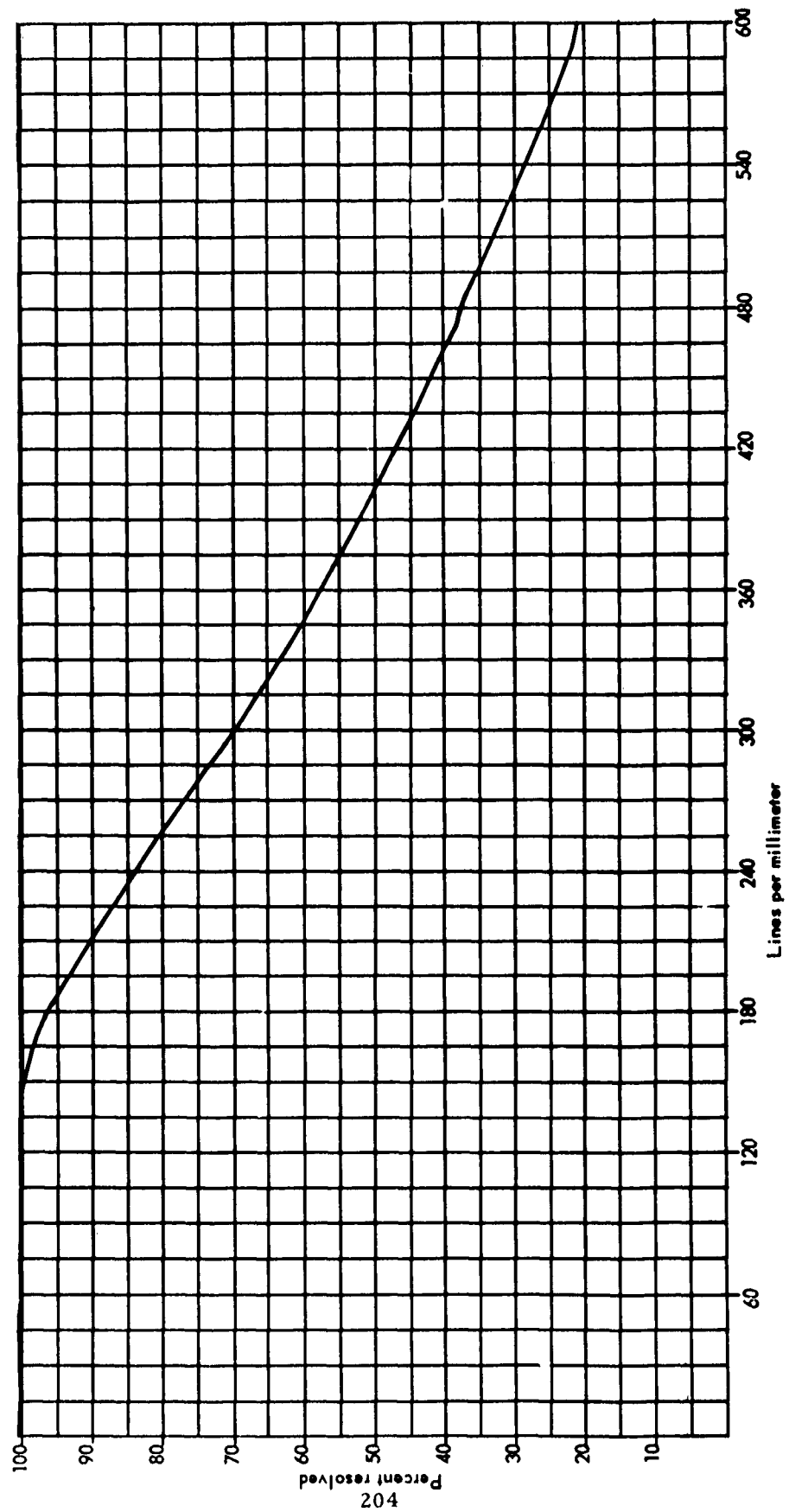
Figure 83. Performance of Zeiss Planapochromat Optics and a Photochromic Coating.

ASD TR 61-70
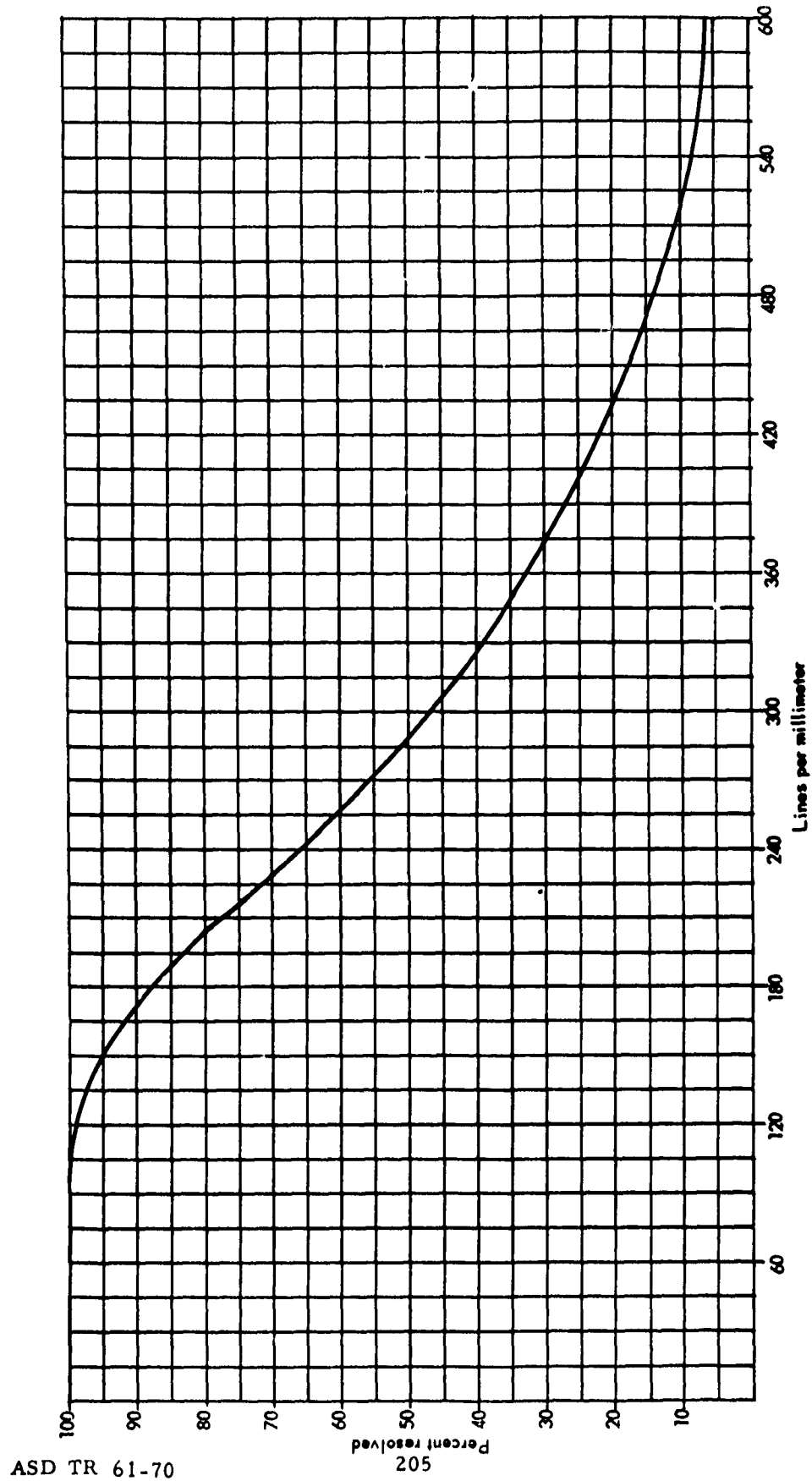
Figure 84. Performance of Luminar and Simpson Optics with a Photochromic Coating.

ASD TR 61-70

205

of experiments finally yielded the best method of contact printing. Some of the problems encountered and their solutions will be discussed before presenting the results.

Initial experiments were conducted with Kodak High Resolution Plates which are coated with a 649 GH emulsion. The photochromic plate and the photographic plate were pressed firmly together and various methods of illumination tried. The results were frustrating since sometimes they were excellent and other times poor. Observations showed that even though the plates were firmly held under pressure a good contact was not always insured. This problem was overcome by substituting film for plates and pressing the photochromic plate against the film which was backed by a fairly stiff felt pad on a flat steel table which was mounted on springs (see Figure 85). Repeated tests under such conditions showed that reliable and good contact between the film and the photochromic plate was being effected. Next the method of illumination was varied from diffuse to very specular . Results showed that the more specular the illumination the better the transfer factor up to a certain point. Making the illumination more specular after this point had been reached caused interference fringes to "confuse" fine detail. Still further increase in the specularity of illumination caused additional fringing patterns from dirt or blemishes present within any portion of the photochromic glass plate to be transferred to the photographic emulsion.

Another problem, which is not related specifically to contact printing, that of matching the characteristic D log E curve of the high resolution emulsion to suit the contrast range present in the photochromic pattern, was also attacked. The D log E characteristic of photochromic materials can generally be described as low gamma with a contrast range from 1.0 to 1.7. The effective gamma at peak contrast may be varied downward by viewing the image under different spectrums of illumination since the image is colored. The maximum gamma and contrast occur when illuminated with green light, and under these conditions produce a gamma of one or slightly less. Examination of the D log E characteristics of 649 GH emulsion

206
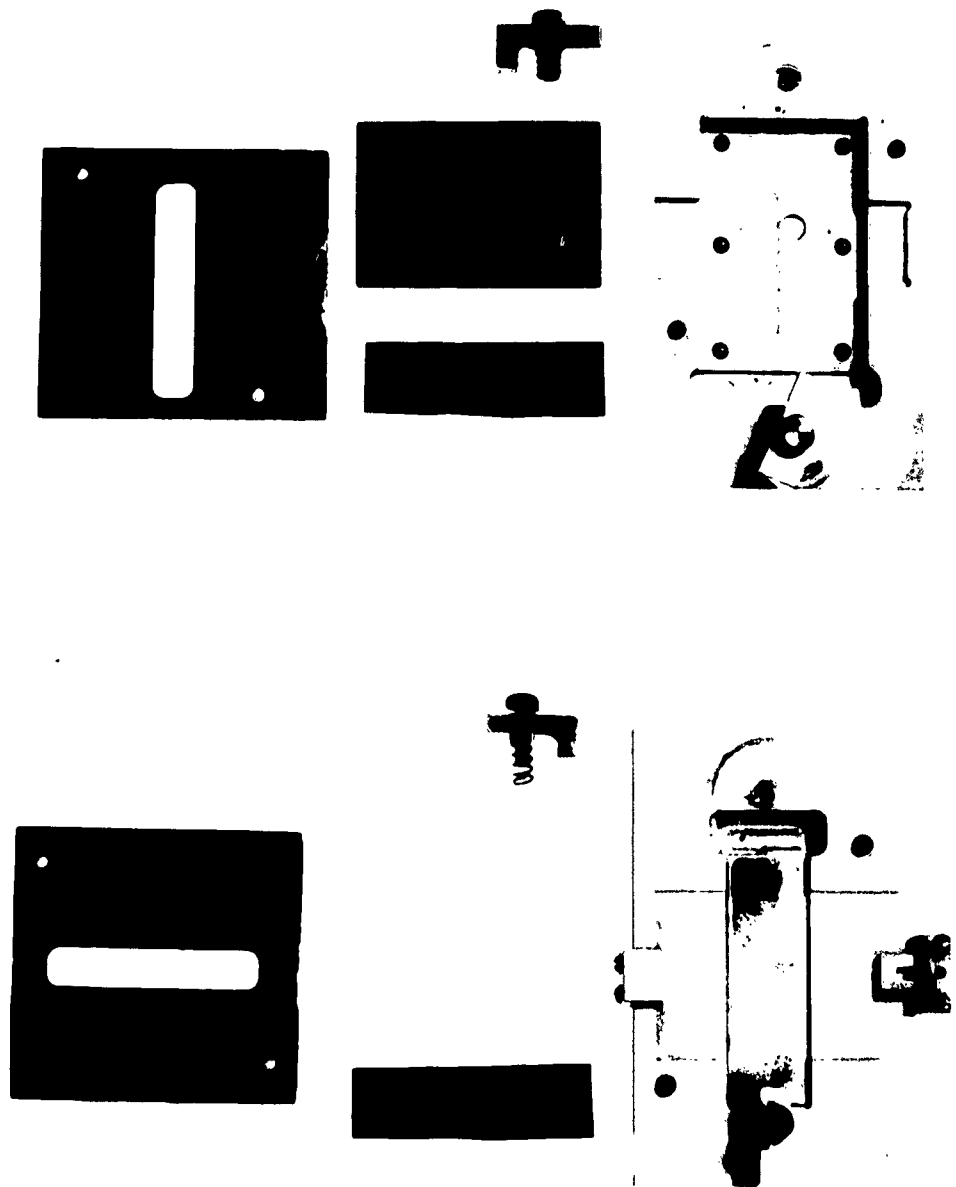
Figure 85. Contact Printers Used for
Contact Printing Studies.

ASD TR 61-70

when developed in D19 for five minutes at 68°F show that a gamma of six to eight is effected. This is certainly too high except for the transfer or unusual images where a high clipping level is desired. Communication with Kodak in Rochester revealed the existence of:

1) A special high definition low gamma film designated SO-105 (special order only)

2) A special developing kit designated PS471A for use with the above film

Arrangements were made with Eastman Kodak of Rochester, N. Y., to supply a sample of this film and developer for evaluation. The developer turned out to be the solution to the problem, with which 649 GH emulsion was processed satisfactorily with a gamma of 1 to 1.3. The special order SO105 film was also tried and it too yielded good results, but exhibited slightly larger grain size than 649 GH. It was also about an order of magnitude faster. This special film does not have any advantage for the photomemory application since there is no restriction from speed considerations. Another set of D log E curves was also obtained for medium gamma processing of 649 GH emulsion by development in a solution of D19 diluted 6:1 and yielded D log E curves for the various times with gammas ranging from two to three.

Depending upon the contrast of the information carried in the micro-image, it is now possible to process the film to give an enhanced degree of contrast. This, together with the previously determined optimum illumination and contact requirements, allows methods of measuring the transfer factor to be described.

The transfer factor sought is the ratio of the resolution measured in lines/mm resolved in the transferred photographic micro-pattern to those resolved in the original photochromic micro-pattern. The 10 percent point on the resolution curve was judged by eye under the microscope for both photochromic and photographic mirco-patterns. Figure 86 shows a graph of the results,

ASD TR 61-70
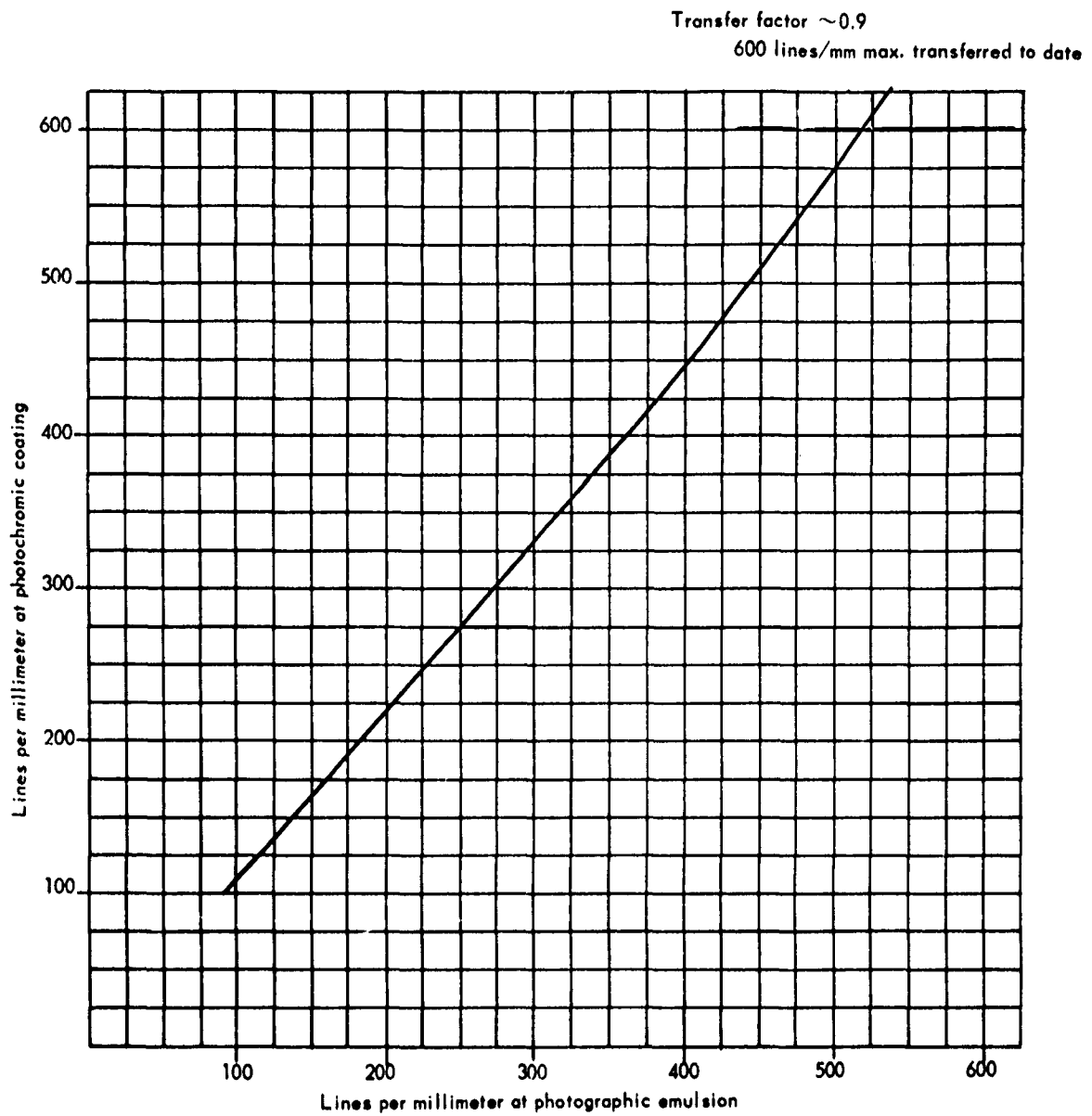
Figure 86. Photochromic-Photographic Contact Print Transfer Factor.

209

the vertical ordinate in lines/mm at the photochromic micro-pattern and the horizontal axis resolution transferred to the photographic micro-pattern, 600 lines/mm representing the highest resolution so far consistantly obtained with available optics at the photochromic micro-pattern. It is hoped that this curve may be extended on up to 800 lines/mm in due course when it is expected that the transfer factor will gradually get smaller and smaller.

Another experiment in direct transfer involved reversing the procedure, i.e., transferring by contact a photographic micro-pattern back to a photochromic coating. All the same problems were encountered as described for the forward process, and the transfer function was essentially the same in either direction. Micro-patterns containing a range of gray scales are the hardest to control, as the range of gray scales transferred becomes less and less with each successive transfer if the product of the two gammas is more than one. To illustrate the severity of this, Table XIV tabulates the transferred resolution for six forward and backward steps and in addition shows the number of gray scale steps observed at each phase of the step. Both 10 percent and 30 percent resolution by contrast transfer observation are listed. Some idea can now be obtained for how the image quality degrades from one generation to another. At this time it was felt that there would be little use for image quality obtained after a third generation photographic transfer had been reached. This will, however, depend upon the initial quality of the virgin photochromic micro-pattern and the final resolution required. The digital patterns will very somewhat from the norm in contrast; the test described indicates the maximum variation allowable for a given number of transfers without the use of high contrast clipping.

210

TABLE XIV

TRANSFER RESOLUTION DATA

Step No.	Generation Description	Partially Resolved, 10%	Fully Resolved, 30%	Grey Scales Carried
1	Virgin photochromic image	420	352	6.5
2	1st generation photographic image	391	328	5.8
3	2nd generation photochromic image	364	306	5.1
4	2nd generation photographic image	339	285	4.4
5	3rd generation photochromic image	316	266	3.7
6	3rd generation photographic image	294	248	3.0

G. SPECIAL ACCESSING STUDIES

1. Introduction

In order to be cognizant in the area of accessing, the photochromic memory program had anticipated a rotating disk-CRT memory. The initial accessing studies were primarily concerned with the development of digital control equipment for achieving track location simply for the feasibility model. It was assumed this model would use a servoed CRT spot, at least in the read mode of operation, if not in write or erase.

In line with the above reasoning, the digital equipment was designed around a modified commercial servoed CRT spot device, the Option Displacement

ASD TR61-70

Follower (described in Appendix X). This then required a minimum CRT design effort in the initial stages of the program before the CRT capabilities and optimum operating modes were well defined.

On completion of the design, construction, debugging and initial testing of the CRT track seeking equipment, it was felt that the accessing studies should be de-emphasized until further information was available on a final memory configuration. This decision was also in line with the reduced manpower assignments during the latter portion of the contract.

The investigation of "colored track" accessing is described under "Dichroic Gratings" in part F of this Section; accessing studies carried out with respect to the final systems selected for investigation can be found in part H.

2. Technical Description of Equipment Constructed

A test unit that allowed a single multiplier phototube (MPT) to be used in multiplex for track accessing and edge-locking servoing was designed, constructed and tested. Figures 87 and 88 are simplified block diagrams of the equipment constructed. Figure 89 is a photograph of the equipment and power supplied on a relay rack. As this was experimental research hardware, no great effort was made to minimize the power supply requirements. The lower six units in Figure 89 are power supplied. The plug-board layout, for ready changes in operation, is shown in Figure 90. Figures 91 through 100 give the circuitry and other details and are self-explanatory. The plug-ins are identified in Table XV.

Figure 101 is a more detailed diagram which includes the logical inter-connections between the basic blocks within the accessing unit.

The track-seek and servo unit operates by controlling both the MPT output signal and the servoed CRT input (control) signal. In the track-holding state, the MPT feeds directly into the servoed CRT unit. In the track-accessing state, the MPT provides a series of pulses corresponding to track crossings while the control unit provides a ramp function to the

212
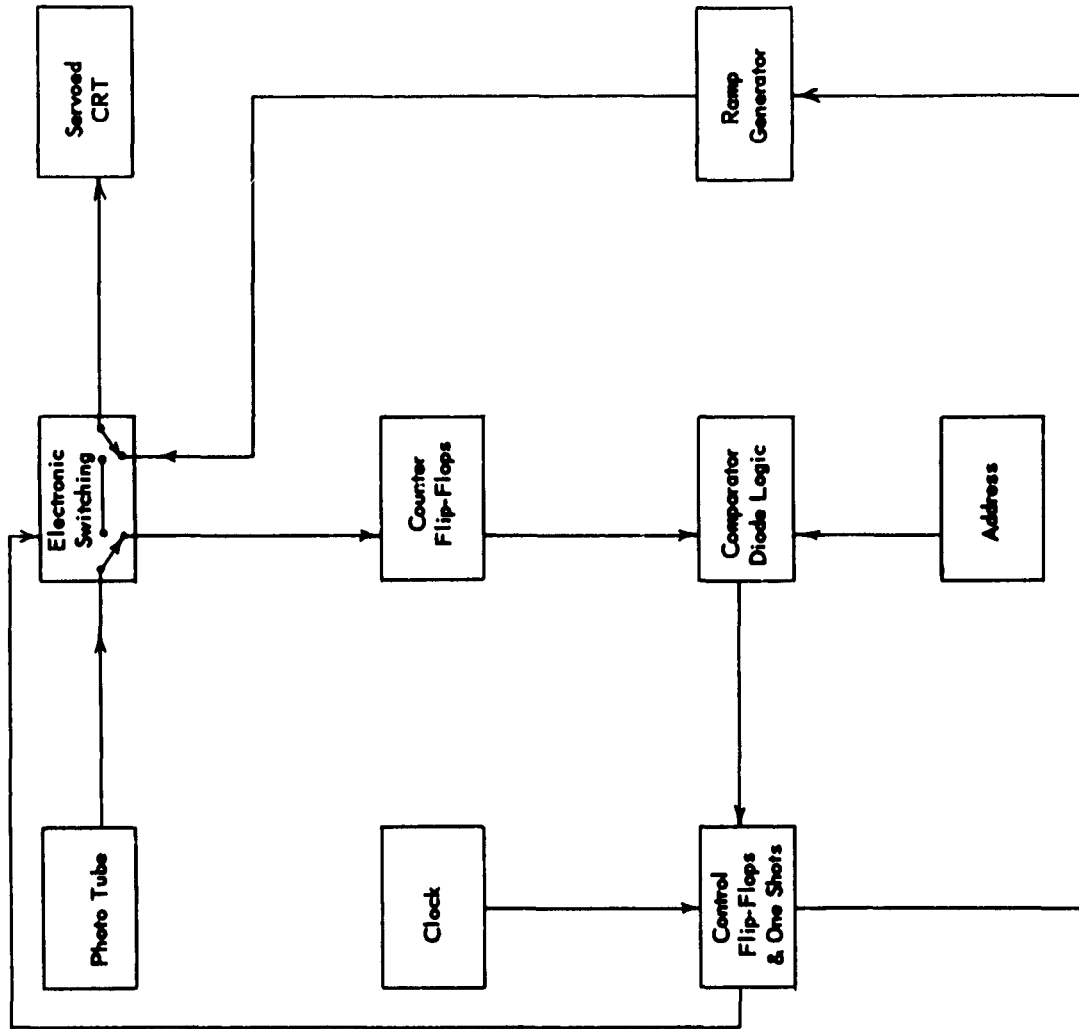
Figure 87. Photo-Tube Multiplexing CRT Servo and Track Location Simplified Block Diagram.

213

$f_1 = (M_2 + M_3) F_1$

$\phi f_1 = P_3 F_1 K_3'$

$f_2 = F_1 F_2' C_1$

$\phi f_2 = P_3 F_2$

$f_3 = F_1 F_2 F_3' C_1$

$\phi f_3 = F_1 F_2 F_3 C_1 + B_2$

$f_4 = F_1 F_2 F_3 F_4' C_1$

$\phi f_4 = F_1 F_2 F_3 F_4' C_1 + B_2$

$f_5 = F_1 F_2 F_3 F_4 F_5' C_1$

$\phi f_5 = B_2 F_5$

$f_6 = F_5 F_6' C_1$

$\phi f_6 = B_2 F_6$

$q_1 = P_4 Q_1'$

$\phi q_1 = P_4 Q_1$

$q_2 = P_4 Q_1 Q_2'$

$\phi q_2 = P_4 Q_1 Q_2$

$q_3 = P_4 Q_1 Q_2 Q_3'$

$\phi q_3 = P_4 Q_1 Q_2 Q_3$

$q_4 = P_4 Q_1 Q_2 Q_3 Q_4'$

$\phi q_4 = P_4 Q_1 Q_2 Q_3 Q_4$

$P_3 = (D_1 Q_1 + D_1' Q_1')(D_2 Q_2 + D_2' Q_2')$
$\quad\quad (D_3 Q_3 + D_3' Q_3')(D_4 Q_4 + D_4' Q_4')$

$k_1 = P_3 K_1'$

$\phi k_1 = Q_1 Q_2 Q_3 Q_4 K_1 C_1$

$k_2 = M_2 K_2'$

$\phi k_2 = M_3 K_2$

$P_4 = \left[(K_1 + \overline{F_2})(K_1' + \overline{C_1})(K_4' + \overline{C_1})\right]' M_1 P_3$

$P_2 = F_1 F_2 F_4' F_5' C_1$

$0 = (K_2 + F_5' + R)(K_2 + P_1 + F_1)$

$k_3 = M_2 K_3'$

$\phi k_3 = B_2 K_3$

$k_4 = M_2 K_4'$

$\phi k_4 = B_2 K_3' K_4$

$b_2 = P_3$

Figure 88 Photo-Tube Multiplexing CRT Servo and Track
Location Block Diagram.
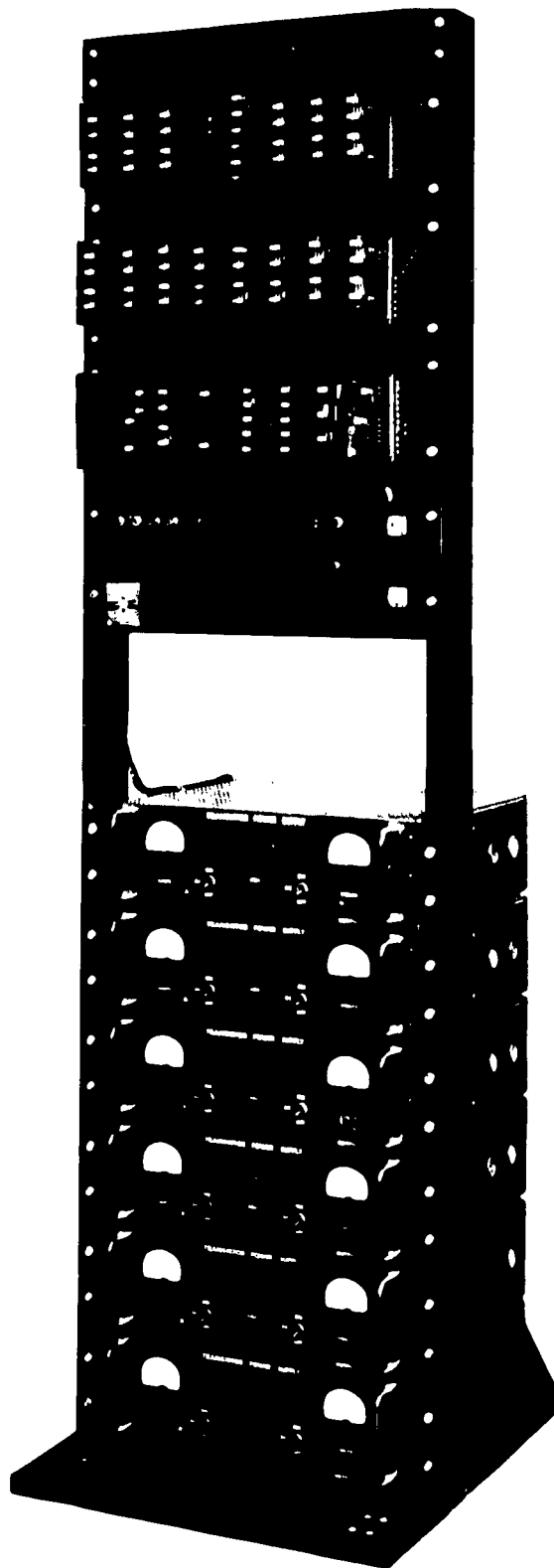
Figure 89. Track-Seek and Servo Control
Circuitry (with Power Supplies).

215

K₂ ▭   Q₄ ▭   P₃ ▭

K₃ ▭   Q₃ ▭   R ▭

K₄ ▭   Q₂ ▭   DRVR C₁ ▭

M₁ ▭   Q₁ ▭   B₂ ▭

P₄ ▭   F₃ ▭   M₃ ▭

K₁ ▭   F₄ ▭   M₂ ▭

F₂ ▭   F₅ ▭   C₀ ▭

F₁ ▭   F₆ ▭   O ▭
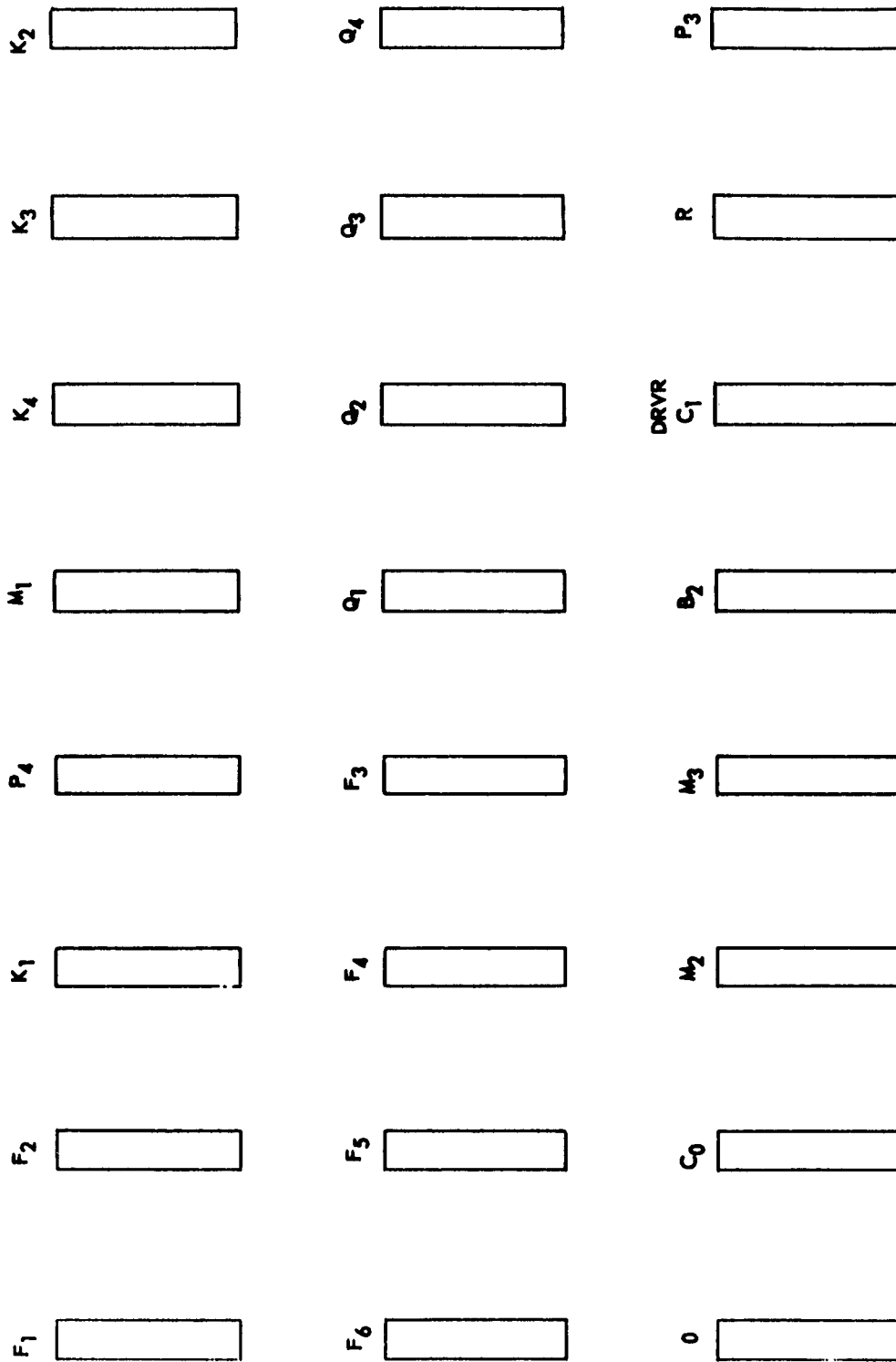
Figure 90. Layout (Rear) View of Panels in Figure 89.

216
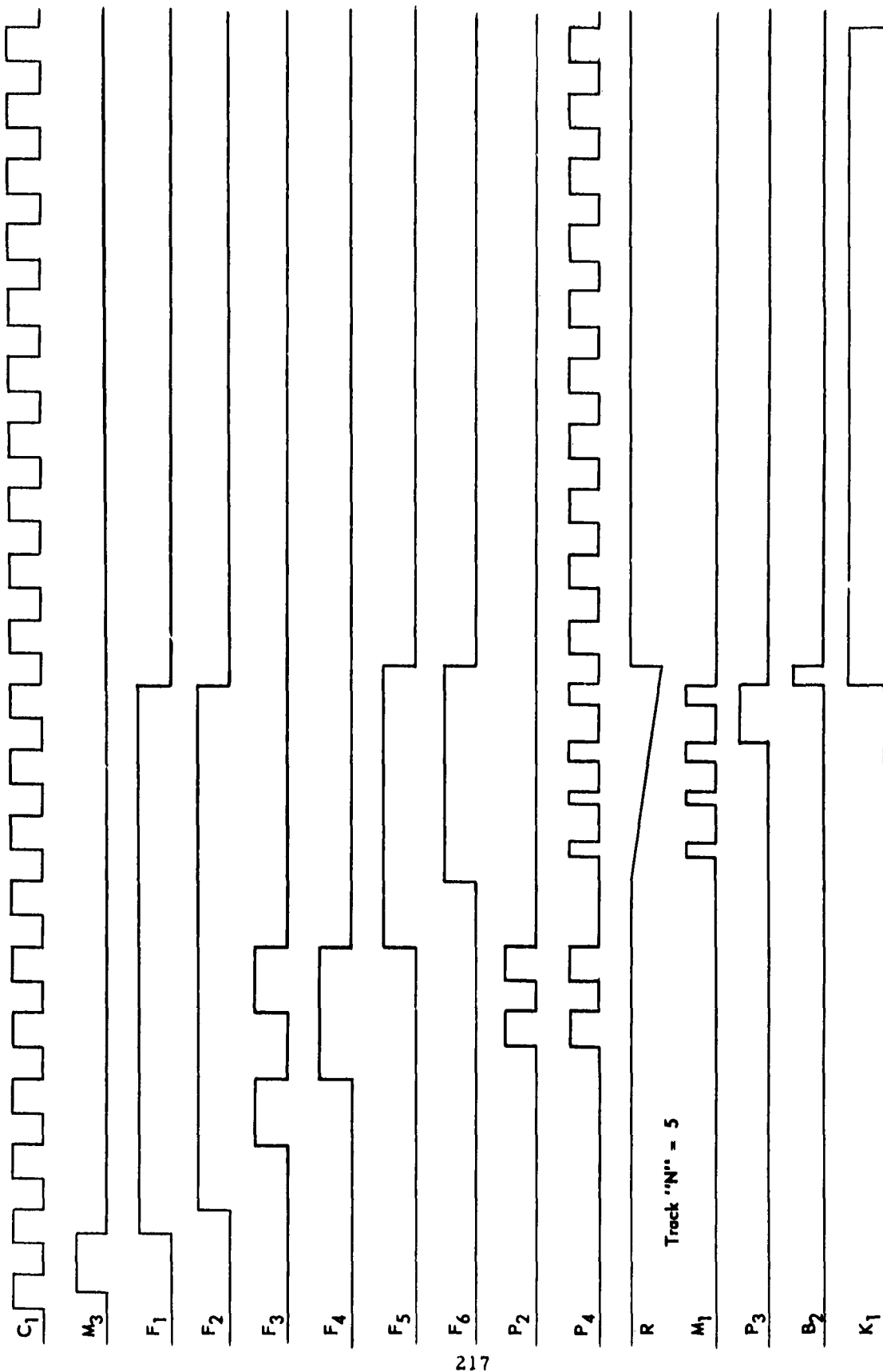
Figure 91 Control Circuitry Waveforms for Track-Seek and Servo Unit.

Track "N" = 5

C₁ M₃ F₁ F₂ F₃ F₄ F₅ F₆ P₂ P₄ R M₁ P₃ B₂ K₁

217

ASD TR 61-70
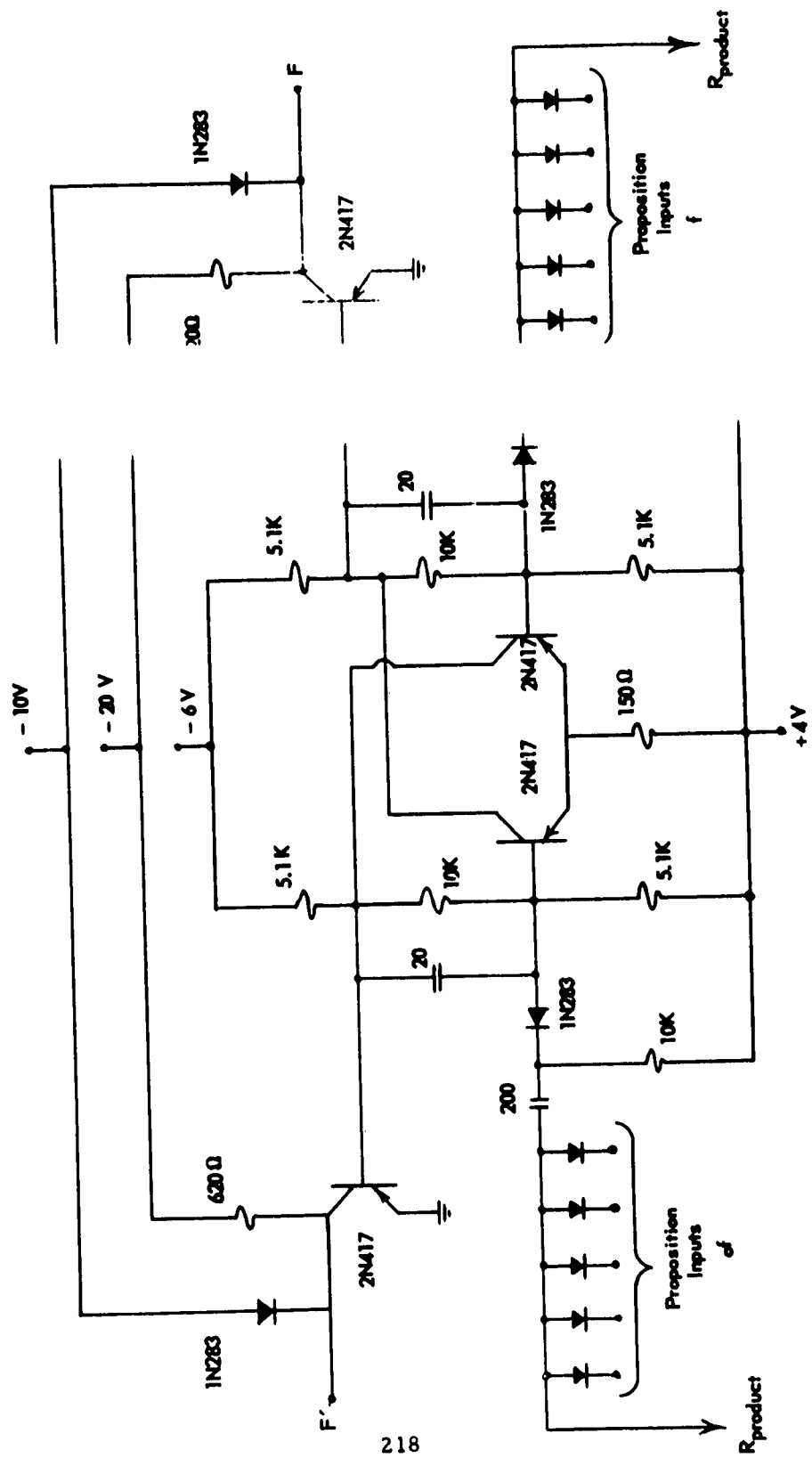
Figure 92. Basic 100 KC Flip-Flop.

218

The circuit is activated by a negative step.
Output is a positive pulse, 5 μsec duration.

Figure 93. One-Shot.

219

ASD TR 60-71
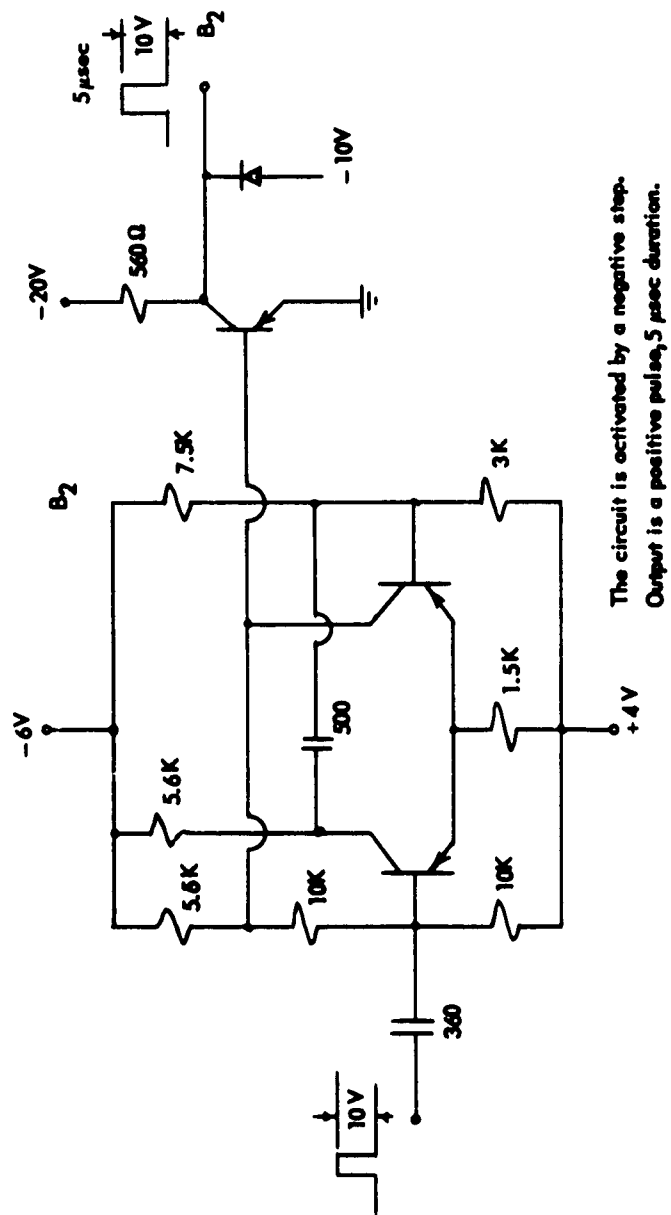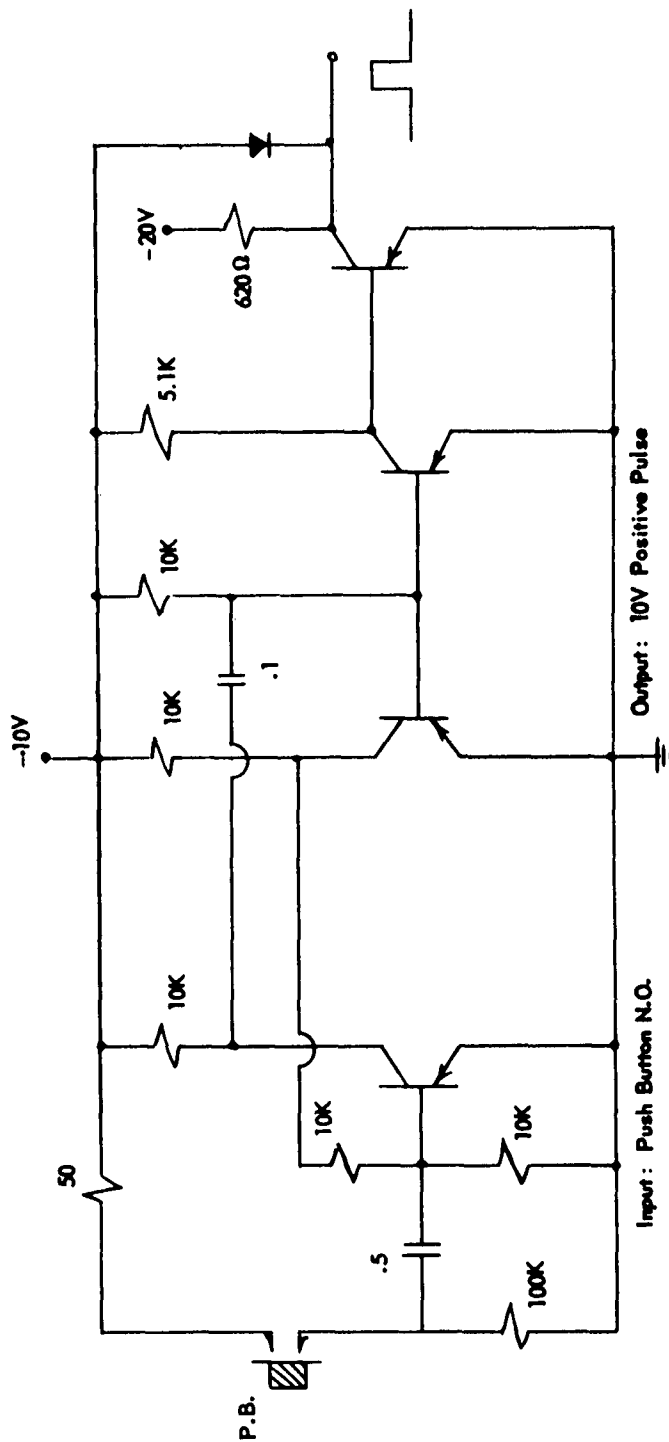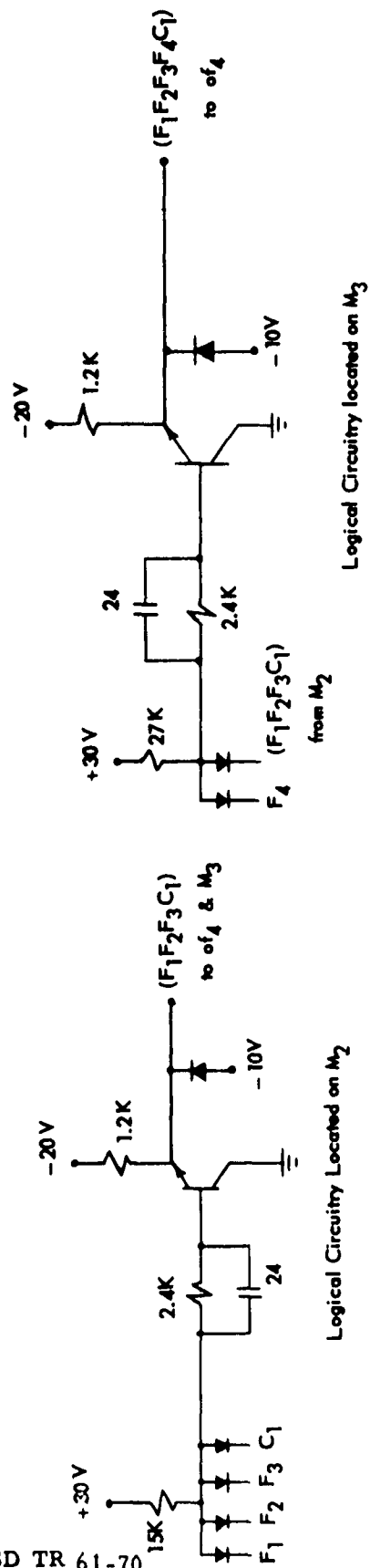
Figure 94. Push-Button One-Shot.

Logical Circuitry located on M_3

Logical Circuitry Located on M_2

$(F_1F_2F_3F_4C_1)$ to of$_4$

$(F_1F_2F_3C_1)$ from M_2

$(F_1F_2F_3C_1)$ to of$_4$ & M_3

Input: Push Button N.O.

Output: 10V Positive Pulse

Comparator $P_3 = (D_1Q_1 + D_1'Q_1')(D_2Q_2 + D_2'Q_2')(D_3Q_3 + D_3'Q_3')(D_4Q_4 + D_4'Q_4')$

Output is a 10V Positive Pulse

Figure 95. Comparator.

221

Figure 96. Logic Board "P_4".

$$P_4 = \left[(K_1' + \bar{C}_1)(K_1 + \bar{P}_2)(K_4' + \bar{C}_1) \right]' + F_5 M_1$$

ASD TR 61-70
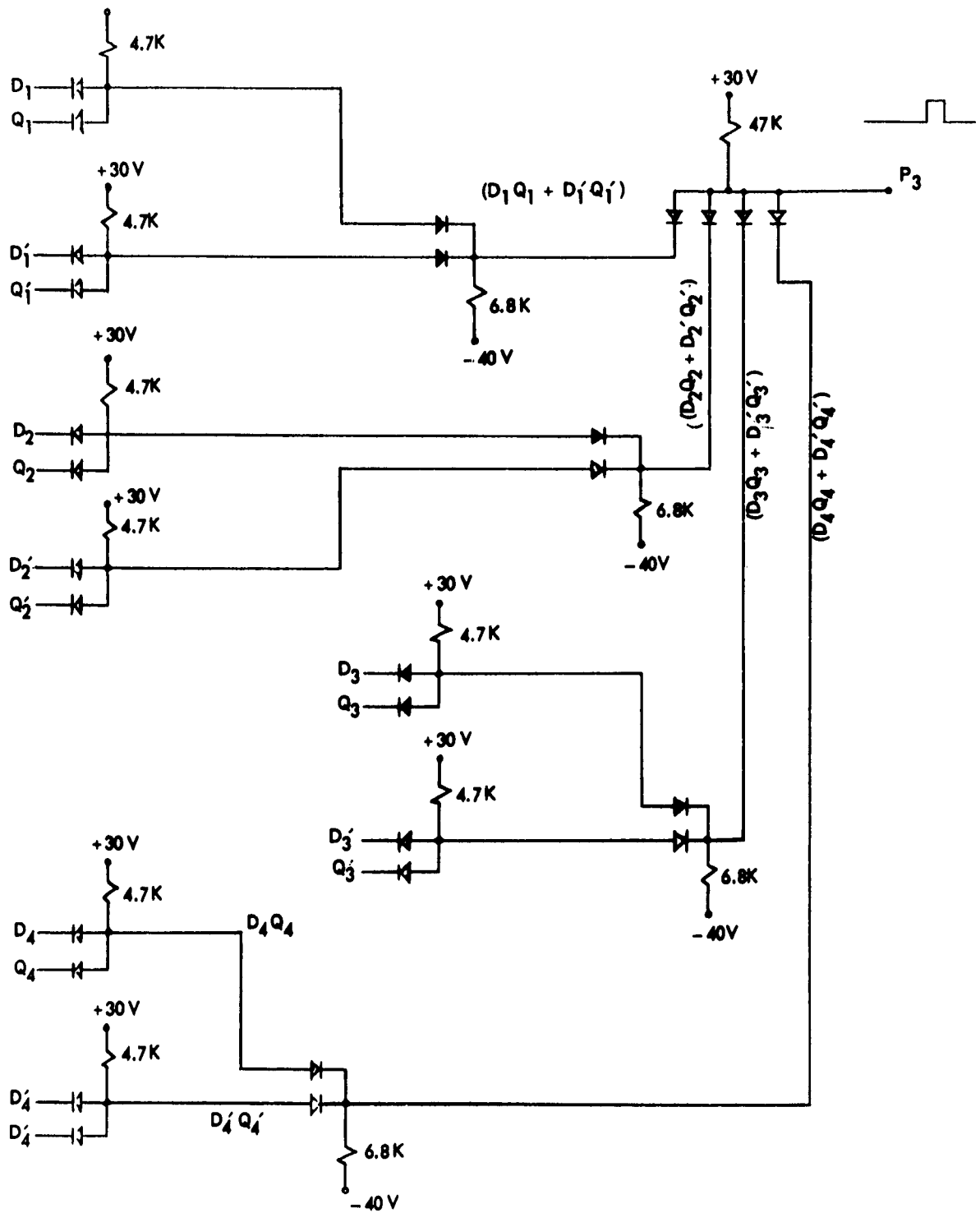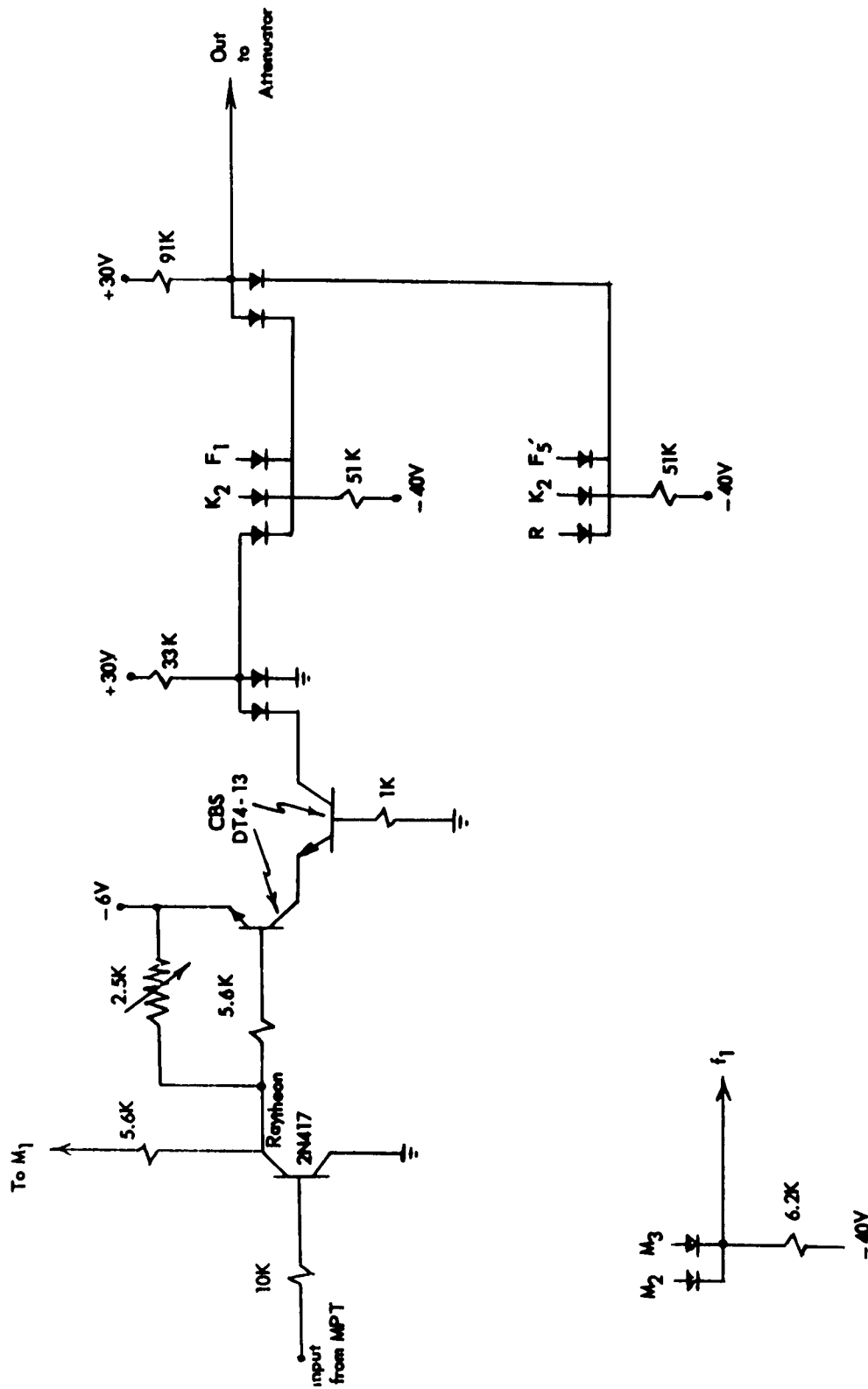
Figure 97. MPT Amplifier and Logic Board "O".

223
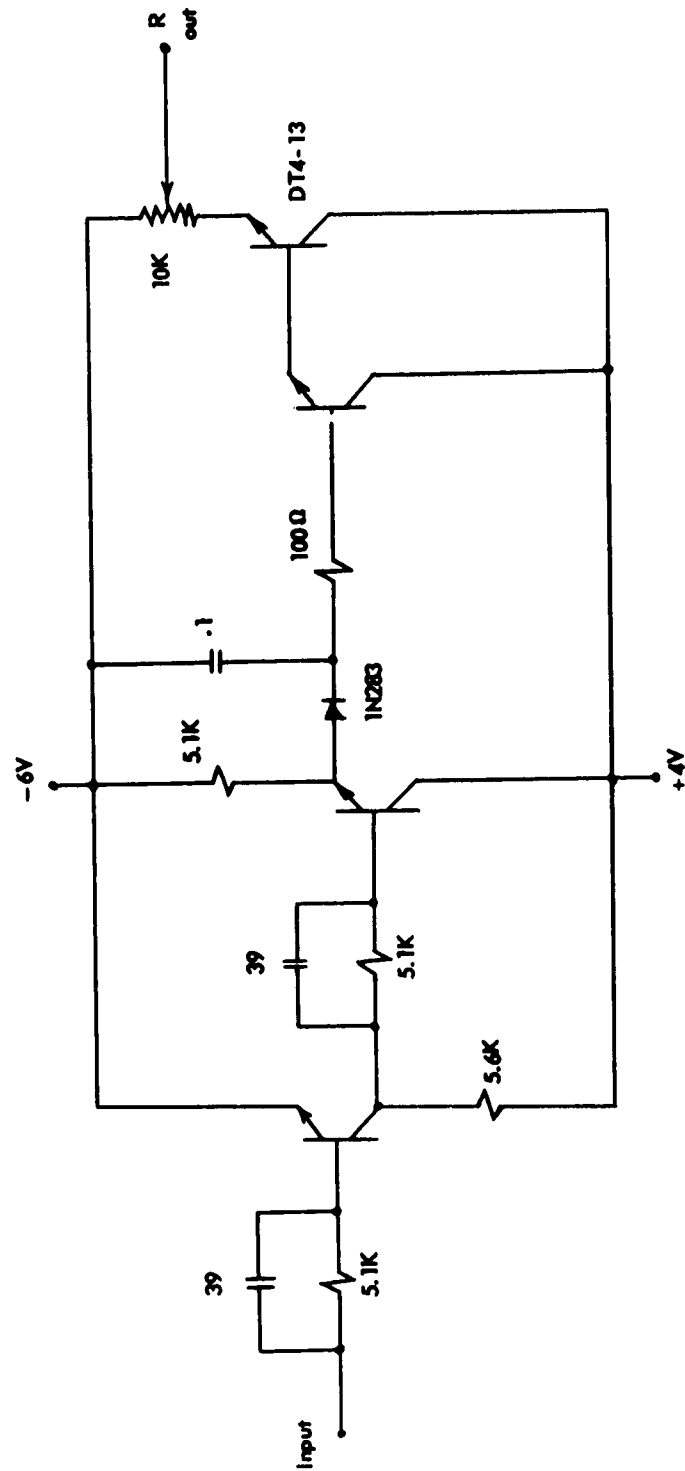
Figure 98. Ramp Generator.

224
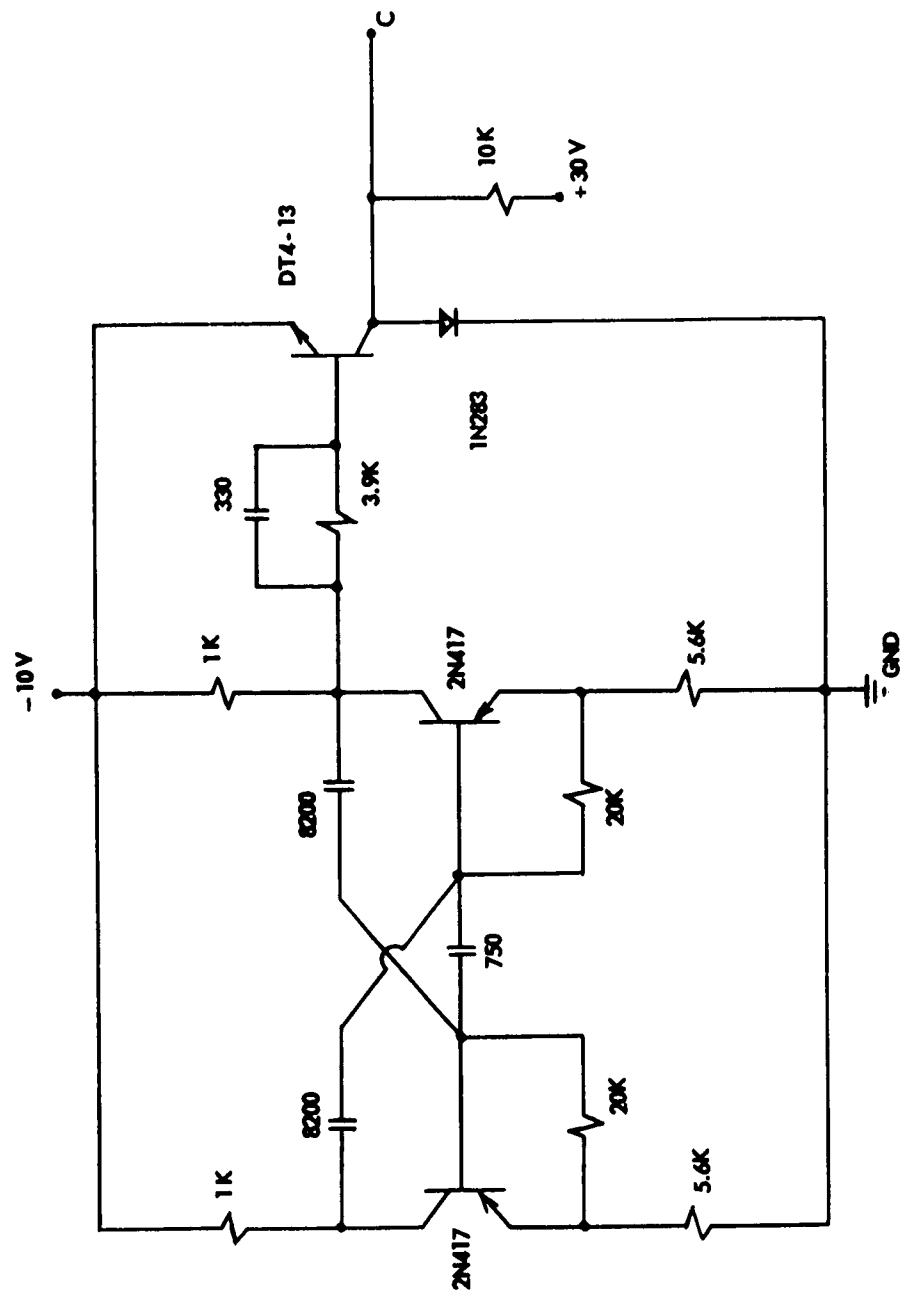
Figure 99. 200 KC Clock "C_1".

225

ASD TR 61-70
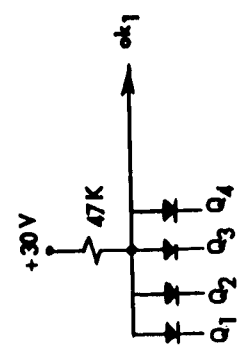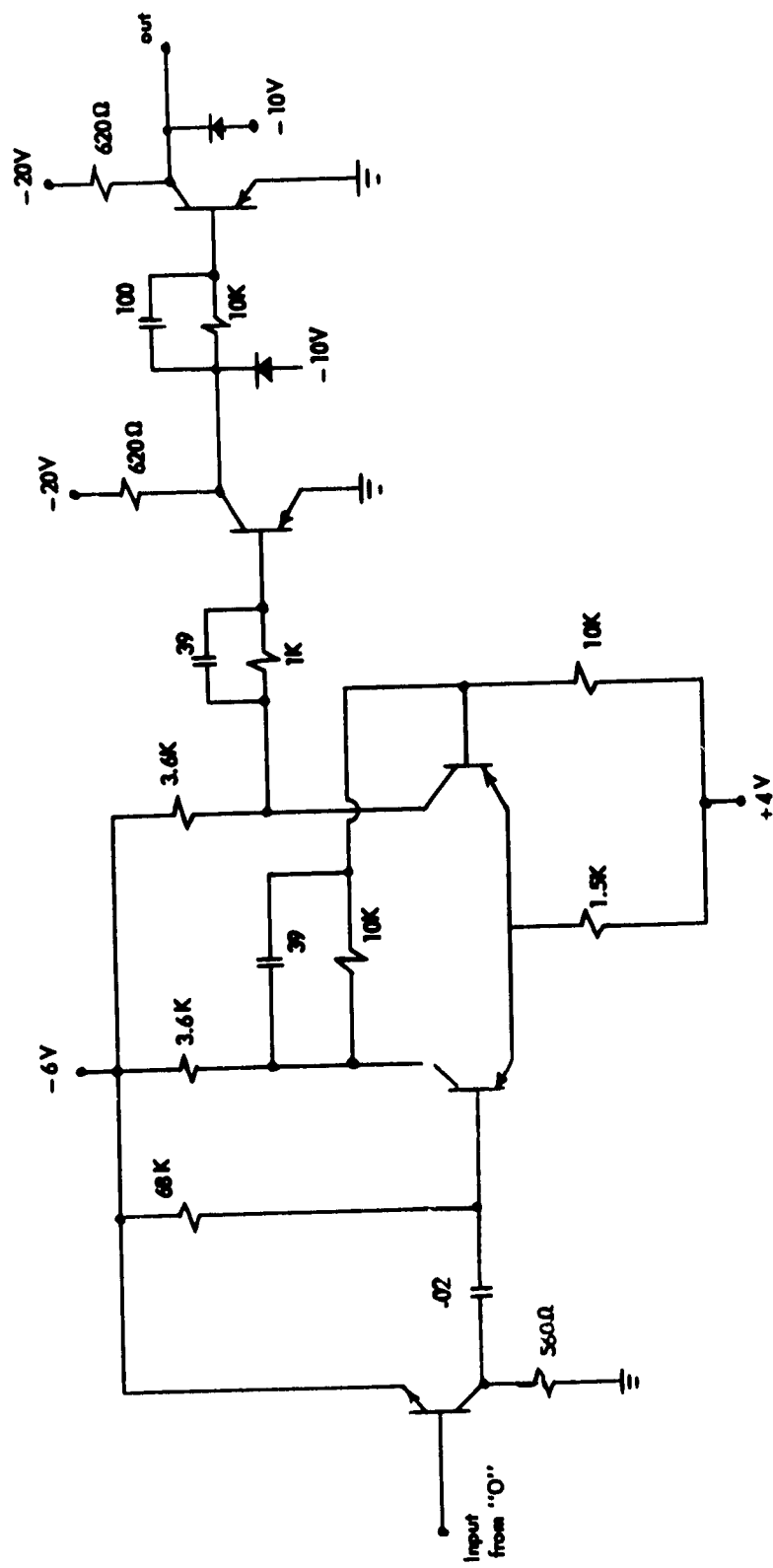
Figure 100. Access Pulse Shaper.

226

ASD TR 61-70
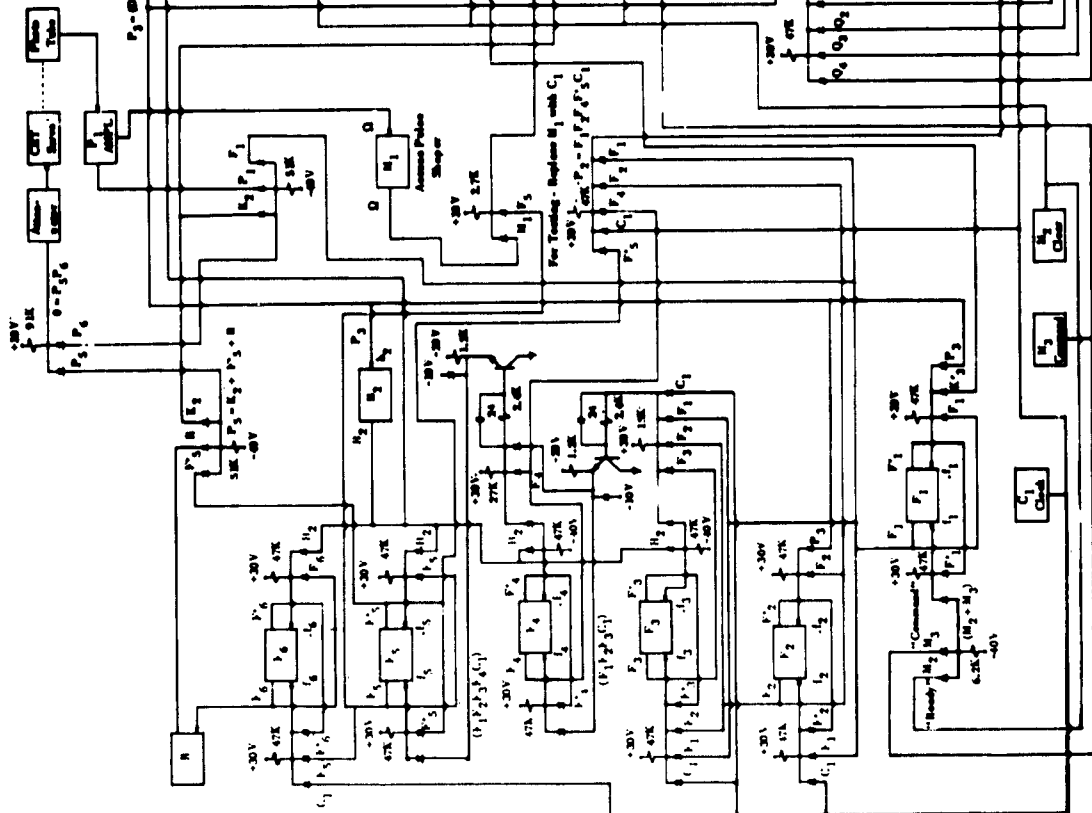
FIGURE 101. TRACK-SEEK AND SERVO UNIT BLOCK DIAGRAM.

ASD TR 61-70

TABLE XV

PLUG-INS

Unit	Description	Figure No.
F_1 - F_6	Flip-Flop	92
Q_1 - Q_4		
K_1 - K_4		
B_2	One-Shot	93
m_2		
m_3	Push-Button One-Shot	94
P_3	Comparator	95
P_4	Logic Board	96
O	Logic Board	97
R	Ramp Generator	98
C	Clock	99
m_1	Access Pulse Shaper	100

servoed CRT's input to drive the beam normal to the tracks. When seeking track N, the control unit switches to the track-folding state immediately after sensing N-1 track crossings. The beam then locks onto the next track edge, track N.

The control unit can be subdivided into the following listed groups along with descriptions of their various functions.

228

a. Electronic Switching

K_2 inhibits any signal and isolates the CRT while the control unit is in the "clear" state. F_1 inhibits P_1 from the CRT until the control unit is ready to return the CRT to the servo state. F_5' gates the ramp to the CRT.

b. Sequences

Flip-Flops F_1 through F_6 sequence the action of the control unit from receipt of the command signal until track "n" has been located.

$$f_1 = (M_2 + M_3) F_1' \qquad f_4 = F_1 F_2 F_3 F_4' C_1$$
$$of_1 = P_3 K_3' F_1 \qquad of_4 = F_1 F_2 F_3 F_4 C_1 + B_2$$

$$f_2 = F_1 F_2' C_1 \qquad f_5 = F_1 F_2 F_3 F_4 F_5' C_1$$
$$of_2 = P_3 F_2 \qquad of_5 = B_2 F_5$$

$$f_3 = F_1 F_2 F_3' C_1 \qquad f_6 = F_5 F_6' C_1$$
$$of_3 = (F_1 F_2 F_3 C_1) + B_2 \qquad of_6 = B_2 F_6$$

F_1 goes high and inhibits P_1. F_3 and F_4 make up a counter which is used to put a count of 2 into the track counter. F_5 opens the gate to the Optron for R. F_6 turns the Ramp Generator ON and OFF.

c. Track Counter

Flip-Flops Q_1 through Q_4 are used as a track counter and their outputs fed to a comparator.

$$q_1 = P_4 Q_1' \qquad q_3 = P_4 Q_1 Q_2 Q_3'$$
$$oq_1 = P_4 Q_1 \qquad oq_3 = P_4 Q_1 Q_2 Q_3$$

229

$$q_2 = P_4 Q_1 Q_2' \qquad\qquad q_4 = P_4 Q_1 Q_2 Q_3 Q_4'$$

$$oq_2 = P_4 Q_1 Q_2 \qquad\qquad oq_4 = P_4 Q_1 Q_2 Q_3 Q_4$$

M_1 a Schmitt trigger is used to generate the count-pulses from the MPT.

d. Comparator P_3

The comparator utilizes diode-resistor logic and compares the address with the track counter.   The output is low for inequality and high for equality.

$$P_3 = (D_1 Q_1 + D_1' Q_1')(D_2 Q_2 + D_2' Q_2')(D_3 Q_3 + D_3' Q_3')(D_4 Q_4 + D_4' Q_4')$$

In view of the fact that the control unit must return the CRT to servo between track (N-1) and track "N", and because the circuitry is designed to operate upon the fall of P_3, the aforementioned count of two is placed in the counter to allow the use of track No. 1 as indicated in Table XVI.

TABLE XVI

COMPARATOR LOGIC

Address	Counter	P_3
0 0 0 1	0 0 0 0	0 Off
0 0 0 1	0 0 0 1	1 On
0 0 0 1	0 0 0 2	0 Off

The CRT unit is thus returned to serve on track No. 1 before the ramp has been turned ON.

230

e. Ramp Generator (r = F_6)

The ramp generator is designed to produce a waveform with a slope of
-a t, beginning at +4 volts. (Diode-Resistance logic circuits prevent
any voltage above GND to appear at the CRT unit). This waveform is
applied to the input of the CRT unit and causes the CRT spot to move
downward in a linear manner.

f. Analog-to-Digital Converter

This circuitry amplifies the signal from the MPT to a level that can be
recognized by the diode-resistor logical circuits and then attenuates the
signal until it is usable at the input to the CRT unit.

g. Clearing Circuitry

Flip-Flops K_1 through K_4, and associated logic circuits of both transistors
and the diode-resistance type, are used to assure proper clearing of the
control unit.

$$k_1 = P_3 K_1' \qquad\qquad k_3 = M_2 K_3'$$
$$ok_1 = (Q_1 Q_2 Q_3 Q_4) C_1 K_1 \qquad ok_3 = B_2 K_3$$

$$k_2 = M_2 K_2' \qquad\qquad k_4 = M_2 K_4'$$
$$ok_2 = M_3 K_2 \qquad\qquad ok_4 = B_2 K_3' K_4$$

M_2 is the ready push button one-shot. M_3 is the command push button
one-shot. M_3 is interchangeable with M_4 which is a pulse activated one-
shot.

A description of the clearing can be given by assuming the flip-flops come
on in random states when the power is first applied.

If the configuration is such that the unit does not clear itself, then M_2
is activated. The sequencing flip-flops will be cleared and turned OFF.

231

The clock and K_1 will make the track counter count to 1111 and then turn OFF with the next clock pulse.

K_2 will remain ON to inhibit the Optron until turned OFF by the command one-shot.

Logical levels are 0 and -10V. Operating voltages are: +30V, +40V, -6V, -10V and -40V. The clock rate is 100 kc. All circuitry works well at or below $25^{\circ}C$. Above $25^{\circ}C$, leakage develops in both diodes and transistors.

Figure 102 illustrates the operation of the circuitry in the track-seeking switching and track-locking modes. The signals presented consist of the CRT deflection voltage and the MPT signal.
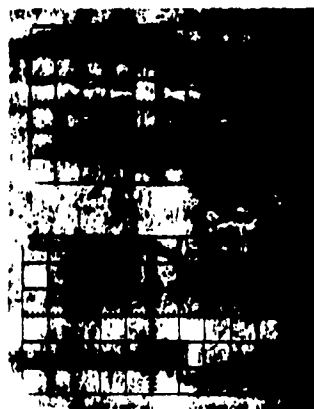
Figure 102.   Multiplier Phototube and CRT Deflection
Plate Waveforms During the
Track Seeking Operation.

3. Results of Experimental Evaluation

Tests of the equipment described with the Optron unit indicated that the design was adequate for experimental studies. The studies did reveal that if the operating speed of a photochromic memory were low enough,

a more reliable servo operation could be achieved by modulating the CRT spot at a relatively high frequency (compared to servo response time). This then provided an a-c servo signal which could be demodulated in the servo amplifier. This mode of operation was especially useful for experimental work. Stray light pick-up by the multiplier phototube became quite an operating handicap for the d-c servo loop case.

H.   SYSTEMS STUDIES

1.   Introduction

Before the start of the contract, members of the photochromic memory project had been asked to prepare preliminary systems designs on the two most promising photochromic memory systems as of that date. The systems were identified by their auxiliary components. The first, and most desirable, made use of a cathode-ray tube as both a light source for write-erase and as a light shutter. The second made use of an ultrasonic diffraction grating as a light switch in conjunction with an intense continuous source for providing the write-erase function. Two preliminary systems designs were made using postulated data, where necessary, and abbreviated versions are included as Appendix XVIII of this report. As more data was generated, these systems were seen to be entirely unrealistic.

As the program neared its final phases, it was necessary to specify a general system on which the final effort would be expanded with regard to a synthesis effort. In order to assist the monitoring personnel in their decision with regard to the final system (s), a number of systems were presented in one of the formal reports to the monitoring agency.

These were divided into two categories, cathode-ray tube write and/or erase and fixed light source write and/or erase. These systems are described below.

A follow-up discussion with the personnel of the monitoring agency led to the decision to concentrate the final effort on the two systems as described under "Final Objectives" in Section I of this report. It was understood that because of the request for two systems instead of a single system, and the unlikelihood that the cathode-ray tube system would have enough promise to lead to a hardware effort to follow this program, the design effort would be somewhat less detailed than originally anticipated. Because of the implications of the laser as a photochromic memory light source, a laser study was also undertaken during this final period.

Even as serious as the low write-erase rates are, the most serious limitation by far is the fatigue associated with photochromic materials. This is not a serious problem for some special purpose applications, such as the up-dating system for a photographic memory, but for applications of the more general purpose type it imposes severe restrictions on the programmer. The fatigue limitation will not be treated further in this section as no memory organization has been generated which might tend to by-pass this restriction. It is understood that the CRT system chosen for the synthesis effort would only be applied within the constraints of life as determined by the dynamic fatigue characteristics of photochromic material. Thus even a high intensity continuous laser light source which could be modulated in a shutter-like fashion would not overcome this major obstacle to the realization of a general purpose photochromic memory capable of repeated write-erase operations.

234

2. Systems Configurations

a. Introduction

Work on specific memory systems began later than was originally anticipated. This was associated with a lack of fundamental data early in the program. It was felt somewhat premature to expand effort on the basis of "educated" guesses at that point in the program. It was more important to continue gathering the data necessary for a sound approach to the problem.

The cathode-ray tube offered so many advantages as a switchable, movable light source that it almost appeared to be a mandatory component in the system for the write, read, and erase functions. For example, if CRT's were found to be lacking in resolution, or if they were found to be too grainy, it was possible to use a larger spot which could be reduced optically to the required size at the photochromic surface. In fact, it was desirable to relax the requirements on the CRT as much as possible. This helped to insure that a proposed system did not go beyond the state of the art in this area and would help keep this component within economic bounds. Such a loss of resolution at the CRT face would, at the limit, result in a single spot over the whole face with a complete loss of spot mobility. It appeared then, that for a given system (depending on other parameters as well, e.g., phosphor burn), there was a region of optimum compromise in trading spot mobility and resolution for reliability and economy. In the case of the photochromic memory, only when the data was available on the use of a CRT with the photochromic coatings was it possible to finally establish CRT requirements and capabilities. These specifications greatly influenced the final form of the memory.

When the low CRT writing speed became apparent it was reasonable to ask whether a servoed mirror-fixed light source type system might not be preferable. An Osram HBO-109 had at least an order of magnitude increase in writing rate over the 5ZP16 with respect to photochromic coatings. While there appeared to be a natural dislike for mechanical systems among digital

235

(electronic) engineers, at this stage of research, all the systems were in need of an objective evaluation.

b.   Investigation of a Mechanical System

In line with the above policy, preliminary investigation of the non-CRT (at least for writing) type of photochromic store was conducted. The layout used is shown in Figure 103. Only a single mirror was used for the servo operation instead of the two shown (for simplicity in drawing). This mirror was mounted to rotate around two perpendicular axes which coincided with the plane of this front surface mirror and intersected at its center. A non-concentric, fixed-speed motor drive was used to rotate the mirror so as to generate an ellipse similar in shape to that described under "Cathode-Ray Tube Studies" in part E of this Section and shown projected in Figure 70. By changing motors, cycle time for the ellipse was varied from 30 to 1 rpm, and, through use of the shutter and moving the photochromic plate, single ellipses or sections of the ellipse were easily isolated. It was from this equipment that the fatigue measuring device described in Appendix XIII was derived. Reference to the figure in that appendix should help clarify the description given above.

Experiments with this device indicated that a writing rate of 100 spot diameters/sec was feasible. At this speed it was quite reasonable to make use of mechanical (moving) shutters, shutters which are by far cheaper than the ultrasonic cell which had been investigated in some detail for use as a microsecond shutter. This general reasoning was felt to hold true up to a writing rate of about an order of magnitude greater than the 100 spot diameters/sec. (By the term mechanical is included electro- and magneto-strictive shutters, i.e., any shutters which involve mechanical displacement.) Thus, it was concluded that the mechanical optical device could work better than a CRT write memory when writing speed is of paramount importance.

236
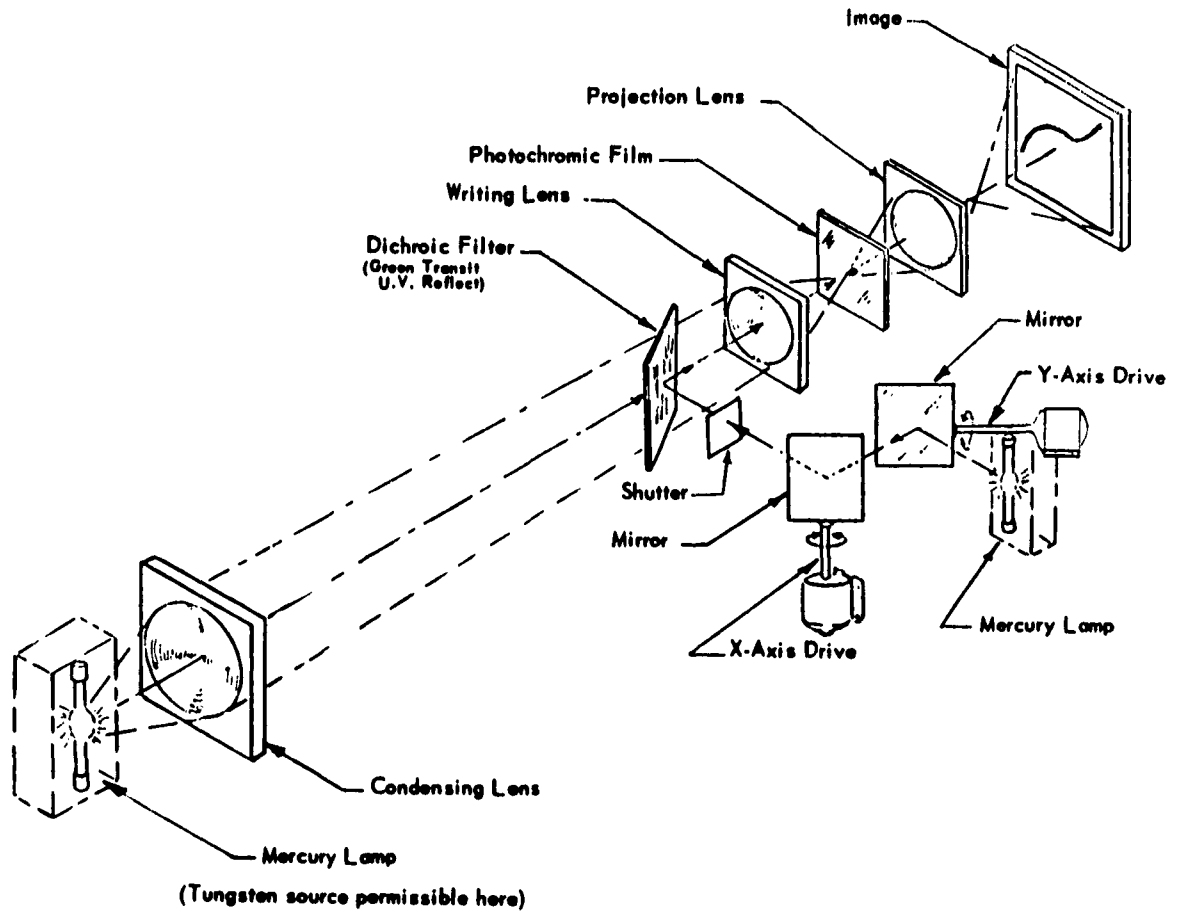
Figure 103.   Fixed Source - Photochromic System with Simultaneous Read Capabilities.

237

The most pertinent experimental data on photochromic material systems, optical components, CRT's, servos, light sources, etc., was collected and was available prior to the preliminary design phase. In general, the characteristics of a digital photochromic memory system which could be designed around existing materials and components are given in Table XVII.

An examination of Table XVII shows that Items 1, 2, and 7, namely the speed of writing and erasing information plus the irreversible fatigue exhibited by the photochromic material, represents significant performance limitations. In other words, any digital photochromic memory designed around existing materials and techniques necessarily has a limited capability.

It was recognized by the contractor that another approach to the preliminary design phase could have been taken. In this approach assumptions could have been made with respect to future improvements which might become available at a later date through improved materials and/or components, e.g., better light sources of CRT's. While this approach to the preliminary design of a photochromic memory could have been undertaken, the contractor did not recommend that this be done on the basis that it did not represent normal engineering practice.

The photochromic memory systems described in the remainder of this section are all considered to be within the state-of-the-art of present photochromic materials and related components. These estimates are deliberately on the optimistic side in order that no potentially useful system would be eliminated on cursory examination only.

TABLE XVII

PARAMETERS OF A DIGITAL STORE (AS DEFINED BY KNOWN PHOTOCHROMIC MATERIALS) USED IN

SYSTEMS SYNTHESIS[*]

	CRT	Osram HBO 109
Serial writing rate (bits/sec)[**]	5-50	20-200
Serial erasing rate (bits/sec)[**]	5-50	20-200
Serial read rate (bits/sec)	10^6	10^6
Capsular packing density (2 marks/bit)	$1/4 \times 10^6 - 10^6$ bits/in^2	
Non-capsular packing density (2 marks/bit)	$> 10^6$ bits/in^2	
Memory surface temperature	-15°C to 0°C	
Number of useful switching cycles[***]	1,000 - 10,000 cycles	
Capsular optical density (written)	0.5 - 1.0	
Non-capsular optical density (written)	1.0 - 2.0	
Bulk transfer (seconds)	0.1	

* Representative values from the above table were used for photo-chromic memory system analyses.

** Not necessarily maximum contrast operation.

*** To one-half initial written density

239

4. Systems Using Cathode-Ray Tube Write and/or Erase

Two different approaches to a CRT photochromic memory system will be discussed in the following paragraphs. The major emphasis is placed on the compatibility of each system with the properties of photochromic coatings.

With open-loop accessing, a number of configurations are possible which are not considered. When using such accessing techniques, severe requirements on tolerances, both electrical and mechanical, are called for, e.g., the Williams tube memory system. At the present state-of-the-art, it is generally agreed that high resolution digital operation requires a closed-loop servo system. In line with this general conclusion, a closed-loop servo system was an accessing requirement.

a. Rotating Disk Cathode-Ray Tube Photochromic Memory

A rotating disk system is discussed in Appendix XVIII. Disregarding any other technical difficulties associated with this system, a comparison of the assumed photochromic properties at that time with those known presently is enlightening. A comparative chart is given in Table XVIII.

The first entry in Table XVIII all but rules out the disk memory. Writing a circular track of 36,000 marks (a reasonable figure) is measured in hours. If a continuous speed mechanism was used, this would also be the access time. The alternative is to step the disk from mark-to-mark with a rapid access mode for locating the region of interest. Such a system would be more complex mechanically and it does not offer any particular advantages over an alternate system to be described later.

ASD TR 61-70

TABLE XVIII

BASIC PHOTOCHROMIC PROPERTIES

		Assumed	Present (Non-capsular coatings)
1)	Write-Erase Times	5×10^{-6} sec.	0.1 sec
2)	Operating Bit Size (includes smear)	0.001 x 0.002 inch	0.001 x 0.001 inch (or less)
3)	Write Wavelength	3800 Å	3300 Å - 3800 Å
4)	Erase and Read Wavelength Band	4500 Å - 5500 Å	5000 Å - 6000 Å
5)	Low Intensity Read, Erasure?	No	Small
6)	Fatigue	Unknown	1000 cycles

Since an increase in writing speed of as much as two or three orders of magnitude would still lead to relatively long access times; therefore, there appeared to be little merit in pursuing the disk (or drum for that matter) type of memory any further. The system which follows is more compatible with the write-erase and fatigue characteristics of photochromic coatings. The latter characteristic, fatigue, dictated that replacement of the storage surface must be both economically feasible and a relatively simple operation.

b.   Photochromic Analog of the Digital Storage Tube

The digital storage tube can take on a variety of forms, but the basic feature of such tubes remains the same. An electron beam is used to write the information on the storage surface, with the same beam,

ASD TR 61-70

or another beam, used for reading out this information. By and large, the storage surface is stationary and the beam traverses this surface in two dimensions. At any rate, this is the type of storage tube around which the photochromic analog device to be described was synthesized.

In the photochromic version, a photochromic coating is used as the storage surface. The phosphor on a CRT is used as a transducer from electron beam energy to radiant energy, and a photosensitive detector is the transducer in the reverse direction. The system to be described can be developed from the basic system of Figure 69 described under "Cathode-Ray Tubes" in part E of this Section.

A photochromic analog of the storage tube is shown in Figure 104 and is the system to be described. Referring to Figure 104, the dichroic beam combiner affords a means for registration of the two cathode-ray tubes with respect to the photochromic material. This same dichroic beam combiner provides additional registration of the two CRT's for the servo channels. With considerable optical reduction at the photochromic plate, the depth of field of the "write" lens allows considerable tolerance in the positioning of the CRT's.

A rather sophisticated servo system for positioning a CRT beam has been described in the literature[*] and might be used here in a modified form. However, it calls for a multiplicity of multiplier phototubes, an undesirable feature. In the present system it is proposed that digital location be obtained and held by noting crossings of the opaque gratings in x and y accessing channels and edge locking the spot. The CRT faces are imaged on the access plates.

A troublesome feature has to do with the light integrating property of photochromic materials. Thus, during accessing it is possible to lay

---

* Gallaher, L. E. , "Beam-Positioning Servo System for the Flying Spot Store," B. S. T. J. , 38, p. 425 (March 1959).

242
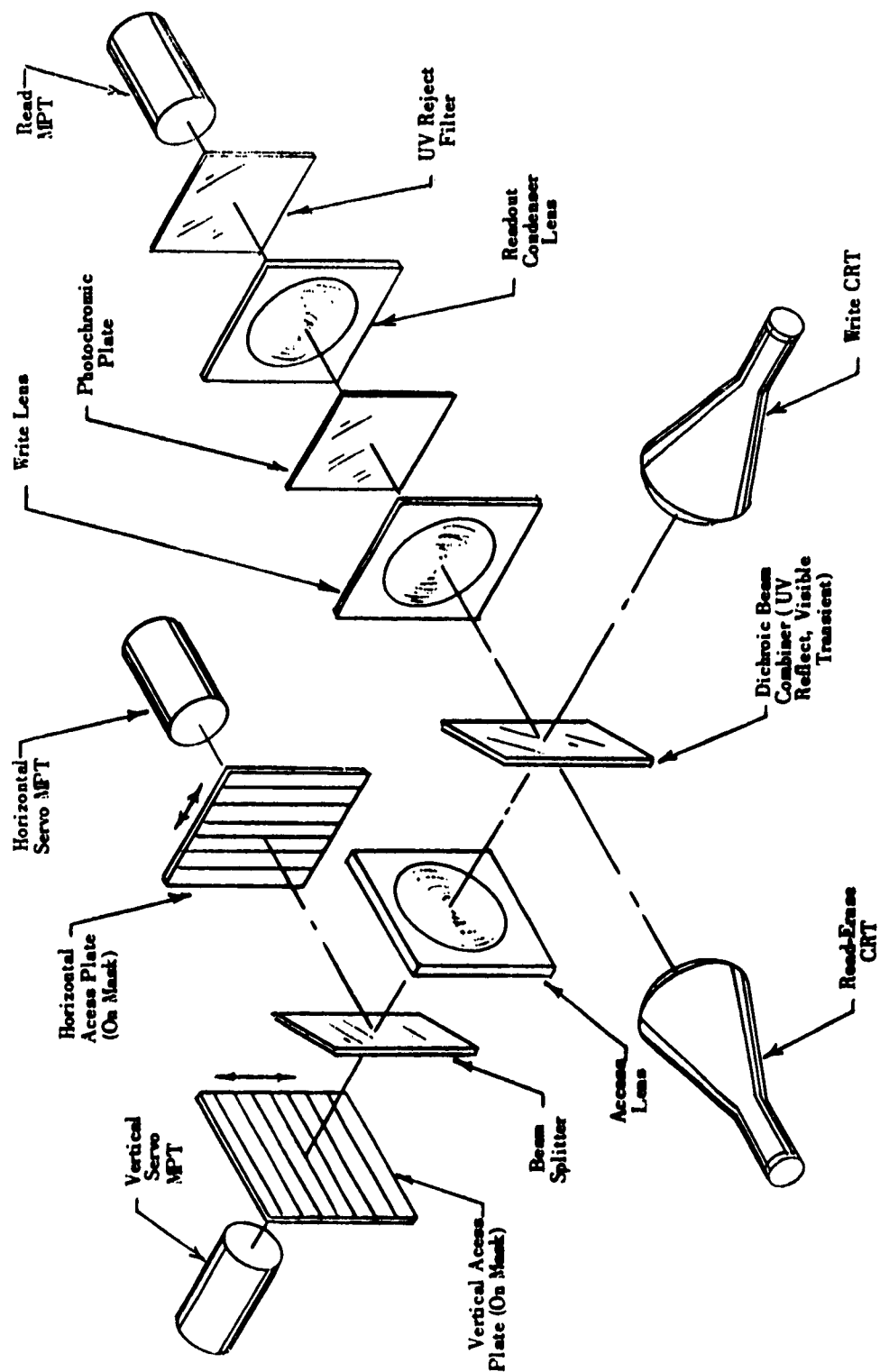
Figure 104. CRT-Photochromic Memory.

243

down faint patterns in a random fashion over the photochromic surface which could eventually build up to higher contrast. If, on the other hand, accessing and recorded information areas are interleaved on the photochromic surface, there should be relatively little interaction. This arrangement would appear as indicated in Figure 105.
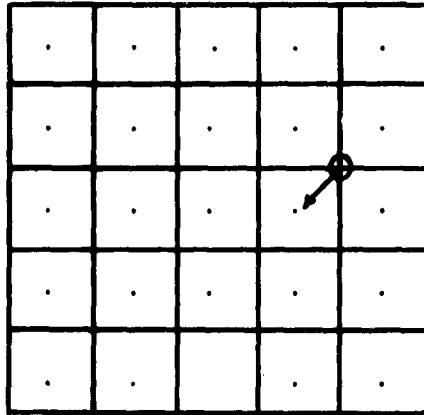
Figure 105. Servo Access Scheme.

The solid dots represent recorded information (these areas could be recorded on two marks/bit basis as well as in the manner shown).

The solid lines represent paths which the image of the CRT spot follows to reach a given area. The spot actually seeks line intersections, but, as illustrated by the dashed circle and arrow, a slight mechanical displacement of the access masks can force the spot into an information location. Since it takes 0.1 second to write or erase a spot, it is not unreasonable to take some fraction of this much time for mechanical shift of the access masks.

ASD TR 61-70

When reading, the masks can be left in the shifted position so as to cause the read spot to pass through the center of the recorded spots. If a fast horizontal sweep is used to read a horizontal line, the vertical grating in the other channel can be used to generate clock (or position) pulses to indicate when the spot is in the proper location for reading.

The literature[*] indicates that it is reasonable to expect a spot array of 256 x 256 elements from a cathode-ray tube. Cutting this down to 128 x 128, because of the access interleave feature, provides a total of 16,384 spots. While this represents a limited number of bits, it is relatively easy to move a new section of photochromic material into the read-write position and then repeat the operation. At a 25 to 1 reduction, a 5 inch CRT is reduced to a 0.2 inch field. This provides space for at least 25 arrays of 128 x 128 spots/inch^2. The above estimates are conservative, but not inconsistent with the results obtained in the studies under this contract.

It is reasonable to consider a 5 x 5 inch photochromic slide, or 25 square inches of useful surface. We would then have a total capacity of 25 x 25 x 128 x 128 or, approximately, 10^7 bits. The access time to a 128 x 128 block should be possible in somewhat under 1/2 second with a reasonable servo drive. The read-out rate is then limited by the servo control and spot intensity. A read rate of 100 kc should be readily achieved. Replacement of the plates, or automatic selection of plates from a bin, should also prove to be a relatively straightforward operation.

Although more detailed systems work was needed, the preliminary specifications in Table XIX proved helpful in evaluating the potential usefulness of this system.

---

* Hoover, C. W., Jr., Haugk, G., and Herriott, D. R., "Systems Design of the Flying Spot Store," B.S.T.J., 38, p. 365 (March 1959).

ASD TR 61-70

TABLE XIX

CRT DIGITAL PHOTOCHROMIC MEMORY
PRELIMINARY SPECIFICATIONS

Capacity (per 5 x 5 inch plate)	10^7 bits
Random Access	0.5 sec.
Access within a Block	0.001 sec.
Packing Density	400,000 bits/in^2
Write-erase Speed	10 bits/sec.
Write-erase Life Before Replacement*	~1000 cycles
Readout Rate	10^5 bits/sec.
Write CRT	5XP16
Read-erase CRT	5AUP24
Photochromic Plate Servo, x-y Positions (Detented)	25 x 25
Over-all Length Along Optical Axes	48 inches

* Replacement of the photochromic memory surface should be a relatively simple and inexpensive operation.

5. __Systems Using a Fixed Light Source Write and/or Erase__

Two different types of approaches to a fixed source write-erase photo-chromic memory system will be described next. The rather novel drum system presented in Appendix XVIII will not be considered since it suffers from the limitations described previously under the rotating disk cathode-ray tube system. As before, the emphasis is to be placed on the compatibility of the system with the properties of present

photochromic coatings. The closed-loop type of servo operation will be
a requirement for these systems for the same reasons as given under
the cathode-ray tube discussion.

a.   Servoed Mirror, Fixed Light Source Photochromic Memory

It is possible to replace the cathode-ray tubes in Figure 104 with an
Osran HBO-109 source and a servoed mirror. By using filters, the
same source can be used to serve the three functions, write, erase
and read. Such a system is shown in Figure 106. Aside from the
change in the method of moving the spot and switching dichroic filters,
the layout is identical to that in Figure 104. For the present, a 128 x
128 array is postulated (per field).

Because of the mechanical servo of the beam, beam positioning time
within a block would average about 100 milliseconds. This is not
unreasonable since it is the same order as the writing time.

Stepping to an adjacent position should be possible in about 30 milli-
seconds. By accelerating to reading speed and sweeping a full line,
a readout rate of about 10 kc should be practical. Writing need not
be any faster than the time it takes to step to an adjacent position,
30 milliseconds, or about 30 spots/second.

Figure 107 includes the features of Figure 106, but with provision
for bulk entry of information, if desired. This feature can be used
with an array of shutters whose pattern is transferred in parallel
or it can be used with punched tape or film containing digital patterns
in an appropriate format. This feature will allow loading a 128 x 128
array in 0.1 second, or an effective writing rate of the order of 100 kc,
if new information is sequenced into position rapidly enough.

Note that the servoed beam in Figure 107 is capable of providing an
updating feature by operating on the data that has been transferred
in bulk (parallel) form. It will be necessary to register the patterns

247
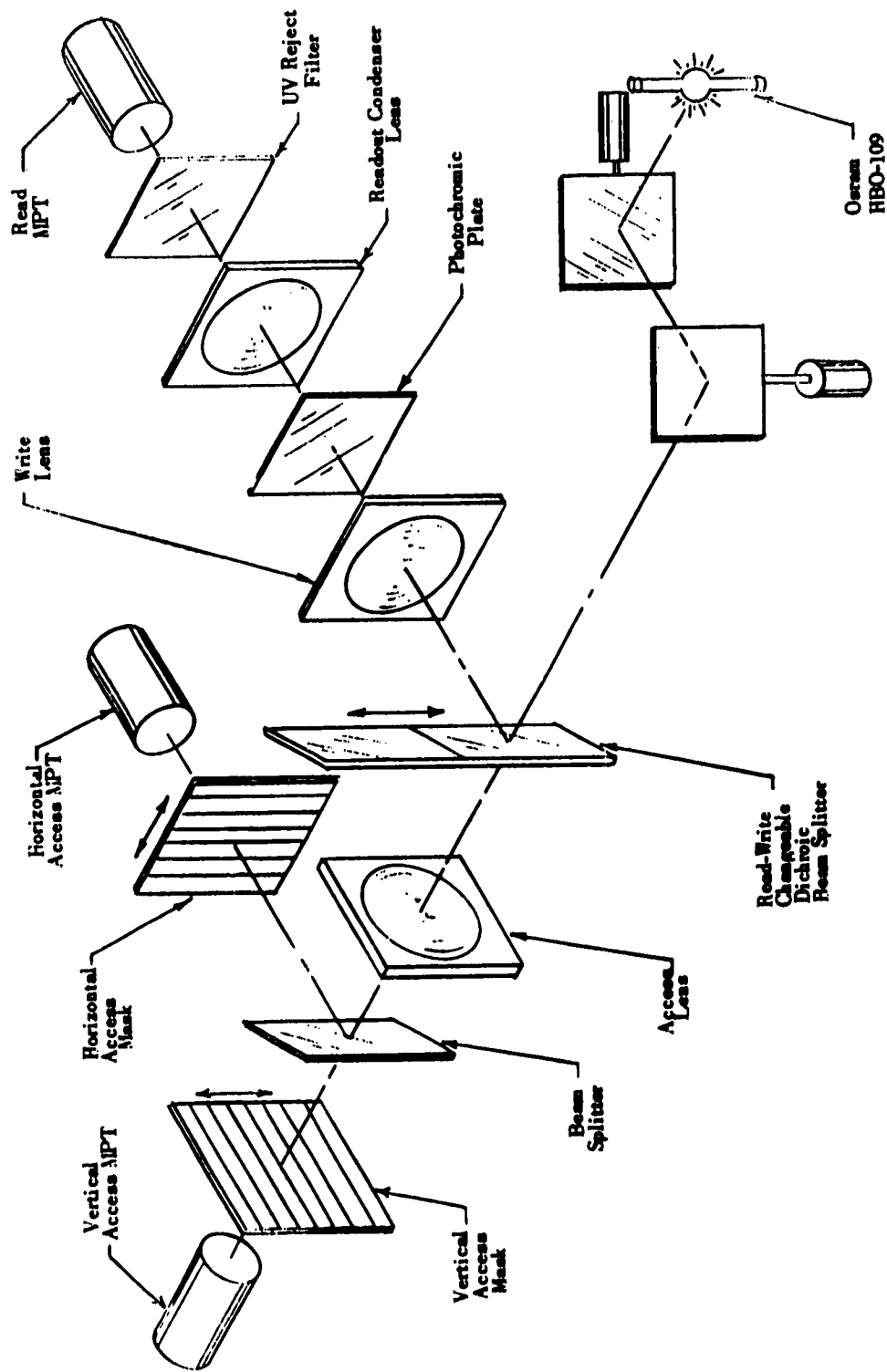
Figure 106. Servoed Mirror Photochromic Memory.

248
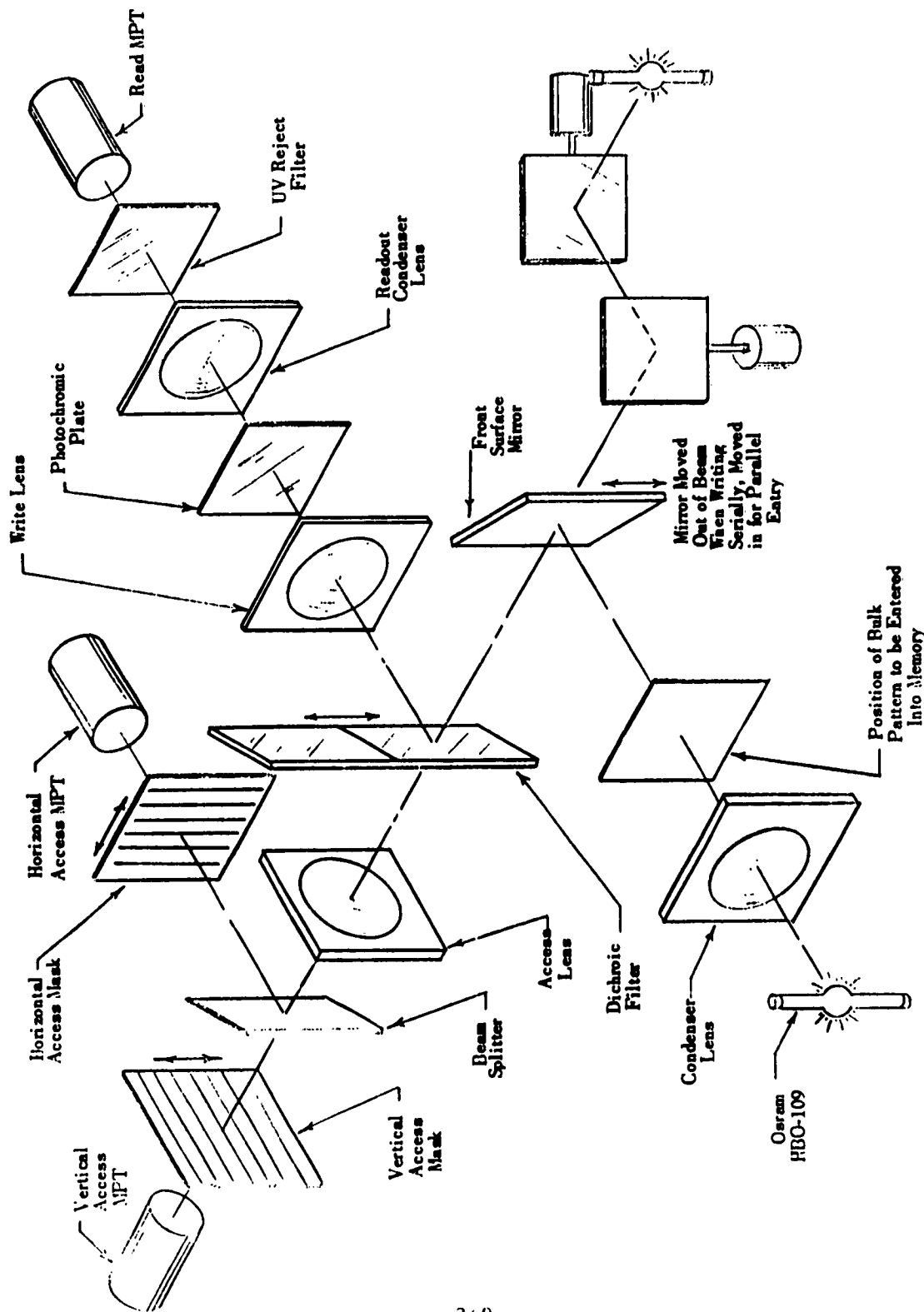
Figure 107. Servoed Mirror Photochromic Memory with Bulk Entry.

249

ASD TR 61-70

to about one mil when entering data in parallel by unit media. Special registration holes can be provided on the servo accessing masks for verifying that the master transparency is properly registered for data transfer. The bulk transfer feature can also be included in the system of Figure 104, if desired.

A much faster read-out might be desirable than is available from the servoed mirror system. This can be accomplished by means of the system shown in Figure 108. Here the read path is in the reverse direction and operates similar to C. Baumann's rotating mirror photo-memory as described in Appendix XVIII. The servo lights in Figure 108 are imaged in the reverse direction on the vertical access mask and the images are moved to a given location on this mask by the y access mirror. Motion of the y access mirror in turn places a given series of track images in register and rapidly sweeps them by the photodetectors. Thus, parallel read-out is readily achieved.

Use of the far red or far blue part of the spectrum for servoing allows the dichroic beam splitters to reflect the useful part of the information carrying spectrum as defined by the absorption characteristic of the photochromic material, while passing that part which cannot sense the data written on the photochromic coating. This read-out feature also can be included in the systems of Figures 104 and 107, if desired.

There are other possible variations of the basic system, but those presented seem to offer the greatest promise. The specifications for Figures 106, 107, and 108 which differ from those given in Table XIX are given in Tables XX, XXI, and XXII.

250
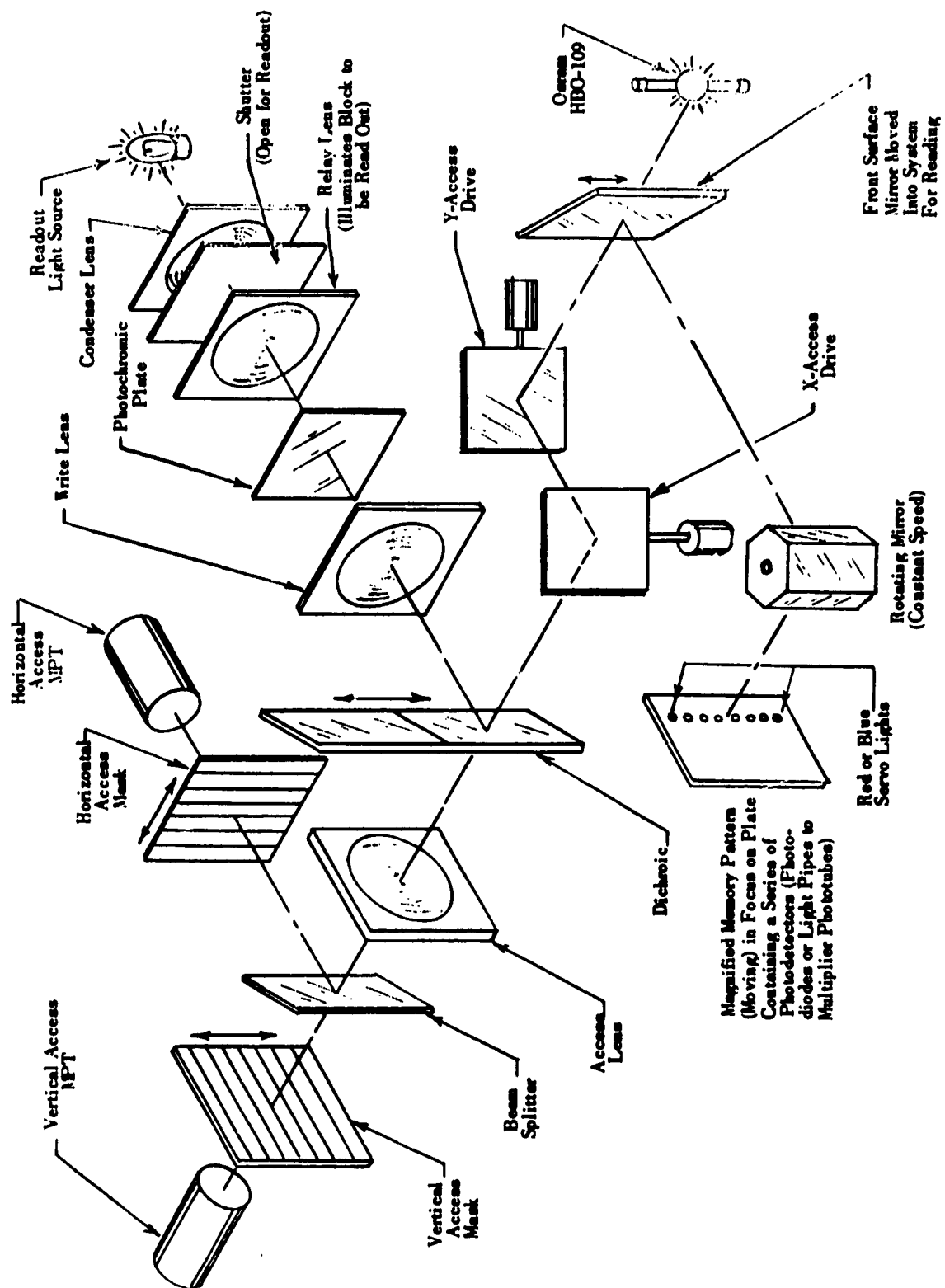
Figure 108. High Speed Read-out of a Servoed Mirror Photochromic Memory.

251

TABLE XX

SERVOED MIRROR PHOTOCHROMIC MEMORY
(Specifications differing from Table XIX)
(Figure 106)

Access Within a Block	0.1 second
Write-Erase Speed	30 bits/second
Readout Rate	10^4 bits/second
Read Write-Erase Source	Osram HBO-109

TABLE XXI

SERVOED MIRROR PHOTOCHROMIC MEMORY WITH BULK ENTRY
(Specifications Differing from Table XIX)
(Figure 107)

Serial Access Within a Block	0.1 second
Serial Write-Erase Speed	30 bits/second
Bulk Write-Erase Speed	10^5 bits/second
Readout Rate	10^4 bits/second
Read-Write-Erase Source	Osram HBO-109

252

TABLE XXII

SERVOED MIRROR PHOTOCHROMIC MEMORY WITH HIGH SPEED READOUT

(Specifications differing from Table XIX)

(Figure 108)

Serial Access Within a Block	0.1 seconds
Write-Erase Speed	30 bits/seconds
Readout Rate (n tracks)	$>10^5$ bits/second/track
Write-Erase Source	Osram HBO-109
Read Source	Tungsten (optional)

b.   High Capacity Photochromic File Memory

Critchlow[*] and Litz[**] have described a high capacity file type photo-memory using Chalkly film, a film which does not require development. It differs from photochromic coatings in that it is not reversible and that it requires harder ultraviolet for writing (2400 $\overset{o}{A}$ - 3200 $\overset{o}{A}$). Since many of the system details have been described, it is possible to generate realistic estimates of how photochromic materials might perform in such a high capacity digital file system. The writing speed limitation exists with both Chalkly film and photochromic coatings, so that they are compatible in this respect.

The reader is referred to the Critchlow and Litz article for the general system details. Erasing would be a bulk (by track) operation in a manner similar to that used for writing. This is necessary since the

---

[*] Litz, F.A., "A Direct Access Photomemory Part I, Phototype Machine System,". Proc. of Western Joint Computer Conf., p. 53, (May 6-8, 1958).

[**] Critchlow, A. J., "Direct Access Photomemory Part II, System Considerations," ibid, p. 56.

253

servo guide tracks are written with the information to be recorded.
The information format would be as shown in Figure 109 and the optical
system as shown in Figure 110.
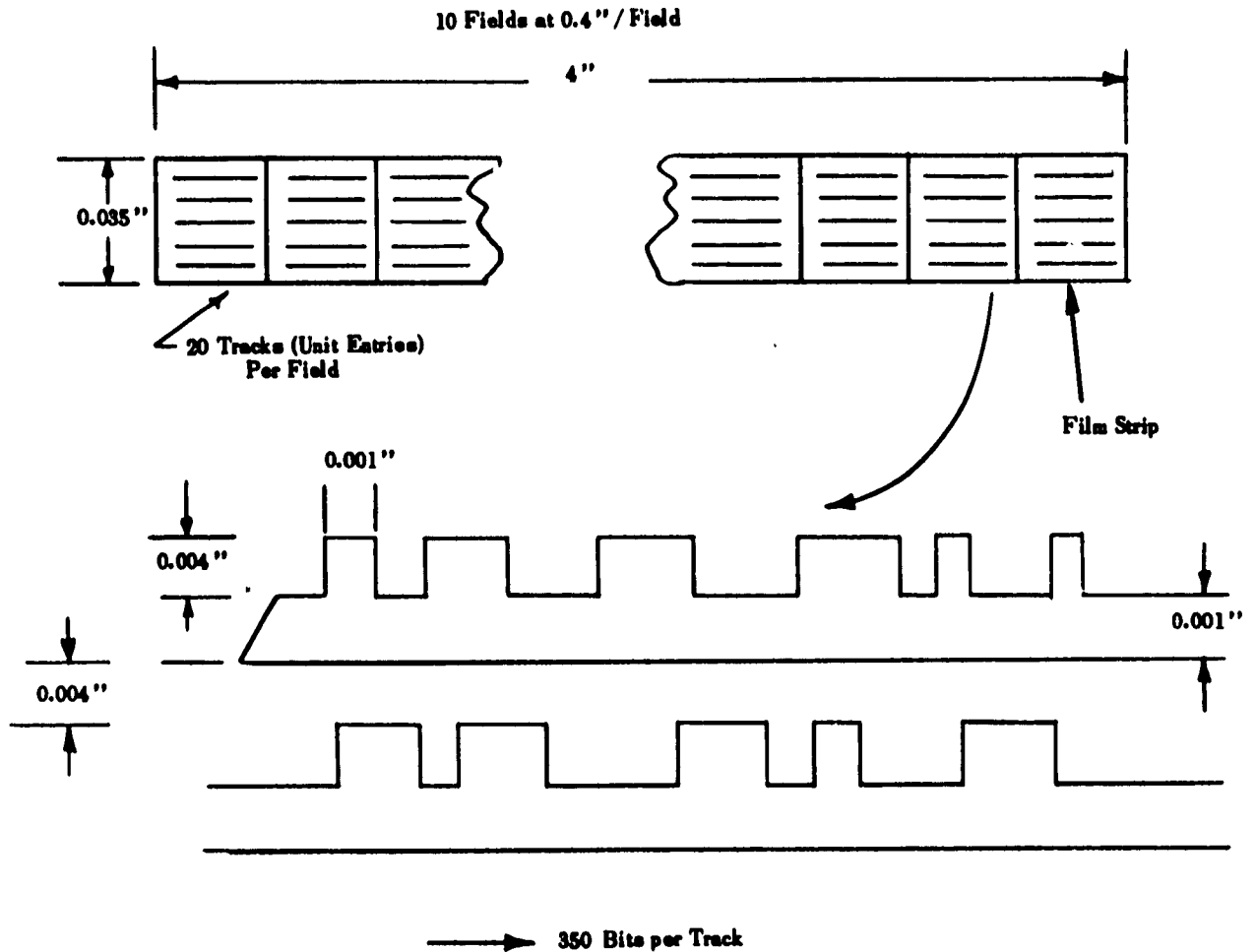
Figure 109.   Photochromic File Film Strip Format.

The tolerances of the format described here have been somewhat re-
laxed over that described by the authors Critchlow and Litz, who
did not have the erasure and re-entry problem.

ASD TR 61-70
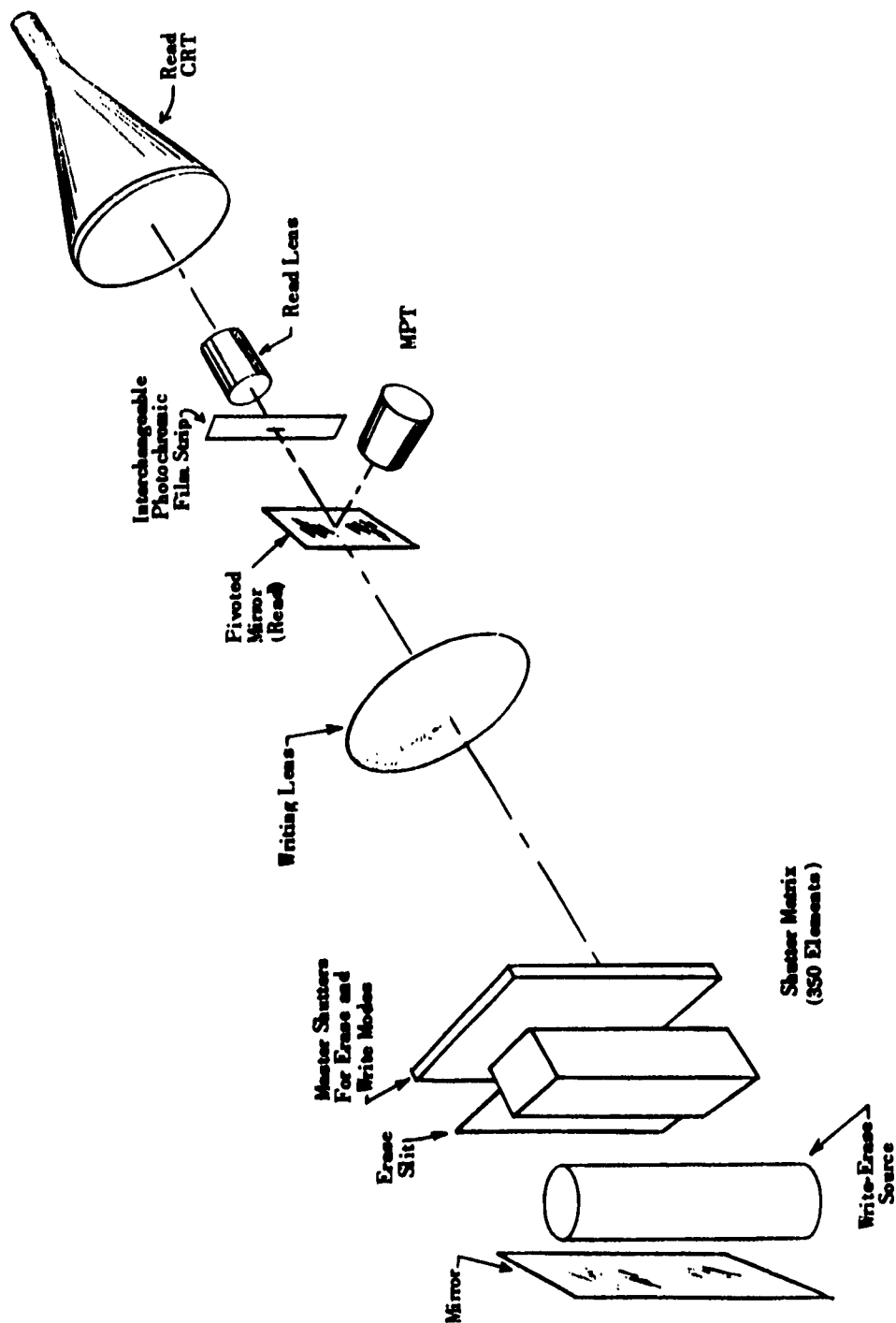
Figure 110: Unfolded Optical Layout of Photochromic File Memory.

255

The write time and erase time for the light source has not been checked, but one second appears reasonable for non-capsular materials, and is in accordance with the original file photomemory. Table XXIII outlines the specification for such a memory which should help determine its potential for Air Force applications. Of course, refrigeration is also required. This feature is more easily incorporated into the systems described previously.

TABLE XXIII

PHOTOCHROMIC FILE MEMORY SPECIFICATIONS

(Figure 110)

Capacity	140×10^6 bits
Unit Entry (bulk)	350 bits
No. of Entries per Field	20
No. of Fields per Film Strip	10
No. of Film Strips per Bin	20
No. of Bins per Drawer	20
No. of Drawers per File	10
Random Access Time	0.5 sec.
Write-Erase Times	1 sec.
Reading Rate	10 kc
Packing Density	10^5 bits/inch^2

6. **A Photochromic System for Up-dating Permanent Photographic Memories**

This portion of the report wil' lescribe one of the systems selected for synthesis, the up-dating of permanent photographic type memories. This

256

application is well within the present capabilities of photochromic materials.

a.   Introduction

Digital photographic storage devices are now making their appearance in industry, and are renowned for their high packing density capabilities. Depending upon the application of the system, the storage devices will exhibit wide ranges of performance with regard to capacity and access time.   A few examples will show what orders of magnitude and what variations might be encountered.

1)   Computer Set AN/GSQ-16 (King Disc)
Capacity 30 x 10^6 bits
Random Access Time - 35 milliseconds
Read-out rate - 1 megacycle

2)   Bell Flying Spot Store
Capacity from 1 to 100 x 10^6 bits
Random Access Order of 5 x 10^{-6} seconds
Read-out rate depends on use

3)   Proposed new King Disc
Capacity - 10^8 bits
Random Access - 1 millisecond
Read-out Rate - over 20 megacycles implied

These examples are listed as a guide to the number variations that may be encountered and are not meant to compare the merits of the systems. The main point to be established is the vast number of bits handled by any of these systems, and the fact that they are all placed on permanent photographic film or plates.   Notwithstanding the time involved in the pre-paration of the information to be placed in the store, which is extremely lc..g, it also takes a relatively long time to actually transfer the compiled ir_ormation into a suitable photographic format.   The King discs, when fully loaded for purposes of translation, will have taken about five eight-hour days to film and have required some ten separate photographic processings.   During these processings, the film is exposed to damage in several ways and may have to be redone if only a small portion is damaged.   So far, no provision for computer errors in transforming

257

the information have been taken into account. Hence, the chances of finally ending up with a perfect fully-loaded disc are infinitesimal. Fortunately, when the store is used for purposes of language translation, quite a large percentage of errors are permissible without detriment to the final performance of the store. However, it is these errors, which at this time are present, acknowledged and lived with, that really prevent this particular device from being practical where accuracy is really necessary, such as the banking and bookkeeping areas. These same problems apply to all of the systems mentioned to a lesser extent because the other systems break up their information into small packages. Nevertheless, any one of these systems would be greatly enhanced if errors could be corrected without the necessity of rewriting a whole block of information that is already correct. This, therefore, defines a need for being able to correct an original error.

By the same reasoning of the inability to alter the permanent photographic image, data that may require changing could also present a formidable problem if the whole store has to be rephotographed to accommodate the change, not to mention the possibility for compounding of errors during the new processing steps required. Hence, there is a need to be able to insert a change of data.

So far in the digital photographic stores mentioned, no mention has ever been made of reproducing the whole storage medium, possibly for use in reading machines at other locations than that of the parent unit. However, if the use of photographic digital storage devices could be improved as suggested by correction of all errors in a relatively simple manner, than the scope of their use would undoubtedly require that the whole store be reproducible, thus creating the need for an original master. The combination of being able to change data and have an original master could lead to a feature embodying the deleting and adding of data when preparing multiple copies. If the changeable entry and reproduction of originals outlined to date are indeed possible then

258

one could say that refinements of editing, inspection, and multiple copies of originals have been added to the existent photographic storage techniques which should expand their usefulness tremendously.

b.   The Indexing Problem

Before going into the feasibility of a photochromic up-dating system, it would be well to consider the indexing problem associated with such a system. In this discussion, the problem is one of organization and, in order not to confuse the issue, the photochromic up-dating system will be assumed to have reached the state of an operating device. Indexing here is defined as the task of location, recognition, alteration, and checking of the digital patterns in need of change.

Consider a typical (and difficult) situation which might arise for, say, up-dating the King disc language translator. The complete disc has been perfectly transferred to a photochromic coating. Equipment is available for erasing and writing single marks and transferring the whole store in bulk to a permanent medium.

One correction might require that on track 540 a word requires changing, precisely the 54th entry on track 540. The operator is then required to locate this entry, which is buried within the 30×10^6 bits over-all, and reliably recognize that it is truly the entry sought. Though difficult enough, track 540 could probably be located. However, from that point on things really become difficult. It is not apparent on the disc where one entry stops and the next starts. When the methods for locating the entry sought are considered, one soon finds he requires something akin to the original disc reader which can be accurately stopped at a given spot.

Although the problem as outlined is not impossible to implement, to make it practical for the particular case considered suggests something akin to a research program in its own right. Thus, the photographic

259

memory most likely to take advantage of a photochromic up-dating system is one in which the up-dating concept will have been considered in the original design.

It should not be assumed that all present photographic memories are as difficult to up-date as the one described. In general, however, the bigger the store and the greater the packing density, the more difficult the problem.

The system to be described here will not be concerned with the format of the store or the techniques necessary for successfully performing the indexing operation. Rather, the purpose is to describe the capabilities and limitations of photochromic materials and the associated techniques developed to accomplish this task. Once this capability is known and understood, there is reason to believe that the advantages inherent in such a system will not be overlooked.

c. General Capabilities of Photochromic Techniques

Investigations with the solid-solution photochromic materials have demonstrated that their resolution capabilities are extermely high; indeed, to date, the optical system has set the limit. With a small field, more than 700 lines/mm have been recorded at the photochromic material, the resolution by contrast was somewhere in the neighborhood of 10 percent to 15 percent. The smallest digital photographic marks to date are projected in the new large capacity King disc unit where mark sizes of 1.5 μ are anticipated. It is estimated that marks of such a size could be handled by the photochromic materials; however, the question of sufficient contrast must also be considered. At this time, it seems reasonable to take, as the smallest mark likely to be encountered in a practical photographic store, a square 7.5 μ on a side. This is the size of marks regularly in use in the King disc language translator. Most other photographic systems have marks considerably larger than this. In order to edit, change, or erase such marks, it will be necessary to be able to:

ASD TR 61-70

1) Write such a mark individually

2) Erase such a mark individually

3) Transfer such writings and erasures outlined in (1) and (2) to the photographic medium and compare the resultant marks for resolution, size, and contrast with the original marks.

The first two steps of writing and erasing such mark size has been accomplished. Transfer of information from the photochromic material has also been accomplished for marks of this size by contact printing and projection printing to a photographic medium, and correct arrangement of processing and gamma control in the film have provided a clean transfer of marks compatible in quality to the original. Since these steps can be carried out without serious detriment to the final marks, the basic steps of up-dating and transfer of digital photographic marks have been achieved. All experimental data to date indicate that such transfers are practical.

d. Bulk Transfer of High Density Photographic Stores

Two types of bulk (parallel) transfer have been considered in this program. The first is concerned with transfer by projection imagery through an optical system. The second is concerned with the bulk transfer of data by the simple process of contact printing. These two systems will be considered in turn below.

(1) Projection Transfer. The capabilities of optical systems and photochromic materials acting together for bulk transfer of data from one medium to another is described under "Optical Studies" in part F of this Section. Two modes of operation are possible. The first, the imaging of a stationary object pattern on a stationary image surface, has been studied in this program. The second, which makes use of moving object and image surfaces, also has merit, but has not been studied in the laboratory on this program.

The stationary object-image case is limited in the number of bits which can be transferred in parallel. This is due to the limit in the number of lines,

261

or marks, per field which can be imaged and resolved adequately by an optical system. As can be ascertained from the studies reported in part F, for a reasonably good lens, it is reasonable to assume 1400 lines per field resolution with 10 percent response. This can be reduced to about 600 lines per field in order to maintain a good response. A square field of 600 divided by 1.4 or 430 lines per side can be placed within the 600 line field diameter. Now, assuming a full photographic line per bit (this implies one bit requires both a black and transparent mark), the number of bits which might be bulk transferred in the fashion indicated is $430^2 = 0.185$ megabits. This figure is conservative as it has been found possible to bulk transfer five to ten times this many bits in the laboratory.

However, as the response falls off, it becomes more and more difficult to process the high gamma, high resolution emulsion so as to clip the marks at the right size. Failure to do this results in either the dark marks being larger than the white or the white marks being larger than the dark. This obviously can lead to a read-out problem. The stationary object-stationary image case is considered further as part of the cathode-ray tube preliminary systems study.

The moving object-moving image case results when both the object and image are moved in a synchronous fashion so as to eliminate an image smear effect on the moving photosensitive surface. This is really a parallel-serial mode of operation as the optical system is time-shared by the memory surface transferred during the exposure period. The limit to this mode of transfer is the lines per field (as defined by a square or rectangle to insure equal exposure to patterns tranversing the edges as well as the center of the field). Assuming a square field, as before, the bulk transfer rate is then 600 tracks, where it is assumed that two marks per track are necessary. It is meaningless to attempt to quote a total bit transfer. As before the figure quoted is conservative and could be extended somewhat.

262

It should be noted that extreme resolution is not required of the photo-chromic material for projection transfer. It is quite feasible to use magnification in going from a photographic pattern to the photochromic version. After alteration, de-magnification can be used to reproduce a photographic storage surface of the original dimensions. Writing rates must of course be gauged to the magnification used.

(2) <u>Contact Transfer</u>. The case of contact transfer is actually the case of greatest interest as it requires only relatively simple equipment. Since the transfer is one-to-one, resolution capabilities are quite important in the photochromic material. This type of transfer is considered parallel only, even though it is possible to scan the surface with a light beam as well as to provide simultaneous over-all illumination when transferring the data.

As described in part F of this section, contact printing has been found to be a reliable method of transferring high density digital data from transparencies. The results indicated that it is necessary that at least one of the patterns be placed on a non-rigid backing, e. g. , mylar or cronar. It appears that this allows the non-rigidly backed coating to follow the undulations of the rigidly backed coatings, insuring good contact. A transfer factor about 0. 9 was effected over a range from 100 lines per mm to 600 lines per mm. This means that if the finest patterns discernible are X lines per mm, after transfer the finest patterns discernible are 0. 9 X lines per mm.

What is actually required is a sine wave response transfer function, but this has not as yet been established. Another problem here is that digital pattern transfer back to photographic film is accompanied by high gamma processing (or a clipping of the signal) to give good contrast. Sine wave response is a linear function (measured at low gamma) and is not representative of the case of a clipped signal. The multiple transfer case described in part F was a lower gamma. All these difficulties have

263

not been resolved, but it has been demonstrated that a transfer from a photographic master to photochromic and back to photographic can be made to appear about as good as the original. In this case, the marks were of the order 0.003 inches on a side. Although further studies are necessary before contact print up-dating systems could be termed completely feasible, the system to be described below is certainly within the basic capabilities of photochromic materials.

e. Kalvar Film as the Permanent Storage Medium in a Photochromic Up-dating System

As basic information on Kalvar film is available from the manufacturer,[*] the discussion here will be limited to a brief technical description of Kalvar film before considering its application in a photochromic up-dating system.

Kalvar film is a near-U.V. sensitive film which contains diazo-type material in a transparent plastic medium on a mylar backing. Exposure requirements are quite similar to that of the non-capsular photochromic coatings. Kalvar quotes 0.1 watt-second per square centimeter, but laboratory measurements on this program have indicated approximately twice the sensitivity of photochromic coatings, or 0.16 watt-seconds per square centimeter, which is near enough, considering other factors.

After exposure (which creates a latent image), the image is developed by heating to around 240°F. Heat causes small voids (or bubbles) to form because of expansion of the nitrogen gas released during exposure. Cooling fixes these voids which then act as light scattering centers. When viewed by transmitted light, the scattering centers deflect light from the transmitted beam and appear dark. The main advantage of Kalvar film is that it does not require chemical development. Developing is ordinarily

---

* Kalvar Corporation, 909 S. Broad St., New Orleans 25, Louisiana.

264

accomplished by two seconds contact with a heated plate. Immersion in a heated water bath containing salts to raise the boiling temperature is also possible.

Kalvar high resolution film contains voids from three to five microns in diameter. Since gas diffusion occurs in the film, both exposure and development should be accomplished in the shortest possible time for highest resolution. It is also recommended that the temperature during exposure not exceed 110°F. Recommended developing time is from 1/2 to 2 seconds, and it is determined experimentally. Exposures longer than one minute are considered unrealistic. The coating and mylar backing have almost negligible temperature coefficients. Coating thickness is 10-15 microns.

Kalvar-to-Kalvar prints can be made by clearing the unexposed Kalvar film after development. This is accomplished by simple U.V. exposure and allowing sufficient time for the nitrogen gas to diffuse out of the coating. If viewing does not involve heating (e.g., as in an ordinary projector), viewing can be immediate. Thus, a Kalvar copy can be made from a Kalvar original as soon as the diazo breakdown has progressed sufficiently. Because of similar characteristics, this also applies for a Kalvar-to-photochromic print.

Since a Kalvar-photochromic system would use Kalvar for the permanent memory and photochromic material for the up-dating medium, there would be no requirement for chemical processing and the operations could be carried out in a lighted room (but with the blue end of the spectrum filtered out to keep from destroying the diazo dye in Kalvar). A number of techniques could be used for heating the Kalvar film and this does not appear to be a serious problem.

Experimental studies were carried out using a sample quantity of Kalvar film X-129D, a high gamma, high resolution film still in the development stage. A later request for a low gamma, high resolution film resulted in receipt of a sample of X-129H, but this was received too late to be included in the study.

265

The first tests were run to establish a crucial point, the possibility for a photochromic-to-Kalvar contact transfer. Since photochromic materials absorb in the near U. V., and in fact are written; any attempt to write through them onto Kalvar film with U. V. would not only result in U. V. absorption, but it would also color the photochromic material in previously uncolored regions.

Two approaches were tried with respect to the photochromic-to-Kalvar contact transfer. The first took cognizance of the fact that Kalvar actually was somewhat sensitive out to 440 millimicrons while an unwritten-photochromic coating was transparent in the 400-440 milli-micron range and some written photochromic coatings are partially absorbing in this region. It was not found possible to pass enough energy through even an unwritten photochromic coating in the 400-440 millimicron range to effect Kalvar exposure. This could have been partially due to the blue filters used in that they were not highly transmissive in their pass bands. As noted before, unless a sufficiently rapid exposure is made, the latent image diffuses as rapidly as the diazo breakdown proceeds and this was probably occurring here. This approach might still work, but special laboratory equipment must be set up to insure that sufficient energy density passes through the photochromic coating. At any rate, it has been established that this approach is not readily implemented. Such a condition helps to defeat one of the primary purposes for which the Kalvar-photochromic system was investigated, i.e., a simple, easily implemented, reliable up-dating system.

The second approach was a brute force approach. It was predicted on the possibility for a difference in absorption between the written and unwritten states which could be detected in the transmitted U. V. Again, no exposure was effected on the Kalvar film no matter what technique was tried in illuminating the photochromic with intense U. V. To be sure, this situation always completely colored the photochromic film, but it was the initial differences that were being sought in this transfer method.

266

This problem was discussed with the Dayton group, but they knew of no photochromic material which might fit into either of these techniques. An extremely thin photochromic coating could possibly succeed, but this would introduce many new problems. As of the end of the contract, a photochromic-to-Kalvar transfer had not been effected.

The reverse process, Kalvar (after clearing)-to-photochromic, worked quite well, as was expected. Although good resolution was maintained, the slight diffusion in the transfer process tended to fuse the voids together to give a more uniform image under microscopic examination. With photochromic material, exposure time offered no problem and the quality of the image did not appear to vary, even with minutes of exposure to arrive at the standard density used for viewing.

While the problem of photochromic-to-Kalvar transfer was under investigation, the resolution capability of X-129D film was also under study. The edge spread was found to be just under one micron for a knife-edge test as claimed by the manufacturer. This appears odd as the voids are at least three times this large. However, on examination, the voids are found right up to the edge of the exposed area and tend to make it ragged (under a high power microscope). With other types of tests, where two edges approach each other, rather disturbing effects occur. What in high resolution silver halide would amount to a gradual filling in between the edges with very fine particles, appears in this case as random occurrences of large voids. In other words, a grey scale is accompanied by a very grainy structure. For a digital store where edges are sufficiently far apart, three to four microns or more, there should be no problem. With a pattern of small squares riding on a reference bar, there is a problem in the corner areas where two written edges meet. Relatively large voids can occur at random in these positions.

The reading density can be as high as 3.0 with high resolution Kalvar in a properly illuminated reading system taking advantage of the

scattering properties. In summary, it can be said that from the investigations made on X-129D film, this film meets the resolution capabilities for the packing densities typically used in existing photographic stores as outlined previously. It has not shown itself to be compatible with the characteristics of photochromic materials, and the limited latent image life imposes further restrictions on the techniques and equipment for exposing and developing the images.

As a matter of interest, a photochromic-to-photochromic transfer has been accomplished by contact printing with a visible light pattern from non-light erasable coating P-112 to light erasable coating P-105 which had been previously completely exposed. However, a high sensitivity material such as silver halide is needed to transfer out of the P-105 coating.

The results of the investigations described have led to the conclusion that the permanent medium in an up-datable photographic-type store must have the properties presently exhibited by silver halides. This being the case, high resolution silver halide is considered to be the medium on which the permanent memory is recorded in the following system for up-dating photographic memories.

f. A System for Correcting and Up-dating Permanent Photographic Memories

(1) Introduction. Rather than consider a system for up-dating a specific photographic memory presently in existence, the approach here was to pick an arbitrary photomemory which best illustrates the principles involved in developing a system. It is then a relatively straightforward procedure to adapt the techniques presented to some alternate system.

The description will follow the sequence that would be required in actually proceeding through an up-dating sequence of operations. While it is recognized that the actual photomemory cou. ι be used for data location,

268

it will be assumed that the up-dating is an off-line operation and that the memory could be working on-line with an alternate photographic plate. In other words, it is assumed that the memory contains a file of plates upon which might be contained many hundreds of megabits. The individual plates will periodically go through an up-dating procedure.

As pointed out under the "The Indexing Problem" previously, indexing is a difficult problem and a solution will not be attempted here. It will be understood that by one means or another the actual data in need of change is reliably located. The actual change of data will be made one or a few bits at a time by means of projection transfer. Thus, though basically a contact transfer system, it is actually a hybrid system which makes use of both of the techniques studied under this program - contact and projection transfer.

The methods illustrated may not be the optimum for any particular step in the operation, but they do illustrate some of the care which must be practiced and the pitfalls which must be kept in mind.

(2) Contact Printing. Figures 111 and 112 illustrate the primary features of the contact printing operation. The photographic memory glass plate is loaded into a plate carrier at the main memory file (not shown) with due precautions to minimize dirt pick-up. On being brought to the contact printer, the plate carrier is latched onto the dehydration and cooling chamber and the sliding cover door is withdrawn from the plate carrier.

Using the rubber gloved box, the operator internally opens the plate entrance sliding door and removes the photographic plate and places it emulsion side up on a small table and replaces the door. The clean, pre-cooled, dry nitrogen used to keep a positive pressure on the chamber also provides a blast of air with which the surface is swept clean. When the plate is dehydrated and cooled, the operator, using the rubber gloves, re-moves the door between the pre-cooling chamber and the refrigeration-contact printing chamber. He then transfers the plate to the contact printer, Figure 112, in the refrigeration-contact printing chamber. Emul-sion up, he references the photo plate against the photo plate reference

269
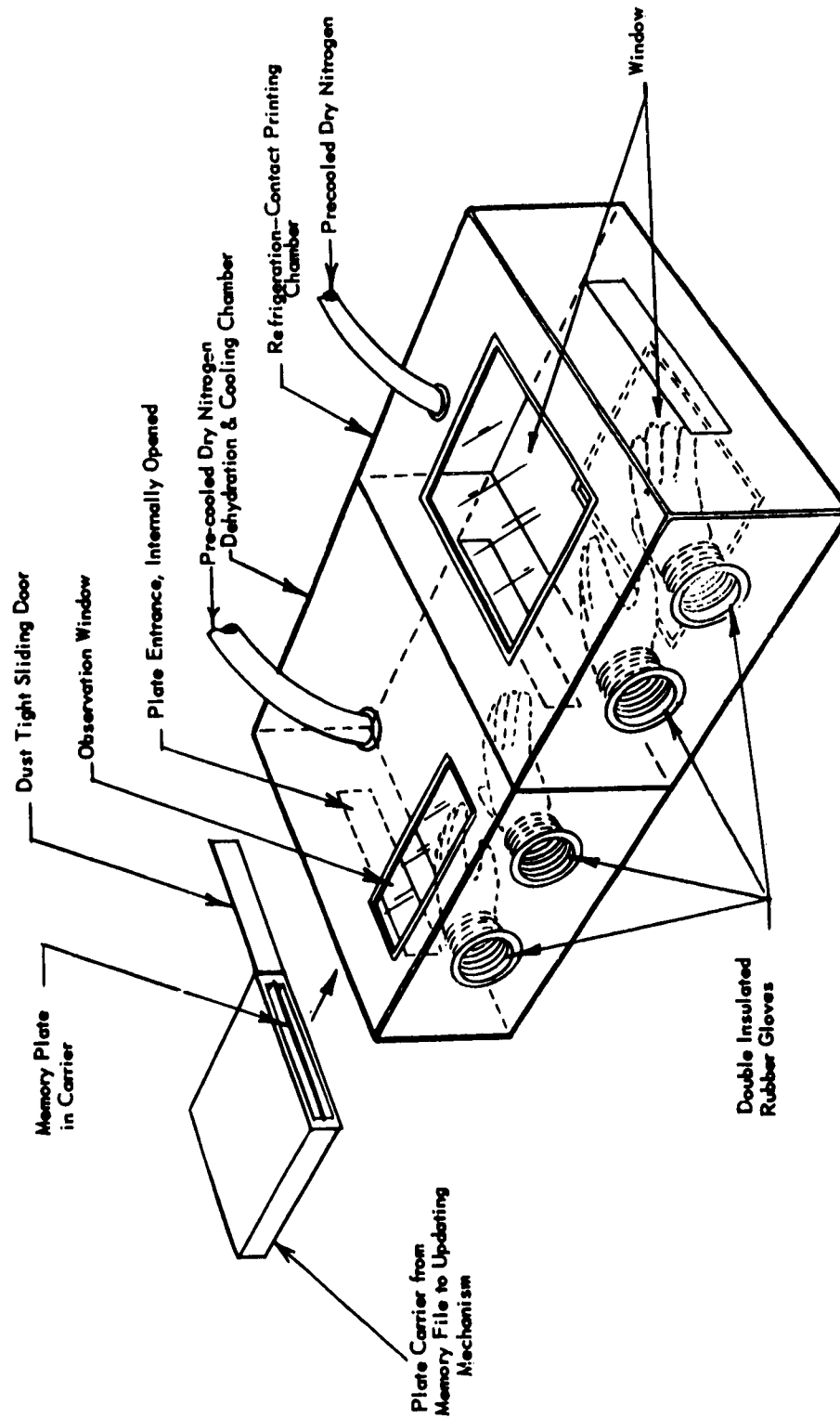
Figure 111. Plate Carrier and Contact Printing Chambers.

Window

Precooled Dry Nitrogen

Refrigeration—Contact Printing Chamber

Precooled Dry Nitrogen Dehydration & Cooling Chamber

Plate Entrance, Internally Opened

Observation Window

Dust Tight Sliding Door

Memory Plate in Carrier

Plate Carrier from Memory File to Updating Mechanism

Double Insulated Rubber Gloves

270
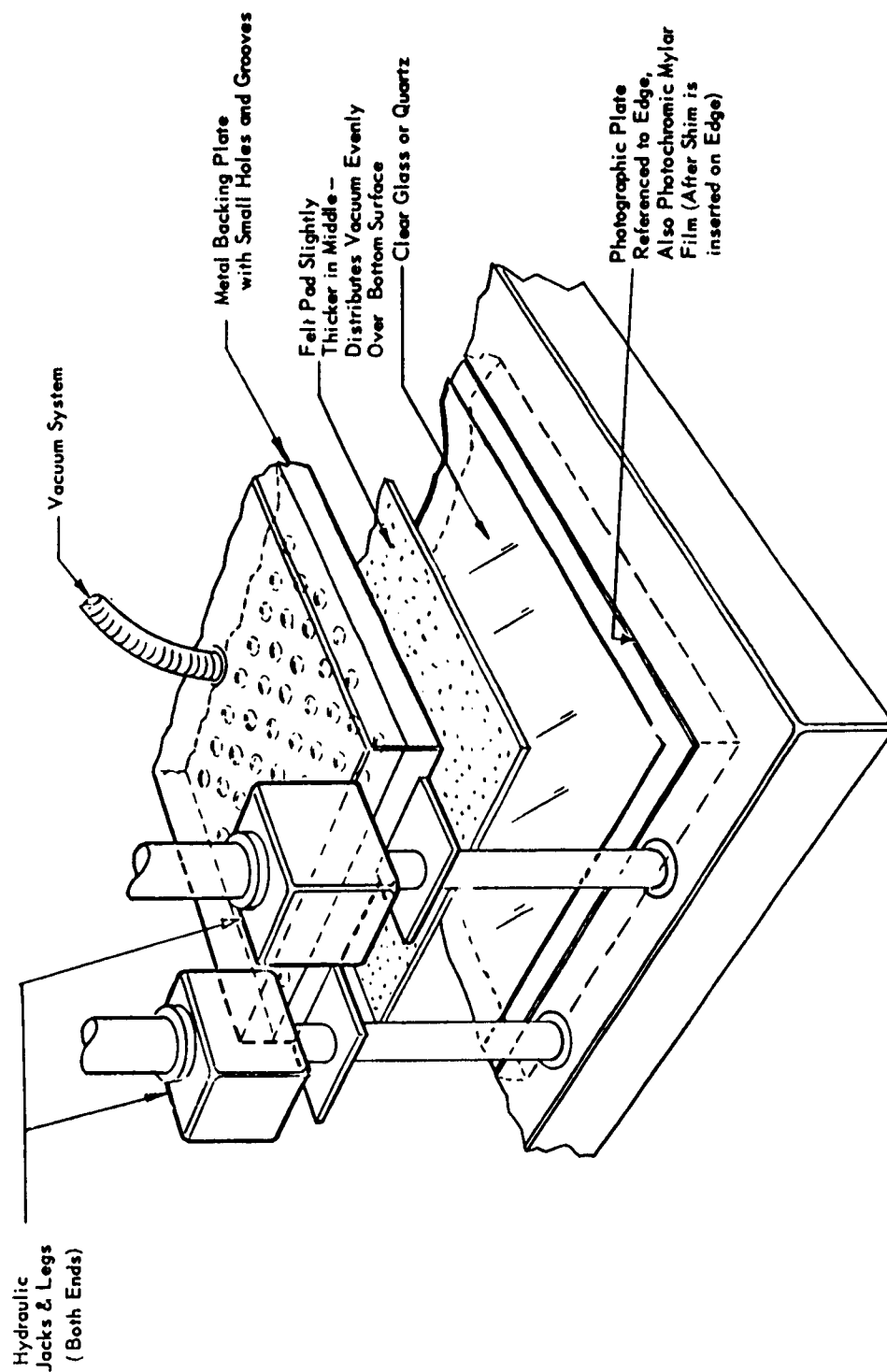
Figure 112. Contact Printer.

Vacuum System

Metal Backing Plate
with Small Holes and Grooves

Felt Pad Slightly
Thicker in Middle —
Distributes Vacuum Evenly
Over Bottom Surface

Clear Glass or Quartz

Photographic Plate
Referenced to Edge,
Also Photochromic Mylar
Film (After Shim is
inserted on Edge)

Hydraulic
Jacks & Legs
(Both Ends)

271

ASD TR 61-70

edges of the contact printer and locks it in position. Next, reference shims are placed on the reference edges and a photochromic coating (on a mylar backing) is placed face down and referenced to the reference shim.

With the photo plate and photochromic film in position, the hydraulic jack is activated so as to make the raised central portion of the stiff felt backing pad make contact with the photochromic film and apply a slight pressure. The operator removes the reference shims to allow the film to move slightly if needed so as not to buckle and separate from the photo plate. The hydraulic jack is again activated and the felt pad is made to apply pressure over the whole recorded surface. The system is now ready for exposure of the photochromic coating.

Exposure is accomplished by sweeping the light from a mercury arc, elongated tube light source across the photochromic plate. This light is located under the chamber and moves along with its associated optical system across the field (e.g., as in the Xerox 914 copier). Because of the motion of the light source, it will be required to produce somewhat more collimated illumination than was required during the laboratory tests with a stationary system. The integrated result of the specularity should be equivalent to that of the laboratory runs. A stationary source could also be used in the system under consideration, but it would most likely be large and unwieldy.

Light source intensity is manually monitored by a light meter and adjusted to the correct level by the operator. Exposure is not critical so this method should suffice.

On completion of exposure, the vacuum system is activated to remove the photochromic film normal to the emulsion surface. There is a tendency to stick, and any side motion would tend to tear and scratch the coatings. Conditions within the chamber should also be helpful in minimizing the tendency to stick together. The operator activates the hydraulic system and removes the photochromic film from the plate. He then takes hold of the film and releases the vacuum.

272

(3) <u>Updating.</u>. The photochromic film is replaced on the holder on which it was placed in the contact printing chamber. The holder contains eight pins which fit into eight holes in the mylar film. Four are spring loaded to provide a slight tension. It is then removed from the chamber by inserting it into a film carrier (in a manner similar to that described previously).

To prevent heating the film to room temperature, the carrier was previously cooled to near or below the refrigeration chamber's temperature. The film is rapidly transferred to the photochromic up-dating chamber shown in Figure 113. The film is mounted on pins similar to those in the carrier and accessed correctly into the field of the viewing microscope.

Using the auxiliary illumination reflected off the beam splitter (this could be Saran wrap which reflects 3-5 percent, is very transparent and does not unduly affect imagery), the operator is able to see the complete field of view. He then inserts the correct mask plate or opens the proper shutter (a few or many of many shutters which cover the field). The use of the proper filters provides only a small increase of illumination in those regions of the field where the mask is transparent and allows for focusing and registration. All this takes place at very low levels of illumination, which is possible because of the viewing method. It does not introduce appreciable erasing of the information over a reasonable period of time. The operator now closes the over-all shutter, puts in an erase filter and opens the shutter for erase. He then closes the over-all shutter, changes to the viewing filter and checks erase. The shutters and/or masks are then changed to the writing configuration and registered and focused.

To write, it is first necessary, most likely, for the operator to adjust the writing lens a fixed amount to compensate for the difference in U. V. and visual focus. He then closes the over-all shutter, places the writing filter into position and shutters the over-all shutter for the correct writing interval. The viewing operation is repeated once again to verify the correct results. If desired, a camera can be swung into the viewing position to record the final results for later verification.

273
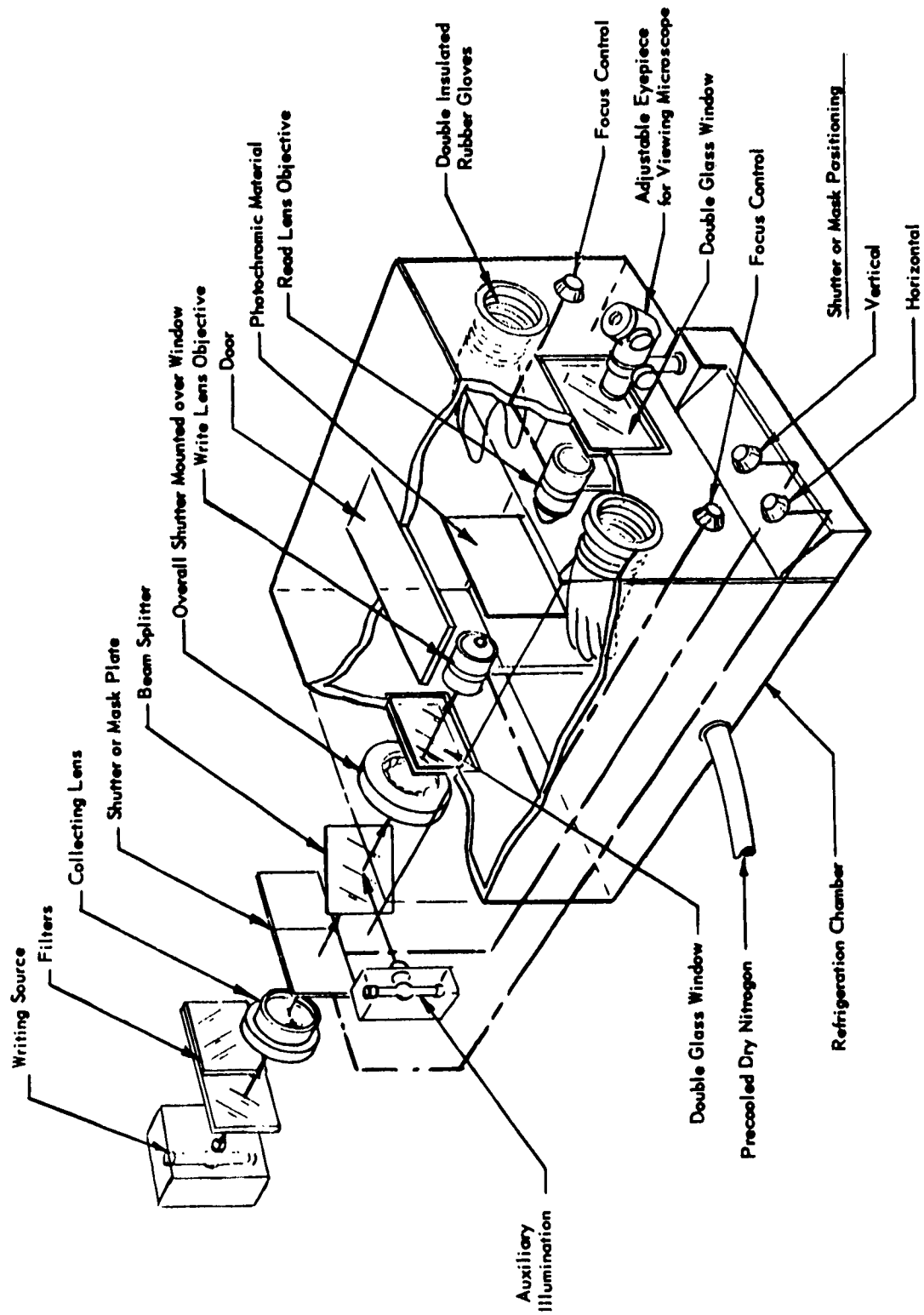
Figure 113. Photochromic Updating Mechanism.

274

The preceding was a rather lengthy description, but a trained operator could perform quite a few up-dating procedures in the time it takes to describe a single such operation. There are advantages to making the procedure automatic, or semi-automatic, but the registration and focusing tolerances could be rather difficult to hold. An operator should have little trouble holding very tight tolerances.

To transfer back to an unexposed high resolution photographic plate, the film is put back into the refrigeration chamber and set up just as before. However, this time the procedure is used to make the film stick to the unexposed plate and the pressure used is considerably higher than before. The sandwich is then turned over so as to have the film on the bottom so the exposing light will pass through it first. The jack pressure is again applied, but not as high as that used for causing the plate and film to stick to one another. The exposing source has its filter changed to the case for exposing film and the film is exposed. The sandwich is once again turned over, pressure applied, vacuum applied and the film and plate are then pulled apart. The plate is removed and processed in a plate processing machine or dark room.

The last procedure described is the weakest link in the system. Other alternatives are the use of only flexible backing media in the main store, use of transparent film with some give at the bottom glass surface of the contact printer (a good one not known at the present time), use of a transparent liquid in a clear very thin flexible container at the bottom surface, and the use of a transparent liquid sealed between the glass surface and the mylar film. The last suggestion appears the best as it would most readily force the film to follow the plate contour when under pressure. It provides some fabrication and operational problems, however, and would require further study before implementation.

Recapitulating, the system described really provides just four basic functions: cleanliness, good contact between the surfaces to be transferred, refrigeration, and projection transfer. Any other system providing these

ASD TR 61-70

functions adequately would also serve the purpose. Although provided, refrigeration is not actually a necessity if the up-dating procedure is not overly lengthy. It could possibly take up to one half hour at room temperature if illumination levels were carefully controlled.

7. A Cathode-Ray Tube Photochromic Memory System

a. Introduction

The second of the two systems selected for systems design is the modification of the system described above as the photochromic analog of the digital storage tube, Figure 104. In order to allow loading of this memory at high effective bit transfer rates, the bulk entry feature of Figure 107 was also included.

There was some concern shown by the personnel of the monitoring agency with respect to the need for mechanically moving the access plates to change from the accessing mode to the read, write, or erase modes of operation, or the reverse. Some thought and discussion was given to this problem and led to the system shown in Figure 114, which does not require mechanical motion during operation of the store within a single field (by the CRT's).

Before proceeding with the following description, it is recommended that the reader re-orientate himself with the material in parts 4-b and 5-a, presented earlier. The information in these paragraphs is pertinent to the present discussion and will be assumed to be known by the reader and will not be repeated in this portion of the report.

b. Description of Operation

Referring to Figure 114, a brief description of the system is in order here. Assume the memory is to be loaded and operated for the first time. First, the memory is loaded by bulk transfer of a whole field in parallel (128 x 128 bits per field), one field at a time. During this

276
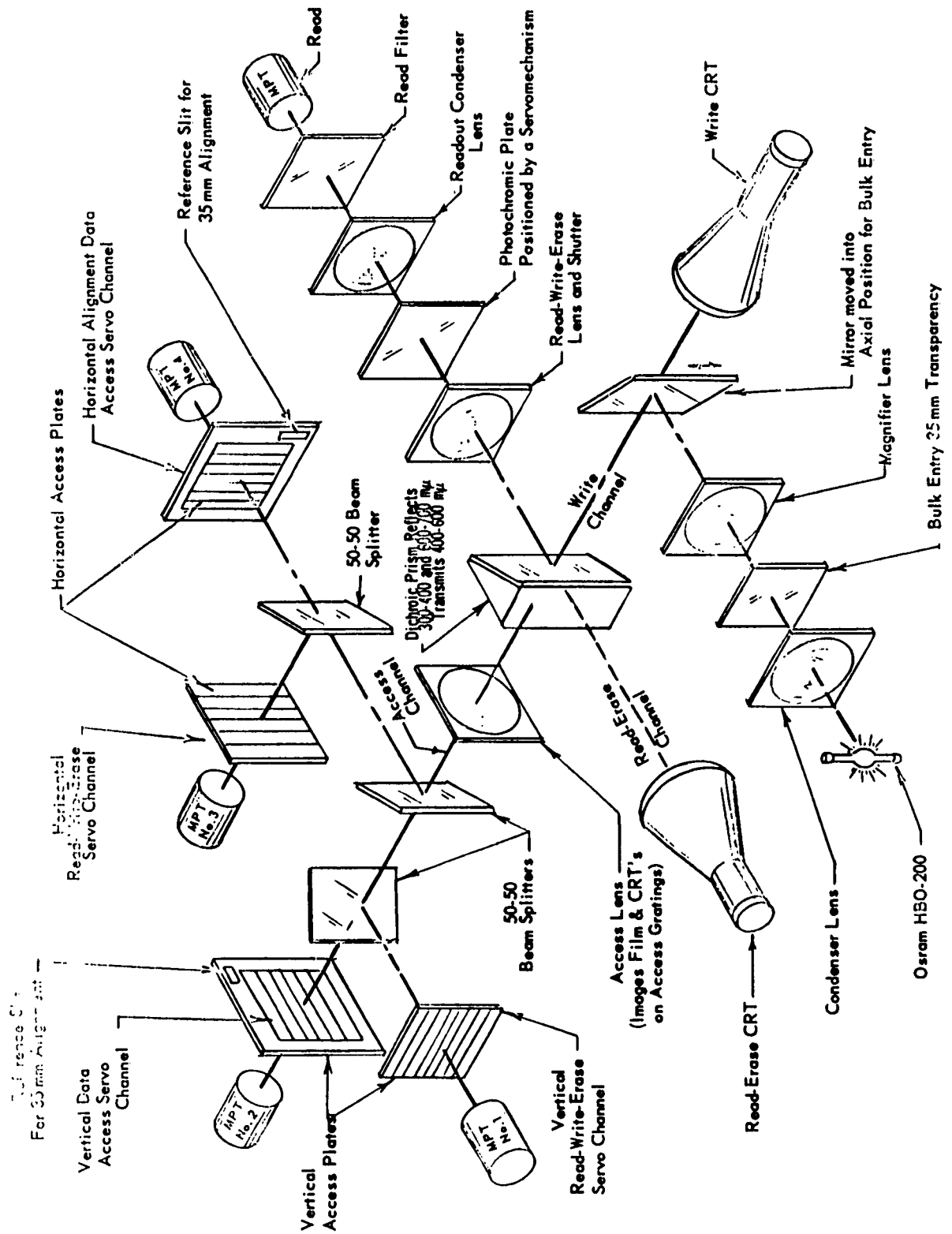
Figure 114. Cathode-Ray Tube Photochromic Memory System.

277

operation, a front surface mirror is used to direct the beam down the "write" channel. As each new 35-mm frame is replaced, the servo-mechanism advances the photochromic plate to an empty position. The writing shutter is not opened for writing until film registration signals from the phototubes indicate that the border registration slits in the access channels are registered with corresponding slits on the film borders.

The photochromic plate is servoed into position and detented into the operating position. Thus, repeatability is a function of the detent mechanism, and absolute position is relatively unimportant. After loading the memory, the mirror in the write channel is removed. Since the 35-mm film and the CRT's are all at the same optical distance from the read-write erase lens, they will all focus simultaneously on the photochromic material (with a properly corrected lens). The magnifier lens serves to make the 35-mm film appear of the same dimensions as the CRT's, thus allowing the use of standard, easily-obtained film and film handling mechanisms. Read-out occurs by sensing the transmitted illumination with the read MPT when in this mode of operation.

Accessing is somewhat different from that for the similar system of Figure 104. Spot control is still maintained by the edge locking technique, but the shift from the access mode to the read-write-erase mode is obtained by electronically switching to the parallel set of access gratings and MPT's which are displaced one effective spot diameter from the first set of gratings and MPT's. A prism dichroic beam splitter is used to minimize the multiple image effect which occurred with the parallel (more or less) plate dichroic filters used in the laboratory studies.

Read-out of the data within a field to permanent film can be accomplished by replacing the read-out MPT with a light source and putting a 35-mm camera and shutter at the bulk entry position for 35-mm transparencies.

The photochromic plate, read-write-erase lens, and read-out condenser lens are all in a refrigeration chamber similar to that shown in Figure 113. In this case, the viewing eyepiece is replaceable with a MPT or a 35-mm read-out camera.

c.   System Component Considerations

(1) The Plate Servomechanism. A serious limitation to a high packing density appeared in the requirement to repeatedly register the photochromic plate accurately for each of the fields on the photochromic surface. The first approach to the servo problem follows.

The block diagram in Figure 115 is one channel of the plate servo system which has received consideration. An array of 25 x 25 fields was proposed with digital counts of x and y gratings located next to the plate to establish which field is in the operating position. Bi-directional counters allow counting from any position in either direction. Photocell channels No. 1 and No. 2 are used to establish a fine position control for holding a closer tolerance in final position. These photocells require the dual grating structure, as shown, to produce the proper directional instruction to the servo amplifier.

The glass substrate is to be a 5 x 5 inch glass plate of 1/8 inch thickness. The inertia is represented by

$$J_G = \frac{L^4}{3} \, pd \, \frac{1}{g}$$

and

$$= \frac{5^4}{3} \times \frac{161 \times 16}{12^3} \times \frac{1}{8} \times \frac{1}{32 \times 12}$$

$$= 0.101 \text{ inch - oz.} / \text{sec}^2$$

where J_G = inertia for the glass plate d = thickness = 1/8 inch

   L = glass dimension = 5 inches g = acceleration of gravity

   p = glass density = 161# /ft^2 = 32 ft/sec^2
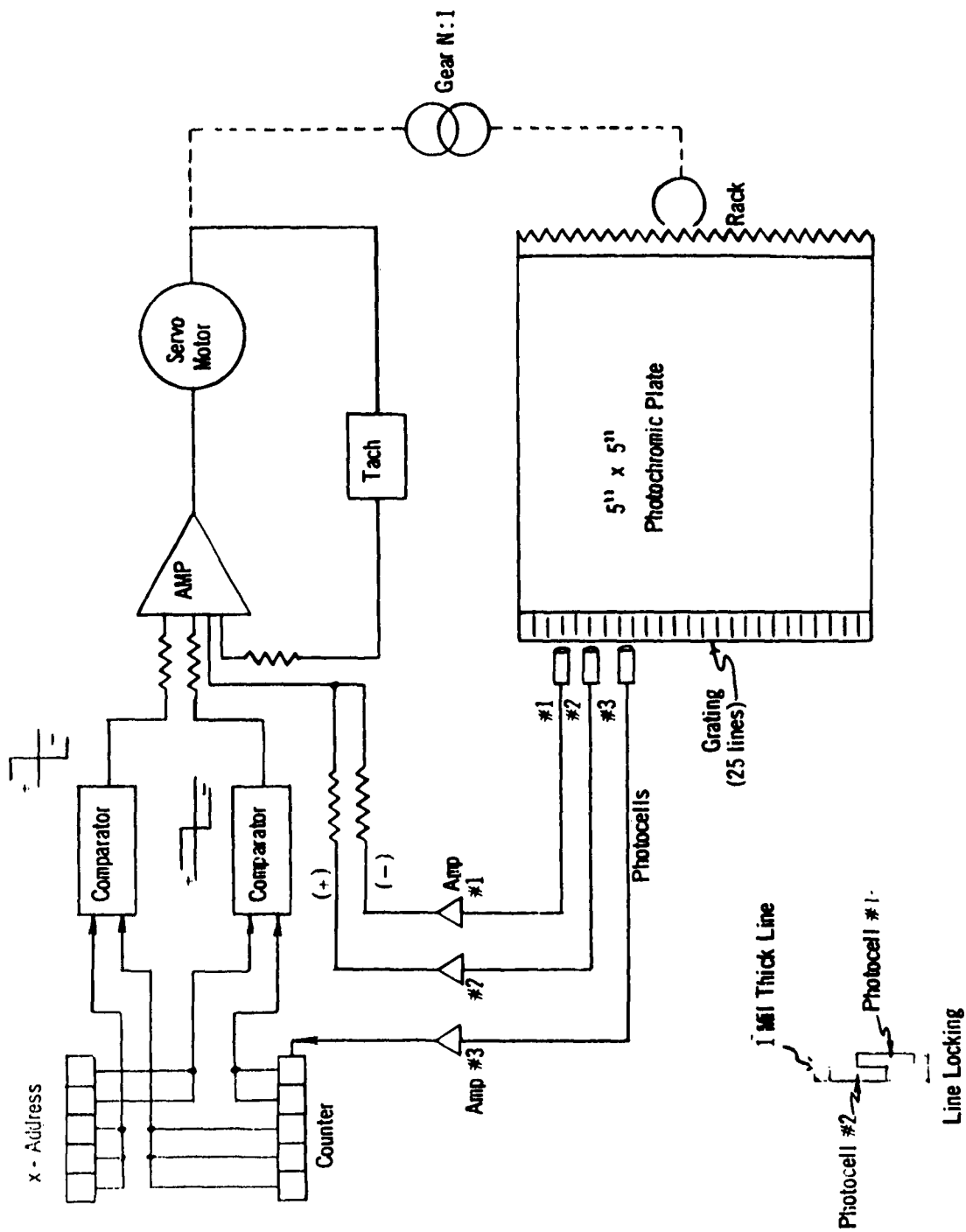
Figure 115. Block Diagram of One Channel of Plate Servo System.

280

A servo motor has been located with the following specifications:

No load speed   4800 rpm

$(\omega_s = 503 \text{ rod/sec})$

Stall torque   2.4 in.-oz. $= (T_s)$

Rotor inertia 5×10^{-5} in.-oz./sec^2

Size   18

Input power   9 watts

Voltage   115V @400 cps

The total inertia is then essentially that of the plate, or $J_{total} = J = 0.001$ in.-oz. sec^2.

The servo will be operating in the non-linear region, i.e.,

$$J \frac{d^2\theta}{dt} = T_s - \frac{T_s}{\omega_s}(\frac{d\theta_o}{dt})$$

for the initial condition that

$$\left[\frac{d\theta_o}{dt}\right]_{t=o} = 0.$$

Therefore,

$$\frac{d\theta_o}{dt} = \omega_o (1 - e - \frac{T_s}{J\omega_s})$$

$$\theta_o = \omega_s \left[t + \frac{J\omega_s}{T_s} (e^{-T_s/J\omega_s} - 1) \right]$$

where θ_o is the angular displacement on the motor shaft.

281

Solving the equation for different values of t, we arrive at the data
(plotted in Figure 116) indicated in Table XXIV.

TABLE XXIV

SERVO RATE OF DISPLACEMENT

t (in sec.)	θ_o (in radians)	Linear Displacement[*] of photochromic plate in inches
0.1	10.6	0.53
0.2	37	1.85
0.3	73	3.58
0.4	114	5.70
0.5	160	7.96

[*]A one inch diameter spur gear is used to drive the rack.

It is seen that the servo positioning time is compatible with the writing
time which will be on the order of one second or so for the bulk transfer.
It is also compatible with the time to write or to erase a few bits by the
cathode-ray tubes. It is quite slow when considering only the read mode
which can be very fast.

A preliminary estimate of the accuracy of the servo system described
above is that it is capable of registration to within one-half of a mil
on reaccess to the same field. This figure required considerable
tightening up; it called for an increase in the basic mark size to insure
reliability.

282
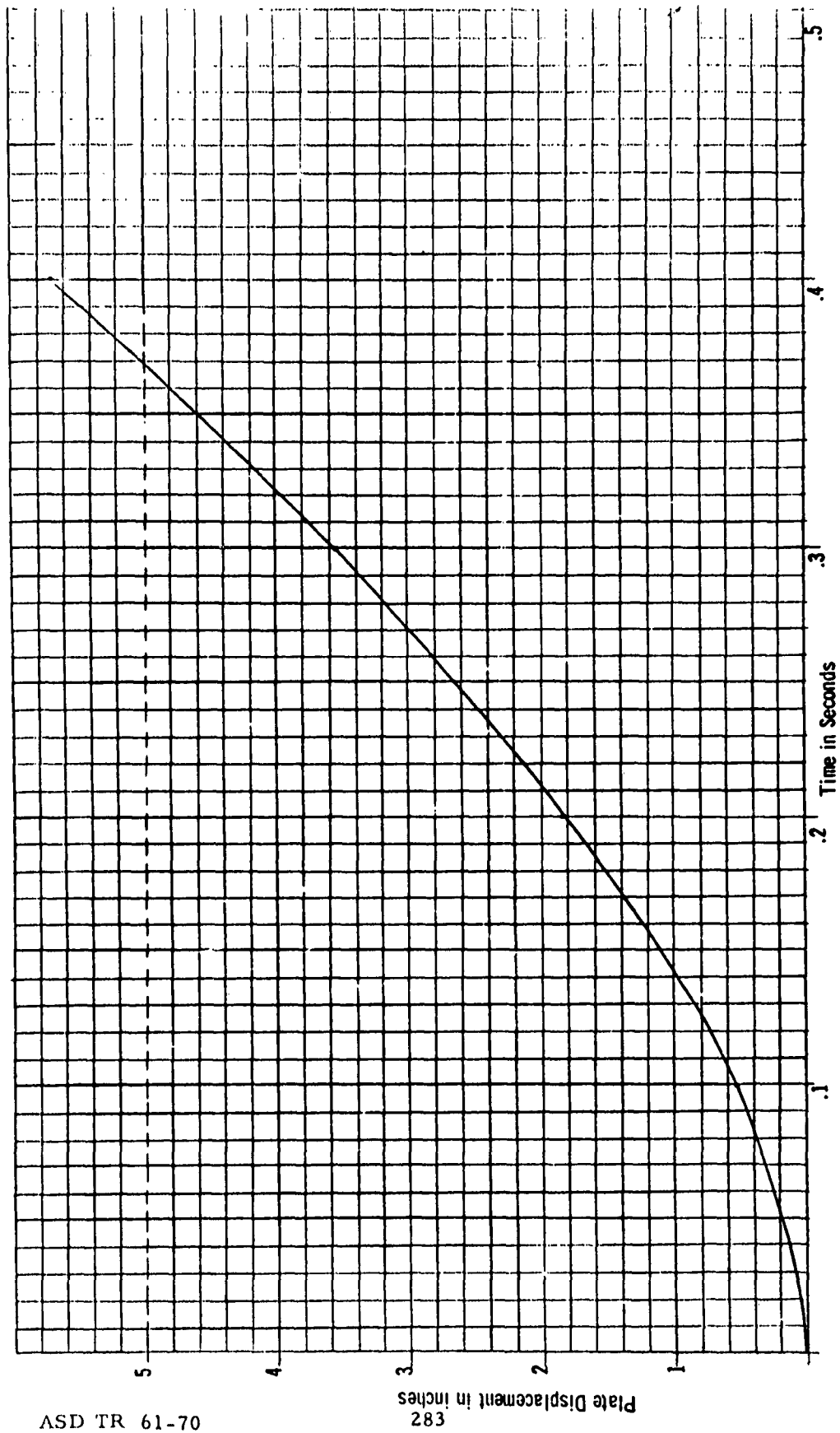
Figure 116. Photochromic Plate Positioning Time.

Time in Seconds

Plate Displacement in inches

The simplest expedient to finer positioning of photochromic plate was felt to be through the use of a detent mechanism in conjunction with the servo described above. At least a five-fold increase in accuracy appears reasonable, or better than 0.1 mil in repositioning error.

(2) <u>Packing Density at Photochromic Plate.</u> The attainable accuracy in repositioning a plate, estimated at 0.1 mil, determines the spot size limit at the photochromic plate. Since this is not meant to be a conservative design, and has not been so far, the spot size on the photochromic material is set at 0.5 mil. With a square field of 256 x 256 equivalent spots, the circular field becomes 0.18 inch. Since the equivalent resolution is 40 lines per millimeter at the photochromic material, and the Simpson lens is capable of much greater resolution, the increase in field size is well within the region of adequate response for this lens, whose full field is at least 0.25 inch. To minimize the flare overlap of fields, the fields will have image free borders of 0.02 inch or the fields will occupy areas 0.2 x 0.2 inch or 0.04 $inch^2$. The total number of fields then becomes, for a 5 x 5 inch plate, effective area 25 $inches^2$, 625 fields. At 16,404 bits per field, this leads to 10,252,500 bits per plate. For comparative purposes, this comes out to be about 410,000 bits per $inch^2$. It should also be noted that such a store could easily be transferred by contact printing, as well.

(3) <u>Light Sources.</u> The light sources included in this device are the 5ZP16, 5AUP24, and the Osram HBO-200 (see Table XXV). Use of the HBO-200 leads to faster writing and less of a specularity problem from the optics in the system. It does not have as great a power supply problem as the HBO-109, in addition.

284

TABLE XXV

LIGHT SOURCE DATA

	HBO-200	5ZP16	5AUP24
Volts	220	27 Kv	27 Kv
Current	4	0.2 Ma	0.2 Ma
Writing Rate - Spots/sec.	- - -	5	5
Spot Size - mils	- - -	10	10
Writing Rate - Field	0.5 sec.	-	-

The value of five spots per second differs somewhat from the data obtained from the detailed CRT studies, but the grosser tests (and under different conditions) gave something of this order. It will be assumed that the tubes are being pushed to their limit (as they are) and frequent replacement is required. It should be recalled that this writing rate does not appear so extreme for the new rotating anode tube. For the case under consideration, however, the tubes indicated shall be retained.

With the 10-mil spots on the CRT's, and the 0.5 mil spots on the photochromic material, it follows that the system will be working at a reduction factor of 20 to 1.

(4) Lenses. The read-write-erase lens is assumed to be the Simpson f/1.6, 3/4 inch focal length lens described in part F of this Section. The access lens is chosen as an f/1.6 lens also, partially to simplify comparison of the light acting on the phototubes in the different channels. This lens works at 1:1 magnification for two reasons; first to keep the spot servo masks and alignment problems to relative coarse requirements,

285

and, second, to allow the capture of light over a greater solid angle such that sufficient signal is available to the servo channels.

The magnifier lens allows use of standard 35-mm film for bulk entry rather than some other not-so-readily available type. This lens magnifies the field of the 35-mm frame to properly register with the spot array structure dictated for the cathode-ray tubes. No tests were run on lenses operated in this manner, but such a lens appears to offer no great difficulties.

Although not shown, condenser lenses are postulated for each MPT. These lenses are arranged so as to image the access lens, or the read-write-erase lens, onto the photocathode surface of each MPT. They have no particular requirements beyond that of standard condenser lenses.

The bulk writing channel condenser lens will probably offer little difficulty with the use of good quality glass and the HBO-200 light source. The mottling effect noted in the laboratory studies is reduced by the use of a source of larger physical size. Unless high bulk transfer rates are required, the use of a quartz condenser is not called for.

(5) Filters and Beam-Splitters. The multiplicity of 50-50 beam-splitters in the beam servo channels serve to channel the light to the individual access plates. The price paid for the electronic jog feature when going from between-spot access to the spots is the loss due to the additional beam-splitters required. A 50-50 beam-splitter can be made to provide about 45 percent of the incident light into each of the channels it is servicing. Although multiple reflections can occur between the surfaces of the beam-splitters, it is predicted that they can be kept to reasonable values for the accessing channels.

In the case of the U.V.-visible dichroic beam-splitter, a beam splitting prism is proposed to minimize multiple reflection effects which could be integrated by the light integrating properties of the photochromic

286

memory plate. The dichroic filter breaks the spectrum into a U.V. region (300-400 mμ) and a red region (600-700 mμ) which reflect, and a visible region, (400-600 millimicrons) which is transmitted. These spectral bands are compatible with the required characteristics of the photochromic material and light sources for providing their various functions. A read filter is provided for removing the 400-500 mμ illumination from the reading beam. This leads to a higher contrast read signal output.

The write channel mirror is an optically flat front surface mirror and should offer little difficulty.

(6) Multiplier Phototube Considerations. Sufficient energy must reach the access multiplier phototubes for correct operation of the servo systems.

The signal-to-noise ratio at the output of the MPT's defines the accuracy of the servo system. Noise will cause the spot to fluctuate in position.

The ideal transfer characteristic of a spot traversing the edge of a line on an access plate can be represented by the following:
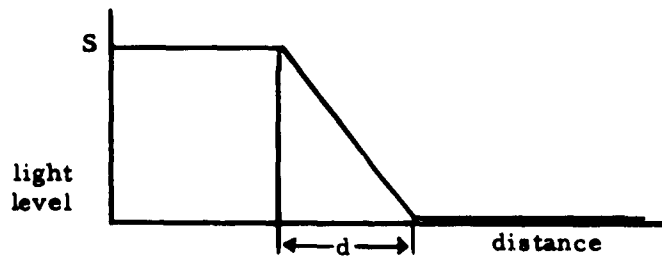
where   S = the change in signal obtained when going from on a line to off of it,

d = the distance over which the system is in a transition from the white to black regions and is equal to the diameter of the spot (idealized).

287

To achieve edge locking the system will attempt to settle midway up the ramp. Noise on the signal will cause the apparent mid-point to shift displacing the spot.

The displacement caused by noise can be represented by the following:
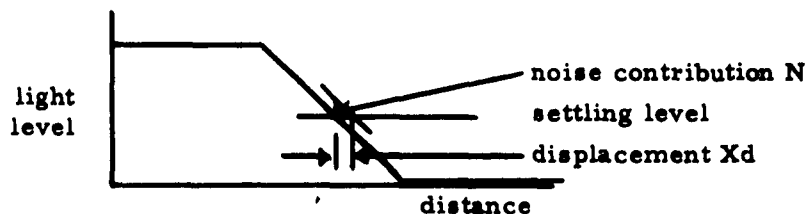
where N = the noise

d = the diameter of the spot

X = the displacement expressed as a percentage of the spot diameter.

The displacement then can be related to the signal-to-noise ratio by use of similar triangles.

$$\frac{N}{Xd} = \frac{S}{d} \text{ or } \frac{S}{N} = \frac{1}{X}$$

In the case of a gaussian spot the slope at the mid-point of the ramp is 1.6 times S/d[*]. Therefore, the signal-to-noise ratio of 1/1.6X is required to register a spot within Xd.

Noise at the output of the PMT's will be 80 percent shot noise. Equation 1 expresses this noise.

---

[*] Bell System Tech. Journal, March 1959, p. 430.

ASD TR 61-70

$$\bar{i}_n^2 = 2e\bar{i}\Delta F \qquad (1)$$

Equation 2 expresses the total signal-to-noise ratio.

$$S/N = \frac{0.8\sqrt{\bar{i}}}{\sqrt{2e\Delta F}} \qquad (2)$$

where $\bar{i}$ = the average photo current

ΔF = the bandwidth

e = the charge of an electron

In order to have the required registration accuracy Equation 3 must then be satisfied

$$\frac{1}{1.6X} \geq \frac{.8\sqrt{\bar{i}}}{\sqrt{2e\Delta F}}$$

or

$$\bar{i} = \frac{1.95 \times 10^{-19}\Delta F}{X^2} \qquad (3)$$

Since the sensitivity of PMT's, S-11 response, is 0.056 amps per watt, then,

$$\overline{W} = \frac{\bar{i}}{0.056} \geq \frac{3.48 \times 10^{-18}\Delta F}{X^2}$$

Approximately 20 percent of the light will be lost in the beam-splitters if dichroic beam-splitters are used. Another 20 percent of the light will be lost in the access lens. The total light entering the access lens must then be

$$\overline{W} \geq \frac{2.18 \times 10^{-17}\Delta F}{X^2}$$

289

This wattage is required at the mid-point of the ramp. Therefore, twice as much is required at the maximum level.

$$\overline{W} \geq \frac{4.36 \times 10^{-17} \, \Delta F}{X^2}$$

The bandwidth required to track an edge when reading is 20 kc or 62.8×10^3 radians. The spot should be registered to within a tenth of a diameter or better; therefore, $X = 0.1$. W must then be greater than 2.7×10^{-10} watts.

The wattage available is the product of the energy of the spot, the percentage of the energy gathered by the access lens, the percentage leaving the central dichroic beam-splitter, and the percent off the peak of the PMT's S-11 response.

If the dichroic beam splitter passes 400-600 mμ, 20 percent of the energy of the 5ZP16 CRT will pass through the beam-splitter and 15 percent of the 5AUP24 CRT will be reflected.

Therefore, the P16 spot will have a brightness of 7 watts/cm^2 - steradian and the P24 spot will have a brightness of 9.5 watts/cm^2 - steradian to the access system. A spot size of 0.025 cm and an f/1.6 access lens used at 1:1 magnification will yield 2.2×10^{-4} watts of 400-500 mμ light for the 5ZP16 CRT and 2.9×10^{-4} watts of 600-700 mμ light for the 5AUP24.

The S-11 response is at its maximum in the 400-500 mμ region; therefore, all 2.2×10^{-4} watts from the 5ZP16 are useful. This is a factor of 10^6 greater than that required.

The S-11 response will be down to five percent in the 600-700 mμ region so that the useful wattage is 1.5×10^{-5} watts for the 5AUP24 which is 10^5 greater than required.

(7) **Refrigeration Requirements.** For operation over extended periods of time (e.g., one year) the operating temperature is specified as -40°F.

290

This temperature can be maintained by a refrigeration unit of the home freezer type and requires no special care or treatment.

(8) **Beam Servo Masks.** The beam servo masks are best made by photography on 4 x 5 inch glass plates. In order that they all be the same, a master plate can be made from which contact plates can be produced for the working memory. The relatively coarse structure of these plates (10-mil lines) offers no foreseeable manufacturing difficulties.

(9) **35-mm Film Handling Equipment.** For many applications, it appears as if an automatic 35-mm feed mechanism would be advantageous. Therefore, it is proposed that single frame advance film handling equipment be used. This can be purchased with an accuracy in registration of 0.2-mil from frame-to-frame. With this mechanism, the operator could manually check registration with the slits in the access plates, after loading a reel of film, and thereafter proceed to step through the loading cycle at the maximum rate of loading.

An additional feature which would be easy to implement would unload the memory, field-by-field, onto 35-mm film by replacing the read filter and phototube with a collector lens, light source and shutter. Of course, contact print unloading is also feasible as in the first system described.

d. General Discussion of System

Before proceeding into a more detailed discussion of the system just outlined, a brief comment on the philosophy behind the present systems design appears warranted. The cathode-ray tube system effort was undertaken at the direction of the personnel of the monitoring agency. It was felt that the ultimate potential of systems employing mechanical accessing were too limited and that mechanical wear and breakdown were serious problems in such systems. In line with this approach, objection was raised to the mechanical "jog" feature described previously (Figure 104), but the servo-to-a-field mechanical servomechanism appeared tolerable.

291

The original system as shown in Figure 104 was felt to include those features which made presently available CRT's most compatible with photochromic materials. Fortunately, as shown above, the use of the 1:1 magnification system in the accessing channel provided sufficient light to allow the elimination of the mechanical means for accessing between the address seeking and the read-write-erase modes of operation in the access channel. The colored nature of the photochromic materials is such that the light used for accessing would not be useful for the read-write-erase operations. Thus, the rather unusual condition occurred where light used for accessing did not prove detrimental to the operation of the main memory channel, either in signal-to-noise ratio or in packing density (by requiring a specific type of memory format). Within a field, the reading rate is determined by the capability of the CRT control circuitry and signal-to-noise considerations of the readout phototube.

The primary disadvantage of the system proposed is related to the registration problems at the photochromic plate. The magnification of the system with respect to the other components, bulk transfer, CRT's and accessing, makes their alignment and tolerances much less critical. Another disadvantage is related to the predicted writing and erasing speeds. The quoted rates are conducive to rapid phosphor fatigue and slower rates appear in order for many applications.

The advantages of bulk transfer have been discussed previously. The ultimate potential of a system with this feature seems great. However, it must be recognized as such during the systems application study or it will, most likely, prove to be of little advantage in the field.

The system study described has not been as extensive as originally intended, but it was felt that the time would be more profitably spent on the other areas which have received study. This was due both to manpower limitations and to the rather all-encompassing nature of photochromic memory research with respect to the various scientific and

technical disciplines involved. Since it had been indicated that there would be no attempt to construct the device just described, little was to be gained by resorting to a complete system design which, as can be deduced from the above description, requires nothing more than state-of-the-art electronic circuitry. The additional results obtained in the other areas of research activity appear to have fully justified this approach.

The preliminary specifications for a CRT photochromic memory are given in Table XXVI, which represents a revision of data given in Table XIX.

TABLE XXVI

CRT-PHOTOCHROMIC MEMORY SPECIFICATIONS

Capacity (per 5 x 5 inch plate)	$\sim 10^7$ bits
Random access (To a field)	~ 0.2 sec
Access within a field	0.001 sec
Packing Density	~ 400 K inch^2
Write-Erase Speed-Rapid Phosphor Fatigue	5 bits/sec
Write-Erase Speed-Recommended	.1 - 1 bit/sec
Switching Life-Photochromic Plate	1000 cycles
Read-out Rate, Maximum	10^5 bits/sec
Write CRT	5ZP16
Read-Erase CRT	5AUP24
Photochromic Plate Servo	25 x 25
x-y Positions (Detented)	

293

TABLE XXVI (Continued)

CRT-PHOTOCHROMIC MEMORY SPECIFICATIONS

Phototube Photocathode	S11
Photochromic Material	P-113
Light Source, Bulk Transfer	HBO-200
Write-Erase-Read Lens	Simpson f/1.6 fl. 3/4 inch
Temperature	-40°

294

SECTION V
SUMMARY, CONCLUSIONS, AND RECOMMENDATIONS

A. SUMMARY

The work undertaken on this program has properly placed the greatest stress on the determination of the properties of photochromic materials for use in a digital memory system. Both positive and negative results were obtained during this investigation. On the negative side, the sensitivity of photochromic materials, about 1/3 watt-second per square centimeter in general, was found to be a number of orders of magnitude less than that required. More important, photochromic materials were found to have a limited dynamic switching life which automatically limited them to special purpose applications. Temperature characteristics, though not what was desired, were found to be compatible with relatively simple environmental equipment.

On the positive side, resolution capabilities of photochromic coatings were found to be optics limited in the non-capsular coatings. This also provided a very great improvement in the optical quality of the photochromic coatings. The success of contact printing with the resolution obtained in the experimental studies is felt to be a major achievement. Because of the basic simplicity of the operation, this is more of an achievement in the recognition that it can be done reliably than in any great technological breakthrough. It is doubtful that the contact printing studies would have been carried to their present state if photochromic coatings had not been available. The ease with which high resolution micro-imagery can be handled with these coatings can not be overemphasized.

295

The work on light sources did not uncover a source that was capable of switching photochromic materials continuously at high speeds. The laser, studied briefly at the very end of the contract, has some promise in this respect, but, at the present time, no known laser has the required characteristics. The cathode-ray tube was found to rate favorably in brightness as compared to all of the sources investigated except the high pressure mercury arc. The phosphor burn problem, however, is a severe one and is difficult to overcome.

Light shutters were found to suffer from many drawbacks. All of the shutters which do not actually turn off the source, or block it completely by an opaque housing, were found to be "leaky." That is, low flare and scattered light could be integrated by a light sensitive material causing it to become completely exposed. The ultrasonic light shutter, one of the latter type of shutters, was investigated extensively for possible high-speed shuttering service. Because of it's modest power requirements and capability for continuous operation, it was the one of greatest interest. Ordinary camera shutters were used when the low-speed limitation of the material was fully recognized.

With the advent of the high resolution, non-capsular coatings, the field and resolution capabilities of the optics became problems of much greater severity than they had been previously. Rather detailed studies were carried on late in the program with respect to determining these capabilities.

The original systems studies were found to be completely unrealistic. These were replaced later in the program by systems compatible with the characteristics of photochromic materials. A method was developed for achieving high transfer rates with essentially slow-speed photochromic material. This was termed bulk transfer. It related to the optical transfer, in parallel, of a full field of information, or a whole memory (by contact printing). Of the systems

296

developed, most of them appear of greatest use as quasi-photographic memories capable of periodic up-dating, but with low rates of up-dating activity.

B. CONCLUSIONS

There are a number of general conclusions to be drawn from this research program. The first is that, in spite of certain superior characteristics shown by the photochromic material, it is tru y a medium for a special purpose memory only. This will remain the case until the problem of fatigue is overcome. It would be most properly used in a very low activity digital store, or in one which is essentially an up-dateable photographic-type memory. The concept of bulk transfer and the use of photographic "slave" memories seems to be a powerful concept, intuitively speaking, but no specific applications have been uncovered.

Another conclusion to be drawn is that the only "non-leaky" shutter capable of high-speed, continuous operation is a directly switchable source. With the limited capabilities of the cathode-ray tube, this appears feasible only as a laser which can be pulsed at a high rate, or a continuous laser capable of 100 percent amplitude modulation. In lieu of a laser, the high pressure mercury arc offers the highest writing rates over extended periods of time.

With the exceedingly high resolving power demonstrated by photochromic materials, and with the extreme ease of handling, there are undoubtedly numerous applications for these materials; for example, in display systems and photographic systems. In practically all cases, however, the optical systems will have to be designed with the photochromic medium in mind and high energy densities must be provided to achieve the required operations in reasonable times.

297

ASD TR 61-70

C. RECOMMENDATIONS

The following recommendations for future research on photochromic technology, for application to data processing, are based upon the results detailed in the final report:

1) There is a need for further system studies on the potential use of photochromic techniques for generating and up-dating high-density photographic digital stores. Significant over-all savings in cost as well as improved system performance appear to be possible.

2) There is a need for a research program to be undertaken to develop a LASER which would be compatible with the spectral and energy requirements of photochromic materials.

3) There is a need to conduct research on various aspects of photochromic materials in parallel with any future system and application studies. Such research would include work on the detailed photochemistry of photochromic reactions, the fatigue problem, the quantitative relationship of the effect of ambient temperature upon the switching characteristics of photochromic materials, and chemical techniques for reproducibly making high-quality solid-solution photochromic films.

298

APPENDIX I

AN EARLY PAPER ON
THE NCR PHOTOCHROMIC CHEMICO-OPTICAL SWITCH
AND ITS
POTENTIAL APPLICATION
TO
COMPUTER STORAGE SYSTEMS

Research and development of two-state devices (flip-flops) has been an integral part of the development of electronic computers and data processing equipment. At the International Symposium on the Theory of Switching held at Harvard University[1] in 1957, it was pointed out that major advances in the science of computing technology would be highly dependent upon the development of better two-state switching devices. Advanced laboratories in the computer field have concentrated upon broadening the base of switching research to include more physical and chemical phenomena. Vacuum tubes have become relatively obsolete in computer design, having been replaced by various solid-state devices such as transistors and magnetic cores.

An entirely new approach to two-state switching devices is the photochromic chemico-optical switch[2-4]. This development originated in the Dayton research laboratory of The National Cash Register Company. The NCR chemical switch and storage system is a combination of two company developments: micro-encapsulation of liquids and a new class of light-sensitive dyes.

A. ENCAPSULATION AND NCR PAPER

The NCR micro-encapsulation process and subsequent development of NCR paper (see Exhibit) resulted from the need for a neater and simpler office duplicating process to replace carbon paper methods. Years of fundamental research in colloid science were required to perfect, on a large commercial scale, the very closely controlled emulsification process used.

The basic principle is to coat or encapsulate tiny oil droplets with a gelatin-like material. Size and stability of the resultant capsules can be very closely controlled. (Technically, the name for this technique is "coacervation") Figures 117 and 118 are photomicrographs of actual capsules.

Dependent upon the desired application, size of capsules can range from one-tenth micron to one-half centimeter in diameter. Rupture stability of the capsule wall can be controlled from a fraction of a psi to several hundred psi. Permeability of the capsule wall to vapors can also be controlled. In essence, then, capsules can be considered as "liquids in the solid state" which can be handled like powdered materials.

B. LIGHT-SENSITIVE DYES AND THE PHOTOCHROMIC CHEMICO-OPTICAL SWITCH

During the development of NCR paper considerable research was conducted upon organic dyes and color reactions. Out of this work was discovered a new family of photochromic materials. Chemically, these are materials which exhibit reversible absorption effects upon exposure to electromagnetic energy[5,6].

The absorption of electromagnetic (radiant) energy by molecules, within the ultraviolet and visible regions of the spectrum, is a combination of the rotational and vibrational effects produced by the molecular absorption of photons. These effects in turn are superimposed upon by electronic

300

WHAT IT IS!

"NCR Paper" is a revolutionary new product based on a chemical system developed after many years of work by the Research Laboratories of The National Cash Register Company at Dayton, Ohio.

Colorless chemical coatings on the paper itself eliminate the need for carbon paper. The normal pressure or impact of inscribing on the top sheet automatically reproduces data on subsequent sheets.

The system can be used for making handwritten, typewritten or machine printed copies.

HOW IT WORKS!

"NCR Paper" makes use of the reaction between two different chemical coatings which are applied to the paper. The bottom side of the first sheet in a business form is coated with one chemical and the top side of the second sheet is coated with another chemical

When someone writes or types on the first sheet, the two chemical coatings are pressed together. The reaction between the two instantly reproduces on the second sheet the data that is inscribed on the first sheet. A similar reaction takes place between the coatings of the remaining collated sheets.

This system is protected by United States and foreign patents

---

VALUES OF "NCR PAPER" (no carbon required)

PROVIDES SHARP, CLEAR COPIES. The number of sheets is greatly reduced by the elimination of carbon paper, resulting in sharp, clear copies

SMEAR AND SMUDGE RESISTANT. Unlike prints from carbon paper, copies on NCR Paper are smudge and smear resistant.

SOIL FREE "NCR Paper" will not soil hands, clothing or other objects; the color reaction only takes place when the chemical elements are in direct contact with one another.

SAVES TIME, ELIMINATES CARBON PAPER DISPOSAL. Elimination of extra carbon tissues saves both time and effort in handling and collating, and because there are no extra sheets of carbon, there is no problem with their disposal.

PROTECTED BY U. S. & FOREIGN PATENTS
OF THE NATIONAL CASH REGISTER CO.
DAYTON, OHIO. U. S. A.

Topside of this sheet is coated with clay-like material and underside is uncoated.   A-229
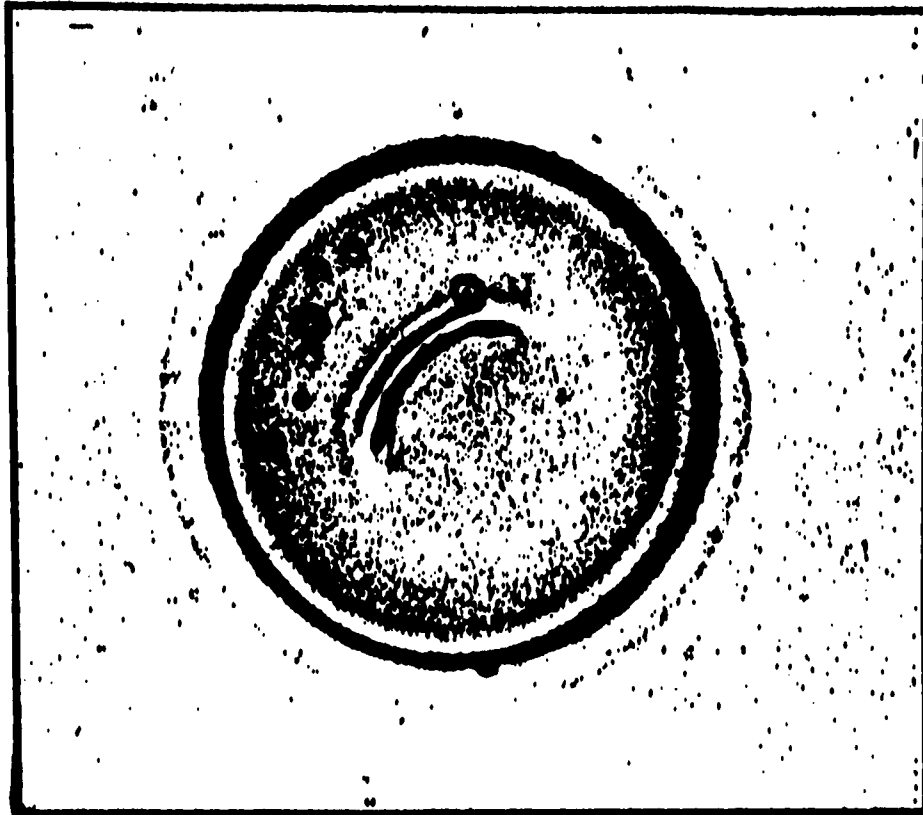
EXHIBIT. Samples of NCR (No Carbon Required) Paper.

301

ASD TR 61-70

Figure 117. Photomicrograph of Randomly Distributed and
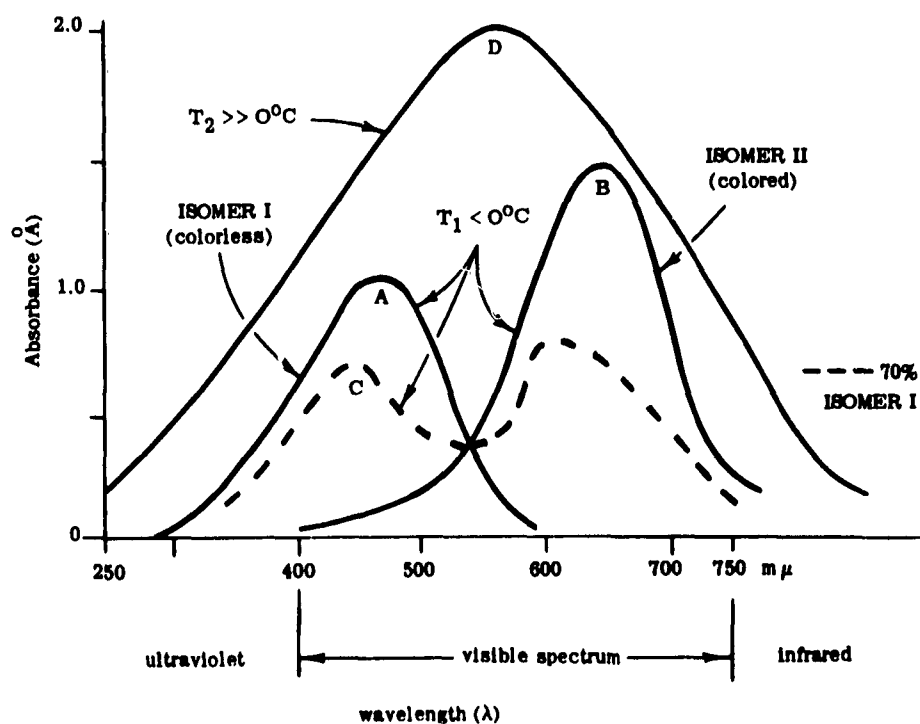Agglomerated Capsules (particle size approxi-
mately 15 microns).

ASD TR 61-70

Figure 118. Photomicrograph of a Single Encapsulated Oil Drop
Showing the Transparent Gelatine Capsule Wall
Structure (capsule size approximately 30 microns).

303

vibrational energy level changes. All three effects are additive in a complex manner which spectrally can be resolved for only a few simple gases. Spectra of molecules in solution are further complicated by "damping" effects or hindrances caused by inter-molecular interferences. This results in a spectral absorption band which is generally smooth and reasonably symmetrical with a shape approaching a probability curve. Combination of molecular states or absorption centers results in unsymmetrical or irregularly-shaped bands (Figure 119).

Curve shape and resolution of spectral bands depends upon many factors (Refs 5, 6). Reproducible results are only possible under precisely controlled experimental conditions. Good instrumentation techniques can usually effect improved resolution. Often lowering the temperature at which the spectral bands are measured will improve resolution.

Photochromic materials require considerable dilution in order to accurately measure their absorption bands. Thus, solvent and solution effects are most important experimental variables. Solvent effects may be induced effects or may be the direct result of chemical reaction. Polar solvents tend to react with the measured material whereas nonpolar solvents are in general non-reactive but limited in their ability to dissolve the complex photochromic materials. Trace quantities of additives or impurities in the solvent can affect the spectral band considerably. Other factors requiring careful control and measurement are concentration and temperature. Solution effects are often interpreted as physical effects and result in only minor shifts in spectral bands. These effects result from changes in refractive indices, dielectric constant, and other physical properties of the solvent.

Considerable influence can be exerted upon the spectral character and properties of photochromic materials by chemically altering their molecular structure and composition. This has been done in various ways by standard organic chemical synthesis techniques. In recent years several research

ASD TR 61-70

Figure 119. Generalized Absorption Band Spectra of a Typical Light Sensitive (Photochromic) Dye in Solution.

1) Curves A and B are for solutions containing only pure isomers.

2) Curve C is for a solution containing a combination of the two isomeric (molecular) forms.

3) Curve D illustrates the influence of temperature on the resolution of component structure in absorption ba ls.

305

papers have discussed the chemistry of photochromic dyes. (An example is the work of Brode and his co-workers (Ref. 7) on indigo dyes.)

The composition of the NCR photochromic materials has not been disclosed though public demonstrations have been performed to show what they can do in conjunction with encapsulation techniques. A sheet of paper is first coated with transparent capsules containing a colorless solution of one of the photochromic dyes. Next, the coated paper is exposed to a bright short-wave blue light. The paper reacts by turning dark (blue) wherever the incident light radiation strikes it. Exposure to a second light source of longer-wave yellow color promptly returns the dark portions of the paper to their original colorless state.

Basically, the effect caused by the incident light radiation is the excitation of the photochromic dye molecule from its ground state, colorless form into its excited state, colored form. These two molecular forms can best be described as geometrical isomers. Upon being excited the two isomeric forms oscillate back and forth from one state to the other. From the absorption curves in Figure 119, it can be seen that each isomer has a maximum absorption of radiant light energy over a relatively narrow wavelength. Within this particular wavelength region only one isomeric form is stable, the other being unstable.

C. POTENTIAL APPLICATION OF THE NCR PHOTOCHROMIC CHEMICO-OPTICAL SWITCH TO REVERSIBLE BISTABLE STORAGE

From the preceding discussion it can readily be seen how a two-state, reversible chemico-optical switch can be effected by combination of encapsulation techniques and the new family of light-sensitive dyes. Surfaces other than paper, such as glass or plastic, can be coated with a uniform thin film of transparent capsules containing a suitable photochromic dye in solution. Such a surface would then represent the chemico-optical analog of magnetic surface storage devices such as tapes and drums.

306

"Writing" is done by scanning the surface with a discrete light beam of the proper wavelength to produce only the stable colored state. "Erasing" would result from scanning with a second discrete light beam of the appropriate wavelength to return the photochromic dye to its stable colorless form.

In order to be useful in computers this stored information -- the discrete colored patterns on the surface -- must be "read". Theoretically, this can be accomplished by scanning with a third discrete light beam of a "neutral" wavelength. This "neutral" light beam would have an energy content such that it would cause negligible "writing" or "erasing" to occur. Response to the color pattern would be amplified by photomultiplier circuits and would be converted to electronic signals for use by other circuits in the computer. Dependent upon the system requirements "reading" could be done either by reflection or transmission.

In principle, it would appear that an ultra high density of surface storage could be effected since the capsules can be made so small. Practical limitations on density are imposed by optical resolution and other system factors as well as capsule size. For example, whether or not a storage system employed servo techniques would have a marked influence on the effective storage density. At the present stage of research development, it is not possible to state quantitatively what realistic values for storage density will be possible using this new technique. To date, on a qualitative basis, it does look very promising.

As indicated in the previous discussion on the variables influencing spectral band characteristics, the temperature at which switching takes place can be an important factor. With present NCR photochromic materials the colored state is relatively stable (after irradiation) only below $0^{\circ}C$. This temperature does not represent a sharp transition point such as the Curie temperatures of ferromagnetic and ferroelectric materials. In addition, the rate of color loss (fading) is not linear with rising temperature but an exponential function.

307

At the present time the switching properties of photochromic material systems, i.e., the dye plus the solvent, are under intensive research investigation at NCR. Theoretically, in a nonpolar solvent, very fast switching times ($\sim 10^{-8}$ sec.) are possible. Practical speeds will be a function of the solvent system used and the brightness or intensity of illumination (watts/cm^2) which can be obtained from the light source used for switching. Further, at the present time it is believed that the rate of switching for a single molecule is independent of temperature but that the quantum efficiency of switching photochromic materials is a "weak" function of temperature.

It is interesting to compare the quantum efficiency of the photographic (irreversible) process with that of the photochromic (reversible) process. On photographic film one photon (quantum) of light energy can effect 10^{10} molecules by cascade action during development. With photochromic materials an incident photon of light can activate a maximum of only one molecule. Unfortunately, the probability of this occurring is highly dependent upon the particular solvent-dye system being irradiated and for most systems studied to date is relatively low. The net result is that in order to switch photochromic materials at speeds significant for computer storage applications ($\sim 10^{-6}$ sec.) very intense light beams must be provided. This in itself is a sizable research problem considering the fact that specific wavelengths of illumination must also be provided with associated switching and indexing methods.

Practical photochromic memory systems for computer application have not yet been built. Many systems approaches and accessing schemes have been studied at NCR in parallel with the materials research. In addition, considerable work has been accomplished on the study of components and techniques suitable for effecting the complex functions of "writing," "erasing," and "reading."

308

Successful photochromic memories should have all of the potential advantages of high density photographic memory schemes (Ref. 8). The very powerful additional feature would be that of reversibility. Potentially, its memory application could be in the form of tapes, cards, drums, discs, and various large capacity random access (RAM) systems.

D.   OTHER POTENTIAL APPLICATIONS

Switching and storage devices are not the only potential uses for NCR capsules and light-sensitive dyes. Already the NCR duplicating paper has become a multimillion dollar a year business. Encapsulation techniques are now being studied for application to such widely different fields as drugs, food, fuels, cosmetics, and adhesives to list but a few.

As for the light-sensitive dyes it seems possible that irreversible switching processes can be readily worked out. This would provide simple and inexpensive means for optical printing and "dry" photography with direct light-to-paper reactions.

E.   FUTURE STATUS

The technical problems remaining to be solved before practical applications of the new two-state chemico-optical switch can be realized are both many and complex. In general, they include both basic materials research for the memory or printing surface and the development of suitable input and output systems and components. While these problems look as though they can be solved, the first practical application of the chemico-optical switch to either memory (reversible states) or printing (irreversible states) appears to be still some time in the future.

309

F.   BIBLIOGRAPHY

1)   "Switching Theory - An Expanding Field," British Communications
      and Electronics, p 365 (June, 1957).

2)   "The Magic Capsules," Time, p 79 (May 13, 1957).

3)   "Chemical Capsules Never Forget," Ind. and Eng. Chem.,
      49 p 23A (December 7, 1957).

4)   "Chemicals Can Remember, Too," Business Week, p 120
      (December 7, 1957).

5)   Brode, W. R., "Chemical Spectroscopy," Proc. ASTM, 50
      p 513 (1950) (61 references).

6)   Ibid, "Color and Chemical Constitution," American Scientist, 42,
      pp 259-84 (1954) (11 references).

7)   Brode, W. R., et al, "The Relation Between Absorption Spectra
      and Chemical Constitution of Dyes. XXVII. Cis-trans Isomerism
      and Hydrogen Bonding in Indigo Dyes," J. Am. Chem. Soc., 76,
      p 1034 (1954). (See also earlier papers in this series)

8)   King, G. W.; Brown, G. W.; and Ridenour, L. N., "Photographic
      Techniques for Information Storage," Proc. IRE, pp 1421-8
      (October, 1953).

February 1958

APPENDIX II

THE BASIC CHEMICAL AND PHYSICAL PRINCIPLES
INVOLVED IN SWITCHING PHOTOCHROMIC MATERIAL

A. PHOTOCHROMIC MATERIAL

Photochromic material can exist in one form as a solution of photochromic dye in gelatin capsules as small as five microns in diameter or less. In the solution there are two isomers. One isomer, call it A, absorbs light mainly in the near U. V. and thus appears colorless. This is the more stable form and is therefore taken as the ground state of the molecule. The other isomer, B, absorbs in the green region of the spectrum and therefore appears purple by transmitted light. When isomer A absorbs energy it can change to isomer B. When isomer B absorbs energy it can change back to A. This is the switching mechanism.

B. ENERGY CONSIDERATIONS

A molecule, a collection of atomic nuclei held together by electron inter- actions, can only have certain discrete energy values, the so-called quantum energy states. If a molecule is in the ground or lowest energy state it must absorb a certain minimum amount of energy to make the transition to a higher energy state (see Figure 120). The frequency of the light absorbed enables us to calculate the amount of energy absorbed according to the equation,

$$E = \frac{NhC}{\lambda} = \frac{2.859 \times 10^5}{\lambda} \quad K \ cal/mole$$

where λ is the wavelength in Angstrom units.

ASD TR 61-70

A molecule can possess vibrational, rotational, and electronic energies. The energy required for transition of each of these types has been well established. Thus any molecule that absorbs in the visible and ultraviolet regions must experience an electronic transition because of the relatively large energy involved. The energy differences between electronic states are in the range one to two electron volts. By electronic energy is meant the sum of the potential and kinetic energy of the electrons. The sum of the electronic energy and the coulomb potential of the nuclei acts as the potential energy under whose influence the nuclei carry out their vibrations. Only if this potential energy, in its dependence on the internuclear distance, is at a minimum is the electronic state considered a stable state of the molecule under ordinary conditions.
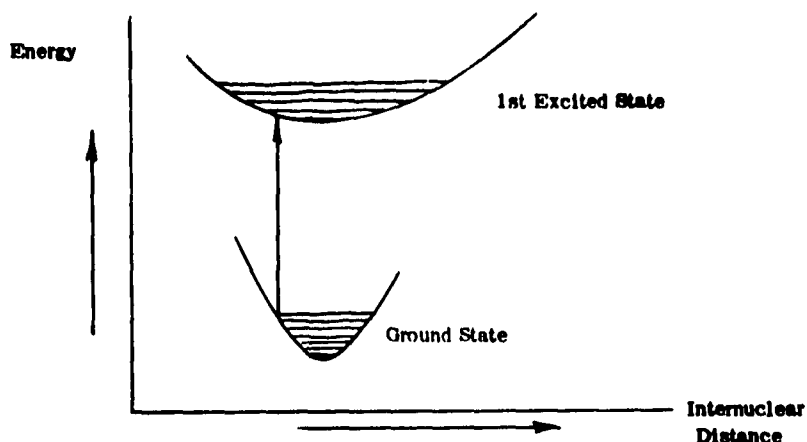

Figure 120. Internuclear Distance vs. Energy Level of a Molecule.

The energy required to make an electronic transition may come not only from irradiation by light but also from thermal collisions, electron bombardment, etc. The only requirement is that enough energy must be supplied to make the transition; there is no such thing as a partial transition.

312

C.   ISOMERIC EQUILIBRIUM

In a solution of photochromic material, both isomers are present in a state of dynamic equilibrium. The position of equilibrium is a function of the temperature and illumination. That is, depending on changes in the intensity and wavelength of the absorbed light or the heat energy absorbed. the relative concentration of the isomers will change and a new position of equilibrium will be reached. This photo-chemical equilibrium position is different from normal thermal equilibrium such that when the source of radiation is removed, the system will tend to change to the true, thermodynamic equilibrium for the given temperature. If the temperature is low, however, an unstable condition may persist for a considerable time because of the slow rate of attainment of equilibrium. This state exists for most NCR photochromic materials at the region of $0^{o}C$ and below, and accounts for the fact that in order to preserve the material for long periods of time in the written or colored state, refrigeration is required.

D.   CHEMICAL AND SPECTRAL ANALYSIS

A chemical analysis of the structure of one of the most promising photochromic materials to date reveals that in the stable ground state there is a closed ring and that absorption of radiant energy causes re-arrangement of the atoms and an opening of the ring is shown in the simplified diagram of Figure 121.
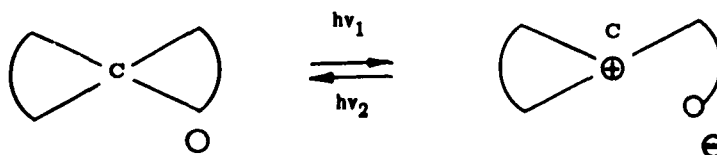

Figure 121.   Molecular Structure of Photochromic
Material in Ground and Excited States.

313

Absorption spectrograms taken of this material in the unwritten and written states are shown in Figure 122.

In connection with these curves, the following facts were established:

1) A new absorption band appears at 525 mμ after exposure to light of about 366 mμ wavelength.

2) There is no writing with light of wavelength longer than about 400 mμ.

3) Thermal effects cause erasure so that even at $0^{\circ}C$ the material was unreadable after two days. Other materials can have longer life spans.
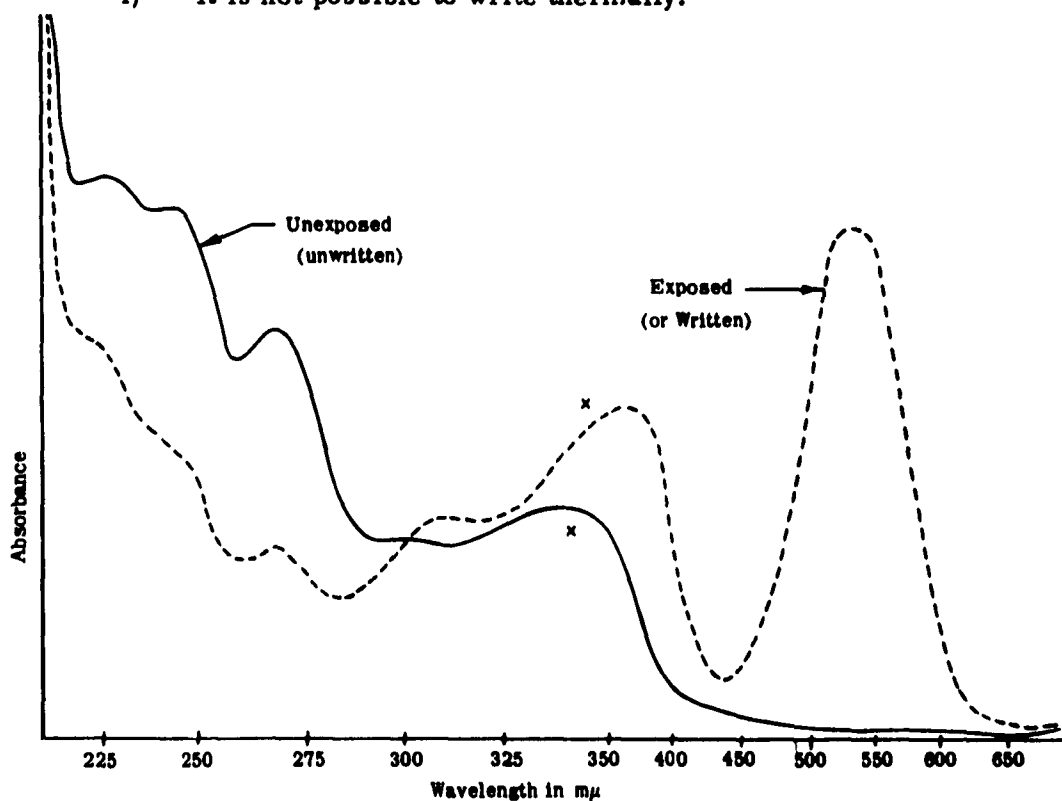
4) It is not possible to write thermally.

Figure 122. Absorption Curves of Photochromic Material in Written and Unwritten States.

314

Several mechanisms have been suggested to explain the previous facts.
The most probable, in our opinion, is similar to that proposed by Olson
as described in "Photochemistry" by Rollefson and Burton for the
cis-trans isomerization. Applying this model to our photochromic
material, we have the diagram of Figure 123.

Before exposure, the molecules are in any of the vibrational states at A.
Absorption of radiation corresponding to at least 72 K cal per mole
energy will raise molecules into the vibrational states of the first excited
state at B. They may now either fall back to the ground state with the
emission of radiation (flourescence) or after vibrating to C, fall into the
switched states at D with the emission of radiation hv_2. The switched
molecules may now return to the original state by absorbing thermal
energy of at least 22 K cal/mole as in the route DEFA. Or they may
absorb radiant energy hv_2 (45 K cal) and proceed by the route DCBA.
The height of the thermal barrier in the unwritten state indicates that it
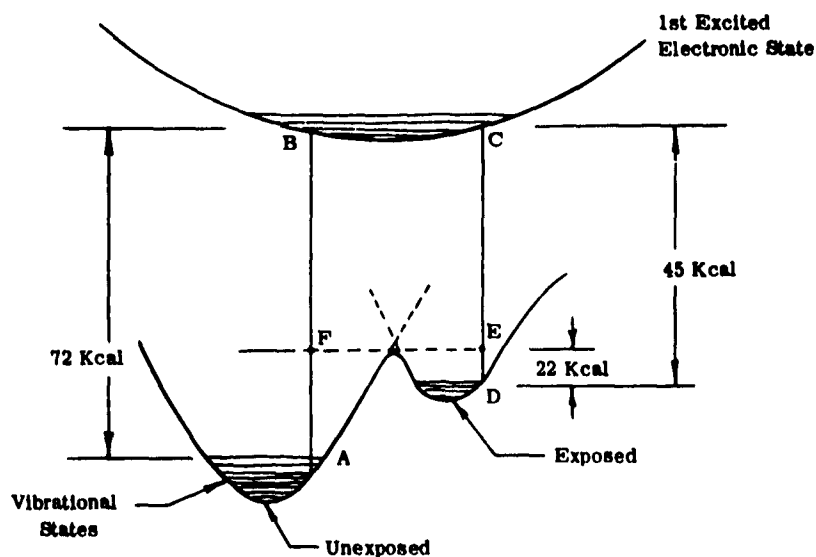is not likely to go thermally from A to D (AFED).

Figure 123. Molecular State of Photochromic Material
During Exposed and Unexposed Periods.

315

E. EFFECT OF HEAT

The thermal erase energy of 33 K cal/mole was found using the Maxwell-Boltzmann distribution of energies as shown in Figure 1240.

In Figure 124, the shaded area represents the number of molecules at temperature T_1 that have minimum energy E_1 to overcome the potential barrier. Raising the temperature to T_2 allows a greater number of molecules to make the transition. The variation of the equilibrium constant with temperature will be proportional to the area under the exponential curve:

$$k = AE^{-\frac{E_1}{RT}} \quad \text{or ln } k = \text{const.} - \frac{E_1}{RT}$$
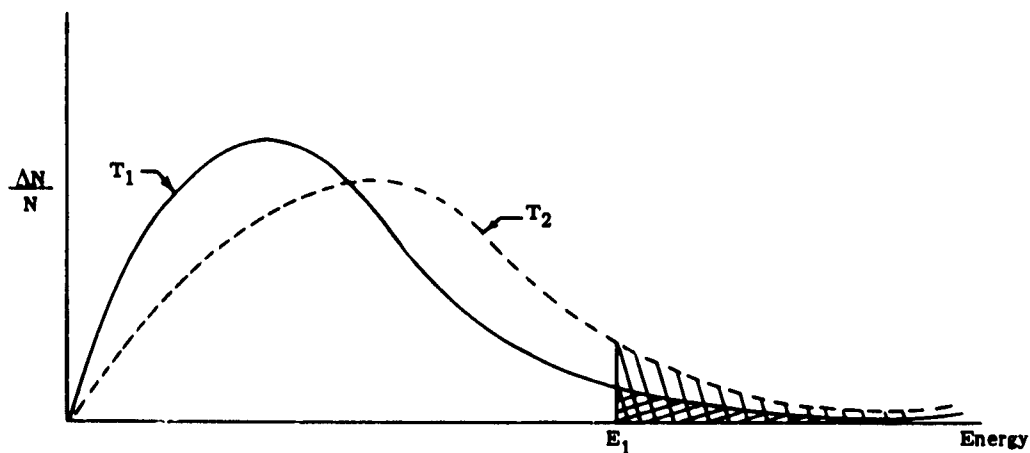
This is the Arrhenius law.

Figure 124. Maxwell-Boltzmann Distribution of Energies.

The equilibrium constant k at various temperatures can be found experimentally and the slope of the $\ln$ k vs. $\frac{1}{T}$ curve gives E_1 the minimum energy required for the thermal transition. Measurements establish this energy at about 22K cal per mole for the material under discussion. The ideal material, of course, would not be able to be erased thermally.

F. EFFECTS OF RADIANT ENERGY

Not all the incident light is absorbed by the material. The amount absorbed depends on the concentration and the path length as given by Beer's law:

$$\log \frac{I_o}{I_t} = \epsilon \, c \, l$$

where I_o and I_t are intensities of radiation before and after passage through the material, l = path length, ϵ = extinction coefficient, and c = concentration.

The quantity $\log \frac{I_o}{I_t}$ is the absorbance and is read directly by the spectrograph, so that extinction coefficients for all the photochromic materials have also been obtained.

However, not all the molecules which absorb radiant energy take part in the chemical change. Referring again to Figure 123, only a fraction of the molecules which reach level B proceed to C and then to D; many drop back to A. The percentage efficiency in producing the switched form is called the quantum yield:

$$\Psi = \frac{\text{molecules decomposed per sec.}}{\text{quanta absorbed per sec.}} = \frac{\text{rate of photochemical reaction}}{\text{quanta absorbed per sec.}}$$

317

APPENDIX III

THE NATIONAL CASH REGISTER COMPANY
ENCAPSULATION PROCESS -
COACERVATION

The term "coacervation" was first used by H. R. Kruyt and H. G. Bungenberg deJong in 1929 to describe the partial miscibility of optically isotropic liquids in which at least one of the liquids is macromolecular or colloidal in nature. The macromolecular or colloidal equilibrium liquids are known as coacervates.

If a solution of sodium sulphate is added to a warm gelatin solution, the gelatin solution can be made to contract so that it no longer fills the entire volume occupied by the water and sodium sulphate. Droplets of more concentrated gelatin solution first separate. On standing, these coalesce to form a separate liquid layer of the more concentrated gelatin solution.

A warm solution of gelatin and gum arabic, in which each constituent has a concentration of about 10 percent, forms a single phase solution at a pH 4.5. If this solution is diluted, the gelatin - gum arabic solution can be caused to contract and two liquid phases form.

Starting with the same 10 percent mixed solutions of gelatin and gum arabic, two liquid layers also form if the system is concentrated. One of the layers is rich in gelatin and the other rich in gum arabic. Both liquids are coacervates.

318

If chloroform is added to a three percent solution of cellulose diacetate in certain alcohol-chloroform mixed solvents, a more concentrated solution of cellulose acetate can be caused to separate.

These are examples of coacervation. The phenomena are of very wide occurrence and apply to many macromolecular solutions. They give rise to dispersed systems in which, in a certain sense, the dispersed phase is the same as the continuous phase such as water in water. More specifically, the same continuous liquid phase exists throughout two immiscible liquids, the discontinuity between the phases being caused by an expanded liquid such as gelatin.

To define an expanded liquid will clarify the nature of the coacervation process and the physical differences underlying liquid immiscibility involving coacervates and liquid immiscibility involving ordinary liquids.

In many ordinary solutions, the solute or dissolved material is considered to be present in a gas-like state. Among macromolecular materials, the so-called solute, such as gelatin in the above examples, can be present in a liquid-like state even at very low concentrations.

The liquid state is chiefly characterized by cohesion or continuity and flow while the gaseous state does not have cohesion or continuity but does flow. A gas tends to fill the entire space available. A liquid has a limited volume and tends to take the shape of the container. Gases are miscible in all proportions while liquids can exhibit partial miscibility.

The chain-like or randomly kinked nature of many macromolecular materials permits them to form a continuous network throughout the solution. The forces between the molecules or particles of the polymer are continually shifting but at any instant the continuity or cohesion characteristic of the liquid state is holding the polymer network together. The network is expanded and the voids are filled with water or solvent. This is what is meant by the "solute" being present in an expanded liquid state.

319

In the first example cited above the gelatin solute at first fills the entire space available, i. e. , the entire volume of the solvent. On addition of sodium sulphate the gelatin solution contracts and no longer fills the entire volume of the solvent. Such contraction is characteristic of the liquid-like nature of the solute. If the solute were in a gas-like state, it could not contract but would continue to fill the entire space available. Since, however, the gelatin is an expanded liquid and the voids are filled with water, water in the liquid state is common to both liquid layers.

In the case of ordinary liquid immiscibility the two liquid layers do not have a liquid that is common to both layers. There are no expanded liquids involved. Solutes, if present, are in a gas-like, not a liquid-like, state.

Coacervation might therefore, be defined as partial miscibility of optically isotropic liquids in which at least one of the liquids consists of two constituents both of which are in the liquid state. Since macromolecular materials tend to fulfill the above requirements better than low molecular weight materials, the commonly accepted definition first cited may be accepted until more accurate criteria for determining if a solute is present in a gas-like or liquid-like form are available. It has been suggested that such differences may ultimately be differentiated thermodynamically in terms of entropy and interaction.

The coacervate state is only one, albeit a very important one, of several equilibrium states of colloid systems. It is of extreme importance in biological phenomena and doubtlessly will find many industrial and commercial applications as the phenomena become better known.

320

BIBLIOGRAPHY

1)   H. G. Bungenberg deJong and H. R. Kruyt, <u>Proc. Koninklijke Nederlandse Akademie Van Wetenschappen</u>, Amsterdam <u>32</u> 849 (1929).

2)   H. G. Bungenberg deJong, <u>Kolloid Zeitschrift,</u> <u>79</u>, 223, 334; <u>80</u> 221, 350 (1937).

3)   D. G. Dervichian, <u>Research,</u> <u>2</u> 210 (1949).

4)   A. Dobry, <u>J. Chem. Phys.</u> <u>35</u> 387 (1938).

5)   A. C. S Lawrence, <u>Discussion of the Faraday Society No. 18,</u> page 229 (1955)

6)   <u>Ibid,</u> D. G. Dervichian, p. 231.

321

APPENDIX IV

THE NATIONAL CASH REGISTER COMPANY
MICROENCAPSULATION PROCESS

A. INTRODUCTION

A number of years ago a project was started at The National Cash Register Company to develop a paper coated on one side with all of the necessary reactants to synthesize a dye when subjected to impact. Essentially, this involved the study of techniques for keeping reactive materials apart until it was desired that the reaction occur. The reaction in question involved a colorless form of an oil-soluble dye in a non-polar solvent which would react with acidic adsorbents to produce the colored form of the dye. The first approach to the problem was to disperse the reactive oil in a solution of gelatin-in-water and form an oil-in-water emulsion which was coated over a clay coating on paper. If was found, however, that such systems would not function reliably; that is, the reaction would occur prematurely without the need for impact when the emulsion was coated on the acidic clay adsorbent. It was found that during the coating operation the molecular protective film about each oil drop would rupture and the resulting structure was thus rendered porous. It was thus apparent that emulsion coatings of this type were not suitable for separating reactive substances.

To solve this problem, it was concluded that the only way to get a completely protected system would be to build a strong wall about each oil drop which would remain intact during the drying operation. In addition, it was concluded that the submicroscopic porosity of such a dry wall would

322

have to be controlled to make it impermeable to the contained oil. After
several years of extensive research, a suitable capsule system was
developed.

B. MICROSCOPIC ENCAPSULATION OF REACTIVE OILS

The microscopic capsules are produced by a novel application of the
phenomenon termed "coacervation." Bungenberg deJong and Kruyt
have used the word "coacervation" to describe phase separation or
"demixing" in colloid systems. Mr. B. K. Green of The National Cash
Register Company has defined coacervation in the Encyclopedia of
Chemistry (Reinhold, 1957) in a comprehensive manner and states in
part, "Coacervation might, therefore, be defined as partial miscibility
of optically isotropic liquids in which at least one of the liquids consists
of two constituents, both of which are in the liquid state. Since macro-
molecular materials tend to fulfill the above requirements better than
low molecular weight materials, the commonly accepted definition first
cited may be accepted until more accurate criteria for determining if a
solute is present in a gas-like or liquid-like form are available."

Several distinct types of phenomena have been described as coacervation.
Kruyt has classified them as follows:

1) Simple coacervation

2) Mono-complex coacervation

3) Di-complex coacervation

4) Tri-complex or multi-complex coacervation

Kruyt does not attempt a rigorous definition of the above terms, but con-
fines himself to giving examples where the terms seem to be appro-
priate. The writings of Kruyt and Bungenberg deJong indicate that all
four types of phenomena can occur in an aqueous media, but only simple
coacervation can occur in a non-aqueous media. Simple coacervation is
sometimes used to describe coacervation in aqueous media when "salt-like"

323

ASD TR 61-70

valence forces are not supposed to be involved. The various manifestations of complex coacervation occur only in aqueous or ionizing media and are believed to involve intra-molecular salt-bonding of one form or another. The following discussion will be concerned with the encapsulation of oils utilizing the principle of complex coacervation.

When high isoelectric point gelatin, gum arabic and water are mixed together to form a solution, it will be noted that there is a concentration and pH region where phase separation (coacervation) occurs. If a sample of the material is removed when in the coacervate zone, tiny liquid droplets, rich in colloid, can be seen under the microscope. These droplets will flow together and settle, forming a fluid liquid coacervate phase. If a system (gelatin-gum arabic-water) of such a concentration and pH, where all components are compatible, has an oil added to it and the coacervate zone is entered by pH, dilution, or both, a very unique thing occurs. When the oil is first added and mixed to form an oil-in-water emulsion, gelatin molecules are adsorbed at the oil-water interface. In a sense, each droplet now behaves as a very large molecular weight fraction of gelatin, and as the coacervation zone is entered, the coacervate phase (colloid-rich phase) separates or forms the oil-water interface, producing a liquid film. In another sense, the oil droplets serve as seeding points about which the liquid polymer-rich phase forms. Since the coacervate phase is very rich in colloid, the system can be stabilized by lowering the temperature to form a gel. At a subsequent step, the capsule wall can be cross-linked by various chemical additives to render the structure inert to temperature changes, thus permitting high temperature drying operations.

Many variations can be produced; oil-drop size can be varied over a very wide range (0. 1 micron to 0. 5 cm.) without affecting the process. Holding the colloid oil ratio constant, this variation in oil-drop size changes the total surface area; thus the film thickness about each oil drop changes. For example, with large oil drops, the wall thickness is much greater than

would be the case if the same amount of oil were reduced to much smaller oil-drop sizes. The ratio of wall material to contained oil also can be varied over a wide range. To date, the ratio of four parts wall material to one part of oil and one part wall material to sixteen parts of oil, has been studied. If the oil-drop size is held constant, the variation in phase ratio affects the thickness of the wall about each oil drop.

C. PERMEABILITY CHARACTERISTICS OF MICROSCOPIC OIL-CONTAINING CAPSULES

It was mentioned earlier that the encapsulation of materials alone was not sufficient to permit the mixing together of highly reactive materials without reaction. It was found that the permeability of such structures to the encapsulated material was also of vital importance. For example, with the capsule structure just discussed, it is possible to make the protective walls very permeable to the contained oil. When the capsule is dry, the oil, if volatile, will pass out of them rapidly. With the same type structure, a dry capsule can be made having the wall very impermeable to the contained oil. Some of the structures that have been prepared have held very volatile solvents for over three years under varying conditions of temperature and humidity with no measurable loss. Of even more interest is the fact that some of the structures have held solvents for extended periods of time above the boiling point of the solvent. Most of the systems that have been considered above involve structures containing approximately 80 percent liquid. The factors which influence the permeability of such structures are numerous and complex. Some of these factors are:

1) Location within the coacervate phase diagram
2) Rate and method of entering coacervate zone
3) Rate of gel formation and final gelation temperature
4) Concentration, temperature, final pH value, and time
5) Method of water removal

325

6) Cross-linking technique
7) Micelle formation
8) Presence of salts or other solutes

Since gelation of the colloid-rich film about the oil drops is an important aspect of the capsule system, a comment on gel structures and how they contribute to producing impermeable structures is in order. Gels are colloidal states in which fiber-like solid structures completely enclose a liquid to give a rigid mass.

Gels are of two main types: reversible and irreversible. An example of the former are gels formed by gelatin and other organic polymers where the linear gelatin molecule, upon cooling, becomes interconnected at numerous points along the polymer chain, enclosing the solvent within the network of the polymer. The gel, thus, is a mass of tiny pores and holes, the size being governed by such things as concentration, temperature of gelation, rate of gelation, and many other factors. These gels are reversible because the interaction by which the polymer chains are attached, are reversible.

Irreversible gels, such as silica gels, can be obtained by acidulation of water glass (sodium silicate) or hydrolysis of $SiCl_4$. Colloidal silica is formed, which grows in chain-like structures. These structures enclose and surround the solvent in a network as the gelatin polymer molecules do. In this case, however, the gel is irreversible because the formation of the silica is an irreversible reaction.

Since gels are masses of interconnected networks, they can be described as masses of pores of capillary dimensions, and the forces of capillarity come into play in the structure. For example, water in capillary pores exists in an orderly crystalline form approaching that of ice, rather than the form of bulk water. If one attempts to remove water from a gel such as silica gel by evaporating off the water, the surface tension of the liquid will cause the gel structure to collapse. If, however, by successive

326

solvent displacement, water is replaced as the continuous liquid phase
by diethyl ether, and the gel heated under pressure above the critical
point of the ether, the liquid phase can be removed without collapse of
the structure, since the surface tension is zero above the critical point
(no liquid-vapor interface).

The capillary nature of gel structures can be utilized in permeability con-
trol by the nature of the wetting forces of the capillary walls. Selected
adsorbed materials on capillary walls can be used to prevent wetting,
and thereby penetrations of certain liquids into the capillaries (i. e. ,
utilization of hydrophobic and oleophobic monolayers on capillary walls).
The phenomena of structure collapse of gels upon drying can be utilized
in capsular structures. Rapid drying results in the collapse of the outer
wall of the capsule as the solvent is driven out. Meanwhile, the liquid
in the inner pores can be retained to provide a solubility barrier to the
encapsulated liquids. It is possible to utilize drying of the gel walls to
force other materials into the capillaries of the gel. Paraffin wax, for
example, has been forced into the capillaries of the gelatin wall. Upon
drying of the capsule, the paraffin-filled gelatin serves as a moisture
barrier.

In addition, films that are dried by solvent removal can be made with
very small pores which can prevent the movement of materials in much
the same manner as a sieve; i. e. , the pores are too small for the large
molecules to pass through. The size of the pores can be controlled by
mixing the filming material in a solution of a good and poor solvent and
controlling the drying rate. Such methods provide uniform control of the
pores and should have an application to films that form capsular structures.

D.   LIMITATIONS OF COMMERCIAL ENCAPSULATION TECHNIQUES

In a general sense, the more polar the oil to be encapsulated, the more
problems which are encountered. It also follows, that as water sensitivity

or solubility of the oil increases, more problems are encountered. To date, a wide variety of solvents ranging from the pure hydrocarbons and chlorinated hydrocarbons to the very volatile, highly complex flavors, perfumes, etc., have been encapsulated. We have also been able to encapsulate a wide variety of finely divided solid materials, as well as solid material dispersed in oil phases. Again, as the water solubility of the material to be encapsulated increases, the difficulties increase.

E.   PHYSICAL FORM

Early research was concerned, for the most part, with capsules coated on a base material from an aqueous dispersion. It is possible, however, to spray dry the capsule slurry to produce a free-flowing powder which can be used as a powder, re-dispersed in water or dispersed in certain organic solvents, or mixed with fillers and compressed into pellets. Also, if so desired, it is possible to produce a solid chunk of the material. This can be done by filtering off the water and allowing the material to dry. During the drying operation, the capsule wall becomes tacky and sticks together to form an apparent solid, reproducing the shape of the container. With a 4:1 system, such a solid contains approximately 80 percent oil. One of the unusual properties of this solid material is that when it is fractured, the breakage occurs around the capsules and not through them, thus releasing no oil. The oil can be subsequently removed by pressure. Flakes of the dried material have been placed in high-speed blenders for extended periods of time with surprisingly little breakage as the particle size is reduced by fracture.

F. SUMMARY

So far we have discussed, in general terms, only the capsular system now in commercial production at The National Cash Register Company. As was stated, the wall material consists of hydrophilic colloid material,

328

and the amount of oil protected in this manner varies from 0 percent to 95 percent. The oil-drop size has been varied from 0.1 micron to 0.5 cm. and many different and unique structures have been prepared. The permeability of such structures (wall material) can be varied over a very wide range. The limitations as to the oils which can be encapsulated are not completely known, but the more water soluble the oil, the greater the difficulties that are encountered. In short, some of the basic principles that such capsular structures demonstrate are listed below:

1) Separation of reactive components (protection from atmosphere)
2) Retention of very volatile solvents for extended periods of time
3) Formation of structures that have various physical strengths due to wall thickness variations
4) Serve as microscopic reaction vessels
5) Liquids in apparently solid form

December 1958

APPENDIX V

MILITARY SUPPORTED PHOTOCHROMISM AND CAPSULAR RESEARCH AT THE NATIONAL CASH REGISTER COMPANY

Prior to this contract the Air Force had been supporting two different capsular and photochromic material programs at The National Cash Register Company, Dayton, Ohio, since 1 May 1958.

The first program - Research Study on The Application of the NCR Capsular System, Contract No. AF33(616-5510), Project No. 8(76-6272), Task No. 62733, was divided into two phases. Phase I entitled "Marking Inks for Photographic Negatives," was concerned with the application of data and titles to the acetate film base of photographic negatives. Phase II was entitled "Investigations of Non-Silver Halide Photographic Systems Suitable for Airborne Processes." The title is descriptive of the program.

The second program - Research Reports and Test Items Pertaining to Eye Protection of Air Crew Personnel, Contract No. AF41(657)-215, R and D Project No. 7753-36, was concerned with the application of photochromic materials to eye protection from intense light sources.

Work on these programs was reported in regular quarterly reports to the sponsoring agencies.

During 1960, a contract sponsored by the Air Force supported work on the utilization of the best photochromic materials for use in an eye protective device. The Contract number was AF41(657)-322 and was monitored by the School of Aviation Medicine.

330

The Navy has been supporting two programs in encapsulation since 1959. One is entitled "Non-Aqueous Microencapsulation," Contract No. ONR Nomr 2848 (00), and the other program is classified and cannot be described here.

In 1960 the Navy awarded the National Cash Register Company a contract for the "Development of a Reversible-Color Coating for Aircraft Camouflage," (NOas 60-6104-6).

APPENDIX VI

PHOTOCHROMISM RESEARCH AT
THE NATIONAL CASH REGISTER COMPANY
PRIOR TO WADD CONTRACT AF33(616)-6205

A. INTRODUCTION

Studies of photochromic compounds and photopolymenzation were carried out
at The National Cash Register Company for several years prior to the start
of military support in these areas. This part of the report will summarize
the work conducted during the pre-military support period.

B. PRIOR WORK

1. Printing Systems

For many years The National Cash Register Company has been interested
in the photochemical reactions of organic compounds for application to new
printing and data storage concepts.

During the development of NCR (No Carbon Required) Paper, an important
consideration was the photosensitivity of the color reactants. A study was
therefore made of derivatives of N-benzoyl leuco methylene blue with regard
to the effect of substituents in the benzene ring or photosensitivity.

Photochemical reactions in conjunction with a capsular system (see later
section) had been under intensive study for the past four years. In these
photographic systems the capsule was used either as a container or a wall
of changing properties. Processes affecting the capsule were based on wash-
off methods, removal of capsule contents by heat or solvent, differential

332

ASD TR 61-70

extraction of dye, or a photosensitive hectograph system. By use of phosphotungstic acid, reactions were carried out through the capsule wall. Chemical reactions were carried within the capsule which were dependent upon a polymerization or color formation for their printing properties. Finally the study of color formation by light within the capsule led to the investigation of reversible chemical systems in which the two states differed markedly in their light absorption properties (photochromism).

One of the earliest printing systems studied involved the production of an acid within the capsule by virtue of the known reaction (Ref. 1) of o-nitro-benzaldehyde (1) with light to yield o-nitrosobenzoic acid (2):

(1)   (2)
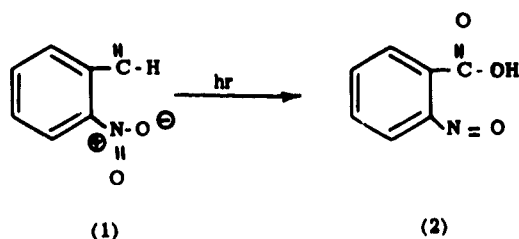
If the capsule also contained a basic color reactant similar to those used in NCR paper, color could be produced. The polar dye being insoluble in the capsule solvent was precipitated and adsorbed on the capsule wall. Such a system required complete precipitation of the dye in the exposed areas to be considered a practical printing process in which the capsule contents would be transferred to a receiving sheet by pressure. If the receiving sheets were reactive to the color reactant used, print would be obtained from the originally unexposed areas and no print obtained from the exposed areas. Since complete precipitation was required to obtain a "clean" process, this system was too slow to be considered, especially for high speed printing paper.

333

A search was then made for a photochemical system which would yield an oil soluble dye so that this color formation could be used directly to produce copies without necessity of "complete" reaction. One system employed xanthylidene anthrone (3) (Ref. 2) which reacted with light to produce (4):

(3)   (4)
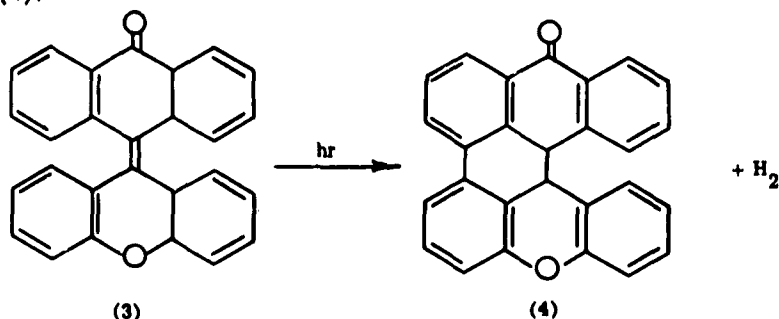
The xanthylidene anthrone was yellow in solution while material (4) was red. The red material (4) was indeed soluble in common capsulable solvents. Although transfer prints could be made with this system, the red prints on a yellow background were not too satisfactory and the reaction seemed to require fairly large amounts of energy.

Xanthylidene anthrone had other properties of interest. The material turned an intense green-black on melting or when in boiling xylene. The material returned to its original yellow color on cooling. In addition to being thermo-chromic, a solution of xanthylidene anthrone in toluene, while yellow at room temperature and virtually colorless at $-80^{\circ}C$, turned green-black when exposed to ultraviolet light for short periods of time. This photochromism was observed at low temperatures only. The thermochromic and photochromic properties of xanthylidene anthrone seemed to demonstrate the possibility of obtaining a large change in the light absorption properties of a material under the influence of a small amount of applied energy. (Ref. 3).

Some time was spent on the study of zanthylidene anthrone (3),

(5)   (6)
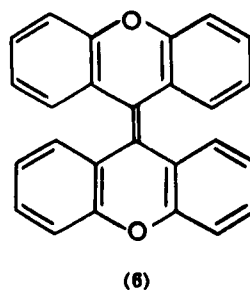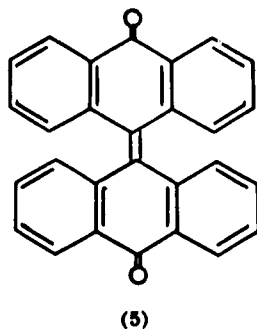
dianthrone (5), dixanthylene (6), and their derivativ?s.

These materials, which have been called thermochromic enthylenes,[2] all appeared to be capable of undergoing the non-reversible reaction with light given above for xanthylidene anthrone, i. e. , (3) to (4). Where a completely reversible photochromic system was required, the thermo-chromic enthylenes were not satisfactory because they underwent an irreversible reaction with light along with the reversible reaction.

2.   Photochromic Spirans

"A spiran is a compound in which a single atom is a common member of two rings with three or more members" (Ref. 4). In spiropentane (7), the central carbon atom is a spiro atom; the compound, a spiran.

(7)

335
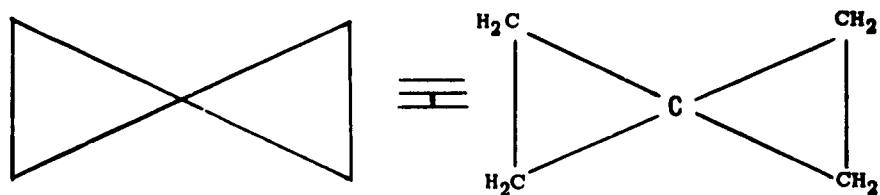
The photochromic spirans are in general spiropyrans, i.e., one of the rings in which the spiro atom is involved is a pyran ring (six-membered ring containing an oxygen), for example, 1,3,3-trimethylindolinobenzopyrylospiran (8) (hereafter referred to as BIPS). The atoms in the spiropyran (8) are numbered as indicated following the nomenclature rule of assigning the number one position to the hetero ring atom. When sufficient energy is absorbed by a photochromic material, such as (8),
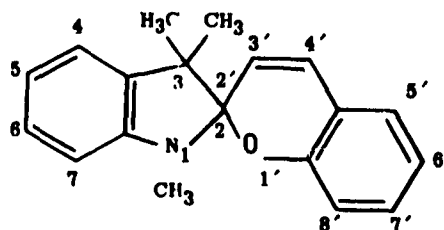
(8)

the 1'-2' C-O bond breaks giving rise to a dye of the merocyanine type (9):

336
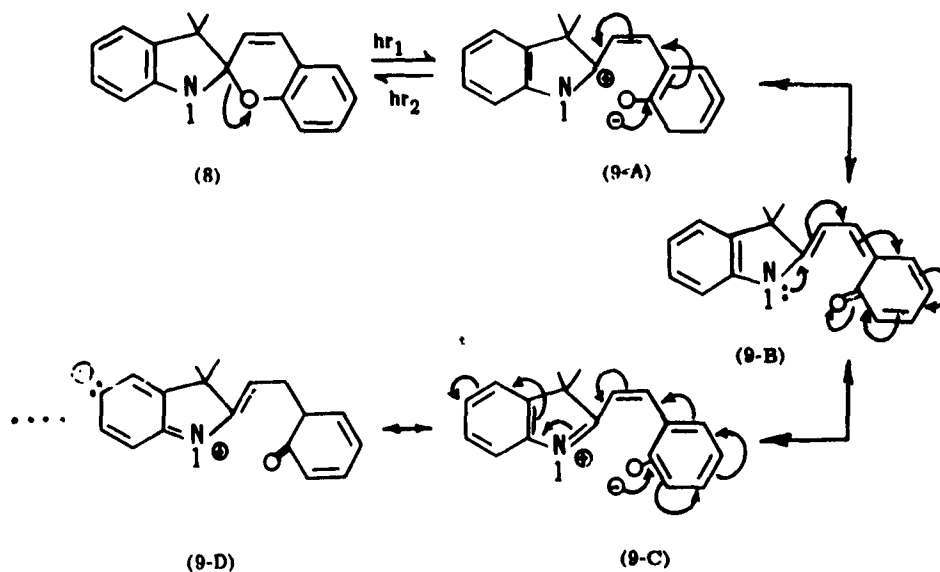
The material (9) is represented in this case by four of the symbolic structure which probably made impo··tant contributions to the hybrid, (canonical forms which are of significance in the wave equation). The geometry of the spiro carbon (Ref. 4) requires that the rings are at right angles to each other as shown in (8-A).
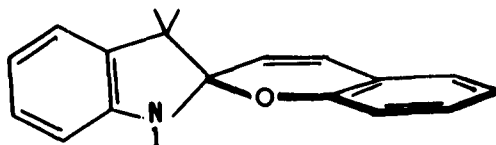
(8-A)

"Resonance" is only of importance between groups lying in the same plane. Therefore, in (8), the spiro carbon serves to insulate the indolino ring from the benzpyrylo ring, and the adsorption spectra will correspond to that of the sum of the spectra of the two halves which absorb only in the ultraviolet portion of the spectrum.

In (9), on the other hand, both ring systems will probably lie in the same plane (i.e., 9-B, 9-D) and forms like (9-C) involving electron movement along fairly long chains will be of importance. The compound (9), therefore, would be expected to absorb visible radiation.

a.   Synthesis Program

The primary goal of the synthesis program was to design materials which would exhibit the following properties:

1)   Have at least two stable states.

2)   Conversion from one state to the other requiring only small amounts of light energy.

337

3) The states should be easily distinguishable with light.

4) Repeated conversions should have no effect on the system (non-fatiguing).

5) The switching wavelengths should not be effected by the reading wavelength (non-destructive readout).

6) The conversion should preferably occur at room temperatures.

7) Possibility of conversion to stable state.

The known photochromic materials (Ref. 5-29) had many of the desirable properties at low (-80° centigrade) temperatures. Therefore, a natural point of departure for the synthesis program was to make derivatives of the reported photochromic spirans and to observe the effect of such derivatives on photochromic properties.

In the early stage of the synthesis program, the derivatives were selected on the basis of availability and imagination. Fortuitously, this method led to compounds with more desirable stability than the reported materials. As the number of derivatives increased, it appeared that the relative stability of the colored form (9) was dependent upon structure in a "regular" manner.

A number of reactions of aromatic derivatives were quantitatively correlated with the Hammett Equation, (Ref. 30, 31):

$$\log \frac{k}{k_o} = \rho\sigma$$

where k_o was the rate constant for the reference compound in the reaction; k, the rate constant for a substituted compound in the same reaction; ρ, a constant for the reaction; and σ, a constant for the substituent. Okamoto and Brown (Ref. 32) modified Hammett's Sigma values for electrophilic reactions. These modified values were referred to as σ^+.

It was found possible to measure the rate constants for the general reaction,
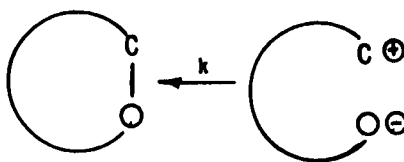
and the valu-s of k for various photochromic compounds were found to be consistent with the Hammett Equation. In Figure 125, the negative logarithm of the rate constant, k, for a specific photochromic compound was plotted against its respective σ^+ value (Table XXVII). The approach of the points to a straight line indicated that the theoretical considerations involved in assigning sigma values were correct and that the stability of the colored form of certain new photochromic materials could be accurately predicted before synthesis.

There was, however, a limit to the increase in stability gained by increasing σ^+ values. The 6', 8' -dinitro BIPS was assigned a σ^+ value of 1.554 and should have been appreciably more stable than any of the BIPS compounds in Table XXVIII. On preparation of the 6', 8' -dinitro BIPS it was found that the colored form was so stable that the colorless form could not be prepared.

Synthesis work was also conducted on the preparation of dipyrospirans, which too had been reported to be photochromic at low temperatures(Ref. 5). In this area, as with the benzoindolinospiropyrans, improved temperature stability of the colored form was attained by the application of Hammett's Rule. However, this series of compounds did not reach the same stability level as the BIPS compounds.

Although, twenty-five new materials were synthesized which exhibited improved photochromic properties over previously known materials. Table XXVIII lists all the photochromic spiro compounds prepared prior to the contract.

<div align="center">339</div>

ASD TR 61-70

Evaluation of the photochromic properties of the various compounds was
complicated by the fact that the properties of a single material were
greatly affected by the media. This effect was of the same order of
magnitude as a distinct change in the structure. The light absorption
properties of photochromic materials varied with the media. The
reversible photochromic reaction was also temperature sensitive. Each
new compound, therefore, had to be evaluated in various solvents and on
various surfaces. These variables indicated the latitude and flexibility
available with photochromic systems.

Figures 126 through 128 give the absorption spectra of typical photochromic
compounds. In Figure 126, for example, it can be noted that there was
strong ultraviolet absorption for the unexposed sample with maxima at
225 mμ and 235 mμ. When this material was exposed to ultraviolet light,
it was partially converted to its colored form and a strong absorption
occurred with a maximum at 532 mμ. The molar extinction coefficient for
the colored form of the material was found to be 5.2×10^4. If the same
compound was dissolved in other solvents, or mixed solvents, the visible
absorption spectra could be shifted appreciably (Table XXIX).

ASD TR 61-70
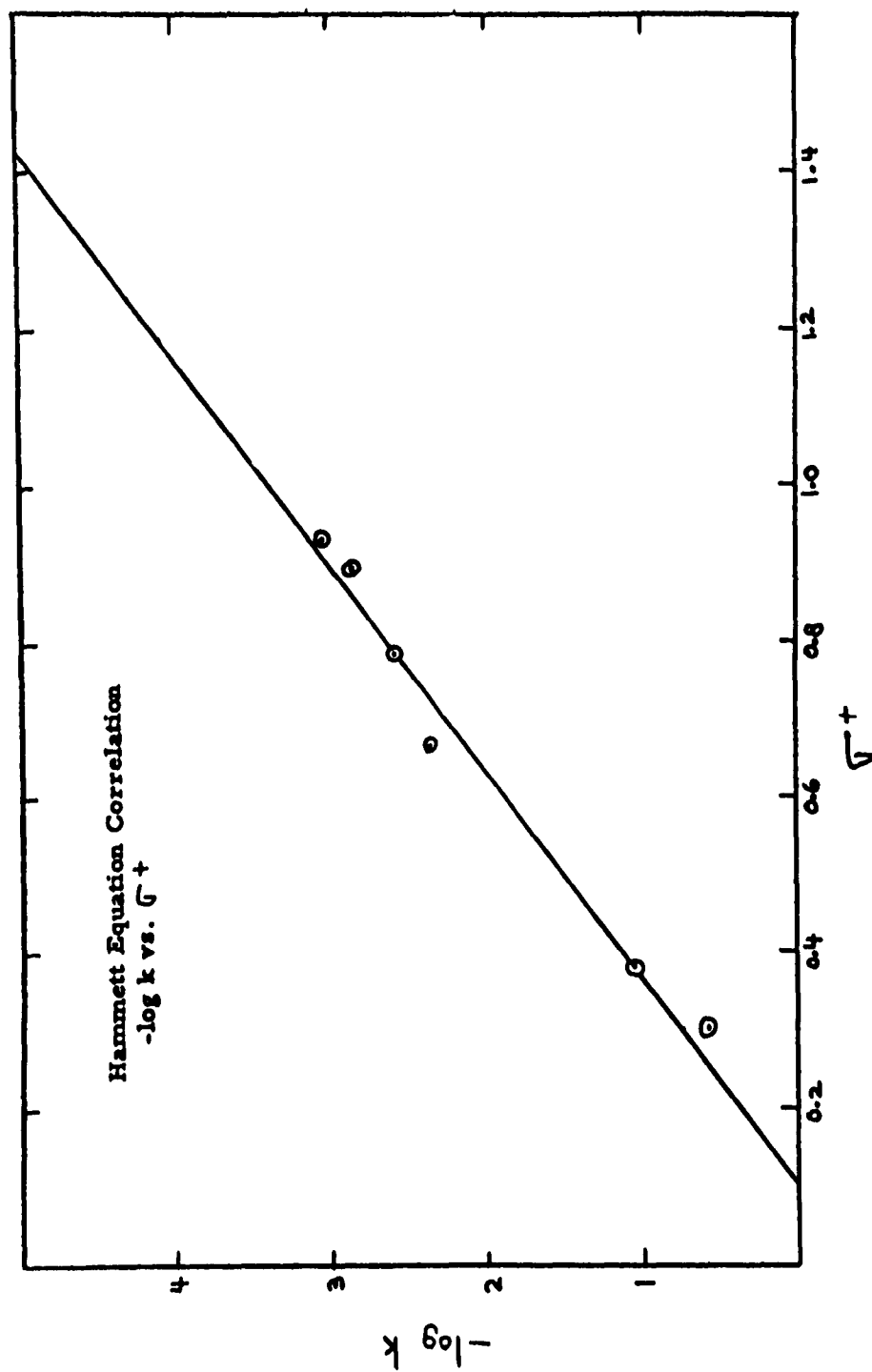
Figure 125. Plot of Rate Constant vs. σ^+ Value.

341
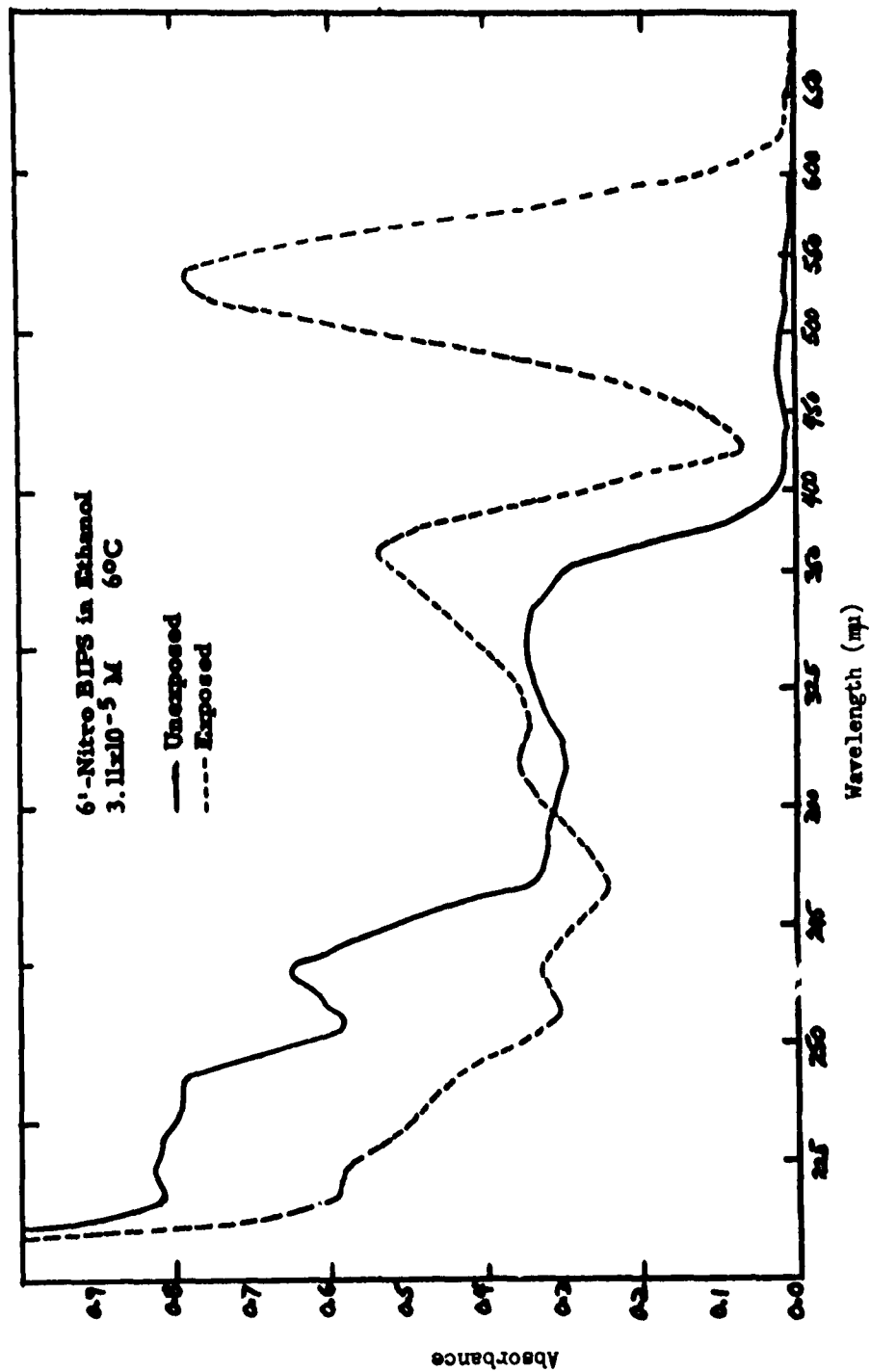
Figure 126. Absorption Spectra of Typical Photochromic Compounds
(6'-Nitro BIPS in Ethanol).

342
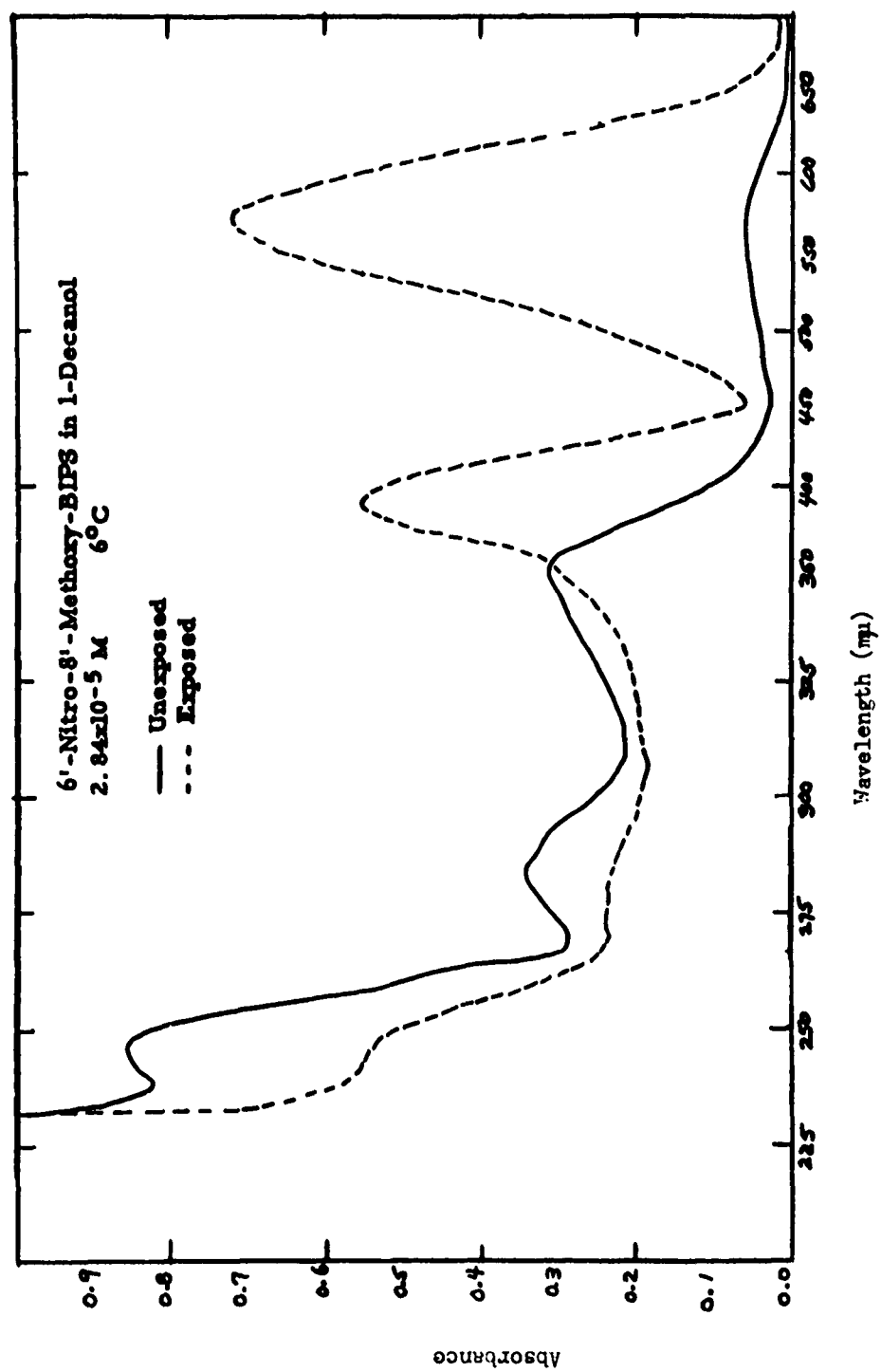
Figure 127.   Absorption Spectra of Typical Photochromic Compounds
(6'-Nitro - 8' - Methoxy-BIPS in 1 - Decanol).

343
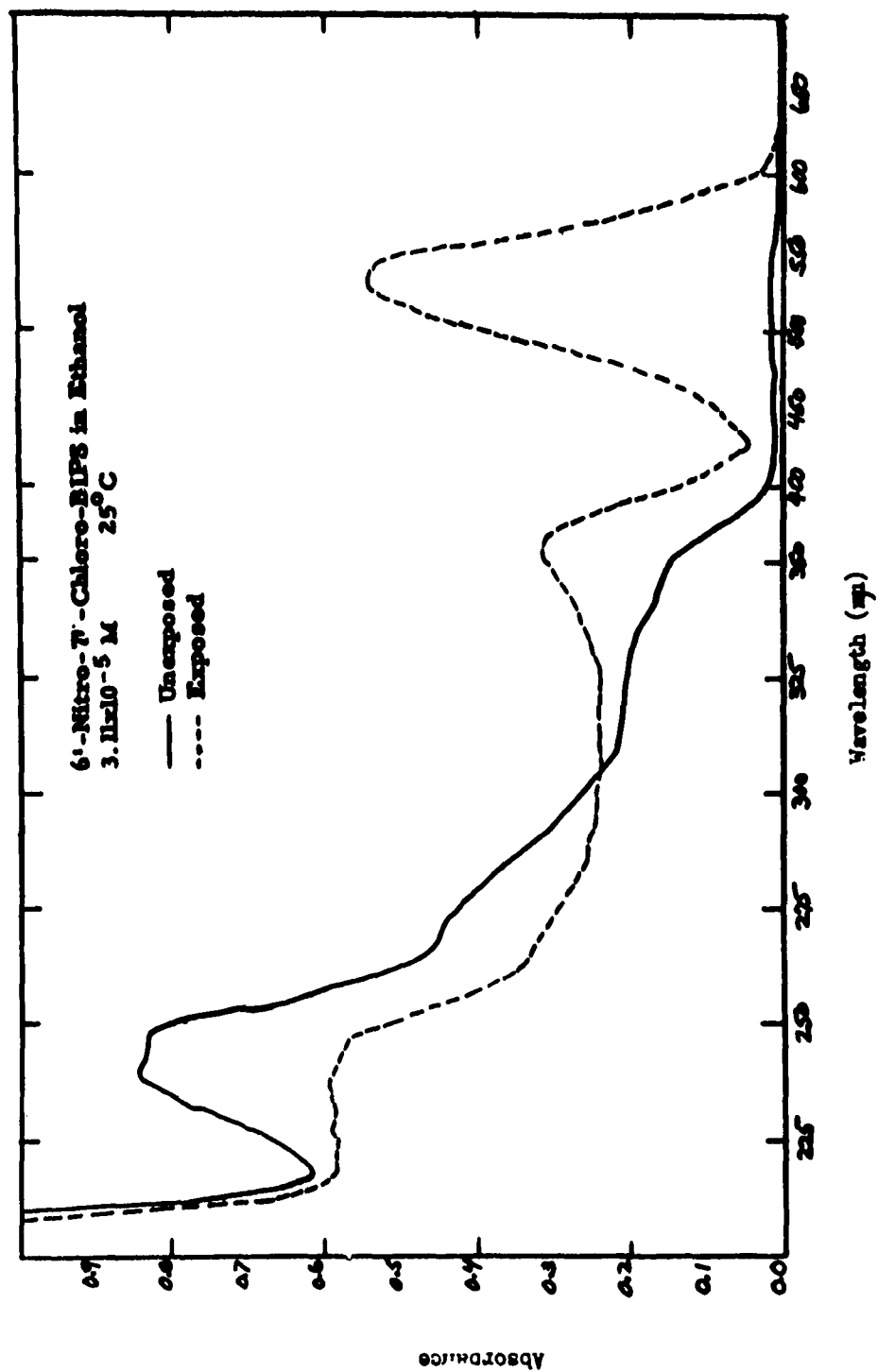
Figure 128. Absorption Spectra of Typical Photochromic Compounds.
(6'-Nitro - 7' - Chloro-BIPS in Ethanol).

ASD TR 61-70

TABLE XXVII

HAMMETT EQUATION CORRELATION

BIPS	σ^+	$k(min^{-1})$*
6',8'-dibromo	0.296	2.53×10^{-1}
7'-chloro	0.373	8.72×10^{-2}
7'-nitro	0.662	4.10×10^{-3}
6'-nitro	0.777	2.57×10^{-3}
6'-chloro-8'-nitro	0.889	1.36×10^{-3}
6'-bromo-8'-nitro	0.925	8.39×10^{-4}

* For the first order rate of disappearance of the colored form of the substituted BIPS compounds at $6^\circ C$ in ethanol.

ASD TR 61-70

TABLE XXVIII

BIPS COMPOUNDS

Material	Formula	Calc.	Found	Calc.	Found
Parent Compound (BIPS)	$C_{19}H_{19}NO$	82.9	82.4	6.9	6.9
5-nitro	$C_{19}H_{18}N_2O_3$	70.8	70.8	5.6	5.8
6'-nitro	$C_{19}H_{18}N_2O_3$	70.8	70.5	5.6	5.6
7'-nitro	$C_{19}H_{18}N_2O_3$	70.8	70.6	5.6	5.8
8'-nitro	$C_{19}H_{18}N_2O_3$	70.8	70.7	5.6	5.7
6',8'-dinitro	$C_{19}H_{17}N_3O_5$	62.1	62.2	4.7	5.0
5'-chloro	$C_{19}H_{18}NOCl$	73.2	73.2	5.8	5.5
6'-chloro	$C_{19}H_{18}NOCl$	73.2	73.0	5.8	5.5
7'-chloro	$C_{19}H_{18}NOCl$	73.2	72.9	5.8	6.0
6'-bromo	$C_{19}H_{18}NOBr$	62.3	62.3	5.0	5.0
6',8'-dibromo	$C_{19}H_{17}NOBr_2$	52.4	52.3	3.9	3.9
8'-fluoro	$C_{19}H_{18}NOF$	77.3	77.1	6.1	6.0
5-nitro-6'-bromo	$C_{19}H_{17}N_2O_3Br$	56.9	56.9	4.3	4.3
6'-nitro-7'-chloro	$C_{19}H_{17}N_2O_3Cl$	64.0	64.2	4.8	4.9
6'-chloro-8'-nitro	$C_{19}H_{17}N_2O_3Cl$	64.0	64.3	4.8	4.8
6'-nitro-8'-bromo	$C_{19}H_{17}N_2O_3Br$	56.9	56.9	4.3	4.5
6'-bromo-8'-nitro	$C_{19}H_{17}N_2O_3Br$	56.9	56.9	4.3	4.3
6'-nitro-8'-fluoro	$C_{19}H_{17}N_2O_3F$	67.1	67.4	5.0	5.0
5'-nitro-6'-bromo-8'-methoxy	$C_{20}H_{19}N_2O_4Br$	55.7	55.8	4.4	4.6
5-nitro-8'-methoxy	$C_{20}H_{20}N_2O_4$	68.2	67.9	5.7	5.9

346

TABLE XXVIII (Cont'd)

BIPS COMPOUNDS

Material	Formula	Calc.	Found	Calc.	Found
5'-nitro-8'-methoxy	$C_{20}H_{20}N_2O_4$	68.2	68.1	5.7	5.8
6'-nitro-8'-methoxy	$C_{20}H_{20}N_2O_4$	68.2	68.2	5.7	6.0
6'-methoxy-8'-nitro	$C_{20}H_{20}N_2O_4$	68.2	67.8	5.7	5.9
5-amino-8'-methoxy	$C_{20}H_{22}N_2O_2$	74.5	74.7	6.9	6.9
5'-amino-8'-methoxy	$C_{20}H_{22}N_2O_2$	74.5	74.7	6.9	7.0
6'-hydroxy	$C_{19}H_{19}NO_2$	77.8	77.6	6.5	6.3
7'-hydroxy	$C_{19}H_{19}NO_2$	77.8	77.8	6.5	6.4
5',7'-dihydroxy	$C_{19}H_{19}NO_3$	73.8	73.7	6.2	6.1
6'-nitro-7'-hydroxy	$C_{19}H_{18}N_2O_4$	67.4	67.6	5.4	5.4
6'-amino-7'-hydroxy	$C_{19}H_{20}N_2O_2$	74.0	73.8	6.5	6.5
6'-methoxy	$C_{20}H_{21}NO_2$	78.1	78.1	6.9	6.6
5',7'-dimethoxy	$C_{21}H_{23}NO_3$	74.8	74.9	6.8	6.9
6'-phenylazo	$C_{25}H_{23}N_3O$	78.7	78.3	6.1	6.2
6'-p-nitrophenylazo	$C_{25}H_{22}N_4O_3$	70.4	70.6	4.8	5.1
6'-o-nitrophenylazo	$C_{25}H_{22}N_4O_3$	70.4	70.6	4.8	4.8
8'-allyl	$C_{22}H_{23}NO$	83.0	83.0	7.6	7.6
6',8'-diallyl	$C_{25}H_{27}NO$	84.0	84.2	7.6	7.5
7'-hydroxy-8'-formyl	$C_{20}H_{19}NO_3$	74.7	75.0	6.0	6.1
8'-carbomethoxy	$C_{21}H_{20}NO_3$	75.2	75.6	6.3	6.1

TABLE XXVIII (Cont'd)

BIPS COMPOUNDS

Material	Formula	Calc.	Found	Calc.	Found
6'-hydroxy-8'-methoxy	$C_{20}H_{21}NO_3$	74.3	74.2	6.5	6.3
5'-nitro	$C_{19}H_{17}N_2O_3$	70.6	70.9	5.6	5.8
6',8'-diiodo	$C_{19}H_{17}NOI_2$	43.1	43.4	3.2	3.2
6'-NO$_2$-8'-carbomethoxy	$C_{21}H_{19}N_2O_5$	66.5	66.3	5.1	5.0
7'-hydroxy-8'-bromo	$C_{19}H_{21}NO_2Br$	61.5	61.7	4.6	4.4
6'-nitro-8'-allyl	$C_{22}H_{21}N_2O_3$	73.1	73.3	5.9	6.0
6'-nitro-8'-iodo	$C_{19}H_{16}N_2O_3I$	51.0	51.0	3.6	3.7
1,3,3-trimethylindolino-7'-nitro-β-naphthopyrylospiran	$C_{23}H_{20}N_2O_3$	74.2	73.8	5.4	5.2

DIPYROSPIRANS

Material	Formula	Calc.	Found	Calc.	Found
6-nitro-3-methylbenzo-β-naphthospiropyran	$C_{22}H_{15}O_4N$	73.9	73.6	4.2	4.1
6-nitro-8-methoxy-3-methylbenzo-β-naphthospiropyran	$C_{23}H_{17}O_5N$	71.2	71.1	4.3	4.6
3,3'-dimethylene-di-β-naphthospiropyran	$C_{23}H_{18}O_2$	86.6	85.9	4.8	4.7
3,3'-trimethylene-di-β-naphthospiropyran	$C_{28}H_{20}O_2$	86.5	86.8	4.9	5.2
6,6'-dinitro-3-3'-diphenyl-dibenzospiropyran	$C_{29}H_{18}O_8N_2$	71.0	71.3	3.7	3.8

TABLE XXVIII (Cont'd)

BIPS COMPOUNDS

Material	Formula	Calc.	Found	Calc.	Found
3-phenylbenzo- β -naphthospiro-pyran	$C_{29}H_{18}O_2$	86.5	86.3	4.9	5.0
6-chloro-3-methylbenzo- β -napthospiropyran	$C_{22}H_{15}O_2Cl$	76.2	76.0	4.4	4.7
3'-methylbenzo- β -naphtho-spiropyran	$C_{22}H_{16}O_2$	84.5	84.8	5.2	5.4
benzo- β-naphthospiropyran	$C_{21}H_{14}O_2$	84.7	85.1	4.7	4.7

349

TABLE XXIX

SHIFT OF ABSORPTION MAXIMUM IN A MIXED SOLVENT SYSTEM[*]

Percent volume of ethanol	Absorption Maximum, $m\mu$
0.00	600
0.40	594
0.79	585
1.57	579
3.47	573
100.0	532

[*] 6'-Nitro EIPS in benzene with varying amounts of ethanol.

350

b. Energy Studies

The photochromic and thermochromic processes in spiropyrans involve one or more of the following transformations:
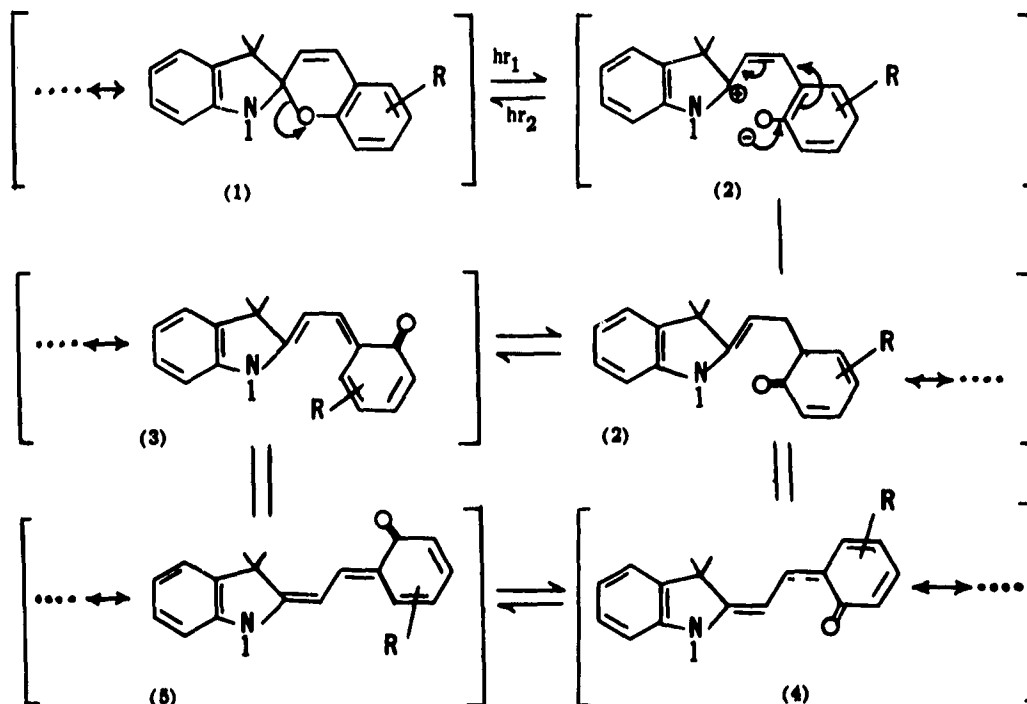
In most photochromic spiropyrans, two materials have been observed; one being colorless or light yellow, the other highly colored. The colorless form has structure (1) since the spiro structure prevents resonance interactions between the two aromatic moieties. The colored form is either one or more of structures (2 - 5). Since one of structures (2 - 5) has an absorption peak at 575 ± 50 millimicrons, (2 - 5) would be expected to be colored, as the absorption peaks of cis-trans isomers commonly do not differ by more than 50 mμ. On steric grounds, one would expect the stable

351

colored form to be the trans-trans compound (5) or perhaps the trans-cis compound (4).

In the photo or thermochromic color formation process, therefore, compound (1) absorbs light or thermal energy which converts it to (2). Compound (2) then isomerizes more or less rapidly to (4) or (5). In the reverse process, compound (5) or (4) absorbs light or thermal energy to convert it eventually to compound (2) which forms a carbon-oxygen bond to give compound (1).

The kinetics of the thermal process form colored spiropyran to colorless spiropyran were studied for a number of systems. In general, a first order rate law was followed. If the reaction under consideration followed Arrhenius' temperature dependence,[33] then,

$$d (\ln k) / dT = E_a / RT^2$$

where k was the rate constant, E_a the Arrhenius activation energy, R the "Gas constant" and T the absolute temperature. If E_a was a constant with respect to temperature, then integration gave

$$\ln k = -E_a / RT + \text{constant}$$

It was known that a plot of -log k versus 1/T should give a straight line if the assumptions made were applicable to the system.

Plot of -log k where k is the first order rate constant versus 1/T for 6'-nitro-7'-chloro BIPS in p-isopropylbenzyl alcohol is given in Figure 129. Since the plotted data closely approached a straight line, the Arrhenius activation energy (24.42 Kcal/mole) was calculated from the slope of the line. Chaude'[13] had found heat of reaction, ΔH, values of about two Kcal/mole for the same type transformations.

In the photochemical transformations, conversion from colorless to colored (1 → 5) is possible with light of wavelength 405 mμ or less while light from 575 mμ to 425 mμ causes conversion from colored to colorless (5 → 1). Therefore, the activation energy for formation of the colored form

6'-Nitro, 7'-chloro BIPS in p-Isopropylbenzyl Alcohol
$E_a = 24.42$ Kcal/mole
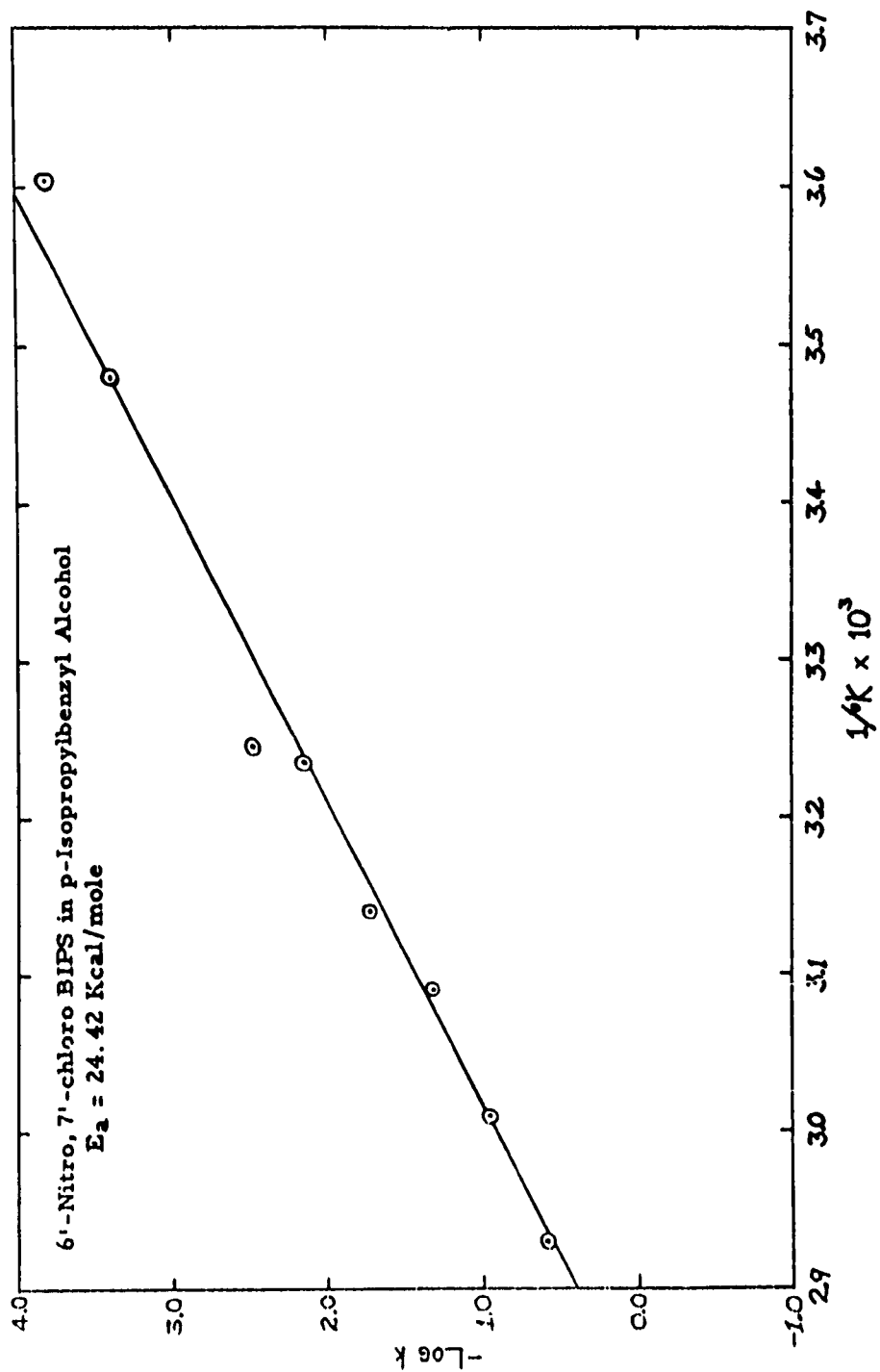
Figure 129. Plot of Rate Constant vs 1/T.

353

is equal to or less than 70 Kcal/mole (405 mμ light) while the activation energy for the formation of the colorless form from the colored is equal to or less than 49 Kcal/mole (575 mμ light).

The energy relationships for typical photo and thermochromic spiropyran systems are summarized in Figure 130. The lower energy curve represents the ground states of the colored (5) and colorless (1) forms and the thermally activated state while the upper energy curve represents the photochemically activated state. It was found that the thermal energy of the order of 25 Kcal/mole supplied to the colored form (5) will raise it from the potential energy well to the activated state and then to the colorless form (1) by evolution of about 27 Kcal/mole. The thermal energy barrier of 25 Kcal/mole is close to an ideal barrier, for if it was much less than 20 Kcal/mole, some molecules would, at room temperature, due to normal Gaussian energy distribution, have sufficient energy to pass this barrier (Ref. 4). When a photon having energy of 405 mμ light or higher is absorbed by a colorless molecule (1) in its ground state the molecule is brought to the photochemical activated state from which it may give up energy (as visible light or heat) and become a colored molecule (5). Similarily, when a colored molecule (5) in its ground state absorbs a photon of energy corresponding to light between 435-575 mμ it is brought to the photochemical activated state from which it may become a colorless molecule.

c.   Methods of Fixing

In the foregoing discussions emphasis was based on the point that the photochromic spiropyrans exhibited reversible color changes, which would make them suitable as chemical switches applicable for data storage devices and light filters. On the other hand, if a compound were switched from one state to another irreversibly, it would become a tool for photographic systems such as films, oscillograph recording paper, and printing systems. Studies were made to find methods which would aid in stabilizing or "fixing" the exposed image in a previously reversible system and thereby attain a possible non-silver halide system.
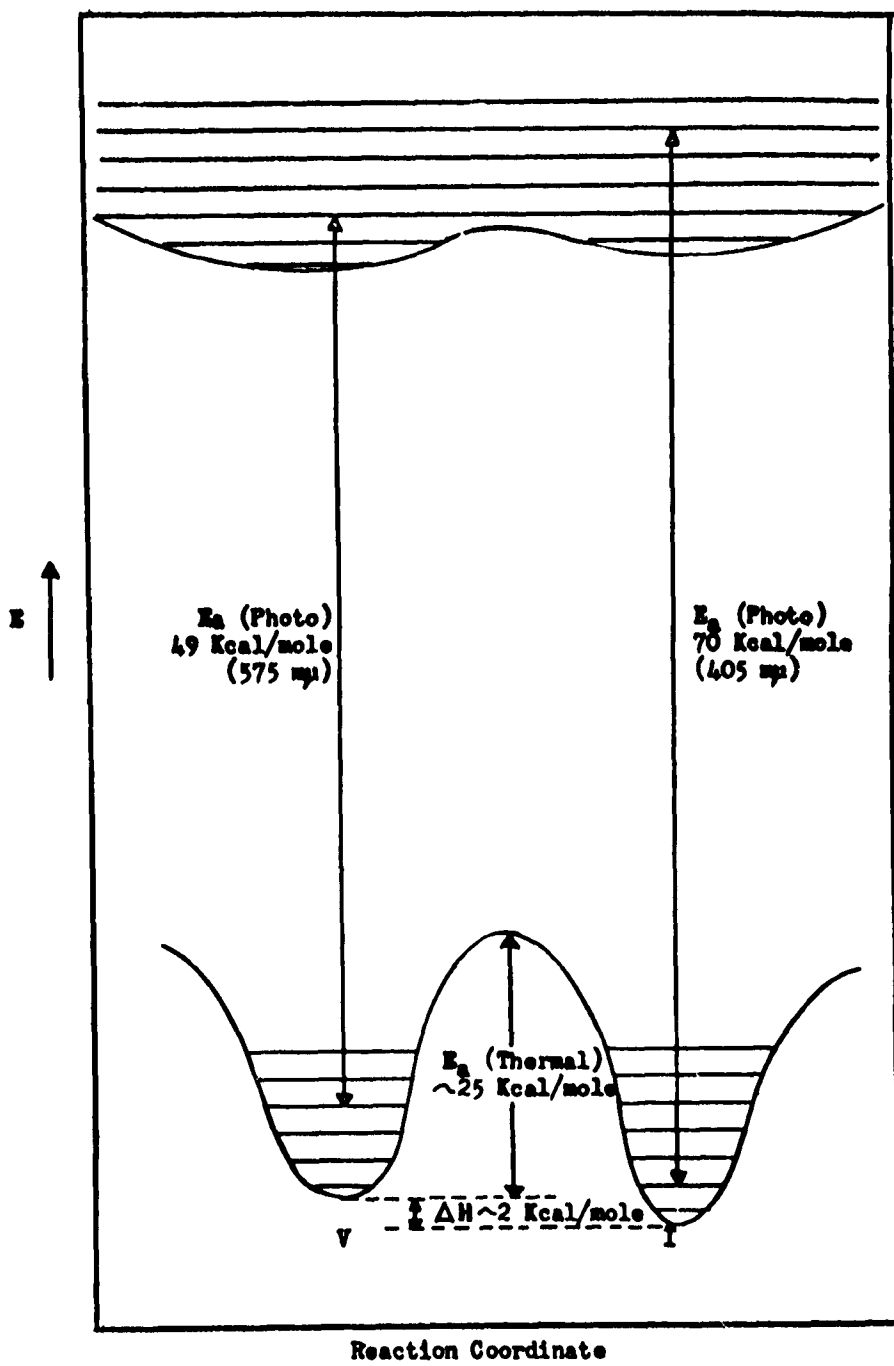
354

Figure 130. Potential Energy Diagram.

355

(1) Preferential Adsorption. It was first observed that the 6'-nitro
BIPS in its colored form could be preferentially adsorbed on Solk-Floc
α -cellulose, when the adsorbent was suspended in cyclohexane containing
the spiropyran and the solution exposed to an ultraviolet light source. After
the exposure, as the adsorbent settled, the supernatent liquid was colorless
and the solid colored grayish-black. A similar experiment carried out in
benzene resulted in no adsorption of the colored form onto the adsorbent.

It was known that this phenomena potentially offered a method of fixing,
if the adsorbent could be encapsulated along with the solution of the
photochromic compound. Upon exposure, the colored form would prefer-
entially be adsorbed into the adsorbent and render the image fixed. It was
still necessary, however to deactivate the unexposed areas.

(2) Chemical Reactions. Coatings of the encapsulated BIPS compounds
were as sensitive as the solution in bulk. After an image was formed on the
coated sheet, the image was stabilized by moistening the sheet with dilute
acidic or basic solutions. The degree of stability varied with the composi-
tion of the internal phase of the capsules.

This method did not require the rupture of the capsules, but it still left
the sheet sensitive to subsequent exposures.

(3) Removal of the Solvent. To take advantage of the fact that the photo-
chromic spirans generally did not exhibit their switching properties in the
solid state, the removal of the solvent offered a method for fixing the
compounds in their existing state.

By calendering a sheet coated with the photochromic capsules, the solvent
was permitted to evaporate thereby fixing the image previously produced.
It was also possible to apply a solution of the photochromic compound into
the proper receiving sheet, make an exposure, and drive off the solvent to
fix the print. A 2:3 percent solution of the BIPS compound in benzene
generally offered the best results. A modified method of this principal was

356

to have an organic compound with the above properties coated in contact with capsules containing the necessary solvent. Under these conditions the coated sheet was passed through pressure rolls to rupture the capsules, the solvent was released and dissolved the compound which in solution was light-sensitive similarly as the system described above.

3.   Encapsulation

A technique was developed by The National Cash Register Company in which a thick film (0.1 μ) of a colloid material was deposited about tiny individual oil drops (1-2 μ diameter) (Ref. 34-38). This process was based on the principle known as coacervation. When these films were hardened, they provided protection for each oil drop, and when coated and dried on base material, the microscopic capsules retained their form, holding the oil in place. There was no tendency for the encapsulated oil to migrate to the surface or into the base stock, even over extended periods of time under extreme environmental conditions.

It was also found that the submicroscopic porosity of the capsular wall in the dry state could be varied over a wide range, so that very volatile solvents could be encapsulated and retained in the "dry" form for years without loss of solvent. With the same system, if desired, the porosity could be so adjusted that the volatile solvent would gradually leave the structure during storage.

The oil drop range was studied between 0.1 μ to 0.5 cm., and the ratio of colloid to oil was varied from four parts colloid - one part oil to one part colloid - eight parts oil. By the variation of these parameters, oil drop size and phase ratio, the wall thickness of the capsule was varied.

With this technique, it was possible to encapsulate a wide variety of oils, solids, and solids dispersed or dissolved in the oil phase. It was also shown that these materials have wide application in industries either as coated materials on various base materials or as "solid" liquids in powdered or chunk form.

357

A variety of photochromic materials were encapsulated and coated on base materials. By variations in the composition of the internal phase (solute and solvents), coatings of different photographic characteristics were obtained.

4. Capsular Systems Involving Photopolymerization of Contained Oils

Systems were studied which involved the encapsulation of an oil in which was dissolved a dye and an organic compound capable of photopolymerization or photo-cross linking. It was found that when the surface of a paper coated with the capsules was subjected to light, polymerization in the oil phase was induced, and the internal phase viscosity increased rapidly to a high value. The degree of polymerization was a function of the exposure; thus, the system offered the possibility of producing a continuous tone reproduction. To develop the image, the exposed sheet was passed through pressure rolls in contact with a receiving sheet. The amount of oil with dissolved dye that was transferred was a function of the internal oil phase viscosity; that is, where considerable light reached the surface the viscosity of the oil was very high and little or no oil and dye would be transferred, the reverse being true where little or no light fell on the surface. A very interesting feature was that a system of this type produced a direct positive master from which a number of copies could be made. The system offered extreme simplicity in that no image development beyond the exposure was necessary, followed only by the transfer of the image to obtain a print. In addition the chemistry of photopolymerization reactions suggested the possibility of developing systems as sensitive as the silver halide systems to light, as well as systems that were sensitive to a very limited region of the spectrum.

5. Materials Evaluation Studies (Dayton)

Rather extensive experimental studies were carried out with respect to measuring the parameters of photochromic systems. Equipment was built and purchased as the program proceeded in order to refine the measurements

and obtain more precise data. Spectral curves were regularly run on the liquid systems from the ultraviolet region of the spectrum to the infrared, both in the colorless and colored states.

Some very specialized equipment for obtaining data was evolved from experimental work on the photochromic memory problem. The most interesting was the fatigue tester pictured in Figure 131. Both liquid and coating samples were mounted on the disk. As the disk was rotated, the samples were exposed to writing, reading and erasing stations to closely simulate certain types of memory operations. The rack of electronic equipment provided automatic and semi-automatic control for continuous operation.

In the fatigue tester, liquid materials under test were held in a hanging drop slide with a 1 x 3 inch microscope glass slide used as a cover plate, and sealed, or in another special holder which can be seen on the disk. The sample was placed on the rotating disk which periodically rotated the sample past the writing and erasing sources. The read station determined the change in transmission of the sample after the write and erase operations. The material was considered fatigued when it reached the point where very little change occurred on exposure to switching radiation. This point was usually at about one-tenth that of the original written density. Since the absolute optical density was highly dependent on the specific read source and filter used, relative densities were used in the fatigue experiments and were adequate to convey the data of significance.

The tester was also subjected to various environmental conditions in the deep freeze box shown in Figure 132. Tests were ordinarily run at reduced temperature in the refrigeration chamber. Other environmental chambers were also available at the Dayton facility for more exacting tests.

359
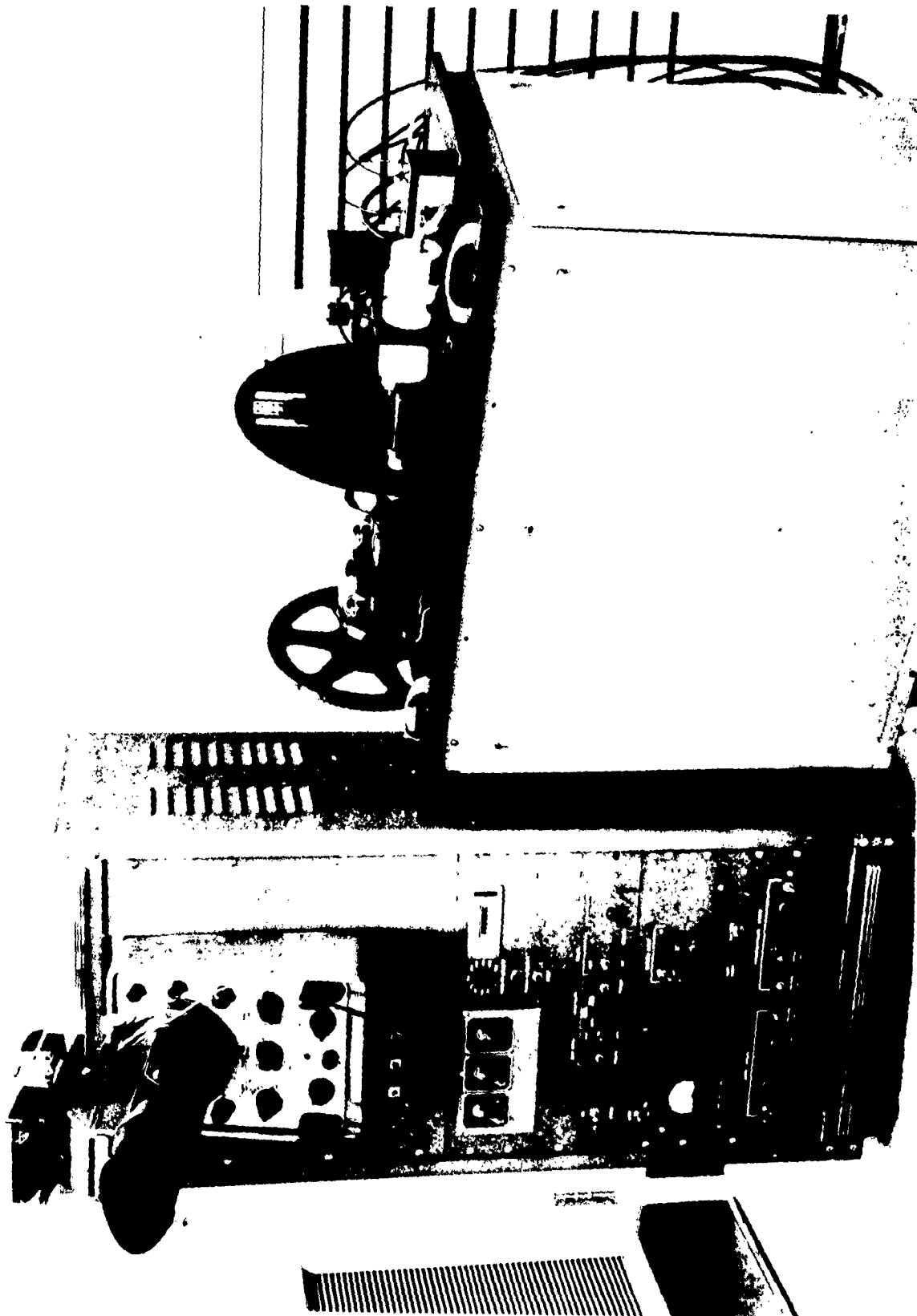
Figure 131. Fatigue Tester.
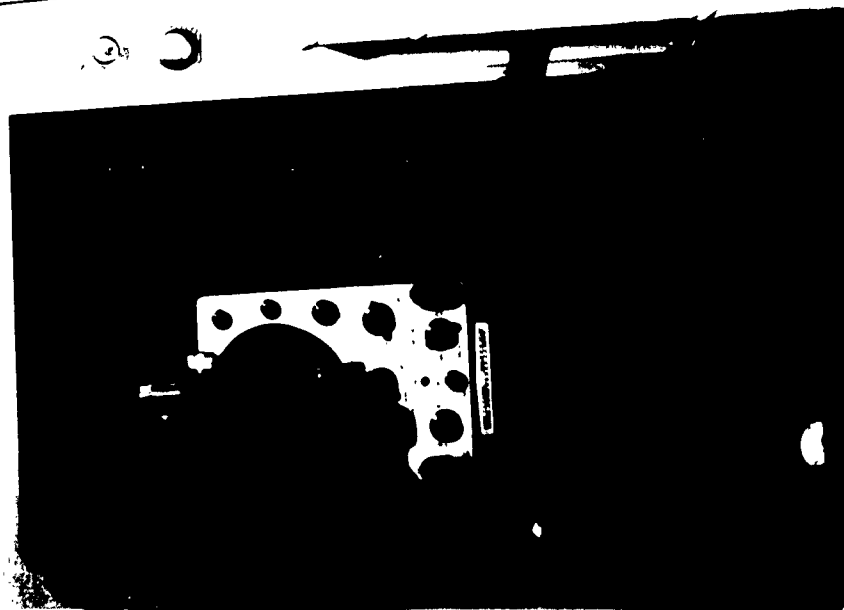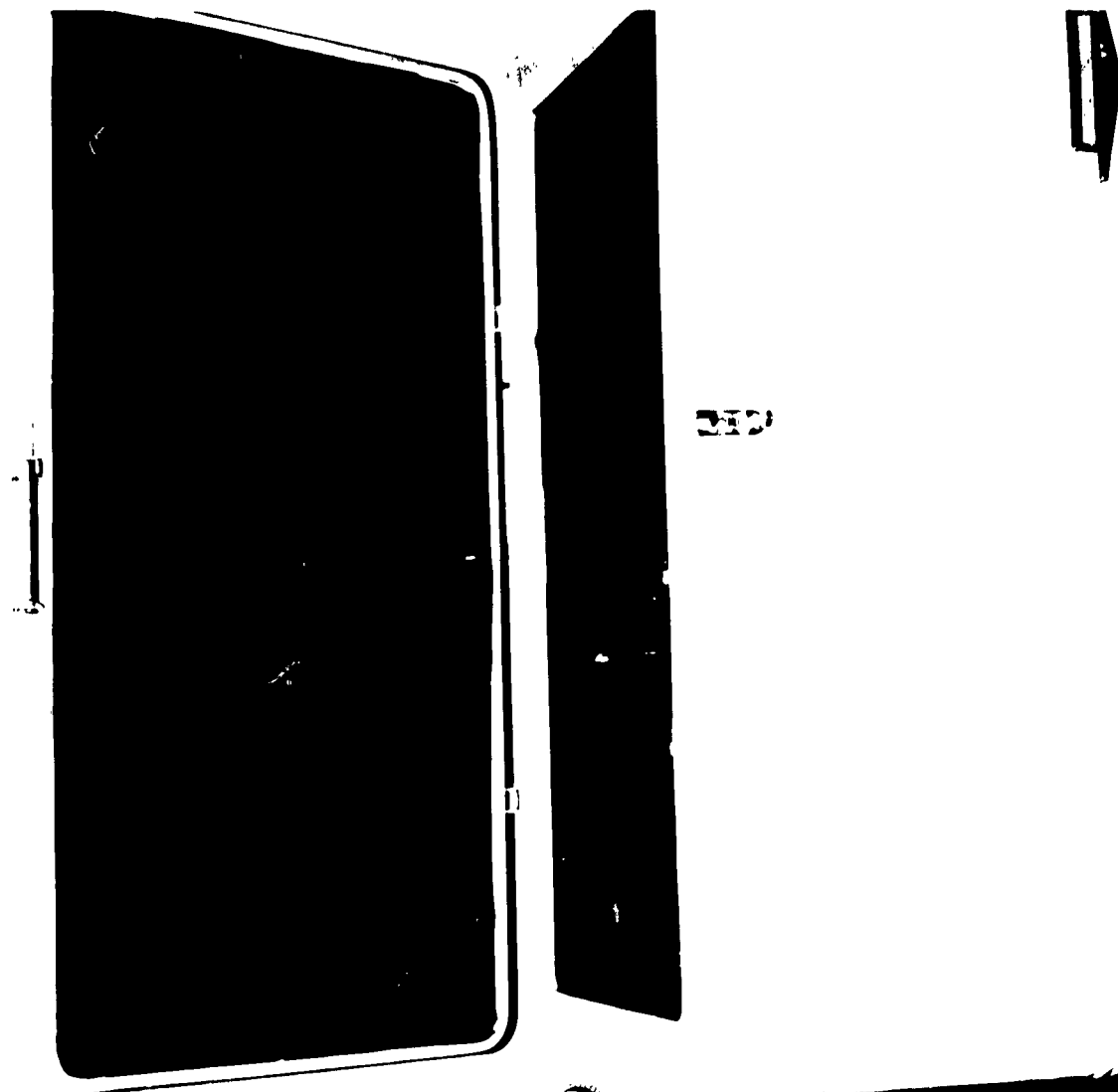
Figure 132. Fatigue Tester and Deep Freeze Box.

C. REFERENCES

1) P.A. Leighton and F.A. Luey, J. Chem. Phys. 2, 756 (1934),
   L. Kúchler and F. Patat, Z. Electrochem. 42, 529 (1936).
2) A. Schönberg et al., J. Chem. Soc., 14, 442 (1946).
3) E. Harnik, J. Chem. Phys. 24, 297 (1956).
4) G.W. Wheland, Advanced Organic Chemistry, John Wiley and Sons,
   Inc., New York pp. 200, 178 (1949).
5) Y. Hirshberg, Compt. Rend. 231, 903 (1950).
6) Y. Hirshberg and E. Fischer, J. Chem. Soc., 21, 629 (1953).
7) Y. Hirshberg and E. Fischer, J. Chem. Phys., 21, 1619 (1953).
8) Y. Hirshberg and E. Fischer, J. Chem. Soc., 22, 297 and 3129 (1954).
9) Y. Hirshberg, J. Am. Chem. Soc. 78, 2304 (1956).
10) Y. Hirshberg, J. Chem. Phys. 27, 758 (1958).
11) Y. Hirshberg, E.H. Frei and E. Fischer, J. Chem. Soc., 21, 2134 (1953).
12) E. Fischer and Y. Hirshberg, J. Chem. Soc., 20, 4522 (1952).
13) O. Chaudé, Cahiers Phys. 50, 17 (1954).
                                51, 6 (1954).
                                52, 3 (1954).
14) O. Chaudé and P. Rumpf, Bull. Soc. Chim, 18, 342 (1951).
15) O. Chaudé and P. Rumpf, Compt. Rend. 233, 405 (1951).
16) P. Rumpf and O. Chaudé, Ibid 1274 (1951).
17) O. Bloch-Chaudé, P. Rumpf, and J. Sadet, Ibid 1426 (1955).
18) O. Bloch-Chaudé and J.W. Masse, Bull. Soc. Chim., 22, 625 (1955).
19) R. Wizinger and H. Wennig, Helv. Chim. Acta. 23, 247 (1940).
20) A.A. Huckins and R.J.W. LeFevre, J. Chem. Soc. 17, 2088 (1949).
21) E.D. Bergmann, A. Weizman, and E. Fischer, J. Am. Chem. Soc. 72,
   5009 (1950).
22) A. Mustafa, Chem. Review 43, 509 (1948).
23) C.Y. Koelsch and W.R. Workman, J. Am. Chem. Soc. 74, 6288 (1952).
24) E.B. Knott, J. Chem. Soc. 19, 3038 (1951).
25) C.F. Koelsch, J. Org. Chem. 16, 1352 (1951).
26) A. Schönberg, A. Mustafa, and W. Asker, J. Am. Chem. Soc. 73, 2876
   (1951).
27) J.L. Masse, Compt. Rend. 238, 1320 (1954).
28) O. Chaudé and P. Rumpf, Compt. Rend. 236, 697 (1953).
29) Y. Hirshberg, E.B. Knott, and E. Fischer, J. Chem. Soc. 23, 3313
   (1955).
30) L.P. Hammett, Physical Organic Chemistry, McGraw-Hill Co. Inc.,
   New York, Chap. VII (1940).
31) R.W. Taft, Jr. in M.S. Newman Steric Effects in Organic Chemistry,
   John Wiley and Sons, Inc., New York p. 556 (1956).
32) Y. Okamoto and H.C. Brown, J. Am. Chem. Soc. 79, 485 (1957).
33) A.A. Frost and R.G. Pearson, Kinetics and Mechanism, John Wiley
   and Sons, Inc., New York p. 23 (1953).
34) B.K. Green and L. Schleicher, U.S. 2,800,457 (1957).
35) B.K. Green, U.S. 2,800,458 (1957).
36) B.K. Green, U.S. 2,712,507 (1955).

362

37) B. K. Green and L. Schleicher, U.S. 2,730,456 (1956).
38) B. K. Green and L. Schleicher, U.S. 2,730,457 (1956).
39) C. E. K. Mees, The Theory of the Photographic Process, Macmillan Company, New York p. 203 (1942).
40) F. E. Bartell, Laboratory Manual of Colloid and Surface Chemistry, Edwards Brothers, Inc., Ann Arbor, Michigan, pp. 101-102 (1949).
41) H. B. Weisen, Colloid Chemistry, John Wiley and Sons, Inc., New York, pp. 49-54, 89-90 (1950).
42) T. A. Berson and E. Brown, J. Am. Chem. Soc., 77, 448 (1955).
43) L. E. Hinkel, E. E. Ayling, and W. H. Morgan, J. Chem. Soc. p. 1855 (1931).
44) H. H. Hodgson and T. A. Jenkinson, J. Chem. Soc. p. 1740 (1927).
45) Bert, Bull. Soc. Chem., (4) 37, 1406.
46) A. H. Blatt, Organic Syntheses, Collective-Volume II John Wiley and Sons, Inc., New York, p. 590 (1947).
47) G. A. Lutz et al., J. Am. Chem. Soc., 70, 4139 (1948).
48) R. W. Taft et al., Ibid, 74, 4735 (1952).
49) M. C. Brown and M. Berkowski, Ibid, 74, 1894 (1952).
50) N. Zelensky and S. Namjetkin, Ber., 35, 2683 (1902).
51) C. T. Redeman and C. E. Redeman, Organic Syntheses, John Wiley and Sons, Inc., New York, p. 8, 78 (1949).
52) E. H. Huntress et al., J. Am. Chem. Soc., 56, 241 (1934).
53) R. C. Elderfield and S. L. Wythe, Heterocyclic Compounds R. C. Elderfield, Editor, Vol. 6, John Wiley and Sons, Inc., New York, p. 229 (1957).
54) L. F. Fieser, Experiments in Organic Chemistry, 3rd Edition, D. C. Heath and Company, Boston (1955).

APPENDIX VII

TESTING AND EVALUATION OF PHOTOCHROMIC MATERIALS (HAWTHORNE) PRIOR TO WADD CONTRACT AF 33(616)-6205

The Hawthorne photochromic materials testing program originally used coatings prepared in Dayton. This was followed by some experimental studies on the production of uniform coatings of encapsulated photochromic systems at Hawthorne. The microscopic as well as macroscopic uniformity required of a high density memory coating made the coating problem especially difficult.

It was found that during shipment of the bulk photochromic capsules to Hawthorne, severe aggregation occurred. It was not possible to sufficiently deaggregate the samples by either a chemical stirring motor or a liquidizer, even though the latter was effective in actually rupturing the capsules (determined by the odor of the released solvent). Experimental coatings on glass were made with the available samples; however, both spray coatings, Figure 133, and evaporation coatings, Figure 134, were made which exhibited pin holes, clumps of material and very poor uniformity of thickness. As can be seen from the photomicrographs, the evaporation coating has a much finer texture (the same magnification was used in both photographs) than the spray coating. The edges of the coatings were formed by scratching the surface with a sharp needle.

During writing studies, it was found that experimental measurements did not give reproducible results, and, in fact, some of the photochromic material lost the switching property completely. These measurements were made at room temperature, and erasing to the colorless state was accomplished through ordinary thermal decay of the colored state (10 to 15 minutes). Some of the troubles were ultimately traced to poor capsule structure, with eventual
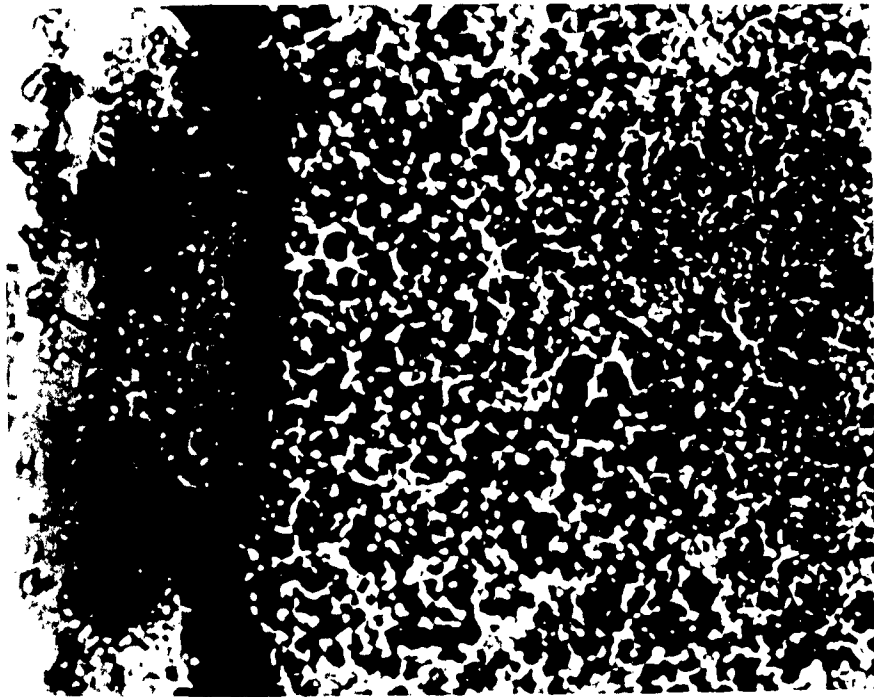
Figure 133. Capsular Spray Coating.
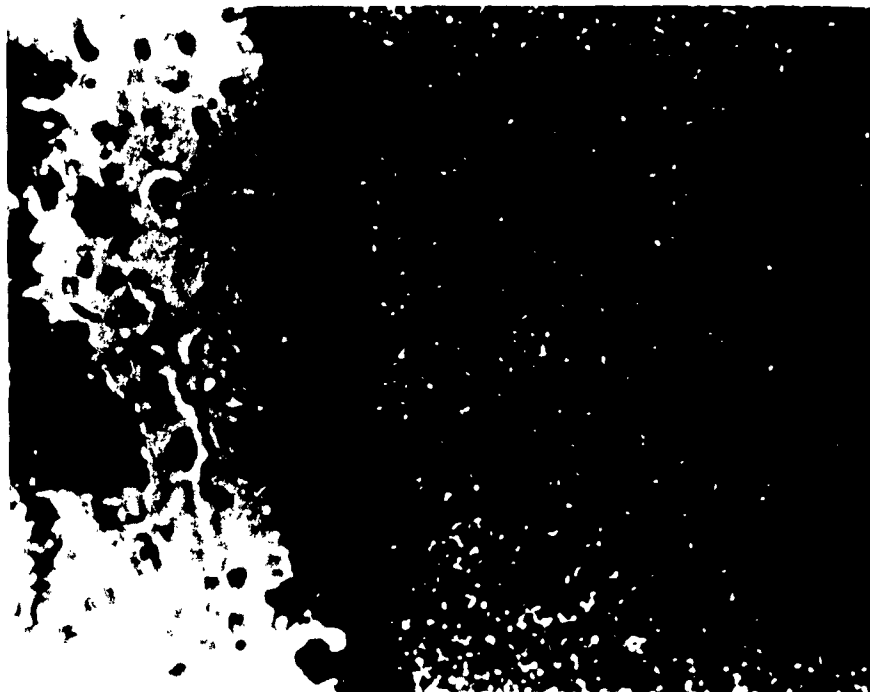
Figure 134. Capsular Evaporation Coating.

evaporation of the solvent. It was noted that the "good" capsules which lost their switching properties had an accompanying increase in color as they "fatigued." It was decided to conduct conclusive experiments to establish if this fatigue actually occurred.

Figures 135 and 136 show the experimental fatigue set-up for writing and reading a small spot. The spot was written with the disk stationary. Immediately after write,the disk was rotated and read by the "read" photo-multiplier. After allowing sufficient time for adequate thermal decay, the pattern was read again. This process was repeated a number of times taking care to always write at the same spot.

Typical results are shown in Figures 137 and 138. The central neutral density calibration steps represent densities of 0, 0.1, 0.2, 0..4, 0.8 and 1.0. It can readily be seen that there were two effects: a loss of writing ability and a build-up of the base level.

Most of the materials continued to show the loss of writing ability under dynamic excitation. However, one material did not show either type of fatigue in the limited dynamic tests to which it was subjected. Improvement in capsule structure was obtained through the use of larger capsules (from 3 microns to 15 microns). This fact implied a need to contend with a much more coarsely grained coating, but this situation has greatly improved since the experiments were run.

It was subsequently found in Dayton that the build up of the base level was due to a permanent precipitation of the colored photochromic material. This effect was largely eliminated by reducing the concentration of the photochromic material in the solvent. The slight base build-up now experienced is attributed to other factors.

The loss of writing ability was due to a fatigue that still persists. This has led to extensive synthesis and testing programs in order to eliminate the condition.

ASD TR 61-70
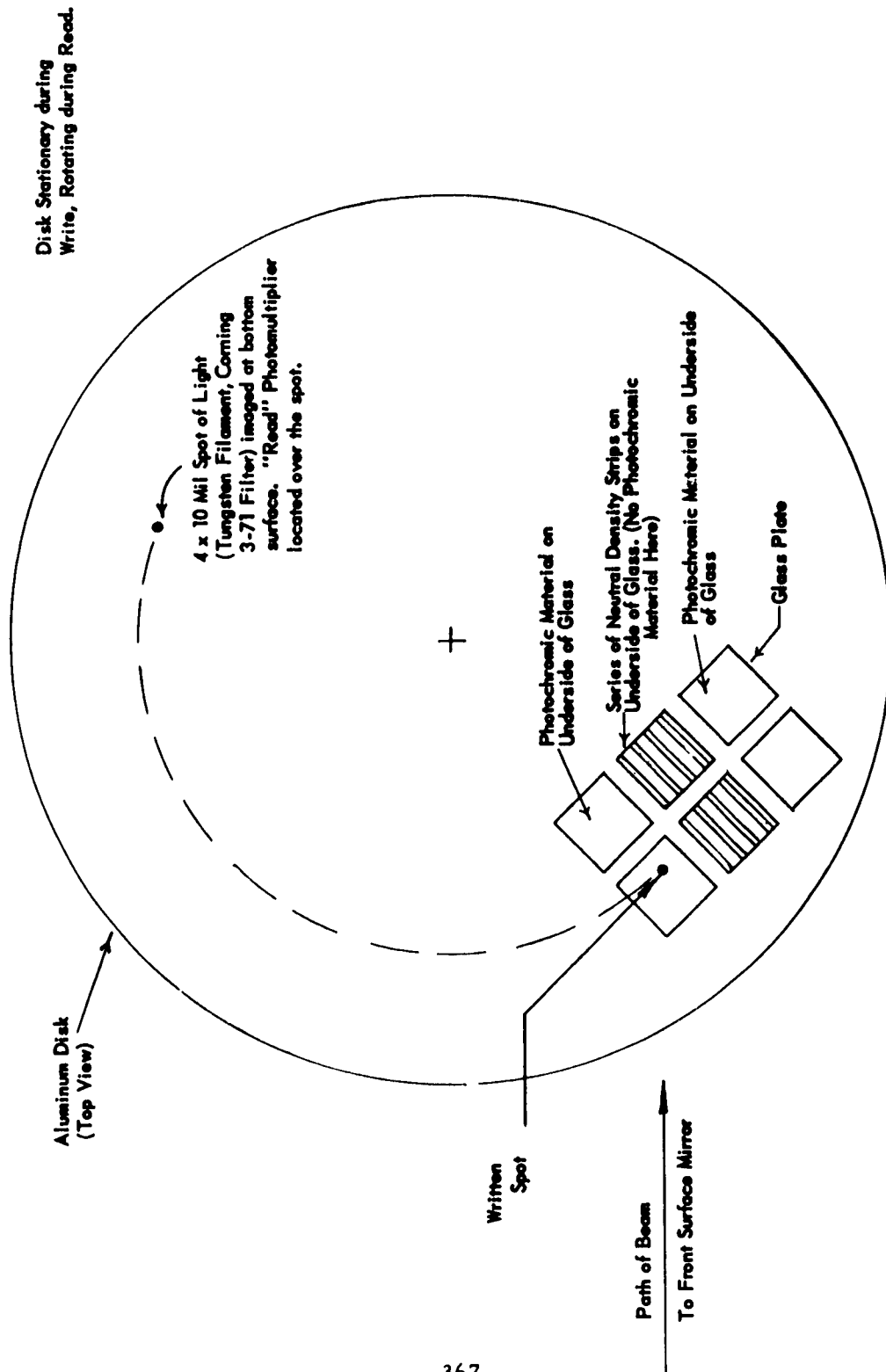
Figure 135. Experimental Disk Set-up.

367
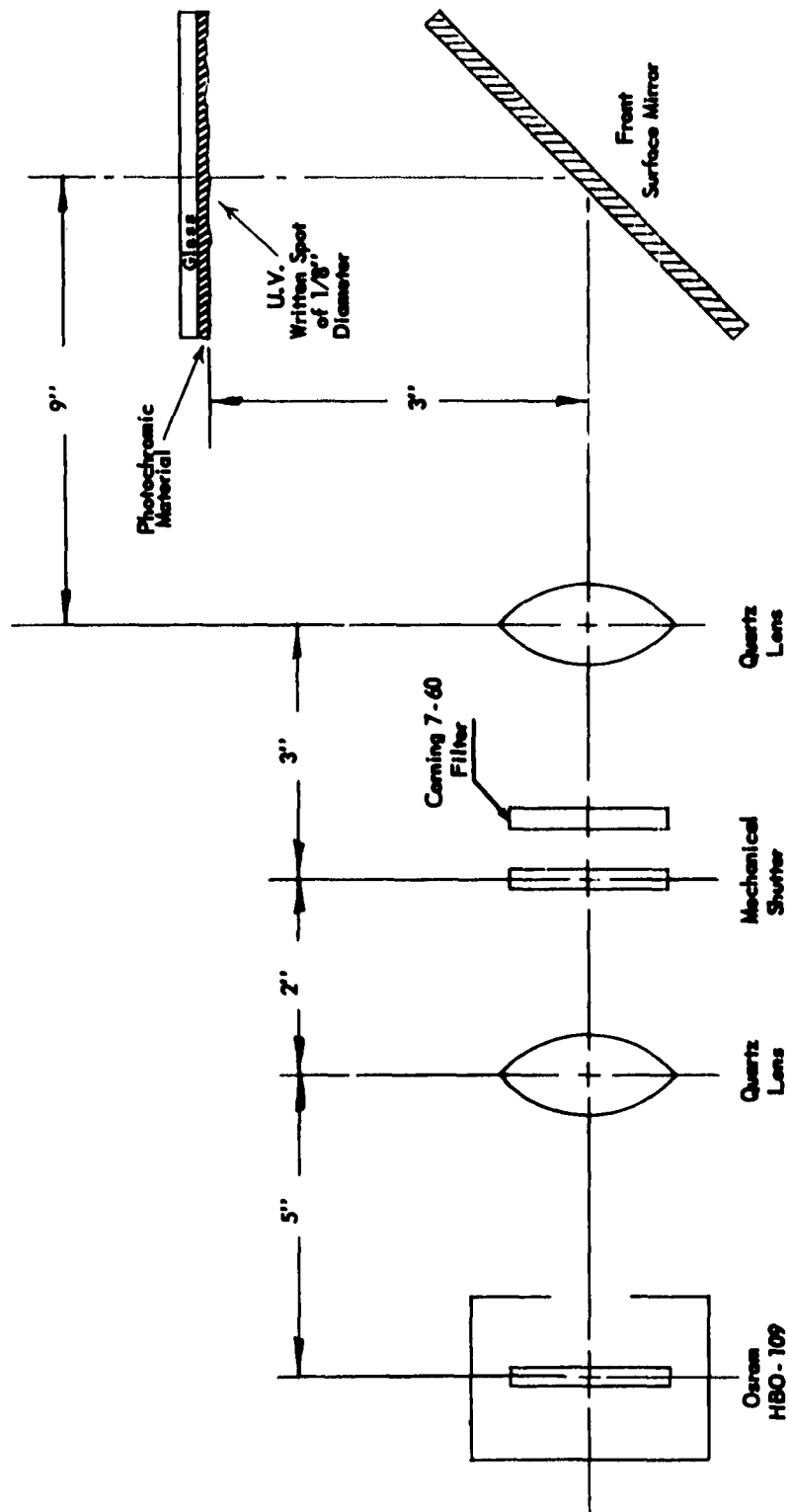
Figure 136. Optical Set-up for Writing.

Immediately After
First "Write"

After Thermal Decay

Figure 137. Fatigue Testing Waveforms.

Immediately After
12th "Write"

After Thermal Decay

Figure 138. Fatigue Testing Waveforms.

APPENDIX VIII

LIGHT SOURCE AND OPTICAL REQUIREMENTS
FOR OBTAINING OPTIMUM PERFORMANCE
IN A PHOTOGRAPHIC MEMORY

A.   INTRODUCTION

Optimum performance from any optical system used with photochromic material requires that it deliver the most energy per unit area at the material. (It is convenient to think in terms of "bits" 1 mil^2 in area.) The various factors which influence optical design will be evaluated to indicate what is required to produce over-all maximum performance for this particular application.

Objective terms and absolute units will be used as distinguished from the more commonly used subjective photometric units which refer to the sensation in the consciousness of a human observer. The reason for this choice is that subjective terms lose their meaning when dealing with ultra-violet radiation.

B.   MAXIMUM ENERGY PER UNIT AREA

Energy in the form of photons flows from an extended source as shown in Figure 139.
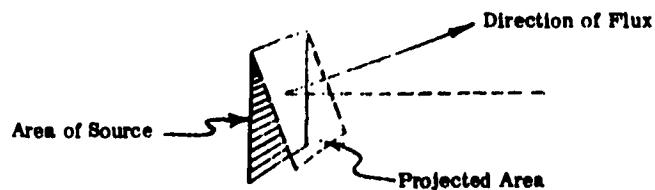
Figure 139.   Photon Energy Flow.

370

The intensity per unit of projected area of the source is called the luminance[1] of the source and may be measured in watts/cm^2 steradian. Similarly, the intensity of radiation falling upon a unit of projected area of the image is called the illuminance[1] of the image, again in watts/cm^2.

For a perfectly diffuse source the luminance of a source is independent of the angle θ or is a constant. Thus a perfectly diffuse disc appears equally bright from whatever angle it is viewed.

The f/number[*] of an optical system measures its ability to gather radiation and is the ratio of the object distance divided by the free aperture of the lens.[2] Now, the system has an f/number rating for its image side also, and this is equal to the image distance divided by the same free aperture. Thus,

$$\text{f/number (image side)} = \frac{\text{image distance}}{\text{free aperature}}$$

$$\text{f/number (object side)} = \frac{\text{object distance}}{\text{free aperature}}.$$

The relationship between the two f/numbers is therefore

$$\frac{\text{f/number (image side)}}{\text{f/number (object side)}} = \frac{\text{image distance}}{\text{object distance}}.$$

But since the ratio of image distance to object distance is equal to the magnification at which the system is being used, $f_i/f_o = M$.

Of the total energy radiated by the source only the fraction passing through the solid angle subtended by the lens will be used (see Figure 140). It can be shown (see section D-1) that, to a good approximation, the fraction intercepted

---

[*] This is not the lens manufacturer's f/number which is defined as the lens focal length divided by the free aperture. To avoid confusion, this will be denoted by $\bar{f}$.

371

ASD TR 61-70
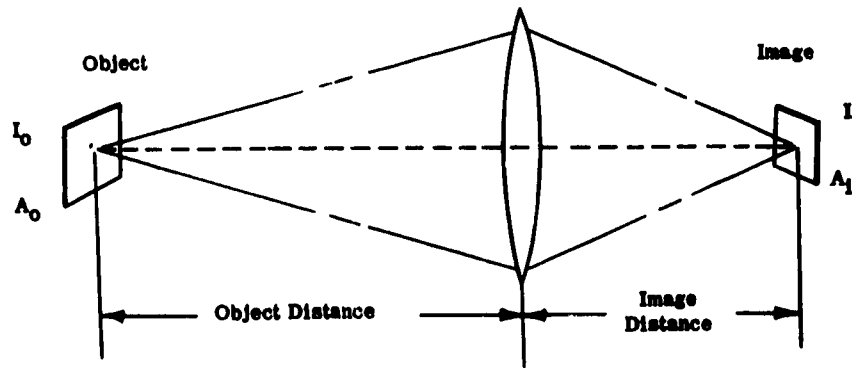
Figure 140. Basic Optical System.

is given by $\dfrac{F_o}{16 f_o^2}$ where f_o is the f/number (object side) and F_o is the total emitted flux from the source.

If K is the transmission coefficient of the lens, then the radiant flux falling upon the image of Figure 140 is given by

$$F_i = K \cdot \frac{1}{16 f_o^2} F_o.$$

The magnification, $M = \dfrac{f_i}{f_o} = \dfrac{\text{size of image}}{\text{size of object}}$

$$\therefore M^2 = \frac{\text{area of image}}{\text{area of object}} = \frac{A_i}{A_o} = \frac{f_i^2}{f_o^2}.$$

It follows then that flux per unit area of the image or the illuminance is

$$\frac{F_i}{A_i} = \frac{K}{16 f_o^2} F_o \cdot \frac{f_o^2}{f_i^2 A_o} = \frac{K}{16 f_i^2} \cdot \frac{F_o}{A_o}. \tag{1}$$

Thus we have the important result that intensity per unit area at the image depends upon the f/number (image side) of the lens[*] and the intensity per unit area of the source.

The introduction of faster lenses (low f/number) however, introduces some new problems.

---

[*] This f/number can approach the f/number determined by the lens focal length which is the limiting case.

ASD TR 61-70

1. Resolution Performance

The result of diffraction of light through a lens is that for a point source there corresponds, in the image plane, a patch of light called the Airy disc.[3] The diameter of the Airy disc (see Section D-2) determines the theoretical limit of resolution (density of bit storage). If it is too large there is overlapping. However, the lower the f/number, the better the resolution performance of a lens, at least theoretically. For example, an f/2 lens will have an Airy disc diameter of only 0.0001 in. which is better than that required for this application.

For two reasons, then maximum energy per unit area and good resolution we desire low f/number lens systems. Because the higher-speed lens (low f/number) is inherently more difficult to correct in the design stage and more difficult to produce in the manufacturing stage, a general lowering in predicted resolution performance is to be expected in higher-speed lenses. However, even an average f/1.4 lens may be expected to resolve 40 lines per mm (1000 lines per inch).

2. Depth of Focus

The term "depth of focus" is usually taken as the distance along the lens axis through which an object can be moved forward or backward without causing a detectable change in focus of the image of that object. Its practical importance in a photochromic memory is that it is indicative of how much relative run-out can be tolerated between the coated surface and the imaged spot.

$$\text{Depth of focus} = \pm\ 0.000043 \times (f/\text{number})^2 \text{ in.} \qquad (2)$$

For comparison purposes, the depth of focus for several lens f/numbers is listed in Table XXX.

373

TABLE XXX

DEPTH OF FOCUS FOR SEVERAL LENS F/NUMBERS

f/number	‡ Depth of Focus, in.
2.5	0.00027
2.0	0.00017
1.8	0.00014
1.6	0.00011
1.4	0.00008

If a run-out tolerance of ± 0.0001 inch is imposed, then a lens of f/number as low as f/1.5 may be used.

3. Factors Affecting the Choice of Lenses

It appears that lens aberrations such as spherical, chromatic, astigmatism, coma, etc. , can be overcome satisfactoriiy in a f/1.5 lens used for photographic purposes with visible light. Usually these lenses are corrected for two wavelengths, one in the blue and the other in the red visible region. In the near ultraviolet (360 mμ) a loss in resolution and a 15 percent loss in transmission is to be expected for the optical glass lenses available as off-the-shelf items.

Another type of lens is the reflecting retrofocus objective shown in Figure 141 which is completely achromatic; that is, it has the advantages of high resolution at all wavelengths from the far U. V. to the infrared. It can have a low f/number and negligible reflection loss. Such an objective is the A. O. #1200 with f/0.74 (image side) at 50 X magnification.[4]
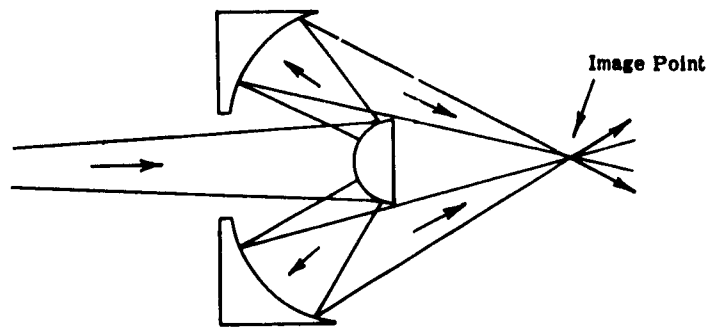
Figure 141. Reflecting Objective.

In Formula (1) the transmission coefficient K of the lens system appeared.
The value of K depends on the number of air-glass surfaces and whether
these surfaces are coated. Referring to the graph shown in Figure 142[5], it
is apparent that even coated, highly corrected lens systems suffer a
substantial loss of transmission. For example, a coated six-element lens
transmits 73 percent of the incident radiation.

4. Experimental

The formula derived above for intensity per unit area of an image as a
function of f/number was experimentally verified by actually measuring
the image size with a microscope graticule and measuring the radiant
energy by means of a thermopile calibrated against an NBS standard lamp.
The agreement between theory and experiment was quite satisfactory.

C. AN ALTERNATIVE DERIVATION FOR IMAGE POWER DENSITY

It is common practice to state the brightness of a source in terms of watts
per square centimeter per steradian. The image power density is then
readily found by a simple calculation, recognizing that the brightness of
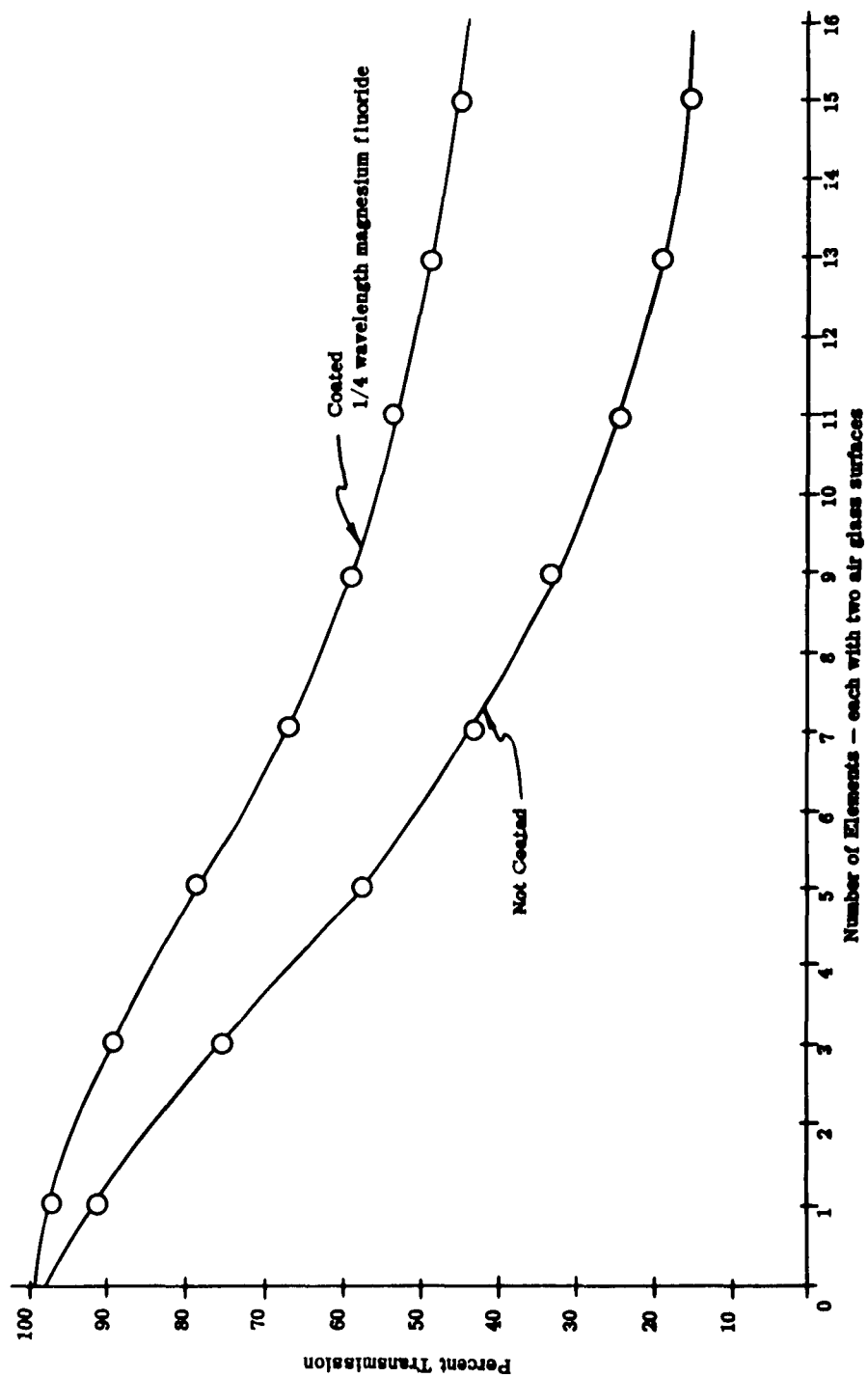
Figure 142. Transmission Loss Through Glass Optics.

376

the image equals that of the object.[*]

Consider the optical system in Figure 143.

K = Lens Transmission
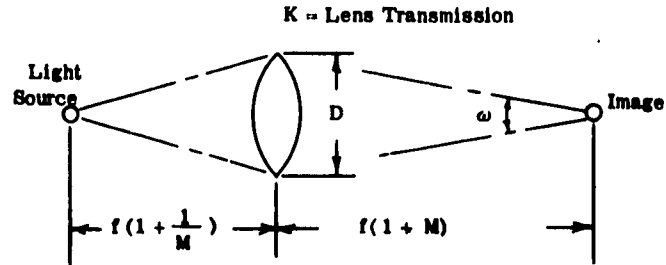
Figure 143. System for Calculating Image Power Density

For reasonable image distances, the area of the intercepted sphere can be approximated by the area of the lens aperture. Thus, ω, the solid angle, is given as,

$$\omega = \frac{\pi D^2}{4} \cdot \frac{1}{f^2 (1+m)^2}$$

$$\omega = \frac{\pi}{4} \frac{1}{(1+m)^2 \bar{f}^2}$$

where $\bar{f} = \frac{f}{D}$

Given the source brightness as B_o, the image power density, P. D., becomes,

$$P. D. = \frac{\pi}{4} \frac{K}{(1+m)^2 \bar{f}^2} B_o \qquad (3)$$

---

[*] Jenkins, F. A. and White, H. E. , "Fundamentals of Optics," McGraw-Hill Book Co. , pp. 111-112 (1957).

ASD TR 61-70

where K = transmission of the lens.

For small "m" this reduces to

$$P.D. = \frac{\pi}{4} \frac{K}{f^2} B_o.$$ (4)

This checks with equation (1) by recognition of the following relationship:

$$\frac{F_o}{A_o} = 4\pi B_o.$$ (5)

Then, substitution gives,

$$\frac{I_i}{A_i} = \frac{K}{16 f_i^2} 4\pi B_o$$

or

$$P.D. = \frac{K\pi}{4(1+m)^2 f^2} B_o.$$ (6)

Equations (3) and (6) are consistent. However, with B_o given, equation (3) affords a very simple means for the calculation of the power density. For example, let,

$$K = \frac{1}{\pi}$$

$$1+m \cong 1$$

$$f^2 = (1.6)^2 \cong 2.5.$$

Then,

$$P.D. = 0.1 B_o.$$ (7)

378

D.   CALCULATIONS

1.   Lens Collection Efficiency

The solid angle (see Figure 144) $\Omega = \dfrac{A}{(S + h)^2}$
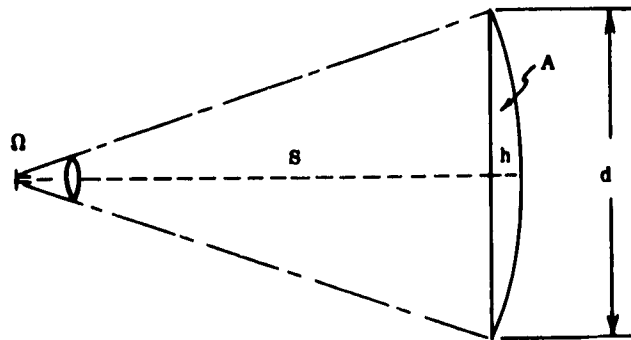
Figure 144.   Lens Calculation Diagram.

Now, h is usually small and A, the area of the spherical surface section, is very nearly equal to $\pi d^2/4$.

Even at f/1, the inaccuracy introduced by these approximations amounts to only seven percent.   Thus,

$$\Omega \sim \frac{\pi d^2}{4S^2} \; .$$

Assuming that the source is small, spherical, and perfectly diffuse, i.e., it radiates uniformly in all directions, then the fraction of emitted flux intercepted by the lens is

$$\frac{\Omega}{4\pi} \;\; \text{or} \;\; \frac{d^2}{16S^2} \; .$$

379

But,

$$\frac{S}{d} = \text{f/number.}$$

Therefore, the fraction of the total emitted flux, F_o, intercepted by a lens from a source which radiates with spherical symmetry is

$$\frac{1}{16 f_o{}^2} F_o.$$

2. Airy Disc

The diameter of the Airy disc is given by the formula

$$D = \frac{1.22 \lambda}{n \cdot \sin u}$$

where λ is the wavelength of the light used, n the refractive index of the medium into which the light emerges, and u is the angle with the axis made by the extreme ray of the bundle transmitted by the system when it emerges into the final medium. Taking a mean wavelength of light as 0.00002 in., n = 1 for air, and letting $\sin^2 u = \frac{1}{4f^2 + 1}$, we have at f/2

$$D = 1.22 \ (2 \times 10^{-5}) \ \sqrt{17} = 10^{-4} \text{ in.}$$

E. REFERENCES

1) Sears, A. W., Principles of Physics III, pp 286 ff. (1946).

2) Posenburger, H. E., JSMPTE, 67, 378 (1958).

3) Habell and Cox, Engineering Optics, Pitman and Sons, p. 104 ff. (1956).

4) American Optical Bul. NO.1200, Buffalo 15, New York.

5) Wollensak Lens and Shutter Guide, p. 26.

THEORETICAL INVESTIGATION OF THE
ULTRASONIC DIFFRACTION GRATING LIGHT SHUTTER

A. THE DIFFRACTION OF LIGHT BY ULTRASONIC WAVES IN A TRANSPARENT MEDIUM

1. Introduction

When a beam of plane light waves (parallel rays) crosses a beam of
high frequency plane sound waves (which exhibit compression and
rarefaction in the acoustic medium), a Fraunhofer-type of interfer-
ence pattern results, not unlike the pattern produced by a diffra-
ction grating (see Figure 145). The spacings of the orders in the
resultant pattern are the same as that which would result when
using a diffraction grating whose line spacings are equal to the
wave length of the ultrasonic beam. However, the light intensity
distributions amongst the various orders are quite different. These
distributions have been the subject of many papers.
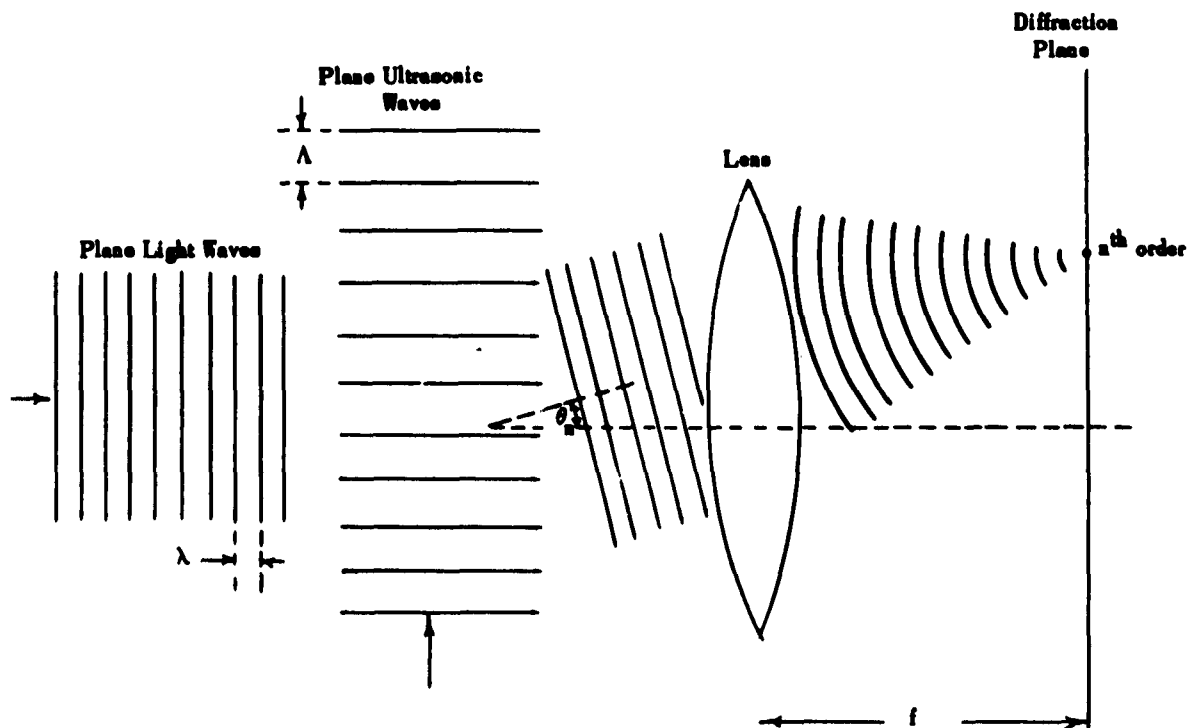
Figure 145. Example of Ultrasonic Diffraction.

ASD TR 61-70

The first papers describing experimental results appeared in 1932 in the United States by Debye and Sears[1] and in France by Lucas and Biquard[2]. Debye and Sears, at that time, suggested that the phenomenon might be the result of Bragg reflections, but they could not explain the intensity distributions. Lucas and Biquard assumed a sinusoidal distribution of index of refraction in the liquid and calculated trajectories of normally incident light rays. They also could not explain the light intensity distributions.

The first theory offering an explanation of the intensity distributions encountered experimentally appeared in a series of five papers by Raman and Nath[3] beginning in 1935. In their first paper they assumed that the optical path of the light rays through the sound beam is small enough so the curvature of the light rays may be neglected. Then, as the incident light wave front traverses the medium, the sinusoidal variations of index of refraction caused by the ultrasonic waves cause variations in the "optical path" of adjacent portions of the light wave front. Thus, the emergent wave front has phase variations, or as Raman and Nath call it "a corrugated wave front". They consider this treatment analogous to Lord Rayleigh's[4] treatment of the diffraction of plane waves by periodically corrugated surfaces. For the case of normal incidence they derive the equation giving the angular displacement of the orders ($\Lambda \sin \theta_n = n \lambda$). They also show that the relative intensities of the various orders can be expressed in terms of Bessel functions whose independent variable is a function of a change in the index of refraction of the medium, $\Delta \mu$.

$$\frac{I_m}{I_n} = \frac{J^2_m(v)}{J^2_n(v)}$$

Where: $v = v(\Delta \mu)$

382

Raman and Nath's second paper treats the case of oblique incidence of the light waves. Their calculations show that varying the angle of incidence should produce variations of intensity amongst the orders similar to the effects produced by varying the ultrasonic intensity.

In their third paper, they consider the effects of the time variation of the index of refraction. This was ignored in their first two papers to avoid unnecessary complications at that time. A Doppler effect is shown to exist for both traveling and standing ultrasonic waves. In particular, for ultrasonic standing waves, (using monochromatic light) the odd and even orders are shown to contain different groups of Doppler-shifted light frequences. Thus, any odd order is incoherent with any even order, while any two odd (or even) orders are partly coherent.

Their fourth paper is a more general treatment of the phenomenon described in the previous papers. They take the case of normal incidence of the light beam and derive some general relationships. Then assuming a sinusoidal variation of the index of refraction of the medium, they derive a complex differential-difference equation. Then by eliminating the imaginary term of the equation by assuming that its coefficient is "small", the solution of the resulting equation is shown to be the same as the Bessel function solution derived in their first paper. The validity of these assumptions will be discussed later.

In their fifth paper, they treat the case of oblique incidence of the incoming light beam. They show that for this case, the light intensity distribution is not symmetrical about the zeroth order.

In 1936 N. S. Nagendra Nath[5] solved the general differential-difference equation (derived jointly with C. V. Raman[3]) in series form. P. H. Van Cittert[6] solved the problem for normal incidence of 1937 using a different approach. It was later shown by K. Nagabhushana Rao[7] that both solutions were compatible.

383

In 1951 O. Nomoto[8] pursued the geometrical ray-tracing approach further and obtained graphical solutions for the intensity distributions for both normal and oblique incidence.

Numerous papers have appeared in the literature describing various experiments and their correlation with theory. There seems to be a great deal of confusion as to the scope of the Raman-Nath theory and the validity of its approximate solution.

An excellent summary of the work done in this field up to 1954 including a very large bibliography appears in L. Bergmann's book "Der Ultra-schall"[9]. Unfortunately, this book is not yet available in English. Bergmann's earlier book[10] was translated into English and is an excellent summary of the work done up to 1938.

2. Theory

The experimental setup used to examine the phenomenon of diffraction of light by ultrasonic waves is shown in Figure 146.

Lens L_1 focuses an image of the source upon the slit forming a secondary source whose width can be controlled. Lens L_2 is located such that the slit is in its primary focal plane. Thus the light rays from each point in the slit are rendered parallel after passing through lens L_2.

The light beam then passes through an acoustic field of plane traveling waves. Since a sound wave is propagated by compressions and rare-factions of the transmitting medium, the light rays encounter a medium having variations of index of refraction. Thus, a particular light ray in passing through the acoustic field may suffer any one or all of the following effects (relative to other rays):

1) change of direction
2) change of phase
3) change in amplitude

384
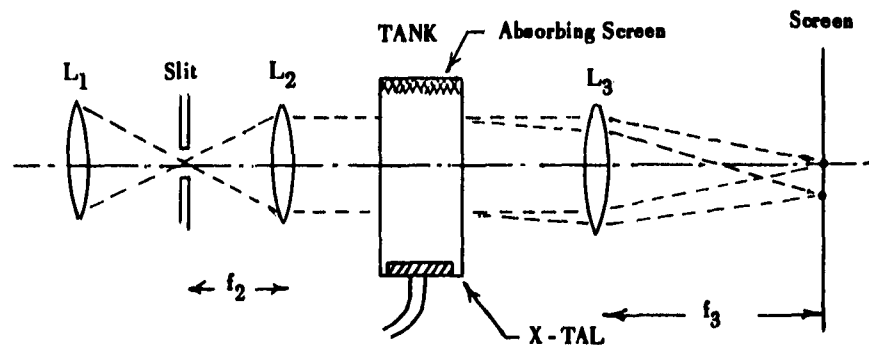
Figure 146. Experimental Set-up.

The emerging light consists of many diverging bundles of parallel rays whose individual rays vary in both amplitude and phase.

Lens L_3 focuses the Fraunhofer pattern (located at infinity in a system without lens L_3) on a screen placed in its focal plane.

The angular spacings of the resultant spectral orders are given by the following equation[3]:

$$\Lambda \sin \theta_n = n \lambda \qquad (1)$$

Where:

Λ = wavelength of the sound beam

λ = wavelength of the incident light rays

n = spectral order (central order, $n = 0$)

θ_n = angular displacement of the nth order

Equation (1) is very similar to the equation describing the "diffraction grating," given below [3]:

$$d \sin \theta_n = n \lambda \qquad (2)$$

where "d" is the distance between adjacent rulings on the grating.

385

The intensities of the various orders are functions of the acoustic
intensity. The resultant intensity distributions are quite different than
those produced by a diffraction grating. For a diffraction grating,
the intensity distribution is of the principle orders, and is contained in
a $\frac{\sin^2 x}{x^2}$ envelope which is a function of the elemental transparent
region of the grating. A typical example is shown in Figure 147.
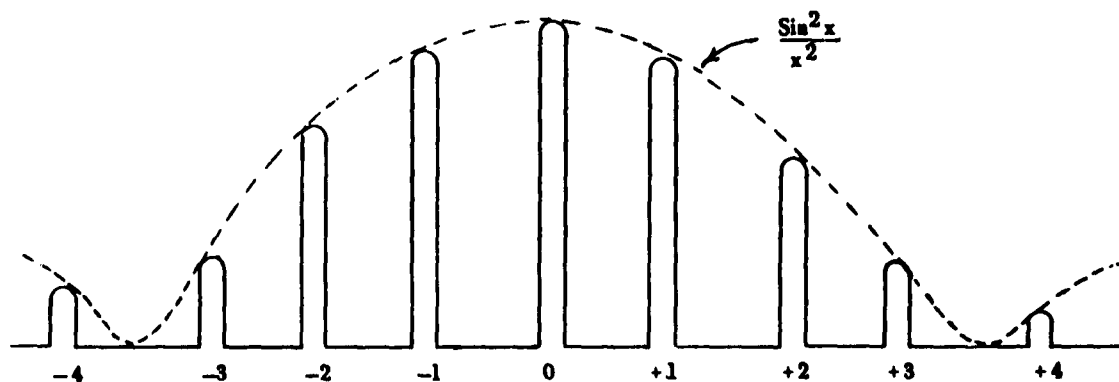
Figure 147. Example of an Ordinary $\frac{\sin^2 x}{x^2}$ Envelope.

For diffraction by ultrasonic waves, each order is a function of the
ultrasonic intensity. At zero ultrasonic intensity, only the "zeroth"
order is present in the diffraction pattern. As the ultrasonic intensity
is increased, the "zeroth" order begins decreasing in intensity and
the +1 and -1 orders appear and begin increasing. As the ultrasonic
intensity continues to increase, the +2 and -2 orders appear and increase.
Further increases in ultrasonic intensity show the "zeroth" order
passing through a null and the appearance of other higher orders. This
is illustrated in Figure 148 which is a copy of Raman and Nath' s
calculated values (normalized).

Calculations based on the approximate solution to the Raman and Nath
general equation predict the experimental results very well, provided
that the experimental conditions and parameters are in accord with the
theoretical assumptions and approximations.
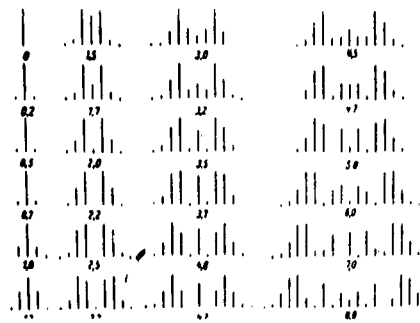
Figure 148 Normalized Intensities of Diffraction Orders
(calculated by Raman and Nath).

In Raman and Nath's fourth paper the following complex differential-difference equation is derived for light incident normal to the direction of the sound beam.

$$2 \frac{d\phi_n}{d\xi} - (\phi_{n-1} - \phi_{n+1}) = \frac{\ln^2 \lambda^2}{\mu_0 \mu \lambda^{*2}} \phi_n \qquad (3)$$

Where: $\phi_n(\xi)$ = desired amplitude function

$\xi = \frac{2\pi\mu z}{\lambda}$

μ = maximum change of index of refraction

μ_0 = index of refraction of the liquid

z = special coordinate normal to the diffraction plane

λ = wave length of the incident light

λ^* = wave length of the ultrasonic beam

The above equation, was derived from the general partial differential equation of wave motion given on the following page.

$$\frac{\delta^2 \psi}{\delta x^2} + \frac{\delta^2 \psi}{\delta y^2} + \frac{\delta^2 \psi}{\delta z^2} = \left[\frac{\mu(x, y, z, t)}{c}\right]^2 \frac{\delta^2 \psi}{\delta t^2} \qquad (4)$$

The sound beam is assumed to be sinusoidal and of uniform cross-sectional area and the time-variation of $\mu(x, y, z, t)$ is assumed very slow compared to the time-variation of the wave-function of light.

The solution is assumed to be of the form of a periodic plane-wave whose amplitude is a function of position and time. Thus,

$$\psi = e^{i\omega t} \phi(x, z, t) \qquad (5)$$

By using recognized techniques of eliminating terms that are negligible for all envisioned conditions, they derive the basic formula describing the angular positions of the diffracted orders (Equation 6) as well as the frequency of the light present in the orders due to Doppler shift (Equation 7).

$$\sin \theta = \frac{n\lambda}{\lambda^*} \qquad (6)$$

$$v_n = v - nv^* \qquad (7)$$

Continuing the derivation for the case of progressive waves, they arrive at Equation (3). They recognized that if the term on the right were equal to zero, the solution could be written as a series of Bessel functions, which upon inserting boundary conditions would simplify to:

$$\phi_n(\xi) \approx J_n\left(\frac{2\pi\mu z}{\lambda}\right) \qquad (8)$$

It will now be shown that it is not permissible to eliminate the right hand term when using ultrasonic frequencies approaching the megacycle region, and therefore experimental results will necessarily vary from the approximate solution given.

388

In order for the solution to be valid, the coefficient of the right hand term of Equation (3) must be small.

$$\frac{n^2 \lambda^2}{\mu_o \mu \lambda^{*2}} \ll 1$$

or

$$\left(\frac{\lambda}{\lambda^*}\right)^2 \ll \frac{\mu_o \mu}{n^2} \tag{9}$$

If it is desired that this solution be valid for 10 orders, and since in general $\mu_o \approx 1.4$ and $\mu \approx 10^{-5}$,

$$\left(\frac{\lambda}{\lambda^*}\right)^2 \ll 10^{-7}$$

Arbitrarily assuming that a coefficient of 0.1 for the term on the right hand side of Equation (3) will make it negligible, we find an upper limit of 300 Kc for the ultrasonic vibrations for the Raman and Nath approximation to remain valid up to the appearance of the 10th order.

$$\left(\frac{\lambda}{\lambda^*}\right)^2 \lesssim (0.1)(10^{-7})$$

$$\lambda^* \gtrsim 10^4 \lambda$$

$$\nu^* = \frac{c}{\lambda^*} \lesssim \frac{c}{10^4 \lambda}$$

For visible light at 500 mμ,

$$\nu^* \lesssim \frac{1.5 \times 10^3}{(10^4)(5 \times 15^7)}$$

$$\nu^* \lesssim 3.0 \times 10^5 \text{ cycles}$$

For use up to the appearance of the 5th order, the approximation remains valid up to about 600 Kc. For use up to the appearance of the 3rd order, the approximate solution remains valid up to about 900 Kc.

389

The fact that the approximation is invalid in the megacycle region does not imply that the results obtained are necessarily useless, but indicates that some unknown amount of error exists which can only be determined by comparison with the results of a solution of equation (3) in its entirety.

This equation was solved in series form by Nagendra Nath[5] and independently in a Bessel function series by Van Cittert[6]. These solutions were shown to be compatible by Nagabhushana Rao[7] and appear in Sub-Appendixes 1 and 2. Nagandra Nath states that his series is rather slowly convergent and difficult to use. Bhagavantam and Rao[11] in working at very high ultrasonic frequencies (177.2 Mc.) found that Nath's series was not convergent at that frequency. The Bessel function series solution of Van Cittert is also very slowing converging (or non-convergent in some cases).

A different approach used by Nomoto[8] involves the calculation of ray trajectories through the sonic beam and the graphical determination of the resultant phases upon emerging. He claims good agreement with experiments when operating at 1.395 Mc. and at large ultrasonic intensities.

Poor results have been reported in the literature when the experimental conditions resulted in light rays crossing each other. This crossing occurs, according to Lucas and Biquard, when the path length of the light beam and the peak change in index of refraction are related as follows:

$$y_o = \frac{\Lambda}{4} \sqrt{\frac{n_o}{\Delta n}}$$

Where: y_o = path length of the light beam through the ultrasonic beam for crossing of light rays to occur.

Λ = ultrasonic wave length

n_o = index of refraction of the sonic medium

Δn = peak change of index of refraction

390

Figure 149 illustrates paths of light rays through the ultrasonic beam
(from Lucas and Biquard). The parameter "K" is defined in terms of
the path length "y" by:

$$K = \frac{2\pi}{\Lambda} \, y \sqrt{\frac{\Delta n}{n}}$$

It has been pointed out in the literature that Raman and Nath failed to
account for this curvature in their earlier papers. However, the concept
of bending of rays becomes irrelevent in the solution of the general
wave equation derived in their fourth paper.
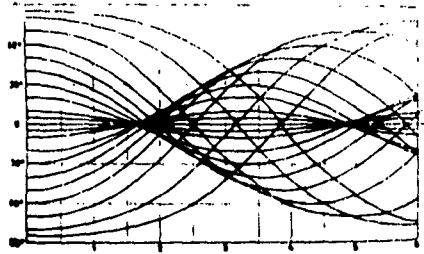
Figure 149. Light-Ray Trajectories in Liquid Medium
(Lucas and Biquard).

It is possible that the poor results obtained when the path length exceeds
y_o may be attributed to reflections and multiple reflections due to the
necessity of using a tank to contain the ultrasonic medium.

Evan for normal incidence some reflection occurs both at the inner and
outer surfaces of the exit wall of the tank. This is due to the light rays
encountering two changes of index of refraction before reaching the exit
lens.

ASD TR 61-70

Since the percentage reflection is a function of the angle of incidence, those rays incident at larger angles to the normal suffer a greater percentage of reflection. This results in amplitude differences. However, in most cases, this deviation from the normal is so slight that the effect is probably negligible.

When the path length becomes long enough for some rays to begin crossing each other, they are inclined enough to cause multiple reflections spreading transversely over a distance of one or more ultrasonic wave lengths causing superimposed effects.

The effects of these reflections can be reduced by (1), using a liquid whose index of refraction matches that of the tank to eliminate reflections from the inner surface, and (2), by coating the outer surface of the exit wall with an anti-reflection coating.

At large ultrasonic intensities, it appears that the sinusoidal waveform becomes distorted, thus resulting in the presence of harmonics (by Fourier analysis). This produces a superposition of diffraction patterns of each harmonic.

For future theoretical advances in ultrasonic diffraction, a solution of the Raman-Nath equation in either closed form or as a rapidly converging series would certainly be useful.

392

3. Nath's Solution as Extended by Rao.

The first four terms of the Nath[5] solution for the amplitude of the nth and $-n^{th}$ order as extended by Rao[19] is given below.

$$\psi_n = \left(\frac{x}{2}\right)^n \frac{1}{n!} \left\{ 1 + i\rho \left[n\frac{(2n+1)}{12} + \frac{\alpha}{4}n \right] x \right.$$

$$- \left[\frac{1}{4(n+1)} + \frac{\rho^2}{2} \left\{ \frac{n(2n+1)(2n+3)(5n-1)}{720} + \frac{\alpha}{12}n^2(n+1) + \frac{\alpha^2}{48}n(3n+1) \right\} \right] x^2$$

$$- \frac{i\rho}{8(n+1)(n+2)(n+3)} \left[\left\{ \frac{n(n+2)(n+3)}{2}\alpha + \frac{n(n+1)(n+2)(2n+5)}{6} + n+2 \right\} \right.$$

$$+ \frac{\rho^2}{6} \left\{ \left[\frac{n(n+1)(2n+1)}{6} + \frac{\alpha}{2}n(n+1) \right]^3 \right.$$

$$+ 2\left[\frac{n(n+1)(2n+1)(3n^4+6n^3-3n+1)}{42} + \frac{\alpha}{4}n^2\left(n+1\right)^2\left(2n^2+2n-1\right) \right.$$

$$\left. + \frac{\alpha^2}{10}n(n+1)(2n+1)(3n^2+3n-1) + \frac{\alpha^3}{4}n^2(n+1)^2 \right]$$

$$+ 3\left[\frac{n(n+1)(2n+1)}{6} + \frac{\alpha}{2}n(n+1) \right] \left[\frac{n(n+1)(2n+1)(3n^2+3n-1)}{180} \right.$$

$$\left.\left.\left. + \frac{\alpha}{2}n^2(n+1)^2 + \frac{\alpha^2}{6}n(n+1)(2n+1) \right] \right\} \right] x^3 + \ldots\ldots$$

$$\psi_{-n} = (-1)^n \left(\frac{x}{2}\right)^n \frac{1}{n!} \left\{ 1 + i\rho \left[\frac{n(n+1)(2n+1)}{6} - \frac{\alpha}{2}n(n+1) \right] x \right.$$

$$- \left[\frac{1}{4(n+1)} + \frac{\rho^2}{2} \left\{ \frac{n(2n+1)(2n+3)(5n-1)}{720} - \frac{\alpha}{12}n^2(n+1) + \frac{\alpha^2}{48}n(3n+1) \right\} \right] x^2$$

393

$$-\frac{i\rho}{8(n+1)(n+2)(n+3)}\left[\left\{-\frac{n(n+2)(n+3)}{2}\alpha + \frac{n(n+1)(n+2)(2n+5)}{6} + n+2\right\}\right.$$

$$+\frac{\rho^2}{6}\left\{\left[\frac{n(n+1)(2n+1)}{6} - \frac{\alpha}{2}n(n+1)\right]^3\right.$$

$$+2\left[\frac{n(n+1)(2n+1)(3n^4+6n^3-3n+1)}{42} - \frac{\alpha}{4}n^2(n+1)^2(2n^2+2n-1)\right.$$

$$\left.+\frac{\alpha^2}{10}n(n+1)(2n+1)(3n^2+3n-1) - \frac{\alpha^3}{4}n^2(n+1)^2\right]$$

$$+3\left[\frac{n(n+1)(2n+1)}{6} - \frac{\alpha}{2}n(n+1)\right]\left[\frac{n(n+1)(2n+1)(3n^2+3n-1)}{180}\right.$$

$$\left.\left.\left.-\frac{\alpha}{2}n^2(n+1)^2 + \frac{\alpha^2}{6}n(n+1)(2n+1)\right]\right\}\right]x^3 + \ldots\ldots$$

Where:

ψ_n = amplitude of the nth order

ψ_{-n} = amplitude of the $-n^{th}$ order

n = integer $\geqq 0$

$\alpha = \frac{\mu_o\lambda^*}{\lambda}\tan\phi$

$\rho = \frac{\lambda^2\cos^2\phi}{\mu_o\mu\lambda^{*2}}$

μ_o = index of refraction of the medium with no ultrasonic excitation present.

μ = peak variation of index of refraction for a given sinusoidal ultrasonic excitation.

394

ASD TR 61-70

λ = wave-length of the incident light

λ^{*} = wave-length of the ultrasonic wave.

ϕ = angle of incidence (from the normal) of the incident light beam.

The independent variable "x" is given by:

$$x = \frac{2 \pi \mu z}{\lambda}$$

where z is the path length through the ultrasonic beam.

395

4. Van Cittert's Solution as Extended by Rao.

The first four terms of the Van Cittert[6] solution for the amplitude of the nth order, as extended by Rao[7][19] to include oblique incidence is given below:

$$\psi_n = J_n + i\rho \left\{ \frac{n(n+1)(2n+1)}{6} + \frac{\alpha}{2} n(n+1) \right\} J_{n+1}$$

$$- \frac{\rho^2}{2} \left\{ \frac{n(n+1)(2n+1)(n+2)(2n+3)(5n+1)}{180} + \frac{\alpha}{3} n^2 (n+1)^2 (n+2) \right.$$

$$\left. + \frac{\alpha^2}{12} n(n+1)(n+2)(3n+1) \right\} J_{n+2}$$

$$+ \left\{ -i\rho \left[\frac{(n+1)(n+2)(2n+3)}{6} + 1 + \frac{\alpha}{2} n(n+3) \right] \right.$$

$$- \frac{i\rho^3}{6} \left[\left\{ \frac{n(n+1)(2n+1)}{6} + \frac{\alpha}{2} n(n+1) \right\}^3 \right.$$

$$+ 2 \left\{ \frac{n(n+1)(2n+1)(3n^4 + 6n^3 - 3n + 1)}{42} \right.$$

$$+ \frac{\alpha}{4} n^2 (n+1)^2 (2n^2 + 2n - 1)$$

$$+ \frac{\alpha^2}{10} n(n+1)(2n+1)(3n^2 + 3n - 1)$$

$$+ \frac{\alpha^3}{4} n^2 (n+1)^2 \right\}$$

$$+ 3 \left\{ \frac{n(n+1)(2n+1)}{6} + \frac{\alpha}{2} n(n+1) \right\} \left\{ \frac{n(n+1)(2n+1)(3n^2 + 3n - 1)}{180} \right.$$

$$\left. \left. \left. + \frac{\alpha}{2} n^2 (n+1)^2 + \frac{\alpha^2}{6} n(n+1)(2n+1) \right\} \right] \right\} J_{n+3} + \ldots$$

396

Where:

ψ_n = amplitude of the nth order

n = integer $\geqq 0$

J_n = n^{th} order Bessel Function of the first kind

$\alpha = \dfrac{\mu_0 \lambda^*}{\lambda} \tan \phi$

$\rho = \dfrac{\lambda^2 \cos^2 \phi}{\mu_0 \mu \lambda^{*2}}$

μ_0 = index of refraction of the medium with no ultrasonic excitation present.

μ = peak variation of index of refraction for a given sinusoidal ultrasonic excitation.

λ = wave-length of the incident light

λ^* = wave-length of the ultrasonic wave.

ϕ = angle of incidence (from the normal) of the incident light beam.

The independent variable " ξ " is given by:

$\xi = \dfrac{2 \pi \mu z}{\lambda}$

where z is the path length through the ultrasonic beam.

397

5. Surface Displacement

The calculations on the displacement of the crystal surface as a function of the applied voltage are given below. The short-circuit polarization of a strained crystal is given by Hueter and Bolt[14]:

$$P_i = e_{ik} x_k$$

Where:

$$x_k = \text{strain} = \frac{\xi}{l}$$

$$e_{ik} = e_{11} = 0.17 \text{ coul.}/m^2$$

Since $P_i = \frac{q}{S} = \frac{CV}{S}$

Where:
q = charge
S = surface area
V = potential difference

Equation (1) becomes:

$$\frac{CV}{S} = e_{11} \frac{\xi}{l}$$

or $\quad \xi = \frac{Cl}{e_{11}S} V$

For the crystal used:

C = 72×10^{-12} farads
l = 3.51×10^{-4} m.
S = 6.42×10^{-4} m^2

Giving:

$$\xi = (2.32 \times 10^{-10}) V$$

B. ILLUMINATION OF THE FINAL IMAGE OF THE DIFFRACTED FIRST ORDER IN THE ULTRASONIC OPTICAL SWITCH SYSTEM
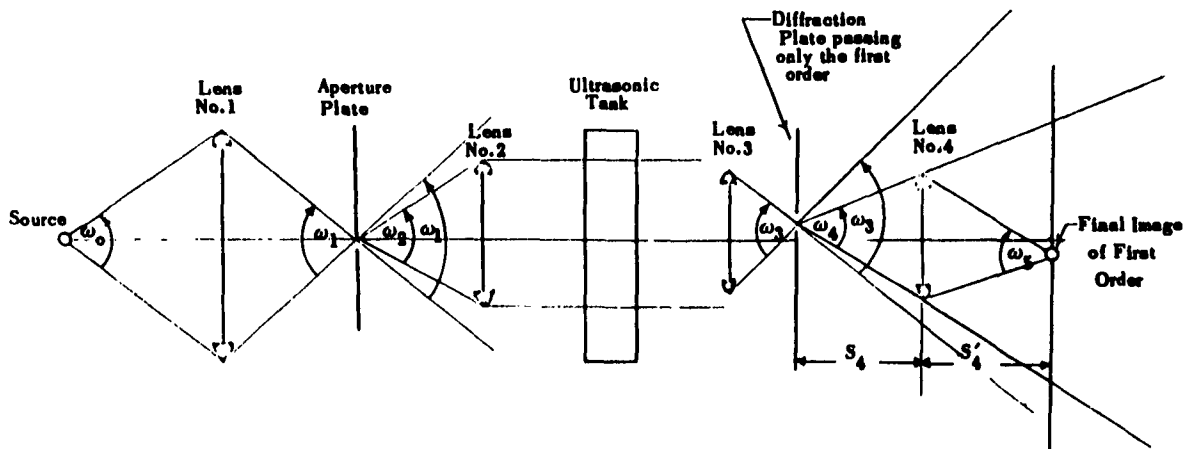
Figure 150. Ultrasonic Optical Switch System

The illumination of the final image of the first order of the diffraction pattern in Figure 150 is given by:

$$E = L_o \omega_f \beta \tau \, e^{-\alpha x} \qquad (1)$$

Where:

E = the illumination of the final image (watts/cm^2)

L_o = the luminance (brightness) of the source (watts/cm^2-steradian)

ω_f = the solid angle subtended by the exit pupil of the system at the image (steradians)

β = the fraction of light flux contained in ω_3 which is passed by the diffraction plate

τ = the net transmittance of the optics

α = the absorption coefficient of the liquid in the ultrasonic tank

X = the length of the path through the ultrasonic tank

Provided that the following conditions prevail, lens #4 is the exit pupil of the system:

$$\omega_2 \lesssim \omega_1 \qquad (2a)$$

$$\omega_4 \lesssim \omega_3 \qquad (2b)$$

$$D_3 \lesssim D_2 \qquad (2c)$$

Where D_3 and D_2 are the diameters of lenses #3 and #2, respectively. For this case,

$$\omega_f = \omega_5 \qquad (3)$$

When the ultrasonic intensity is adjusted so that the first order of the diffraction pattern reaches its first maximum, approximately 30 percent of the available light flux is diffracted into each of the first orders. Therefore,

$$\beta \approx 0.3 \qquad (4)$$

For paraxial rays (i.e., rays for which the approximation $\sin \theta = \tan \theta = \theta$ can be made) the transmission through a <u>single</u> dielectric surface is given by:

$$\tau_i = 1 - \left(\frac{n' - n}{n' + n} \right)^2 \qquad (5)$$

For an air-glass or air-quartz boundary, for which $n' \approx 1.5$,

$$\tau_i \approx 0.96 \qquad (6)$$

Since there are six lenses in the system (including the plates forming the sides of the ultrasonic tank) a total of 12 boundaries are crossed. The net transmittance is, therefore:

$$\tau = (\tau_i)^n = (0.96)^{12} \approx 0.61 \qquad (7)$$

400

The absorption coefficient of an alcohol-water mixture is quite small, so that:

$$\alpha \approx 0$$

$$e^{-\alpha x} \approx e^0 \approx 1 \tag{8}$$

Substituting these values into equation (1) we find:

$$E = (0.18) \, L_o \, \omega_5 \tag{9}$$

If the final image is the result of at least a 5:1 reduction of the diffraction image, the image distance is approximately equal to the focal length of lens #4, and we can express equation (9) in terms of the "F-number" of lens #4.

i.e., if $\quad \dfrac{S_4'}{S_4} \leqq \dfrac{1}{5} \quad$ then $S_4' \approx f_4$

And $\qquad \omega_5 = \dfrac{A_4}{f_4^2} = \dfrac{\pi D_4^2}{4 \, f_4^2} = \dfrac{\pi}{4} \left(\dfrac{D_4}{f_4} \right)^2$

But $\qquad f_4/ = \dfrac{f_4}{D_4}$

$\therefore \qquad \omega_5 = \dfrac{\pi}{4} \left(\dfrac{1}{f_4/} \right)^2$

And $\qquad E = 0.14 \left(\dfrac{1}{f_4/} \right)^2 \, L_o$

If conditions given in (2) are met and lens #4 were an f/2 lens:

$$E = 0.035 \, L_o$$

401

C. REFERENCES

(1)   P. Debye and F. W. Sears; Proc. Nat'l Acad. Sci, 1932, 18, 409.

(2)   R. Lucas and P. Biquard; Jour. de Physique et le Radium, 1932, 3, 464

(3)   C. V. Raman and N. S. Nagendra Nath; Proc. Ind. Acad. Sci.,
        1935, 2, 406
        1935, 2, 413
        1936, 3, 75
        1936, 3, 119
        1936, 3, 459

(4)   Lord Rayleigh: Theory of Sound, Vol. 2, 89.

(5)   N. S. Nagendra Nath; Proc. Ind. Acad. Sci., 1936, 4, 222.

(6)   P. H. Vancittert; Physica, 1937, 4, 590.

(7)   K. Nagabhushana Rao; Proc. Ind. Acad. Sci., 1938, 8, 124.

(8)   O. Nomoto; Bull. Kobayasi Inst. Phys. Res.,
        1951, 1, 42
        1951, 1, 189

(9)   L. Bergmann; Der Ultraschall und Seine Anwendung in Wissenschaft
        und Teknik, 1954, 263.

(10)   L. Bergmann; 'Ultrasonics and Their Scientific and Technical
        Applications, 1938, 63.

(11)   S. Bhagavantan and B. Ramachandra Rao; Proc. Ind. Acad. Sci.,
        July 1948, 54.

(12)   W. D. Dye; Proc. Roy. Soc. Lond., 1932, A138, 1.

(13)   R. W. Ditchburn; Light, Interscience Publishers, 1957.

ASD TR 61-70

(14) Hueter and Bolt; *Sonics* .

(15) B. Carlin; *Ultrasonics.*

(16) R. Bar; *Helv. Phys. Acta;* 1933, 6, 570.

(17) S. Parasarathy; *Proc. Ind. Acad. Sci.*,
1936. 3, 442
1936, 3, 594

(18) F.H. Sanders; *Canadian Jour. Res.*, 1936, 14, 158

(19) K. Nagabhushana Rao; *Proc. Ind. Acad. Sci.*, 1939, 9, 422.

(20) G. W. Willard; *J.A.S.A.;* 1940, 12, 438.

(21) G.W. Willard; *J.A.S.A.;* 1949, 21, 101

APPENDIX X
LABORATORY EQUIPMENT

A. EQUIPMENT ACQUIRED PRIOR TO CONTRACTUAL PERIOD

A variety of laboratory equipment was obtained for experimental work
on the photochromic memory project, both by purchase and by construc-
tion on the project. The major portion of the equipment not likely to
be found in a standard laboratory is listed below.

1. Specially Constructed Equipment and Facilities

1) Photographic darkroom with hot and cold running water.

2) Optical darkroom.

3) Large, Rigid Triangular Optical Bench.
    Permanently mounted in the optical (darkroom) with variable
    speed motor and component mount for rotating components
    of experimental optical systems (see Figures 151 and 152).

4) Word Generator (Figure 153).
    17-bit word set up by toggle switches generates the number of
    words set up on the Berkeley Pre-set EPUT Meter.

5) PEDAL (Photochromic Experimental Disk Apparatus, Lineated).
    (Figure 154).
    Variable speed drive. Removable sample holders take test
    samples of photochromic material on standard 1 x 3 inch or
    2 x 3 inch microscope slides.

6) Read Light Source.
    Read optical system and read photomultiplier optically aligned
    at all times on bed which can be moved to locate center of track
    written on photochromic slides.

    Provisions available for accurate synchronizing of signals for
    writing and erasing.

404
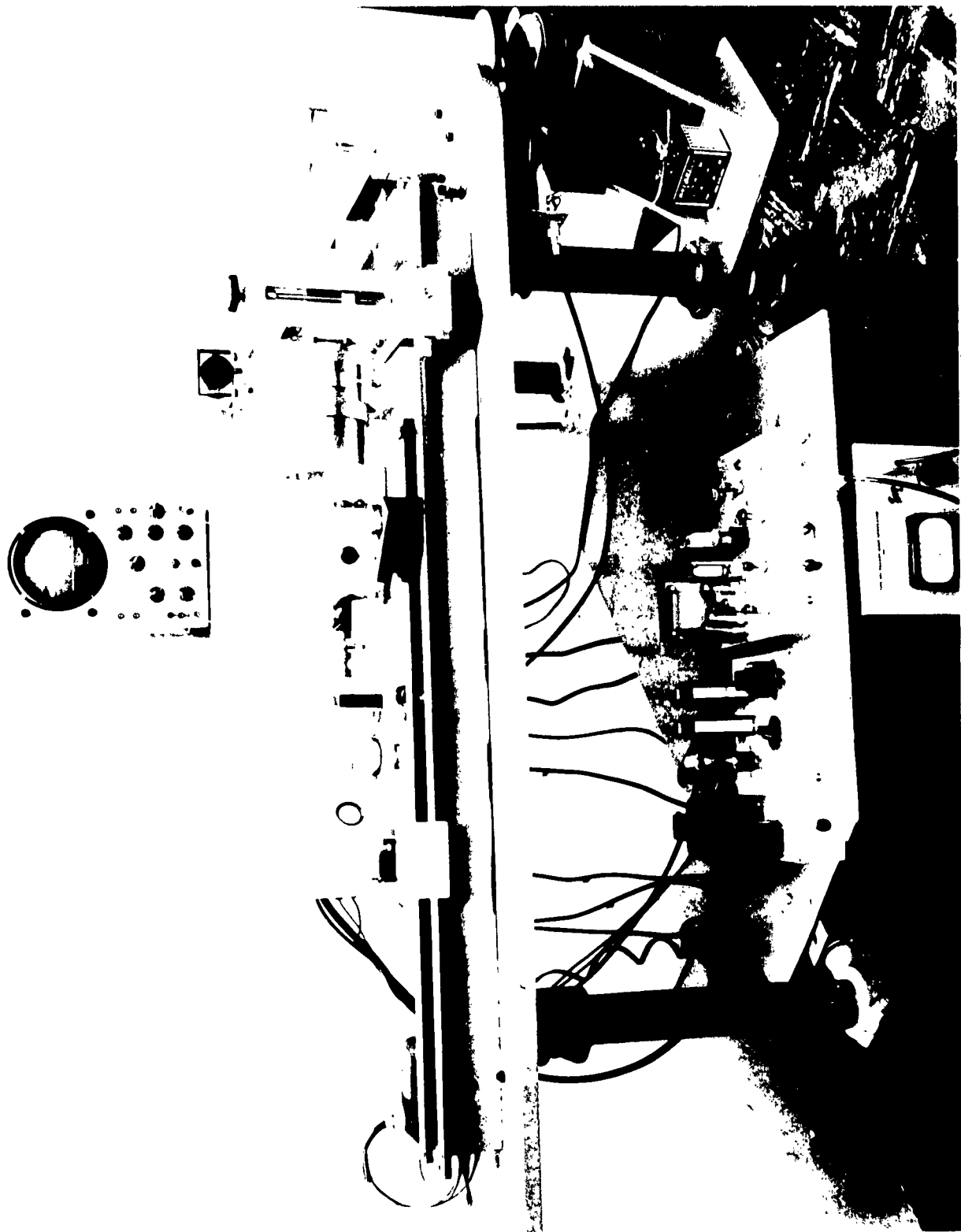
Figure 151. Rigid Optical Bench

405
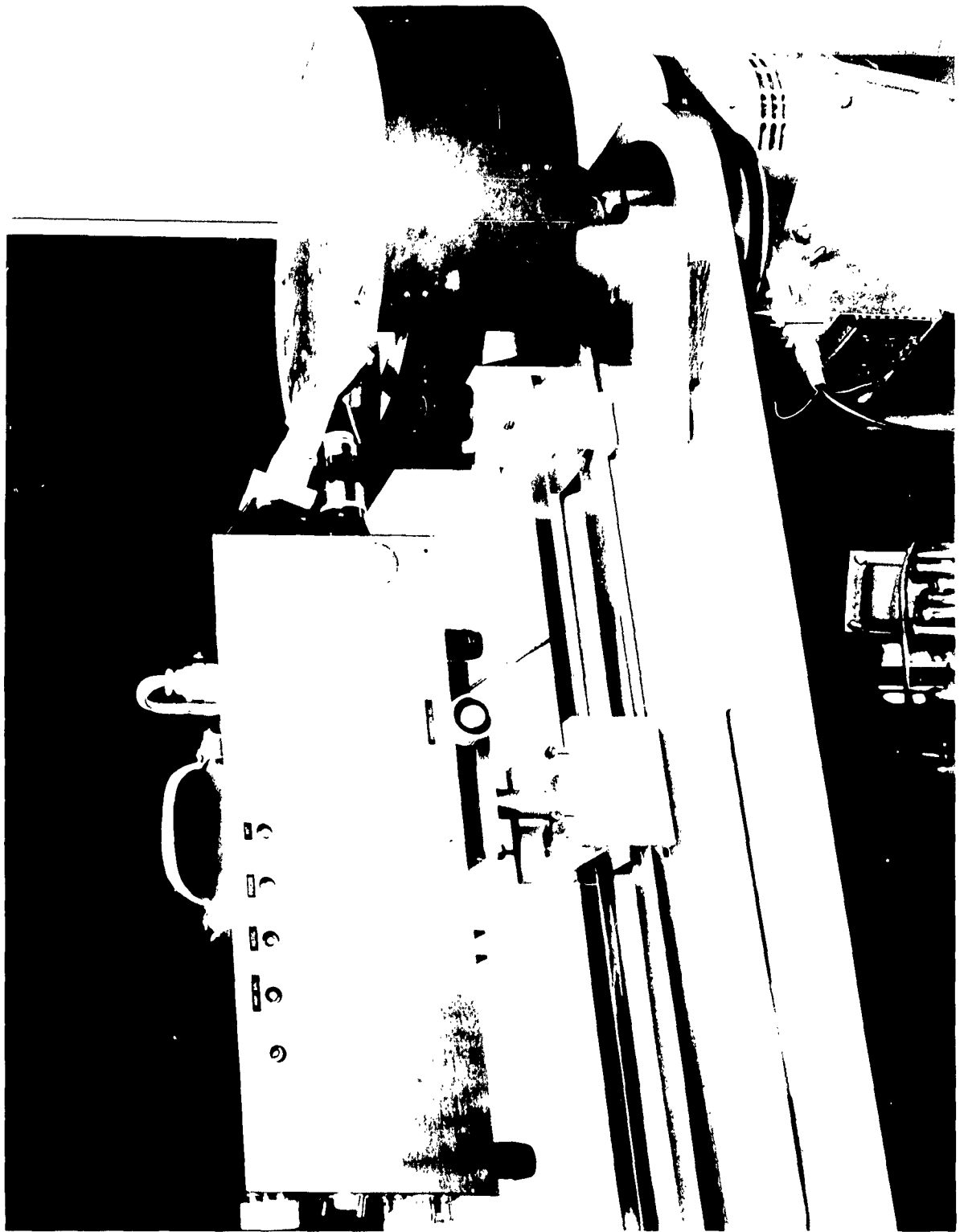
Figure 152. Optron and Disk (with shielding).
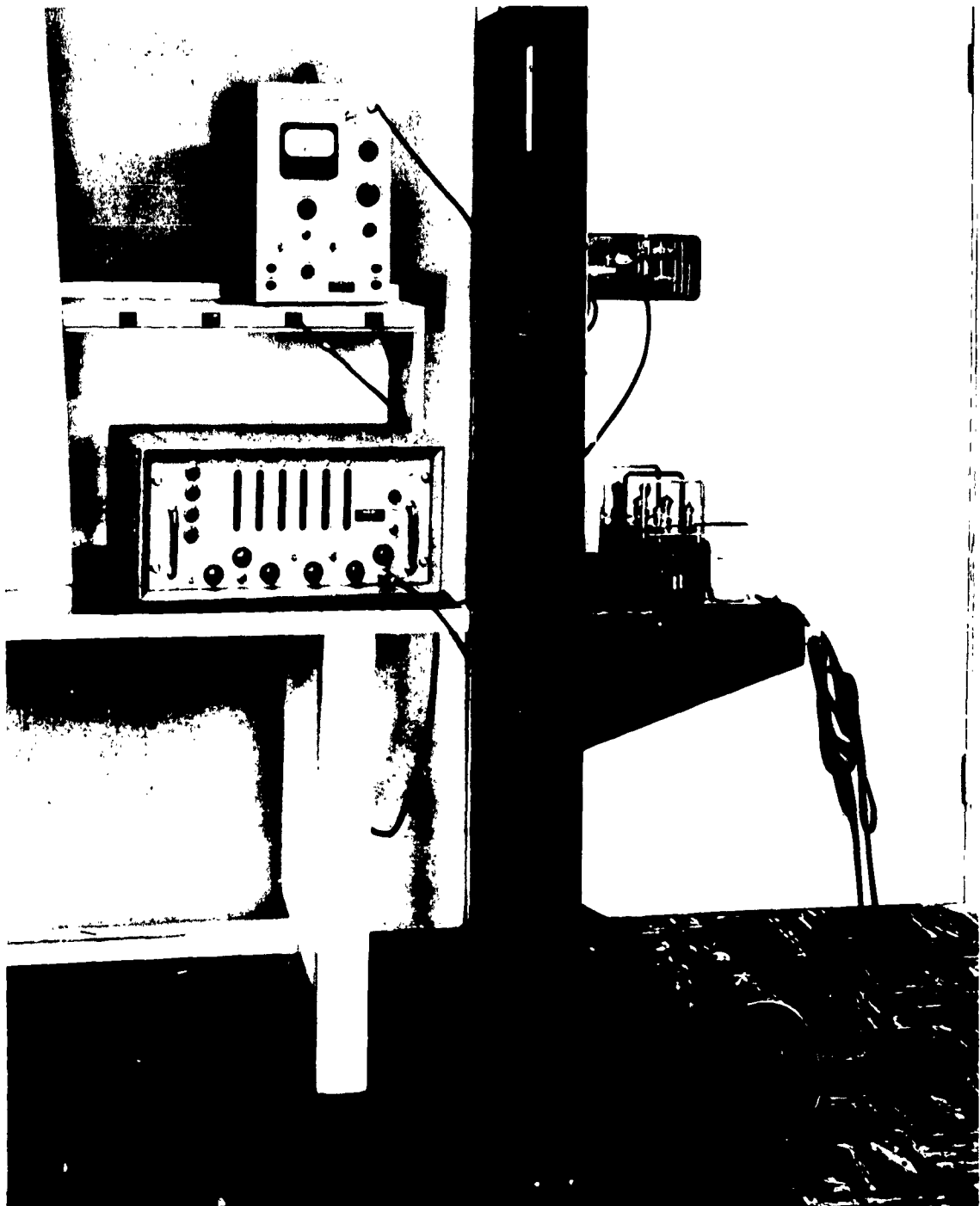
Figure 153. Special Word Generator.
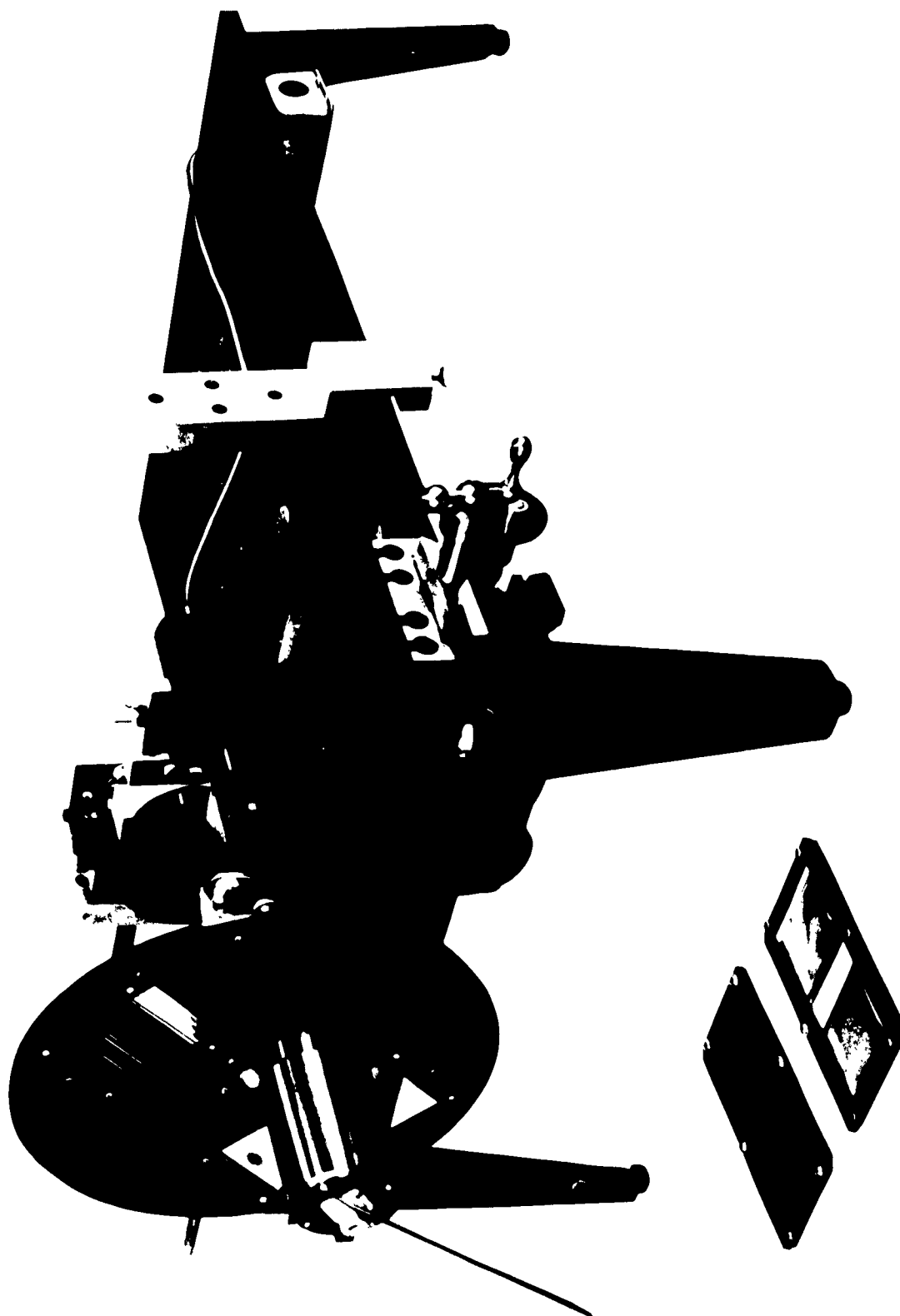
Figure 154. PEDAL.

7)   Lenses, Quartz (Texas Instruments)

Collimator: F. L. = 40 cm, Dia. = 2 inches (2 each).
Doublet: F. L. = 8 cm, Dia. = 1 inch (1 each).

8)   Sync Pulse Generators

Provide a constant rise time and amplitude output pulse for
input pulses in the range 0.2 volt to 50 volts.

9)   Variable width Pulse Generator

Input-push button (single shot) or square wave generator input.
Output No. 1 - negative pulse variable in amplitude from 0 to 0.6
volts, 100 ohms output impedance, 0.2 microsecond rise time.
Output No. 2 - negative pulse variable in amplitude from 0 to 50
volts, 7000 ohms output impedance, 0.3 microsecond rise time.

10)   Dual Pulse Generator

Provides two outputs and two output pulses for each input pulse.
These outputs may be selected as:
   a)   Identical positive pulses at the two outputs.
   b)   Identical negative pulses at the two outputs.
   c)   Single positive pulses, output A leading output B by
        the delay setting.
   d)   Single negative pulses, output A leading output B
        by the delay setting.

2. Optical Equipment

1)   Lenses
        a)   Kodak, Ektanon Enlarging 135 mm f/4.5
        b)   Goez, Tricolor 5 inch f/4.5
        c)   Elgeet Camera Lens (Optron) 13 mm f/1.5
        d)   Santar Camera Lens (Optron) 3 inch 5/1.9
        e)   Ross, Homocentric (2 each) 15 inch f/8

409

f)   Applied Research Quartz Condenser Lens 33-84-28-01.

g)   Edmund Optics - Miscellaneous.

h)   American Optical Reflecting Objective No. 1200.

2)   Corning Glass Filters

a)   Metascope, Type B - Infrared Receiver (purchased for optical components).

b)   Technicolor sine wave transmission plate.

c)   Spectrolab interference filters (3 each).

d)   Texas Instruments Polygon mirror (on loan).

e)   Numerous front surface mirrors.

f)   Wollensak shutter, Century graflex No. 1.

g)   Rapax shutter No. 2.

h)   Baush and Lomb 1.5 meter grating spectrograph.

i)   Stellite bi-laterial spectrographic slit #4098.

j)   Central scientific optical benches.

k)   Central scientific polarizing filters # 610A.

l)   Unitron microscope Model MMV.

3.   Photographic Equipment

1)   Standard darkroom supplies.

2)   Polaroid photographic equipment and supplies readily available.

3)   Beseler enlarger Model 45M.

4)   Graflex IV stroboflash 50-200 watt-seconds.

4.   Light Sources

1)   Sylvania concentrated arc lamp and power supply with 0.003 inch dia. point source 36,000 candles/inch^2.

2)   GE-H6 lamp with housing and facilities for water cooling in optical darkroom - 1000 watts.

3)   Osram HBO-109 Hg point source and power supply.

4)   Ultra-violet products Blak-Ray (U.V.) lamp - Model XX-4.

5)   G. E. Sun Lamp.

6)   Applied Research low pressure Hg Arc #7518.

7)   Various tungsten sources.

8)   NBS 50 watt calibrated carbon lamp.

5.   <u>Electronic Equipment</u>

    1)   Viking Adventurer CW Transmitter (modified) with 50 watts input power.

    2)   Viking Courier RF Power Amplifier with 500 watts plate input for CW.

    3)   Leeds and Northrup Galvanometer #2284B.

    4)   Berkeley Preset Universal EPUT Meter and Timer - Model 7631.

    5)   Keithley Electrometer Model 200A and Voltage Divider - Model 2007.

    6)   Optron Displacement Follower Model 301 (extensively modified).

When used to lock on an edge by reflected light the Model 301 has the following specifications:

Range No. 1	Range - full scale	0.1 inch
	Resolution	0.0001 inch
	Working Distance	1/2 inch
Range No. 2	Range - full scale	1/4 inch
	Resolution	0.0002 inch
	Working Distance	2 inches
Range No. 3	Range - full scale	1 inch
	Resolution	0.001 inch
	Working Distance	3-1/2 inches
Range No. 4	Range - full scale	4 inches
	Resolution	0.004 inch
	Working Distance	9 inches

The following specifications are common to all four ranges:

| Linearity | 0.2 percent of full scale over central 75 percent of range. |
| Repeatability | 0.1 percent of full scale over central 75 percent of range. |

411

Signal Output	40 volts full scale, push-pull.
Output Impedance	Approximately 1000 ohms.
Noise	10 mv rms, push-pull.
Bandwidth (3db)	0 to 5000 cps.
Power Requirements	Optron Model 301 Power Supply.
Focusing Adjustment	Fore and aft $\pm$ 1 inch.
Ambient Light Requirements	Low Ambient.

6. **Miscellaneous**

1) Thermopile (Eppley): circular, bismuth-silver, 8 junction sensitivity 0.110 microvolts/microwatt per cm^2.

2) Liquidizer, Multi-Speed (Knapp-Monarch).

B. **ADDITIONAL EQUIPMENT ACQUIRED DURING CONTRACTUAL PERIOD**

The following list is not all-inclusive, but is primarily intended to provide a list of additional equipment which was obtained and was of some significance in the laboratory program. General electronic laboratory equipment is not included in this listing.

1. **Purchased Equipment**

1) Air Gauge (focus to 50 microinches).
2) High Current P-16 CRT - Litton Industries.
3) Kodak RT Densitometer.
4) Leiss GFL Microscope.
5) Graff-Apsco GK-3 Microscope.
6) Bausch and Lomb Inspection Microscope.
7) Microscope Objectives and Eyepieces - (a number of these).
8) Refrigeration test unit - four chambers.
9) RCA P-16 Pulsed Source - C73687A.
10) FX-12 Xenon Flash Tube.
11) Various Optical Absorption Filters.

412

12) Special 45° U. V. Reflecting, Visible Transmitting Dichroic Filter.

13) Kodak Aero-Ektar f/2. 5 7 inch lenses (2 each).

2. Specially Constructed Equipment

1) Test Equipment for CRT Studies.

2) Test Equipment for Optical Resolution Studies.

3) Test Equipment for Photochromic Material Evaluation.

4) Improved Optical Bench Apparatus.

5) High Resolution Contact Printers.

The improved optical bench set-up is shown in Figure 155 along with some of the apparatus used for checking field and resolution of objectives lenses. This equipment has worked quite well.

Much of the specially constructed test equipment was breadboarded from available components whenever required for specific applications. The application of this equipment is described in the main body of this report.

The simplicity of the equipment used for measuring square wave response is worth describing in more detail here. Except for very high resolution systems, this equipment should suffice. At any rate, it provided more data in a shorter time than alternate schemes tried on this program. Although the precision was not all that could be desired, reliable results were obtained from which general conclusions could be drawn. Of the two techniques used, square wave response and knife edge response, the former was found to be preferable, generally. However, the latter is inherent in square waves, so both types of data are available from square wave response tests.

Figure 156 illustrates the set-up used for square wave response evaluation. The multiplier phototube responds to the light fluctuatio , as the

ASD TR 61-70

Light Source

Filter Mount

Condenser Lens

Transparency Mount

Dry Nitrogen (for air gauge)

Photochromic Plate Mount

Microscope

Air Gauge Indicator

Shutter

Air Gauge (for focus)

Writing Lens and Air Gauge Mount
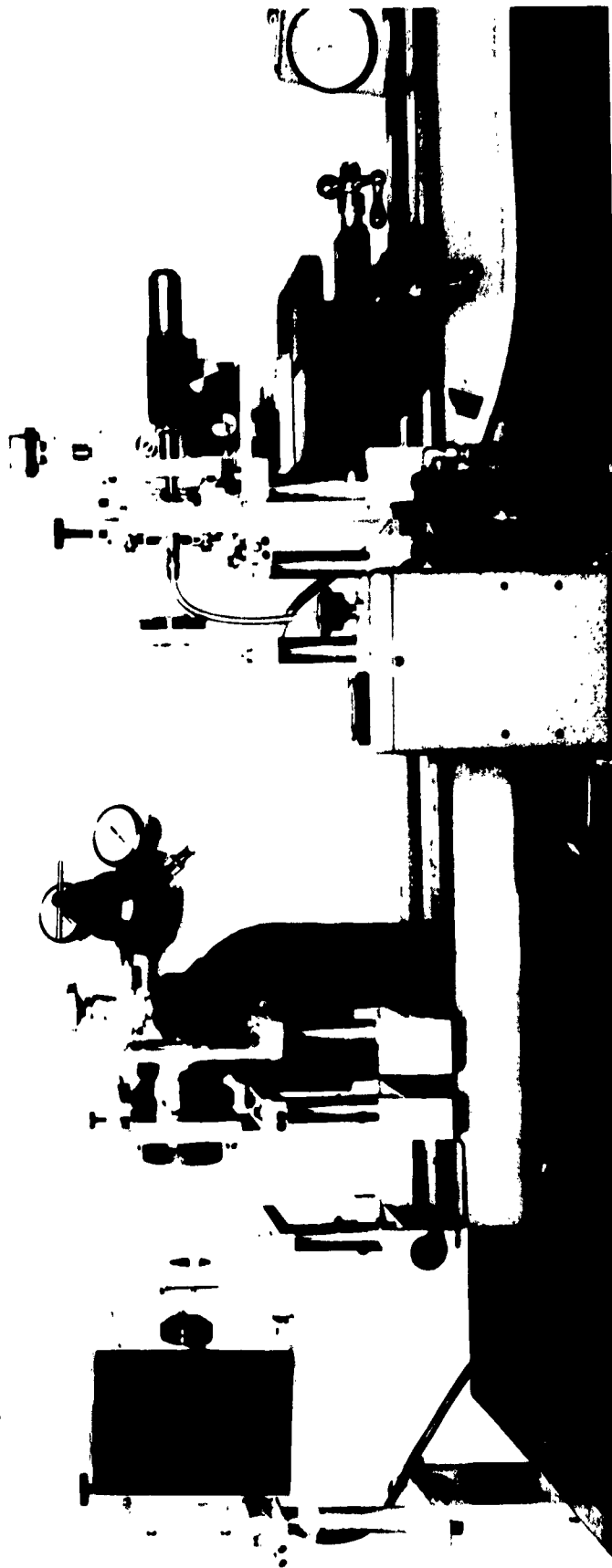
Figure 155. Optical Bench Set-Up.

projected image of the pattern under test scans the sensing hole. When a slit is used, provision is included for slit rotation and slit width adjustment. All elements are aligned axially. Use of only the axial region of a high resolution microscope objective insures a minimum image degradation from this component. Course alignment is achieved by projecting the pattern on the screen with the disk stationary. Fine alignment is accomplished by focusing while observing the oscilloscope for optimum output. A master test pattern or knife edge is readily mounted alongside the pattern under test and can be referred to during a test (without stopping the disk) to insure that optimum operation is being maintained.

In the initial arrangement used for checking resolution (described in Appendix XI), a small spot was imaged on the rotating pattern and the transmitted light was sensed by a phototube. The disadvantages of this technique are described in part F of Section IV (Volume I).
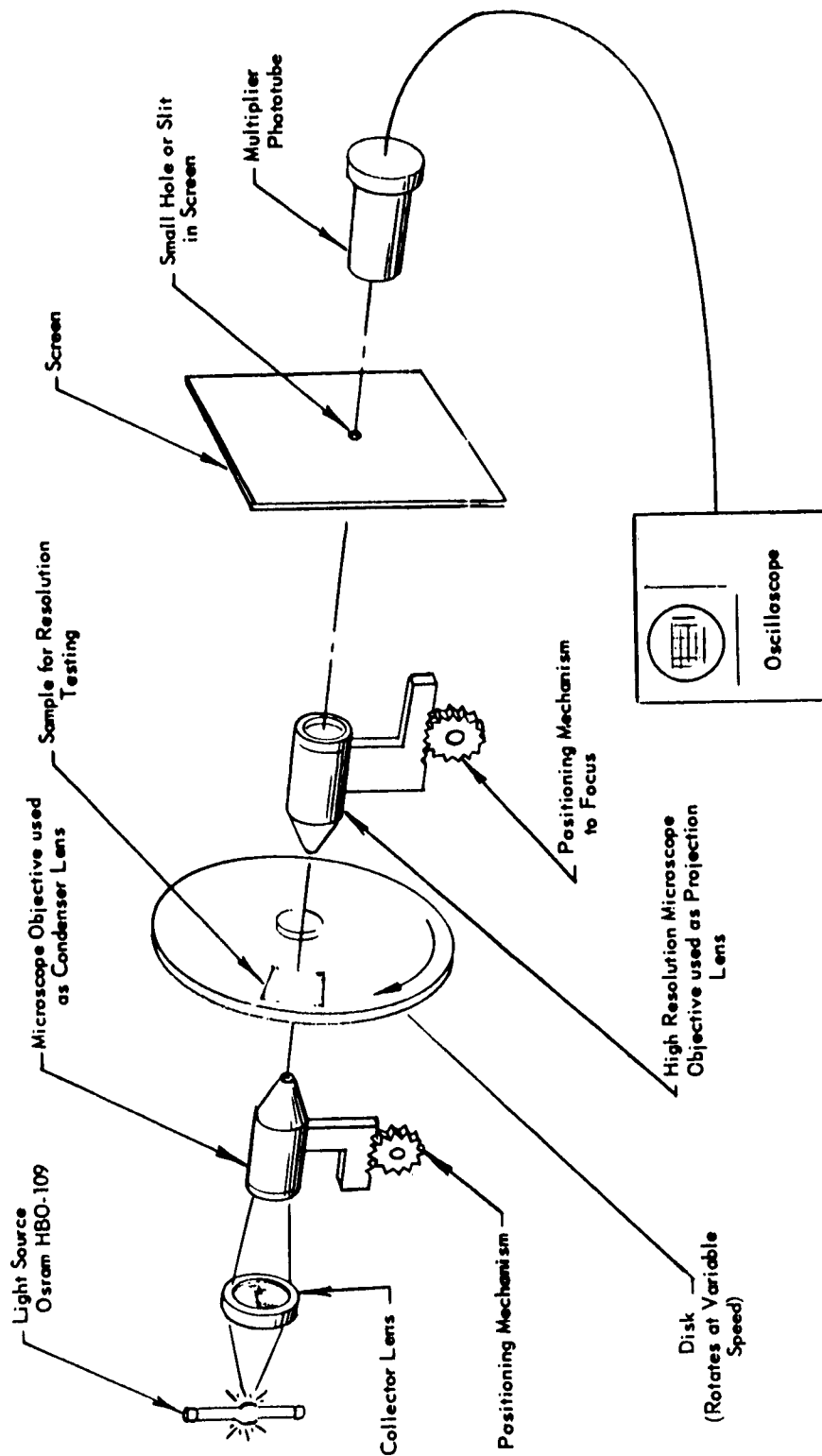
Figure 156. Set-Up used for Testing Square Wave Response.

Multiplier Phototube

Small Hole or Slit in Screen

Screen

Oscilloscope

Sample for Resolution Testing

Positioning Mechanism to Focus

Microscope Objective used as Condenser Lens

High Resolution Microscope Objective used as Projection Lens

Light Source Osram HBO-109

Collector Lens

Positioning Mechanism

Disk (Rotates at Variable Speed)

416

APPENDIX XI
EXPERIMENTAL SET-UP AND PROCEDURE FOR
CONDUCTING TESTS ON PHOTOCHROMIC SAMPLES
HSP-208, HSP-209 AND HSP-210

The experimental set-up used for conducting the investigations on capsular coatings HSP-208, HSP-209 and HSP-210 is described in Section IV of this report and was designed for use on PEDAL (see Section A in Appendix X). The coated microscope slides were placed in holders and attached to the disk. They were then rotated into position at the ''write'' station and held stationary during the write operation. Immediately following the write exposure, the disk drive motor was turned on and the written spot was caused to rotate past the "read" station (located one-half a revolution away on the other side of PEDAL). The readout multiplier phototube (DuMont 6467) and the read spot imaging objective were optically aligned and mounted on a common rigid platform which could be positioned radially along the disk. Thus, it was a relatively simple operation to align the read spot with the written spot(s) by observing the output of the multiplier phototube on an oscilloscope and positioning the " read" station for maximum output. A continuously adjustable focusing control was also provided for the readout objective to insure optimum focus for readout of high resolution patterns.

The microscope used on the original PEDAL " read " station was found to image rings as well as the desired spot. The rings appeared to be due to reflections from the edges of the various microscope elements and their respective mounts. Use of a number of field limiting dia-phrams within the microscope barrel gave some improvement, but enough light, though faint, appeared as rings to reduce the effective read spot size appreciably. In order to facilitate measurements, this read spot problem was bypassed by use of an objective sans barrel for imaging a spot of light (the filament of a small pilot lamp as seen through a small hole located at the rear of PEDAL) on the photochromic material. A large light shield was placed between the light source and

417

the objective to eliminate stray light. The objective was a Simpson Fl. 6, 3/4 inch focal length lens. It was the same type as used for the "write" operation.

Calibration of the effective size of the read spot was accomplished by scanning a series of known-width opaque lines on a high resolution photographic slide. The photographic slide had standard microscope slide dimensions (1 inch x 3 inches) and was mounted adjacent to the photochromic slide under test. This allowed for a cons ant monitoring of the resolution capabilities of the read system while conducting experimental readout investigations on the photochromic coatings. The calibrated slide indicates that the read system for this experiment was capable of providing full white-to-black resolution of lines 0.7 mil wide (the smallest measured). For the purpose of the discussions in this report, a read spot size of 0.5 mil was assumed. Except where noted, no spectral filters were used in the "read" beam.

Exposure was accomplished through the imaging of an Osram HBO-109 mercury arc on the photochromic material. To properly define the written spot, the arc was first magnified and imaged on a 50-mil circular aperture in a thin brass shim and then reduced by a Simpson Fl. 6, 3/4 inch focal length lens to the final size of 9 mils. A Corning glass filter, No. 7-60R, was placed in front of the aperture to provide a more desirable spectral characteristic (similar to P-16 phosphor) for the "write" source. Exposure control was accomplished by means of a photographic shutter placed in front of the circular aperture. A mechanism was provided to allow for accurate focusing of the "write" objective onto the photochromic material.

Thermopile energy measurements were made on the "write" light beam after the imaging process and with the photochromic material removed from the optical path. These measurements automatically take into account the factors affecting the energy in the "write" spot

418

image and were made immediately after any sensitometeric data was recorded.

The measurements described were carried out in the dark at room temperature. No discernable erasure was noted due to the spectral distribution and energy density of the "read" spot.

419

APPENDIX XII

EXPERIMENTAL DETERMINATION OF
D LOG E CURVES FOR
NON-CAPSULAR PHOTOCHROMIC COATINGS

A.   INTRODUCTION

For the sake of convenience, the following D log E curves of non-capsular photochromic coatings were plotted against exposure time. Multiplication of the time coordinate by the energy density given for each curve will give the actual exposure.

The data was obtained by exposing a number of areas on the photochromic slides to different densities of light. These spots were then scanned by a reading spot, with the transmitted light being picked up by a multiplier phototube. The resulting phototube output waveforms were displayed on an oscilloscope and photographed. The data was then scaled off the photographs and recorded in tabular form.

420

B.   LIGHT SOURCE CALIBRATION

A calibrated energy light source as described below, was used in obtaining the data on the photochromic materials presented in the following pages.

1. **Thermopile Deflections**

$$4.75 \text{ to } 9.50 \longrightarrow 4.75$$
$$4.00 \text{ to } 8.50 \longrightarrow 4.50$$
$$3.80 \text{ to } 8.25 \longrightarrow 4.48$$
$$3.50 \text{ to } 8.00 \longrightarrow 4.50$$
$$3.50 \text{ to } 8.00 \longrightarrow 4.50$$

2. **Solid Angle Data**
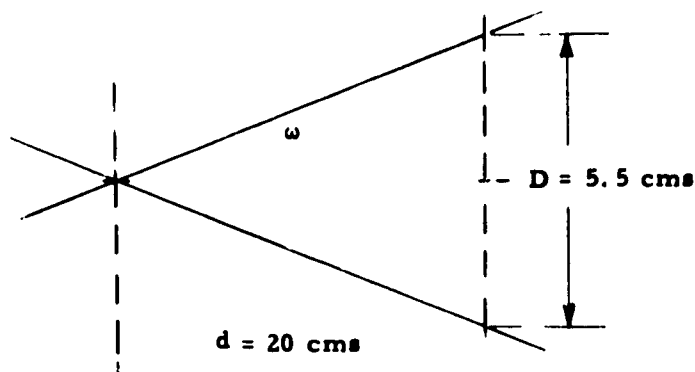
D = 5.5 cms

d = 20 cms

Note: Spectral distribution of energy controlled
by Corning Filter #7-37.

3. Light Source Calculations

Measurement of 20 cms from the emulsion plane showed a circle of light some 5.5 cms in diameter.

$$\omega = \frac{A}{d^2} = \frac{\pi D^2}{4} \times \frac{1}{d^2} = \frac{3.14 \times (5.5)^2}{4 \times 20^2}$$

$$= 5.93 \times 10^{-2} \text{ steradians}$$

ASD TP. 61-70

The average thermopile deflection was found to be 4.5 cms at a distance of 20 cms. Energy density at the thermopile was equal to:

$$\frac{4.5}{0.118} = 38 \ \mu watts/cm^2$$

Effective area was equal to:

$$\omega d^2 = 5.93 \times 10^{-2} \times 400$$
$$= 23.7 \ cm^2$$

Total energy passing the image plane was equal to:

$$38 \times 23.7 = 900 \ \mu watts$$

Area of the image at the emulsion was equal to:

$$0.031 \ in. \ dia. = 49.3 \times 10^{-4} \ cm^2$$

Therefore, the energy density at the emulsion was equal to:

$$\frac{900}{49.3 \times 10^{-4}} = 18.3 \times 10^{-4} \ \mu watt/cm^2$$

$$= \underline{0.18 \ watts/cm^2}$$

422

C. EXPERIMENTAL DATA

1. Characteristics of Photochromic Material No. P102 (Contrast vs. Exposure with Tungsten Light)

TABLE XXXI

Exposure Time in Seconds	Density	Base & D
10	$\frac{15}{2}$ = 7.5:1 = 0.876	1.176
5	$\frac{15}{2.8}$ = 5.35:1 = 0.730	1.030
3	$\frac{15}{3}$ = 5.0:1 = 0.700	1.000
2	$\frac{15}{3.2}$ = 4.7:1 = 0.673	0.973
1	$\frac{15}{4.8}$ = 3.14:1 = 0.497	0.797
.50	$\frac{15}{5.8}$ = 2.6:1 = 0.415	0.715
.20	$\frac{15}{9.3}$ = 1.62:1 = 0.210	0.510
.10	$\frac{15}{10.5}$ = 1.43:1 = 0.155	0.455
.04	$\frac{15}{12.5}$ = 1.2:1 = 0.080	0.380

Figure 157

(Base Density = $\frac{30}{15}$ = 2:1 = 0.3)

NOTE: The D Log E curve based on the above data will be found in Figure 37 of the main body of the report.

2. Characteristics of Photochromic Material No. P102 (Contrast vs. Exposure with Tungsten Light and Green Read Filter)

TABLE XXXII

Exposure Time in Seconds	Density			Base & D
10	$\frac{13.8}{5}$	= 27.5:1	= 1.440	1.740
5	$\frac{13.8}{.7}$	= 19.7:1	= 1.290	1.590
3	$\frac{13.8}{1}$	= 13.8:1	= 1.140	1.440
2	$\frac{13.8}{1.1}$	= 12.5:1	= 1.095	1.395
1	$\frac{13.8}{1.7}$	= 8.14:1	= 0.910	1.210
.5	$\frac{13.8}{2.2}$	= 6.3:1	= 0.800	1.100
.2	$\frac{13.8}{5.4}$	= 2.56:1	= 0.408	0.708
.1	$\frac{13.8}{8.5}$	= 1.63:1	= 0.210	0.510
.04	$\frac{13.8}{11}$	= 1.25:1	= 0.097	0.397

$$\text{(Base Density} = \frac{27.5}{13.8} = 2:1 = 0.3)$$

Figure 158.

NOTE: The D Log E curve based on the above data will be found in Figure 37 of the main body of the report.

3. **Characteristics of Photochromic Material No. P105** (Contrast vs. Exposure with Tungsten Light)

TABLE XXXIII

Exposure Time in Seconds	Contrast			Base ΔD
15	$\frac{26}{2.8}$ =	9.3:1	= 0.970	1.030
10	$\frac{26}{2.9}$ =	9:1	= 0.955	1.015
5	$\frac{26}{3}$ =	8.7:1	= 0.940	1.00
3	$\frac{26}{4.8}$ =	5.42:1	= 0.735	0.795
2	$\frac{26}{5}$ =	5.2:1	= 0.717	0.777
1	$\frac{26}{6.2}$ =	4.2:1	= 0.625	0.685
.50	$\frac{26}{8}$ =	3.25:1	= 0.510	0.570
.20	$\frac{26}{13}$ =	2:1	= 0.300	0.360
.10	$\frac{26}{17.5}$ =	1.47:1	= 0.167	0.227
.04	$\frac{26}{22.5}$ =	1.15:1	= 0.060	0.120

(Base Density = $\frac{30}{26}$ = 1.15:1 = 0.06)
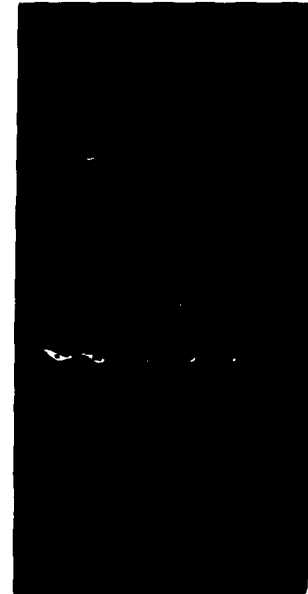
Figure 159.

4. Characteristic of Photochromic Material No. P105 (Contrast vs. Exposure with Tungsten Light and Green Read Filter)

TABLE XXXIV

Exposure Time in Seconds	Contrast			Base & D
15	$\frac{26}{0.6}$	= 43:1	= 1.630	1.690
10	$\frac{26}{0.6}$	= 43:1	= 1.630	1.690
5	$\frac{26}{0.6}$	= 43:1	= 1.630	1.690
3	$\frac{26}{1.5}$	= 17.3:1	= 1.230	1.290
2	$\frac{26}{1.5}$	= 17.3:1	= 1.230	1.290
1	$\frac{26}{2.4}$	= 10.8:1	= 1.030	1.090
.50	$\frac{26}{3.8}$	= 6.85:1	= 0.835	0.895
.20	$\frac{26}{10}$	= 2.6:1	= 0.415	0.475
.10	$\frac{26}{17}$	= 1.53:1	= 0.180	0.240
.04	$\frac{26}{20}$	= 1.3:1	= 0.114	0.174

Figure 160.

(Base Density = $\frac{30}{26}$ = 1.15:1 = 0.06)

(a) Density to Tungsten
(b) Peak Density with Green Read Filter
Exposed with Osram H100 and Corning Filter 7-37 with
calibrated energy density of 0.18 watts/cm²
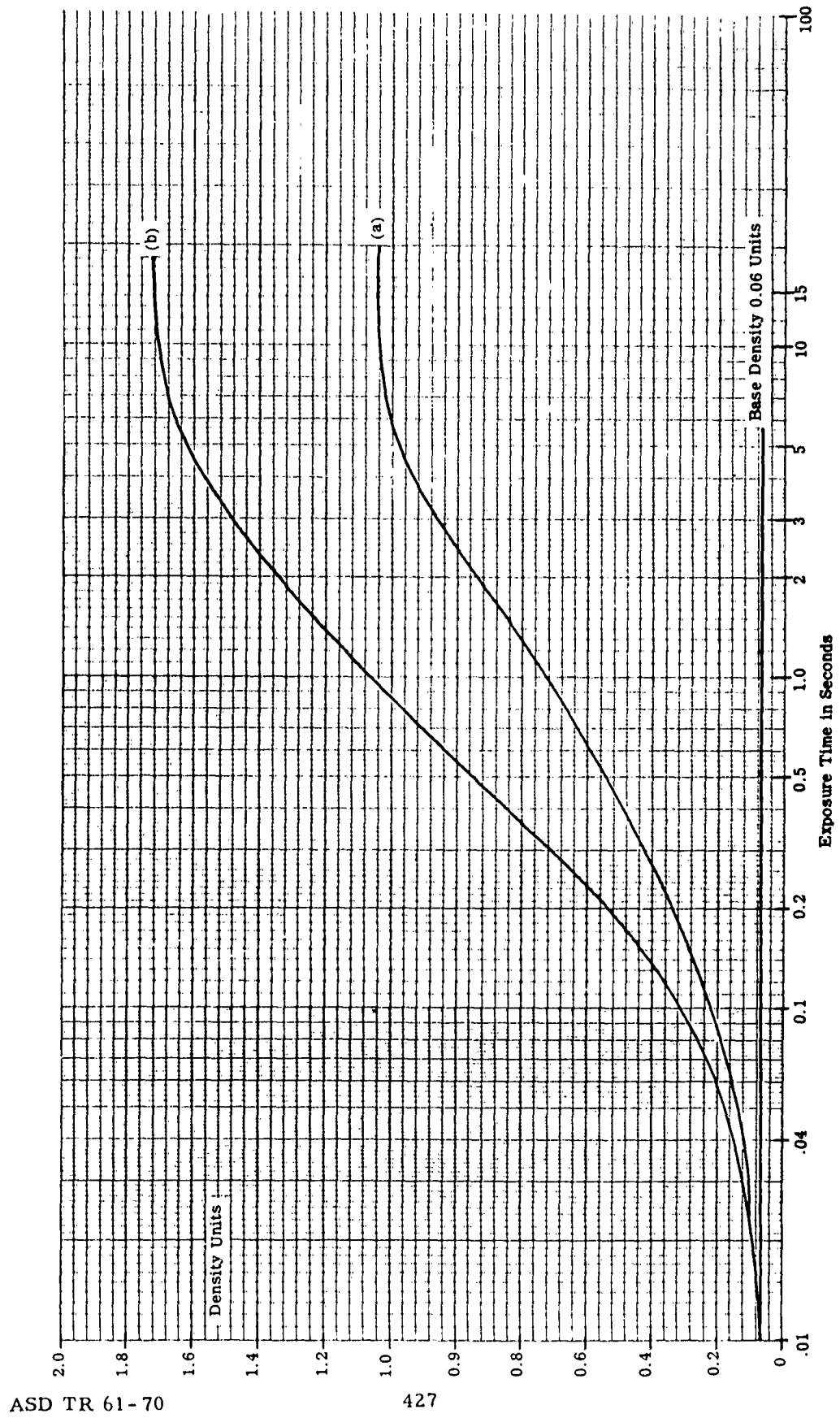
D Log E Characteristic Curves for Photochromic Solid Solution Material No. P105

Figure 161.

5. **Characteristics of Photochromic Material No. P108** (Contrast vs. Exposure with Tungsten Light)

TABLE XXXV

Exposure Time in Seconds	Contrast				Base &D
15	$\frac{21}{4}$	= 5.27:1	=	0.720	0.855
10	$\frac{21}{4.5}$	= 4.67:1	=	0.670	0.805
5	$\frac{22}{6}$	= 3.67:1	=	0.565	0.700
3	$\frac{22}{7}$	= 3.14:1	=	0.497	0.632
2	$\frac{22}{8}$	= 2.75:1	=	0.440	0.575
1	$\frac{22.5}{11}$	= 2.05:1	=	0.312	0.447
.50	$\frac{23}{14}$	= 1.64:1	=	0.215	0.350
.20	$\frac{23}{19}$	= 1.21:1	=	0.083	0.218
.10	$\frac{23}{22.5}$	= 1.02:1	=		0.175
.04	$\frac{24}{23}$	= 1.04:1	=		0.135
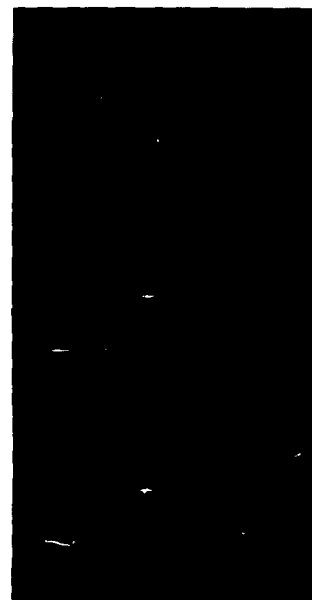
Figure 162.

(Base Density = $\frac{30}{22}$ = 1.36:1 = 0.135)

6. **Characteristics of Photochromic Material No. P108** (Contrast vs. Exposure with Tungsten Light and Green Read Filter)

TABLE XXXVI

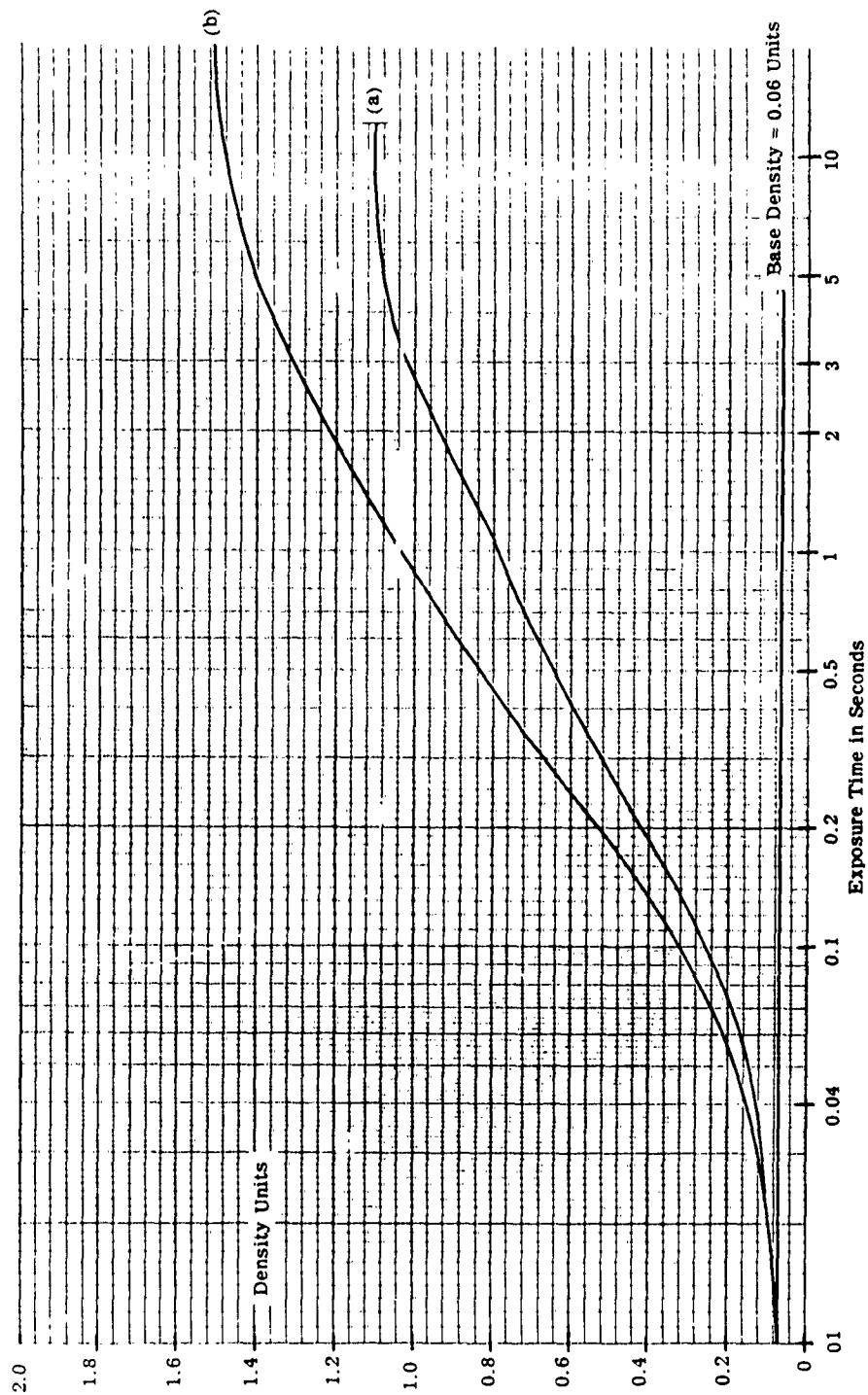| Exposure Time in Seconds	Contrast	Base & D
15	$\frac{24}{2}$ = 12:1 = 1.08	1.160
10	$\frac{24}{2.8}$ = 8.6:1 = 0.934	1.014
5	$\frac{24}{3.5}$ = 6.87:1 = 0.835	0.915
3	$\frac{24}{5}$ = 4.8:1 = 0.680	0.760
2	$\frac{25.5}{6.5}$ = 3.92:1 = 0.593	0.673
1	$\frac{26}{10}$ = 2.6:1 = 0.475	0.495
.50	$\frac{26}{13}$ = 2:1 = 0.300	0.380
.20	$\frac{26.5}{20}$ = 1.33:1 = 0.124	0.204
.10	$\frac{26.5}{22.5}$ = 1.18:1 = 0.072	0.152
.04	$\frac{26.5}{24}$ = 1.11:1 = 0.047	0.127

(Base Density = $\frac{30}{25}$ = 1.2:1 = 0.08)
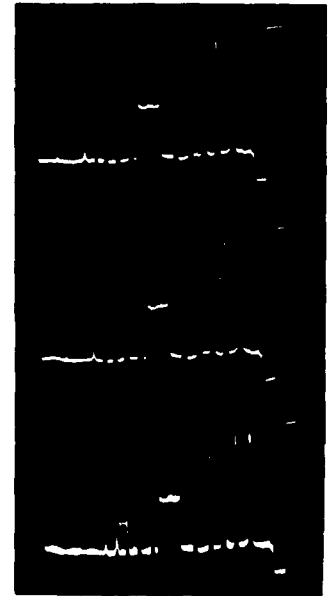
Figure 163.

(a) Density to Tungsten

(b) Density with Green Read Filter

Exposed with Osram H100 and Corning Filter 7-37 with Calibrated energy density of 0.18 watts/cm²
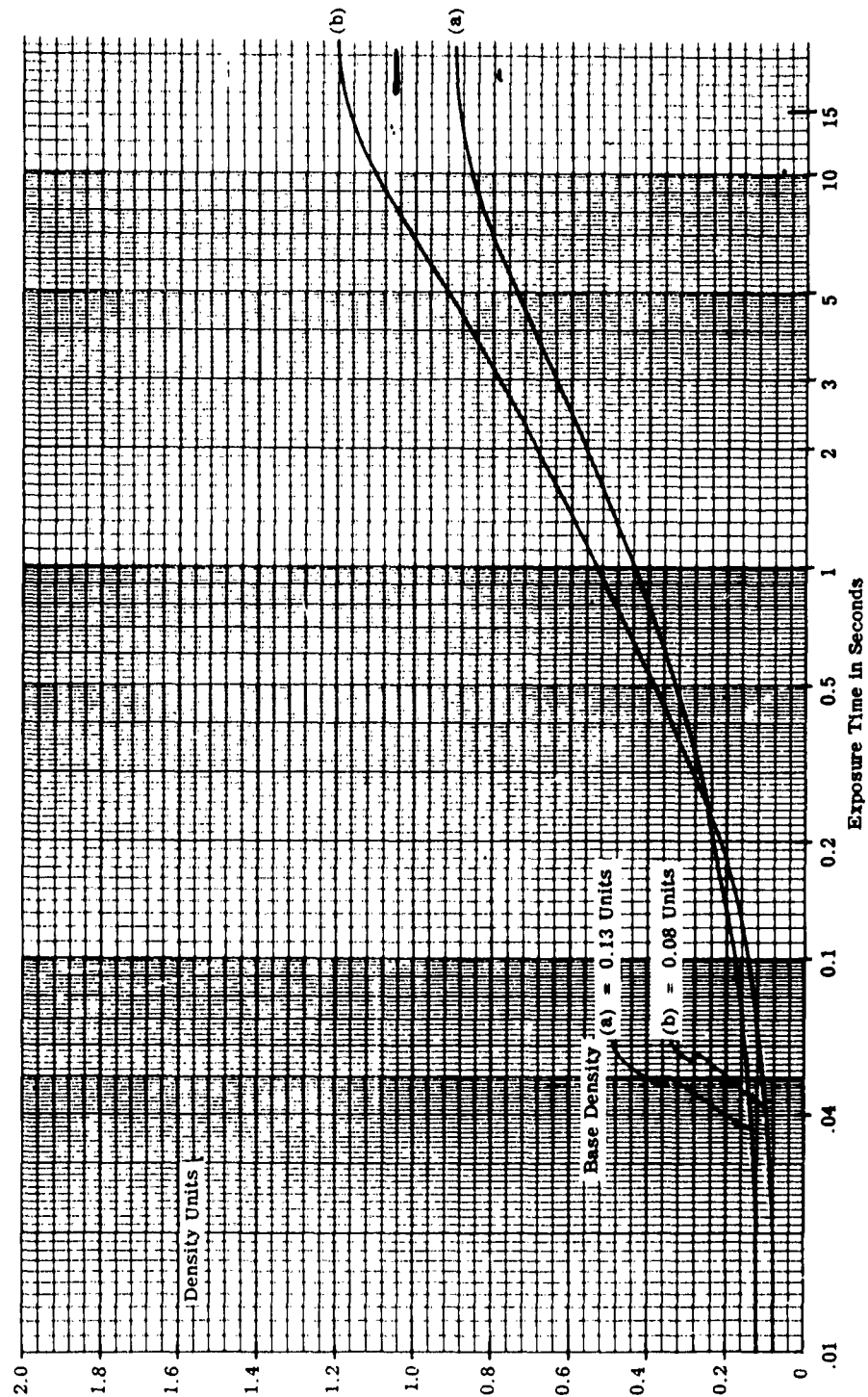
D Log E Characteristic Curves for Photochromic Solid Solution Material No. P108.

Figure 164.

7. **Characteristics of Photochromic Material No. P112**(Contrast vs. Exposure with Tungsten Light)

TABLE XXXVII

Exposure Time in Seconds	Contrast				Base & D
10	$\dfrac{20}{1.1}$	=	18.2:1	= 1260	1.536
5	$\dfrac{20}{1.2}$	=	16.7:1	= 1.230	1.506
3	$\dfrac{20}{2}$	=	10:1	= 1.000	1.276
2	$\dfrac{20}{3.2}$	=	6.26:1	= 0.800	1.076
1	$\dfrac{22}{5}$	=	4.4:1	= 0.645	0.921
.50	$\dfrac{20}{6}$	=	3.3:1	= 0.520	0.796
.20	$\dfrac{20}{11}$	=	1.81:1	= 0.258	0.534
.10	$\dfrac{21}{16}$	=	1.31:1	= 0.117	0.393
.04	$\dfrac{20}{16}$	=	1.25:1	= 0.097	0.373

(Base Density = $\dfrac{30}{20}$ = 1.5:1 = 0.176)

Figure 165.

8. **Characteristics of Photochromic Material No. P112** (Contrast vs. Exposure with Tungsten Light and Green Read Filter)

TABLE XXXVIII

Exposure Time in Seconds	Contrast			Base & D
10	$\dfrac{20}{.40}$ =	50:1 =	1.700	1.976
5	$\dfrac{20}{.45}$ =	44:1 =	1.650	1.926
3	$\dfrac{21}{1}$ =	21:1 =	1.330	1.606
2	$\dfrac{21}{1.1}$ =	19.1:1 =	1.280	1.556
1	$\dfrac{19}{2.1}$ =	9.1:1 =	0.955	1.231
.50	$\dfrac{20}{4}$ =	5:1 =	0.700	0.976
.20	$\dfrac{19}{10}$ =	1.9:1 =	0.278	0.554
.10	$\dfrac{19}{14}$ =	1.36:1 =	0.133	0.409
.04	$\dfrac{21.5}{17.5}$ =	1.23:1 =	0.090	0.366

Figure 166.

(Base Density = $\dfrac{30}{20}$ = 1.5:1 = 0.176)

(a) Density to Tungsten

(b) Density with Green Read Filter

Exposed with Osram H100 and Corning Filter 7-37 with
Calibrated Energy Density of 0.18 watts/cm^2
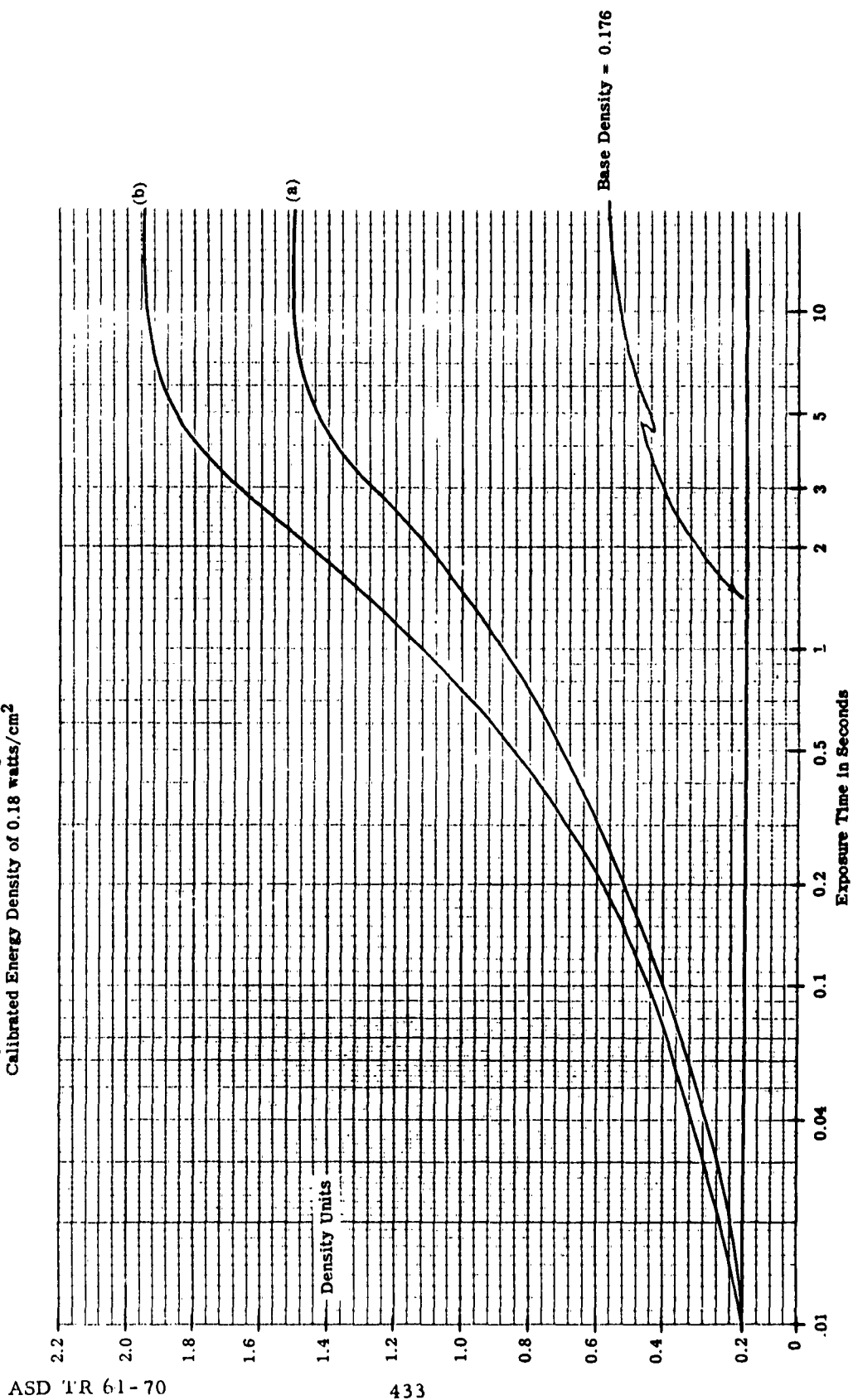
D Log E Characteristic Curves for Photochromic Solid Solution Material No. P112

Figure 167.

9. Characteristics of Photochromic Material No. P113 (Contrast vs. Exposure with Tungsten Light)

TABLE XXXIX

Exposure Time in Seconds	Contrast				Base & D
10	$\frac{26}{2.5}$	=	10.4:1	= 1.020	1.080
5	$\frac{26}{2.6}$	=	10:1	= 1.000	1.060
3	$\frac{26}{2.8}$	=	9.3:1	= 0.968	1.028
2	$\frac{26}{35}$	=	7.43:1	= 0.870	0.930
1	$\frac{26}{5}$	=	5.2:1	= 0.715	0.775
.50	$\frac{26}{5.7}$	=	4.67:1	= 0.670	0.713
.20	$\frac{26}{9.9}$	=	2.63:1	= 0.420	0.480
.10	$\frac{26}{15}$	=	1.73:1	= 0.238	0.298
.04	$\frac{26}{21.5}$	=	1.21:1	= 0.083	0.143

(Base Density = $\frac{30}{26}$ = 1.15:1 = 0.06)

Figure 168.

10. Characteristics of Photochromic Material No. P113 (Contrast vs. Exposure with Tungsten Light and Green Read Filter)

TABLE XL

Exposure Time in Seconds	Contrast			Base & D
10	$\frac{26}{1}$ =	26:1 =	1.420	1.480
5	$\frac{26}{1.2}$ =	21.6:1 =	1.340	1.400
3	$\frac{26}{1.7}$ =	15.3:1 =	1.190	1.250
2	$\frac{26}{1.8}$ =	14.7:1 =	1.170	1.230
1	$\frac{26}{2.5}$ =	10.4:1 =	1.020	1.080
.50	$\frac{26}{3.5}$ =	7.42:1 =	0.870	0.930
.20	$\frac{26}{8.2}$ =	3.16:1 =	0.500	0.560
.10	$\frac{26}{15}$ =	1.73:1 =	0.240	0.300
.04	$\frac{26}{20}$ =	1.3:1 =	0.114	0.174

Figure 169.

(Base Density = $\frac{30}{26}$ = 1.5:1 = 0.006)
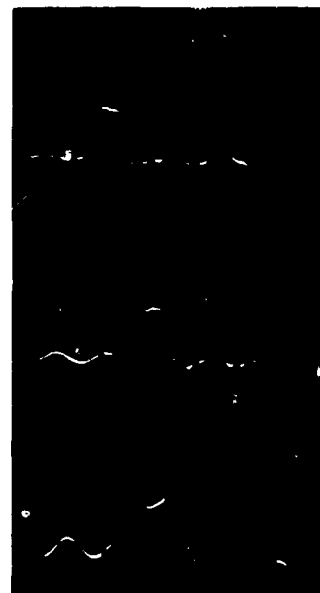
(a) Density to Tungsten

(b) Density with Green Read Filter

Exposed with Osram H100 and Corning Filter 7-37 with
Calibrated energy Density of 0.18 watts/cm²

D Log E Characteristic Curves for Photochromic Material No. P113

Figure 170.

436

11. **Characteristics of Photochromic Material No. H62** (Contrast vs. Exposure with Tungsten Light)

TABLE XLI

Exposure Time in Seconds	Contrast	Base & D
10	$\frac{18}{1.7} = 10.5:1 = 1.020$	1.298
5	$\frac{18}{2} = 9:1 = 0.955$	1.231
3	$\frac{18}{2.2} = 8.2:1 = 0.914$	1.190
2	$\frac{18}{2.7} = 6.7:1 = 0.826$	1.102
1	$\frac{18}{4} = 4.5:1 = 0.653$	0.929
.50	$\frac{18}{6} = 3:1 = 0.477$	0.753
.20	$\frac{18}{11} = 1.63:1 = 0.212$	0.478
.10	$\frac{18}{13} = 1.38:1 = 0.140$	0.416
.04	$\frac{18}{16} = 1.13:1 = 0.057$	0.333

$$\text{(Base Density} = \frac{27}{18} = 0.176)$$

Figure 171.

12. Characteristics of Photochromic Material No. H62 (Contrast vs. Exposure with Tungsten Light and Green Read Filter)

TABLE XLII

Exposure Time in Seconds	Contrast			Base & D
10	$\dfrac{20}{.57}$ =	35:1 =	1.545	1.821
5	$\dfrac{20}{.67}$ =	30.5:1 =	1.485	1.751
3	$\dfrac{20}{.9}$ =	22.5:1 =	1.350	1.626
2	$\dfrac{20}{1.1}$ =	18.2:1 =	1.250	1.526
1	$\dfrac{20}{2.5}$ =	8:1 =	0.905	1.181
.50	$\dfrac{20}{4}$ =	5:1 =	0.700	0.976
.20	$\dfrac{20}{11}$ =	1.82:1 =	0.260	0.536
.10	$\dfrac{20}{14.7}$ =	1.36:1 =	0.134	0.410
.04	$\dfrac{20}{16}$ =	1.25:1 =	0.100	0.376

(Base Density = $\dfrac{30}{20}$ = 1.5:1 = 0.176)

Figure 172.

(a) Density to Tungsten
(b) Density with Green Read Filter
Exposed with Osram H100 and Corning Filter 7-37 with
Calibrated Energy Density of 0.18 watts/cm²
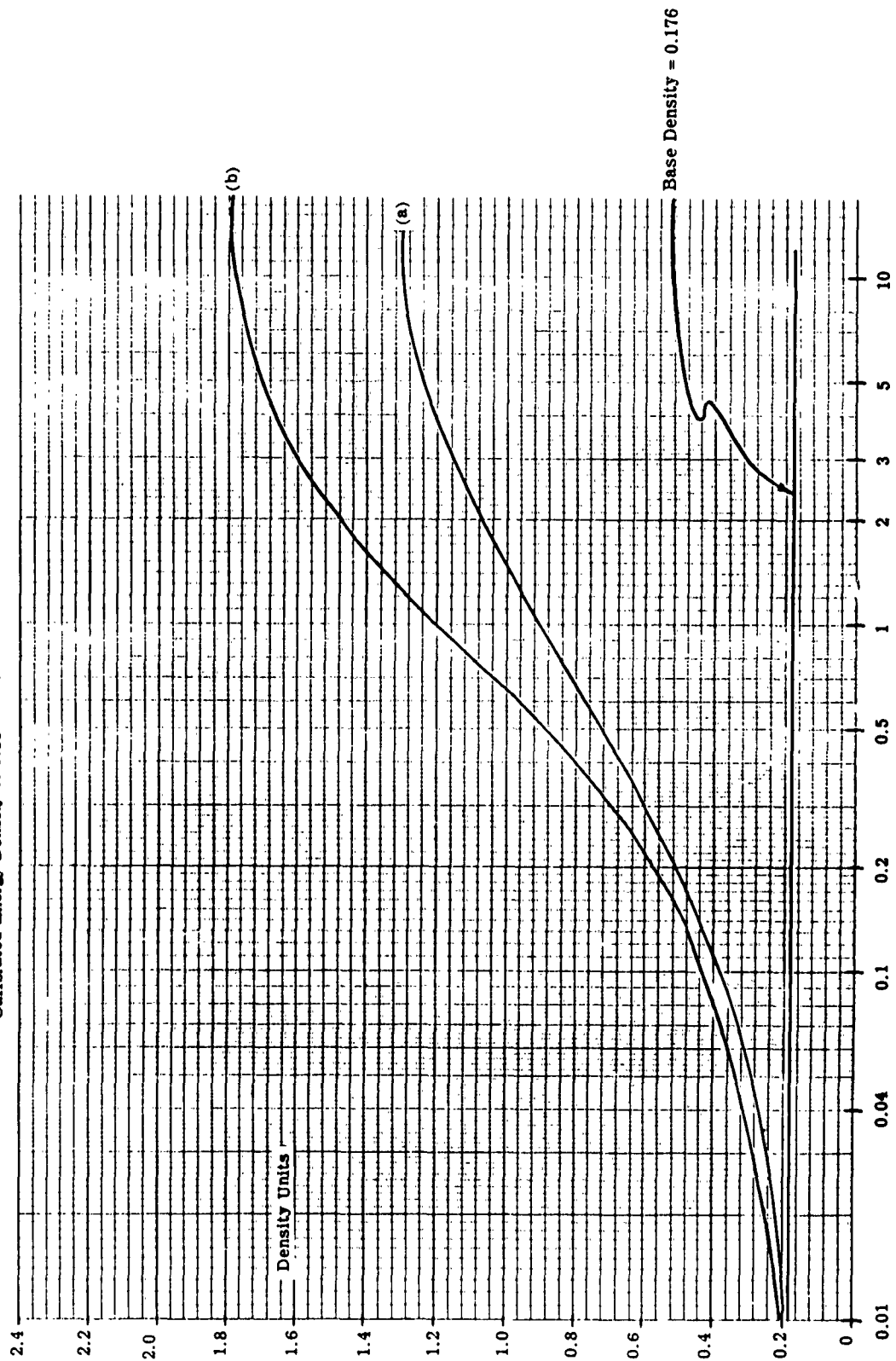
D Log E Characteristic Curves for Photochromic Material No. H62

Figure 173.

13. **Characteristics of Photochromic Material No. 94** (Contrast vs. Exposure with Tungsten Light)

TABLE XLIII

Exposure Time in Seconds	Contrast		Base & D
20	$\dfrac{12.5}{1.2}$ =	10.4:1 = 1.020	1.400
10	$\dfrac{12.5}{1.7}$ =	7.35:1 = 0.855	1.235
5	$\dfrac{12.5}{2.6}$ =	6.25:1 = 0.796	1.176
3	$\dfrac{12.5}{2.3}$ =	5.44:1 = 0.736	1.116
2	$\dfrac{12.5}{2.8}$ =	4.47:1 = 0.651	1.031
1	$\dfrac{12.5}{3.8}$ =	3.3:1 = 0.518	0.898
.50	$\dfrac{12.5}{6.4}$ =	2.32:1 = 0.364	0.744
.20	$\dfrac{12.5}{7.2}$ =	1.74:1 = 0.240	0.620
.10	$\dfrac{12.5}{9}$ =	1.39:1 = 0.143	0.523
.04	$\dfrac{12.5}{10.5}$ =	1.19:1 = 0.077	0.457
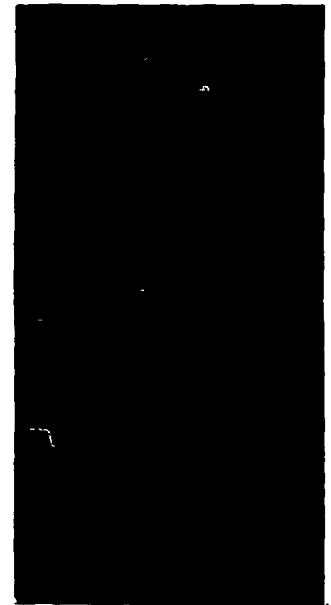
Figure 174.

(Base Density = $\dfrac{30}{12.5}$ = 2.4:1 = 0.38)

NOTE: The D log E curve based on the above data will be found in Figure 37 of the main body of the report.

14. **Characteristics of Photochromic Material No. 94** (Contrast vs. Exposure with Tungsten Light and Green Read Filter)

TABLE XLIV

Exposure Time in Seconds	Contrast	Base & D
20	$\frac{35}{.42}$ = 84:1 = 1.920	2.300
10	$\frac{35}{.52}$ = 68:1 = 1.830	2.210
5	$\frac{35}{.66}$ = 53:1 = 1.720	2.100
3	$\frac{35}{1.32}$ = 26.5:1 = 1.420	1.800
2	$\frac{35}{2}$ = 17.5:1 = 1.240	1.620
1	$\frac{35}{4}$ = 8.75:1 = 0.940	1.320
.50	$\frac{35}{8.5}$ = 4.13:1 = 0.615	0.995
.20	$\frac{35}{16}$ = 2.19:1 = 0.340	0.720
.10	$\frac{35}{24}$ = 1.46:1 = 0.165	0.545
.04	$\frac{35}{29}$ = 1.20:1 = 0.079	0.459

Figure 175.

(Base Density = $\frac{30}{12.5}$ = 2.4:1 = 0.38)

NOTE: The D log E curve based on the above data will be found in Figure 37 of the main body of the report.

APPENDIX XIII
EXPERIMENTAL INVESTIGATION OF FATIGUE IN NON-CAPSULAR PHOTOCHROMIC COATINGS

The experimental set-up for the fatigue measurements is shown in Figure 176 and the data obtained in Table XLV. The data is qualitative rather than quantitative because of a visual estimate for the end-of-useful-life deter-mination, but it does offer a means for rapid evaluation of samples. The continuous track insures that a few hundred spot diameters are exposed, giving a better average estimate of the expected life. With certain modifications, the equipment should be able to produce quantitative results as well.

The only erasing feature in the device is the same illumination that is used for viewing. For most samples, it was found that erasure occurred before the writing spot had completed a traversal of the ellipse. A degradation of the part of the visual field not being traversed by the writing spot was noted (hereinafter called visual fatigue) after prolonged exposure of the sample to the intense viewing beam. The field at the photochromic sample was about 60-mils in diameter. Visual fatigue was determined by slight displacement of the photochromic slide and exposing the complete field (easily accomplished by removing the dichroic filter). The area of the field which had been under continuous illumin-ation (500-600 millimicrons) for a period of hours was observed to write to a lower density than the fresh material which had been inserted into part of the field. Introduction of a green filter over part of the field was found to decrease the visual fatiguing appreciably in that part of the field. The visual fatigue is most certainly much less severe than the effect due to U.V. exposure.

442
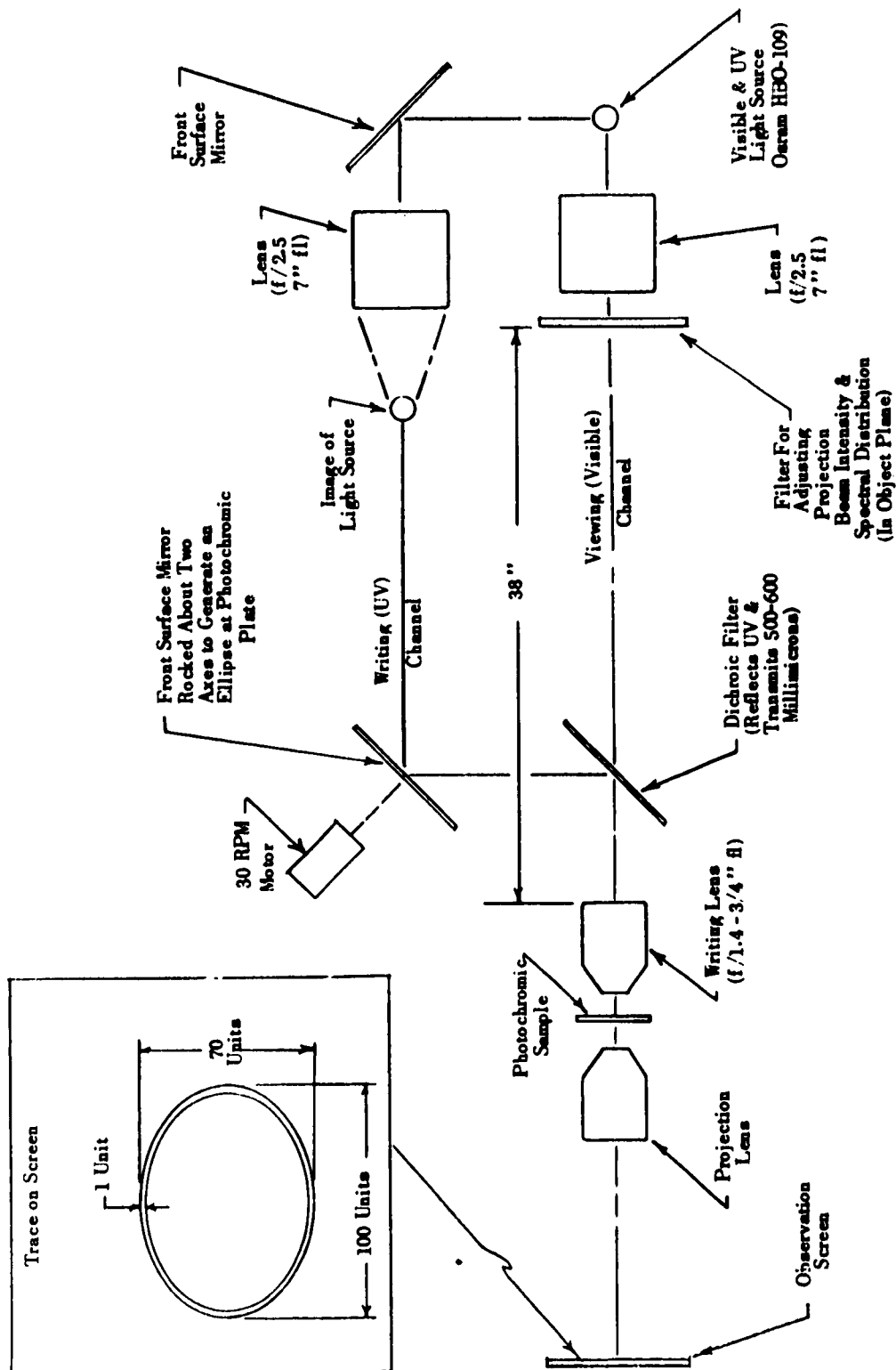
Figure 176. Fatigue Measuring Equipment.

443

TABLE XLV

SOLID SOLUTION FATIGUE DATA

Slide No.	Life (in region being switched visually determined)			Approximate Time to Erase Seconds *	Comments **
	Cycles	Hours	Min.		
94	10,000	6	10	> 2	Good contrast. Tends to be heat erasable only. Slight visual fatigue.
P-105	1,800	1	00	0.1 - 0.2	Average contrast. Appreciable visual fatigue.
H-61	1,800	1	00	0.5	Good contrast. Burning in of track noted at 25 minutes. Slight visual fatigue.
P-123	1,350	0	45	0.2	Average contrast. Slight visual fatigue.
P-120	1,050	0	38	0.4	Good contrast. Burning in of track apparent in 6 minutes. Heavy visual fatigue in yellow, but only slight in green filter region.

* Estimated from length of trace and known ellipse traversal time (2 seconds).

** Visual fatigue determined at end of test period for each sample.

APPENDIX XIV

THE LASER - A LIGHT SOURCE CAPABLE OF
EXTREME POWER DENSITIES

A. INTRODUCTION

The optical MASER, or LASER, has been announced only very recently
as a realizable device in the laboratory. This device, because of the
electromagnetic coherency of its output, can be used to create minute
spots of light with many orders of magnitude greater power densities
than ever before achieved. Thus, the LASER appears potentially capable
of switching photochromic materials orders of magnitude faster (in an
operating system) than the other light sources discussed in this report.

At the present time, LASERS with a potential for continuous operation,
or at least a high duty cycle (~50 percent), and the proper spectral dis-
tribution for a photochromic memory, have not been announced. However,
the implications of a LASER-photochromic system are such that it was
deemed important to at least review the LASER in this final report and
estimate the order of improvement possible in a photochromic memory
through the use of such a light source. The purpose of this appendix
is to provide a fundamental understanding of LASER operation for the
reader who is not familiar with quantum theory. Mathematical and
physical rigor have been sacrificed for greater clarity. Although the
examples contain exaggerations and over-simplifications, the general
conclusions reached are essentially correct. In order to establish a
basis for comparison, a brief treatment of non-coherent illumination
precedes the discussion of coherent illumination and LASER theory.

1. **Incoherent Light Sources**

The radiation emitted by conventional light sources is primarily due to the spontaneous emission of photons from atoms in excited states. Since these occurrences are entirely random, the instantaneous amplitude of the output is also random. If "a" is the amplitude of one atomic "oscillator" and there are "n" oscillators present, the instantaneous amplitude varies as follows:

$$0 \leq |A| \leq na \tag{1}$$

Thus, the instantaneous phases could be such that the net amplitude is zero, or possibly all oscillators could be exactly in phase resulting in a maximum amplitude "na." In general, however, the magnitude of the resultant amplitude "A" will lie somewhere between these limits. The intensity is proportional to the square of the amplitude, and it can be shown that for an array of "n" oscillators radiating with randomly varying phase, the resultant average intensity is given by

$$I_{av} = na^2 \tag{2}$$

Conventional light sources are referred to as incoherent sources. It is well known that the power density obtainable in the image of an incoherent source cannot exceed the power density of the source (see Appendix VIII). The commonly used terms "brightness" or "luminance" refer to the power density of the source per unit solid angle (steradian). A source which radiates in all directions in space radiates over a solid angle of 4π steradians.

The super-pressure mercury arc is amongst the brightest known lamps. It radiates energy in the ultraviolet, visible, and infrared regions. Its over-all brightness is several thousand watts per square centimeter per steradian. Ordinarily, one is interested only in a small part of the output spectrum, so that the "useful" brightness can be much less than 1,000 watts/cm^2-ster. If one is interested only in a very narrow portion of the spectrum, this limitation becomes severe.

446

2. Coherent Light Sources

An electromagnetically coherent light source would be one in which the atomic "oscillators" radiated in phase. If this were possible, the output intensity would be:

$$I = n^2 a^2 \qquad (3)$$

Comparing this intensity with the intensity of an incoherent source, we find that

$$\frac{I \text{ (coherent)}}{I \text{ (incoherent)}} = \frac{n^2 a^2}{n\, a^2} = n \qquad (4)$$

Thus, if it were possible to achieve <u>complete coherence</u> of all atomic oscillators present, the increase in intensity would be a factor equal to the number of atoms present!!

The LASER is a device in which atoms in an excited state are stimulated to give up their energy by emitting photons that are in phase with the incoming radiation. By using a "cavity" from which only a limited number of modes are emitted, a fairly plane, monochromatic wave is obtained. These "plane" waves can be focused into a very small spot (the order of a wave-length) thus resulting in enormous power densities.

The word "LASER" is an acronym for "Light Amplification by Stimulated Emission of Radiation." As a light source, we would be primarily interested in using this device as an oscillator rather than an amplifier.

447

B.   THE LASER

1.   Quantum Concepts

The theory contained in this section will be kept to a bare minimum and is intended to help the reader not familiar with quantum theory to appreciate the basic phenomena involved in LASER action.

In contrast to the continuous range of energies allowed by classical mechanics, the atom contains discrete energy levels in which bound electrons may exist.   The number of electrons which may exist in an uncharged atom is determined by the net nuclear charge.   Sodium, for example, has a net nuclear charge of +11 and therefore contains 11 bound electrons when uncharged.   For a given nuclear charge, when the bound electrons fill the lowest energy levels, the atom is said to be in the ground state.

The instantaneous locations of the bound electrons determine the instantaneous energy state of the atom.   For convenience, the magnitudes of the allowed energy states can be shown graphically on energy level diagrams.   An isolated atom contains sharply defined discrete energy levels which are represented by horizontal lines on the energy level diagram.   An energy level diagram of an arbitrary, hypothetical isolated atom might look something like the diagram in Figure 177.

$$E_4 \quad \rule{8em}{0.4pt}$$

$$E_3 \quad \rule{8em}{0.4pt}$$

$$E_2 \quad \rule{6em}{0.4pt}$$

$$E_1 \quad \rule{7em}{0.4pt}$$
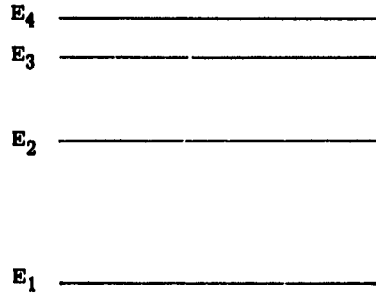
Figure 177. Energy Level Diagram of a
Hypothetical Isolated Atom.

In a solid, atoms are closely spaced and individual energy levels are affected by interaction with neighboring atoms. For the solid state LASER, we are concerned with substitutional impurities in single crystal lattices. If any of the energy levels of the impurity atom are close to an energy level of the host atoms, broadening of these levels will occur. In general, we are interested in crystals in which the upper energy states of the impurity atoms are broadened, while the lower energy states remain fairly sharp. The reason for this requirement will subsequently become clear. A hypothetical example of this type of energy level diagram is shown in Figure 178 showing the broadening of levels 3 and 4.
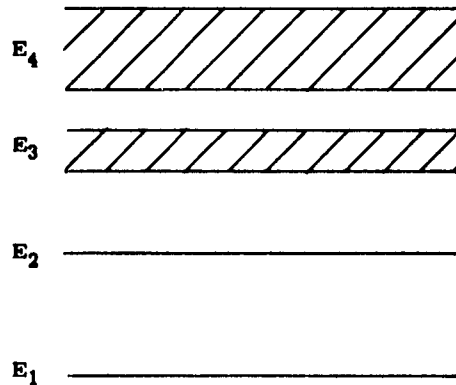
Figure 178. Energy Level Diagram of a
Hypothetical Impurity Atom.

449

Radiant energy exists in discrete quanta called "photons" or "wave
packets." The energy of a photon is given by the following equation:

$$E = h\nu \qquad (5)$$

where ν = frequency of the radiation
         h = Planck's constant = 6.6252×10^{-34} joule-sec.

There are three important processes involved in the interaction of
radiation and matter. These processes will be explained by consider-
ing two particular energy levels of an isolated, hypothetical atom.

Consider an atom in the ground state E_1 and an incoming photon in
close proximity to the atom. If the energy $h\nu$ of the photon is exactly
equal to the energy difference between energy states E_1 and E_2, the
photon may be absorbed by the atom, exciting it to energy state E_2
(see Figure 179-a). The probability of this happening is a function of
the Einstein "B_{12}" coefficient. The subscripts of the "B" coefficient
refer to the initial and terminal states.

An atom in state E_2 may spontaneously drop to energy state E_1 thereby
emitting a photon of energy $h\nu$ exactly equal to the energy difference
$E_2 - E_1$ (see Figure 179-b). This process is called spontaneous
emission and its probability of occurrence is a function of the Einstein
"A" coefficient.

A process much less well known but extremely important in LASER
action is that of stimulated emission, illustrated in Figure 179-c.
In contrast to the process of absorption, an incoming photon whose
energy $h\nu$ is exactly $E_2 - E_1$ may cause an atomic transition from the
upper state E_2 to the lower state E_1 thereby emitting a second photon.
Since the energy of the second photon is exactly equal to that of the in-
coming photon, their frequencies are exactly equal. Even more impor-
tant is the fact that the two photons are "coherent," i.e., in phase.

450

E_2 ———— ·— —(⌀)—·— · ——————

$h\nu_{12}$ 〜〜〜 "B_{12}" $\left[\dfrac{\text{Transitions}}{\text{Second-Atom-Photon Density}} \right]$

E_1 ———— —◉— — —————

(a) Absorption

E_2 ———— ·—◉— —·— · ——————

$h\nu_{12}$ "A" $\left[\dfrac{\text{Transitions}}{\text{Second - Atom}} \right]$

E_1 ———— ·—(⌀)— —·— · ——————

(b) Spontaneous Emission

E_2 ———— ·—◉— —·— · ——————

$h\nu_{12}$ 〜〜〜〜〜〜 ←→ Photons in Phase "B_{21}" $\left[\dfrac{\text{Transitions}}{\text{Second-Atom - Photon Density}} \right]$

E_1 ———— ·—(⌀)— —·— · ——————

(c) Stimulated Emission
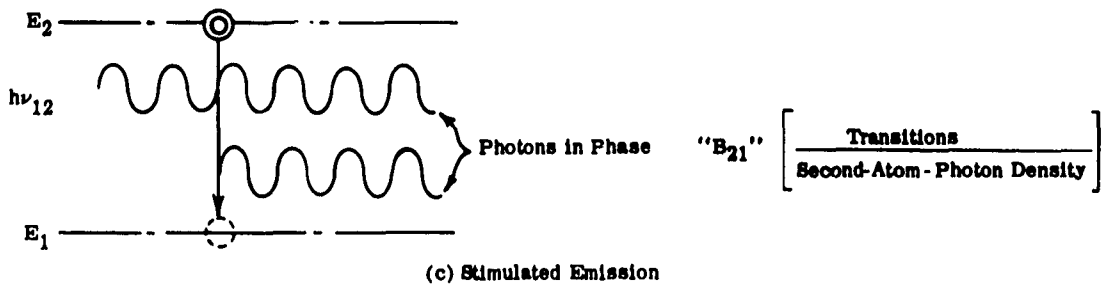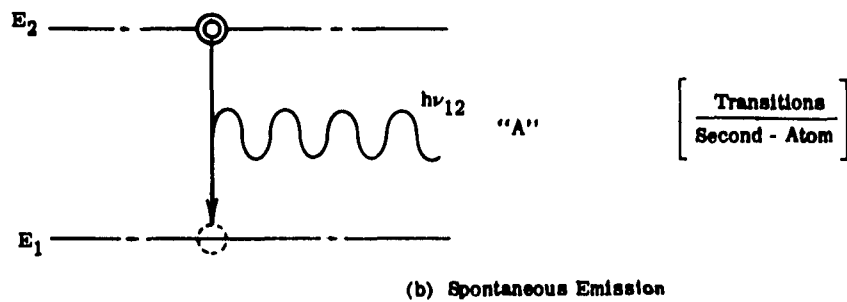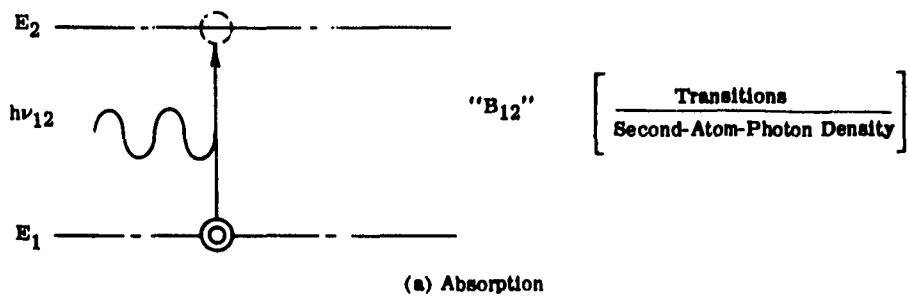
$B_{12} = B_{21}$

Figure 179. Atom - Photon Interactions.

451

The probability of stimulated emission is a function of the Einstein B_{21} coefficient. This coefficient is exactly equal to the B_{12} coefficient pertaining to the absorption probability. The actual probabilities, however, are not equal due to differences in energy level population densities. Ordinarily, the stimulated emission probabilities are so low that the process is negligible. This will be explained in more detail in the next section.

2. Statistics

A substance in thermal equilibrium has its atoms distributed in the various allowed energy states. If only discrete quantum states are allowed, the ratio of the number of atoms in any given state to the number in the ground state is given by the simplified Boltzmann distribution

$$\frac{N_j}{N_1} = e^{-\frac{E_j - E_1}{kT}} \qquad (6)$$

where

N_1 = number of atoms in the ground state E_1

N_j = number of atoms in energy state E_j

k = Boltzmann's constant = 1.38×10^{-23} joules/oK

T = absolute temperature

Close examination of the Boltzmann distribution reveals the following:

a) The ground state has the largest population.

b) The higher energy states have progressively smaller populations.

c) As "T" approaches zero, N_j approaches zero. This indicates that relative depopulation of the upper energy states can be accomplished by cooling.

452

3. Requirements for LASER Action

Let us consider a hypothetical assembly of "N" atoms and examine the conditions for which the process of stimulated emission predominates.

Let the number of atoms in energy states E_1 and E_2 be N_1 and N_2 respectively, and consider an incoming radiation density "p".

$$N_1 B_{12} \rho = \text{absorptions per second} \tag{7a, b, c}$$

$$N_2 A_{21} = \text{spontaneous emissions per second}$$

$$N_2 B_{21} \rho = \text{stimulated emissions per second}$$

We require that the ratio of stimulated emission to both spontaneous emission and absorption be greater than one. Recalling that $B_{21} = B_{12}$, the following two expressions result:

$$\frac{\text{Stimulated Emission}}{\text{Spontaneous Emission}} : \quad \frac{B_{21}}{A_{21}} \rho \gg 1 \tag{8}$$

$$\frac{\text{Stimulated Emission}}{\text{Absorption}} : \quad \frac{N_2}{N_1} \gg 1 \tag{9}$$

The requirement given by equation (8) is less easily met at optical frequencies than at microwave frequencies. This is due to the B/A ratio ordinarily being a function of the cube of the wavelength. However, there are a great many materials (such as those exhibiting fluorescence) for which the "A" coefficient is very small, thereby meeting the requirement of equation (8).

Ordinarily, for a substance in thermal equilibrium, the ratio N_2/N_1 is many orders of magnitude less than one. Thus, to meet the requirement given by equation (9), the normal population densities must somehow be inverted, so that the upper energy levels are more densely populated

ASD TR 61-70

than the lower energy levels. The process by which this is accomplished is called "pumping" and will be discussed later.

If the requirement of equation (9) is met, we may speak of the substance as having a "negative temperature." This arises directly from the Boltzmann distribution. Solving equation (6) for "T" and letting $j = 2$, we find

$$T = - \frac{E_2 - E_1}{k \log_e \frac{N_2}{N_1}} \tag{10}$$

For $N_2 > N_1$, T is negative. Note also that when $N_2 = N_1$, the temperature is infinite.

4. **Pumping**

The examples given in this section are grossly over simplified. Technicalities have been avoided so that the basic concepts will not be obscured.

Figure 180 illustrates pumping two discrete levels to saturation. Only incoming photons of energy $h\nu$ exactly equal to $E_2 - E_1$, which cause an interaction, are considered. Arbitrary populations of 6 and 12 were chosen for simplicity.

454

E_2 —OOOOOO——— — — — $\left[N_2 = 6 \right]$

E_1 —OOOOOOOOOOO—— — $\left[N_1 = 12 \right]$

(a) Equilibrium

E_2 —OOOOOOⒸⒸ—— — — — $\left[N_2=6 \right] \rightarrow \left[N_2=7 \right]$ —O-OOOOOO—— —

E_1 —ⒸOOOOOOOOOOOO— $\left[N_1=12 \right] \rightarrow \left[N_1=11 \right]$ —O-OOOOO-OOO-OOO—

(b) For 3 Incoming Photons $\nu_{12} = \dfrac{E_2 - E_1}{h}$

E_2 —OOOOOOⒸⒸⒸⒸ—— $\left[N_2 = 6 \right] \rightarrow \left[N_2 = 9 \right]$ —O-OOOOO-OOO—— —

E_1 —ⒸⒸⒸOOOOOOOOOOOO— $\left[N_1 = 12 \right] \rightarrow \left[N_1 = 9 \right]$ —O-OOOOO-OOOO— — —

(c) For 9 Incoming Photons
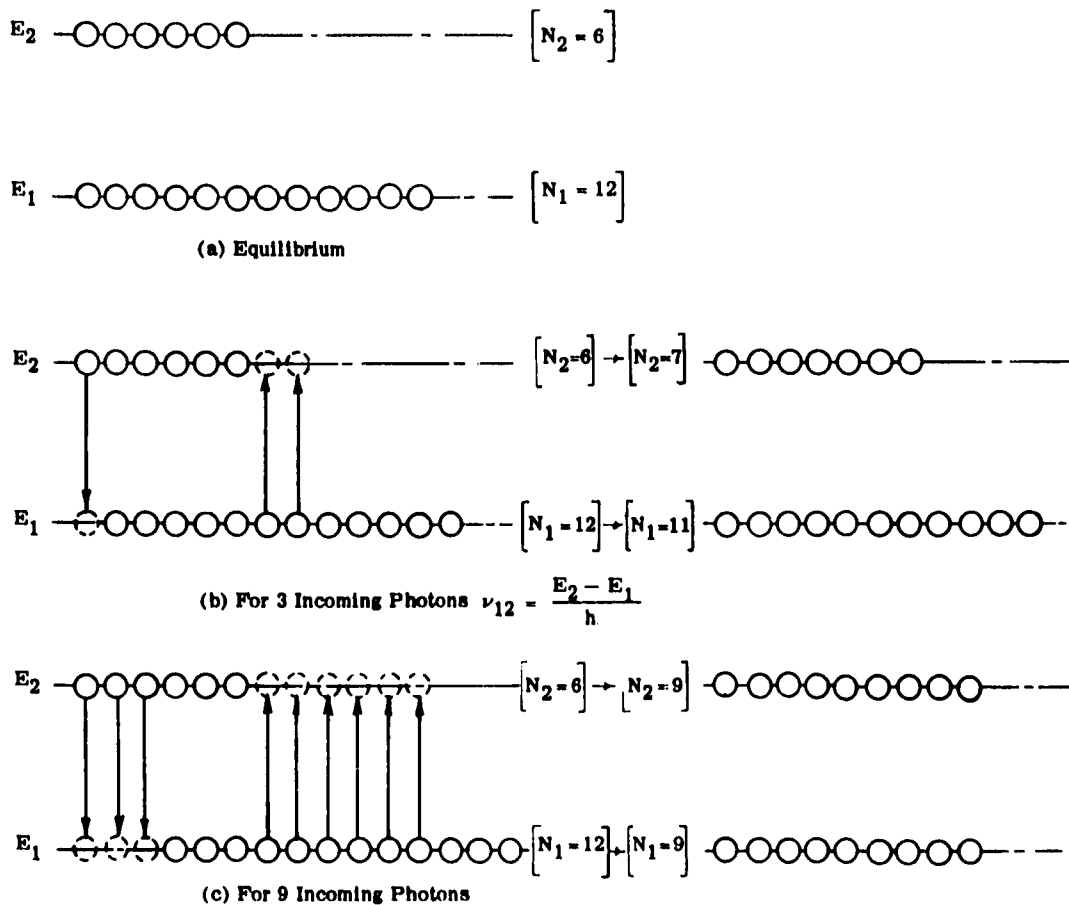
Figure 180. Two-Level Pumping.

The equilibrium distribution is shown in Figure 180 -a. Assuming that spontaneous emission may be neglected, the ratio of absorptions to stimulated emissions is simply N_1/N_2, which in this case equals 2 (eq. 9). Part (b) illustrates the net absorption of one interacting photon by two absorptions and one stimulated emission. Part (c) illustrates the effect for 9 incoming interacting photons. Six absorptions and three stimulated emissions occur, resulting in a net absorption of

455

ASD TR 61-70

three photons. The population densities are now equal and saturation is said to have occurred (T = ∞). (Actually, we could only approach saturation for this hypothetical example, since we have neglected spontaneous emission. Also, we have considered only the interacting photons, rather than the incoming radiation densities).

Pumped states are unstable and will return to equilibrium when the incoming radiation ceases. The decay time constant for return to equilibrium is a function of the "A" and "B" coefficients involved in the transition. This is illustrated in Figure 181.
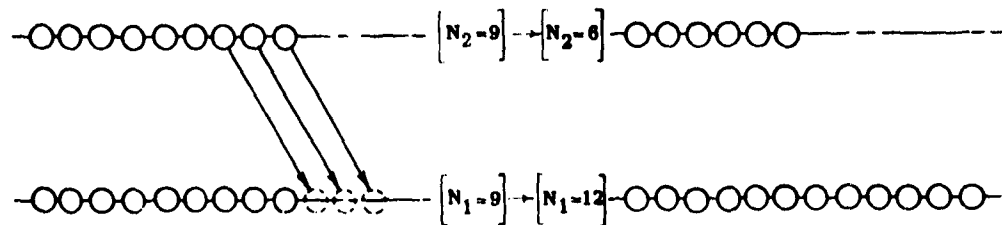
Figure 181. Decay to Equilibrium.

Population inversions can be obtained with multi-level devices. An example of a three-level device is shown in Figure 182. Atoms are pumped from state E_1 directly to state E_3. This requires photons of energy $h\nu_{13} = E_3 - E_1$. Materials are sought for which decay from E_3 to E_2 is rapid, while decay from either E_3 or E_2 to E_1 is slow. Thus, with atoms falling into state E_2 faster than they can return to state E_1, a surplus of atoms can be accumulated in state E_2 exceeding the number of atoms in state E_1.

456

E_3 —O—O———————— — ——— — —————— $\left[N_2 = 2\right]$

E_2 —O—O—O—O——————— ——— ———— $\left[N_2 = 4\right]$

E_1 —O—O—O—O—O—O—O—O—O———— — —— ——— $\left[N_1 = 9\right]$

(a) Equilibrium

—O—O———— OOOOOOOOOO ———————— $\left[N_3 = 2\right] \rightarrow \left[N_3 = 2\right]$

Rapid!

—O—O—O—O—————— OOOOOOOO — —— $\left[N_2 = 4\right] \rightarrow \left[N_2 = 11\right]$

Slow!

—O—O—O—O—O—O—O—O—O—— — —— $\left[N_1 = 9\right] \rightarrow \left[N_1 = 2\right]$

(b) Pumping with Photons $\nu_{13} = \dfrac{E_3 - E_1}{h}$

—O—O———— — ———— —— ———— $\left[N_3 = 2\right]$

—O—O—O—O—O—O—O—O—O—O—O—O———— — ———— $\left[N_2 = 11\right]$

—O—O———— — ———————— — —— $\left[N_1 = 2\right]$
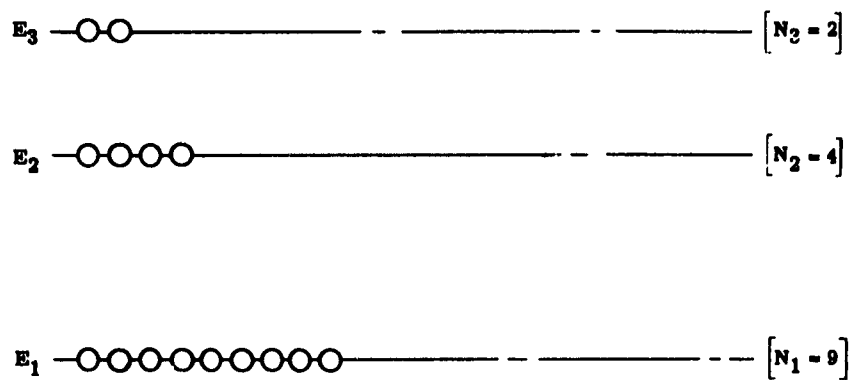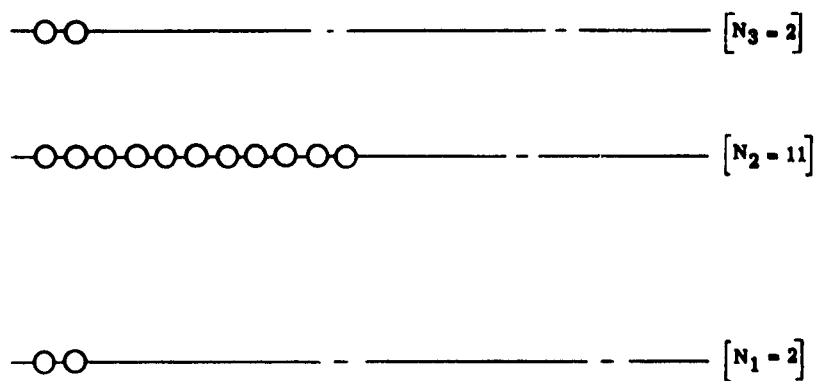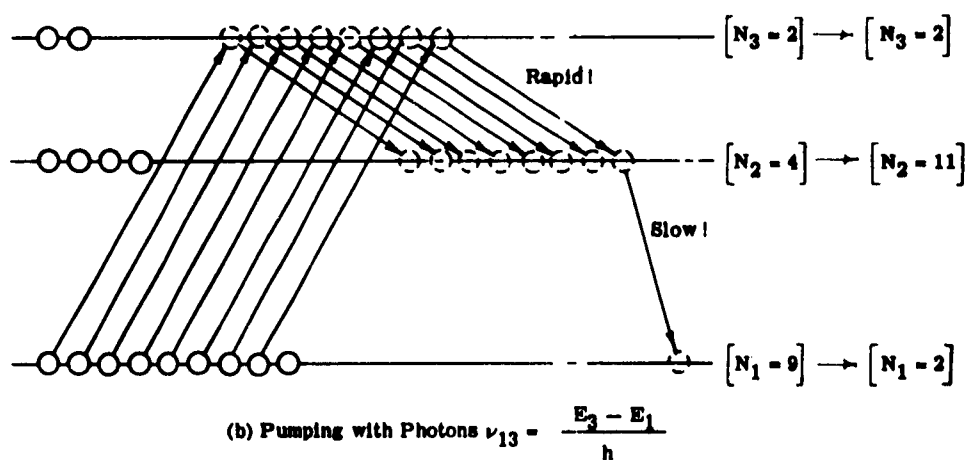
(c) Pumped $N_2 > N_1$

Figure 182. Three-Level Pumping.

5. Amplification by Stimulated Emission

Having created a population inversion by pumping with radiant energy of frequency V_{13}, it is now possible to achieve amplification of radiation of frequency $V_{12} = E_2 - E_{1/h}$. This process is illustrated by the hypothetical example shown in Figure 183.
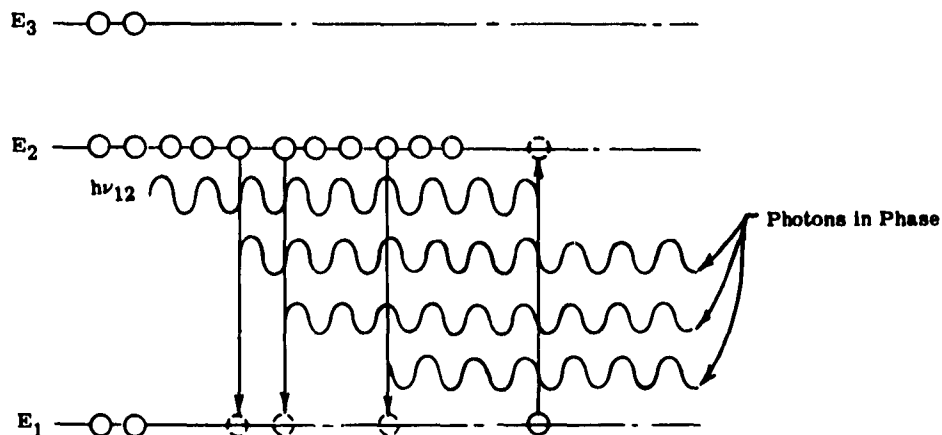
Figure 183. Stimulated Emission.

Each incoming photon of correct frequency V_{12} causes stimulated emission of other photons, which in turn cause other stimulated emissions. These photons add coherently, i. e., in phase. Photons are also absorbed occasionally as determined by the ratio N_1/N_2. Non-coherent, i. e., random phase, addition also occurs occasionally as determined by the ratio $A_{21}/B_{21}P$.

As stimulated amplification continues, depopulation of energy state E_2 occurs. Therefore, in order to achieve continuous stimulated amplification of radiation at a frequency of V_{12}, it is necessary to supply continuous pumping with energy at a frequency of V_{13}.

6. Experimental Devices

A LASER with only discrete energy levels would not be a very practical device, since a monochromatic source of frequency V_{13} would be

458

required for pumping. It is highly desirable to have level three considerably broadened so that pumping may be accomplished with broadband radiation.
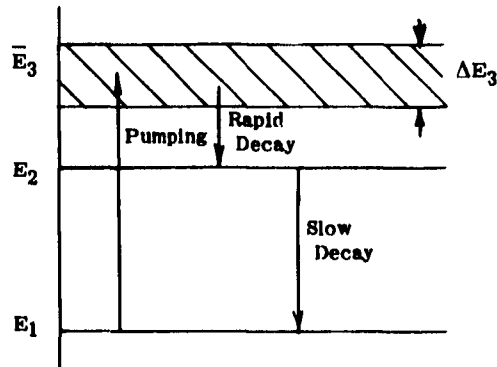
Figure 184. Hypothetical Three-Level Energy Diagram.

In the energy level diagram shown in Figure 184, levels one and two are discrete, while level three has been broadened. Pumping may be accomplished with energy throughout the following range:

$$(E_3 - \frac{\Delta E_3}{2}) - E_1 \leq h\nu \leq (E_3 + \frac{\Delta E_3}{2}) - E_1 \qquad (11)$$

The solid state LASER achieves energy levels as shown in Figure 184 by interaction of the impurity energy levels with those of the host crystal.

Energy levels similar to those in Figure 185 are found in Chromium doped, single crystal aluminum oxide, commonly known as a ruby. LASER action has been achieved in a ruby by both Hughes Aircraft and Bell Laboratories. At this writing, detailed data has not been made available to the public except through news releases to various publications. References are given at the end of this appendix.

LASER action in a ruby seems to have been obtained by "brute force." Pumping was accomplished with a flash tube wrapped around a ruby rod

459

whose silvered ends were very flat and parallel. The transition proba-
bilities of a ruby are such that approximately <u>one megawatt</u> of peak
pumping power was required to obtain approximately 10 kilowatts of peak
output power at 6943 A$^\circ$ with a coherence ratio of only four (coherence
defined as the ratio of stimulated emission to spontaneous emission).

It has been stated that the coherence ratio could be improved to approxi-
mately 100 by cooling with liquid nitrogen. Also, that the efficiency
could be increased from 1 to approximately 15 percent by improved
design. However, because of the high pumping power required, heating
will probably limit the ruby LASER to pulsed operation only. The pre-
sent repetition rate is limited to one pulse every 30 to 60 seconds.

A four level solid state LASER requiring 500 times less pumping power
than ruby has been built by I. B. M. The crystal used was uranium doped,
calcium fluoride. A simplified energy level diagram is shown in Figure 185.
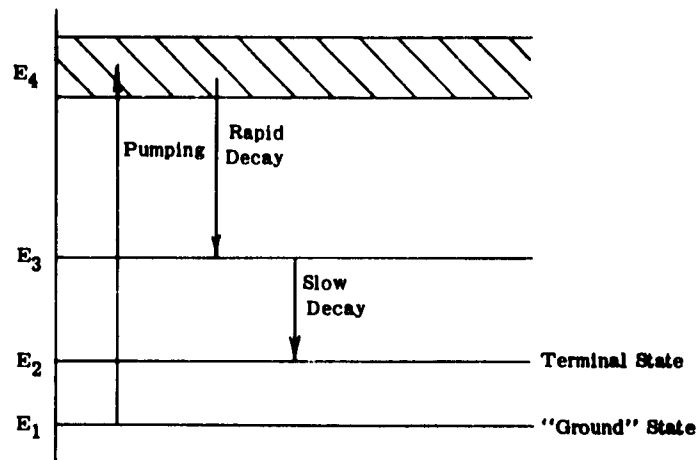
Figure 185. Hypothetical Four-Level Energy Diagram.

460

Atoms are pumped from the ground state E_1 to broadened state E_4. Rapid decay from E_4 to E_3 and slow decay from E_3 to E_2 (and E_1) makes possible a population inversion between states E_3 and E_2. For this device the terminal state is E_2 instead of the ground state E_1. Thus, since the highly populated ground state is not directly involved in the population inversion, much less pumping power is required. The stimulated emission output between states E_3 and E_2 is in the infrared at approximately 2.5 microns. A coherence ratio greater than 2000 was achieved. Doping of the calcium fluoride lattice with samarium instead of uranium results in an output frequency of approximately 0.7 microns (deep red).

Although this is also a pulsed device, the huge reduction of pumping power leaves little doubt that a continuously operating LASER will be developed in the near future.

C. APPLICATIONS

1. Coherent Light Sources

a) It has been estimated that the power output of the first operational continuous LASER will be approximately a few milliwatts. However, since this energy is in the form of a parallel beam, it can be focused into a tiny spot, resulting in enormous power densities. When focused into a spot approximately one micron in diameter, the resultant power density would be approximately 10^5 to 10^6 watts per square centimeter. Further developments will result in even more staggering values.

b) The use of monochromatic light sources will simplify lens design, in that there will be no chromatic aberration to correct.

2. Communications

a) Since the LASER will emit a narrow beam with very little diver-
gence, it can be used for the long distance transmission of informa-
tion at low power levels.

b) Communications from space vehicles could be limited to small
areas on the earth's surface, thus remaining undetected at all
other points on earth.

c) By using a direction detector to receive the highly directional
beam, jamming would be impossible.

d) The present communications spectrum could be extended from
approximately 200 kilomegacycles to approximately 500,000
kilomegacycles.

3. High Resolution Radar

Since the resolution of a radar system is ultimately limited by the wave-
length used, a 10,000 fold increase in resolution is possible by using
optical frequencies.

4. Spatial Filtering

An almost parallel beam of monochromatic light which could be focused
into a spot the order of one wavelength would contribute much to spatial
filtering techniques.

D. CONCLUSIONS

1) Pulsed LASER action has been demonstrated in various solid state
devices (Al_2O_3:Cr; CaF_2:U; and CaF_2:Sm).

462

2) Continuous LASER action is predicted for the near future. The estimated output of the first continuously operating LASER has been estimated at a few milliwatts. When focused into a spot the order of one wavelength, the resultant power density would be 10^5 to 10^6 watts per square centimeter.

3) Spatial coherence has been proven by means of a double slit interference experiment with a ruby $(Al_2O_3:Cr)$ LASER.

4) A large number of active media are possible:

    a) single crystals
    b) metal vapors
    c) inert gases
    d) possibly liquids

5) Biological effects are unknown, although it seems very likely that the parallel beam could cause blindness.

ASD TR 61-70

E. BIBLIOGRAPHY

1. Papers, Semi-Technical

H. E. D. Scovil, "The Three-Level Solid-State Maser," Bell Labs Record, page 243 (July 1958).

George E. Pake, "Magnetic Resonance," Scientific American, page 58 (Aug. 1958).

James P. Gordon, "The Maser," Scientific American, page 42 (Dec. 1958).

M. Brotherton, "Amplifying with Atoms," Bell Labs Record, page 163 (May 1960).

Arnold L. Bloom, "Optical Pumping." Scientific American, page 72 (Oct. 1960).

A. L. Schawlaw and C. H. Townes, "Infrared and Optical Masers," Bell Labs Record, page 403 (Nov. 1960).

2. Papers, Technical

J. P. Gordon, H. J. Zeiger, and C. H. Townes, "The Maser - New Type of Microwave Amplifier, Frequency Standard and Spectrometer," Physical Review, 99, 1264 (1955).

James P. Wittke, "Molecular Amplification and Generation of Micro-waves," Proc. I. R. E. 45, 291 (1957).

H. E. D. Scovil, "The Three-Level Solid-State Maser," I. R. E. Trans. MTT-6, 29 (1958).

A. L. Schawlaw and C. H. Townes, "Infrared and Optical Masers," Physical Review, 29, 1940 (1958).

R. D. Haun Jr. and T. A. Osial, "Low-Noise, Solid-State Microwave Amplifiers," Electrical Manufacturing, page 139 (Oct. 1959).

D. J. Howarth, "Physics of the Solid State Maser," I. R. E. Trans. CP-6, 81 (1959).

P. P. Sorokin and M. J. Stevenson, "Stimulated Infrared Emission from Trivalent Uranium," Physical Review Letters, 5, 557 (1960).

464

Collins, et al, "Coherence, Narrowing, Directionality and Relaxation Oscillations in the Light Emission from Ruby," Physical Review Letters, 5, 303 (1960).

T. H. Maiman, "Optical and Microwave-Optical Experiments in Ruby," Physical Review Letters, 4, 564 (1960).

3. Books

J. R. Singer, Masers, John Wiley & Sons (1959).

C. H. Townes (Editor), Quantum Electronics (A Symposium) Columbia University Press (1960).

4. News Articles

"Optical Maser Held Working at Hughes," Electronic News, July 11, 1960.

"Synthetic Ruby Does New Tricks with Light," Business Week, page 102, July 14, 1960.

"Space Coherence Aim in Optical Maser R & D," Electronic News, page 6, July 18, 1960.

"Optical Maser May Aid Space Avionics," Aviation Week, page 96 July 18, 1960.

"Optical Maser Developed by Hughes Gives 10-KW Coherent Light Output," Electronic Design, July 20, 1960.

"Light Amplifier Extends Spectrum," Electronics, page 43, July 22, 1960.

"Optical Maser Research Programs Nearing Success," Electronic Design, page 14, Aug. 3, 1960.

"BTL Flashed Laser Beam for 23 Miles," Electronic News, Oct. 10, 1960.

"Optics Gets Space Age Cue From Electronics," Business Week, page 144, Oct. 22, 1960.

465

"Optical Maser's Space Potential Probed," <u>Aviation Week</u>, page 75 Oct. 24, 1960.

"Pulsed Ruby Optical Maser," <u>Western Electronic News</u>, page 41, Dec. 1960.

"IBM Sees Laser Closer to Continuous Operation," <u>Electronic News</u>, page 14, Dec. 19, 1960.

466

BIBLIOGRAPHY ON OPTICAL INFORMATION THEORY
WITH SPECIAL REFERENCE TO
OPTICAL SPATIAL FILTERING

(1)   Blanc-Lapierre, A., "Upon Some Analogies Between Optics and
        Information Theory." Symposium on Microwave Optics, McGill
        University, Montreal, Canada, June 1953.

(2)   Cheatham, T. P., Jr., and Kohlenberg, A., "Analysis and
        Synthesis of Optical Systems." Technical Report No. 84,
        Physical Research Laboratory, Boston University, 1952.

(3)   Cutrona, L. J., Leith, E. N., and Porcello, L. J., "Coherent
        Optical Data Processing." 1959 IRE WESCON CONVENTION RECORD,
        Part 4, pp. 141-153.

(4)   Cheatham, T. P., Jr., and Kohlenberg, A., "Optical Filters -
        Their Equivalence to and Difference from Electrical Networks."
        1954 IRE CONVENTION RECORD, part 4, "Electronic Computers
        and Information Theory," pp 6-12.

(5)   Duffieux, P. M., "L'Integrale de Fourier et ses Applications a
        l'Optique." Besancon, Faculte des Sciences, 1946.

(6)   Elias, P., Grey, D. S., and Robinson, Z., "Fourier Treatment
        of Optical Processes." Journal of the Optical Society of America,
        Vol. 42 (February 1952), pp. 127-134.

(7)   Elias, P., "Optics and Communication Theory." Journal of the
        Optical Society of America, Vol. 43 (April 1953), p. 229.

(8)   Gabor, D., "Microscopy by Reconstructed Wave Fronts."

Proceedings of the Royal Society (London) 1949, p. 454.

(9)   Gabor, D., " Lectures on Communication Theory." Technical Report
        No. 238, Research Laboratory of Electronics, Massachusetts Institute
        of Technology, April 1952.

(10)   Goldman, S., Information Theory. New York, Prentice-Hall, 1953.

(11)   Hopkins, H. H., " The Concept of Partial Coherence in Optics."
        Proceedings of the Royal Society A, Vol. 208 (1951), pp. 263-277.

(12)   Hopkins, H. H., " On the Diffraction Theory of Optical Images."
        Proceedings of the Royal Society A, Vol. 217 (1953), pp. 408-432.

(13)   Jacquinot, P., Boughton, P., and Dossier, B. Contributions in La
        Theorie des Images Optiques. Paris, Editions de la Revue d'Optique,
        1949, p. 183.

(14)   Kovasznay, S. G., and Joseph, H. M., "Image Processing."
        Proceedings of the IRE, Vol. 43 (May 1955), pp. 560-570.

(15)   Linfoot, E. H., and Fellgett, P. B., "On the Assessment of Optical
        Images." Royal Society of London Philosophical Transactions, Series A,
        Vol. 247, p. 931.

(16)   Lundberg, R. K., Mathematical Theory of Optics. Providence, R. I.,
        Brown University, 1944.

(17)   Macdonald, D. E., "Air Photography." Journal of the Optical Society
        of America . Vol. 43 (April 1953), p. 290.

(18)   Macdonald, D. E., "Quality Aspects of the Aerial Photographic
        System." National Bureau of Standards Circular 526, Proceedings
        of the N. B. S. Semicentennial Symposium on Optical Image
        Evaluations, 1951.

(19) Mar'echal, A., "The Contrast of Optical Images and the Influence of Aberrations." National Bureau of Standards Circular 526, Proceedings of the N. B. S. Semicentennial Symposium on Optical Image Evaluations, 1951.

(20) Mar'echal, A., and Croce, P., "Un Filtre de Frequences Spatiales pour l' Amelioration du Contraste des Images Optiques." Comptes Rendus de Academic des Sciences, Vol. 237 (September 1953), pp. 607-609.

(21) O'Neill, E. L., "The Modulation Function in Optics." Ph. D. Thesis, Department of Physics, Boston University, 1954.

(22) O'Neill, E. L., "The Analysis and Synthesis of Linear Coherent and Incoherent Optical Systems." Technical Note 122, Boston University, Physical Research Laboratory, September 1955.

(23) O'Neill, E. L., "Transfer Function for an Annular Aperature." Journal of the Optical Society of America, Vol. 46 (1956), p. 285.

(24) O'Neill, E. L., "Spatial Filtering in Optics." IRE Transactions of the Professional Group on Information Theory, I T-2, No. 2, June, 1956.

(25) Osterberg, H., and Wilkins, J. E., Jr., "The Resolving Power of a coated Objective." Journal of the Optical Society of America, Vol. 39 (1949), p. 553.

(26) Page, C. H., "Application of the Fourier Integral in Physical Science." IRE Transactions of the Professional Group on Circuit Theory CT-2, No. 3, September 1955, pp. 231-237.

(27) Porter, A. B., "On the Diffraction Theory of Microscopic Vision." Philosophical Magazine, Vol. 11 (1906), p. 154

(28) Rhodes, J. E., Jr., "Analysis and Synthesis of Optical Images." American Journal of Physics, Vol. 21 (May 1953), pp. 5 and 337.

469

(29)   Rhodes, J. E., Jr., " Microscope Imagery as Carrier Communication. "
         Journal of the Optical Society of America, Vol. 43 (October 1953), p. 848.

(30)   Schade, O. H., " Electro-Optical Characteristics of Television Systems. "
         RCA Review, Vol. 9, Nos. 1, 2, 3, and 4 (1948).

(31)   Selwyn, E. W. H., " Theory of Resolving Power. " National Bureau of
         Standards Circular 526, Proceedings of N. B. S. Semicentennial
         Symposium on Optical Image Evaluation, 1951.

(32)   Steel, W. H., " Etude des Effects Combines des Aberrations et d'une
         Obturation Centrale de la Pupille Sur le Contraste des Images Optiques. "
         Revue d'Optique, Vol. 32 (1953), pp. 4-26, 143-178, 269-306.

(33)   Strong, J., Concepts of Classical Optics. San Francisco, W. H. Freeman
         Co., 1958, Appendix F.

(34)   Wood, R. W., Physical Optics. Third Edition. New York, The MacMillan
         Co., 1934, Chapter VII.

470

CATHODE-RAY TUBE EVALUATION - EXPERIMENTAL DATA

A.   TEST DATA SHEETS I THROUGH IV

1.   Test Data Sheet I (5 µsec. pulses)

Average Beam Current, µ amps.	Rep. Rate, cps.	Duty Cycle	Galva. Deflec., cms	Peak Beam Current, ma	Remarks
6	2000	100:1	0.75	0.6	Thermopile to
11	3000	67:1	1.25	0.73	tube face distance
16.5	5000	40:1	2.1	0.66	= 4.0625 inches.
27	8000	25:1	3.5	0.675	
35	10,000	20:1	4.1	0.7	CRT spot size
54	15,000	13:1	6.0	0.7	= 0.375 inch dia.
72	20,000	10:1	7.9	0.72	Focus coil in the
92	25,000	8:1	10.5	0.73	forward position.
112	30,000	6.6:1	12.75	0.74	5ZP16 tube
130	35,000	5.5:1	15.25	0.715	with pulse duration
149	40,000	5:1	17.25	0.74	of 5 µsecs.
154	41,000	4.5:1	18.0	0.7	

ASD TR 61-70

2. Test Data Sheet II (15 µsec. pulses)

Average Beam Current, µamps.	Rep. Rate, cps.	Duty Cycle	Galva. Deflec., cms	Peak Beam Current, ma	Remarks
22	2000	33:1	2.4	0.725	Thermopile to
28	2500	28:1	2.9	0.785	tube face = 4.0625 inches
34	3000	22:1	3.4	0.748	CRT Spot size =
47	4000	16..7:1	4.6	0.785	0.375 inch dia.
59	5000	13.3:1	6.1	0.785	Focus coil in the
72	6000	11:1	7.4	0.792	forward position
98	8000	8.3:1	11.0	0.812	5ZP16 tube with
123	10,000	6.7:1	13.5	0.825	pulse duration of 15 µsecs.
145	12,000	5.5:1	16.0	0.798	
175	15,000	4.5:1	19.0	0.785	

472

3. <u>Test Data Sheet III (50 μsec. pulses)</u>

Average Beam Current, μamps.	Rep. Rate, cps.	Duty Cycle	Galva. Deflec., cms.	Peak Beam Current, ma	Remarks
8	300	66:1	1.2	0.53	Thermopile to tube face = 4.0625 inches.
12	400	50:1	1.6	0.6	
19	600	33:1	2.2	0.627	CRT Spot size = 0.375 inch dia.
32	1,000	20:1	4.0	0.64	
50	1,500	13:1	5.5	0.65	Focus coil in the forward position.
67	2,000	10:1	7.25	0.67	
84	2,500	8:1	8.75	0.67	5ZP16 tube with pulse duration of
105	3,000	6.6:1	11.25	0.69	50 μsecs.
137	4,000	5:1	14.0	0.685	
154	4,600	4.4:1	16.5	0.68	

473

4. <u>Test Data Sheet IV (5 μsec. pulses)</u>

Average Beam Current, μamps	Rep. Rate, cps.	Duty Cycle	Galva. Deflec., cms.	Peak Beam Current, ma	Remarks
10	700	286:1	1.2	2.86	Thermopile to tube face = 4.0625 inches
14	1,000	200:1	1.7	2.8	CRT Spot Size = 0.375 inch dia. spreading
28	2,000	100:1	3.4	2.8	slightly at higher average beam currents.
35	2,500	80:1	4.2	2.8	
42	3,000	66:1	5.0	2.78	Focus coil in rear position (Per max peak beam current).
60	4,000	50:1	7.0	3.00	
75	5,000	40:1	8.6	3.00	5ZP16 tube with pulse duration of 5 μsecs.
91	6,000	33:1	10.3	3.00	
126	8,000	25:1	14.5	3.16	
144	9,100	22:1	16.75	3.16	

474

B. CALCULATION SHEETS I THROUGH IX

1. Calculation Sheet I

Analysis of 5 µsec. Pulse in Test Data Sheet I

A typical mid-range value selected from Test Data Sheet I provides
the following necessary data:

1) Rep Rate = 20,000 cps

2) Pulse Duration = 5×10^{-6} secs.

3) Spot Size = 0.712 cm^2 in area

4) Ultor Volts = 27×10^3

5) Galvo Deflection = 7.9 cms

6) Peak Beam Current = 0.72 ma

7) Thermopile to CRT Face = 4.0625 inches

Thermopile/Galvo Calibration: 0.118 Cms Deflection = 1 µwatt/cm^2
Energy Density

Hence, Energy Density at Thermopile $= \dfrac{7.9}{0.118}$ = 67 µwatts/cm^2

Area of Radiation $= 2\pi \times (4.0625)^2 \times 6.45$ = 670 cm^2

Total Average Energy $= 67 \times 670$ = 44,800 µwatts

Average Brightness $= \dfrac{44.8 \times 10^3}{0.712}$ = 63 $\times 10^3$ µwatts/cm^2

Radiant Energy Density per Pulse $= \dfrac{63 \times 10^3}{20,000}$ = 3.14 µwatt-secs/cm^2

Radiant Energy per Pulse $= 3.14 \times 0.712$ = 2.2 µwatt-secs.

Electric Input Power per Pulse $= (27 \times 10^3) \times (0.72 \times 10^{-3}) \times (5 \times 10^{-6})$ = 97.3 µwatt-secs.

Input Energy Density $= \dfrac{97.3}{.712}$ = 114 µwatt-secs/cm^2

Phosphor Efficiency $= \dfrac{2.22}{97.3} \times 100$ = 2.28 percent

ASD TR 61-70

2. Calculation Sheet II

Analysis of 15 μsec. Pulse in Test Data Sheet II

Mid-range selection from Test Data Sheet II provides the following:

1) Rep Rate = 6, 000 cps
2) Pulse Duration = 15 x 10^{-6} secs.
3) Spot Size = 0.712 cm^2 in area
4) Ultor Volts = 27 x 10^3

5) Galvo Deflection = 7.4 cms
6) Peak Beam Current = 0.792
7) Thermopile to Tube Face = 4.0625 inches

Thermopile/Galvanometer Calibration: 0.118 cms Deflection = 1 μwatt/cm^2 Energy Density.

Hence, Energy Density at Thermopile = $\frac{7.4}{0.118}$ = 63 μwatts/cm^2

Area of Radiation = 2π x $(4.0625)^2$ = 670 cm^2
x 6.45

Total Average Energy = 63 x 670 = 42, 800 μwatts

Average Brightness = $\frac{42.8 \times 10^3}{0.712}$ = 60 x 10^3 μwatts/cm^2

Radiant Energy Density per Pulse = $\frac{60 \times 10^3}{6,000}$ = 10 μwatt-secs/cm^2

Radiant Energy per Pulse = 10 x 0.712 = 7.12 μwatt-secs.

Electrical Input Power per Pulse = (27 x 10^3) x = 320 μwatt-secs.

(0.792 x 10^{-3})

(15 x 10^{-6})

Input Energy Density = $\frac{320}{0.712}$ = 450 μwatt-secs/cm^2

Phosphor Efficiency = $\frac{7.12}{320}$ x 100 = 2.22 percent

476

3. <u>Calculation Sheet III</u>

Analysis of 50 μsec. Pulse in Test Data Sheet III

Mid-range value selected from Test Data Sheet III provides the following:

1) Rep Rate = 2,000 cps.

2) Pulse Duration = 50×10^{-6} secs.

3) Spot Size = 0.712 cm^2 in area

4) Ultor Volts = 27×10^3

5) Galvo Deflection = 7.25 cmь

6) Peak Beam Current = 0.67 ma

7) Thermopile to CRT Face = 4.0625 inches

Thermopile/Galvanometer Calibration: 0.118 cms Deflection = 1 μwatt/cm^2
Energy Density

Hence, Energy Density at Thermopile $= \frac{7.25}{0.118}$ = 61.5 μwatts/cm^2

Area of Radiation $= 2\pi \times (4.0625)^2 \times 6.45$ = 670 cm^2

Total Average Energy $= 61.5 \times 670$ = 41,000 μwatts

Average Brightness $= \frac{41 \times 10^3}{0.712}$ = 57.7×10^3 μwatts/cm^2

Radiant Energy Density per Pulse $= \frac{57.7 \times 10^3}{2,000}$ = 28.8 μwatt-secs/cm^2

Radiant Energy per Pulse $= 28.8 \times 0.712$ = 20.5 μwatt-secs.

Electrical Input Power per Pulse $= (27 \times 10^3) \times (0.67 \times 10^{-3}) \times (50 \times 10^{-6})$ = 905 μwatt-secs.

Input Energy Density $= \frac{905}{0.712}$ = 1270 μwatt-sec/cm^2

Phosphor Efficiency $= \frac{20.5}{905} \times 100$ = 2.26 percent

4. Calculation Sheet IV

Analysis of 5μsec. Pulse - High Peak Beam Current

Mid-range value selected from Test Data Sheet IV provides the following:

1) Rep Rate = 4,000 cps.

2) Pulse Duration = 5×10^{-6} secs.

3) Spot Size = 0.712 cm^2 in area

4) Ultor Volts = 27×10^3

5) Galvo Deflection = 7 cm^2

6) Peak Beam Current = 3.00 ma

7) CRT Face to Thermopile = 4.0625 inches

Thermopile/Galvanometer Calibration: 0.118 cms Deflection = 1 μwatt/cm^2 Energy Density.

Hence, Energy Density at Thermopile	$= \dfrac{7.0}{0.118}$	$= 59.4$ μwatts/cm^2
Area of Radiation	$= 2\pi \times (4.0625)^2 \times 6.45$	$= 670$ cm^2
Total Average Energy	$= 59.4 \times 670$	$= 39,800$ μwatts
Average Brightness	$= \dfrac{39.8 \times 10^3}{0.712}$	$= 57 \times 10^3$ μwatts/cm^2
Radiant Energy Density per Pulse	$= \dfrac{57 \times 10^3}{4000}$	$= 14$ μwatt-secs/cm^2
Radiant Energy Per Pulse	$= 14 \times 0.712$	$= 10$ μwatt-secs.
Electrical Input Power per Pulse	$= (27 \times 10^3) \times (3 \times 10^{-3}) \times (5 \times 10^{-6})$	$= 405$ μwatt-secs.
Input Electrical Energy	$= \dfrac{405}{0.712}$	$= 570$ μwatt-sec/cm^2
Phosphor Efficiency	$= \dfrac{10}{405} \times 100$	$= 2.46$ percent

478

5. Calculation Sheet V

Circular Raster Analysis

The following essential data were recorded:

1) Ultor Volts = 27×10^3

2) Average Beam Current = 180×10^{-6} amps

3) CRT Spot Size = 11.3×10^{-4} cm^2 (0.015") dia.

4) Thermopile/Galvo Deflection = 7.7 cms at 4.125 inches CRT

5) Galvanometer Sensitivity = 1 μwatt/cm^2 Energy Density for 0.118 cm deflection.

6) Raster Diameter = 2.5 inches

Hence, Energy Density at Thermopile $= \dfrac{7.7}{0.118}$ = 65 μwatts/cm^2

Area of Radiation $= 2 \pi \times (4.125)^2$
$\times 6.45$ = 690 cm^2

Total Energy $= 65 \times 690$ = 45,000 μwatts

Average Brightness $= \dfrac{45 \times 10^3}{11.3 \times 10^{-4}}$ = 39.8 watts/cm^2.
EFFECTIVE

6. Calculation Sheet VI

Equivalent Pulsed Operation of Circular Raster

Knowing the following;

1) Raster Diameter = 2.5 inches

2) Spot Size = 0.015 inch dia.

3) Rotational Speed = 30 cps.

4) Galvanometer Deflection = 7.7 cms.

Distance Travelled by Spot per Revolution $= \pi \times 2.5$ = 7.85 inches

No. of Spots per Revolution $= \dfrac{7.85}{0.015}$ = 520

No. of Spots per Second $= 520 \times 30$ = 15,600

479

ASD TR 61-70

Duration of One Spot $= \dfrac{1}{15,600} = 64 \times 10^{-6}$ secs.

Percent of Galvo-Deflection per Spot $= \dfrac{7.7}{520} = 0.0148$ cms.

Equivalent pulsed data are as follows:

1) Rep Rate = 30 cps.

2) Pulse Duration $= 64 \times 10^{-6}$ secs.

3) Spot Size $= 11.3 \times 10^{-4}$ cm^2(area).

4) Ultor Volts $= 27 \times 10^3$

5) Galvanometer Deflection = 0.0148 cms.

6) Beam Current = 180 μamps.

7) Tube Face to Thermopile = 4.125"

8) Galvo/Thermopile Calibration:

0.118 cms Deflection $= 1\,\mu$watt/cm^2 Energy Density.

Hence, Energy Density at Thermopile $= \dfrac{0.0148}{.118} = 0.125\ \mu$watts/cm^2

Area of Radiation $= 2\pi \times (4.125)^2 \times 6.45 = 690$ cm^2

Total Average Energy $= 690 \times 0.125 = 86.5\,\mu$watts

Average Brightness $= \dfrac{86.5}{11.3 \times 10^{-4}} = 76.5 \times 10^3\ \mu$watts/cm

Radiant Energy $= \dfrac{76.5 \times 10^3}{30} = 2540\ \mu$watt-sec/cm^2

Radiant Energy per Pulse $= 2540 \times 11.3 \times 10^{-4} = 2.87\ \mu$watt-secs.

Electrical Input Energy per Pulse $= (27 \times 10^3) \times (0.18 \times 10^{-3}) \times (64 \times 10^{-6}) = 310\ \mu$watt-secs.

Electrical Input Energy Density $= \dfrac{3.10}{11.3 \times 10^{-4}} = 270 \times 10^3\ \mu$watt-sec/cm^2

Phosphor Efficiency $= \dfrac{2.87}{310} \times 100 = 0.93$ percent

480

7. <u>Calculation Sheet VII</u>

Beam Current required for 0.375 inch Dia. Spot to Reach T_{max} in 10 μsecs.

Given: 1) Maximum radiant energy density of phosphor as $2540 \mu watt/sec/cm^2$

   2) Ultor Volts = 27×10^3

   3) Spot Dia. .375" or 0.712 cm^2 in area.

   4) Pulse Duration = 10×10^{-6} secs.

   5) Phosphor Efficiency = 2 percent

Radiant Energy per pulse = $\dfrac{2540}{0.712}$ = 3600 μwatt-secs.

Input Electrical Energy = $\dfrac{3600 \times 100}{2}$ = 180×10^3 μwatt-secs.

Beam Current = $\dfrac{180 \times 10^3}{27 \times 10^3 \times 10}$ = 0.67 amps.

From circular raster we know that a duty cycle of 500 provides the necessary cooling time.

$$\therefore \quad \text{Average beam current} = \frac{670}{500} = 1.34 \text{ ma}$$

$\therefore$ Frequency of pulses = 200 times per second.

Answer:

Phosphor heated to T_{max} by 10 μsec pulses requires a peak beam current of 0.67 amps at a repetition rate of 200 cps.

8. <u>Calculation Sheet VIII</u>

Energy Density at CRT Face for Optical Transfer Test

CRT Operating Conditions:

   1) Ultor Volts = 29×10^3 5) CRT Spot Size 0.712 cm^2 area

   2) Average Beam Current = 120 μa   6) Peak Beam Current = 1.5 ma

   3) Pulse Width = 5×10^{-6} secs.   7) Galvometer Deflection = 13 cms.

   4) Rep. Rate = 16,000 cps.   8) Galvo to CRT Face = 4.125 "

Thermopile Calibration/Galvo Deflection: 0.118 cms Deflection = 1 μwatt/cm^2
Energy Density.

481

Hence, Energy Density at Thermopile $= \dfrac{13}{0.118}$ $= 110$ μwatts/cm^2

Area of Radiation $= 2\pi \times (4.125)^2$ $= 690$ cms.
$\times 6.45$

Total Average Energy $= 110 \times 690$ $= 74 \times 10^3$ μwatts

Average Brightness $= \dfrac{74 \times 10^3}{0.712}$ $= 104 \times 10^3$ μwatts/cm^2

Energy Density per Pulse $= \dfrac{104 \times 10^3}{16 \times 10^3}$ $= 6.5$ μwatt-secs/cm^2

Energy per Pulse $= 6.5 \times 0.712$ $= 4.6$ μwatt-secs.

Electrical Energy Input per Pulse $= (29 \times 10^3) \times$ $= 218$ μwatt-secs.
(1.5×10^{-3})
(5×10^{-6})

Phosphor Efficiency $= \dfrac{4.6}{218} \times 100$ $= 2.1$ percent

9. Calculation Sheet IX

Energy Density at Image for Optical Transfer Test

1) Lens = f1.60.75 inch F.L.

4) Image Spot Size $= 155 \times 10^{-4}$ cm^2 (0.055" Dia.)

2) Image Plane to Lens F.L. pt. = 1.85 cms.

3) Thermopile to image plane = 5.0 cms.

5) Galvo Deflection = 1.2 cms.

Hence, Lens Diameter $= \dfrac{f}{f1} = \dfrac{.75}{1.6} = 0.47" = 1.2$ cm^2 Radius = 0.6 cms.

Solid Angle $= \pi \operatorname{Tan}^2 \theta$ where $\tan \theta = \dfrac{0.6}{1.85} = 0.324$

$= \pi \times (0.324)^2 = 0.33$ Steradians.

Energy Density at Thermopile $= \dfrac{1.2}{0.118} = 10.2$ μwatts/cm^2

Area of Radiation = Solid Angle x (Distance)^2 $= 0.33 \times 5^2 = 8.25$ cms.

Total Energy per Unit Time $= 10.2 \times 8.25 = 84$ μwatts
Passing Through Image Plane

Energy Density at Image $= \dfrac{84}{155 \times 10^{-4}} = 5.4 \times 10^3$ μwatts/cm^2

From Sheet No. 8 Energy Density at CRT face $= 104 \times 10^3$ μwatts/cm^2

Ratio Transfer $= \dfrac{5.4}{104}$ or $\dfrac{1}{20}$ th Approximately.

APPENDIX XVII
ACCESSING STUDIES
PRIOR TO CONTRACT AF 33(616)-6205

Paper accessing studies were undertaken during the initial stages of the project to determine the special features of a photochromic memory which might be helpful in providing the optimum accessing schemes. Some rather interesting results were obtained.

Proposals for using relatively non-absorbing regions of the photochromic spectrum for access control and negative feedback stabilization appeared to be important contributions to the solution of these problems. Since these spectral regions would not change with a change in photochromic state, this type of accessing and stabilization would not require a specified method for coding the stored information.

Three such proposal were made, initially:

1) Light beam tracking - A variable density wedge of photographic material with specified spectral absorption (in a region where the photochromic material is non-absorbing) could be deposited directly under (or over) the photochromic material. By proper feedback, filters, and beamsplitters, the light beam could be servoed on the middle density of the wedge while writing, reading, or erasing the photochromic substance.

2) Clocking information - Another photochromic non-absorbing spectral region (different from that in (1) above) would be used. In this case, the proper photographic material would be deposited on the storage surface as a series of lines across each track. Use of this clock information plus the tracking information should allow precise access to a given point on the surface.

483

3) Photomultiplier Compensation - A third photochromic non-absorbing spectral region could be used to compensate for variations and/or drift in the gain of photomultiplier tubes. The scheme requires sampling this third region at some convenient period and correcting the photomultiplier output to a fixed standard.

Figure 186, the Photochromic Tracking Scheme, illustrates a method for keeping the light beam on the average density of a variable density pre-recorded track. The scheme depicted assumes the photochromic material is relatively red transparent, and that this red transparency is independent of photochromically recorded information.

Figure 187, the On-Track Clocking Scheme, breaks the photochromic non-absorbing spectral region into two bands; one is used for servoing as in Figure 186, and the other is used to sense clock marks written along the track. As before, a selective spectral reflector separates the channels. This reflector would be placed just to the left of the reflector shown in Figure 186.

Figure 188, the Compensation Scheme, has regions R_1, R_2, and R_3 of Figure 187 fall within Region A of the rotating disk filter. Additional light is available in Region B which is incapable of being modulated by the photochromic, clock, or servo information. The photomultiplier compensation circuit periodically samples the light in Region B, produces a corresponding voltage, and compares it with a reference. If this supposedly constant brightness signal has changed because of changes in the phototube and/or the light source, the comparison network will produce a change in the photomultiplier high voltage to change the photomultiplier gain to offset the aforementioned change (s).

A system somewhat similar in concept to the preceding systems was also conceived. It is pictured in Figures 189 and 190.

484
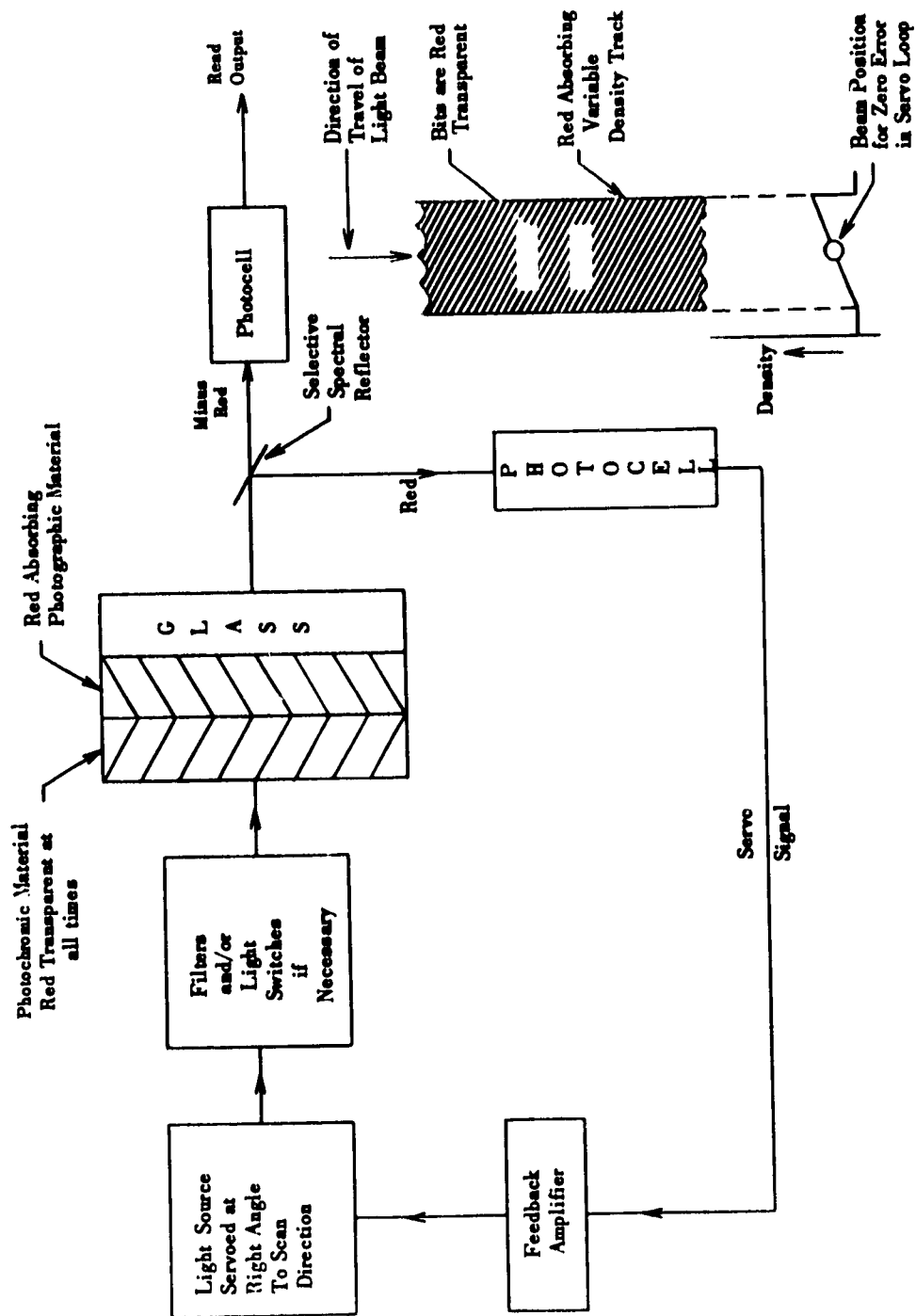
Figure 186. Photochromic Tracking Scheme.
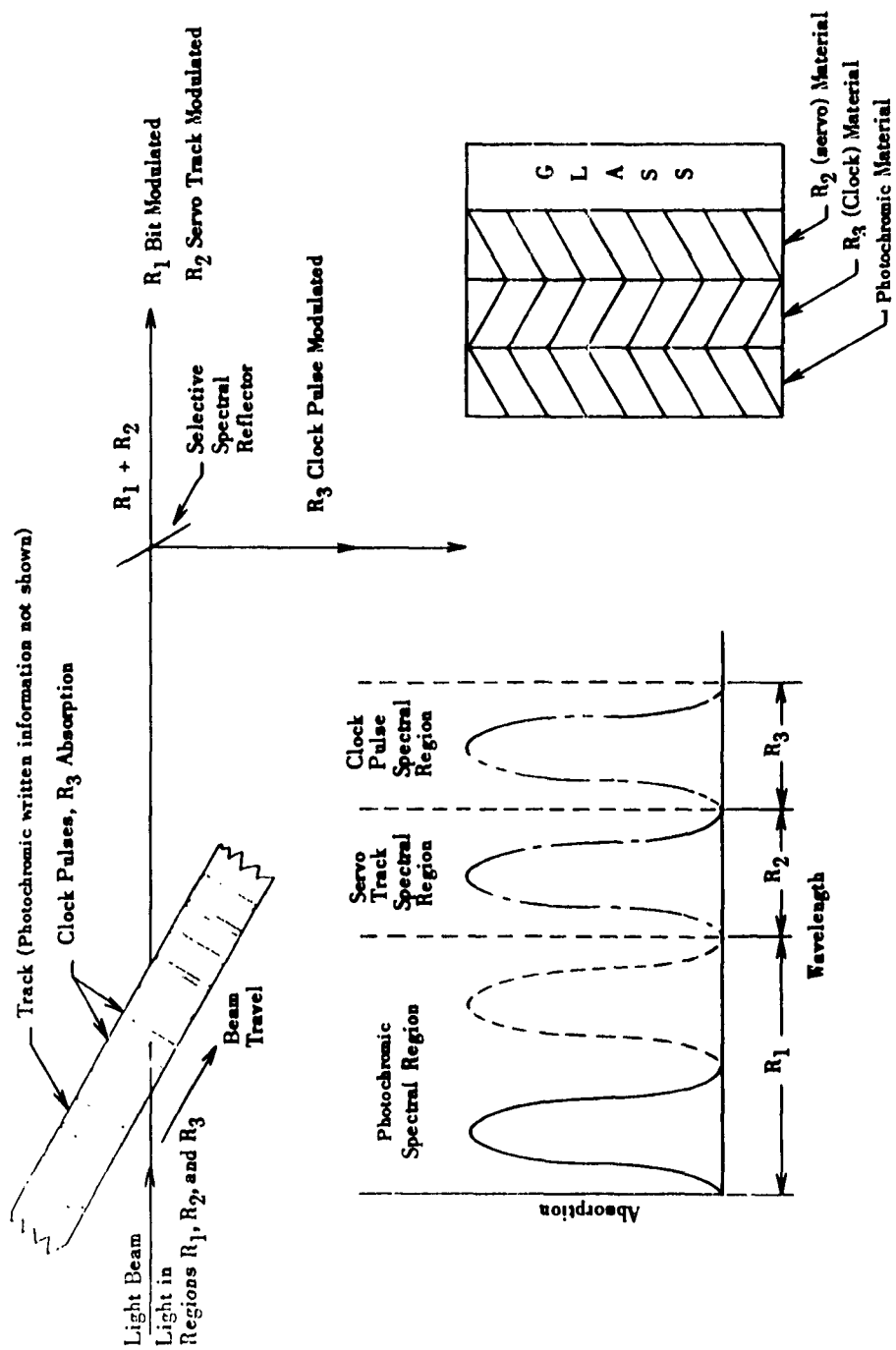
Figure 187. On-Track Clocking Scheme.
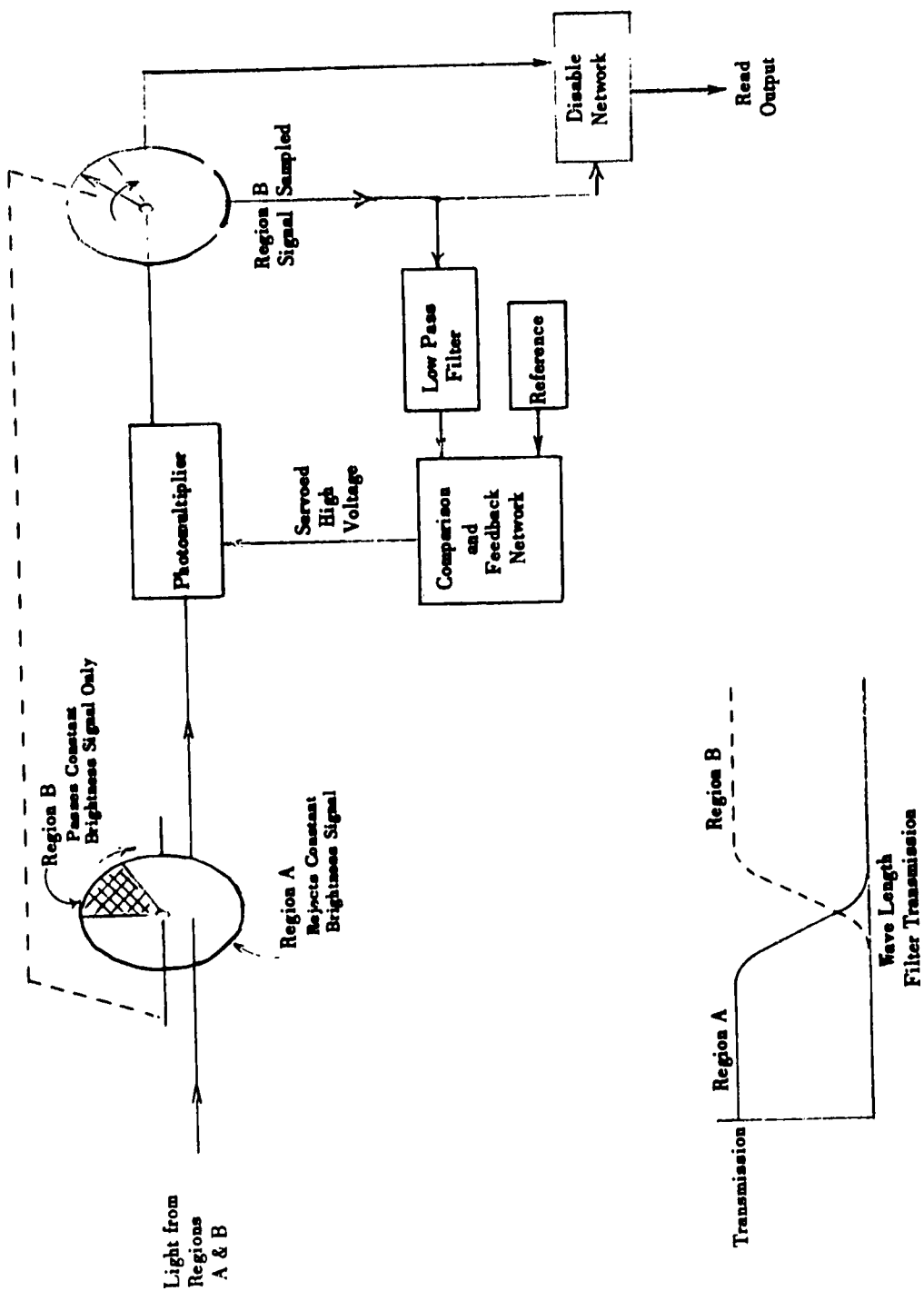
Figure 188. Compensation Scheme.

487
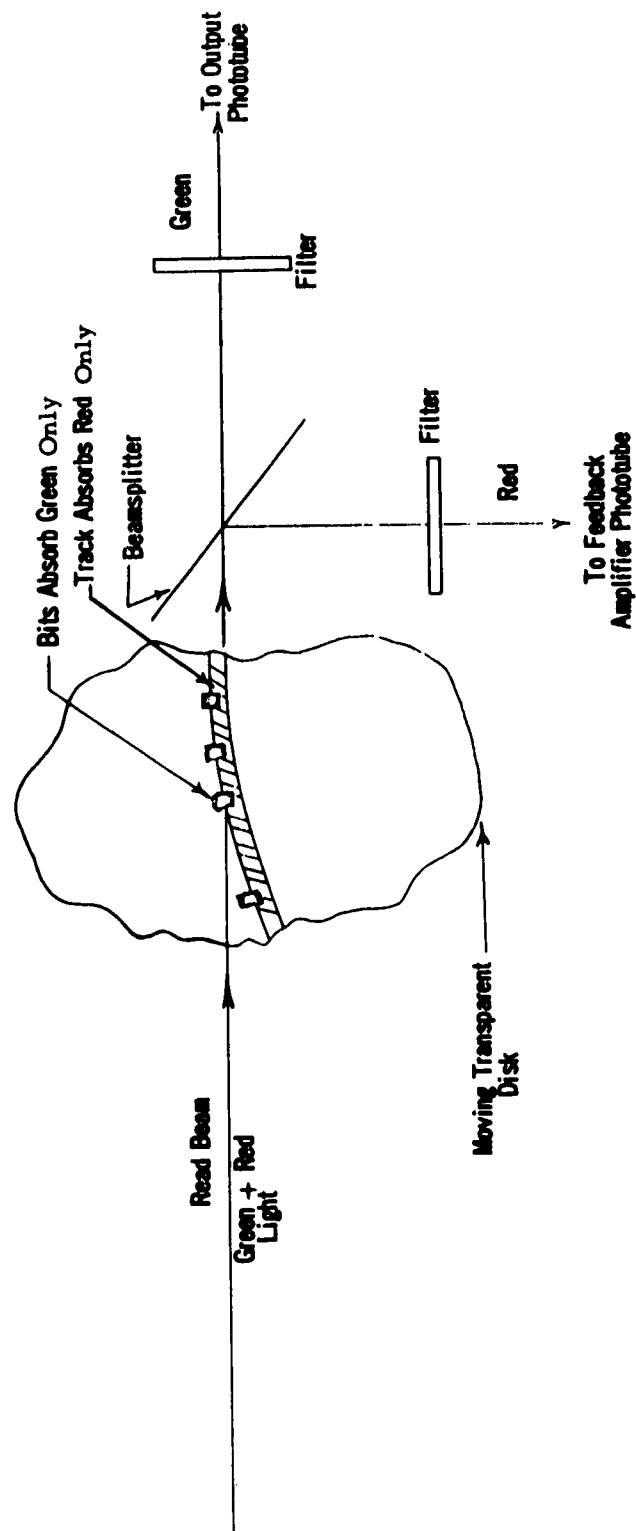
Figure 189. Photochromic (Information) - Photographic (Tracking) Memory.

ASD TR 61-70

Figure 190. Photochromic-Photographic Memory Track Details.
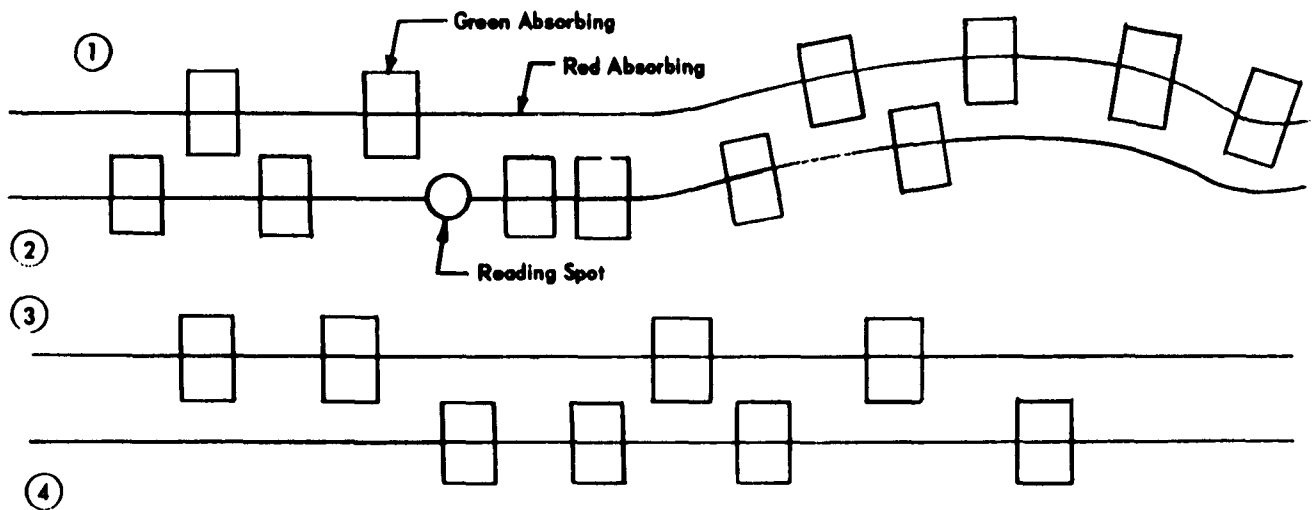
BEAM SERVOED TO STRADDLE EDGE OF TRACKING LINE

VERY FAST ACCESS BETWEEN TRACKS ② AND ③ BY REVERSING SERVO POLARITY

BY OPTICAL FILTERING, TRACKING AND BIT SENSING ARE INDEPENDENT OF ONE ANOTHER

COINCIDENCE DETECTION BETWEEN TRACKING AND BIT SENSING PHOTOTUBES FOR ERROR DETECTION (DIRT OR HOLES IN MATERIAL)

489

The rotating polygon memory of C. Baumann of MIT, depicted in Figure 191 was considered briefly, both theoretically and experimentally. With write and erase sources at the photodiode plane, and with photochromic material at the photographic plane, read can occur as in Baumann's memory, while the write and erase sources are imaged correctly in the reverse direction by the lens pictured. This system appeared to offer both optical and energy transfer difficulties.

A CRT imaged spot, edge-locking device, the Optron, shown in Figure 192 was purchased to aid in initial CRT feedback accessing studies. A number of modifications were made in the basic mechanism in order to make it more versatile for experimentation. This device could be servoed to a dark-light edge by either reflected light or transmitted light, and it was used experimentally in both modes. Control circuitry was designed and constructed in order that this device could be used for track-seeking as well as track-locking studies.

When a CRT is servoed on a track, optimum reliability dictates that the read-write-erase images be related somewhat as in Figure 193 It was found possible to achieve these relationships by use of a ten megacycle sweep on the deflection plates of the Optron. This high frequency, or even higher if need be, is not sensed by the system, and the spot appears to the system just as pictured in Figure 193.

The accessing discussion just presented was not exhaustive in presenting the accessing systems considered (e. g., The Bell System Photomemory, mechanical accessing, etc.), but the accessing problem was to receive further attention in systems studies.

490
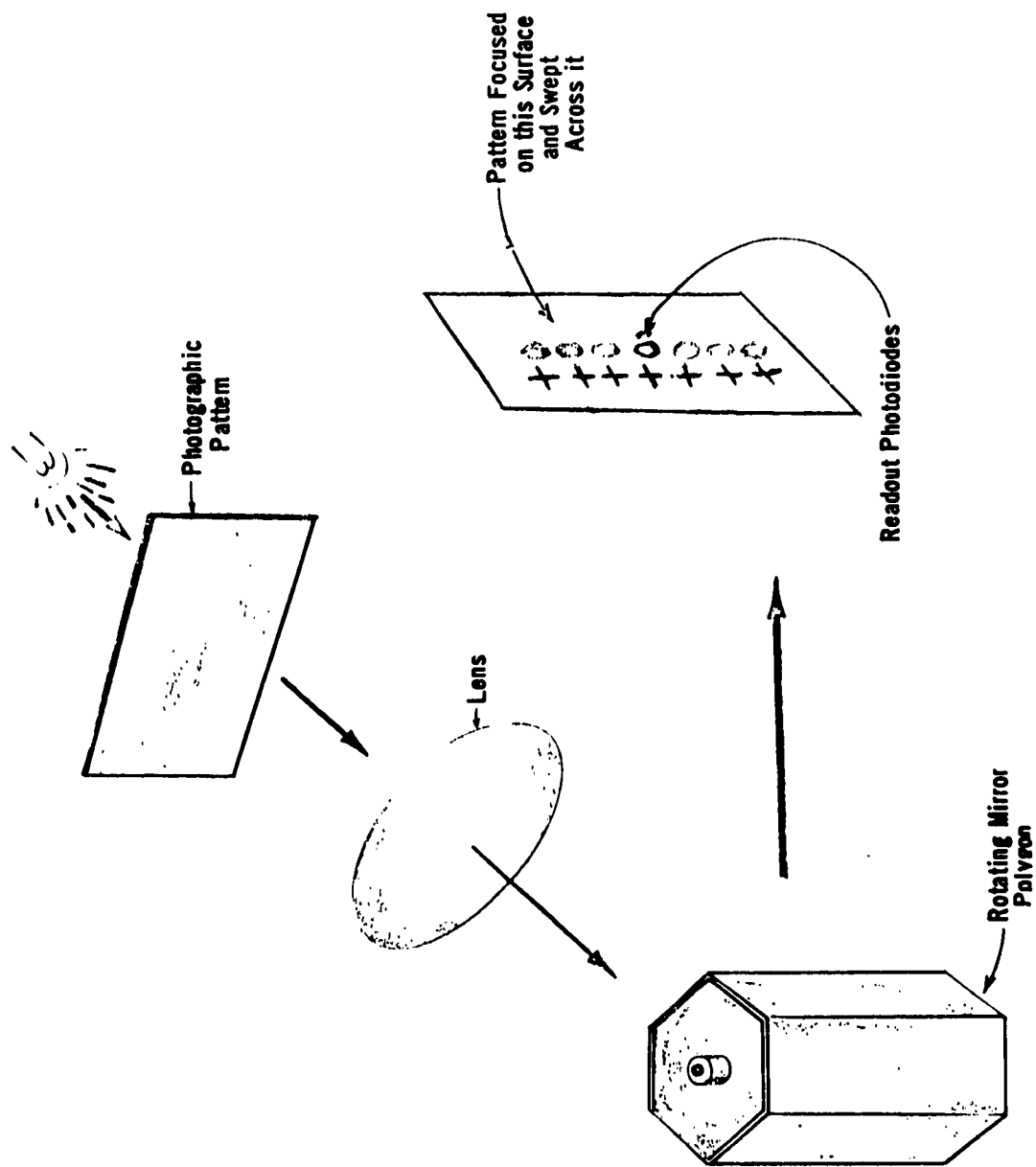
Figure 191. Baumann's Rotating Mirror Photomemory.

491
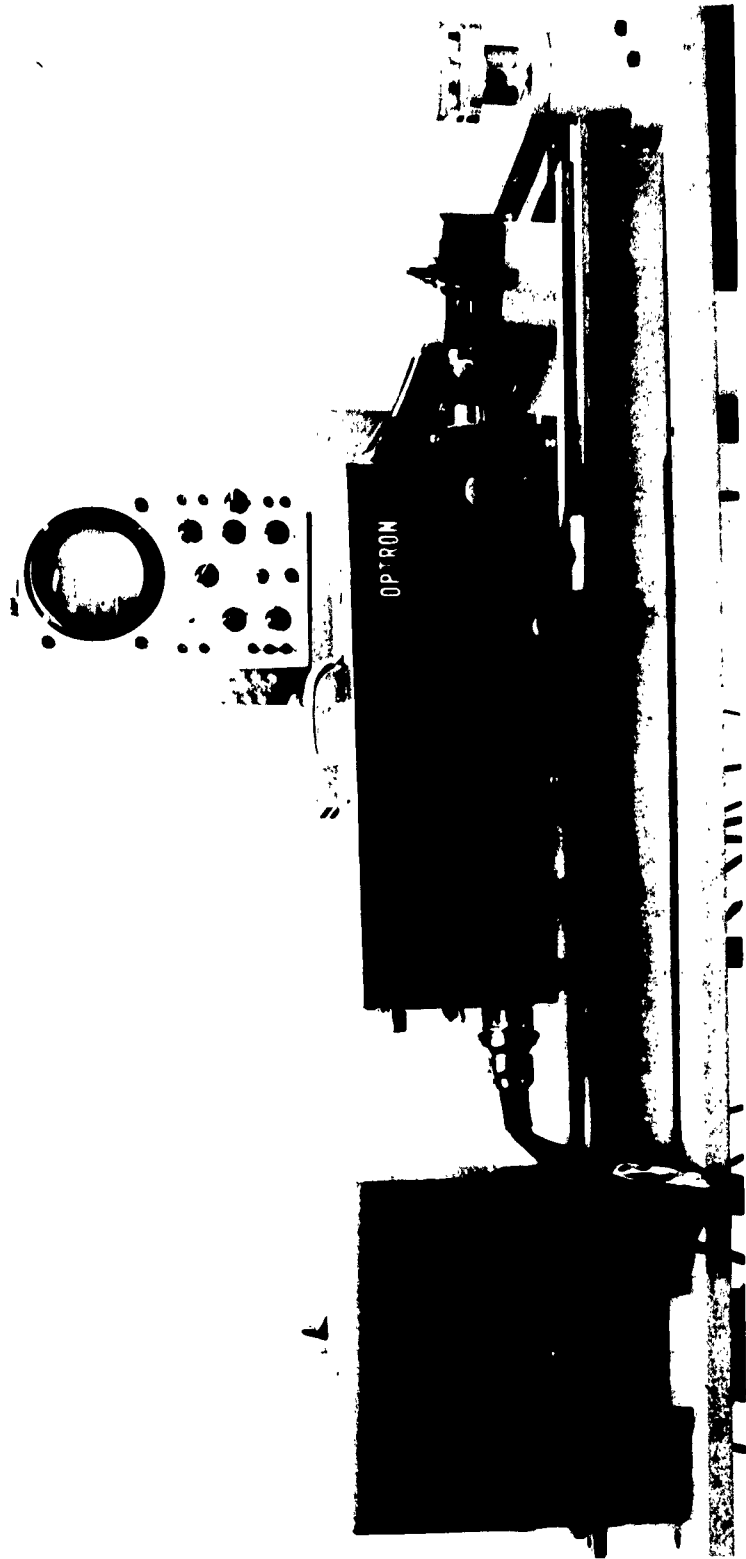
Figure 192. Optron Equipment.

492
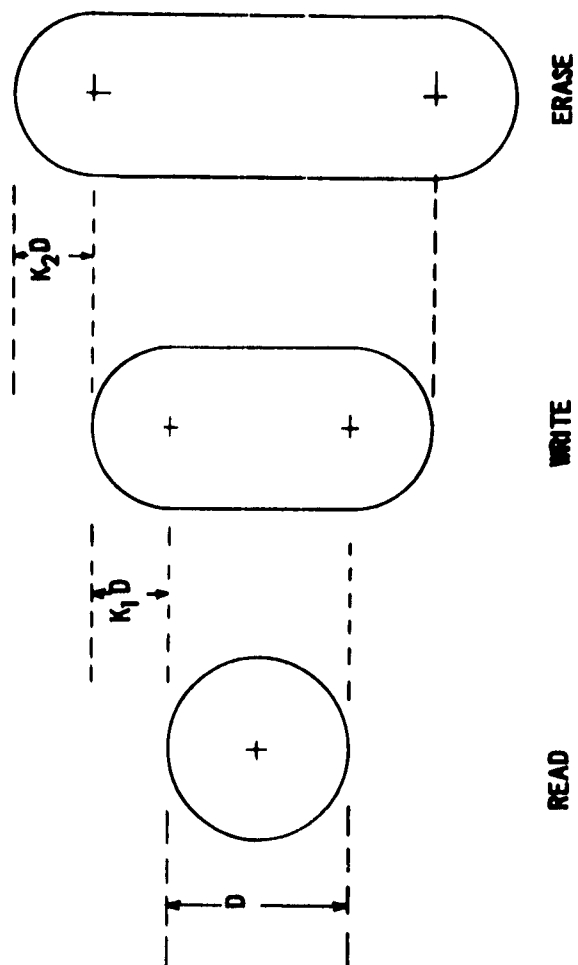
Figure 193. Optimum Shapes for Cathode-Ray Tube Imaged Spot.

493

APPENDIX XVIII

SYSTEMS STUDIES
PRIOR TO CONTRACT AF 33(616)-6205

A. INTRODUCTION

Two preliminary systems proposals were generated prior to receipt of this contract. These proposals were to provide the information necessary for a preliminary evaluation of the potentialities of a photochromic memory. Since physical and chemical data was lacking on the properties of encapsulated photochromic material systems, assumptions were to be made concerning such data to establish detailed specifications for the proposed devices.

The systems which were proposed were based on 1), the use of a cathode-ray tube and 2), on the use of an ultrasonic diffraction grating light shutter. Brief descriptions of these systems follow.

B. CATHODE-RAY TUBE PHOTOCHROMIC MEMORY

This proposed device consisted of a single rotating glass or metallic disk, two cathode-ray tubes, optics, four photomultipliers and associated electronic equipment. Both sides of the disk were to be used to give, essentially, two memory systems in parallel from a single disk. The essential specifications are listed in Table XLVI.

TABLE XLVI
CRT PHOTOCHROMIC MEMORY SPECIFICATIONS

Capacity	50 megabits
Maximum Access Time	0.125 seconds
Transfer Rate	200 KC
Maximum Bit Density Along Tracks	1000/inch

494

ASD TR 61-70

TABLE XLVI (CONT'D)

CRT PHOTOCHROMIC MEMORY SPECIFICATIONS

Bit Capacity/Track	25,000 Bits/Track
Track Density	250 Tracks/inch
No. of Tracks	1000 Tracks/Disk Side
Motor Speed	480 rpm
Track Width	0.002 inch
Between-Track Spacing	0.002 inch
Disk Diameter	17 inches

The characteristics listed in Table XLVII were assumed realizable in a photochromic material.

TABLE XLVII

PHOTOCHROMIC MATERIAL CHARACTERISTICS

Basic Properties:	
Write and Erase Times	5 microseconds
Operating Bit Size (includes smear)	0.001 inch x 0.002 inch
Write Wavelengths	<3800 A^o
Erase and Road Wavelength Band	4500A^o - 5500A^o
Low Intensity Read	No erasure
Coating Uniformity:	
Capsule Size Range	1-3 microns
Maximum Hole Diameter	7 microns
Hole Area per Bit[*]/Total Area per Bit	0.10

[*]Holes smaller than 1 1/2 microns were not considered in this calculation.

Figures 194 through 198 illustrate the important aspects of the system. A reflecting disk would be used. Multiple strip phosphors on the CRT allow the read-write-erase operations to be performed by a single CRT, and optical dissection doubles the CRT resolution. Tracking and recorded information would be separated in spectrally independent channels.

495

ASD TR 61-70
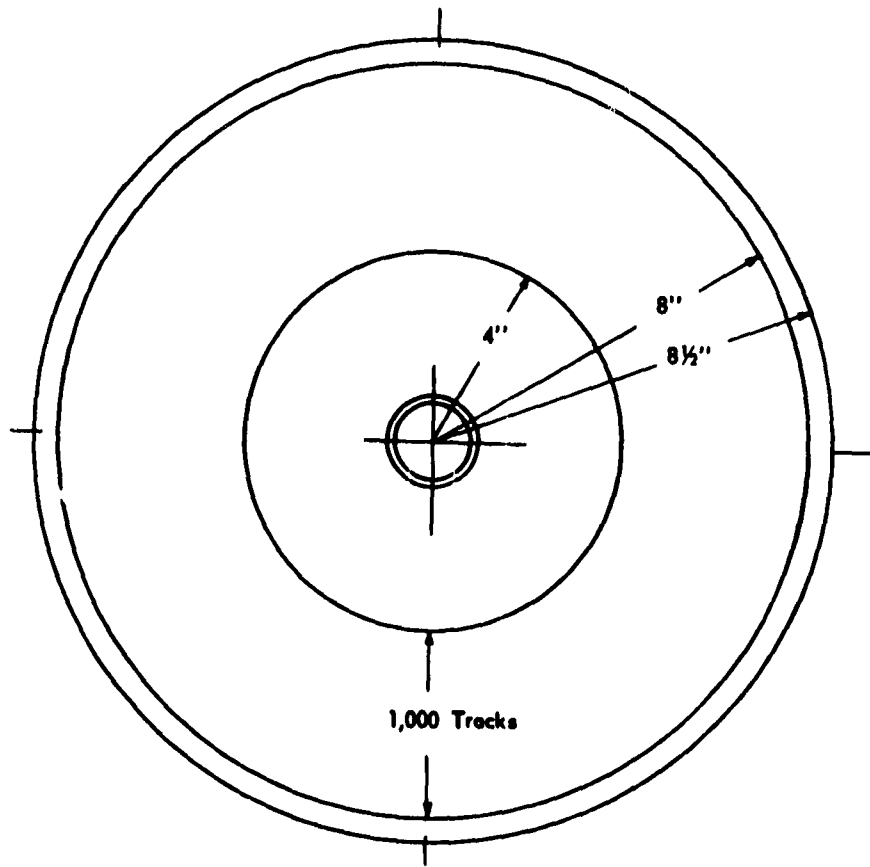
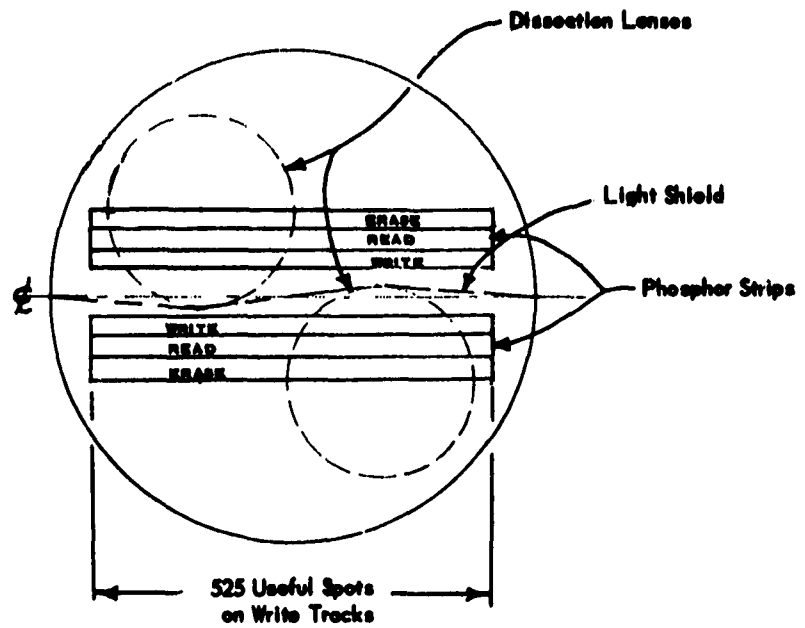Figure 194. Memory Disk (Same Pattern Other Side).

496
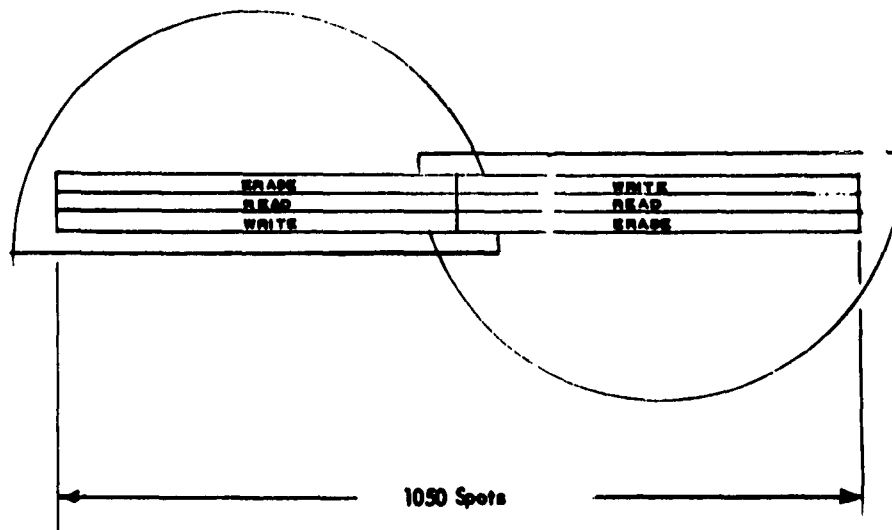
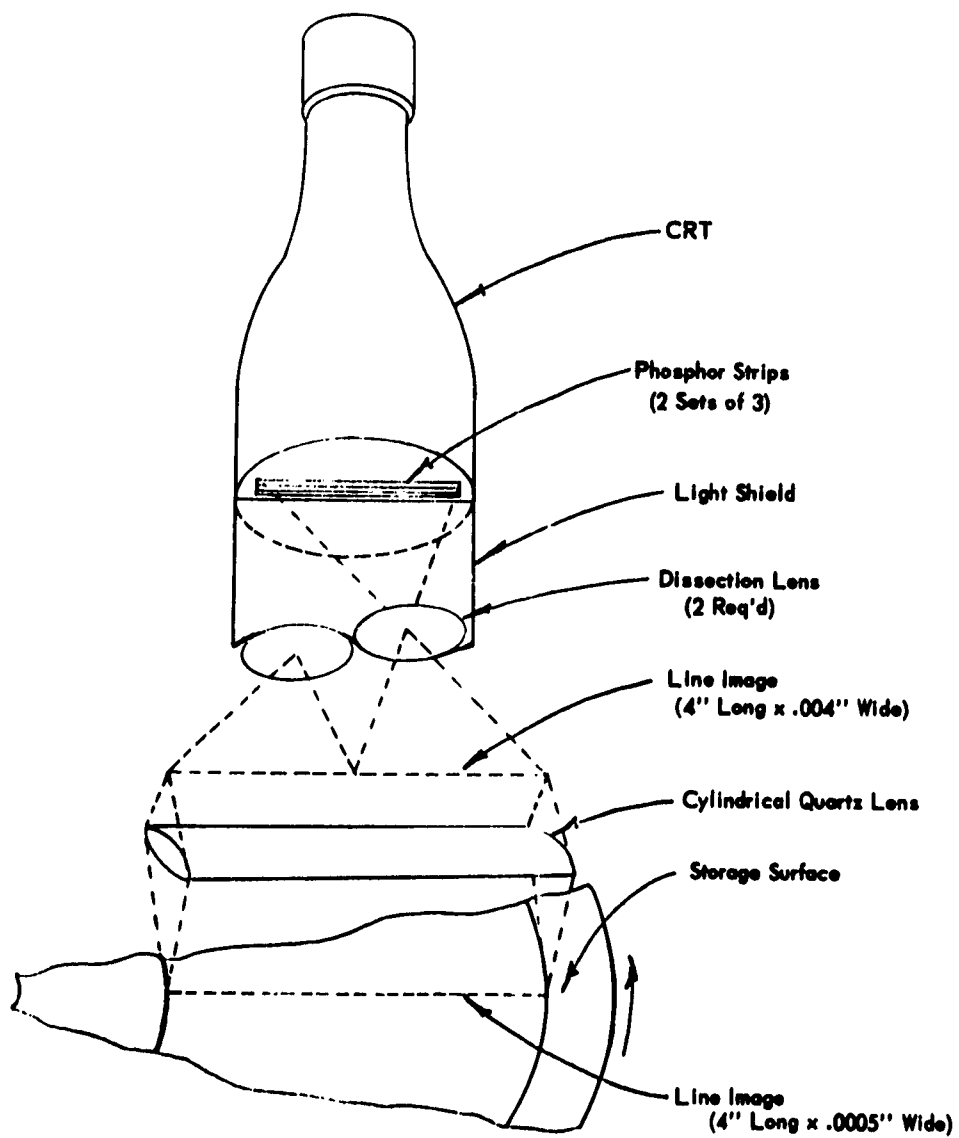Figure 195. CRT Face.

Figure 196. CRT Optical Dissection Image.

497

Figure 197. Optical Dissection and CRT Spot Demagnification.

498

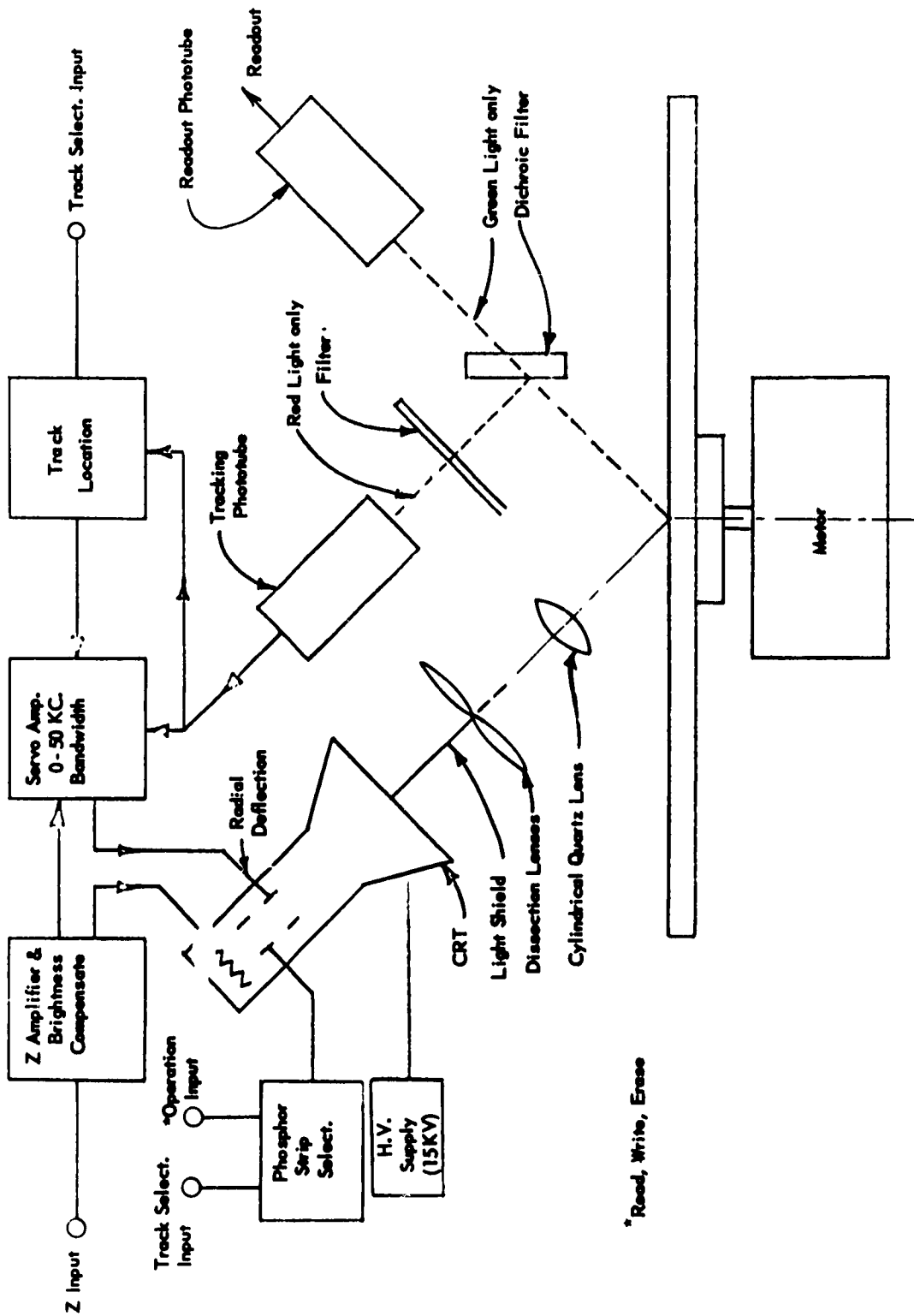Figure 198. Possible Operational Setup for Single Side Storage.

* Read, Write, Erase

499

C. ULTRASONIC DIFFRACTION GRATING LIGHT SHUTTER

This proposed device consisted of a drum whose shape was the central cross-section of a sphere, a servoed mirror, an ultrasonic diffraction grating, a light source, a drive motor, a photomultiplier, and necessary associated electronic equipment (see Figure 199). The specifications for the device are listed in Table XLVIII.

TABLE XLVIII
ULTRASONIC DIFFRACTION GRATING SPECIFICATIONS

|	
Capacity	26 megabits
Maximum Access Time	0.11 seconds
Transfer Rate	300 KC
Bit Density Along Tracks	1250 Bits/inch
Bit Capacity Per Track	43,000 Bits/Track
Track Density	100 Tracks/inch
No. of Tracks	600 Tracks
Motor Speed	456 RPM
Track Width	0.004 inch
Between-Track Spaces	0.002 inch
Drum Dimensions	12 inch Diameter 6 inch long

The characteristics listed in Table XLIX were assumed realizable in a photochromic material to be used in this system.

TABLE XLIX
ULTRASONIC DIFFRACTION GRATING-PHOTOCHROMIC
MATERIAL SPECIFICATIONS

Basic Properties:	
Write and Erase Times	16 microseconds
Operating Bit Size	0.0008 inch x 0.004 inch

500
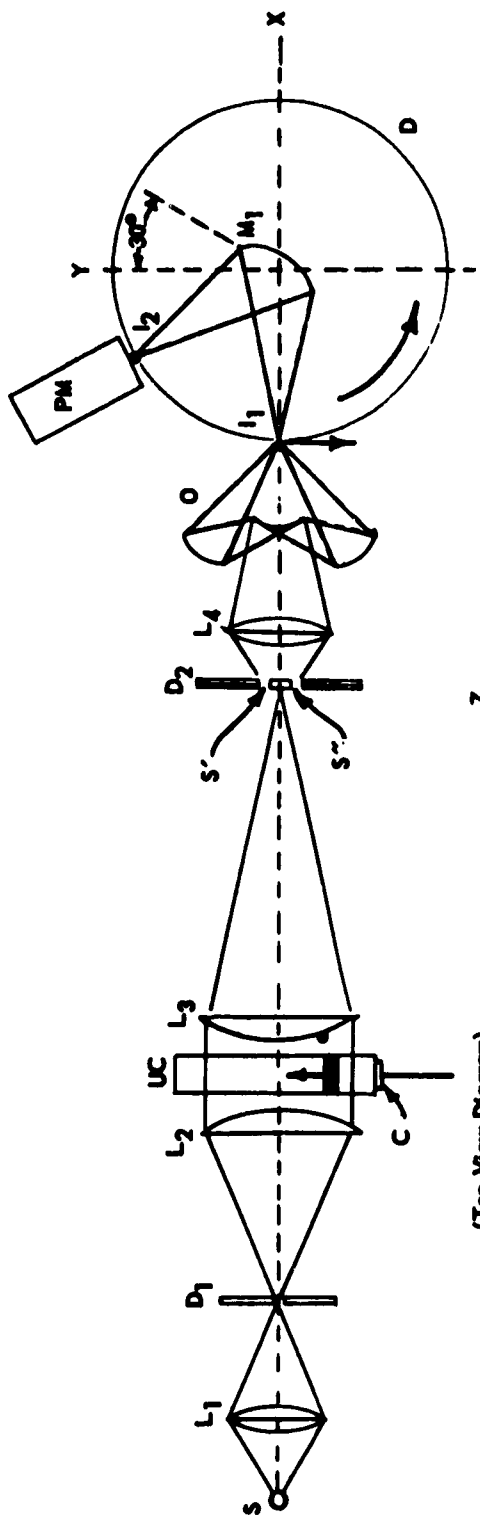
(Top View Diagram)
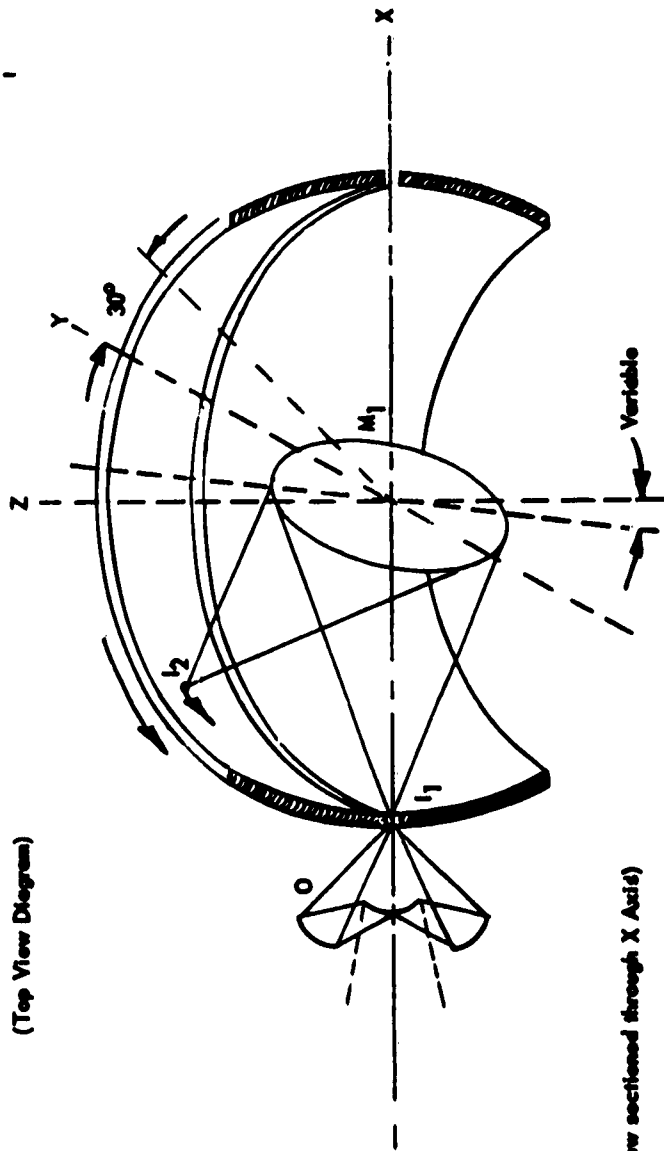
(Side View sectioned through X Axis)

Figure 199. Ultrasonic Grating System.

501

TABLE XLIX (CONT'D)

ULTRASONIC DIFFRACTION GRATING-PHOTOCHROMIC

MATERIAL SPECIFICATIONS

Write Wavelengths	$<3800\text{Å}$
Erase and Read Wavelength Band	$4500\text{Å} - 5500\text{Å}$
Low Intensity Read	No erasure
Coating Uniformity:	
Capsule Size Range	1 - 3 microns
Maximum Hole Diameter	5 1/2 microns
Hole Area Per Bit[*]/Total Area per Bit	0.10

[*]Holes smaller than 1 1/2 microns were not considered in this calculation.

The storage surface would be located on the interior surface of a drum (Figures 199 and 200). As shown, the drum would be equivalent to a central section of a large sphere, which, in turn, would be divided into two sections. This configuration greatly simplified the optical requirements for the reflecting lens located at the center of the drum. The lens was to be used to servo and focus the light beam on the proper track. The light beam was to enter the drum through the slit separating the two drum sections.

For the transmission read-out operation (Figure 194) the drum had to be transparent. An alternate scheme, Figure 200, suggested the use of any suitable drum material which could be coated with a reflecting coating. The read beam would be reflected from this coating to a deflection mirror inside the drum and then passed on to a photomultiplier located at the side of the drum.
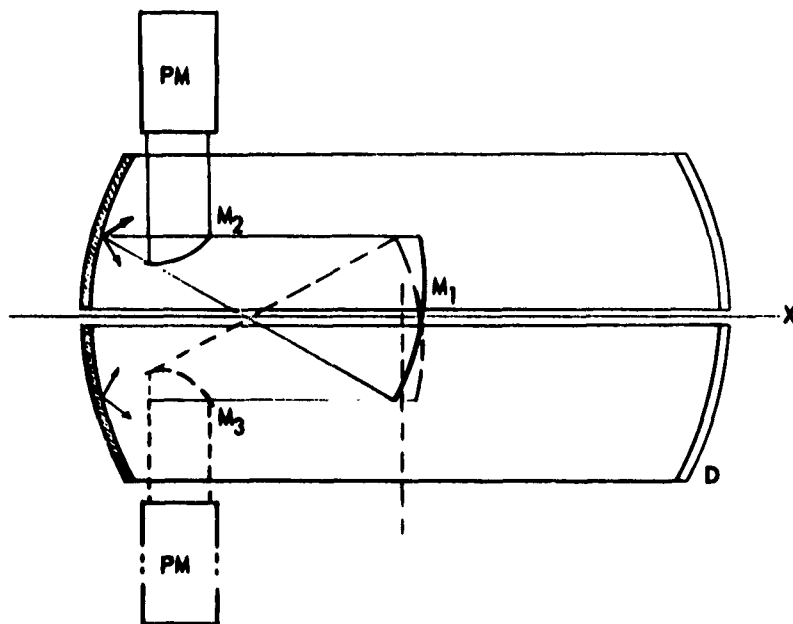
ASD TR 61-70

Figure 200. Reflecting Readout Scheme.

ASD TR 61-70